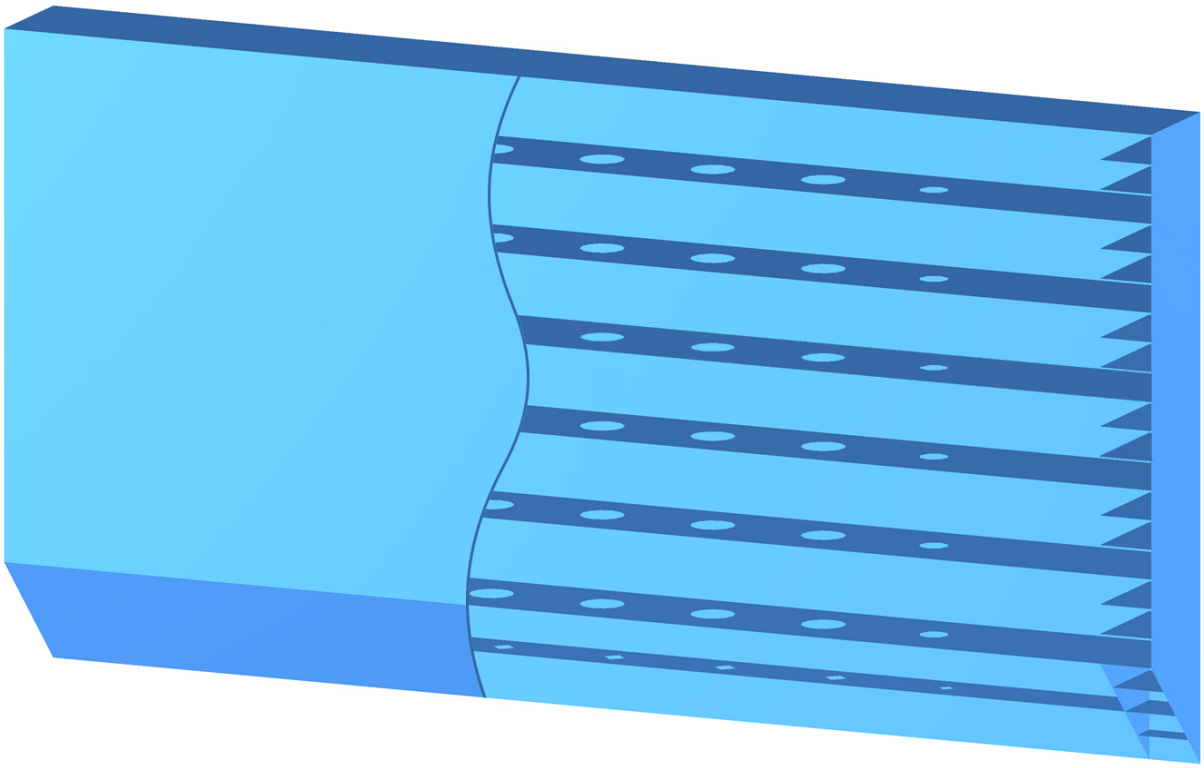
Feasibility study on fibre reinforced polymer slides in the Eastern Scheldt storm surge barrier

Master thesis



Ing. R.W. van Straten
September 2013

TU Delft

Witteveen + Bos

Feasibility study on fibre reinforced polymer slides in the Eastern Scheldt storm surge barrier

Master thesis

Author

Name:	R.W. van Straten
Student number:	1504932
Email:	r.w.vanstraten@student.tudelft.nl

Study

Delft University of Technology
Faculty of Civil Engineering & Geosciences
Department Structural engineering
Stevinweg 1, 2628 CN Delft

Graduate company

Witteveen+Bos
PMC Infrastructural Engineering
Special materials and structures
Leeuwenbrug 27, 7411 TE Deventer

Graduation committee

Chairman:	Prof. ir. F.S.K. Bijlaard	TU Delft, CEG
Committee members:	Dr. M.H. Kolstein	TU Delft, CEG
	Dr. ir. P.C.J. Hoogenboom	TU Delft, CEG
	Ir. W. Claassen	Witteveen+Bos
Graduation coordinator:	Ir. L.J.M. Houben	TU Delft, CEG

September 2013

© Copyright 2013 R.W. van Straten, Delft University of Technology, Delft, the Netherlands
All rights reserved. No part of this document may be reproduced for commercial purposes without written consent from the author. Permission is granted to reproduce for personal and educational use only with the use of proper citation. Commercial copying, hiring, lending and selling is prohibited without written consent from the author.

Preface

This report presents the results of my Master Thesis. This graduation project was performed to obtain my master's degree in Civil Engineering at Delft University of Technology. The project was carried out at the engineering office Witteveen+Bos in Deventer.

I would like to thank some people which supported me during this graduation project. First of all, I want to thank the graduation committee members from Delft University of Technology for their support and advice during the graduation meetings. In addition, I would like to thank Wouter Claassen who has accompanied me from Witteveen+Bos and I want to thank Maarten Visser for his support and advice at various times.

Finally, I want to thank my family which supported me during my study and especially my girlfriend which gave me the time and space to carry out this project.

Deventer, September 2013

Roeland van Straten

Summary

The Eastern Scheldt storm surge barrier is a closeable barrier in Southwest Netherlands, which should protect the Southwestern Delta from flooding from the North Sea. The barrier is constructed with lifting steel slides, which corrode rapidly in the salty environment. The service life of the coating, which should protect the slides, is probably too short, to maintain all the slides before maintenance is necessary. Therefore, the slides can deteriorate such that maintenance costs exceed the costs of replacement of the slides.

Previous researches on new slides in the Eastern Scheldt barrier showed that the replacement of the existing slides could form an attractive solution. Next to that, the rise in use of fibre reinforced polymers in the civil engineering industry, due to their high strength properties, low self weight and low maintenance give occasion to study the feasibility of fibre reinforced polymer slides in the Eastern Scheldt barrier.

Different variants of FRP slides have been investigated. This shows that a box-girder variant with a thickening in the middle is a structural promising design for the slide. The deflection of this variant is such big, that the slide will hit the upper beam of the barrier. Therefore, it's checked whether it's possible to reduce or vanish this deflection requirement.

That investigation shows that there are two options:

- To vanish the deflection requirement a rigorously solution has to be carried out. This option requires extra adjustments on the current barrier. The upper beam should be removed, the sill beam should be replaced and the rabbets should be increased.
- To meet the deflection requirement the stiffness of the FRP slide could be increased by using carbon fibers, a camber can be applied or the leakage gap could be increased. This option does not require extra adjustments on the current barrier.

Since the last option is not feasible by using glass fibres, which are much cheaper than carbon fibres and the first option has some advantages on the long term, the first option is elaborated into more detail. The advantages on the long term are:

- The top of the slide has increased to cope with the sea level rise in the future.
- The sill beam height is halved to increase the trough-flow opening of the barrier. This can contribute to solve the problem of disappearing intertidal zones in the Eastern Scheldt.

The deflection requirement is vanished in this option. This can be done, since nobody had to walk over the slide or is hampered by a large deflection. Therefore, the final design could be dimensioned on strength. The uniform strain criterion is used as criterion in ULS.

The final design is a straight box-girder, without a thickening in the middle, since the thickness should be decreased to apply an oblique bottom of the slide. This oblique bottom should be applied due to hydraulic reasons. It should prevent vibrations of the slide by flow. The final design has a height of 22 m and a uniform thickness of 4 m.

The direct investment costs of the final design are estimated on 225 million euro, including the extra adjustments which are necessary. These costs are in comparison with the costs of dike raising, which could form an alternative on the long run, much lower. Also a life cycle analysis is carried out to compare the investment costs of an FRP slide with the maintenance costs of the current barrier. This

LCA shows that the life cycle costs of an FRP slide are much lower over 100 years, the payback time of the FRP slides is between 40 and 50 years.

Therefore, it's technically feasible and financially attractive to replace the current steel slides with larger FRP slides.

Table of contents

PREFACE ..... **V**

SUMMARY ..... **VII**

LIST OF FIGURES ..... **XV**

LIST OF TABLES ..... **XIX**

1 INTRODUCTION **1**

1.1 BACKGROUND 1
1.2 PROBLEM DESCRIPTION 1
1.3 PREVIOUS RESEARCH 1
1.4 RESEARCH OBJECTIVE 1
1.5 RESEARCH QUESTIONS 2
1.6 STRUCTURE OF THE REPORT 2

PART 1: LITERATURE STUDY

2 THE DESIGN OF THE CURRENT BARRIER **6**

2.1 HISTORY 6
2.2 DELTA PLAN 6
2.3 CLOSABLE STORM SURGE BARRIER 7
2.4 DESIGN OF THE STORM SURGE BARRIER 8
2.4.1 Boundary conditions *8*
2.4.2 Overall design *8*
2.4.3 Bottom consolidation *8*
2.4.4 Piers *10*
2.4.5 Construction of the other parts *10*
2.5 SETTLEMENTS AND MAINTENANCE 10
2.6 FUTURE OF THE BARRIER 11
2.6.1 Future vision of the Delta committee *11*
2.6.2 Sea level rise *11*
2.7 SUMMARIZED 12

3 STRUCTURAL DESIGNS FOR LIFTING SLIDES **13**

3.1 OTHER WATER BARRIERS WITH LIFTING SLIDES 13
3.1.1 Hartel barrier *13*
3.1.2 Storm surge barrier Hollandse IJssel *13*
3.2 CONCEPTS FOR SLIDES IN THE EASTERN SCHELDT BARRIER 14
3.2.1 Concepts Veraart *14*
3.2.2 Concepts Van der Laken *15*
3.2.3 Concepts concrete slides *17*
3.2.4 Analysis of concepts *18*
3.3 HYDRAULIC DESIGN CONSIDERATIONS FOR LIFTING SLIDES 18
3.3.1 Vibrations by flow *18*
3.3.2 Wave impact loads *19*
3.4 SUMMARIZED 20

4 FIBRE REINFORCED POLYMERS **21**

4.1 HISTORY 21
4.2 GENERAL 22
4.3 REINFORCEMENTS 22
4.3.1 Glass fibres 22
4.3.2 Carbon fibres 23
4.3.3 Polyaramid fibres 23
4.3.4 Other reinforcements types 23
4.3.5 Reinforcement forms 23
4.4 RESINS 24
4.4.1 Unsaturated polyester resins 25
4.4.2 Vinyl ester resins 25
4.4.3 Epoxy resins 25
4.4.4 Other resin types 25
4.5 CORES 25
4.5.1 Foam 25
4.5.2 Honeycomb 26
4.5.3 Balsa wood 26
4.6 MANUFACTURING PROCESSES 26
4.6.1 Open mold processes 27
4.6.2 Closed mold processes 28
4.6.3 Continuous processes 31
4.6.4 Comparison manufacturing methods 31
4.7 CHARACTERISTICS OF FIBRE REINFORCED POLYMERS 32
4.7.1 Durability 32
4.7.2 Sustainability 33
4.7.3 Fire resistance 33
4.7.4 Mechanical properties 33
4.7.5 Costs 34
4.8 DESIGN CODES 35
4.9 REFERENCE PROJECTS 35
4.9.1 Kreekrak sluices 36
4.9.2 Spiering sluice 36
4.9.3 Minehunter 'Alkmaarklasse' 37
4.9.4 FRP concept for lifting slide 37
4.10 SUMMARIZED 37

PART 2: MAIN REPORT

5 THE DESIGN OF THE CURRENT SLIDES 40

5.1 THE CLOSURE STRUCTURE 40
5.2 BOUNDARY CONDITIONS 41
5.3 DESIGN CONSIDERATIONS 42
5.4 THE DESIGN 43
5.5 LOADS ON THE SLIDES 46
5.5.1 Horizontal wave and water loads (closed position) 46
5.5.2 Vertical wave loads (during closure) 47
5.5.3 Dead load 47
5.5.4 Torsion 48
5.5.5 Longitudinal loads 48

5.5.6 Ice loads ... *48*
5.5.7 Wind loads ... *48*
5.5.8 Water flows and leakage gaps vibrations ... *48*
5.5.9 Collision ... *48*
5.5.10 Terrorist attack ... *48*

6 DESIGN REQUIREMENTS AND ASSUMPTIONS ... 49

6.1 GENERAL REQUIREMENTS ... 49
6.2 GEOMETRICAL BOUNDARY CONDITIONS ... 49
6.3 LOADS ON THE SLIDES ... 50
6.4 ASSUMPTIONS ... 51

7 MATERIAL SELECTION ... 52

7.1 MANUFACTURING METHOD ... 52
7.2 REINFORCEMENT ... 53
7.3 RESIN ... 53
7.4 CORE ... 53
7.5 LAMELLA PROPERTIES ... 54
7.6 SAFETY FACTORS ... 54
7.6.1 Material safety factor ... *55*
7.6.2 Conversion safety factor ... *55*
7.7 FRACTURE CRITERION ... 56
7.8 MATERIAL PROPERTIES (INITIAL DESIGN STAGE) ... 57

8 STRUCTURAL CONCEPTS ... 59

8.1 DESIGN PHILOSOPHY ... 59
8.2 EVALUATION OF PREVIOUS CONCEPTS ... 59
8.3 SANDWICH ... 60
8.3.1 Hand calculation ... *60*
8.3.2 Finite element analysis ... *61*
8.3.3 Conclusion ... *63*
8.4 HORIZONTALLY CURVED SHELL ... 63
8.5 BOX GIRDER ... 64
8.5.1 Straight box girder ... *65*
8.5.2 Varying thickness ... *69*
8.5.3 Manufacturability ... *75*
8.5.4 Hydraulic adjustments ... *76*
8.5.5 Conclusion ... *76*

9 DEFLECTION REQUIREMENT ... 78

9.1 LESS STRICT REQUIREMENT ... 78
9.2 RIGOROUSLY SOLUTION ... 78
9.2.1 Overall idea ... *79*
9.2.2 Checking the feasibility of the adjustments ... *80*
9.2.3 Concluding ... *84*
9.3 OTHER SOLUTIONS ... 84
9.4 EVALUATION ... 85
9.4.1 Simple comparison of costs ... *85*
9.4.2 Comparison of costs with alternatives on the long term ... *86*
9.4.3 Choice of elaborating short and medium term or long term solution ... *86*

10 FINAL DESIGN 88

10.1 ADJUSTMENTS ON MATERIAL PROPERTIES 88
10.1.1 Safety factors 88
10.1.2 Lamella properties 88
10.1.3 Strain criterion 88
10.1.4 Core properties 89
10.2 STRUCTURE IN GENERAL 89
10.3 STRUCTURAL IMPROVEMENTS 90
10.3.1 Decreasing the peaks in the strains 90
10.3.2 Addition of gaps in horizontal plates 92
10.3.3 Optimizing the laminates 93
10.3.4 Adding some additional load cases 94
10.4 FINAL FEA MODEL 96
10.4.1 Dimensions 96
10.4.2 Constraints 98
10.4.3 Load cases 98
10.4.4 Load combinations 100
10.4.5 Laminate surfaces 101
10.5 FEA ANALYSIS 101
10.5.1 Force distribution 101
10.5.2 Deformations 106
10.5.3 Strains 107
10.6 BUCKLING OF HORIZONTAL PLATES 115
10.7 MANUFACTURABILITY 116

11 COST COMPARISON 117

11.1 COSTS OF VARIANTS 117
11.1.1 Raising dikes 117
11.1.2 Dam 118
11.1.3 Rigorously solution 118
11.2 COMPARISON OF VARIANTS 119
11.3 LIFE CYCLE ANALYSIS 120

12 CONCLUSIONS AND RECOMMENDATIONS 122

12.1 CONCLUSIONS OF LITERATURE STUDY 122
12.2 CONCLUSIONS OF THE MAIN RESEARCH 123
12.3 FINAL CONCLUSION 124
12.4 RECOMMENDATIONS 124

REFERENCES 126

APPENDICES

APENDIX A: CALCULATION OF LAMELLA PROPERTIES 132

APENDIX B: CALCULATION OF SANDWICH VARIANT 134

APENDIX C: COMPARISON LAMINATE STIFFNESS MATRIX 136

APENDIX D: DISTRIBUTION OF SUPPORT REACTIONS 138

APENDIX E: LOADS SPECIFICATION 139

APENDIX F: FINAL DESIGN DLUBAL RFEM..... 166

APENDIX G: EXTRA COSTS RIGOROUSLY SOLUTION 299

APENDIX H: INFORMATION PROVIDED ON DVD 302

List of figures

Figure 1.1 Schematization of the relation between the research questions and the structure of the report 2
Figure 2.1 Overview of the dams of the Delta plan [5] 6
Figure 2.2 Overview of the openings (Hammen, Schaar van Roggenplaat and Roompot) and the artificial islands (Roggenplaat, Neeltje Jans and Noordland) [6] 7
Figure 2.3 Overview of the structure of the storm surge barrier [8] 9
Figure 3.1 Hartel barrier, left: aerial view of the barrier, right: detail of the truss structure of the slide [WEB, www.keringhuis.nl] 13
Figure 3.2 Storm surge barrier Hollandse IJssel [WEB, http://www.flickr.com/photos/alje/] 13
Figure 3.3 Overview of design concepts considered in [3] 14
Figure 3.4 Overview of design concepts considered in [4] 16
Figure 3.5 Adjusted bottom of the slide [4] 16
Figure 3.6 Concepts concrete slides [12] 17
Figure 3.7 Optimized design of the concrete truss girder slide [12] 18
Figure 3.8 Examples of shapes with an undefined release point [13] 18
Figure 3.9 Examples of shapes which cause flow patterns which release and later on lay down again [13] 19
Figure 3.10 Shapes with a favorable flow pattern [13] 19
Figure 4.1 A straw-clay brick [WEB, http://chasingfireflies.typepad.com/chasing_fireflies/2008/09/index.html] . 21
Figure 4.2 Boeing 787 with emphasis on the used materials in this airplane [WEB, http://bintang.site11.com/Boeing_787/Boeing787_files/Specifications.html] 21
Figure 4.3 Stress-strain diagrams of various reinforcement types [16] 22
Figure 4.4 Left: Continuous filament rovings [15] Right: CSM [WEB,http://fiberglassblog.com/category/chopped-strand-mat/] 23
Figure 4.5 Left: CFM [WEB,http://cn.tradekey.com/product_view/id/1810675.htm] Right: Woven glass fibre fabric [WEB, http://www.floratextiles.com/glass-fibre-fabric.htm] 24
Figure 4.6 Honeycomb core (hexagonal shape) [15] 26
Figure 4.7 Hand lamination process [WEB, www.gdecotech.com] 26
Figure 4.8 Spray-up process [15] 27
Figure 4.9 Filament winding process [16] 28
Figure 4.10 Centrifugal casting process [15] 28
Figure 4.11 Vacuum bag process [15] 28
Figure 4.12 Pressure bag process [15] 29
Figure 4.13 Autoclave process [15] 29
Figure 4.14 Cold press process [15] 30
Figure 4.15 Resin injection process [15] 30
Figure 4.16 Injection molding process [15] 30
Figure 4.17 Continuous hand lamination process [15] 31
Figure 4.18 Pulltrusion process [15] 31
Figure 4.19 FRP slide which was applied in the fresh-salt water separation system of the Kreekrak sluices [20] 36
Figure 4.20 Lock gates of the Spiering sluice[S.J. de Waard, Wikimedia Commons] 36
Figure 4.21 Minehunter 'Alkmaarklasse' with a FRP hull [21] 37
Figure 4.22 Overview FRP concept lifting slide (with one arch not displayed) [18] 37
Figure 5.1 Overview of the slides in the openings Hammen, Schaar van Roggenplaat and Roompot [22] 40
Figure 5.2 Span of the slides [22] 41
Figure 5.3 Cross section of the slide with upper beam and sill beam [22] 41
Figure 5.4 Design of the plate girder slide [22] 42
Figure 5.5 Position of the shells used for the flood defense cladding 43
Figure 5.6 Flow pattern, depending on the geometry of the upper beam [23] 43
Figure 5.7 Final design of the slide in the storm surge barrier [22] 44

FIGURE 5.8 COMPONENTS OF THE SLIDE [22] 44
FIGURE 5.9 OVERVIEW OF THE BEARINGS AND GUIDES OF THE SLIDE [22] 45
FIGURE 5.10 DIMENSIONS OF THE RABBET [22] 45
FIGURE 5.11 RESULTANTS LOADS DUE TO WATER PRESSURE AND WAVE CRUST OR WAVE TROUGH [22] 47
FIGURE 6.1 GEOMETRICAL REQUIREMENTS FOR A NEW SLIDE (NOT TO SCALE) 50
FIGURE 6.2 DETAIL OF THE DIMENSIONS NEAR THE RABBETS 50
FIGURE 8.1A SANDWICH WITH SOME PARAMETERS FIGURE 8.1B FIBERCORE PRINCIPLE [25] 60
FIGURE 8.2 MODEL OF A PART OF THE SLIDE (ONLY 1 M HEIGHT) 62
FIGURE 8.3 MECHANICAL SCHEME (TOP VIEW) 62
FIGURE 8.4 DEFORMATIONS IN Y-DIRECTION (MM) 63
FIGURE 8.5 HORIZONTALLY CURVED SANDWICH (TOP VIEW) 64
FIGURE 8.6 IDEA TO ADAPT SIDE OF SLIDE 64
FIGURE 8.7 TWO SANDWICHES WHICH ARE CONNECTED WITH HORIZONTAL PLATES 64
FIGURE 8.8 STRAIGHT BOX-GIRDER VARIANT 65
FIGURE 8.9 DEFORMATIONS IN Y-DIRECTION 66
FIGURE 8.10 SUPPORT REACTIONS IN Y-DIRECTION (KN/M) (SEE EXPLANATION IN APPENDIX D) 66
FIGURE 8.11 NUMBERING OF THE SURFACES OF THE STRUCTURE 67
FIGURE 8.12 STRAIN ε_x AT THE TOP OF LAMELLA 1 IN THE SURFACES 5 TO 9 68
FIGURE 8.13 STRAINS ε_y (LEFT) AND γ_{xy} (RIGHT) AT THE TOP OF LAMELLA 1 IN THE SURFACES 5 TO 9 68
FIGURE 8.14 STRAIN ε_x AT THE BOTTOM OF LAMELLA 9 IN THE SURFACES 10 TO 13 68
FIGURE 8.15 STRAINS γ_{xy} AT THE BOTTOM OF LAMELLA 9 IN THE SURFACES 10 TO 13 69
FIGURE 8.16 BOX-GIRDER WITH THICKENING IN THE MIDDLE 70
FIGURE 8.17 SUPPORT REACTIONS IN Y-DIRECTION (KN/M) (SEE EXPLANATION IN APPENDIX D) 70
FIGURE 8.18 STRAIN εy AT THE BOTTOM OF LAMELLA 7 IN SURFACE 5. (LEFT) STRAIN γxy AT THE BOTTOM OF LAMELLA 9 IN SURFACES 10 TO 13. (RIGHT) 72
FIGURE 8.19 STRAIN γxy AT THE BOTTOM OF LAMELLA 7 IN SURFACES 5 TO 9 72
FIGURE 8.20 STRAIN εx AT THE TOP OF LAMELLA 1 IN SURFACES 14 TO 17 (LEFT) STRAIN γxy AT THE BOTTOM OF LAMELLA 7 IN SURFACES 14 TO 17 (RIGHT) 72
FIGURE 8.21 EXTRA THICKENING OF THE SLIDE TO 8.5M IN THE MIDDLE 74
FIGURE 8.22 DEFORMATIONS IN Y-DIRECTION (TOP VIEW) 74
FIGURE 8.23 NORMAL FORCE IN X-DIRECTION (TOP VIEW) 74
FIGURE 8.24 ADDITION OF HOLES IN THE HORIZONTAL PLATES NEAR THE NEUTRAL AXIS (NORMAL FORCES DO CORRESPOND TO A HORIZONTAL PLATE WITHOUT HOLES) 75
FIGURE 8.25 ILLUSTRATION OF OPTION 1 [WEB, HTTP://WWW.SCIENCEDIRECT.COM/SCIENCE/ARTICLE/PII/S1359836808000061] 75
FIGURE 8.26 ILLUSTRATION OF OPTION 2 76
FIGURE 9.1 SCHEMATIC REPRESENTATION OF A LARGER DEFLECTION BETWEEN THE SILL BEAM AND THE UPPER BEAM 78
FIGURE 9.2 RIGOROUSLY SOLUTION OF ONE VERY HIGH SLIDE 79
FIGURE 9.3 GLOBAL DIMENSIONS OF A PIER [27] 80
FIGURE 9.4 CROSS-SECTION OF BARRIER JUST BEFORE THE PIER [22] 81
FIGURE 9.5 SIDE VIEW OF THE SILL BEAM [27] 81
FIGURE 9.6 TROUGH-FLOW OPENING OF THE BARRIER [22] 82
FIGURE 9.7 LEFT: CURRENT SITUATION, RIGHT: NEW POSSIBILITY 83
FIGURE 9.8 COMPARISON OF SHORT OR MEDIUM TERM AND LONG TERM SOLUTION 85
FIGURE 10.1 OVERVIEW OF DIMENSIONS OF FINAL STRUCTURE IN CLOSED POSITION 89
FIGURE 10.2 SUPPORT REACTIONS IN DIFFERENT FEA MODELS 91
FIGURE 10.3 STIFFENED END STRUCTURE 91
FIGURE 10.4 STRUCTURE WITH GAPS (LEFT: 1ST SITUATION, RIGHT: 2ND SITUATION) 92
FIGURE 10.5 STRAIN εxy IN OPTIMIZED MODEL IN SITUATION 1 93
FIGURE 10.6 STRAIN εx IN OPTIMIZED MODEL IN SITUATION 1 93

Figure 10.7 Strain εy in model without extra horizontal plate 95
Figure 10.8 Strain εy in model with extra horizontal plate 95
Figure 10.9 3D view of the FEA model of the structure with dimensions 96
Figure 10.10 Top views of the horizontal plates with gaps 96
Figure 10.11 Cross-sections of the slide with dimensions 97
Figure 10.12 Constraints of the final structure 97
Figure 10.13a Water pressure load positive drop (LC1) Figure 10.13b Wave pressure load positive drop (LC2) 98
Figure 10.14 Water pressure load negative drop (LC2) Left: total loading, middle: water pressure on outer wall, right: water pressure on inner wall 98
Figure 10.15a Wave pressure load negative drop (LC5) Figure 10.15b Ice load (LC6) 99
Figure 10.16a Collision load (LC7) Figure 10.16b Wave impact load (LC8) 99
Figure 10.17 Overview of compositions in structure (composition number is shown in legend) 100
Figure 10.18 N_x in outer walls (ULS positive drop) 102
Figure 10.19 N_y in outer walls (ULS positive drop) 102
Figure 10.20 N_{xy} in outer walls (ULS positive drop) 103
Figure 10.21 M_x in outer walls (ULS positive drop) 103
Figure 10.22 M_y in outer walls (ULS positive drop) 104
Figure 10.23 N_x in horizontal plates and vertical end plates (ULS positive drop) 104
Figure 10.24 N_y in horizontal plates and vertical end plates (ULS positive drop) 105
Figure 10.25 N_{xy} in horizontal plates and vertical end plates (ULS positive drop) 105
Figure 10.26 Deformation in y-direction (SLS positive drop) 106
Figure 10.27 Deformation in y-direction (SLS negative drop) 106
Figure 10.28 Strain εx at the top of layer 1 in comp. nr 1 for positive drop (CO1) 107
Figure 10.29 Strain εy at the top of layer 1 in comp. nr 1 for positive drop (CO1) 108
Figure 10.30 Strain εxy at the bottom of layer 9 in comp. nr 6 for positive drop (CO1) 108
Figure 10.31 Strain εx at the top of layer 1 in comp. nr 1 for negative drop (CO3) 109
Figure 10.32 Strain εy at the top of layer 1 in comp. nr 1 for negative drop (CO3) 109
Figure 10.33 Strain εxy at the top of layer 1 in comp. nr 7 for negative drop (CO3) 110
Figure 10.34 Strain εx at the bottom of layer 9 in comp. nr 5 for ice load (CO5) 110
Figure 10.35 Strain εy at the bottom of layer 9 in comp. nr 1 for ice load (CO5) 111
Figure 10.36 Strain εxy at the top of layer 1 in comp. nr 2 for ice load (CO5) 111
Figure 10.37 Strain εx at the bottom of layer 9 in comp. nr 1 for collision load (CO6) 112
Figure 10.38 Strain εy at the top of layer 1 in comp. nr 1 for collision load (CO6) 112
Figure 10.39 Strain εxy at the bottom of layer 9 in comp. nr 1 for collision load (CO6) 113
Figure 10.40 Strain εx at the top of layer 1 in comp. nr 1 for wave impact load (CO7) 113
Figure 10.41 Strain εy at the top of layer 1 in comp. nr 1 for wave impact load (CO7) 114
Figure 10.42 Strain εxy at the bottom of layer 9 in comp. nr 1 for wave impact load (CO7) 114
Figure 10.43 Way of supporting and associated stability formula [19] 115
Figure 10.44 Stability formulas for pure bending load [31] 115
Figure 10.45 Idea to integrate the connection of the outer sandwiches in the total structure 116
Figure 12.1 Final FRP slide design 123
Figure C.1 Lamella stiffness matrix from DLUBAL RFEM 136
Figure C.2 Lamella stiffness matrix from Kolibri 137
Figure C.3 Laminate stiffness matrix from DLUBAL RFEM 137
Figure C.4 Laminate stiffness matrix from Kolibri 137
Figure D.1 Distribution of reaction forces over the height (left: line support, middle: nodal supports, right: surface calculation of line support) 138
Figure E.1 Water pressure difference loads due to positive drop (situation without holes) 140
Figure E.2 Water pressure difference loads due to positive drop (situation with holes) 141

FIGURE E.3 WATER PRESSURE DIFFERENCE LOADS DUE TO NEGATIVE DROP (SITUATION WITHOUT HOLES) 141
FIGURE E.4 WATER PRESSURE DIFFERENCE LOADS DUE TO NEGATIVE DROP (SITUATION WITH HOLES) 142
FIGURE E.5 WAVE LOADS ACCORDING TO MODEL OF SAINFLOU [35] 143
FIGURE E.6 WAVE PRESSURES DUE TO POSITIVE DROP (LEFT: WAVE CREST, RIGHT: WAVE TROUGH) 144
FIGURE E.7 WAVE PRESSURES DUE TO NEGATIVE DROP (LEFT: WAVE CREST, RIGHT: WAVE TROUGH) 144
FIGURE E.8 COLISISION SURFACE ACCORDING TO NEN-EN 1991-1-7 NB 145
FIGURE G.1 DIMENSIONS NEW SILL BEAM (IN METERS) 300
FIGURE G.2 DIMENSIONS PIER (IN METERS) 301

List of tables

TABLE 4.1 MECHANICAL PROPERTIES OF DIFFERENT RESIN TYPES [17] 24
TABLE 4.2 COMPARISON OF DIFFERENT MANUFACTURING PROCESSES [18] 32
TABLE 4.3 MECHANICAL PROPERTIES OF A FRP MATERIAL WITH DIFFERENT REINFORCEMENTS AND AN EPOXY RESIN [17] 33
TABLE 4.4 POSSIBLE SUBDIVISIONS OF FIBRES IN EACH DIRECTION OF A LAMINATE 34
TABLE 4.5 OVERVIEW OF THE COSTS OF DIFFERENT REINFORCEMENTS [18] 35
TABLE 4.6 OVERVIEW OF THE COSTS OF DIFFERENT RESINS [18] 35
TABLE 4.7 OVERVIEW OF THE CONSTRUCTION COSTS OF DIFFERENT FIBRES AND RESINS [18] 35
TABLE 5.1 DECISIVE CASES FOR CLOSED SLIDES 46
TABLE 7.1 SELECTION OF MANUFACTURING PROCESSES FOR COMPOSITE SLIDES 52
TABLE 7.2 MANUFACTURING METHODS WHICH ARE SUITABLE FOR THE COMPOSITE SLIDES 53
TABLE 7.3 PROPERTIES PMI FOAM CORE 71S [18] 54
TABLE 7.4 STRAIN LIMITS OF A UNI-DIRECTIONAL (UD) LAMINA [24] 56
TABLE 7.5 APPLYING OF SAFETY FACTORS IN INITIAL DESIGN STAGE AND IN THE FINAL DESIGN 58
TABLE 8.1 DIMENSIONS OF SANDWICH WHEN STRENGTH OR DEFLECTION REQUIREMENT IS GOVERNING 61
TABLE 8.2 STACKING SEQUENCE OF LAMELLAS 62
TABLE 8.3 MAXIMUM STRAINS IN THE STRUCTURE (NOT CORRESPONDING TO ONE SPECIAL POINT) 63
TABLE 8.4 LAY-UP OF SANDWICH WALLS 65
TABLE 8.5 MAXIMUM STRAINS WHICH OCCUR IN THE STRUCTURE (NOT CORRESPONDING TO ONE SPECIAL POINT) 66
TABLE 8.6 MAXIMUM STRAINS IN EACH SURFACE 67
TABLE 8.7 MAXIMUM STRAINS WHICH OCCUR IN THE STRUCTURE 71
TABLE 8.8 MAXIMUM STRAINS WHICH OCCUR IN EACH SURFACE 71
TABLE 8.9 MAXIMUM STRAINS COMPARISON BETWEEN DIFFERENT MESH SIZES 73
TABLE 10.1 LAMELLA STIFFNESS PROPERTIES IN ULS AND SLS 88
TABLE 10.2 STIFFNESS PROPERTIES FOAM CORE 89
TABLE 10.3 MAXIMUM STRAINS IN THE FEA MODELS (NOT CORRESPONDING TO ONE SPECIAL POINT) 90
TABLE 10.4 MAXIMUM STRAINS IN THE FEA MODELS (NOT CORRESPONDING TO ONE SPECIAL POINT) 92
TABLE 10.5 OVERVIEW OF LOAD CASES 99
TABLE 10.6 OVERVIEW OF LOAD COMBINATIONS 100
TABLE 10.7 LAYERS OF EACH COMPOSITION (L=LAMINATE NR., T=THICKNESS,D=DIRECTION) 101
TABLE 10.8 MAXIMUM STRAINS PER LOAD COMBINATION (DO NOT CORRESPOND TO ONE POINT IN THE STRUCTURE) 107
TABLE 11.1 COSTS OF INCREASING THE DIKES [32] 117
TABLE 11.2 COSTS OF A DAM [32] 118
TABLE 11.3 COSTS OF RIGOROUSLY SOLUTION 119
TABLE 11.4 COMPARISON OF INVESTMENT COSTS OF DIFFERENT VARIANTS *) PRICE LEVEL 1976 119
TABLE 11.5 CALCULATION OF PRESENT VALUES 120
TABLE C.1 LAMELLA STACKING 136
TABLE E.1 LOAD FACTORS ACCORDING TO NEN-EN 1990 CC3 139
TABLE E.2 LOAD FACTORS ACCORDING TO LEIDRAAD KUNSTWERKEN 139
TABLE E.3 LOAD FACTORS PER LOAD 139
TABLE E.4 LOAD COMBINATIONS 145
TABLE G.1 EXTRA COSTS SPECIFICATION RIGOROUSLY SOLUTION 299
TABLE G.2 CALCULATION OF COSTS FOR NEW SILL BEAM 299
TABLE G.3 SURFACE NEW SILL BEAM 300
TABLE G.4 CALCULATION OF COSTS FOR INCREASING A RABBET 300
TABLE G.5 SURFACE PIERS 300
TABLE H.1 FEA MODELS OF THE VARIANT STUDY (CHAPTER 8) 302
TABLE H.2 FEA MODELS OF THE FINAL DESIGN (CHAPTER 10) 302

1 Introduction

1.1 Background

The Eastern Scheldt storm surge barrier is a closeable barrier which can be closed at expected high sea levels. The barrier is constructed with movable steel slides to save the tidal movement in the Eastern Scheldt and do not interfere with the nature in the Eastern Scheldt. The barrier is constructed as part of the Deltaplan and was taken in use in 1986. The slides in the barrier are exposed to heavy weathers at sea and are therefore conserved to protect the slides against their environment.

1.2 Problem description

Already a few years after the opening of the storm surge barrier problems with the coating arise. Cracks in the coating are visible and corrosion occurs. The corrosion was removed and the slides were conserved with a new coating. This maintenance takes a lot of time since only a few slides can be maintained simultaneously to restrict the failure probability of the barrier. Next to that, the service life of the coating is probably too short, to maintain all the slides before maintenance is necessary. The slides can deteriorate such that maintenance costs exceed the costs of replacement of the slide. Therefore research to possibilities, which have lower maintenance costs or for which maintenance is required less often, was carried out.

Due to present cutbacks by the Dutch government, the directorate-general for public works and water management (Rijkswaterstaat), which maintain the barrier, should cut in their budgets. Therefore it's really attractive to find new possibilities for the slides.

1.3 Previous research

In 1998 a graduation work was carried out on high strength concrete slides in the Eastern Scheldt storm surge barrier by Keuzenkamp [1]. In 2000 and 2002 other graduations works were carried out on this subject, of which the results can be read in [2]. They showed that replacement of the slides was financially competitive with the maintenance costs of the slides, but the self weight of the slides threatens to exceed the capacity of the lift cylinders of the slides.

In the same time period, in 1998, a graduation work on glass fibre reinforced slides in the Eastern Scheldt storm surge barrier was carried out by Veraart [3]. And in 1999 a continuation on this graduation work was carried out by Van der Laken [4]. These graduations works are mentioned in chapter 3.

1.4 Research objective

According to [2], the replacement of the existing slides could form an attractive solution. Next to that, the rise in use of fibre reinforced polymers in the civil engineering industry, due to their high strength properties, low self weight and low maintenance give occasion to study the feasibility of fibre reinforced polymer slides in the Eastern Scheldt barrier. The objective of this research is therefore defined as follows:

Determine the possibilities to apply fibre reinforce polymers into the slides of the Eastern Scheldt storm surge barrier.

A proof of the excellent resistance of FRP in the environment of the Eastern Scheldt barrier in comparison to steel is the replacement of steel gratings in 2000. The galvanized steel gratings, which

facilitate maintenance of the Eastern Scheldt barrier, were replaced by gratings of FRP because of rapid corrosion due to the salty environment. There was a lot of saving in maintenance, since the steel gratings must be galvanized every five years. Next to that, the directorate-general for public works and water management (Rijkswaterstaat) has taken in 2013 the lead to inform the civil engineering industry about the different aspects of constructing with fibre reinforced polymers. They mention that FRP helps to make the replacement task of Rijkswaterstaat more sustainable, cheaper and more efficient.

1.5 Research questions

The following research question is derived from the problem definition and objective:

Is it feasible to replace the current steel slides in the Eastern Scheldt barrier by slides made of FRP?

Four sub-questions are defined to answer the main research question. These sub-questions are defined as follows:

1. How is the current barrier designed?
2. Which structural designs are feasible for lifting slides in the Eastern Scheldt barrier?
3. Which reinforcement, resins and manufacturing methods are suitable to apply for the slides and what are the characteristics of fibre reinforced polymers?
4. What is technically the most promising design for the slide made of FRP?
5. Is it financially attractive to replace the current slides by slides made of FRP over the total life of the barrier?

1.6 Structure of the report

In Figure 1.1 is shown which sub-research questions are threated in which chapter.

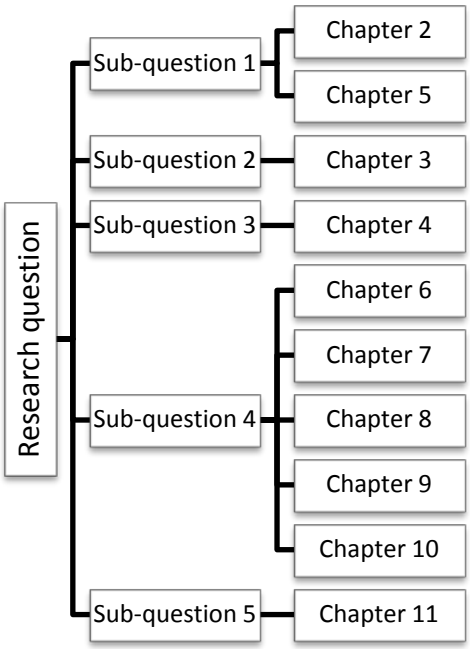


Figure 1.1 Schematization of the relation between the research questions and the structure of the report

The total report consists of two parts: a literature study and a main report. In the literature study the general aspect of the Eastern Scheldt barrier, lifting slides and FRP are described. The main report starts with a description of the design of the current slides, where after the design requirements are

forming the basis for a new design. In the subsequent chapters a FRP design will be developed. In the next paragraphs a short description of each chapter is given.

Part 1: Literature study

Chapter 2
This chapter describes the current design of the Eastern Scheldt barrier in general to get some understanding of the total structure. This will help to understand the concepts from previous researches on new slides in the barrier, which will be threatened in chapter 3. The design of the current slides is described in chapter 5.

Chapter 3
The structural design of other lifting slides are mentioned in the beginning of this chapter, where after the conceptual designs from previous graduation works and researches for slides in the Eastern Scheldt barrier are mentioned. Also the hydraulic design considerations which are applicable to lifting slides are mentioned.

Chapter 4
This chapter is a general introduction on fibre reinforced polymers (FRP). The reinforcements, resins and cores used in fibre reinforced polymers are described. Next to that the manufacturing processes are described and the achievable properties of FRP materials are mentioned. At the end some reference projects are mentioned.

Part 2: Main report

Chapter 5
This chapter describes the current design of the slides, which determines mainly the boundary conditions for the new slides. Also the loads on the slides are considered.

Chapter 6
In this chapter the design requirements and assumptions for a new slide are listed. These requirements are extracted from chapter 5.

Chapter 7
In this chapter, a selection is made on the materials (resin, reinforcement and core) which could be used for FRP slides. Thereafter, the material properties are determined.

Chapter 8
In this chapter different structural variants are compared. These variants are compared with the results of a FEA analysis.

Chapter 9
This chapter examines whether it's possible to reduce or vanish the deflection requirement, since this requirement is quite strict. At the end of this chapter a choice is made, which design will be further elaborated in chapter 10.

Chapter 10
This chapter described the final design of an FRP slide and presents the results of the final FEA analysis.

Chapter 11

In this chapter the final FRP slide is compared with other solutions for the long run. Next to that, a life cycle analysis is carried out to compare the investment costs of an FRP slide with the maintenance costs of the current steel slides.

Chapter 12

This chapter presents the conclusions and recommendations of this research.

Part 1:
Literature study

2 The design of the current barrier

In this chapter the first sub-research question will be partly answered: 'How is the current barrier designed?'. This chapter describes in general the current design of the Eastern Scheldt barrier and chapter 5 describes especially the design of the current slides.

First of all, the process to a closeable storm surge barrier is described in this chapter, where after the current design of the barrier is described in general. Finally, the maintenance and the future of the barrier are described.

2.1 History

The directorate-general for public works and water management (Rijkswaterstaat) mentioned in 1937 that the safety during storms and high sea levels in the Netherlands could not be guaranteed. In the South-west part of the Netherlands it was rather difficult and expensive to build new dikes or to increase existing ones to prevent flooding. Therefore it was a better option to close all the estuaries: the Western Scheldt, the Eastern Scheldt, the Haringvliet, and the Brouwershavense Gat. This first idea was called the 'Delta plan'. In 1950 a start was made to execute this plan, but there was no need to build the dams in a short time period. The flood of 1953 in the night of February 1st has made a change. During that flood 1835 people died and 150,000 hectares of land were flooded. The need for safer dikes and dams against flooding was there.

2.2 Delta plan

On February the 21th 1953 the Delta committee was inaugurated to give advice about the execution of a Delta plan to increase the safety of the delta in the long run. The restriction was: the seaways the Nieuwe Waterweg and the Western Scheldt should stay open because of the economic interest for the ports of Rotterdam and Antwerp.



Figure 2.1 Overview of the dams of the Delta plan [5]

The Delta committee advised in 1954 to close the Haringvliet, the Brouwerhavense Gat, the Eastern Scheldt and the Veerse Gat. This will shorten the coastline, creating better connections in the South-west of the Netherlands, freshwater basins and some recreation areas. Along the Western Scheldt and the Nieuwe Waterweg dikes should be increased.

Part of the plan is to create some compartmentalization dams to divide the water in smaller compartments, such as: Zandkreekdam, Grevelingendam and Volkerakdam. In 1958 the Delta law, which describes these ideas, was passed the Dutch parliament. The dams could be built within 25 years.

In 1958 the storm surge barrier Hollandse IJssel was finished and after that the Zandkreekdam (1960), Veerse Gatdam (1961), Grevelingendam (1965), Volkerakdam (1969), Haringsvlietdam (1971) and Brouwersdam (1971) were built. More information about construction of these delta works can be found in [5]. The smaller dams were built as first to gain experience with closing the sea arms. The biggest sea arm, the Eastern Scheldt, was planned to be closed as last.

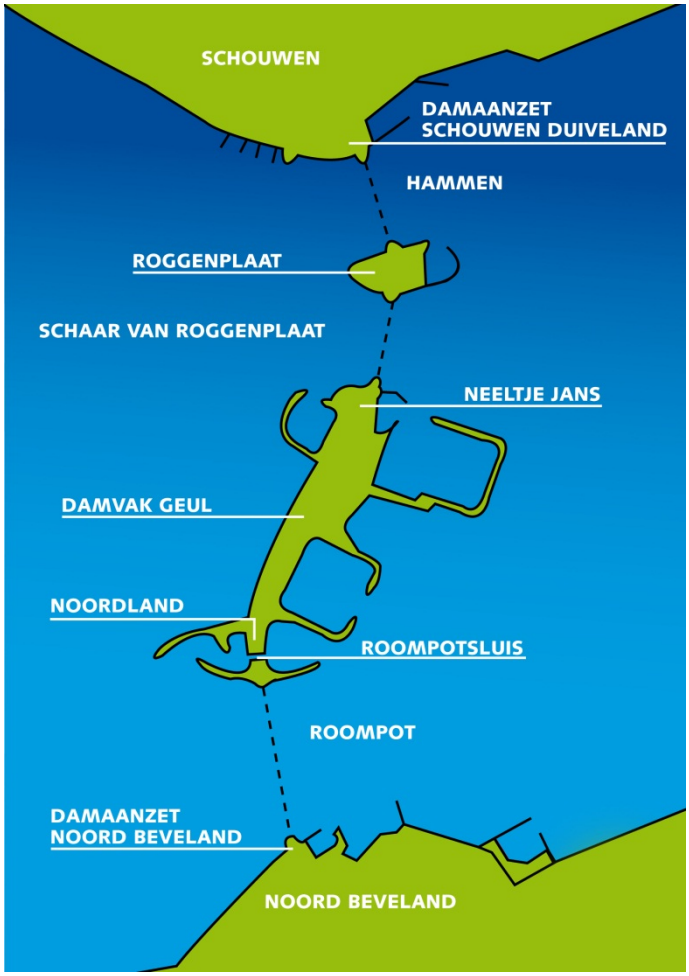


Figure 2.2 Overview of the openings (Hammen, Schaar van Roggenplaat and Roompot) and the artificial islands (Roggenplaat, Neeltje Jans and Noordland) [6]

2.3 Closable storm surge barrier

Already in 1960 a start was made with closing the Eastern Scheldt. In 1969 the artificial island Roggenplaat was created in the sea arm of the Eastern Scheldt. After that the islands Neeltje Jans (1970) and Noordland (1971) were created. In 1973 5 of the 9 kilometer of the Eastern Scheldt was closed and the plan was to finish the dam in 1978, but that didn't happen.

Fishermen, environmental organizations and oyster- and mussel farmers protest against the Eastern Scheldt dam. The Eastern Scheldt was an area with high tide differences and thereby unique ecological processes which should be preserved. The high plankton production and the big variety of other life are examples of that. For the places Yerseke en Bruinisse fishing was an important source of income. For these reasons, the government decided in 1976 to build a closable storm surge barrier. When high sea levels are expected, the barrier could be closed. During normal circumstances the barrier is open and the tide in the Eastern Scheldt remains for the most important part. Besides that, two compartmentalization dams, the Philipsdam and the Oesterdam, should be built, also to ensure a tide free shipping route between Antwerp and the Rhine. The parliament agrees with that in 1979. A closable storm surge barrier in the openings Hammen, Schaar van Roggenplaat and Roompot, see Figure 2.2, will be built. The barrier should be finished in 1985 and should cost up to 3 billion gulden.

2.4 Design of the storm surge barrier

The final design of the barrier depends mainly on the conditions in the Eastern Scheldt. Only the final design is presented here, without all the design considerations and design alternatives of the barrier. Information on that can be found in [5] and [7]. The design considerations of the slides are presented in chapter 5.

2.4.1 Boundary conditions

To preserve the ecosystem in the Eastern Scheldt, enforcement of the tidal movement in the Eastern Scheldt was necessary. Full enforcement was far too expensive, but a restricted decrease in tide difference in Yerseke to 70% of the original tide difference was feasible. Therefore the minimum flow opening of the closeable storm surge barrier is 15,000 m^2.

The storm surge barrier should resist a storm with probability of occurrence of 1 in 4000 years. The corresponding flood defense height is calculated as 5.80 m above NAP[1], and for the opening Hammen adjusted to 5.60 m above NAP. Next to that the storm surge barrier should be designed for a lifetime of 200 years.

2.4.2 Overall design

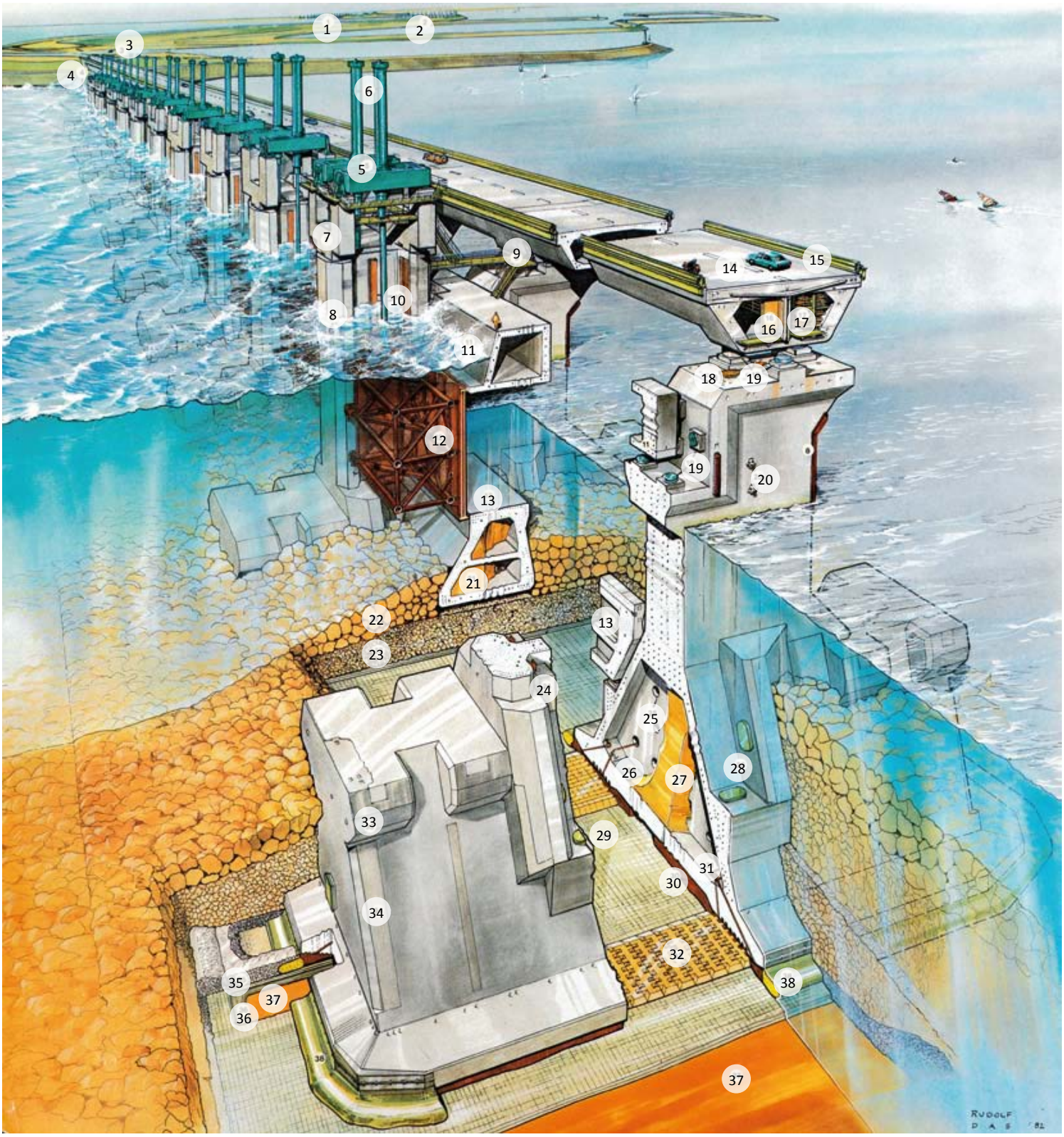
The barrier consists of 65 concrete piers and 62 steel slides, of which 15 slides in the opening Hammen, 16 in Schaar van Roggenplaat and 31 in Roompot. In case of expected high sea levels the water retaining part of the barrier consist of an upper beam, a slide and a sill beam between the piers, see Figure 2.3. The slides are moveable in the vertical direction by cylinders, to ensure the tidal movement in the Eastern Scheldt. The piers transfer all the loads to the bottom of the Eastern Scheldt.

Between the piers there is also a concrete box girder bridge to create a connection between Schouwen-Duiveland and North Beveland. The inside of the traffic box girder is used to place the installations for moving the slides and is used as cable and pipe duct.

2.4.3 Bottom consolidation

Research to the properties of the bottom of the Eastern Scheldt showed that de bottom was too weak to carry the barrier. Therefore a soil layer of silt is replaced with sand. After that, the bottom of the Eastern Scheldt is consolidated with the ship Mythilus with vibrators.

[1]Normaal Amsterdams Peil (Amsterdam Ordnance Datum) is a reference height used in the Netherlands



1 opening Hammen
2 opening Schaar van Roggenplaat
3 sluice Roompot
4 rubble as land abutment
5 cardan girder carries cylinders
6 lift cylinders
7 extending part of pier
8 wood fender
9 platforms and stairs for maintenance
10 conduction of slide
11 upper beam
12 slide
13 sill beam
14 traffic road
15 guardrail
16 devices gallery
17 cable and pipes duct
18 access pier
19 bearings
20 anchor points for maintenance sill beams
21 sand filling sill beam
22 top layer threshold
23 core layer threshold
24 bearing top slide
25 partition holes for filling with sand
26 piers bottom
27 sand filling
28 bearings sill beam
29 upper mat
30 grout
31 grout pipes
32 foundation mat
33 lifting lugs
34 protective layer against bulk stones
35 extending of gravel bag
36 lower mat
37 consolidated soil Eastern Scheldt
38 gravel bag

Figure 2.3 Overview of the structure of the storm surge barrier [8]

To ensure that the storm surge barrier has a perfect flat and strong foundation, mats with sand and gravel were placed at the bottom of the Eastern Scheldt at the location of the barrier. Thereafter the piers were placed on it.

2.4.4 Piers

The hollow concrete piers have a wide base to carry the loads to the bottom. The piers, upper beams, slides and sill beams were prefabricated to minimize the risky work in the openings of the Eastern Scheldt and to disrupt the tidal movement in the Eastern Scheldt as little as possible during construction. The concrete piers were built in 3 construction docks below sea level near Neeltje Jans. When all the piers in one dock were finished, these piers were placed into their position in the Eastern Scheldt. Thereafter the hollow piers were filled with sand to increase the stability of the piers. Also plenty heavy stones were put among the piers.

2.4.5 Construction of the other parts

After placing the piers, the traffic box girders and some extending parts on the piers were placed. On these extending parts the movement components of the slides were placed. Thereafter, the slides were placed between the piers. As last, the sill beams and the upper beams were placed and the sill beam was filled with sand. The construction was finished, with a delay of 1 year, in 1986 and cost 5.5 billion gulden.

2.5 Settlements and maintenance

The settlements of the piers were monitored. That research showed settlements of 4-6 cm in vertical direction, 1-2 cm in the direction of the North Sea and a small tilt in the direction of the Eastern Scheldt. Although the settlements were small after the initial settlements, Rijkswaterstaat does not exclude somewhat bigger settlements after a storm.

To protect the slides from the aggressive environment of the North Sea the slides were conserved during construction. In the openings Hammen and Schaar van Roggenplaat a coal tar epoxy coating of 3 layers was used for the slides. During construction it was decided to use another coating to speed up the drying process of the different layers, otherwise the official opening date of the barrier would not be reached. Therefore the slides in the opening Roompot were conserved with an epoxy coating of 2 layers. But already a few years after the opening of the storm surge barrier problems with this coating arise. Cracks in the coating are visible and corrosion occurs. The corrosion was removed and the slides were conserved with a new coating. This maintenance takes a lot of time since only a few slides can be maintained simultaneously to restrict the failure probability of the barrier. The service life of the coating is probably too short, to maintain all the slides before maintenance is necessary.

The maintenance of the slides consists mainly of removing rust and coating application. The total costs of maintenance for the barrier are 17 million euro per year. [9] Totally 4 slides can be maintained outside the storm season, therefore the maximum maintaining costs are 4 to 4.5 million euro per slide when other maintaining parts are neglected, what is actually not the case.

During the 26 years that the Eastern Scheldt barrier exists there are, already, some small parts of the barrier replaced by FRP parts. The gratings which facilitate maintenance of the cylinders and slides were initially made of galvanized steel, but were affected rapidly by the salty environment. Therefore these gratings are replaced by gratings of FRP in 2000. There was a lot of saving in maintenance,

since the steel gratings must be galvanized every five years. Also some steel protection cabs are already replaced by FRP caps.

2.6 Future of the barrier

2.6.1 Future vision of the Delta committee

In 2007 a new Delta committee was inaugurated to give advice about the protection of the Netherlands against the consequences of climate changes. Especially the sea level rise and the probability of flooding were of interest. The committee has also advised on the Eastern Scheldt storm surge barrier.

The storm surge barrier can resist a sea level rise of 50 cm and is therefore at least safe until 2050. Thereafter additional measures are necessary, such as: other locking regimes or closing the gaps between the slides and the upper- and sill beam. The expectation is that the storm surge barrier can resist a sea level rise of 1 m by taking additional measures. This sea level is estimated to appear not earlier than 2075, but it could also appear not until 2125.

Besides the advice about the safety of the Eastern Scheldt storm surge barrier against flooding, the committee gave advice about the ecosystem in de Eastern Scheldt. Without additional measures the intertidal zones disappear before 2050. To prevent this it is, on the short-term, necessary to compensate the intertidal zones with sand from outside the Eastern Scheldt. On long term the advice is to restore the tidal movement as much as possible. Already a few decades before the end of the lifetime of the current barrier, a decision for that should be made, to have enough time for increasing the dikes, when for example an open Eastern Scheldt is chosen.

The other advises of the Delta Committee can be read in [10].

2.6.2 Sea level rise

In [11] a long-term exploration is carried out on the southwestern delta in the Netherlands. Also the future of the Eastern Scheldt barrier is mentioned. It is suggested that the height of the slides can be increased (adjusted to the sea level rise), when the slides are replaced by new slides. The new height of adjusted slides is not mentioned, but an indication of the potential height can be derived from the current slide design.

The current slides have the freedom to be lifted for another 120 cm from their open position, to facilitate maintenance. It is therefore possible to lift the upper beam for 60 cm and increase the height of the slides with 60 cm, without additional measures on the movement works. Only the upper beam should be lifted, which will increase the flow opening of the barrier. The slides can be increased, and the upper beam lifted, with another 12.5 cm, which ensures that the bottom of the slides is equal to the top of the upper beam. This is not preferable due to ice loading on the slides and the risk of collision. It should be mentioned that an increase of the flow opening, which is relatively small, will probably have almost no effect on the disappearing intertidal zones.

The increase of the height of the slides is a measure which is dependent on the increase of the dikes around the Eastern Scheldt. If dikes around the Eastern Scheldt are increased, the reserve capacity of the Eastern Scheldt increases and the slides could be increased less. Therefore, increasing the slides, which ensures a longer resistance against the sea level rise, should probably be done in combination with dike increments. The assessment level is near Sint-Annaland, so the dikes should be increased there first.

Another measure was closing the leakage gaps, which was advised by the Delta Committee. According to Rijkswaterstaat, this measure will not ensure a much longer service life due to the restricted assessment level by Sint-Annaland, which will be decisive after a certain time. Next to that, it is almost not possible to reduce the leakage gaps considerably, only a small reduction could be possible, which seems to be unachievable by using FRP slides due to their low stiffness.

2.7 Summarized

The Eastern Scheldt barrier was designed as part of the Deltaplan, which should prevent the safety of the Southwestern Delta in the long run. Due to protests against a dam a closeable storm surge barrier was constructed, whereby the most important part of the tide remains and which does therefore not interfere with the nature in the Eastern Scheldt. The barrier is designed with lifting steel slides which are placed between concrete piers, these piers are placed on the consolidated soil of the Eastern Scheldt.

The coating, which should protect the slides against their environment, corrodes rapidly and the slides were conserved with a new coating. This maintenance is restricted by the failure probability of the barrier. Next to that, the service life of the coating is probably too short, to maintain all the slides before maintenance is necessary. The slides can deteriorate such that maintenance costs exceed the costs of replacement of the slide. This give occasion to study alternatives which have lower maintenance costs or for which maintenance is required less often. It's advised to take into account the sea level rise and the disappearing tidal zones in the Eastern Scheldt, if possible, in these alternatives.

3 Structural designs for lifting slides

In this chapter the second sub-research question will be answered: 'Which structural designs are feasible for lifting slides in the Eastern Scheldt barrier?'. First of all, other projects with lifting slides are mentioned, after which design concepts from previous researches for lifting slides in the Eastern Scheldt barrier are mentioned. Finally some hydraulic design considerations which are applicable to lifting slides are mentioned.

3.1 Other water barriers with lifting slides

3.1.1 Hartel barrier

The Hartel barrier is a storm surge barrier in the Hartel canal and consists of two slides. The slides are elliptical truss structures, with various dimensions. At one side, the defense cladding is placed on the truss structure. The spans are respectively ca. 50 and ca. 100 m.



Figure 3.1 Hartel barrier, left: aerial view of the barrier, right: detail of the truss structure of the slide [WEB, www.keringhuis.nl]

3.1.2 Storm surge barrier Hollandse IJssel

The storm surge barrier Hollandse IJssel is situated in the same river near Krimpen aan de IJssel. There are 2 slides positioned behind each other.



Figure 3.2 Storm surge barrier Hollandse IJssel [WEB, http://www.flickr.com/photos/alje/]

The slide structure consists of a truss arch with the defense cladding placed on the straight side. The span of the slides in approximately 80 m.

3.2 Concepts for slides in the Eastern Scheldt barrier

In 1998, a graduation work on glass fibre reinforced slides in the Eastern Scheldt storm surge barrier was carried out by Veraart [3] and in 1999 a continuation on this graduation work was carried out by Van der Laken [4]. The concepts for lifting slides which were considered in these graduation works are mentioned in the first subsections.

In the same time period, in 1998, a graduation work was carried out on high strength concrete slides in the Eastern Scheldt storm surge barrier by Keuzenkamp [1] and in 2000 and 2002 other graduations works were carried out on this subject. Finally, Rijkswaterstaat did research to concrete slides in the Eastern Scheldt barrier. Particularly that last research is mentioned in the last subsections.

3.2.1 Concepts Veraart

In [3] some concepts for the design of new FRP slides for the Eastern Scheldt barrier are mentioned. These concepts are (see Figure 3.3):

1. Horizontally curved shell
2. Vertically curved shell
3. Horizontally and vertically curved shell
4. Stacking of round tubes

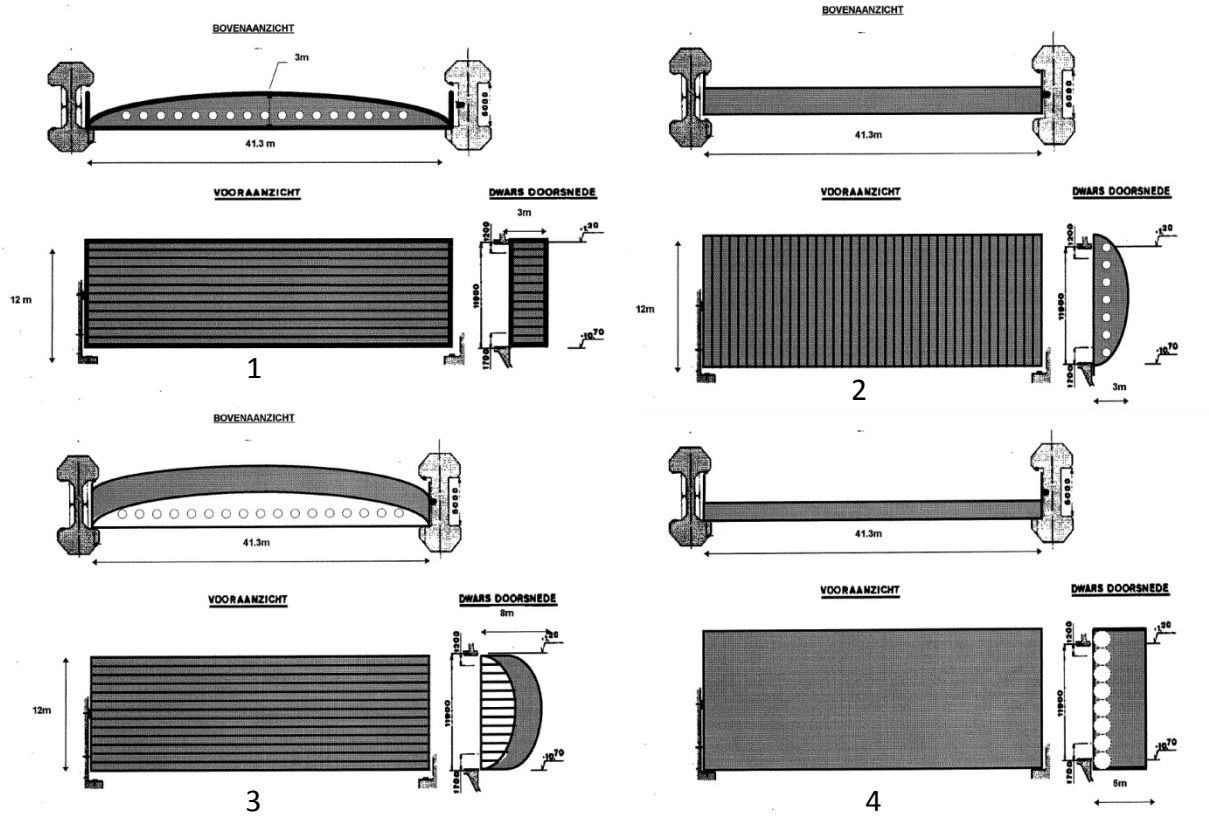


Figure 3.3 Overview of design concepts considered in [3]

The horizontally curved shell in concept 1 carries the wave loadings and the defense cladding carries the water pressure difference loads. These loads are transferred through horizontal walls to the

curved shell. The shell transfers the loads to the piers and the tension rod. The principle of concept 2 and 3 is the same, the forces are just transferred in another direction. In concept 4 round tubes are stacked and a defense cladding is placed in front of the tubes. Every tube can be interpreted as a beam on 2 supports.

Concept 3 was not interesting because the loads were mainly transferred in vertical direction to the top and bottom of the slide. This is almost the same principle as concept 2, but with the use of more material caused by the double curved slide. Therefore concept 3 was not a good alternative.

Concept 2 transfers the loads to the top and bottom of the slide. These parts should transfer the loads to the piers, which are highly loaded at the top and bottom due to the vertically curved slide. The piers are designed for a constant distributed load from the slides. Next to that, manufacturing concept 2 in various heights is difficult, because the absence of a repeated part in vertical direction. For these reasons, concept 2 was not considered to be a good alternative.

Calculations of concept 4 showed that thick tubes were necessary to reduce the deformations of the slide, and prevent contact with the upper beam. It's not possible to manufacture tubes with the required thickness, therefore this concept was not a good alternative.

Concept 1 is sensitive for buckling of the shell and anti-symmetric loads. This behavior of the shell is improved by increasing the moment of inertia of the shell. This is in [3] realized by using curved stacking beams as shell, which was developed into more detail in this graduation work.

3.2.2 Concepts Van der Laken

Also in [4] some concepts for the design of new FRP slides for the Eastern Scheldt barrier are mentioned. The following concepts are considered (see Figure 3.4):

1. Truss arch
2. Stacking of square tubes
3. Truss with U-profiles
4. Sandwich with plate elements

These concepts are mainly based on filament wound tubes and the dimensions were roughly calculated. Concept 1 is a truss compression arch with a tension rod. During positive drop, the hangers are loaded in tension. But during negative drop, the hangers are loaded in compression and can buckle very easily. There are a lot connections in this design, which was considered as unfavorable. The advantages of this concept are low impacts of wave loads and low material usage.

In concept 2 square tubes are stacked. The only disadvantage of this concept is the sensitivity to wave impacts loads, caused by the wide bottom of the slide. Concept 3 consists of two walls stacked of U-profiles with in between a truss of U-profiles. These profiles are difficult to connect and the design is more sensitive to wave impacts loads than concept 1. Therefore this concept was not a good alternative. Concept 4 consists of 2 walls with a core of Z-shaped plates. The walls are connected with diagonal plate elements, which are sensitive to buckling. This design concept requires a lot material and is therefore not a good alternative.

To ensure a high simplicity and therefore an expected high reliability there was chosen to develop concept 2 into more detail. The straight bottom of the slide could experience high vertical wave impact loads and may cause an unfavorable flow pattern. The bottom of the slide is therefore adjusted to another shape, see Figure 3.5.

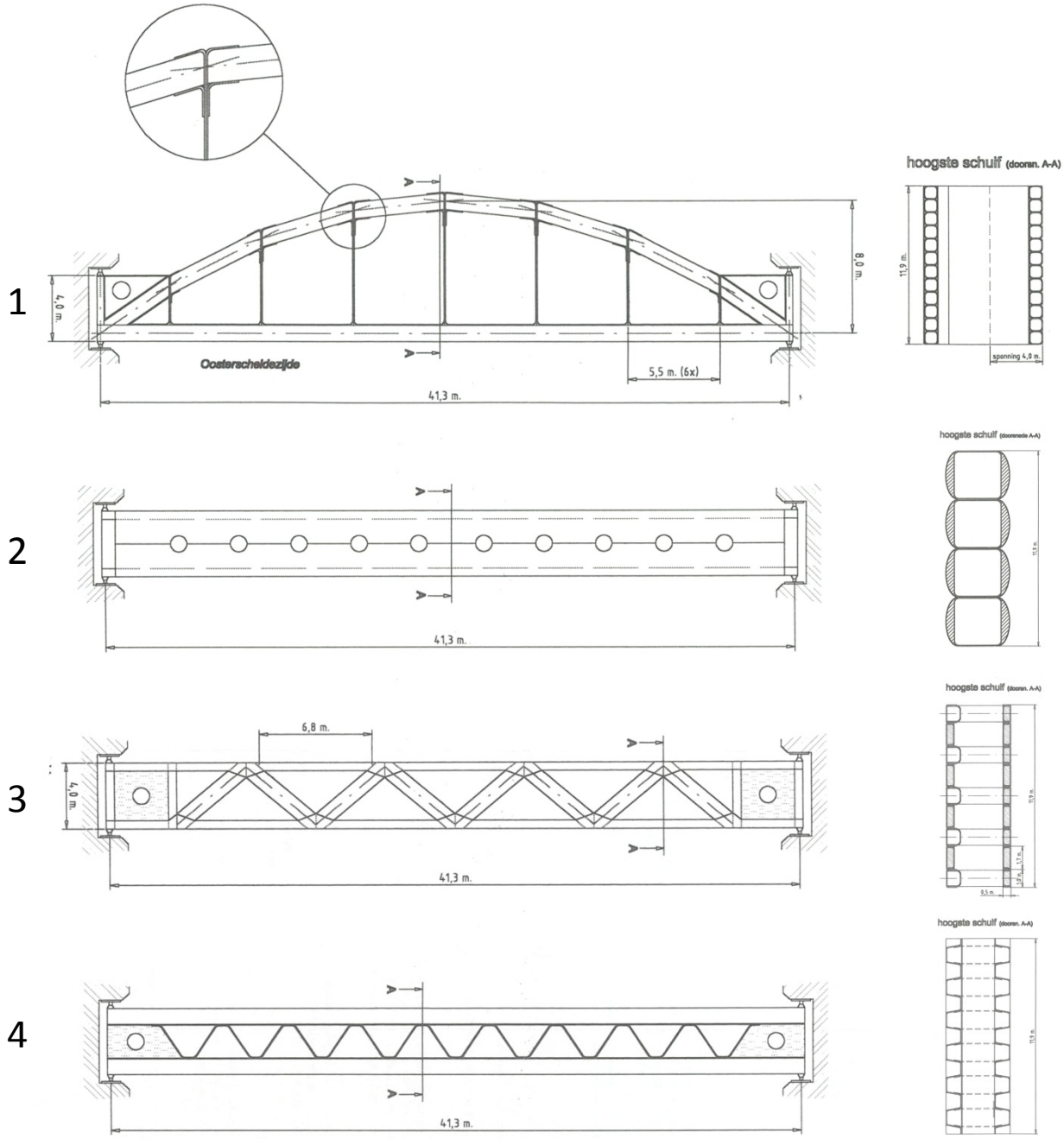


Figure 3.4 Overview of design concepts considered in [4]

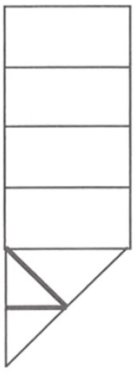


Figure 3.5 Adjusted bottom of the slide [4]

3.2.3 Concepts concrete slides

In [12] some concepts for new concrete slides for the Eastern Scheldt barrier are mentioned. The following concepts are considered (see Figure 3.6):

1. Box structure
2. Plate girder
3. Truss girder

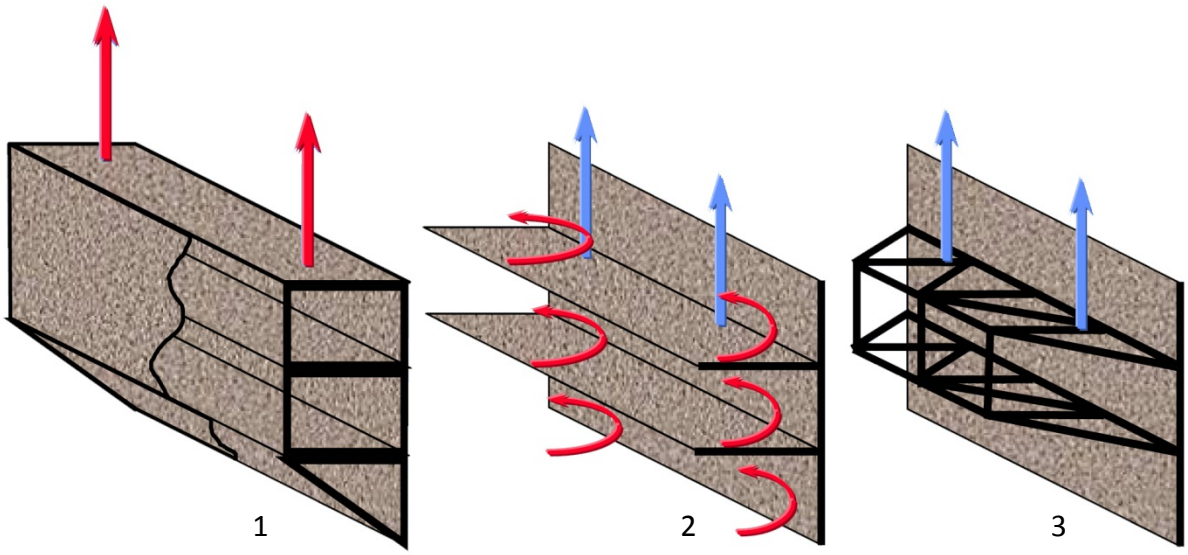


Figure 3.6 Concepts concrete slides [12]

The box structure has the same cross sectional shape as the adjusted concept of Van der Laken. This design in concrete was too heavy for the current movement works, which could carry a maximum slide weight of 700 ton. The box structure had a weight of ca. 1100 ton and was therefore not a good solution for a concrete slide.

The plate girder solution saves a lot of weight, but is sensitive to vertical wave impact loads and therefore not interesting.

The truss girder (totally of concrete) forms an open structure which is lighter than the box concept and is not sensitive to vertical wave impacts loads. The truss girder could have a straight form or could have an arch form. The optimized design was a straight truss girder as shown in Figure 3.7.

In [1] also a box structure and a plate girder solution were considered, which were not explicitly shown in this chapter. The plate girder solution experienced also high wave impacts loads. The box structure is designed in more detail in [1], but without adjusted shape to improve the flow pattern and the sensitivity to vertical wave impact loads.

The researches for concrete lifting slides in the Eastern Scheldt barrier showed that replacement of the slides was financially competitive with the maintenance costs of the slides, but the self weight of the slides threatens to exceed the capacity of the lift cylinders of the slides. [2]

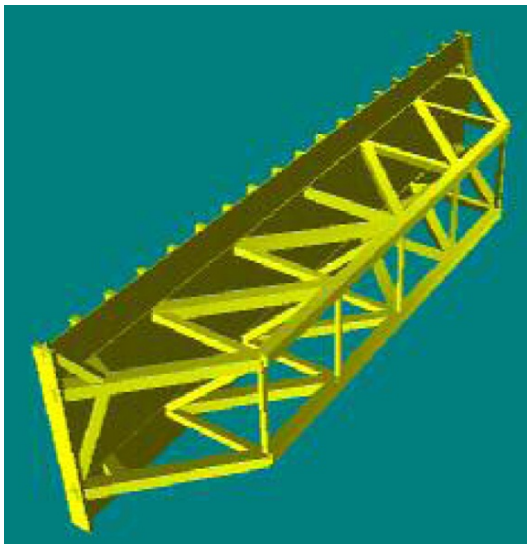


Figure 3.7 Optimized design of the concrete truss girder slide [12]

3.2.4 Analysis of concepts

The previous researches showed that there are a lot of possibilities to make a new lifting slide for the Eastern Scheldt barrier in FRP or concrete. Some of these concepts are not feasible due to hydraulic reasons or manufacturability, but there are concepts which are financially competitive with the maintenance costs of the current slides.

Since concept 1 of the concrete concepts was too heavy for the current movement works, this concept can offer opportunities in FRP since the self weight of a FRP slide will be much lower. Therefore, in the next chapter of this literature study information on the material FRP is mentioned.

3.3 Hydraulic design considerations for lifting slides

Some important design considerations for slides to prevent vibrations by flow and high wave impact loads are mentioned in the next subsections.

3.3.1 Vibrations by flow

The cross sectional shape of the slide can be optimized to prevent vibrations. Some aspects which are important during design are: [13]

- Avoiding of flow patterns with an undefined release point, which is determined by the cross sectional shape and can cause vibrations. Examples of these are shown in Figure 3.8. A sharp or thin edge is preferable.

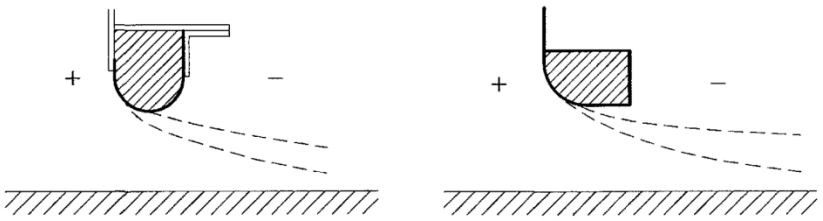


Figure 3.8 Examples of shapes with an undefined release point [13]

- Avoiding of flow patterns which release and later on lay down again. These are causes of instability problems, examples are shown in Figure 3.9. A sharp edge without additional stiffeners in an area of minimal 45° at the downstream side or a sharp edge at the downstream side are solutions with a favorable flow pattern, see Figure 3.10.

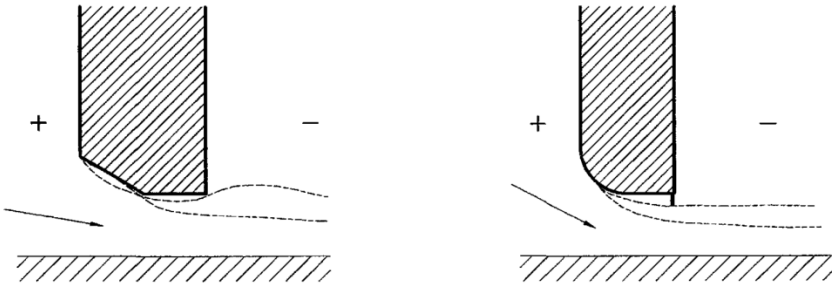


Figure 3.9 Examples of shapes which cause flow patterns which release and later on lay down again [13]

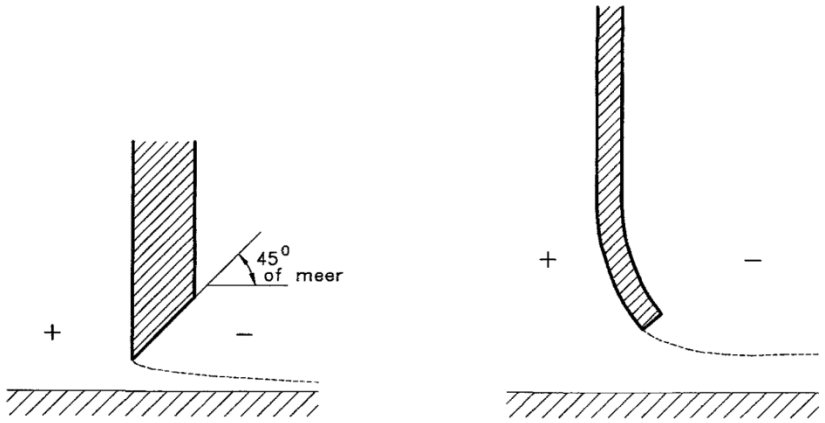


Figure 3.10 Shapes with a favorable flow pattern [13]

3.3.2 Wave impact loads

Additional measures to a structure can be done to reduce the impact of wave loads. Some general measures which could be taken during design and are applicable to lifting slides are: [14]

- Avoid horizontal or inclined construction parts which are placed near the average water level, where the vertical water velocity is greatest.
- If avoiding of these parts is not possible, it's advisable to design an open construction (e.g. truss structure). Perforations in plated structures reduce the loaded surface, but the magnitude is not reduced.
- If slides are designed with horizontal plates at the wave side, it's advisable to use a second vertical plate to prevent wave impact loads on the horizontal plates.
- Corners where waves run in should be avoided, the water flow can't run away sideways which can lead to high water impact loads.
- Air inclusions can lead to a lower response of the slide, but it's not advisable to take this aspect into account since the effect of an air inclusion is difficult to predict.
- The response of a structure is depending on the ratio between the impact time and the eigen vibration time. A low stiffness or a high mass of the structure could reduce the response, but this will be unattractive due to stiffness and strength requirements. This flexibility is mostly restricted by economic considerations, it is therefore more attractive to optimize the shape of the structure.
- Damping can lead to a lower response of the structure, both structural damping and damping from the water can be effective in this way.

3.4 Summarized

The existing water barriers with lifting slides which were considered have both a truss structure. Such an open structure is in favor because of wave impact loads and the ability to sink the structure. But there are other possibilities to reduce vertical wave impact loads, e.g. avoiding horizontal construction parts at wave side. The issue of vertical wave impact loads should be considered as a dominant factor in design of lifting slides.

A lot of structural systems for slides in the Eastern Scheldt barrier were mentioned. In a later stage a choice should be made on the possibilities of re-use of these concepts. The underside of these concepts may have to be adjusted to an inclined underside to avoid vibrations by flow.

These previous researches showed also that there are concepts which are financially competitive with the maintenance costs of the current slides. Concept 1 of the concrete concepts was too heavy for the current movement works, but this concept can offer opportunities in FRP since the self weight of a FRP slide will be much lower. Therefore, in the next chapter of this literature study, information on the material FRP is mentioned.

4 Fibre reinforced polymers

In this chapter the third sub-research question will be answered: 'Which reinforcement, resins and manufacturing methods are suitable to apply for the slides and what are the characteristics of fibre reinforced polymers?'. The previous chapter gave occasion to study this material.

In the first sections, some general aspects of FRP are mentioned, where after the different materials of which FRP is made are mentioned. Also the manufacturing process and the characteristics of FRP are mentioned to get insight in the possibilities of FRP. Finally, some reference projects are mentioned. This chapter, except the first section, focuses on the use of FRP in civil engineering industry.

4.1 History

In the past, composite materials were already made from straw and clay used in bricks. Later on, twigs were coated with clay and used in ceilings. In these applications a kind of reinforcement was used in a brittle natural occurring material, which should strengthen this material and carry the tensile forces.



Figure 4.1 A straw-clay brick [WEB, http://chasingfireflies.typepad.com/chasing_fireflies/2008/09/index.html]

This idea is still applied in fibre reinforced polymers (FRP), which were developed in the 20th century. FRP was mainly used in the aircraft industry, due to their low weight and high strength characteristics. Later on FRP was also used in shipbuilding industry and automotive industry. Their use in structural applications in the civil engineering industry has increased in the last decades. Illustrated examples of the use of FRP in civil engineering industry can be read in [15].

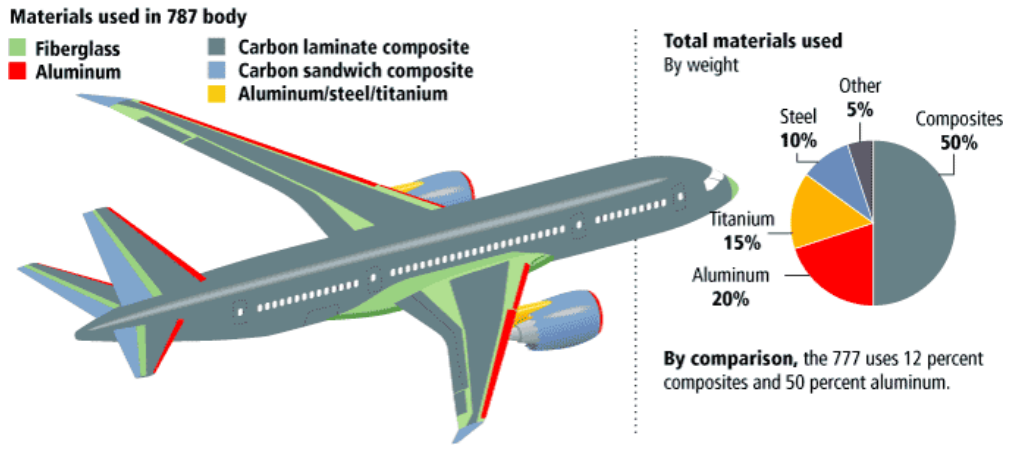


Figure 4.2 Boeing 787 with emphasis on the used materials in this airplane [WEB, http://bintang.site11.com/Boeing_787/Boeing787_files/Specifications.html]

4.2 General

Fibre reinforced polymers are considered to be a durable material with a low need for maintenance. Preservation costs, which are needed for e.g. steel structures, can be saved. The material has high strength characteristics in combination with a low weight. Next to that good fatigue properties can be achieved. FRP structures are mainly attractive when making a comparison of life cycle costs.

Fibre reinforced polymers are a composite of fibres (reinforcement) and a polymer matrix (resin). The fibres carry the load and the matrix binds them together. The matrix should hold the fibres in their position (and prevent them from buckling), protect them against the humidity and transfer the loads to the fibres. The mechanical properties are dominated by the material design. Next to the reinforcement and resin type used, the amount of fibres, the angle of the reinforcement with the loading direction and the adhesion between the fibres and the matrix are influencing the mechanical properties of the FRP.

4.3 Reinforcements

The most used reinforcements are glass fibres, carbon fibres and polyaramid fibres. The stress-strain diagram of different reinforcement types is shown in Figure 4.3. These types are described in the next subsections.

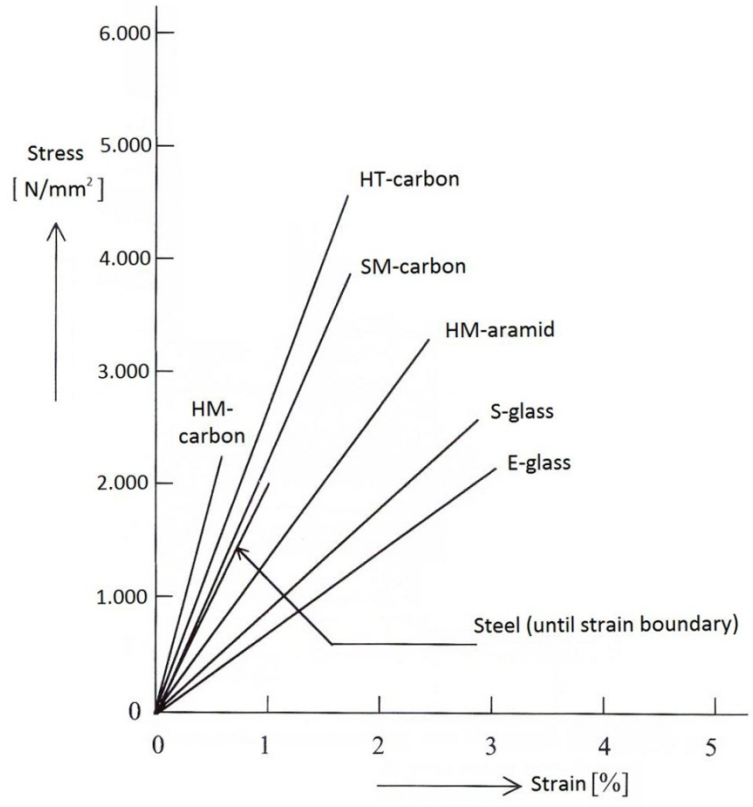


Figure 4.3 Stress-strain diagrams of various reinforcement types [16]

4.3.1 Glass fibres

Glass fibres are manufactured by pulling molted glass through a platinum brushing into continuous filaments. These filaments are coated and brought together in strands. Various types of glass fibres are produced. The most popular type is E-glass (electrical grade glass). Other types of glass are A-glass (alkali glass), C-glass (chemical resistant glass) and R- and S-glass (high strength glass).

Glass fibres have a relatively low price, but the stiffness is lower than the other fibre types. The density of glass fibres is higher than the other fibre types.

4.3.2 Carbon fibres

Carbon fibres are manufactured by controlled oxidation and carbonization of a precursor fibre at a high temperature. As precursor fibres polyacrylonitrile, cellulose, lognin or pitch is used.

Carbon fibres are the most expensive fibre type, but have a very high young's modulus. These fibres can be subdivided into HM (High Modulus) fibres and HS (High Strength) fibres, which have respectively a high young's modulus and a high strength. The disadvantage of the HM fibre is a low elongation at rupture.

4.3.3 Polyaramid fibres

Polyaramid fibres are manufactured by extrusion and spinning processes. The polymer is placed in a solvent at a very low temperature where after the polymer is extruded into a hot cylinder where the solvent evaporates. Thereafter the fibre is drawn. Polyaramid fibres have a high tensile strength, but have a very low compression strength.

4.3.4 Other reinforcements types

Other reinforcement types are polyester fibres, jute fibres, sisal fibres, nylon fibres and boron fibres. These fibres are rarely used, but can have advantages for some purposes. These are mentioned in [15] and [16].

4.3.5 Reinforcement forms

The strand form is restricted for apply in fibre reinforced polymers. Other reinforcement forms are: continuous filament rovings, chopped strand mats, continuous filament mat and woven glass fabric. These are described below.

4.3.5.1 Continuous filament rovings

A continuous filament roving consist of parallel wound strands. A roving is a subassembly which is used in final products, such as pultruded profiles, and in reinforcement forms mentioned below.

4.3.5.2 Chopped strand mats

Chopped strand mats (CSM) consist of rovings which are cut to a certain length and bonded with each other in a random orientation.



Figure 4.4 Left: Continuous filament rovings [15] Right: CSM [WEB,http://fiberglassblog.com/category/chopped-strand-mat/]

4.3.5.3 Continuous filament mat

Continuous filament mats (CFM) consist of multiple layers of continuous filaments in a random orientation.

4.3.5.4 Woven fabrics

Woven fabrics can be made from untwisted rovings or from twisted continuous filaments. The different weave types are: plain weave, twill weave, satin weave and unidirectional wave. A satin wave has the best mechanical properties in all directions, the unidirectional weave has the best properties in the main weaving direction.



Figure 4.5 Left: CFM [WEB,http://cn.tradekey.com/product_view/id/1810675.htm] Right: Woven glass fibre fabric [WEB, http://www.floratextiles.com/glass-fibre-fabric.htm]

4.4 Resins

A resin is necessary to form a material which can be used for structural applications, which ensures that it resists next to tension also compression and shear. There are two resin types which can be used: thermoset and thermoplastic. A thermoset cannot be re-softened with heat after curing, a thermoplastic can. A thermoset is initially liquid at room temperature and a thermoplastic is initially solid. Thermosets are mainly used in fibre reinforced polymers and are described in the next subsections. In the last subsection the advantages and disadvantages of thermoplastics are mentioned. The most used resin types are described in the next subsections. In Table 4.1 the properties of two resin types are shown. The epoxy resins shown have different curing temperatures.

Table 4.1 Mechanical properties of different resin types [17]

Property	Unit	Uns. Polyester	Epoxy 20°	Epoxy 80°+140°	Epoxy 120°+160°
Curing temperature	°C	-	20	80+140	120+160
Density	kg/m^3	1150-1250	1150-2000	1150-2000	1200-1300
Modulus of elasticity	10^3 N/mm^2	2.4-4.6	3.5	3.5	3.5
Poisson's ratio	-	0.35	0.35	0.35	0.35
Tensile strength	N/mm^2	40-85	50-70	60-80	80-90
Compressive strength	N/mm^2	140-150	90	130	120
Rupture strain	%	1.2-4.5	2-4	3-5	4-5
Lin. Them. Exp. Coeff.	$10^{-6}/K$	80-150	90	60	65

4.4.1 Unsaturated polyester resins

Unsaturated polyester resins are the most applied resin in FRP. Polyesters are formed by dissolving polymer chains in a reactive solvent. A catalyst and accelerator is added, which causes a chemical reaction and forms a solid structure. The chemical reaction takes place in a cold state without using pressure. Curing starts when an initiator is added, the curing speed depends upon the temperature and the reactivity of the resin and the catalyst. The chemical resistance isn't easy to quantify, but the general order of increased resistance is: orthophthalics, isophthalics, iso-NPGs and bisphenols.

4.4.2 Vinyl ester resins

Vinyl ester resins can be considered as an extension of polyester resins, because they are also formed using a reactive solvent and are cured using an initiator. The chemical resistance of vinyl esters is higher than polyester resins and the resin structure is tougher. The properties of vinyl esters are similar with those achieved with polyester resins.

4.4.3 Epoxy resins

Epoxy resins are formed by a reaction of epichlorohydrin and bisphenol 'A'. Due to their high viscosity, this resin is mostly used at elevated temperatures or is dissolved in an inert solvent to reduce the viscosity. Curing takes place by using curing agents, preferable above a certain temperature. The properties are determined by the curing agents and the curing temperature. Epoxy resins have better mechanical properties than the other resins: a lower shrinkage affect, better resistant to moister, high temperature stability and good electrical insulation. In seawater there is no difference visible between epoxies and polyesters regarding the resistance to their environment.

4.4.4 Other resin types

Next to the thermosets mentioned in the previous subsections, thermoplastics are in use. Thermoplastics have a high toughness and are resilient. Next to that they have a good corrosion resistance. A disadvantage is the high manufacturing temperature. There is a growing interest in the use of thermoplastics. For structural applications only the 'technical thermoplastics' could be used, such as the amorphous thermoplastics (PS, PI, PEI) and the semi-crystalline thermoplastics (PA, PAI, PPS, PEEK). Almost all thermoplastics are insensitive to moisture, except PA.

Some other resins types are: phenolic resins, silicone resins, polyimide resins and furane resins. All of them offer some specific properties such as fire resistance, good thermal properties or chemical resistance, which can be read in [15].

4.5 Cores

A core material could be used to make a composite sandwich, which is built up from two outer skins and a core material which bonds them together. A core between the outer skins will increase the structural efficiency of a FRP structure, since the skins are placed at a greater distance from the neutral axis. Therefore the bending moment capacity will increase a lot, while the self weight remains almost the same. Some core materials which are used a lot are mentioned shortly in the next subsections.

4.5.1 Foam

Foams can be used as a core material in a composite sandwich. Most foams are made from plastic materials and are attractive due to their low weight. Foams have the advantage that they can be used in almost every shape.

4.5.2 Honeycomb

A honeycomb core, see Figure 4.6, is a core which is build up from hexagonal tubes. This core ensures a high compression and shear resistance. Also other shapes, than a hexagonal, are available.

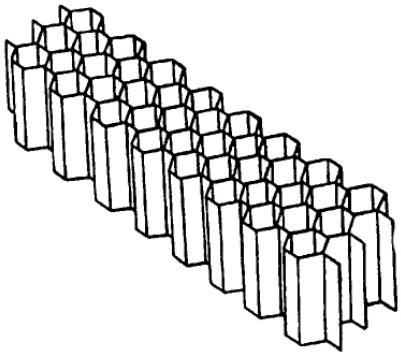


Figure 4.6 Honeycomb core (hexagonal shape) [15]

4.5.3 Balsa wood

Balsa wood is a solid core material which has a light weight and is therefore attractive to use as core material. It's one of the most used materials to create a solid sandwich, although some synthetic materials are emerging.

4.6 Manufacturing processes

To form a composite material, the reinforcement and resin should be merged. Next to these two materials, some additives are used in the manufacturing process which ensures better characteristics of the FRP or which improved the manufacturing process. The fire retardancy can be increased, the shrinkage can be controlled, a pigment can be used or a filler is added to the resin to reduce costs. Additives which are used in the manufacturing process are described the next subsections.

The manufacturing of FRP consists of different processes. First of all, the resin and activator are mixed, where after the resin is dispensed into the mold. This needs to be cured. Thereafter the reinforcement can be placed and impregnated with resin, until the final product is achieved. The manufacturing processes are divided into three categories: open mold processes, closed mold processes and continuous processes, which are described in the next subsections. Finally, a comparison between these manufacturing processes is made in the last subsections.

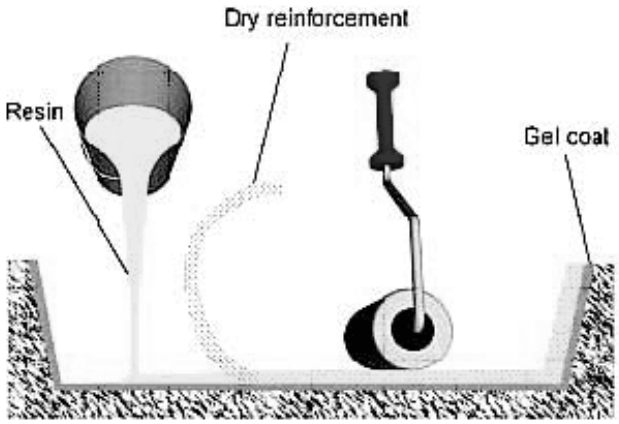


Figure 4.7 Hand lamination process [WEB, www.gdecotech.com]

4.6.1 Open mold processes

4.6.1.1 Hand laminating

The resin and reinforcement are applied manually and are consolidated by hand until the final build-up is achieved. This process is labor intensive, haves a low production rate and the thickness control is bad. The advantages of this process are a lot flexibility and low capital outlay.

4.6.1.2 Saturation

The difference of saturation with hand laminating is the use of a gun to spray the catalyst and resin on to the mold. The resin and catalyst are mixed in the gun to improve control over the resin.

4.6.1.3 Spray-up

During the spray-up process, the resin and fibres are sprayed onto the mold. Only random reinforcement can be manufactured in this way. The thickness control of the product is still bad, but the production rate is increased. Large parts can be manufactured easily with low material and low tooling costs.

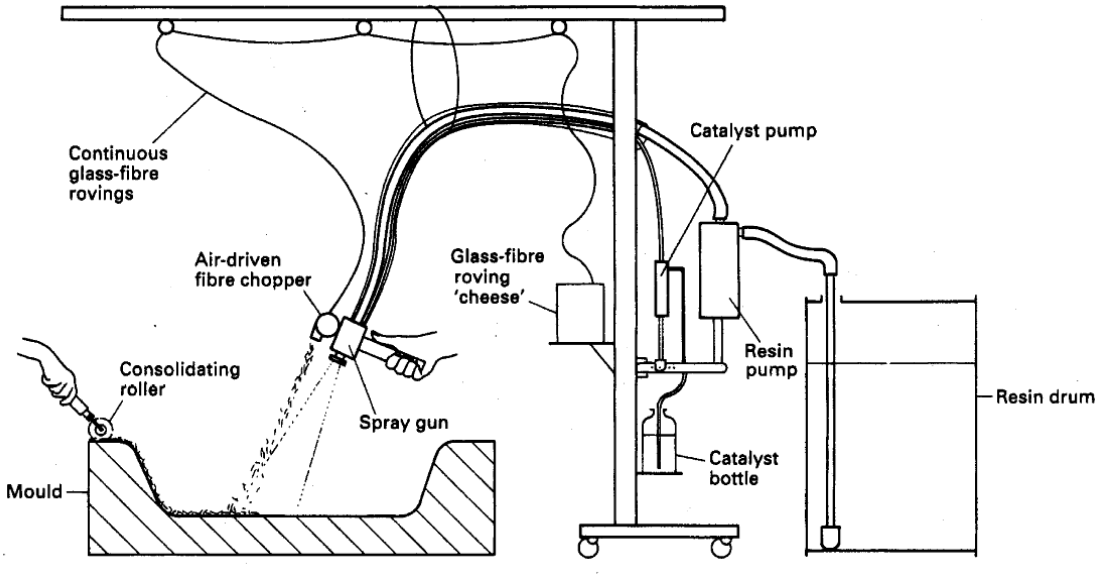


Figure 4.8 Spray-up process [15]

4.6.1.4 Auto spray-up

Auto spray up is an extension of the spray-up process. The gun is controlled by a machine, which can control the thickness. Only random reinforcement can be applied.

4.6.1.5 Filament winding

Filament winding is used to manufacture hollow shapes. Rovings are fed through a resin bath and positioned on a rotating mold. The fibre direction and thickness can be controlled very well. This process is limited to a small range of products and the fibres cannot be placed completely in the longitudinal direction. This process ensures high mechanical properties at high production rate.

4.6.1.6 Spray winding

This process is a combination of auto spray-up and filament winding and can offer a cost-effective manufacture process for some products.

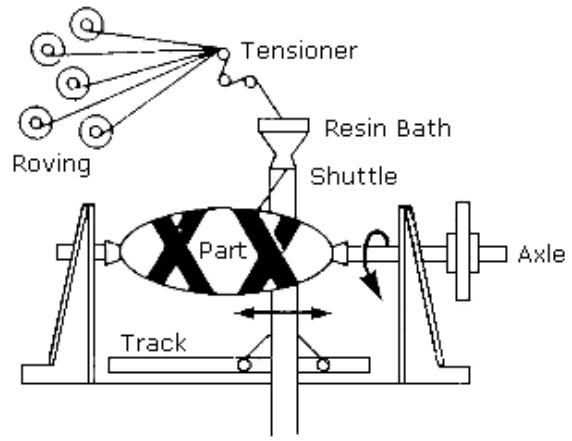


Figure 4.9 Filament winding process [16]

4.6.1.7 Centrifugal casting

During this process random reinforcement is sprayed onto the inside of a rotating mold. The laminate consolidates rapidly due to the rotating mold, which ensures a resin-rich inner surface. This process is characterized by a high production rate and good fibre and thickness control.

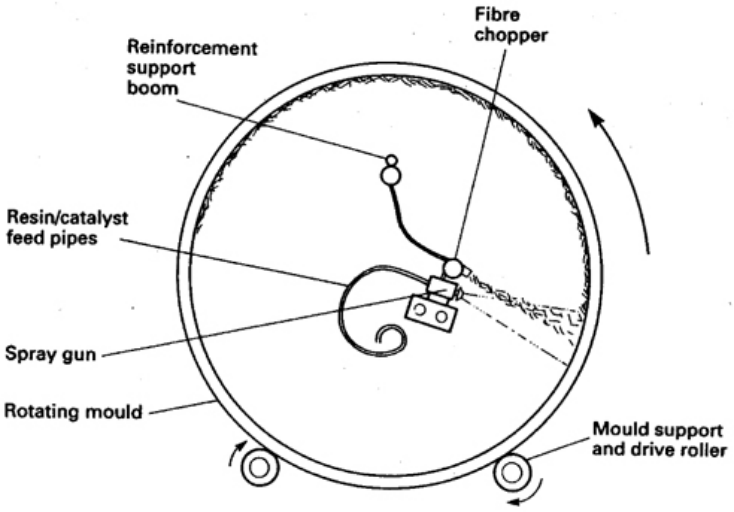


Figure 4.10 Centrifugal casting process [15]

4.6.2 Closed mold processes

4.6.2.1 Vacuum bag

The process starts by applying the resin and reinforcement using the hand lamination process. Thereafter a film is laid over the laminate and this space is pumped vacuum to consolidate the laminate. Besides that, hand rolling is used to achieve complete consolidation. This process is suitable for making sandwich panels.

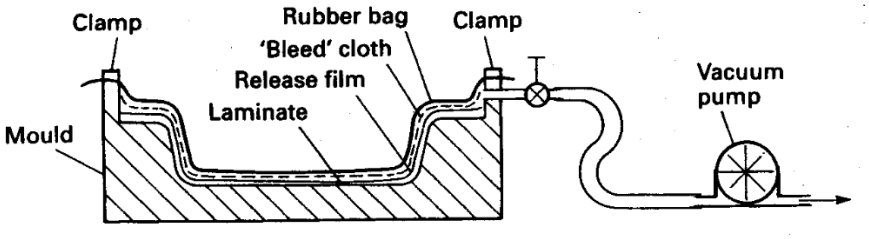


Figure 4.11 Vacuum bag process [15]

4.6.2.2 Pressure bag

This process is very similar to the vacuum bag process, but the pressure is applied on top of the film. This will allow higher pressure and ensures a better consolidation of the laminate. The disadvantage is the use of a more robust mold, due to the higher pressure.

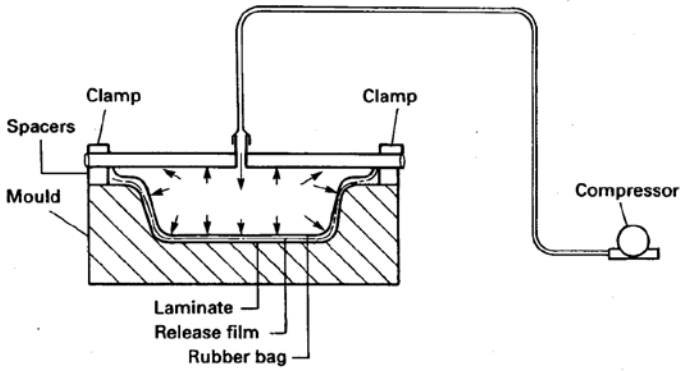


Figure 4.12 Pressure bag process [15]

4.6.2.3 Autoclave

The autoclave manufacturing process is a combination of vacuum and pressure bag molding. Using this process, products with very high quality can be manufactured due to the very high pressure in the autoclave.

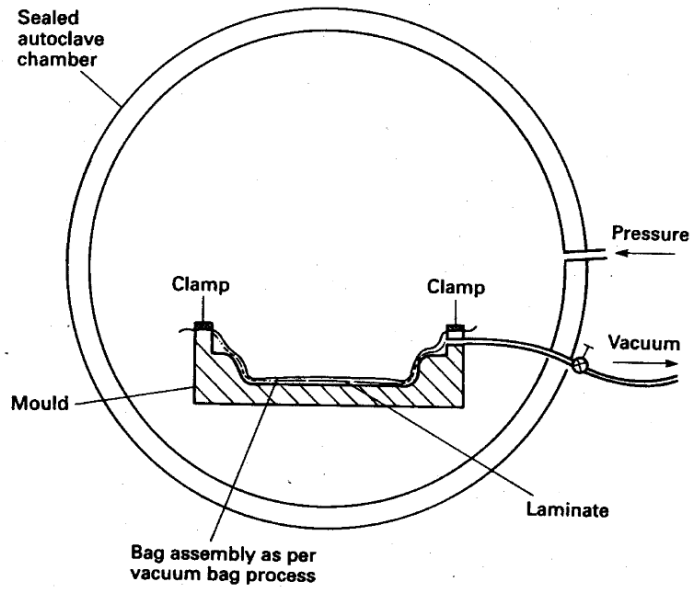


Figure 4.13 Autoclave process [15]

4.6.2.4 Cold press

A cold press consists of a male and a female mold which are placed in a hydraulic press. The reinforcement and the resin are put into the lower mold, thereafter the upper mold will come down and the final product is formed. This process will produce products with accurate dimensions and two molded surfaces at a good production rate. The disadvantages of this process are a limited press size, a low fibre content and a high capital investment.

4.6.2.5 Hot press

This process is similar to the cold press method, with the addition of heat to the mold. This will increase the production rate. The other characteristics are very similar to the cold press process.

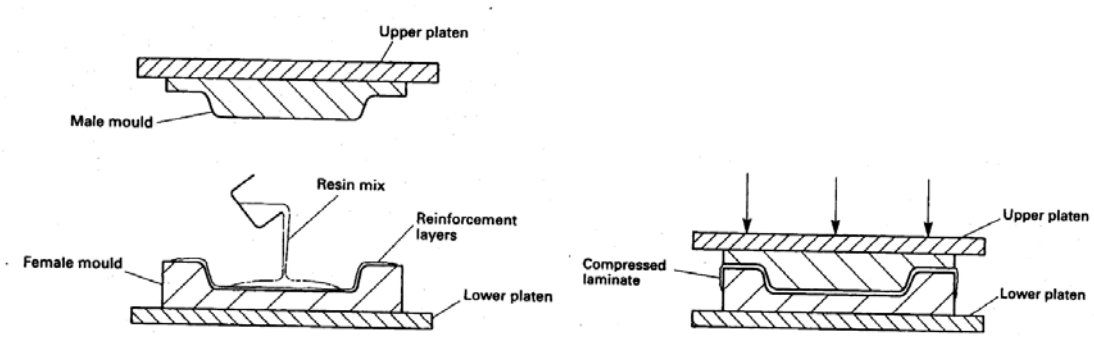


Figure 4.14 Cold press process [15]

4.6.2.6 Resin injection

This process starts with putting the reinforcement into the mold, where after the mold is closed and the resin is injected into the closed mold under a high pressure. This will give accurate dimensions to the products and gives two molded surfaces.

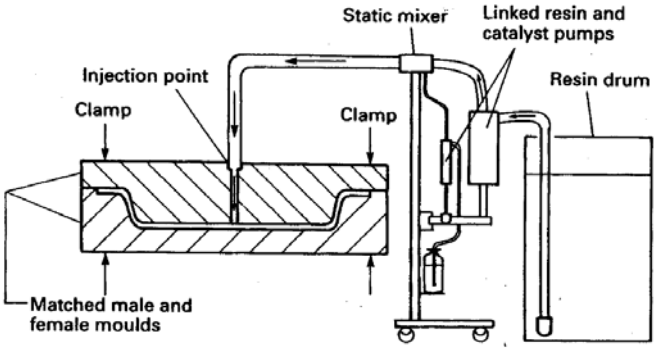


Figure 4.15 Resin injection process [15]

4.6.2.7 Vacuum-assisted resin injection

This process is similar to the resin injection process, but with the addition that a seal is formed around the edge of the mold and the mold is pumped vacuum. This consolidates the laminate and offers the ability of using lager molds and higher fibre contents.

4.6.2.8 Injection molding

The resin and reinforcement are mixed to a dough, which is placed into a closed mold. Only short random reinforcement can be used. Products with accurate dimensions and with complex shapes can be produced with a high production rate.

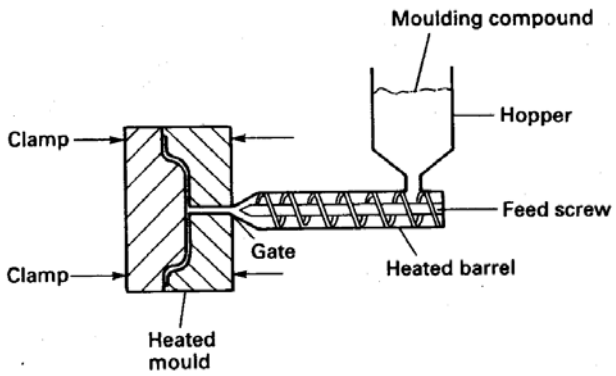


Figure 4.16 Injection molding process [15]

4.6.3 Continuous processes

4.6.3.1 Continuous laminating

The reinforcement is combined with the resin and placed between two layers of release film. This will go through a curing oven, where after the product can be cut at the desired length. The manufacturing characteristics are a very high production rate, good mechanical properties and low costs. The shape which is produced is limited.

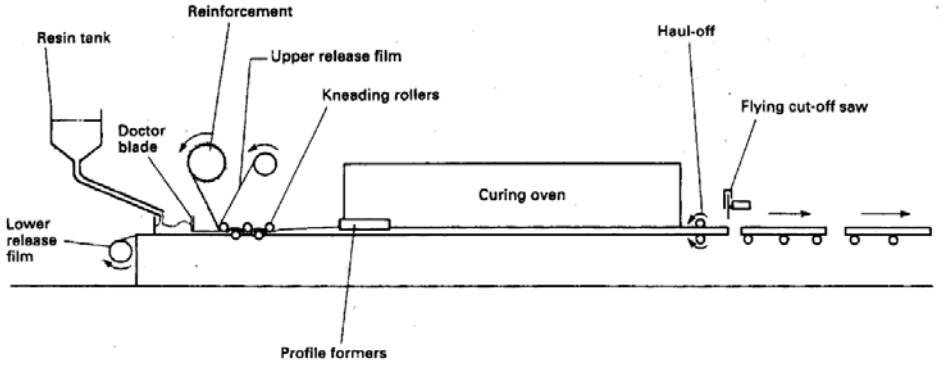


Figure 4.17 Continuous hand lamination process [15]

4.6.3.2 Pulltrusion

The reinforcement is impregnated with resin, where after it's pulled through a headed die which forms the final shape of the product. The continuous profile is cut into the desired length at the end of this process. This process ensures a high production rate, accurate dimensions and high mechanical properties in the longitudinal direction. In the transverse direction, the mechanical properties are limited.

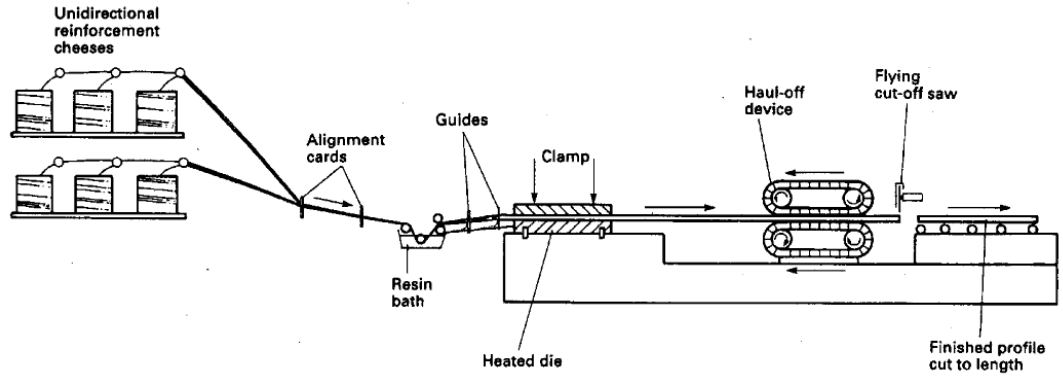


Figure 4.18 Pulltrusion process [15]

4.6.3.3 Continuous filament winding

This process is the extension of the filament winding process in continuous form. The reinforcement is wrapped around a pipe which is moving. Reinforcement under different angles can be applied using multiple winding heads.

4.6.4 Comparison manufacturing methods

An overview of the different manufacturing processes is given in Table 4.2. The characteristic process parameters are mentioned for these processes.

Table 4.2 Comparison of different manufacturing processes [18]

Manufacturing process	Fibre volume [%]	Size range [m^2]	Processing pressure [bar]	Processing temperature [°C]	Core mat.	Detail tolerance [mm]	Relative production cost [-]
Open mold processes							
hand laminating	13-50	0.25-2000	ambient	ambient	Yes	1.0-5.0	High
saturation	13-50	0.25-2000	ambient	ambient	Yes	1.0-5.0	Moderate/High
spray-up	13-21	2.00-100	ambient	ambient	Yes	1.0-3.0	Low
auto spray-up	13-22	2.00-100	ambient	ambient	Yes	2.0-3.0	Very low
filament winding	55-70	0.1-100	ambient	ambient	Yes	1.0-2.0	Moderate/Low
spray winding	40-60	0.1-100	ambient	ambient	Yes	2.03.0	Very low
centrifugal casting	20-60	0.5-100	ambient	40-60	No	1.0-3.0	Moderate/Low
Closed mold processes							
vacuum bag	15-60	0.5-200	ambient	Ambient	Yes	1.0-3.0	Very high
pressure bag	20-70	0.5-200	1-3.5	20-70	Yes	1.0-3.0	Very high
autoclave	35-70	0.25-5.0	1-10.0	20-140	Yes	0.5-1.0	Very high
cold press	15-25	0.25-5.0	2.0-5.0	20-50	No	0.25-1.0	Low
hot press	12-40	0.1-2.5	50-150	130-150	No	0.2-1.0	Very low
resin injection	10-60	0.25-5.0	1-2.0	20-50	Yes	1.0-2.0	Moderate
vacuum-assisted resin injection	15-60	1.0-100	1-2.0	15-30	Yes	2.0-5.0	Moderate
injection molding	5-10	0.01-1.0	750-1500	140	No	0.1-0.5	Very low
Continuous processes							
continuous laminating	10-25	Up to 2m width	Ambient	100-150	No	1.0	Very low
pulltrusion	30-65	Uo to 1m width	Varies	130-150	No	0.2-0.5	Low
continuous filament winding	55-70	Up to 2m diam.	ambient	ambient	No	1.0-2.0	Low

4.7 Characteristics of fibre reinforced polymers

Since the different materials of FRP and the manufacturing processes are mentioned, now the characteristics of the final material can be studied. It should be clear that these characteristics are not fixed, since among other things like the reinforcement, resin and manufacturing process influence these characteristics highly. Therefore the characteristics which are in general achievable are mentioned in the next subsections.

4.7.1 Durability

The maintenance costs are mainly depending on the durability of a structure. Therefore, it is important to mention the durability of FRP. Only accelerated durability tests were carried out on FRP structures, since the material is quite new. Therefore, for various mechanisms the effect of degradation is not known. In general some measures could be taken, which improve the durability of FRP. A resin-rich surface will ensure a lower movement of moisture and chemicals into the composite, which is mostly assured by applying a gel-coat on the outer surface. This can also prevent the FRP of direct exposure to UV-radiation.

FRP structures which are positioned in a wet environment could have a high resistance to moisture. A gel-coat made of the following resins is mostly used in that case: ISO, ISO-NPG or vinyl ester.

4.7.2 Sustainability

The sustainability of FRP can be divided into the sustainability of the reinforcement and the resin. Glass fibre reinforcement is sustainable, due to the low energy consumption of the manufacturing process (one quarter compared to steel). Carbon fibres require high energy consumption and are therefore less sustainable.

Thermosetting resins can be recycled in a limited way, which can be solved using fully recyclable thermoplastics. Provided that last assumption, FRP materials can be considered at least as sustainable as concrete, steel or timber. Different life cycle assessments show a lower environmental impact for FRP structures in comparison to steel or concrete. Especially in the manufacturing and operational phase FRP is in favor, in the end-of-life phase a thermoset isn't.

4.7.3 Fire resistance

FRP have high thermal insulation properties, but are combustible without additional measures. Toxic fumes develop during fire, although some types exists which doesn't. Also fire-retardant types and self-extinguishing types are available today, but there is almost no knowledge available on the loss of strength in fire of FRP.

4.7.4 Mechanical properties

The mechanical properties of the reinforcements are globally mentioned in section 4.3 and those of the resin in section 4.4. The amount of reinforcement determines mainly the mechanical properties of the composite, therefore the resin/fibre ratio is an important parameter in the design of FRP structures. In Table 4.3 some mechanical properties of FRP materials with different reinforcements are shown, for a fibre content of 60% and all with an epoxy resin. These properties are mentioned for a unidirectional reinforced laminate to get some insight in the achievable properties.

Table 4.3 Mechanical properties of a FRP material with different reinforcements and an epoxy resin [17]

Property	Unit	E-glass	SM-carbon	HT-carbon	HM-aramid
Density	kg/m^3	2000	1550	1550	1350
Long. Modulus of elasticity	10^3 N/mm^2	40	130	150	75
Flexural modulus	10^3 N/mm^2	35	125	130	70
Transv. Modulus of elasticity	10^3 N/mm^2	10	9	10	5.5
Long. Transv. Shear modulus	10^3 N/mm^2	4.5	6	6	2.5
Long. Trans. Poisson's ratio	-	0.27	0.30	0.30	0.32
Long. Tensile strength	N/mm^2	800	1550	1700	1400
Long. Compressive strength	N/mm^2	500	1250	1500	270
Bending strength	N/mm^3	850	1600	1750	625
Transv. Tensile strength	N/mm^2	30	70	55	30
Transv. Compressive strength	N/mm^2	140	200	250	55
Long. Transv. Shear strength	N/mm^2	65	90	80	35
Interlaminar shear strength	N/mm^2	40	100	125	60
Long. Lin. Therm. Exp. Coef.	$10^{-6}/K$	7	1.5	0.5	-2
Transv. Lin. Therm. Exp. Coef.	$10^{-6}/K$	20	25	30	60

4.7.4.1 Parameters which influence the mechanical properties of FRP

The resin/fibre ratio is not the only parameter which influences the mechanical properties. Of course, the properties are also determined by the interaction between the fibres and the matrix. The tensile strength depends on both, but the stiffness of FRP is mainly determined by the reinforcement which is used.

4.7.4.2 Laminate design aspects

The laminate build up influences the mechanical properties of FRP and is therefore mentioned here. The properties of one lamella in different directions vary highly due to the fibres, which are placed in one direction. These lamellas can be stacked to a laminate to optimize the mechanical properties in the non-fibre directions, also mats can be used as lamella. The mechanical properties of such a laminate can be derived from the properties of the lamellas. There are 2 calculation methods which describe the calculation of the properties of a laminate: the netting theory and the classical lamination theory. The netting theory is the simplest method, which neglects the properties of the matrix and considers only the reinforcement for the calculation of the mechanical properties. The classical lamination theory considers both the reinforcement and the matrix. This theory assumes that the 'first ply failure' (FPF) means a total failure of the laminate. But actually, the laminate will not lose his load bearing function immediately, because the other laminas could still carry the load. However, first ply failures can cause delamination, so FPF should not occur during normal use.

There are a lot of laminate design tools available, such as MicMac, Kolibri and ESAComp, which can be used for the calculation of the laminate properties. They offer the use of different failure theories. There are also some FEM packages available which have some features for composites, such as Abaqus, Lusas, Nastran and Dlubal RFEM.

Due to the possibility of variation in laminate lay-up, FRP materials enable an extra design flexibility. To optimize the mechanical properties, the next comments are listed from [17]:

- It's advisable to use symmetric laminates, which ensures decoupling of elongation and torsion.
- The stacking of lamellas should have a low variation of direction in height, to reduce stresses.
- A stacking of less lamella placed in the same direction on top of each other will reduce stresses between the lamellas.
- Edges will ensure stresses between the lamellas which can cause delamination. Integrated structures are therefore advisable, with a minimum number of components.

In [19] the minimum amount of fibres which should be placed in all directions is 15% in each direction. This assumption gives generally three subdivisions in amounts of fibres which can be used in every direction of a laminate, see Table 4.4.

Table 4.4 Possible subdivisions of fibres in each direction of a laminate

	0°	90°	+45°	-45°
One main direction	55%	15%	15%	15%
Two main directions	35%	35%	15%	15%
Quasi-isotropic	25%	25%	25%	25%

4.7.5 Costs

Costs are mostly an important factor in design. Therefore the costs of the different reinforcements and resins are mentioned in this section. An overview of the costs per kg material of the different reinforcements is shown in Table 4.5. An overview of the cost of the resin per kg material is shown in Table 4.6.

Since the costs of both reinforcements and resins vary highly per type, the costs will be an important factor in selecting an appropriate type. Of course, the stiffness of each reinforcement will vary also, therefore it's advised to make a selection based on the price per stiffness.

Table 4.5 Overview of the costs of different reinforcements [18]

Reinforcement	Bulk price Euro/kg
E-glass	1,25-2,5
S-glass	15-20
Aramid	18-30
Carbon	10-45

Table 4.6 Overview of the costs of different resins [18]

Resin	Bulk price Euro/kg
Polyester	1,30-2,55
Vinylester	2,55-5.10
Epoxy	3,80-19,50

An overview of the construction costs per fibre/resin combination including labour costs, according to [18], is shown in Table 4.7. The labour costs were estimated to be equal for each composition and were therefore adapted for the different fibre densities.

Table 4.7 Overview of the construction costs of different fibres and resins [18]

Fibre/resin	Material costs range (€/kg)	Mean base material cost (€/kg)	Labour costs(€/kg)	Total costs (€/kg)
E-glass/polyester	1,3 - 2,5	1,9	2 - 5	4 - 7
E-glass/vinylester	1,7 - 3,4	2,6	2 - 5	5 - 8
E-glass/epoxie	2,1 - 8,5	5,3	2 - 5	7 - 10
S-glass/polyester	10,2 - 13,9	12	2 - 5	14 - 17
S-glass/vinylester	10,6 - 14,8	12,7	2 - 5	15 - 18
S-glass/epoxie	11,1 - 19,8	15,5	2 - 5	17 - 20
Aramid/polyester	12,2 - 20,4	16,3	2,8 - 7	19 - 23
Aramid/vinylester	12,6 - 21,3	16,9	2,8 - 7	20 - 24
Aramid/epoxie	13,0 - 26,3	19,7	2,8 - 7	22 - 27
Carbon/polyester	7,0 - 30,1	18,5	2,5 - 6	21 - 25
Carbon/vinylester	7,4 - 31,0	19,2	2,5 - 6	22 - 25
Carbon/epoxie	7,8 - 36,1	22	2,5 - 6	24 - 28

4.8 Design codes

A regular design code for FRP structures, with a legal status, is not available yet, because the material is still in development. Design recommendations for FRP structures are mentioned in the CUR 96 [19]. This current document described the design recommendations for glass fibre reinforce polymers, but is currently being updated to the use of other reinforcements. Other design recommendations are the 'Eurocomp design code and handbook' and the 'Fiberline design manual'.

4.9 Reference projects

Some projects made of FRP in the hydraulic engineering industry are mentioned in the next subsections because of their similarities with the slides in the Eastern Scheldt barrier or their ability to apply FRP in a wet environment.

4.9.1 Kreekrak sluices

The Kreekraksluices in the Scheldt-Rhine canal had a fresh-salt water separation system until 1997. This system consists of 256 steel slides, which corrode rapidly. One of these slides is replaced in 1993 with a slide of fibre reinforced polymers, see Figure 4.19. The slide is manufactured with glass fibre reinforce vinylester using resin injection. The slide functioned well until demolition of the fresh-salt water separation system in 1997. Only the sliding bearings were replaced after a half year.



Figure 4.19 FRP slide which was applied in the fresh-salt water separation system of the Kreekrak sluices [20]

4.9.2 Spiering sluice

Two timber lock gates of the Spiering sluice near Werkendam were replaced by FRP lock gates in 1999. The gates are designed with trapezoidal plates and U-profiles at both sides. The pivots were fixed with stainless steel fittings.



Figure 4.20 Lock gates of the Spiering sluice[S.J. de Waard, Wikimedia Commons]

The gates were made of isophthalics polyester, which has a good resistance in a wet environment. The laminates were manufactured using the hand laminating process, with a fibre volume fraction of 32%. The costs of the FRP gates were 30% higher than a timber alternative, which was partly caused by the costs of the mold.

4.9.3 Minehunter 'Alkmaarklasse'

A good example of a FRP product which has a very good resistant to moister is the minehunters 'Alkmaarklasse'. These minehunters require less maintenance compared to a steel ship and are made of polyester. Since these ships are already for over 20 years in service, they are a good proof of the moister resistance of FRP.



Figure 4.21 Minehunter 'Alkmaarklasse' with a FRP hull [21]

4.9.4 FRP concept for lifting slide

In [18] a concept for a FRP lifting slide in the Hartel barrier has been developed, see Figure 4.22. The slide consists of two curved vertical walls which are connected by horizontal webs. There are gaps made in the web because the slide shouldn't float.

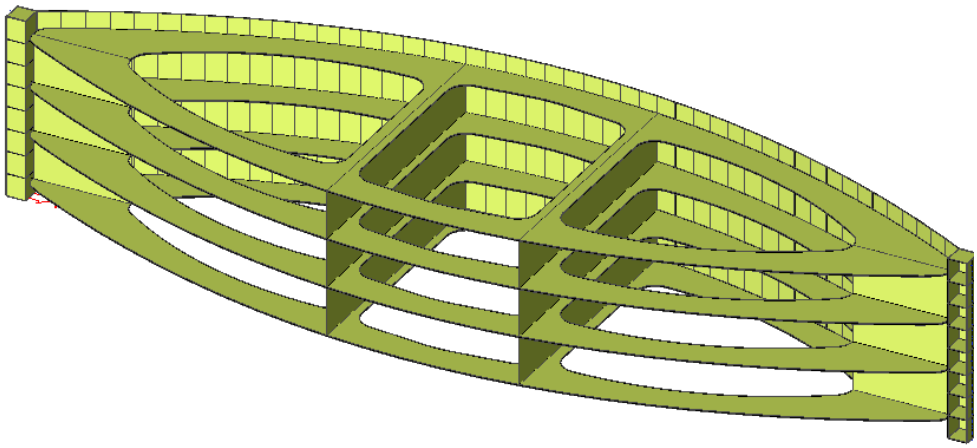


Figure 4.22 Overview FRP concept lifting slide (with one arch not displayed) [18]

4.10 Summarized

In this chapter a short introduction on the material FRP is given. The different materials of which this composite consist of are given in the first sections, where after the different manufacturing processes are described. In a later stage a choice should be made on the reinforcement, resin and manufacturing process which are suitable for a FRP slide, which will be based on the information given in this chapter.

The characteristics of FRP were also described in this chapter. These characteristics show the differences of FRP with other well-known materials as steel, concrete and wood. Since a final FRP

laminate is a mixture of different possible reinforcements, resins, core material, gel-coats, lamina orientations, lamina thickness, lamina stacking and manufacturing process the final properties can be influenced highly. All these design issues could be difficult to oversee, but the opportunities are endless. It is important to take the mentioned comments on the laminate lay-up into account. The most important one is to design a symmetric laminate, which ensures decoupling of elongation and torsion. The material properties of FRP can be determined with the CUR recommendation 96.

The costs of the different reinforcement and resin types are an important factor for selecting an appropriate fibre and resin, since the costs vary highly per type. Finally, the reference projects show the possibilities to use FRP in a wet environment.

Part 2:
Main report

5 The design of the current slides

In this chapter the first sub-research question is answered into more detail: 'How is the current barrier designed?'. The general description of the current design of the barrier was already given in chapter 2. This chapter describes especially the design of the current slides.

The design of the movable slides was mainly depending on a hydraulic research to the behavior of the structure. Only the results of this research are mentioned in this chapter to get insight in the design considerations of the slides. First of all the details of the closure structure are mentioned and thereafter the design of the moveable slides is considered. Finally, the loads which act on the slides are mentioned.

5.1 The closure structure

The slides in de storm surge barrier vary in height between 5.9 and 11.9 m, with step sizes of 1 m. At that way the slides are following the soil profile of the Eastern Scheldt, see Figure 5.1. During normal circumstances, with slides in open position, the top of the slides are showing the reverse soil profile. The step size is chosen to ensure a limited number of standard slide structures. The smaller slides are constructed with two truss beams, the bigger ones with three truss beams.

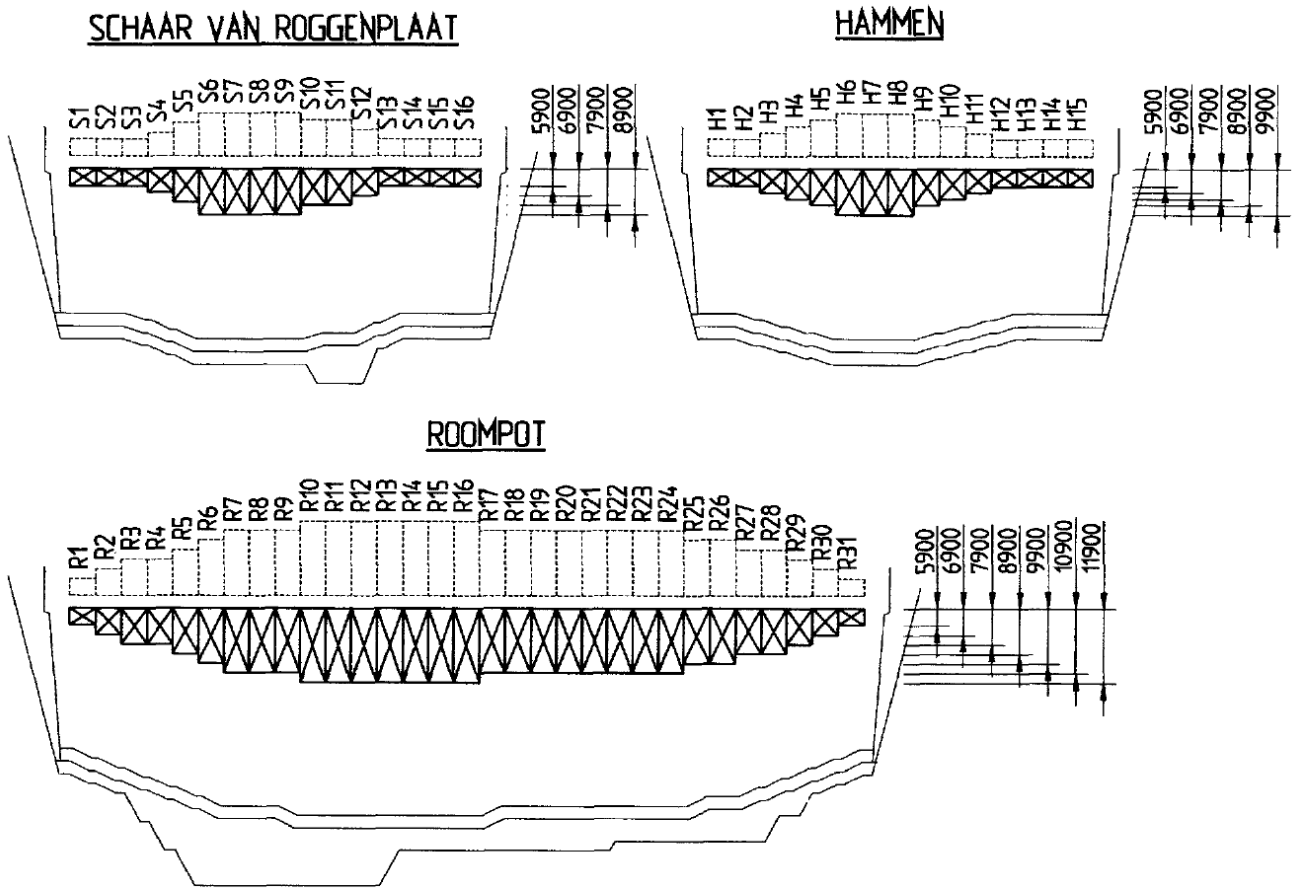


Figure 5.1 Overview of the slides in the openings Hammen, Schaar van Roggenplaat and Roompot [22]

The piers are placed on a center to center distance of 45 m, therefore the theoretical span of the slides is 41.3 m, see Figure 5.2. The slides, in closed position, are placed in front of the sill beam and the upper beam with an overlap of 0.20 m. This overlap is chosen to prevent vibrations due to the water flow and to ensure maximum possible water repellency between the slide and the upper

beam. The space between the slide and the beams is 0.15 m, see Figure 5.3. Therefore the slide is not completely water repelled, but that is accepted through the availability of extra water storage capacity in the Eastern Scheldt during a storm. The bottom of the upper beam lies at 1.0 m above NAP. The top of the sill beam lies at a variable distance below NAP, depending on the height of the slides. The total surface of the flow openings is approximately 20,000 m^2, including the surface above NAP. The surface below NAP is approximately 18,000 m^2.

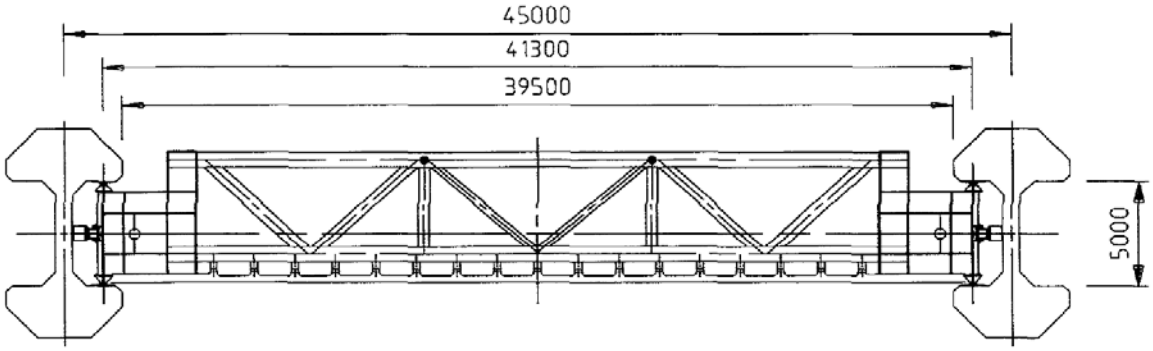


Figure 5.2 Span of the slides [22]

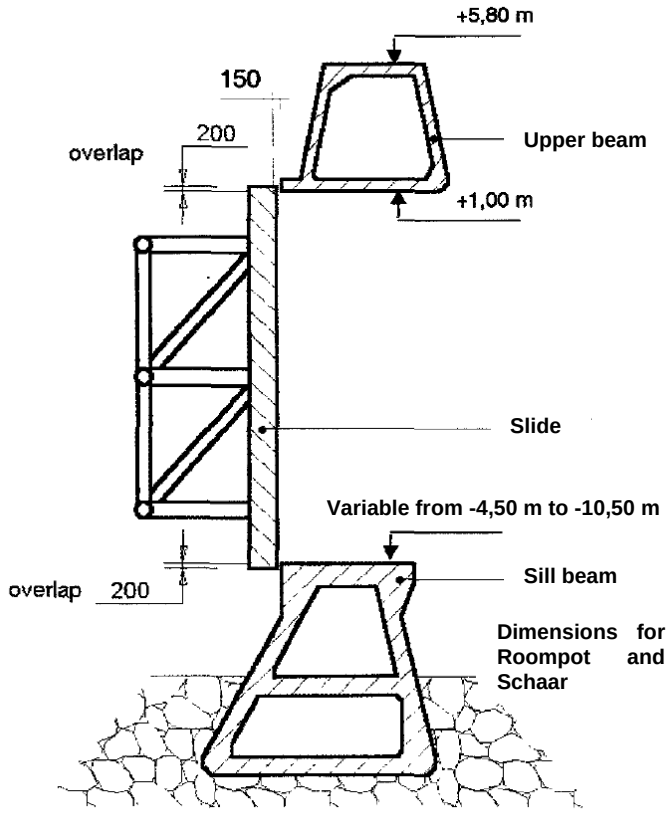


Figure 5.3 Cross section of the slide with upper beam and sill beam [22]

5.2 Boundary conditions

- The lifetime requirement has no consequences for the moveable slides, they are considered to be replaceable. The slides are dimensioned on a fatigue lifetime of at least 50 years.
- The slide should have a low torsional stiffness to carry rotational differences between two piers without high stresses. These rotational differences can occur due to settlements of the piers or due to washing away of sand under the piers.

- The flood defense cladding should be placed at the Eastern Scheldt side of the slides in one plane with the upper beams and the sill beams to ensure a relative waterproof structure. Other alternatives are not feasible due to hydraulic reasons or due to the design planning.
- The lift slides are designed with sliding bearings to ensure lower loads at the bearings.
  The exact slide length is determined after the construction of the piers, because this length can vary due to position inaccuracies. Since the slide manufacture process already started before the piers were placed, the slides were manufactured in 3 components, which could be combined in a later stage. The estimated length of the slides is 41.3 m $\pm$ 0.5 m.
- The slides should be moveable in a temperature range of -10°C to +30°C.

5.3 Design considerations

- During designing the slides a concrete slide has been considered, but the shape of the concrete slide could cause vibrations of the whole slide. Simple changes in de shape of this slide could probably prevent this, but are not considered anymore. There are no figures available of this design.
- There were two alternatives for the lifting slide, a plate girder solution (Figure 5.4) and a truss solution (Figure 5.7). Both solutions had a flood defense cladding. The plate girder solution had plate girders to carry horizontal loads and a truss system in vertical direction. The truss solution had trusses in horizontal and vertical direction. The plate girder solution experienced high loads from the waves, therefore the truss solution is chosen.

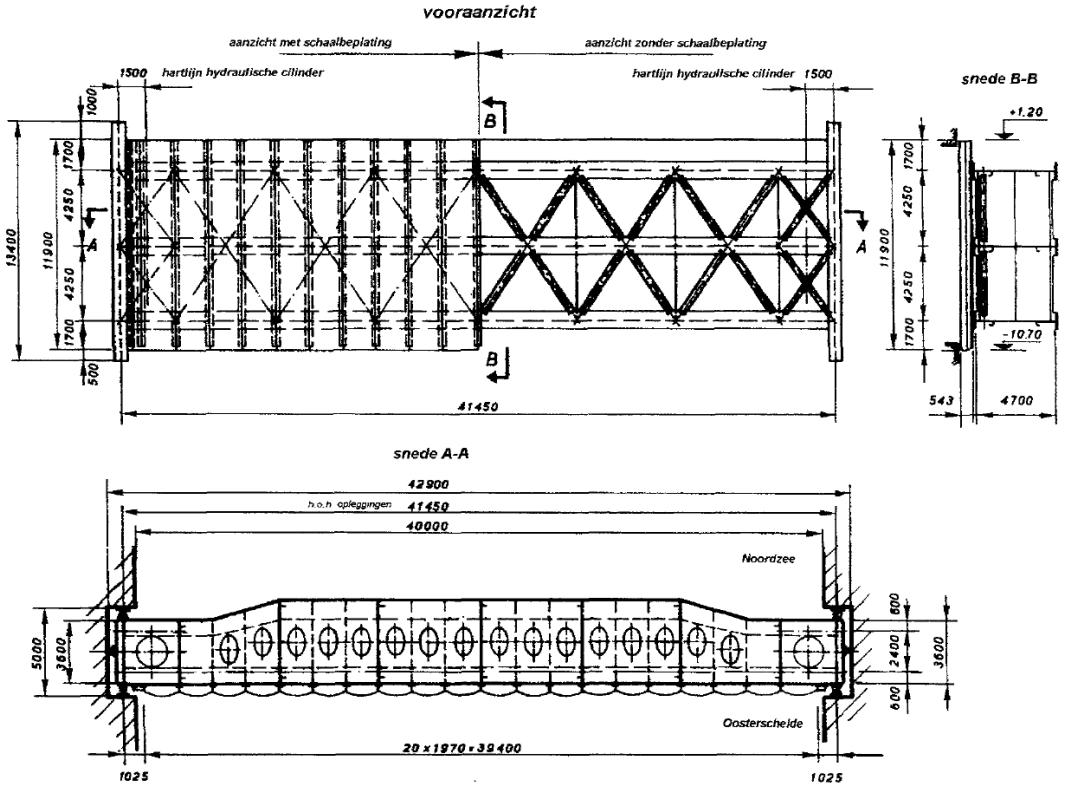


Figure 5.4 Design of the plate girder slide [22]

- For the flood defense cladding a flat cladding could be used or little shells could be used. The little shells were in favor because they can be used without stiffeners. The shells are positioned in such a way, that most of the time tensile stresses occur in the cladding, see Figure 5.5.

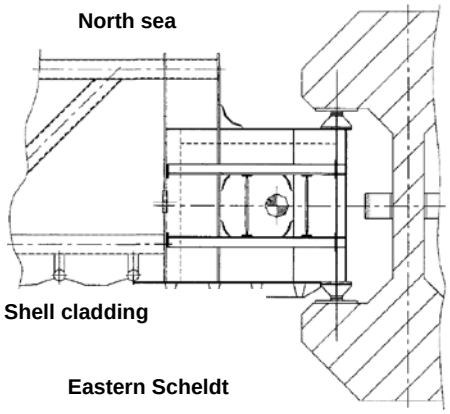


Figure 5.5 Position of the shells used for the flood defense cladding

- The upper beam was extended with a 'little nose' to improve the flow pattern of the water and reducing vibrations of the slide. The flow pattern is illustrated in Figure 5.6.

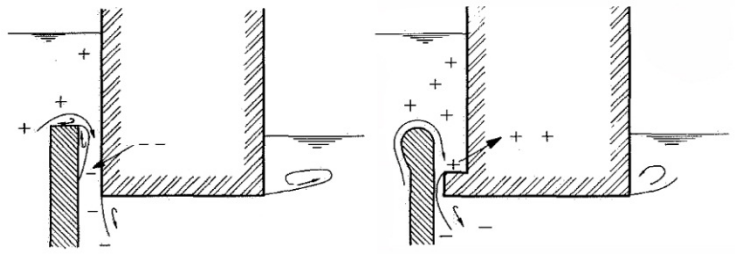


Figure 5.6 Flow pattern, depending on the geometry of the upper beam [23]

5.4 The design

The final design of the slides is in accordance with the dimensions mentioned in section 5.1. Basically, the slides consist of a defense cladding, a truss structure and an 'end structure'. The length of the slide can be varied due to the connection between the truss structure and the 'end structure'.

The horizontal loads due to water pressure and waves are carried by the defense cladding. The shells are in case of storm loaded in tension, only after a storm, in a situation of failing slides, compression can occur in the cladding. The cladding transfers the loads via vertical stiffeners to the truss structure.

The truss structure consists of horizontal, vertical and diagonal truss members. Basically there are 2 or 3 horizontal truss girders to carry the horizontal loads, these are connected with vertical and diagonal members with each other. At the North Sea side the horizontal truss girders are only connected with vertical members, not with diagonal members, to ensure a low torsional stiffness of the truss structure. The truss connections are sensitive for fatigue. Fatigue can cause failure of a structure at a stress level below the material strength, due to varying loads. These loads cause tears, which can grow until the structure finally fails. A tear which is visible after a storm can still carry the loads of 10 storms before failing occurs. Therefore it's aloud that tears occur in the most heavily loaded parts, if inspections are carried out for these parts after each storm. The tear can be repaired easily in the beginning of the growth process.

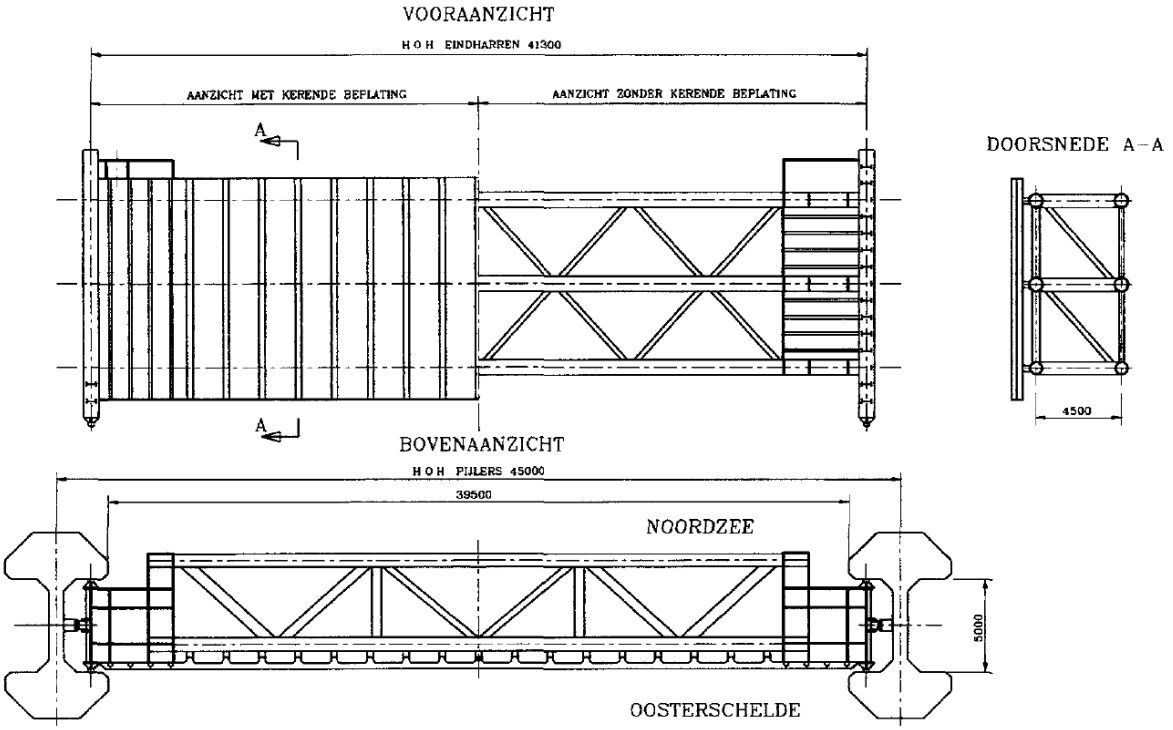


Figure 5.7 Final design of the slide in the storm surge barrier [22]

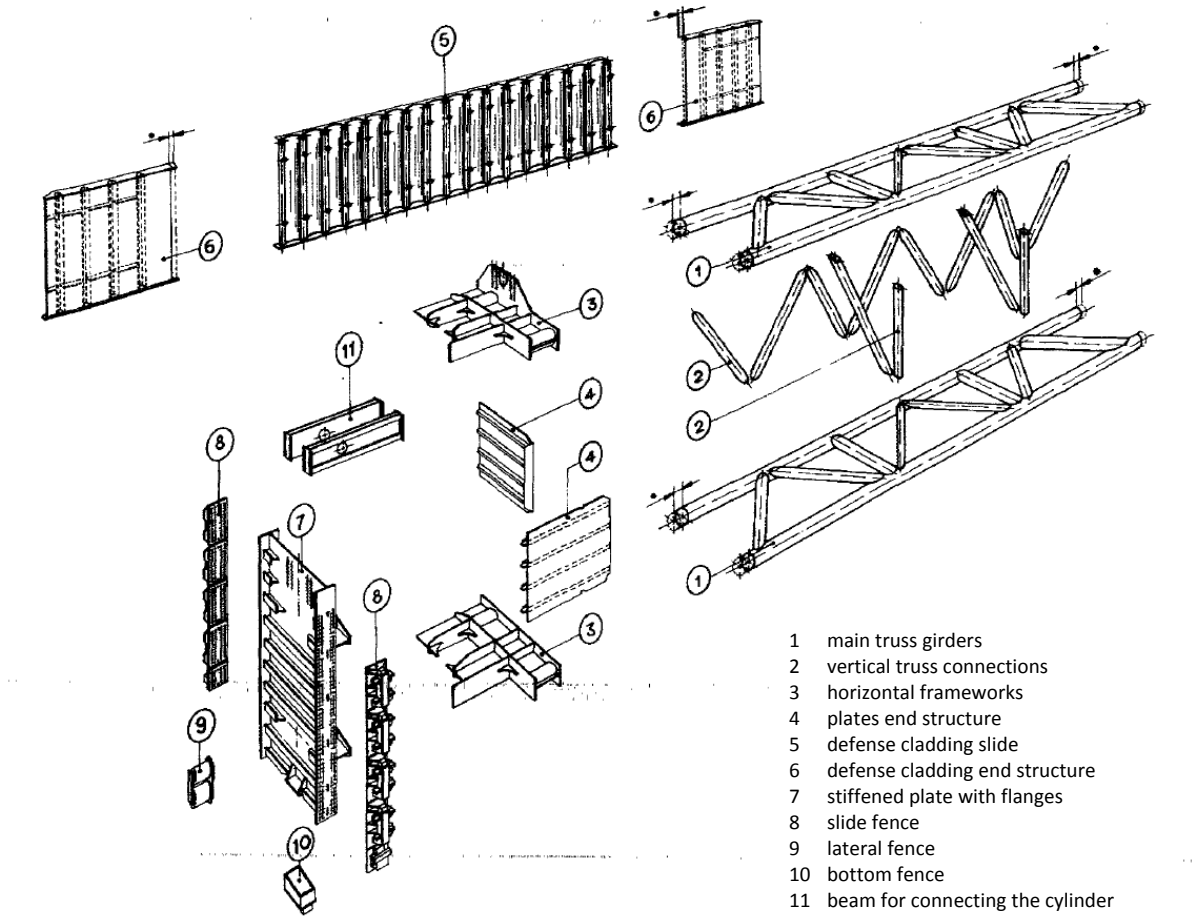


Figure 5.8 Components of the slide [22]

The truss structure transfers the loads to the ‘end structure’. The ‘end structure’ consists of a horizontal stiff frameworks and a stiffened end plate with flanges. The horizontal framework transfers the loads from the horizontal truss girders to the end plate. This end plate finally transfers the loads via the sliding bearings to the piers. An overview of all the components is given in Figure 5.8.

Surrounding the end structure plates are placed to carry the vertical loads. These loads are transferred to the cylinders, in case of an open barrier. If the barrier is closed the cylinders will press the slide onto the bearing block and the vertical loads will be carried by a variation in prestressing force. At the Eastern Scheldt side of the ‘end structure’ a water defense cladding is placed. The stiffened end plate with flanges extends the water defense cladding and will contribute to the water repellency of the slide. The rotational stiffness of the end plate is such big, that a rotation of the pier will be transferred to the slide.

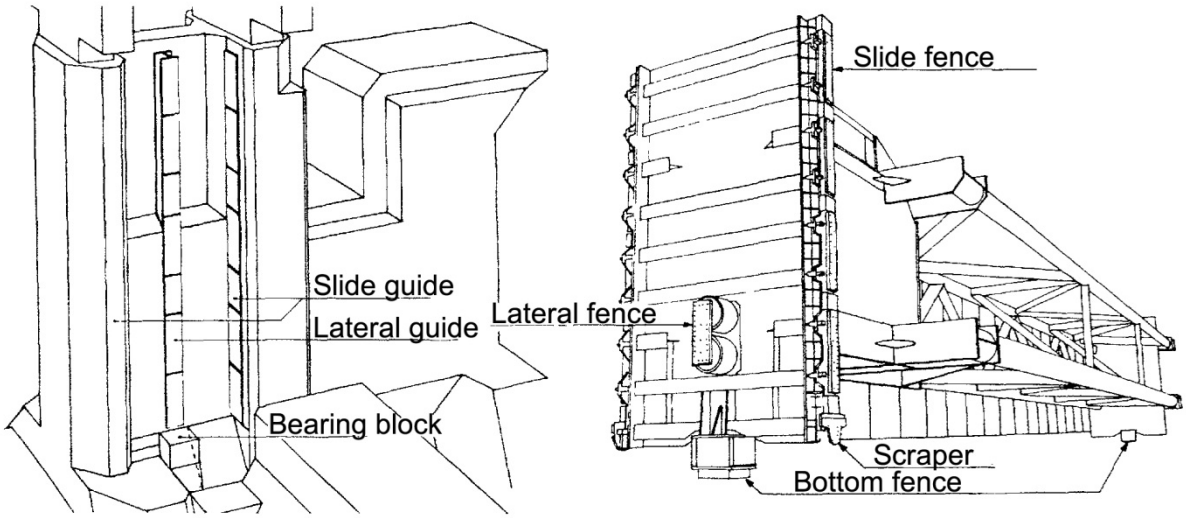


Figure 5.9 Overview of the bearings and guides of the slide [22]

The ‘end structure’ is constrained in the rabbet as shown in Figure 5.9. At the total height of the rabbet a side and lateral guide is present to absorb the forces from the fences. Near the sill beam a bearing block is present. The dimensions of the rabbet are mentioned in Figure 5.10. The slide guides have, according to [23], a thickness of 60 mm. A gap of 50 mm is present between the lateral guide and the fence, to ensure some freedom in longitudinal direction.

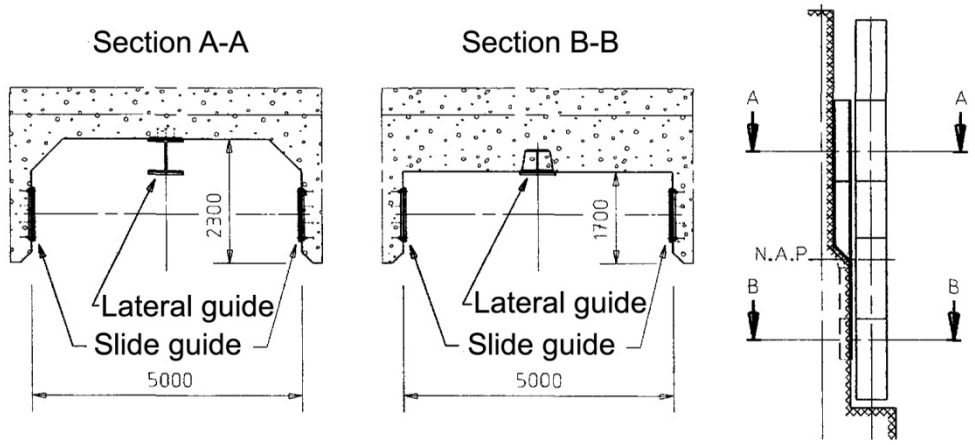


Figure 5.10 Dimensions of the rabbet [22]

5.5 Loads on the slides

In this section the loads on the slides are considered in the different subsections. These loads are determined for the current design of the barrier. It's important to note that loads which are decisive for the current design do not have to be decisive for a new design and vice versa. First of all an introduction is given to get insight in the determination of the loads.

The loads on the slides can be determined in 3 situations: in open position, during closure or opening and in closed position. The loads in closed position were decisive for the slides, the loads during closure or opening were decisive for the movement works.

The loads on the slides, in closed position, are depending on the closure strategy of the barrier. At the decision point, the point at which the decision is taken to close the barrier, the predicted water level should be above a certain limit level. It is assumed that the control members have the full freedom to close the barrier at a certain time before the limit level is expected, to control for example the water level at the Eastern Scheldt. When the barrier is not closed manually, at a certain measured alarm level, the barrier will close automatically.

For the different closure strategies and closure times, different combinations of water levels can occur. The level at the Eastern Scheldt is mainly depending on the closure time/strategy and the water level at the North Sea is mainly depending on the extreme water level during a storm. From these combinations the decisive water levels with a probability of occurrence of 1 in 4000 years can be determined. These loads are considered in the next subsections.

5.5.1 Horizontal wave and water loads (closed position)

The barrier is designed for two decisive water levels, for a closed barrier. In the first case the water level at the North Sea side is higher than at the Eastern Scheldt side of the barrier, this case is called 'positive drop'. The reverse case is called 'negative drop', the decisive water levels for both cases are showed in Table 5.1. The case 'positive drop' was decisive for the truss structure and the case 'negative drop' was decisive for the defense cladding.

Table 5.1 Decisive cases for closed slides

	Closed positive drop	Closed negative drop
Water level North Sea side	NAP + 5.5 m	NAP - 1.0 m
Water level Eastern Scheldt side	NAP - 0.7 m	NAP + 2.4 m
Significant wave height	4.5 m	0.38 m
Wave period	9.5 s	5.0 s

The horizontal loads for these cases consist of a static part, due to the water pressure, and a quasi-static part due to the waves. The resultant load due to the water pressure is in the first part linear ascending with the water depth and thereafter constant. The quasi-static loads due to the waves are maximum by a wave crest or a wave trough.

In the case of 'positive drop' the water pressure and the wave crest loads are in the same direction. According to [1] the total load due to the water pressure and the wave crest can be modeled as a constant load over the height of the slide of 99 kN/m^2. The load due to the water pressure and a wave trough will not be decisive, for the 'positive drop' case.

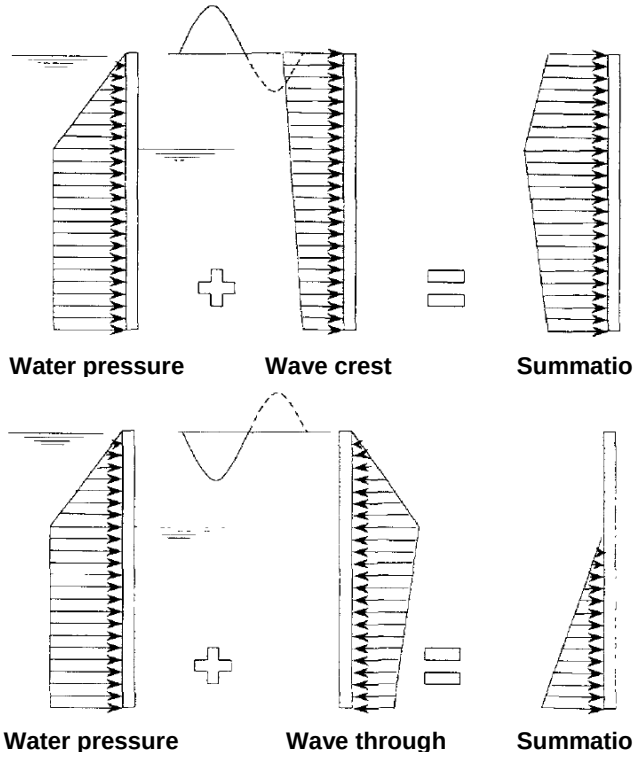


Figure 5.11 Resultants loads due to water pressure and wave crust or wave trough [22]

In the case of 'negative drop' the water pressure will be in the reverse direction, therefore the resultant load due to water pressure and a wave trough will be decisive (in same direction). According to [1] this load can be modeled as a constant load over the height of the slide of 35 kN/m^2.

The horizontal wave impacts loads are much lower than the loads for the cases considered, and will therefore be neglected. The lowest eigen frequency of the slides is 3 times higher than the highest frequency of the waves, therefore the wave loads were modeled as quasi static loads. The loads according to [1], based on a theoretical derivation, are mentioned instead of the loads according to [22], based on hydraulic research, because the results of the hydraulic research were only mentioned in total loads on the slide. These loads are of comparable size.

5.5.2 Vertical wave loads (during closure)

The vertical wave loads are at its maximum around the water level ($\pm$ 0.5 m). Therefore, the loads are maximum during closing the slides. The vertical wave loads are mainly depending on the design of the slides. As already mentioned, the plate girder design experienced 10 times higher vertical wave loads than the truss girder solution. The maximum water pressure for the final design, caused by wave impact in vertical direction, on the bottom flange of the slide is 440 kN/m^2 and on the truss beams 240 kN/m^2.

5.5.3 Dead load

The self weight of the steel slides varies between 2710 and 4790 kN, depended on the slide height. The upward water pressure, in closed situation, reduces the self weight with 40%. This is mainly caused by the hollow truss beams.

5.5.4 Torsion

Settlements of the piers or washing away of sand under the piers can cause rotational differences of the piers. The slides should follow this rotation and can be loaded with torsion. The maximum torsion loading considered in the design is a forced rotation of 0.1 rad.

5.5.5 Longitudinal loads

The direction of the waves does not need to be perpendicular to the barrier, but it can be under a certain angle. In that case the slide is loaded in longitudinal direction and due to some space between the bearings and the slide (in longitudinal direction) the slide can probably move. The impacts loads for this situation were not decisive for the slide.

5.5.6 Ice loads

Ice loads were not considered to be decisive for the design of the slides. Because of the fact that the slides are not permanently closed and therefore not always in contact with water, the ice loads are much lower than for example the Haringvlietdam, were the slides are always in contact with water. Also in open position the slides are protected against ice loading. The bottom of the slides is higher than the bottom of the upper beam, so the last one protects the slides against ice loads. In a closed position the conditions for ice loadings differ from the conditions for a storm surge, therefore they do not have to be considered simultaneously.

5.5.7 Wind loads

The wind pressure loads are negligible in comparison to the horizontal loads from the water pressure and the waves, according to [1]. Therefore the wind loads were not considered during design in [22].

5.5.8 Water flows and leakage gaps vibrations

Hydraulic research was done to the water flows around the slide and to prevent leakage gaps vibrations of the slide. The vertical loads considered in the design at the bottom of the slides due to water flow are 10 kN/m. The design of the slide is adjusted, such that vibrations due to water flows during closure or leakage gaps were not decisive.

5.5.9 Collision

The risk of collision of the upper beam was assumed to be such low that is hasn't been considered in design. The bottom of the slide is placed higher than the bottom of the upper beam, so the upper beam is more sensitive to collision. A collision which occurs when the barrier is closed will have a lower probability of occurrence. The current design of the slide (and also the upper beam) is not designed for a collision impact load.

Although the current barrier was not designed for a collision, a collision takes place in April 2005. A fishing cutter collided against a slide and the upper beam. The fish cutter went along with the flow below the upper beam to the Eastern Scheldt side of the barrier and was damaged a lot. There were no fatalities.

5.5.10 Terrorist attack

A terrorists attack is not considered for the current design of the barrier. The damage of a terrorist attack could be very high when an attack takes place at the moment of very high sea level, but nobody knows when such sea levels occur. Therefore there is no possibility to cause a lot a fatalities in a quick way, which will reduce the risk of a terrorist attack.

6 Design requirements and assumptions

In this chapter a start is made with answering the fourth sub-research question: 'What is technically the most promising design for the slide made of FRP?'. This sub-research question will be investigated in chapters 6, 7, 8, 9 and 10. In this chapter the requirements and the assumptions which have been made for the design of a new FRP slide are described. The requirements are based on the information provided in chapter 5. The requirements are divided into the categories: general, geometrical and loads and are listed in the next sections.

6.1 General requirements

- Lift slides with sliding bearings should be designed to ensure interchangeability of the current slides. The geometrical boundary conditions are specified in section 6.2, Figure 6.1 and Figure 6.2.
- The current slides should be moveable in the temperature range of -10°C to +30°C. According to EN 1991-1-5 the structure is subjected to a larger temperature range in comparison to the current slides. The temperature range according to EN 1991-1-5 has a minimum temperature of -25°C. The maximum temperature depends on the absorption of the structure and is minimal +30°C. Depending on the absorption a value of 20°C, 30°C or 45°C should be added to that minimal value.
- The slides should withstand the loads specified in section 6.3, which have a probability of occurrence of 1 in 4000 years and is based on freedom of closure strategy of the slides.
- The slide, subjected to a load, should not hit the upper beam or sill beam.
- The slides in open position should not reduce the water opening between the piers.
- The new slides must be able to be maintained and inspected in the same way as the current slides.

6.2 Geometrical boundary conditions

- The span length of the slides is 41.3 m.
- The maximum width of the slides near the rabbet is 42680 mm (assuming the same gap as present in the current slides of 50 mm in longitudinal direction at both sides).
- The maximum with of the slides near the piers (outside the rabbet) is 38500 mm (assuming a distance of 500 mm at both sides to the pier)
- The maximum thickness of the slide near the rabbet is 4880 mm. The thickness of the sliding bearings should still be taken into account.
- The thickness of the slide in the middle area (with a width of 38500 mm) can be extended unlimitedly in the direction of the North Sea. It is assumed that the upper beam and sill beam are positioned directly beside the rabbet (at the Eastern Scheldt side), therefore the slide cannot be extended in the direction of the Eastern Scheldt.
- The overlap of the slides with respect to the upper beam and sill beam is 0.20 m. It is assumed that no vibrations due to leakage flows occur with this overlap. Therefore the heights of the slides vary between 5.9 m and 11.9 m.
- The maximum leakage surface is 1250 m^2 according to [12]. Therefore, the leakage gap at the bottom and top of the slides could have a maximum width of $\frac{1250}{(62 \cdot 42.68 \cdot 2)} = 0.236\ m$, when leakage along the sides is neglected. A maximum leakage gap of 200 mm is assumed.

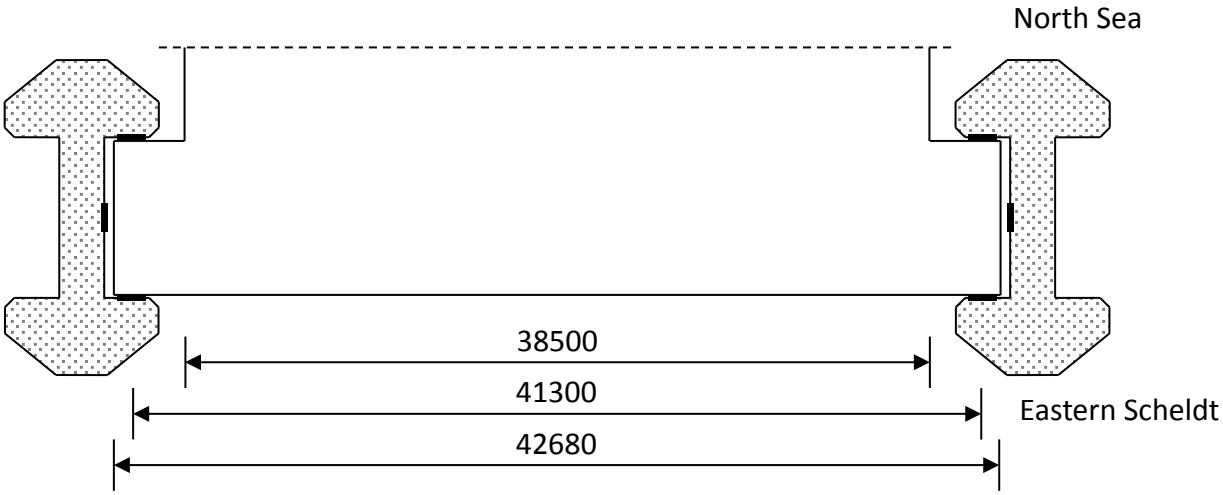


Figure 6.1 Geometrical requirements for a new slide (not to scale)

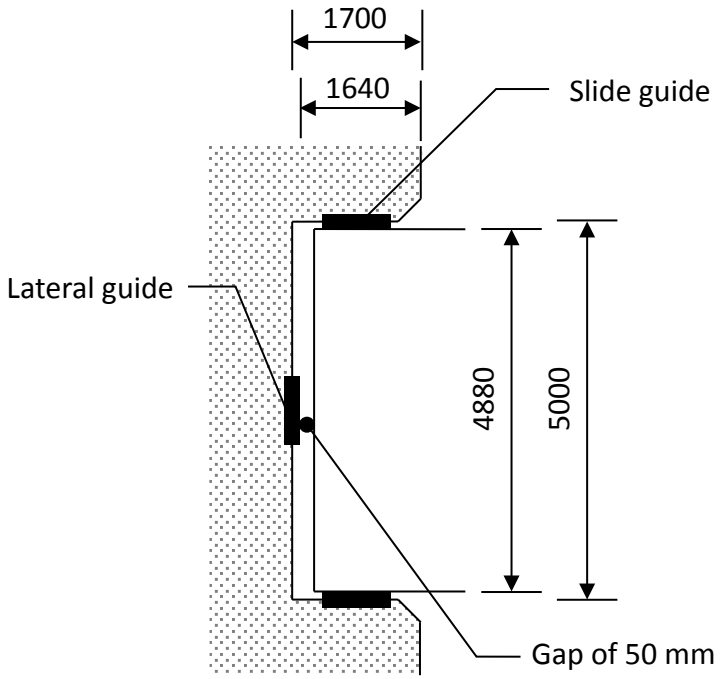


Figure 6.2 Detail of the dimensions near the rabbets

6.3 Loads on the slides

- During positive drop the slide is loaded by the water pressure (water level NSS: NAP + 5.5 m, water level ESS: NAP – 0.7 m) and the wave loads (significant wave height: 5.75 m, wave period: 9.5 s). This could be modeled as a distributed load of 100 kN/m^2 in the direction of the Eastern Scheldt. This load consists of a static part of 63 kN/m^2 and a quasi-static part of 36 kN/m^2. This load is further specified for the final design in appendix E.
- During negative drop the slide is loaded by the water pressure (water level NSS: NAP - 1.0 m, water level ESS: NAP + 2.4 m) and the wave loads (significant wave height: 0.38 m, wave period: 5 s). This load could be modeled as a distributed load of 35 kN/m^2 in the direction of the North Sea. This load is further specified for the final design in appendix E.

- Wind loads are of a smaller order than the loads during positive drop and are therefore not considered. The wind pressure load is 0.72 kN/m^2 according to [1], which is much smaller than the water pressure load of 100 kN/m^2.
- A torsion load isn't taken into account, since the settlements of the piers were small after the initial settlements of the structure. It isn't expected that very big settlements will occur in the future.
- Ice loadings, acting on 35m of the slide, have a magnitude of 8000 kN. This load has a probability of occurrence of $1x10^{-4}$ per year.
- Vertical wave impact loads on horizontal elements near the water level can reach pressures up to 240 kN/m^2 for truss beams and 440 kN/m^2 for horizontal plates.
- A collision load should be taken into account, although it wasn't a design load for the current upper beam and slide. In April 2005 a fishing cutter collided against the slide and the upper beam, therefore a collision is taken into account. This load is further specified for the final design in appendix E.

6.4 Assumptions

- No hydraulic research will be carried out on the new slide design.
- Only a design in fibre reinforced polymers will be considered in this graduation work.
- The slides should function with the current movement works. Therefore the maximum weight of the largest slide is limited to 700 ton [1], which can maximum be lifted with the current movement works.
- The design of the highest slide is considered to be decisive. This slide has a height of 11.9 m. But the design height of the slide should be quite easily adjustable to ensure a functional design for the smaller slides. A repeated construction part in vertical direction could form a solution for that.
- Due to sea level rise the slides height could be increased with 0.6 m, also the upper beam could be lifted with 0.6 m in that case. The design of the slide should be such that the height is increasable. This measure is based on an existing freedom of the slides, which can be lifted another 120 cm from their open position. Therefore this is the maximum measure without adjusting the current movement works, which is discussed with K. Saman from RWS.
- In this initial design stage only the water pressure difference load including the static wave pressure are considered. The total load assumed is an equally distributed load of 100 kN/m^2.
- The upper beam and sill beam are positioned directly beside the rabbet (at the Eastern Scheldt side).

7 Material selection

This chapter is part of the answer of the fourth sub-research question: 'What is technically the most promising design for the slide made of FRP?'. In this chapter, a selection will be made on the materials which could be used in the initial design stage. This selection is based on the information given in chapter 4 of the literature study. First of all, the suitable manufacturing processes will be selected, where after a choice for the reinforcement and resin will be made. Finally, the lamina properties for this choice will be calculated and the material safety factors and design values will be determined.

7.1 Manufacturing method

Manufacturing processes which are suitable for manufacturing of composite slides in the Eastern Scheldt barrier are selected. The manufacturing methods which are suitable should achieve high fibre contents, which improve the strength and stiffness of the material. Manufacturing processes which are only suitable with random reinforcements are excluded. Next to that, the manufacturing size range should be suitable for making large segments (width of a slide is 41.3 m). The selection of manufacturing processes for composite slides is shown in Table 7.1, which is based on Table 4.2 of the literature study. The suitable manufacturing processes satisfy the requirements mentioned above, for the manufacturing processes which are not considered to be suitable the reason is mentioned.

Table 7.1 Selection of manufacturing processes for composite slides

Manufacturing process	Suitable	Reason
Open mold processes		
hand laminating	Yes	
saturation	Yes	
spray-up	No	Only random reinforcement
auto spray-up	No	Only random reinforcement
filament winding	Yes	
spray winding	No	Not cost-effective for highly loaded structures
centrifugal casting	No	random reinforcement + mats of cloths and resin inner surface not especially needed
Closed mold processes		
vacuum bag	Yes	
pressure bag	Yes	
autoclave	No	Limited size
cold press	No	Limited press size
hot press	No	Limited press size
resin injection	No	Limited size
vacuum-assisted resin injection	Yes	
injection molding	No	Limited size
Continuous processes		
continuous laminating	No	low fibre volume fraction
pulltrusion	No	Only suitable for profiles
continuous filament winding	Yes	continuous form not especially needed for the slides

The selected manufacturing methods which are suitable for the composite slides are shown in Table 7.2. The reinforcement types which can be used for each method are mentioned to get insight in the types of reinforcements which can be used. Also the possibility to use polyester, vinyl ester and epoxy as resin is mentioned per method.

The saturation process is only suitable to use resins with a low viscosity, which will have probably negative effects on the mechanical properties and the moister resistance. This process is therefore unlikely to be chosen in a later stage. The continuous filament process cannot make use of a core material. Since the continuous form is also not especially needed, this method is probably not used. In a later stage a choice on the manufacturing process is made, which is also dependent on the structural concept of the slide. The determination of the safety factors in section 7.6 will be based on this provisional choice, taking above comments into account.

Table 7.2 Manufacturing methods which are suitable for the composite slides

Manufacturing process	Polyester	Vinyl ester	Epoxy	Reinforcement
Open mold processes				
hand laminating	X	X	X	most types
saturation	only low viscosity resins			most types
filament winding	X	X	X	only continuous rovings
Closed mold processes				
vacuum bag	as far as know: all			most types
pressure bag	as far as know: all			most types
vacuum-assisted resin injection	as far as know: all			all types
Continuous processes				
continuous filament winding	as far as know: all			only continuous rovings

7.2 Reinforcement

Initially it is assumed to use glass fibres, since these fibres are minimal a factor 4-8 cheaper than aramid or carbon fibres, see Table 4.5 of the literature study. The stiffness of glass fibres is a factor 2-3 lower (see Figure 4.3 of the literature study), but overall it's still cheaper to use glass fibres. If a design with glass fibres is not successful, an alternative with aramid or carbon fibres will be checked.

7.3 Resin

Resins which are resistant to moisture and are therefore suitable for the slides are polyesters resins of the type ISO or ISO-NPG and vinyl ester resins. These resins are earlier used in structures in a wet environment. Epoxy resins should have also a good resistance to moisture, but examples of their application in a wet environment couldn't be found. This is probably caused by their high price, which make them less attractive. Initially it is assumed to use a polyester resin, because of their low price (see Table 4.6 of the literature study).

7.4 Core

Foam is chosen as core material, since it is a widely used and isotropic core material. The properties which will be used are taken over from [18] and are mentioned in Table 7.3.

Table 7.3 Properties PMI foam core 71s [18]

Density (kg/m3)	σ_c (N/mm^2)	E_c (N/mm^2)	Compr. (%)	σ_t (N/mm^2)	E_t **(N/mm^2)**	**Elong. (%)**	τ **(N/mm^2)**	**G (N/mm^2)**
75	1.53	73	8	1.97	157	4.1	2.28	58

7.5 Lamella properties

Since the initial choices regarding the reinforcement and resin are made, the lamella properties can be determined. The average stiffness properties of a uni-directional (UD) lamella composed of glass fibres and polyester is determined according to CUR96 [19]. The semi-emperic equations of Halpin and Tsai can be used, which are valid for a fibre volume content from 40% to 70%. The nominal properties of E-glass and polyester are:

$$E_F = 72\ GPa \quad G_F = 30\ GPa \quad \nu_F = 0{,}22\ GPa$$
$$E_R = 3{,}4\ GPa \quad G_R = 1{,}3\ GPa \quad \nu_R = 0{,}35\ GPa$$

The semi-empiric equations of Halpsin and Tsai for the stiffness properties are:

$$E_1 = E_R + (E_F - E_R) \cdot V_f \tag{7.1}$$

$$E_2 = E_R \frac{1 + \xi \cdot \eta \cdot V_f}{1 - \eta \cdot V_f} \qquad \text{width: } \eta = \frac{E_F/E_R - 1}{E_F/E_R + \xi} \text{ and } \xi = 2 \tag{7.2}$$

$$G_{12} = G_R \frac{1 + \xi \cdot \eta \cdot V_f}{1 - \eta \cdot V_f} \qquad \text{width: } \eta = \frac{G_F/G_R - 1}{G_F/G_R + \xi} \text{ and } \xi = 1 \tag{7.3}$$

$$\nu_{12} = \nu_R - (\nu_R - \nu_F) \cdot V_f \tag{7.4}$$

A reduction factor on these properties, except for ν_{12}, should be applied according to [24]. For uni-directional (UD) lamella the reduction factor is 0,97. This factor is based on a literature research to take some deviations into account, such as: fibre misorientations, fibre damages, fibre undulations, short fibres and air inclusions. Initially a fibre volume content of 60% is assumed. The corresponding nominal properties of a lamella are calculated in appendix A, the results are:

$$E_1 = 43{,}2\ GPa \quad E_2 = 14{,}1\ GPa \quad G_{12} = 4{,}34\ GPa \quad \nu_{12} = 0{,}27$$

The density of a lamella can be calculated according to the rule of mixtures and is:

$$\rho = 0.6 \cdot 2570 + 0.4 \cdot 1200 = 2022\ kg/m^3$$

7.6 Safety factors

The safety factors are determined according to CUR96 [19]. Next to a material safety factor a conversion safety factor should be applied for FRP. These partial safety factors are determined in the next subsections. The design value of the material properties can be calculated with:

$$X_d = \frac{X_k}{\gamma_m \cdot \gamma_c} \tag{7.5}$$

With:

X_k Nominal value of a property
γ_m Material safety factor
γ_c Conversion safety factor

7.6.1 Material safety factor

The material safety factor consists of two partial material safety factors and is calculated with:

$$\gamma_m = \gamma_{m1} \cdot \gamma_{m2} \tag{7.6}$$

With:

γ_{m1} Material factor to take uncertainties into account regarding obtaining the right material properties. This factor should be taken equal to 1,35 according to CUR96 [19]. The exact value was under discussion and should ensure together with the representative material property a certain reliability index β. Next to that, this factor takes also possible differences between the structure and the specimen into account and uncertainties in the calculation models.

Note:
Initially it was assumed that this material factor was equal to 1.5, which came from a misunderstanding. Therefore, the total material safety factor in the initial design stage was equal to 2.1.

γ_{m2} Material factor to take uncertainties into account regarding the material properties due the combination of parts, depended on the manufacturing process. The values are taken according to CUR96 [19], which is based on the average value from the Eurocomp Design Code and the Germanischer Lloyd.

Initially it is assumed that the process of saturation isn't applied. Therefore the highest material factor γ_{m2} for the suitable manufacturing processes, according to [19], is: 1,4. This factors holds for the hand lamination process for a postcured laminate.

The total material factor can be calculated as the product of both partial material safety factors:

$$\gamma_m = \gamma_{m1} \cdot \gamma_{m2} = 1.35 \cdot 1.4 = 1.9$$

7.6.2 Conversion safety factor

The conversion safety factor consists of four different partial conversion safety factors which take all a different aspect into account:

$$\gamma_c = \gamma_{ct} \cdot \gamma_{cv} \cdot \gamma_{ck} \cdot \gamma_{cf} \tag{7.7}$$

With:

γ_{ct} Conversion factor for temperature effects. This factor is equal to 1.1 for resin systems with a heat distortion temperature (HDT) of minimal 30° (according to [19]).

γ_{cv} Conversion factor for moisture effects. This factor takes account of the decrease of mechanical properties which are caused by moisture intrusion. This factor is according to [19] equal to 1.3 for structures which are positioned in a wet environment. For structures which are positioned in a wet-dry environment (alternating dry and wet) this factor is 1.1. A factor of 1.3 is assumed for the slides. In fact the structure is not always wet, but for safety a somewhat higher moisture factor is chosen.

γ_{ck} Conversion factor for creep effects. This factor takes account of creep effects which are caused by long duration loads, this conversion factor is defined by (according [19]):

$$\gamma_{ck} = t^n$$

Width:

t Time of the load in hours

n Exponent depending on the type of reinforcement, equal to 0.01 for a uni-directional (UD) lamina (according to [19]).

Since the decisive load for the slides will have a maximum load duration time of a few hours up to a day. This conversion factor could be taken equal to 1.0.

Note:
Initially it was assumed that the conversion factor should be taken equal to 1.14 (for a load duration of 100 years). Therefore, the total conversion factor in the initial design stage was equal to 1.64.

γ_{cf} Conversion factor for fatigue effects. According to [19] the conversion factor for fatigue effect doesn't need to be taken into account for a ULS check.

The total conversion factor becomes:

$$\gamma_c = \gamma_{ct} \cdot \gamma_{cv} \cdot \gamma_{ck} \cdot \gamma_{cf} = 1.1 \cdot 1.3 \cdot 1.0 \cdot 1.0 = 1.43$$

7.7 Fracture criterion

Initially a strain limit of 1.2 % in all directions will be used. This criterion has been derived in CUR recommendation 96. Some important steps of that derivation will be mentioned here.

This criterion is based on the strain limits of uni-directional (UD) lamina in all different directions, which are mentioned in Table 7.4. The strain limits are average strain limits, which are based on strength data from literature (see references on page 60 in [24]) and stiffness properties calculated with Halpin and Tsai and Manera. The values shown in Table 7.4 are respectively: the tensile strain limit in the first principal direction, the compression strain limit in the first principal direction, the tensile strain limit in the second principal direction, the compression strain limit in the second principal direction and the shear strain limit in the first and second principal direction.

Table 7.4 Strain limits of a uni-directional (UD) lamina [24]

ε_{1tR}	ε_{1cR}	ε_{2tR}	ε_{2cR}	ε_{12R}
2.4	1.6	0.34	1.1	0.58

These strain limits vary for tensile or compression loadings and require that every lamella is checked separately. The CUR recommendation 96 prefers a strain limit which can be used in all direction and which is the same for tensile or compression loading. Therefore the strain limits in Table 7.4 will be used to derive a more simplistic strain criterion.

The average strain limit of all values in Table 7.4 is 1.5%. The consequences of using this average value are investigated in the CUR recommendation 96. Since this recommendation requires that minimal 15% of the fibres is placed in the four main directions (0°, 90°, 45° and -45°), the strain limits $\varepsilon_{2tR} = 0.34$, $\varepsilon_{2cR} = 1.1$ and $\varepsilon_{12R} = 0.58$ of a UD lamella will never be governing for the ultimate strength a laminate. Only in the serviceability limit state the strain limit $\varepsilon_{2tR} = 0.34$ is governing for the first cracks. These cracks can be accepted for the most structures. Especially structures which are exposed to a long-term water pressure, couldn't be designed by using the uniform strain criterion, e.g. storage tanks. Since the slides are exposed to a water pressure, but of short duration, the uniform strain criterion may be applied.

This uniform strain criterion is a simplification. Only during tension the actual strain limit (2.4%) is much higher than 1.5%. During compression the actual limit (1.6%) is just a little bit higher. By using a uniform strain limit, it isn't possible to load the material closer to the limit.

The nominal value of the uniform strain criterion is determined with a coefficient of variation equal to 0.1:

$$\varepsilon_k = \varepsilon_m(1 - v \cdot 2) = 1.5 \cdot (1 - 0.1 \cdot 2) = 1.2 \tag{7.8}$$

The uniform strain limit of 1.2% will be used, since this criterion is very easy to apply. The strain limit should be checked in all directions individually. This means that there is no influence of multi-axial loads. There are some other combined stress criteria which take into account the influence of multi axial loads, e.g. Tsai-Azzi and Tsai-Wu. These criteria are not used in this research.

The first ply failure theory is used to check the laminates. This means that if the strain in the outer fibre reaches the strain limit, the whole laminate is considered to collapse. Therefore, the strains in the outer lamellas should only be checked. According to CUR96 the strains in the direction of the laminate axis because of the design values of the loads should be checked with this criterion. Also the shear strain should be checked with this criterion.

7.8 Material properties (initial design stage)

In the initial design stage, it was assumed that the material safety factor and the conversion safety factor should be applied on the lamella stiffness instead of apply it to the strain limit. The following stiffness properties were used for calculating the structural concepts in chapter 8 (according to [18]):

$$E_1 = 19{,}48\ GPa \quad E_2 = 6{,}36\ GPa \quad G_{12} = 1{,}95\ GPa \quad \nu_{12} = 0{,}27\ GPa$$

Later on, it was found that the safety factors should be applied in another way according to the CUR96, which is schematized in Table 7.5. In ultimate limit state (ULS) the safety factors should be taken into account on the strain limit of 1.2%. In serviceability limit state (SLS) the conversion factor should be taken into account on the stiffness properties of the lamellas. This way of applying the safety factors is used in the final design. In the next paragraph it is made clear what the impact is on the results which are presented in chapter 8.

In ULS there is mathematically no difference in applying the safety factors on the stiffness properties or on the strain limit, since the safety factors are just shifted from the right hand side of equation (7.9) to the left hand side, see equation (7.10).

$$\varepsilon_{max} = \frac{\sigma_{max}}{E} = \frac{1}{E} \cdot \left(\frac{N}{A} + \frac{M \cdot z}{I_{zz}}\right) \leq \frac{1.2}{\gamma_m \cdot \gamma_c} \tag{7.9}$$

$$\varepsilon_{max} = \frac{\sigma_{max}}{E} = \frac{1}{\frac{E}{\gamma_m \cdot \gamma_c}} \cdot \left(\frac{N}{A} + \frac{M \cdot z}{I_{zz}}\right) \leq 1.2 \tag{7.10}$$

In SLS there will be a difference, since only the conversion safety factor should be taken into account on the stiffness properties. Therefore, the deformations in chapter 8 are calculated 55% too high, this percentage is calculated in section 10.1.2. In the conclusion of chapter 8 this fact will be considered.

Table 7.5 Applying of safety factors in initial design stage and in the final design

	Stiffness	Strain limit
Initial design stage		
ULS + SLS	$\frac{E}{\gamma_m \cdot \gamma_c}$	$\varepsilon_{i,ED} \leq 1.2$
Final design		
ULS	E	$\varepsilon_{i,ED} \leq \frac{1.2}{\gamma_m \cdot \gamma_c}$
SLS	$\frac{E}{\gamma_c}$	

8 Structural concepts

This chapter is part of the answer of the fourth sub-research question: 'What is technically the most promising design for the slide made of FRP?'. In this chapter the feasibility of different structural concepts for the slides in the Eastern Scheldt barrier will be investigated. First of all, some guiding principles for the structural concepts will be mentioned, where after the concepts which are mentioned in the literature study are evaluated. Thereafter follows the description and calculation of different variants. Finally, a choice for the most promising variant is made.

8.1 Design philosophy

Aspects which are considered to be important for the development of variants for the slides are:

- There will be as little as possible connections used in the construction.
- A structure which is optimal for wave impacts loads and leakage flows will be designed.
- The structure should transfer the loads pretty equally to the complete height of the slide bearings.

8.2 Evaluation of previous concepts

The concepts which are considered in previous research (see section 3.2 of literature study) are evaluated in this section to get insight in the opportunities of re-use of these concepts.

Regarding the concepts of Veraart:

- The horizontally curved shell transfers the loads in a distributed way to the piers. This principle offers good opportunities for FRP.
- Concept 2 and 3 were not attractive, due to the highly loaded bottom and top of the slide.
- Stacking of round tubes was not attractive, due to the high thickness required.

Regarding the concepts of Van der Laken:

- The truss arch (concept 1) consists of many connections and is therefore excluded.
- Concept 2 is in principle equal to the concrete box girder design, which can offer good opportunities for FRP.
- Concept 3 was difficult to connect and therefore excluded.
- Concept 4 is sensitive to buckling and requires a lot of material.

Regarding the concrete concepts for FRP slides:

- The box girder solution was too heavy, but can offer opportunities when using FRP.
- The plate girder design experienced high wave impacts loads. Therefore this design is excluded.
- The truss girder consists of many connections and is therefore excluded. A design which consists of many connections is considered to be not robust and will be expensive to manufacture.

The concepts which offer good opportunities are the horizontally curved shell and the box girder. Next to that a sandwich structure is considered to offer also good opportunities for the slide. Variants which will be further developed in the next sections are:

- Sandwich
- Horizontally curved shell

- Box girder

8.3 Sandwich

The sandwich variant consists of a core and two skins which are connected by some webs. The skins are positioned at a certain distance from each other to take up the bending moment. The fibercore principle (see Figure 8.1b) could be used for this sandwich. The fibres of the web are then positioned in a Z-shape and connect both skins very good. This principle will prevent that delamination's occur.

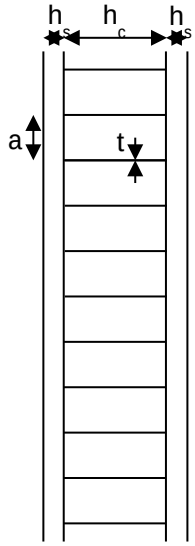


Figure 8.1a Sandwich with some parameters

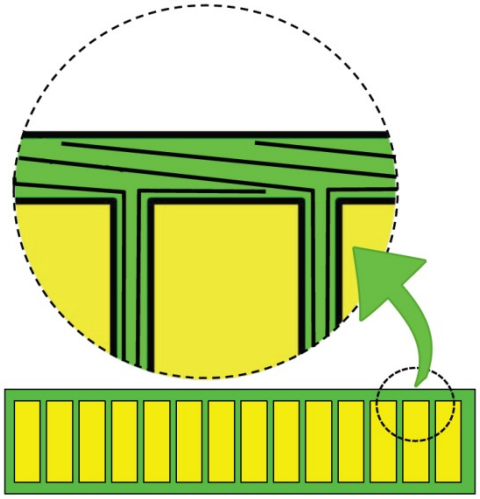


Figure 8.1b Fibercore principle [25]

The possibilities of this variant are investigated in the next subsection by a hand calculation.

8.3.1 Hand calculation

Initially a strain limit of 1% will be used. The young's modulus of the skin is assumed to be 15000 N/mm^2, the young's modulus of the core material is assumed to be 32.9 N/mm^2. The maximum stress in the fibres will be:

$$\sigma = E \cdot \varepsilon = 15000 \cdot 0.01 = 150\ N/mm^2 \tag{8.1}$$

The maximum stress for a foam core is 0.69 N/mm^2 (according to [18]). The flexural rigidity of the sandwich structure can be calculated with:

$$EI = \frac{1}{2} E_s b h_s (h_c + h_s)^2 \tag{8.2}$$

It's assumed that only the skins contribute to the flexural rigidity. The flexural strength M is depending on failure of the skin or the core material and is therefore the minimum value of equations (8.3) and (8.4):

$$M = \frac{EI \cdot \sigma_s^*}{\frac{h}{2} \cdot E_s} \tag{8.3}$$

With:

σ_s^* = maximum stress in skin material

$$M = \frac{EI \cdot \sigma_c^*}{\frac{h_c}{2} \cdot E_c} \tag{8.4}$$

With:
σ_c^* = maximum stress in skin material
E_c = Young's modulus core material

Since only the skin is assumed to be effective for the flexural rigidity, the total thickness of the skins became very thick (up to 300 mm), which was unrealistic. Therefore the bending moment capacity of the webs and core was also taken into account. The equation for calculating the flexural rigidity is:

$$EI = \frac{1}{2}E_s b h_s (h_c + h_s)^2 + E_s \frac{c}{12} t h_c^3 + E_c \frac{1}{12}(1000 - c \cdot t) h_c^3 \quad with: c = \frac{1000}{a} \tag{8.5}$$

With these equations the bending moment resistance is known. The design bending moment is equal to:

$$M_{Ed=} \frac{1}{8}\gamma_q q l^2 \tag{8.6}$$

Initially a distributed load of 100 kN/m^2 is assumed with a safety factor of 1.5. When the design bending moment is equated with the bending moment resistance it's possible to calculate one of the dimensions of the sandwich (when the others ones are known). After some iterations the dimensions of the sandwich were found, see Table 8.1. The calculation is shown in appendix B.

Table 8.1 Dimensions of sandwich when strength or deflection requirement is governing

In mm	Strength	Deflection
h_{tot}	2500	4000
h_s	17	17
h_c	2462	2408
t	17	24
a	100	100

The dimensions are mentioned for 2 situations: to meet the strength requirement and to meet the deflection requirement. A maximum deflection of 250 mm was accepted. The deflection was calculated according to [26]:

$$w = \frac{5}{384}\frac{qL^4}{EI} + \frac{1}{8}\frac{qL^2}{\sum GA} \quad with: \sum GA = G_s \cdot 2 \cdot h_s \cdot b + G_s \cdot c \cdot h_c \cdot t + G_c \cdot h_c \cdot (b - c \cdot t)$$

where b=1000. The deflection of the variant which is dimensioned on strength was 970 mm, the other variant was dimensioned on the maximum deflection requirement. It can be seen that the dimensions will increase a lot when the deflection requirement should be met.

8.3.2 Finite element analysis

To get a somewhat better insight on the deformations a FEA is carried out. A part of 1 m height of the slide is modeled in DLUBAL RFEM, see Figure 8.2. The laminates are modeled as surfaces which get the properties of the laminate by using the module RF-Laminate. The laminate stiffness matrix calculated with RF-Laminate is compared with the matrix of Kolibri in appendix C. This confirms that

it can be assumed that the laminate stiffness matrix of RF-Laminate is calculated correctly with the classical lamination theory. The stacking sequence of lamellas which is applied on each surface is shown in Table 8.2. It should be clear that a real stacking exist of much thinner lamellas, which isn't useful in this calculation. The properties of each lamella are taken equal to the values mentioned in section 7.8. The core material is also modeled, since the thin horizontal webs would otherwise buckle very easily (after stability problems in the program). The core material is modeled as an isotropic solid between the plates.

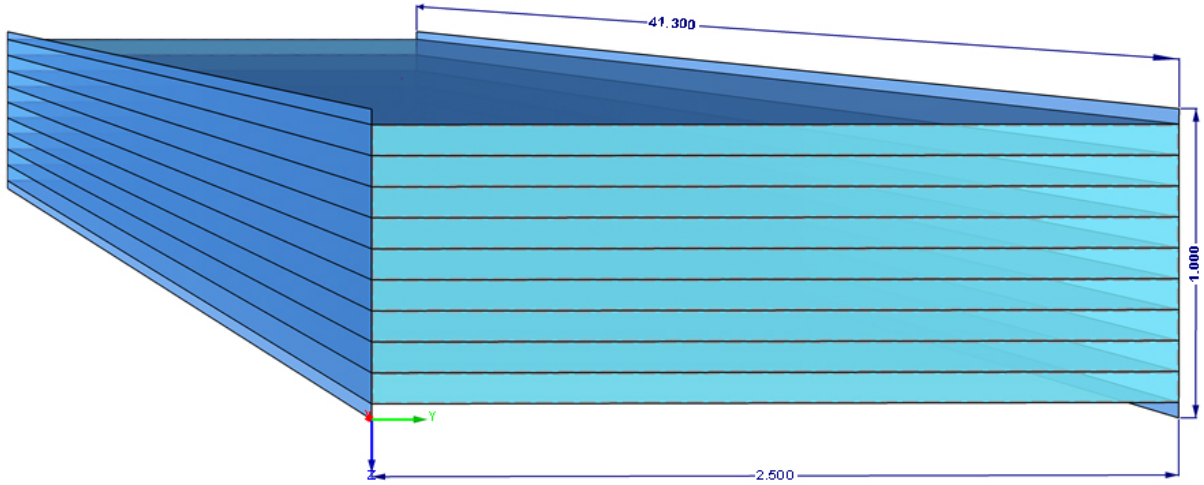


Figure 8.2 Model of a part of the slide (only 1 m height)

At one side of the slide a line support is placed which constraint all translations, at the other side a line support is placed which will allow a translation in the length direction and constraint the other translations. A top view of the mechanical scheme is shown in Figure 8.3. The dimensions in the model are globally taken to meet the strength criterion of the hand calculation, the total thickness of all the lamella surfaces is 20 mm.

Table 8.2 Stacking sequence of lamellas

	thickness (mm)	Direction (°)
1	5.5	0.00
2	1.5	90.00
3	1.5	-45.00
4	3.0	45.00
5	1.5	-45.00
6	1.5	90.00
7	5.5	0.00

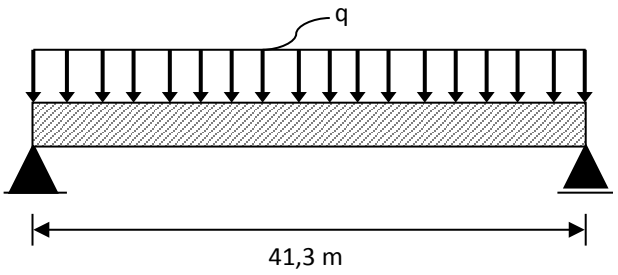


Figure 8.3 Mechanical scheme (top view)

The maximum strains which occur in the structure are shown in Table 8.3. These strains do not correspond to one point in the structure, but are maximum values which correspond to different points. Since the maximum strains are lower than the uniform strain criterion, the strength requirement is met. There is some extra capacity left, since 1.2 % is the maximum strain according to this criterion. This extra capacity is probably caused by the somewhat thicker plates which are modeled in comparison to the hand calculation.

Table 8.3 Maximum strains in the structure (not corresponding to one special point)

Symbol	Maximum strain (%)
ε_x	0,87
ε_y	-0,36
γ_{xy}	0,36

A contour plot of the deformations in y-direction is shown in Figure 8.4. The maximum displacement of this structure is 840 mm. This displacement is somewhat lower in comparison to the hand calculation, but is caused by the thicker plates of 20 mm.

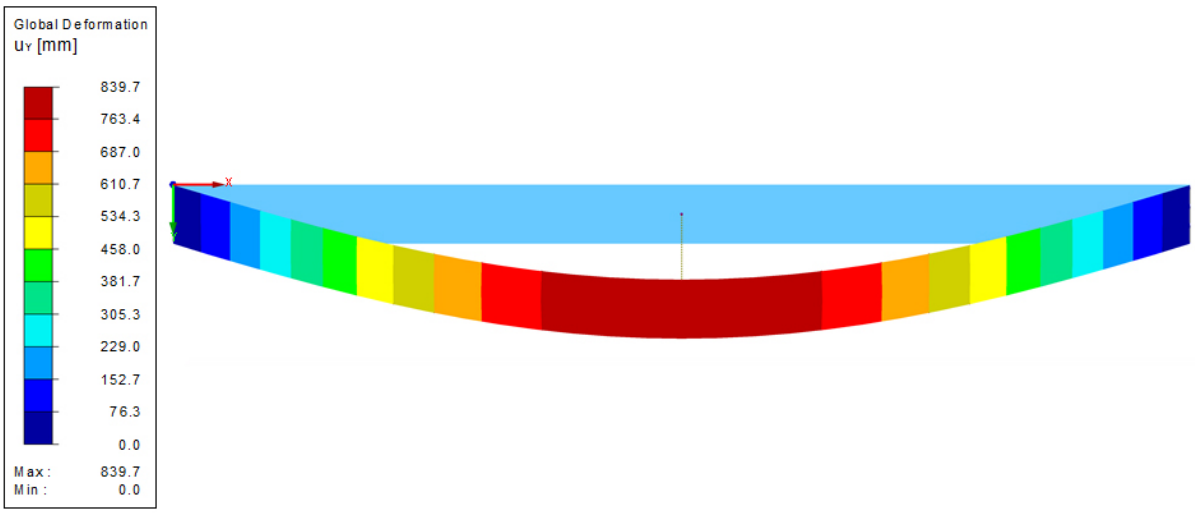


Figure 8.4 Deformations in y-direction (mm)

To meet the deflection requirement, the thickness of the structure should increase. A FEA of a thicker structure isn't performed. Reasons for that could be found in the next subsection.

8.3.3 Conclusion

The calculations of the sandwich variant show that rather big dimensions are necessary to meet the deflection requirement. A sandwich structure with these dimensions isn't applied yet. The minimal thickness according to the strength criterion is around 2.5 m. It is not sure if skin and core can cooperate in the same way as for thinner sandwiches. To meet the deflection requirement, the total thickness should be minimum 4 meters and the webs should have a thickness of 17 mm (every 100 mm) to reduce the thickness of the skins, since the skin thickness is limited by the manufacturing process. These dimensions give the indication that it isn't economic to apply this sandwich for the slide. There should be more material on the outside or the total thickness of the slide should be increased. Also the manufacturing of such a thick sandwich will be difficult, if not impossible. Therefore this sandwich is excluded as variant.

8.4 Horizontally curved shell

A horizontally curved shell can be easily designed as a pressure arc by following the force line. The shell would be loaded in his own plane and is in pressure during positive drop and in tension during negative drop. Since the bending moment in the structure is reduced by a curved shell, the shell is mainly loaded with normal forces, which is attractive for FRP.

A simple horizontally curved shell couldn't be applied directly to the Eastern Scheldt barrier, since:

- The piers are not designed to carry horizontal forces
- The water defense cladding should be placed in one plane with the sill beam and the upper beam

Therefore it's necessary to place a plate between the piers which can function as water defense cladding and can carry the horizontal forces. This idea is applied on the sandwich structure from the previous section. This sandwich could have a varying thickness as shown in Figure 8.5.

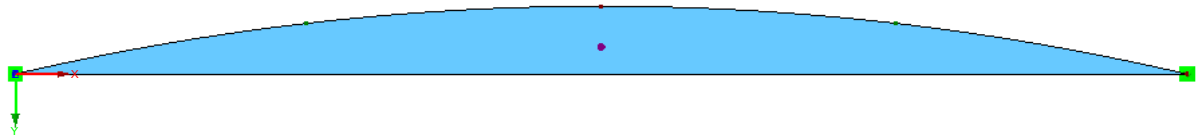


Figure 8.5 Horizontally curved sandwich (top view)

This shape has one major disadvantage, because the sides have a thickness which goes to zero. At the sides there is no thickness needed for the bending moment capacity, but the shear force capacity is too low and the deflection is very big. A horizontal curved shell in this shape isn't a good idea, since there should be some shear force capacity left at the ends. The sides of the slide could be adjusted to a shape as shown in Figure 8.6. But since a sandwich wasn't already a good idea, it makes no sense to adapt the sides of this sandwich. Therefore it would be better to use the advantages of a curved shell in a new concept, e.g. a straight structural system with a thickening in the middle.

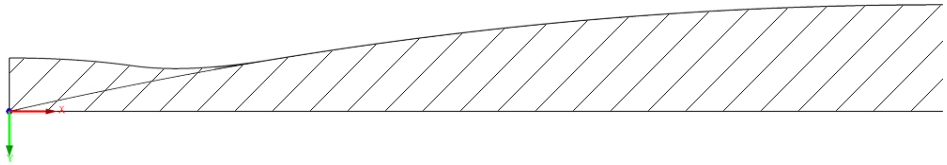


Figure 8.6 Idea to adapt side of slide

8.5 Box girder

The box-girder variant consists of a water defense cladding which is stiffened by some horizontal plates. Since the horizontal plates are susceptible to wave impact loads, a second vertical wall is placed which protects the horizontal plates against wave impact loads.

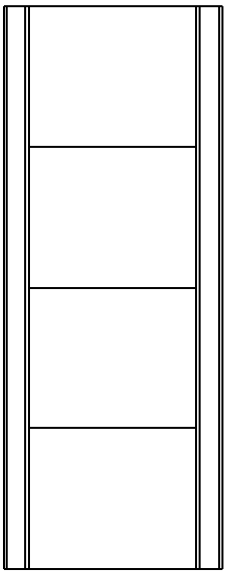


Figure 8.7 Two sandwiches which are connected with horizontal plates

To ensure an equally distributed transfer of forces over the height at the supports, sufficient horizontal plates should be placed between the two walls or a stiff end sleeve should be designed to distribute the forces over the height. For both walls a sandwich could be used. These sandwiches can be connected with horizontal plates which could have also a sandwich layup to prevent buckling of these plates. A schematic representation is shown in Figure 8.7.

8.5.1 Straight box girder

Initially, a straight box girder variant with a total thickness of 6 m has been considered, see Figure 8.8. The outer walls are sandwiches with the lay-up given in Table 8.4. The horizontal plates were initially calculated without a core (the other layers are placed in the same lay-up as in Table 8.4). The properties of the lamellas were equal to the properties in the FEA in subsection 8.3.2. Also the way of supporting the slide and the loads were equal to that FEA.

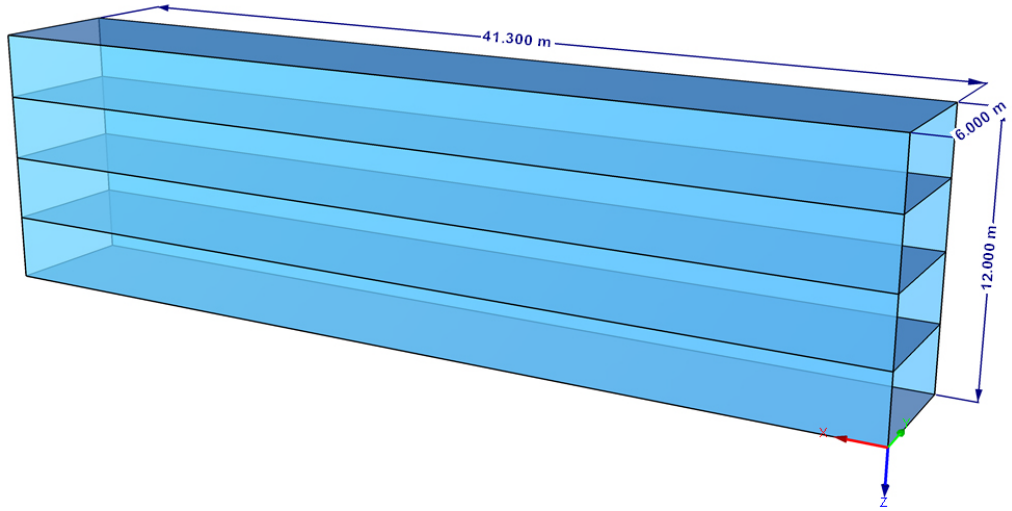


Figure 8.8 Straight box-girder variant

Table 8.4 Lay-up of sandwich walls

Properties	Thickness (mm)	Direction (°)
Lamina	11.0	0.00
Lamina	3.0	90.00
Lamina	3.0	-45.00
Lamina	3.0	45.00
Core	250.0	0.00
Lamina	3.0	45.00
Lamina	3.0	-45.00
Lamina	3.0	90.00
Lamina	11.0	0.00

Since the deflection requirement was considered to be decisive, the deformations of this variant were calculated. In this stage only a horizontal load of 100 kN/m^2 was taken into account. The results are shown in Figure 8.9. The maximum displacement in y-direction is 441 mm, which is more than the deflection requirement allows.

It's also important to check whether the support reactions are pretty equally distributed over the height, since the current piers are designed for that. The support reactions are displayed in Figure 8.10. Since the horizontal plates transfer a lot of the load to the supports, the support reactions are

not pretty equally distributed over the height. A solution for this problem could be the addition of vertical plates near the supports to spread the loads more equally.

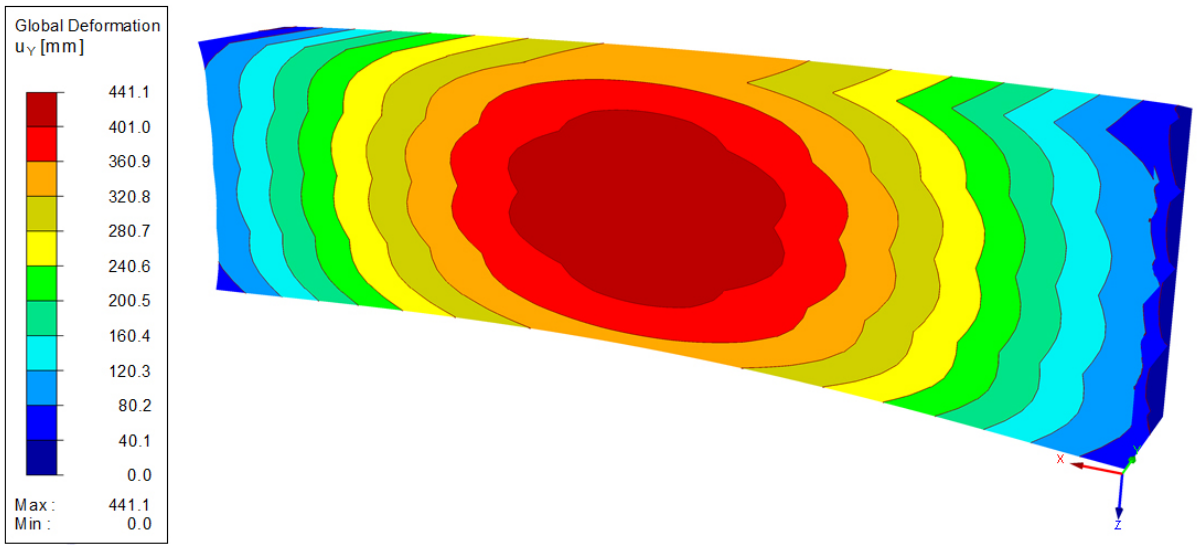


Figure 8.9 Deformations in y-direction

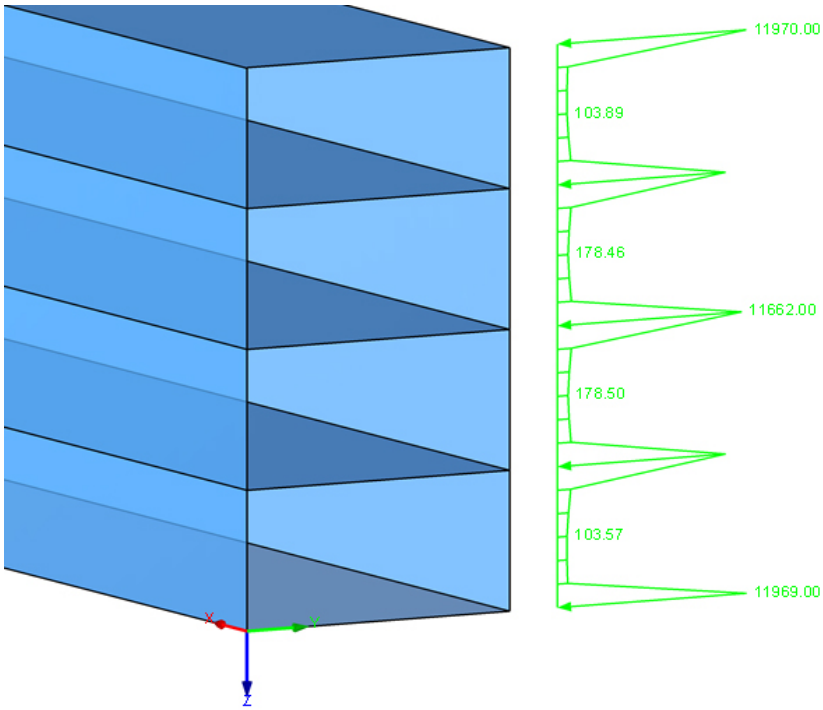


Figure 8.10 Support reactions in y-direction (kN/m) (see explanation in appendix D)

To check whether the deflection requirement is decisive or not, the maximum strains which occur in the structure are shown in Table 8.5. These maximum strains are all (far) above the limit of 1.2%. It is therefore necessary to look into more detail to these maximum strains.

Table 8.5 Maximum strains which occur in the structure (not corresponding to one special point)

Symbol	Maximum strain (%)
ε_x	-1,77
ε_y	-12,42
γ_{xy}	15,18

The maximum strains were only mentioned as maximum strains which occur somewhere in the structure. Therefore it is important to see in which surfaces the maximum strain exceeds the strain limit of 1.2%. Therefore the numbering of the surfaces of the structure is mentioned in Figure 8.11. The maximum strains in these surfaces are mentioned in Table 8.6. These maximum strains do not have to correspond to one special point in the structure, but can correspond to different points. In Table 8.6 is shown at which lamella and where (on the top or bottom of that lamella) the maximum strain occurs. In the table is no information provided about the geometrical location of that point.

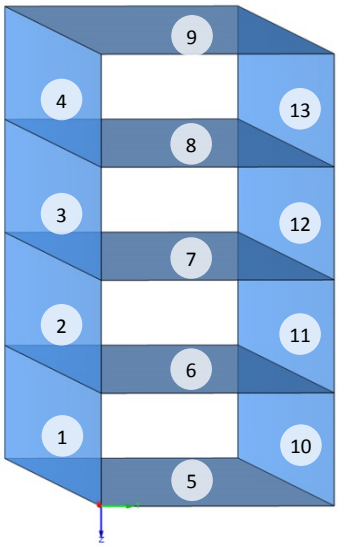


Figure 8.11 Numbering of the surfaces of the structure

Table 8.6 Maximum strains in each surface

Surface No.	Lamella No.	Lamella Side	ε_x (%)	Lamella No.	Lamella Side	ε_y (%)	Lamella No.	Lamella Side	γ_{xy} (%)
1	1	top	-0,72	9	bottom	0,48	1	top	0,50
2	1	top	-0,73	9	bottom	0,43	1	top	0,47
3	1	top	-0,73	9	bottom	0,43	1	top	-0,47
4	1	top	-0,72	9	bottom	0,48	1	top	0,50
5	1	top	-1,77	1	top	-7,37	1	top	13,23
6	7	bottom	-1,39	1	top	-11,38	7	bottom	13,75
7	1	top	-1,54	1	top	-12,42	1	top	15,18
8	1	top	-1,39	1	top	-11,38	1	top	13,77
9	7	bottom	-1,77	7	bottom	-7,37	7	bottom	13,24
10	9	bottom	1,54	1	top	0,96	9	bottom	3,62
11	9	bottom	1,53	1	top	-0,77	9	bottom	3,99
12	9	bottom	1,53	1	top	-0,77	9	bottom	-3,98
13	9	bottom	1,54	1	top	0,95	9	bottom	-3,61

The strains which do not exceed the strain limit of 1.2% are colored green. Thereby, it can be seen that the maximum strains in surfaces 1 to 4 do not exceed this limit. The surfaces 1 to 4 are loaded in compression and are positioned at the North Sea side of the slide. The maximum strains in the horizontal plates (surfaces 5 to 9) do all exceed the strain limit of 1.2%, as well as the strains ε_x and γ_{xy} of the surfaces 10 to 13. These surfaces (10-13) are loaded in tension and are positioned at the Eastern Scheldt side of the slide (where the supports are also placed).

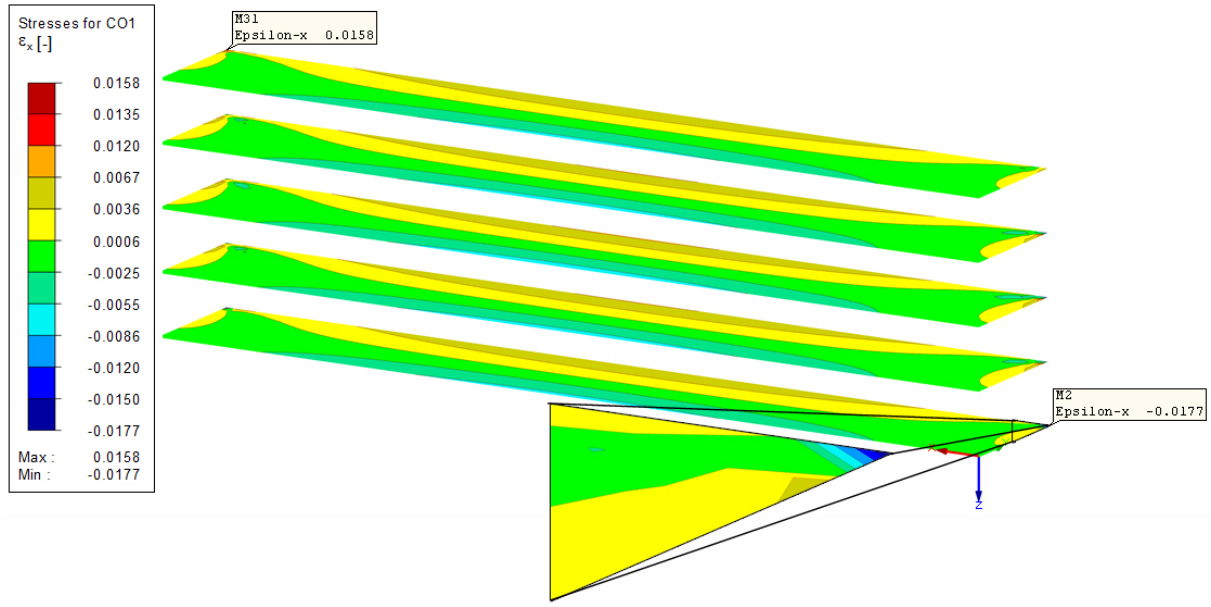


Figure 8.12 Strain ε_x at the top of lamella 1 in the surfaces 5 to 9

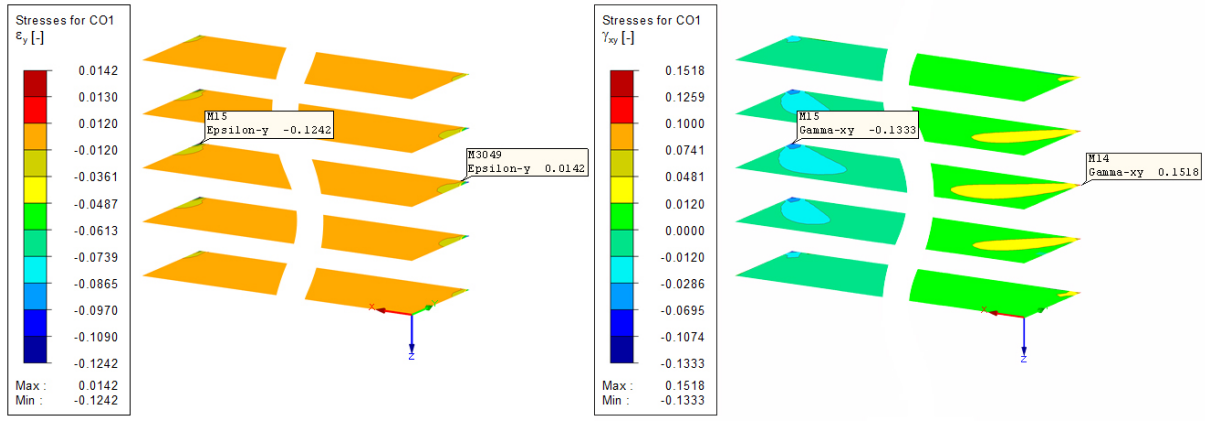


Figure 8.13 Strains ε_y (left) and γ_{xy} (right) at the top of lamella 1 in the surfaces 5 to 9

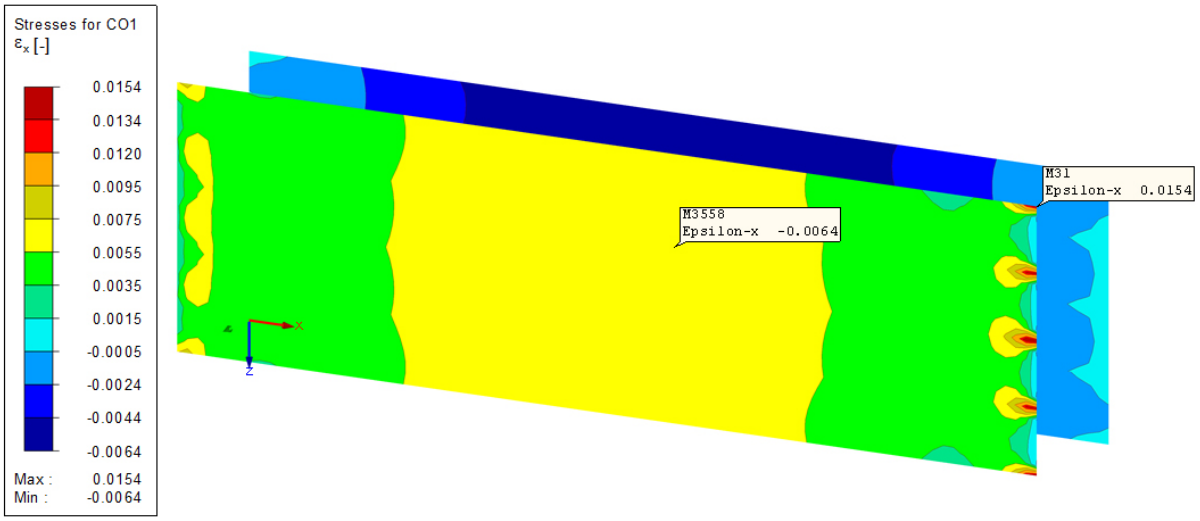


Figure 8.14 Strain ε_x at the bottom of lamella 9 in the surfaces 10 to 13

The strains which exceed the strain limit of 1.2% will also be displayed graphically to understand where these maximum strains occur in the structure. In the surfaces 5 to 9 the maximum strains occur in almost every surface at the top of lamella 1. Therefore the strains at the top of lamella 1 are displayed in Figure 8.12 and in Figure 8.13.

In can be seen that in almost the whole horizontal plate the strain limit is not exceeded. Only very locally, in the corner of the support, the strain limit is reached. Also in Figure 8.13 is shown that the strains ε_y and γ_{xy} do exceed the strain limit only very locally.

The maximum strains, which exceed the strain limit, in the surfaces 10 to 13 are positioned at the bottom of lamella 9. Therefore the strains ε_x and γ_{xy} of these surfaces are graphically shown in Figure 8.14 and in Figure 8.15. Also here, only very locally the maximum strain of 1.2% is exceeded.

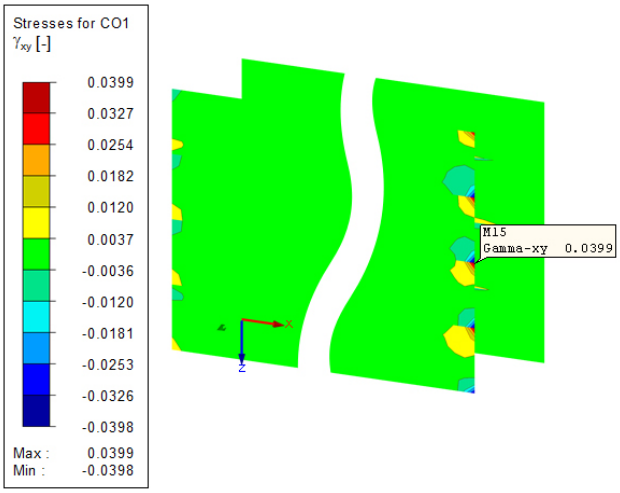


Figure 8.15 Strains γ_{xy} at the bottom of lamella 9 in the surfaces 10 to 13

From the above it can be concluded that the strains do exceed the strain limit only very locally. The strains reach their maximum near the horizontal plates at the supports. This may be caused by the high support reactions near the horizontal plates. Therefore the support reactions should be distributed more equally over the height. If the strains at the support form thereafter still a problem, the core material can possibly be replaced locally by a more stronger material.

Also the deformations of this variant has to be reduced to meet the deflection requirement. Solutions for that are carried out in the next subsections.

8.5.2 Varying thickness

In section 8.4 the possibilities of a curved shell were investigated. The shape shown in Figure 8.5 had the disadvantage that both sides had a too small thickness to carry the shear forces. A box-girder in that shape gives a maximum deformation of 509 mm, which is more than for the straight box-girder. Therefore it would be better to vary the thickness of the box-girder along his length, this idea was shown in Figure 8.6. At both sides the thickness should be enough to take up the shear forces and in the middle the bending moment resistance should be sufficient.

Therefore, there is initially chosen to reduce the total thickness to 4 m at both sides with a thickening in the middle up to 6.25 m, see Figure 8.16. At both ends vertical plates will close the girder to spread the loads more equally to the supports. The support reactions (Figure 8.17) show that the vertical

plates help to transfer the loads more equally to the supports. The peaks are halved and the minimum value is increased more than tenfold. If necessary, it would be possible to place a second vertical wall with maybe some extra horizontal plates between these walls to reduce the peaks in the support reactions even more. The distribution of support reactions over the height is checked in appendix D, since the top and bottom part have much higher peaks then the middle of the slide. This shows that the surfaces of the peaks at the top and bottom part are smaller and therefore the total support reaction at the top and bottom are also smaller (as expected).

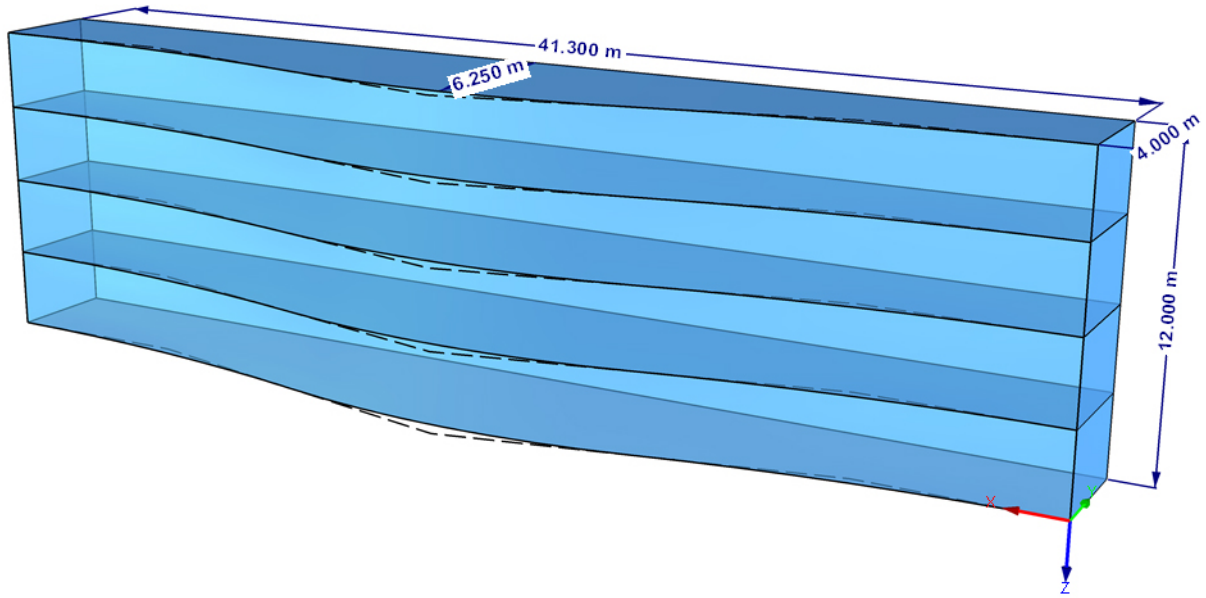


Figure 8.16 Box-girder with thickening in the middle

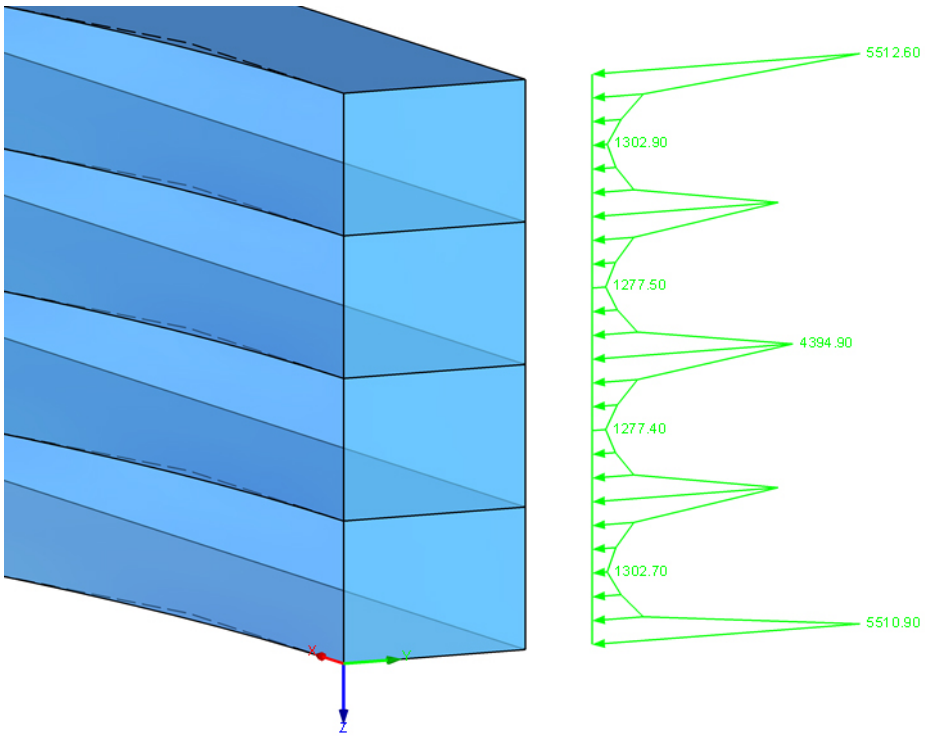


Figure 8.17 Support reactions in y-direction (kN/m) (see explanation in appendix D)

The deformations of this variant shown a very similar pattern as Figure 8.9. The maximum deformation in the y-direction is 439 mm. It's very logic that the deformation hasn't decreased a lot, since a lot of material is removed in comparison to the straight box-girder, which has almost the

same thickness in the middle. But the addition of the vertical walls at both sides has helped to reduce the maximum deformation a little bit.

In order to check the strength requirement, the maximum strains which occur in the structure are shown in Table 8.7. In comparison with Table 8.5 these maximum strains are very well reduced, but not enough to meet the strain limit of 1,2%. Therefore the maximum strains per surface are mentioned in Table 8.8. The values which are colored in green meet the strain criterion of 1,2%.

Table 8.7 Maximum strains which occur in the structure

Symbol	Maximum strain (%)
ε_x	-1,62
ε_y	-1,95
γ_{xy}	3,27

Table 8.8 Maximum strains which occur in each surface

Surface No.	Lamella No.	Lamella Side	ε_x (%)	Lamella No.	Lamella Side	ε_y (%)	Lamella No.	Lamella Side	γ_{xy} (%)
1	1	top	-0,80	9	bottom	0,53	9	bottom	0,83
2	1	top	-0,84	1	top	0,52	9	bottom	-0,76
3	1	top	-0,84	1	top	0,52	9	bottom	0,76
4	1	top	-0,80	9	bottom	0,53	9	bottom	-0,83
5	1	top	0,68	7	bottom	-1,95	7	bottom	2,54
6	1	top	0,69	7	bottom	-1,04	1	top	2,98
7	1	top	0,71	7	bottom	-1,00	7	bottom	3,27
8	7	bottom	0,69	1	top	-1,04	7	bottom	2,99
9	7	bottom	0,68	1	top	-1,95	1	top	2,54
10	9	bottom	0,75	1	top	-0,32	9	bottom	-1,45
11	9	bottom	0,76	1	top	-0,32	9	bottom	0,97
12	9	bottom	0,76	1	top	-0,32	9	bottom	-0,97
13	9	bottom	0,75	1	top	-0,32	9	bottom	1,45
14	1	top	-1,50	1	top	-0,73	7	bottom	-1,18
15	1	top	-1,62	1	top	-0,59	7	bottom	-1,22
16	1	top	-1,61	1	top	-0,60	7	bottom	1,21
17	1	top	-1,49	1	top	-0,72	7	bottom	1,17
18	7	bottom	-1,36	7	bottom	-0,56	1	top	-1,19
19	7	bottom	-1,43	7	bottom	-0,60	1	top	-1,22
20	7	bottom	-1,43	7	bottom	-0,60	1	top	1,22
21	7	bottom	-1,35	7	bottom	-0,56	1	top	1,19

The numbering of the surfaces is the same as mentioned in Figure 8.11, the extra surfaces are the vertical end plates which close the box-girder. These plates are numbered from bottom to top, side by side. The maximum strains in the plates in the first vertical wall (surfaces 1 to 4) meet all the strain criterion. The maximum strains in the horizontal plates (surfaces 5 to 9) do meet the strain criterion with respect to ε_x, but do not completely meet the strain criterion with respect to ε_y and γ_{xy}. The maximum strains in y-direction are located at the bottom of lamella 7 of surface 5 and are shown in Figure 8.18. This distribution is equal to the strain distribution at the top of lamella 1 in surface 9 (which also exceeds the strain limit). Only very locally the strain criterion isn't met.

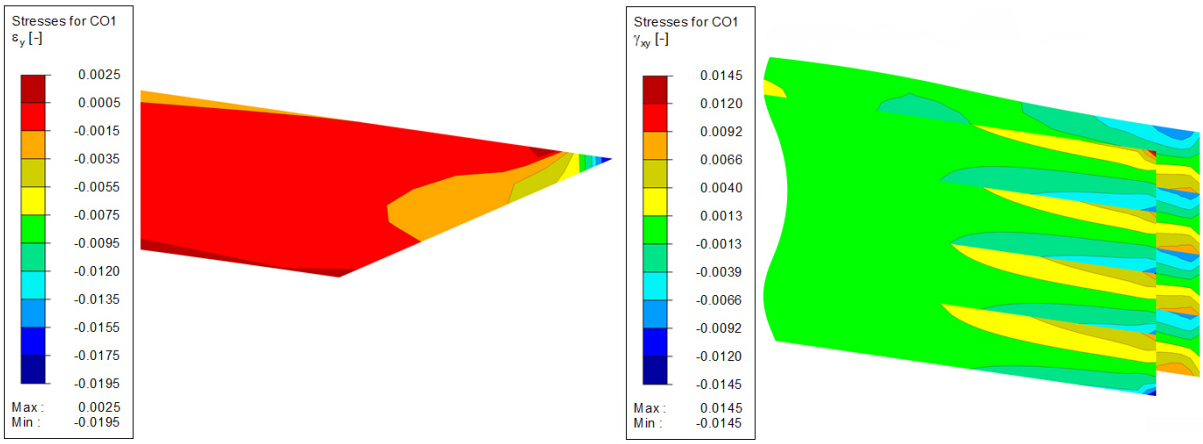


Figure 8.18 Strain ε_y at the bottom of lamella 7 in surface 5. (left) Strain γ_{xy} at the bottom of lamella 9 in surfaces 10 to 13. (right)

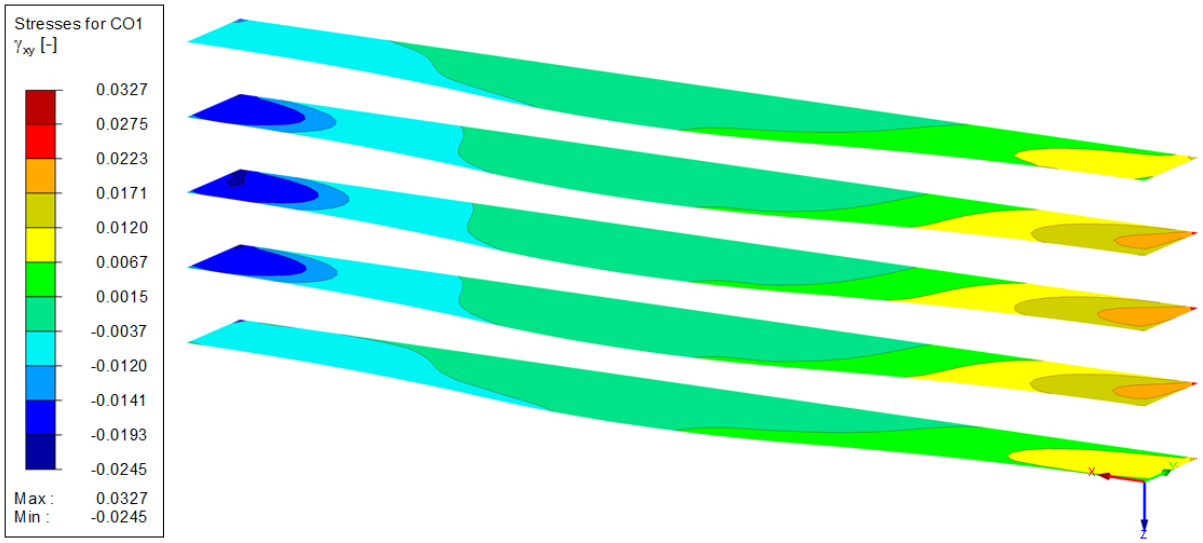


Figure 8.19 Strain γ_{xy} at the bottom of lamella 7 in surfaces 5 to 9

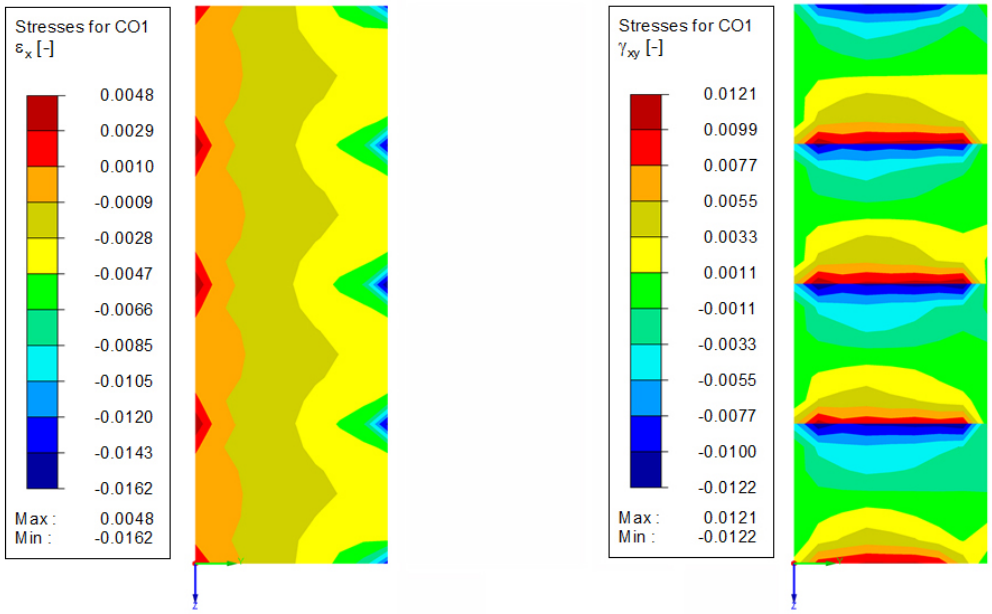


Figure 8.20 Strain ε_x at the top of lamella 1 in surfaces 14 to 17 (left) Strain γ_{xy} at the bottom of lamella 7 in surfaces 14 to 17 (right)

The highest shear strains in these surfaces occur at the bottom of lamella 7, these strains are shown in Figure 8.19. The area's which do not meet the strain criterion are located at the sides of the slide (quite locally).

The shear strains in the surfaces 10 to 13, which do not meet the strain criterion, are positioned at the bottom of lamella 9 (see Figure 8.18) and do not meet this criterion only very locally in the upper and lower corner.

The maximum strains ε_x , which do not meet the strain criterion, in the surfaces 14 to 21 are positioned at the top of lamella 1 or the bottom of lamella 7. The strains at the top of lamella 1 in surfaces 14 to 17 are shown in Figure 8.20, the strains of the other surfaces are mirrored. The maximum strain criterion is, also here, not met very locally to the supports. The shear strains in the surfaces 14 to 17, which do not meet the strain criterion, are located at the bottom of lamella 7. These strains are shown also in Figure 8.20. Only very locally, near the horizontal plates, the strain criterion isn't met (just over the limit).

The peaks in the strains near the supports, which were described above, are increasing with decreasing mesh size. When the mesh size is halved, the maximum strains which occur somewhere in the structure are increasing due to the finer mesh, see Table 8.9. In reality, these peaks do not occur since the peaks will be spread out. These peaks are caused by the simplifications which were made in the FEA model, a more advanced model will not show these peaks. Volume elements could be used to reduce the peaks, next tot that the line support could be spread out to a surface support. To redistribute the support reactions more equally over the height, also the end structure could be modeled into more detail. If the strains near the supports do not fulfill the strain criterion after these improvements have been done, it is possible to replace some part of the core material near the supports with a core material with better characteristics.

Table 8.9 Maximum strains comparison between different mesh sizes

Symbol	**Maximum strain (%)**	
	Mesh size 0.5m	Mesh size 0.25m
$\boldsymbol{\varepsilon_x}$	-1,62	-2,35
$\boldsymbol{\varepsilon_y}$	-1,95	-2,49
$\boldsymbol{\gamma_{xy}}$	3,27	3,86

To reduce the deformation even more the slide will be thickened in the middle up to 8.5 m, see Figure 8.21. The deformations of this slide are shown in Figure 8.22. The maximum deformation of the slide is reduced to 263 mm.

The peaks of the support reactions near the horizontal plates have increased somewhat after increasing the thickening of the slide. Therefore, the maximum strains which occur in the structure have also increased. A more equal distribution of the support reactions over the height will be in favor, to reduce those peaks. A geometrical nonlinear calculation of the model showed that the horizontal plates will be instable. To increase the bending moment capacity of the horizontal plates, these plates should be carried out as a sandwich. Also the vertical plates which close the box girder at both sides should probably be carried out as a sandwich. The thickness of these sandwiches can be optimized in a later stage.

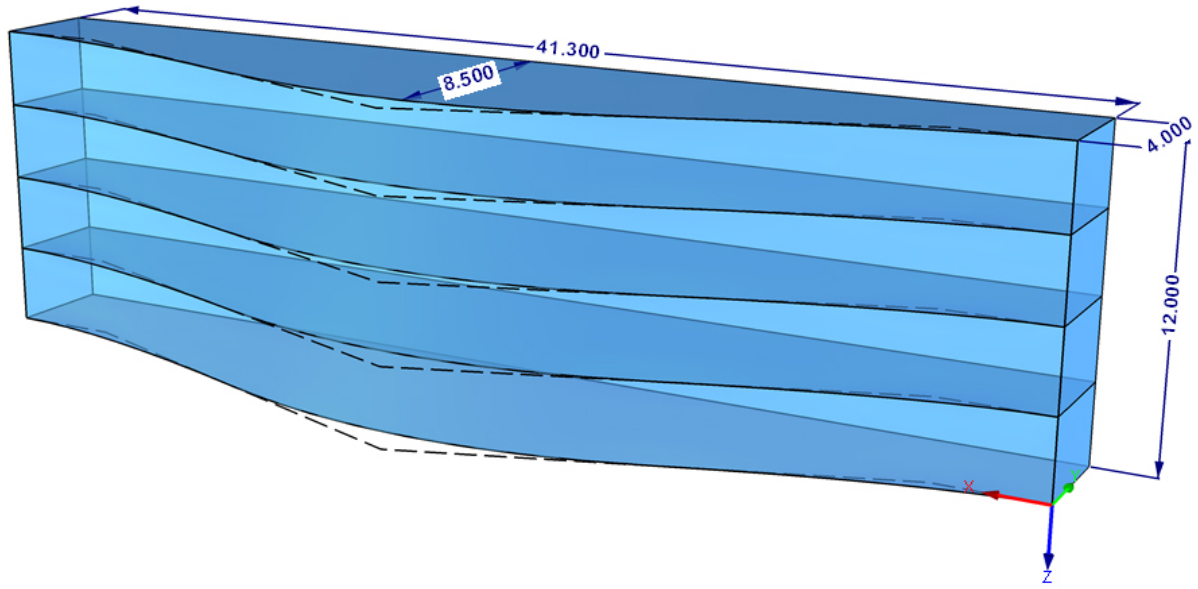


Figure 8.21 Extra thickening of the slide to 8.5m in the middle

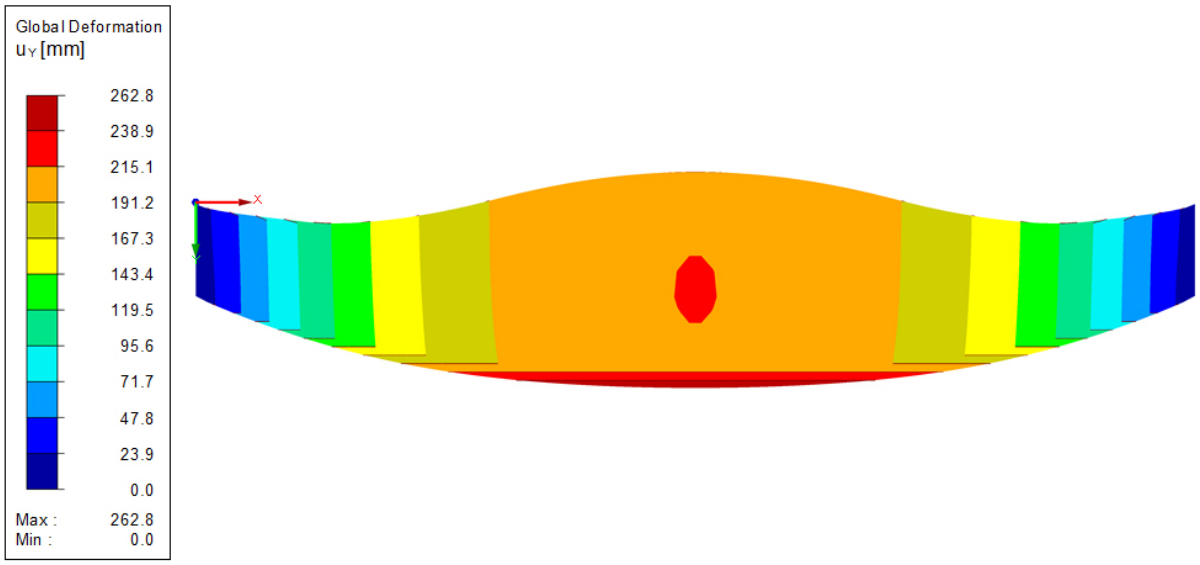


Figure 8.22 Deformations in y-direction (top view)

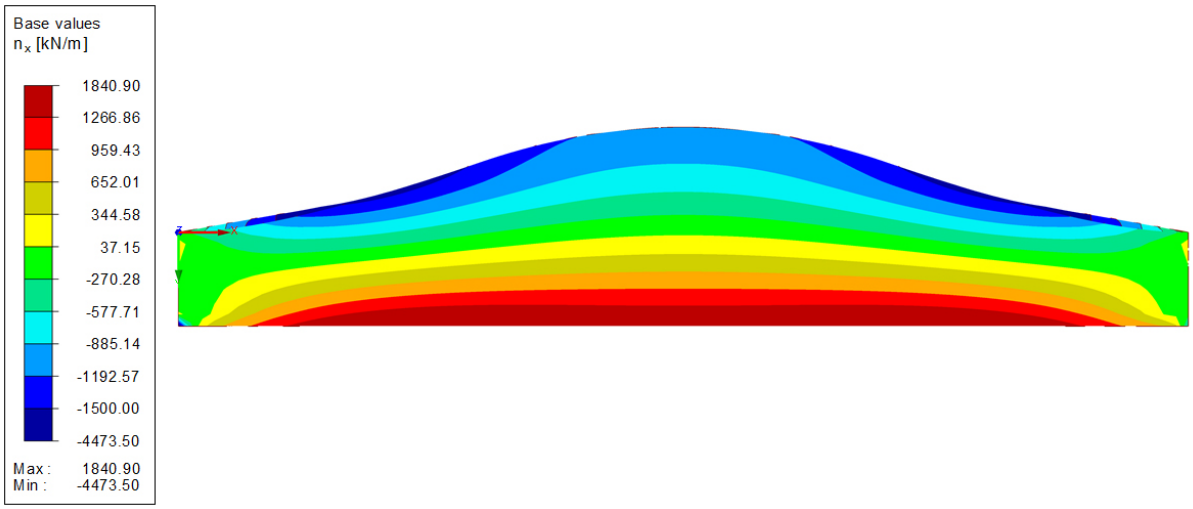


Figure 8.23 Normal force in x-direction (top view)

The normal forces in longitudinal direction (n_x) in the horizontal plates are shown in Figure 8.23. It is clear that the North Sea side of the slide is in compression and the other side in tension. Since a lot of material isn't highly loaded, because this material is placed near the neutral axis, it could be attractive to remove some material near the neutral axis. Some holes in the horizontal places would be sufficient for that. Besides the structural efficiency, some holes will also ensure that the slide will sink. Otherwise, for example water should be pumped into the slide. An example of some holes which could be added is shown in Figure 8.24. The most holes are added in the middle part of the structure where particularly the bending moment is decisive. At the sides there are no holes added, since the shear force will be decisive there. The holes have a varying diameter, which increased up to the middle of the slide and are placed near the neutral axis. The diameter of the holes is based on the stresses in each cross-section. It should be clear that the position and the diameters of the holes can be optimized further. The normal forces shown in Figure 8.24 correspond to a horizontal plate without holes.

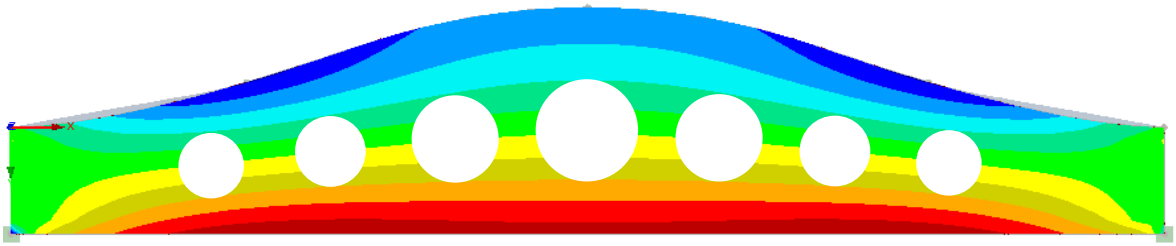


Figure 8.24 Addition of holes in the horizontal plates near the neutral axis (normal forces do correspond to a horizontal plate without holes)

8.5.3 Manufacturability

Since the box-girder concepts looks very attractive, the manufacturability of this concept is investigated. Two possibilities of manufacturing are considered in the next subsections.

8.5.3.1 Option 1

The first option is to manufacture two sandwiches (one straight, one curved) and connect them with the horizontal plates (also small sandwiches). The connection can be carried out as t-joint. This option is illustrated in Figure 8.25.

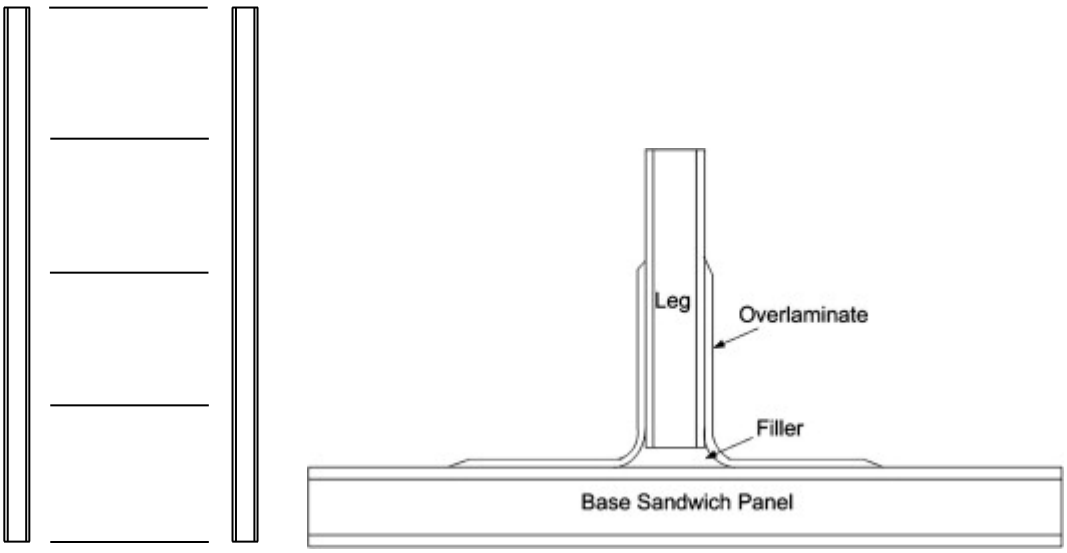


Figure 8.25 Illustration of option 1 [WEB, http://www.sciencedirect.com/science/article/pii/S1359836808000061]

8.5.3.2 Option 2

This option consists of two parts. The first part was mentioned in [4] and consists of winding of some boxes where after these boxes are stacked together. The second part consists of manufacturing the two outer sandwiches (one straight, one curved). These sandwiches can be glued on the stacked boxes, which provide a large surface to glue. This option is illustrated in Figure 8.26. Finally it is possible to finish the complete slide with an overall laminate, which can be winded around the whole slide.

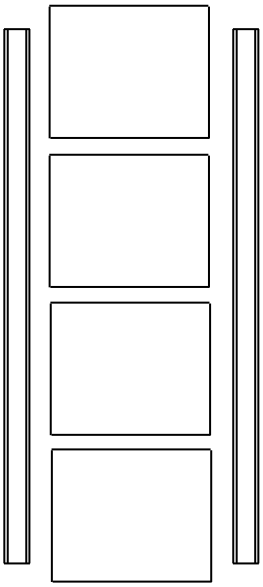


Figure 8.26 Illustration of option 2

8.5.4 Hydraulic adjustments

The hydraulic design considerations, which were mentioned in section 3.3 of the literature study, showed that the bottom of the slide should be adjusted to prevent vibrations by flow. The easiest way of preventing these vibrations is to place the lowest horizontal plate obliquely with an angel of 45°. This should ensure a defined release point and will prevent that the flow pattern will release and later on lay down again.

This way of preventing vibrations by flow was also applied in two previous researches to slides in the Eastern Scheldt barrier and were shown in Figure 3.5 and Figure 3.6. At both figures the bottom of the slide is adjusted over approximately one third of the total slide height (approx. 4 m). Since the thickness of the box-girder variant is already 8.5 m in the middle of the slide, the bottom of the slide should be adjusted over 8.5 m height. That will be very unrealistic, since the thickness couldn't be reduced over such a large part of the slide. The deformations will increase when the bottom of the slide is adjusted over such a large part. Next to that, the lowest slide has a height of 5,9 m, which is too low for this adjustment. Therefore, it is attractive to make the slide thinner. A thickness greater than 4 m is not actually desirable. The most important reason for the great thickness now is the deflection requirement, therefore this requirement should be checked.

8.5.5 Conclusion

The box-girder with varying thickness offers good opportunities in FRP at various aspects. The box-girder could fulfill the strength and deflection requirement and should be manufacturable. There are still some improvements which can be done to the structure, such as adjustments on the end structure to redistribute the support reactions more equally over the height. The FEA model could be

extended into more detail (line supports, volume elements). The strain criterion used could be interpreted as quite rough, probably the use of a combined stress criterion will allow a more efficient structure. The strain criterion is met pretty easily, except for the peak strains near the supports, which are not seen as a big problem. The bottom plate of the slide should be placed obliquely with an angle of 45° to prevent vibration by flow. The thickness of the slide should be reduced to make that a realistic adjustment. Therefore it could be beneficial to check the deflection requirement, because a less strict deflection requirement could save material, since there should be some strength capacity left in the structure.

This conclusion is particularly based on the hydraulic adjustment which is necessary at the bottom of the slide. It is not possible to reduce the slide thickness considerably and meet the deflection requirement with glass fibers. Therefore it doesn't matter that the deformations were calculated 55% too high in this chapter. All the variants were calculated with a too low stiffness, therefore the comparison will not change. In the next chapter, it's checked whether it's possible to reduce the deflection requirement.

9 Deflection requirement

This chapter is part of the answer of the fourth sub-research question: 'What is technically the most promising design for the slide made of FRP?'. In this chapter it's checked whether it's possible to reduce the deflection requirement.

The maximum deflection requirement influences the design of a composite slide very much, since the stiffness of the composite is lower than e.g. steel. Therefore the slide became quite thick. Such a thick slide is not feasible, since the bottom of the slide should be adjusted to an oblique bottom to prevent vibrations by flow. Therefore, in the next sections some solutions to reduce or vanish the deflection requirement are mentioned. This is possible, since nobody has to walk over or is hampered by a large deflection of the slide.

9.1 Less strict requirement

A solution to reduce the deflection requirement would be to accept a larger deflection between the sill beam and the upper beam, see Figure 9.1. Unfortunately, the slide must be able to be lifted during a multiple peak storm (when the slide could be almost fully loaded). Therefore it is not accepted to have a larger deflection between the sill beam and the upper beam, since the slide may not hit the upper beam during lifting.

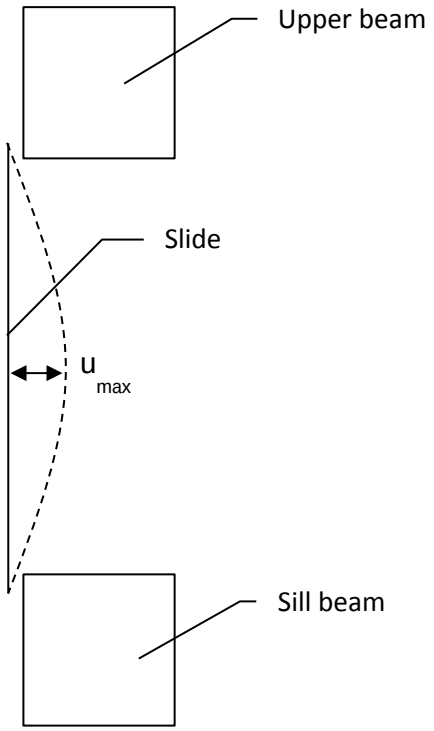


Figure 9.1 Schematic representation of a larger deflection between the sill beam and the upper beam

9.2 Rigorously solution

A rigorously solution to vanish the deflection requirement is to remove the sill beam and the upper beam and make a new, much lower, sill beam in a rectangular shape. A new composite slide could lean on the new sill beam and has no problems of hitting the sill beam or upper beam anymore. The height of the slide has to be increased in this solution.

9.2.1 Overall idea

The sill beam height could be reduced from 8 to 4 meters and the upper beam, with a height of 4.8m, will be completely removed. Therefore, the new slide should have a height of at least $4 + 11.5 + 4.8 = 20.3\ m$. Since the composite slide has a low self weight and could be designed as a hollow structure, it should be possible to make a floating slide. This slide could be closed by pumping water into the slide. The current movement works are therefore not necessary anymore. Next to that, this solution offers some other advantages:

- The height of the new slide could be increased with 1 or 2 meters to cope with the sea level rise. By assuming an extra height of 1.7 m, the total slide height becomes 22 m.
- The reduction of the sill beam height to 4 meters will increase the trough-flow opening by 10.000 m^2 (the current gross trough-flow opening is 18.000 m^2). A larger trough-flow opening of the Eastern Scheldt will increase the intertidal movement and can contribute to solve the problem of disappearing intertidal zones. Also the upper beam is removed, which blocks the trough flow opening in case of high tide. If the new slide is positioned high enough, the trough flow opening can increase even more.

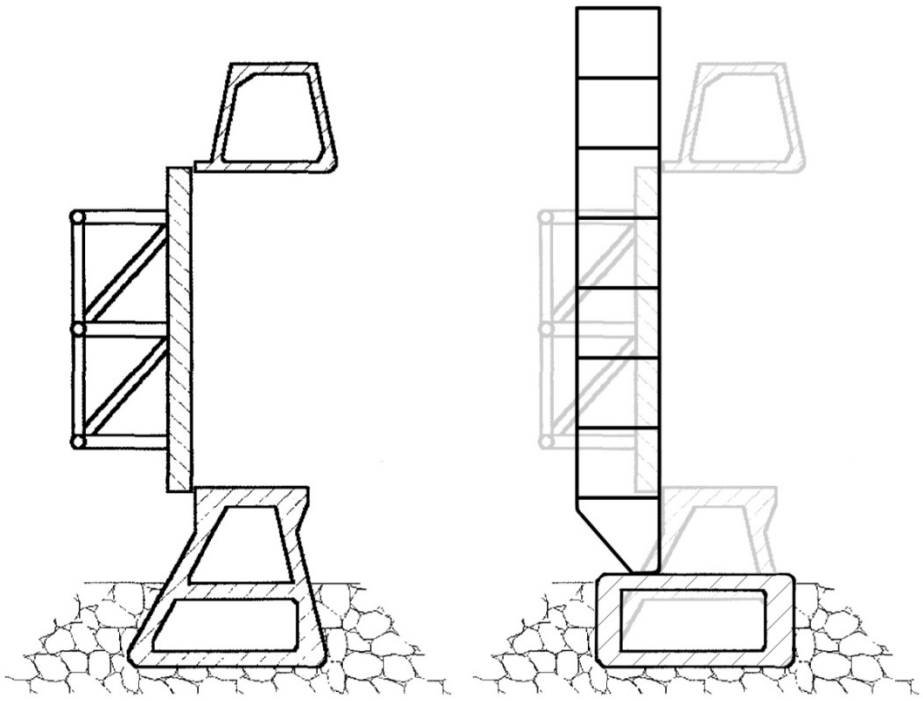


Figure 9.2 Rigorously solution of one very high slide

There are also some disadvantages. The current rabbets are not designed for a slide of 22 meters and should be adapted when this solution is chosen. Next to that, the slide could be horizon polluting, since the top of the highest slide is higher than the road (see Figure 9.3). For lower slides this effect will be lower. In the reverse way: high slides will probably block the wind, which is positive for the cars on the road.

Since, this idea looks attractive, the feasibility of the adjustments on the current barrier are checked in the next subsection.

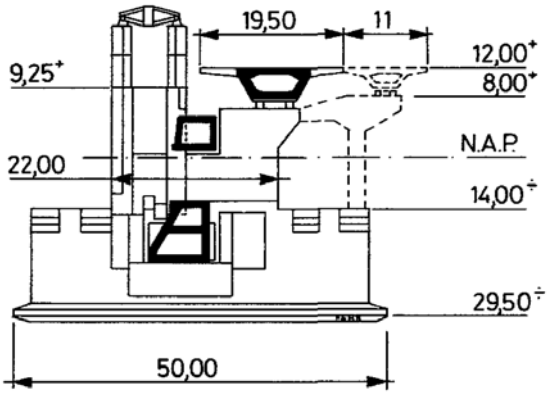


Figure 9.3 Global dimensions of a pier [27]

9.2.2 Checking the feasibility of the adjustments

Since this solution is very rigorous and results in some adjustments on the current barrier, it should be checked whether problems can occur with the adjustments which are necessary. The adjustments on the current barrier are:

1. Removal of the upper beam
2. Replacement of the sill beam
3. Adjustments on rabbet

In the next subsections each adjustment is elaborated and checked on potential problems.

9.2.2.1 Removal of the upper beam

The current upper beam was placed as last part of the barrier. The upper beam was hoisted, between the traffic box girder and the extending parts of the pier, to the supports. Therefore, the beam can be quite easily removed in the reverse way and no big problems will occur due to this adjustment.

9.2.2.2 Replacement of the sill beam

The replacement of the sill beam is intuitively seen a more complex operation than removing the upper beam. Therefore all the steps of replacement are described here. First of all, the sill beam should be removed. To remove the sill beam the stones which were put among the sill beam should be removed or moved away from the sill beam. Next to that the sand in the sill beam should probably be removed, since the weight of the sill beam including sand is probably too heavy to be hoisted. The hoist does not have to be a problem, since the sill beam was placed after the slides were placed. So the beam could be removed, although somewhat more complex than the upper beam.

After the removal of the sill beam a new rectangular lower sill beam could be prefabricated and should be placed. The new slide should lean on this new sill beam. The current sill beam has straight sides near the rabbet, see Figure 9.4, to fit in the rabbet of the sill beam and hit the bearings. The new rectangular sill beam can have a rectangular shape over the complete length with dimensions 9700 x 4000 mm. If possible, the height can be decreased more to increase the trough-flow opening even more, but that depends on the threshold which is minimally necessary between the piers.

Since the new slide should lean on the new sill beam, which top is approximately at the same level of the false floor of the current sill beam, it should be checked whether this is possible or not. In Figure 9.4 is shown that the bearing block (marking 1) of the slide is placed below the top of the current sill

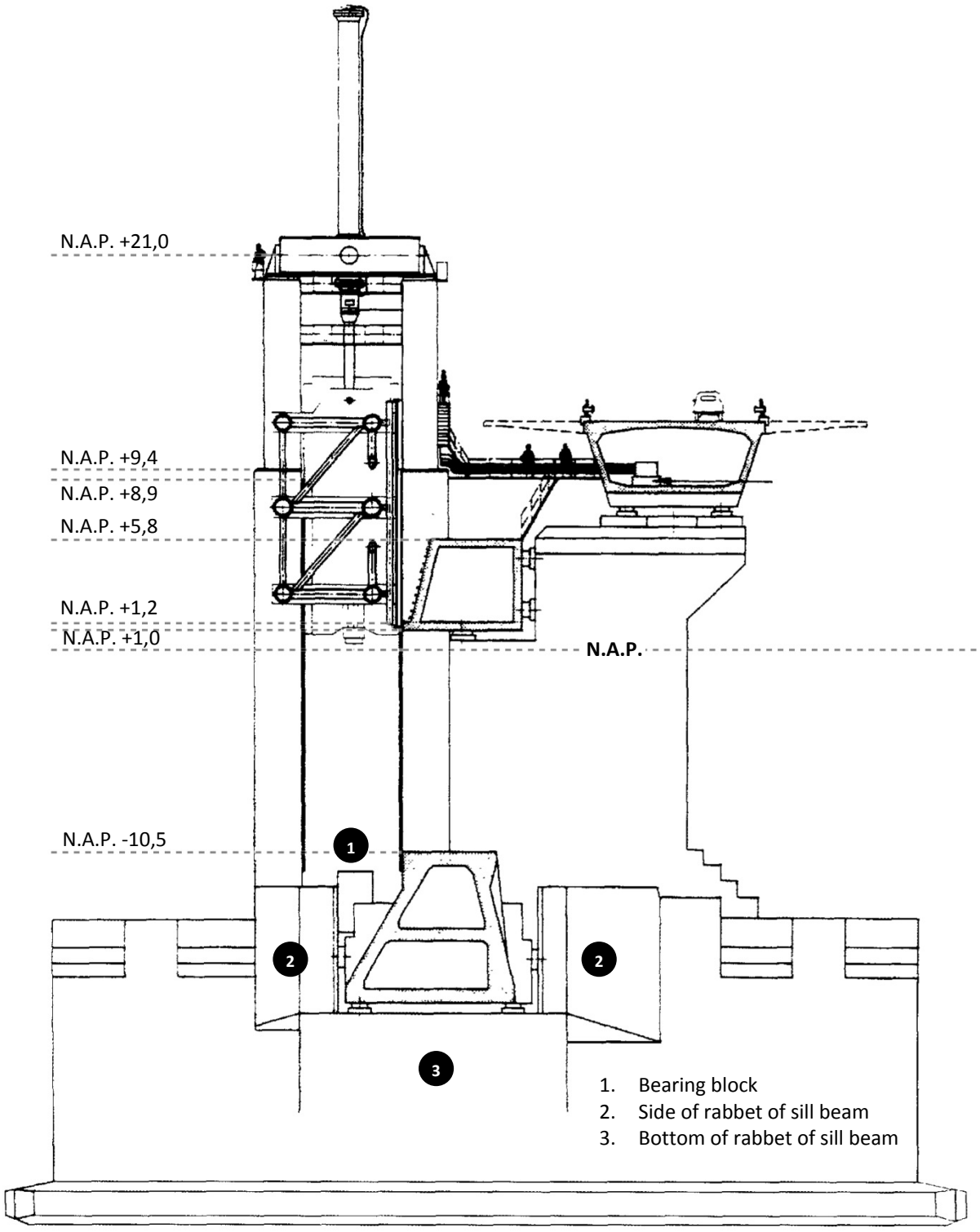


Figure 9.4 Cross-section of barrier just before the pier [22]

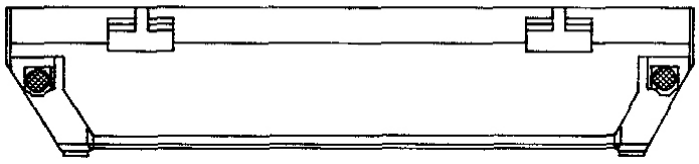


Figure 9.5 Side view of the sill beam [27]

beam, but that this block is positioned such that the top of the new sill beam will be positioned lower. Therefore this bearing block is an obstacle for the new slide, when the slide is in closed position. To solve this, the new slide should have a notch at the position of the bearing block and the bottom fence of the new slide should be positioned at the same level as the bottom fence of the current slide. Otherwise, the concrete in the rabbet should maybe be adapted.

Next to the bearing block, which is an obstacle, the side of the rabbet of the sill beam (see Figure 9.4, marking 2) could form an obstacle when the slide width at the bottom is bigger than 3 m, since the side of the rabbet is positioned approximately 3 m next to the right side of the slide. The sides of the current sill beam are inclined (see Figure 9.5), since the piers are widening to their bottom, so it shouldn't have to be a problem to adapt the side of the new slides.

The replacement of the sill beam is in particular done to contribute to solve the problem with the disappearing intertidal zones. By reducing the height of the sill beam the current trough-flow opening will be increased, as can be seen in Figure 9.6. Another solution which enables the new slide to lean on the sill beam is extending the current sill beam to a rectangular cross section (only necessary at sea side).

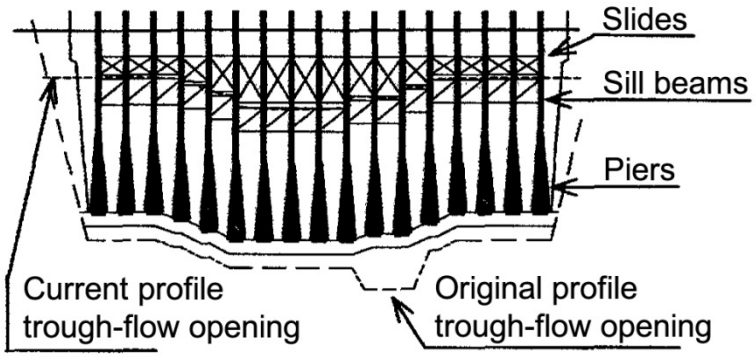


Figure 9.6 Trough-flow opening of the barrier [22]

9.2.2.3 Adjustments on rabbet

First of all, some information about the current rabbets and slide guides is mentioned, after which the adjustments on the rabbets will be investigated. The current slide guides are positioned in the rabbet up to a height of N.A.P. + 8,9 m. The rabbet itself extends to N.A.P. + 9,4 m, see also Figure 9.4. The piers are extended with some additional parts, were the cardan girders are placed on. These girders are carrying the cylinders and the slide isn't supported by these extending parts. The underside of the current slides is positioned at N.A.P. + 1,2 m when the barrier isn't closed and can be lifted another 1,2 m to facilitate maintenance. Therefore, the slide isn't supported over a height of $11.9 - (8.9 - 1.2) = 4.2\ m$ and in case of maintenance over a height of 5.4 m. That is respectively 35% and 45% of the total height of the slide which is unsupported.

It is assumed that the new slide should be supported over minimal 65% of the height, which corresponds to 14.3 m. The current guides in the rabbet have a total height of $8.9 - 1.2 = 7.7\ m$, so the rabbets should be adjusted to support the new slide. Some possibilities for that are listed below.

1. Complete floatable slide
2. Floatable slide with cylinders
3. Only lifting cylinders

Complete floatable slide

A complete floatable slide will always float on the water and will sink by pumping water into the slide. The current extending parts on the piers can be removed and the movement works are also not used in this option. The rabbets should be increased in this case minimal by 6.6 m ($14.3 - 7.7$) minus the height of the slide which is under water and minus the distance below N.A.P. + 1.2 m and the water level. This possibility offers the following disadvantages:

- Some part of the slide will always be under sea level and will therefore block a part of the trough-flow opening.
- Maintenance can be carried out difficult, since the slides are always floating.

These disadvantages make this option less attractive.

Floatable slide with cylinders

This option will re-use the current movement works and the extending parts on the piers. This hybrid option uses the floatable capacity of the slide to be able to float and sink the slide (by pumping water into the slide). When the slide is floating, the cylinders can be connected to the slide and the slide can be lifted up to a level above the water level. To be sure that the slide doesn't block the trough-flow opening and to facilitate maintenance it is assumed that the underside of the slide is positioned at N.A.P. +2.4 m. Therefore, the rabbet should be increased with minimal $14.3 - (8.9 - 2.4 + 1.2) = 6.6\,m$, since the current movement works have a reserve lifting capacity of 1,2 m. Although the minimal increase of the rabbet is 6.6 m, the rabbet and the extending part on the pier should together increase 10,1 m, which is equal to the increase of the slide height. Since it looks attractive to re-use the extending parts, the rabbet should be increased with 10,1 m, see Figure 9.7. Another possibility would be increasing the rabbet somewhat less and to switch some extending parts between different piers and construct some new (higher) extending parts. The connection between the slide and the cylinder could be a critical point in this option. Next to that, the slide weight shouldn't exceed the capacity of the lift cylinders of the slides. Since an FRP slide is probably two

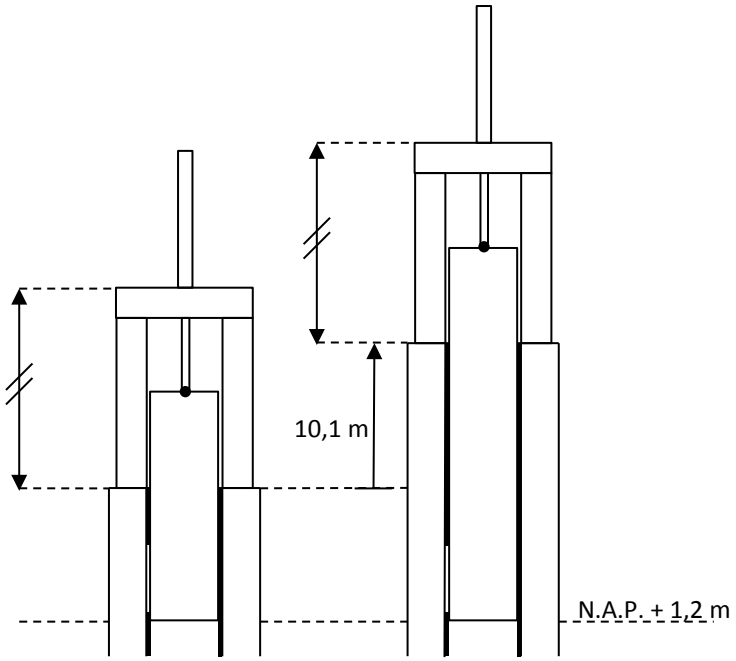


Figure 9.7 Left: current situation, right: new possibility

times as light as a steel slide, the weight of an FRP slide of double height does not reach the capacity of the lift cylinders.

Only lifting cylinders

This option makes only use of lifting cylinders to move the slides in vertical direction. The rabbet should also be increased with minimal 6.6 m, but should be, together with the increase of the extending parts, equal to the increase of the slide. The rabbets should therefore be increased also with 10.1 m, when the extending parts are re-used. The current cylinders can bring the bottom of the slides down to N.A.P. -10.5 m. In the new situation the sill beam height is decreased, therefore the top of the sill beam is positioned at N.A.P. -14.5 m. That means that the current cylinders do not have enough length to close the new slide. It would probably be too expensive to replace all the cylinders, although some of the cylinders at the lower slides can possibly be re-used.

9.2.3 Concluding

When a comparison is made between these options the hybrid option is in favor in terms of costs and the last option is in favor in terms of reliability, since the number of lifting mechanism are reduced to only the cylinders. It's clear that lifting the slide to a level above the water level is in favor, since the trough-flow opening isn't reduced in that case due to the slide. Next to that, the re-use of the current extending parts is probably in favor in terms of costs. Therefore the rabbets should be increased with 10,1 m, which is quite a tough part of reconstructing the barrier, in addition to the replacement of the sill beam. It should be checked whether it is technically feasible to increase the rabbets. Another problem of this solution is that failing of the higher slides could cause more impact, since the through flow opening is increased.

9.3 Other solutions

Other solutions which can increase the stiffness of the slide or which can reduce the deflection requirement are:

- Some part of the glass fibres can be replaced with carbon fibres. This will increase the costs of the structure, since carbon fibres are much more expensive than glass fibres.
- A camber can be applied on the FRP slide to increase the allowable deformation and meet the deflection requirement. The leakage surface of 1250 m^2 is based on water level measurements and hydraulic models of the current barrier. This value holds for a closed barrier for water levels between N.A.P. + 1.0 and N.A.P. + 3.0 m. [28] So the barrier is loaded, when the maximum leakage surface requirement holds. Therefore a camber is possible to apply.

  The camber which can be applied is limited, since a minimum camber should be applied to ensure that the slide does not hit the upper beam at full loading. The camber has also a maximum, which is caused by the maximum leakage surface of 1250 m^2 during water levels between N.A.P. + 1.0 and N.A.P. + 3.0 m. The slide deformation should be such that the leakage surface is not bigger than that. If the water level at the Eastern Scheldt is N.A.P. -0.7 m, the slide is loaded with 1.7 to 3.7 m water column (17 to 37 N/mm^2). This is roughly a third of the full loading. Therefore a camber of 100 mm is maximum possible to apply. If the water level at the Eastern Scheldt will be higher, the load will decrease, but the water pressure difference, which causes a water flow through the leakage opening, will decrease also.

- Increasing the leakage gap with the assumption that the water storage capacity of the Eastern Scheldt will be increased.

9.4 Evaluation

In this chapter different solutions are mentioned which can reduce or vanish the deflection requirement. In general, these solutions can be divided in a short or medium term solution and a long term solution. The short or medium term solution can be described as a FRP slide which can replace the current slide without adjustments on the piers or movement works. The long term solution (rigorously solution) can be described as a FRP slide for which no deflection requirement holds and for which the sill beam and the rabbets should be adapted. In [29] is mentioned the following appropriate sentence: "It is of interest to see choices for the short and medium term in relation to choices on the very long term (after 2100), when a choice on the Eastern Scheldt barrier is necessary."

By applying this sentence a choice should be made by considering both the short or medium and the long term solution. The short or medium term solution should be adapted with some improvements which were mentioned in this chapter. The long term solution takes into account the sea level rise and the problem of disappearing intertidal zones. A simple comparison in terms of cost will be made between the short or medium term and the long term solution (rigorously solution).

9.4.1 Simple comparison of costs

The slide height of the short or medium term solution is 11.9 m. The slide height of the long term solution is 22 m. To make a fair comparison, the slide height of the long term solution will be adapted, since this solution has some extra parts for the sea level rise and the problem with disappearing intertidal zones (the short or medium term solution doesn't). The remaining part of the slide is $22 - 4 - 1.7 = 16.3\ m$, see Figure 9.8. It's assumed that is should also be possible to adapt the current sill beam to enable the new slide to lean on the current sill beam. Therefore, this comparison can be made.

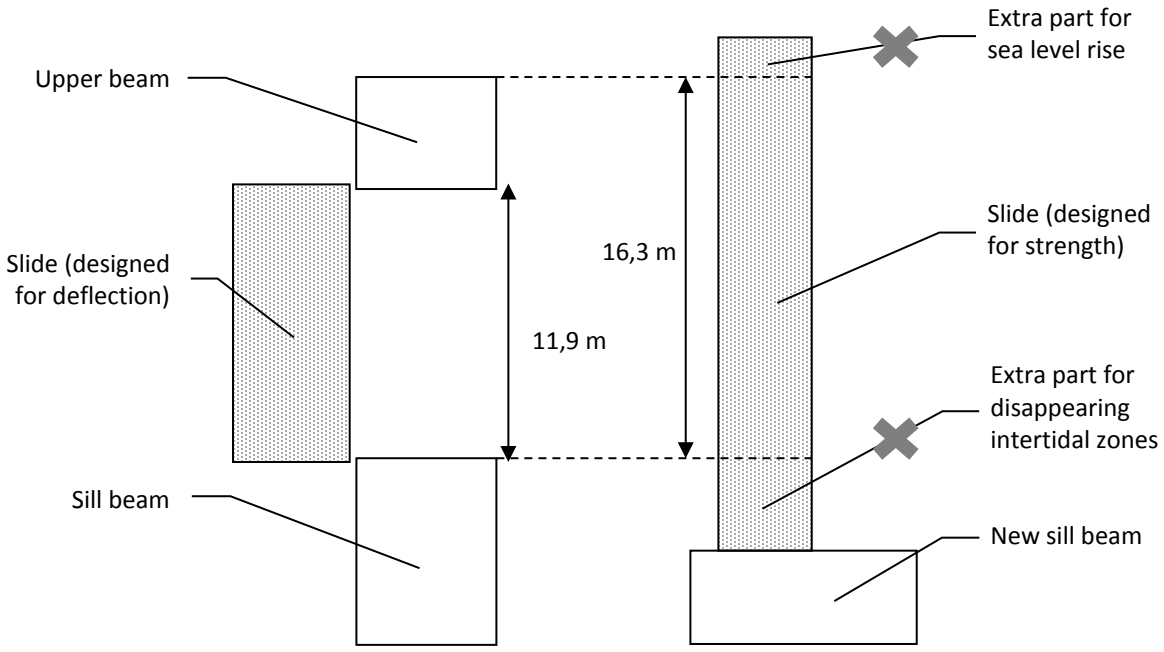


Figure 9.8 Comparison of short or medium term and long term solution

Since the slide heights of both solutions are known and the costs of a slide can be considered as pretty equally distributed over the height, it is possible to make a first comparison of costs. The height of the long term slide is $\frac{16.3-11.9}{11.9} \cdot 100 = 37\%$ higher than the slide of the short or medium term solution. The costs are displayed as an index: the short term solution has a cost index of 100 and the long term solution an index of 137. If it is possible to save $\frac{137-100}{137} \cdot 100 = 27\%$ of the material (or weight), if the costs are assumed proportionally to the weight, the long term solution would be equally in terms of costs. That means that the long term solution, which can be dimensioned on strength, could be a very attractive solution, since only 27% of the material should be saved in comparison to the short or medium term solution to get the same costs. Therefore the costs of the long term solution are calculated more precisely in the next subsection and are compared with other alternatives on the long term.

It should be noted that the costs of increasing the slide rabbet with 4.4 m are not considered in this simple comparison.

9.4.2 Comparison of costs with alternatives on the long term

In this subsection the costs of the short and medium term solution are calculated first to make an estimation of the costs of the long term solution. Thereafter these costs are compared with other alternatives on the long term, as mentioned in chapter 11.

The current FRP slide design has a volume of 96 m^3 of FRP, without the sandwich material. The total weight of this slide will be: $96 \cdot 1885 = 180960\ kg$. Therefore the total costs will be approximately 1.3 million euro per slide (for the highest slide). The average height of all the slides is 8.64 m, therefore the average costs for a slide are estimated on: $\frac{1.3}{11.9} \cdot 8.64 = 0.92$ million euro. The total costs of replacement become approximately 57 million euro.

The new slides for the rigorously solution will become $22 - 11.9 = 10.1\ m$ heigher. It is assumed that 30% material could be saved in comparison to the slide which is dimensioned on deflection. Therefore the average costs of a slide in the rigorously solution becomes: $\frac{1.3}{11.9} \cdot (8.64 + 10.1) \cdot 0.7 = 1.43$ million euro. The total costs of replacement become approximately 89 million euro.

The costs of the extra adjustments which are necessary for the rigorously solution (long term solution) are not taken into account. But when the costs of 89 million euro are compared with the costs of dike raising (1340 million euro) or building a dam (995 million euro) from chapter 11, the costs of the long term solution are quite small. Therefore, the long term solution looks also attractive when compared with other alternatives on the long term.

9.4.3 Choice of elaborating short and medium term or long term solution

In this subsection a choice is made which solution will be elaborated as final design.

The short and medium term solution should have a big thickness when this solution is made with glass fibers. This big thickness is required since the deflection requirement is very strict. But a big thickness isn't realistic, since the bottom of the slide should be adjusted to prevent vibrations by flow. Therefore the thickness of the slide shouldn't become larger than approximately 4 m.

The short and medium term solution could be improved by using carbon fibers, increasing the leakage gap or apply a camber. With a combination of these options it is probably possible to reduce the thickness of the slide. However, the slide will become more expensive, since carbon fibers should

be probably used. A concept which look quite familiar to this solution and which makes use of carbon fibers has been investigated in [4], which is actually a proof that it should be possible to reduce the thickness by making use of carbon fibers (and probably a larger leakage gap).

The long term solution could probably have a lower thickness, since the slide could be dimensioned on strength. Therefore this slide could possibly make use of glass fibers, which are much cheaper than carbon fibers. Therefore, it is much more interesting to elaborate the long term solution into more detail, to investigate the feasibility of this solution. The technical feasibility to improve the rabbets and replace the sill beam will not be investigated. The final design of the long term solution (rigorously solution) is carried out in the next chapter.

10 Final design

This chapter is part of the answer of the fourth sub-research question: 'What is technically the most promising design for the slide made of FRP?'. In this chapter, the design which was chosen in chapter 9 is elaborated into more detail. First of all, some adjustments on the material properties are described. Thereafter, some improvements on the structure are described, after which the final design is described and the FEA results are discussed. Finally, some notes are made on the manufacturability of the slide.

10.1 Adjustments on material properties

Some of the material properties which have been used in the previous chapters have been adjusted in the final design. These adjustments are described in the next subsections.

10.1.1 Safety factors

In chapter 7, the material safety factor γ_{m2}, which takes uncertainties into account regarding the material properties due to the combination of parts, depending on the manufacturing process, was estimated at 1.4 since the manufacturing process wasn't fully selected. From the suitable manufacturing processes, see Table 7.2, the process of vacuum assisted resin injection is now chosen, because the relative low equipment and production costs. This manufacturing process is also a lot used in the construction of FRP bridges and should be suitable for manufacturing composite slides.

Since the final manufacturing process is now selected, the material safety factor γ_{m2} can be determined. This factor is according to [19] equal to 1.2. Thereby the total material safety factor is: $\gamma_m = 1.62$.

10.1.2 Lamella properties

The lamella stiffness properties which will be used in ULS and SLS are mentioned in Table 10.1. In the finite element program Dlubal RFEM it isn't handy to use different lamella stiffnesses as input. Therefore the lamella stiffness properties for ULS are used as input values. These input values are afterwards, for each load combination, adjusted for SLS load combinations with a reduction factor of $\frac{1}{\gamma_c} = \frac{1}{1.43} = 0.699$.

Table 10.1 Lamella stiffness properties in ULS and SLS

	$E_1\ (GPa)$	$E_2\ (GPa)$	$G_{12}\ (GPa)$	ν_{12}
ULS	43,2	14,1	4,34	0,27
SLS	30,2	9,86	3,03	0,27

The lamella stiffness properties used in chapter 8 were $\frac{33.2-19.48}{19.48} \cdot 100\% = 55\%$ too low. Therefore it can be estimated that the deformations were approximately 55% too high. This will have no effect on the conclusions, since it was not possible to reduce the slide thickness considerably and meet the deflection requirement at the same time by using glass fibres.

10.1.3 Strain criterion

Since the material safety factor and the conversion safety factor are determined, the strain limit can be calculated. In ULS the following strain criterion will be used, as was earlier specified in Table 7.5:

$$\varepsilon_{max} = \frac{1.2}{\gamma_m \cdot \gamma_c} = \frac{1.2}{1.62 \cdot 1.43} = 0.52\% \quad (10.1)$$

10.1.4 Core properties

A PU foam core will be used in the final design. The properties of the core are taken from [30] and are mentioned in Table 10.2. In real, some vertical stiffeners are present between the foam, but these stiffeners are not taken into account in these stiffness properties. In [30] no information was provided about these vertical stiffeners, so the effective stiffness of PU foam and stiffened couldn't be calculated. Therefore, the core would react stiffer than in the FEA model. It's assumed that the maximum elongation of the core material will be greater than the strain limit (see also Table 7.3), therefore the strain limit of 0.52% could be used to check the core material.

Table 10.2 Stiffness properties foam core

Ex (MPa)	Ey (MPa)	Ez (MPa)	Gxy (MPa)
310	310	310	120

10.2 Structure in general

The final structure has a height of 22 m and a thickness of 4 m (see Figure 10.1), since the bottom of the slide should be inclined. The bottom of the slide is positioned at N.A.P. -14.5 m in closed position and at N.A.P. + 2.4 m in open position. The inclined part is 4 m height and has 2 horizontal plates between the outer walls (every 2 m). The rest of the slide is divided into 6 pieces of each 3 m height, which is based on an estimation of the author. It is still possible to optimize the number of horizontal plates, but that's outside the scope of this research.

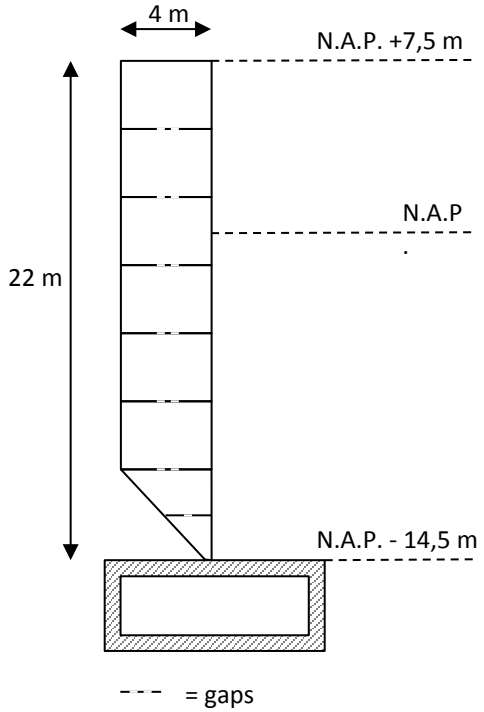


Figure 10.1 Overview of dimensions of final structure in closed position

The slide height is based on the current water defense height and an extra part due to the sea level rise. It's assumed that the new slides should be lifted with a hybrid system. This system consists of

the current movement works and a pumping system to fill the slide with water as was described in chapter 9. This pumping system is not elaborated into more detail in this research.

Since the slide should be filled with water to lower the slide to the sill beam, there are holes in the horizontal plates of the slide, except for the upper one. This will ensure a much more favorable water pressure load, which has been calculated in appendix E. The upper horizontal plate is placed at the top of the slide, because rain water can accumulate when the plate is placed lower.

Since the thickness of the slide is reduced to 4 m, it wasn't attractive anymore to make a thickening in the middle of the slide. That thickening would probably be such small, that the positive effect was small and that the manufacturing costs were quite high. Therefore, there is chosen to make a straight box girder with a thickness of 4 m over the total length.

10.3 Structural improvements

In this section the structural improvements are described which are made between the variant in chapter 8 and the final model which is described in section 10.4.

10.3.1 Decreasing the peaks in the strains

In chapter 8 there were peaks visible in the strains near the supports. An attempt was made to reduce these peaks as much as possible. The results of some different FEA models will be described in the next paragraphs.

Initially, the supports at both sides were modeled as infinity stiff line supports. Since these line supports give very high peaks in the support reactions near the horizontal plates and therefore high peaks in the strains, these line supports are modeled with a finite stiffness of 10^6 kN/m^2 (approximately the stiffness of a rubber bearing). In that model the peaks in the support reactions are reduced, which is shown in Figure 10.2. To model the structure in an even better way, the line support is replaced with a surface support with a supporting width of 200 mm. The surface support has the same finite stiffness. The support reactions of this model are also shown in Figure 10.2. It can be seen that the peaks are reduced even further, and that the support reactions are quite equally distributed over the height.

The maximum strains, which occur anywhere in the structure, of these three models are shown in Table 10.3. The maximum strains ε_y and ε_{xy} are quite well reduced in these models. The maximum strain ε_x isn't reduced, since that maximum value is located in the middle of the slide and does not change much when the side supports are adapted. The last two models in the table are described in the next paragraph.

Table 10.3 Maximum strains in the FEA models (not corresponding to one special point)

Support type	Stiffness (kN/m^2)	ε_x (%)	ε_y (%)	ε_{xy} (%)
Line support	infinity stiff	-0,52	-1,10	-1,69
Line support	1000000	-0,51	-1,08	-1,16
Surface support	1000000	-0,51	-0,75	0,76
End structure	dna	-0,52	-0,76	0,67
Spring support at bottom	dna	-0,52	-0,40	-0,57

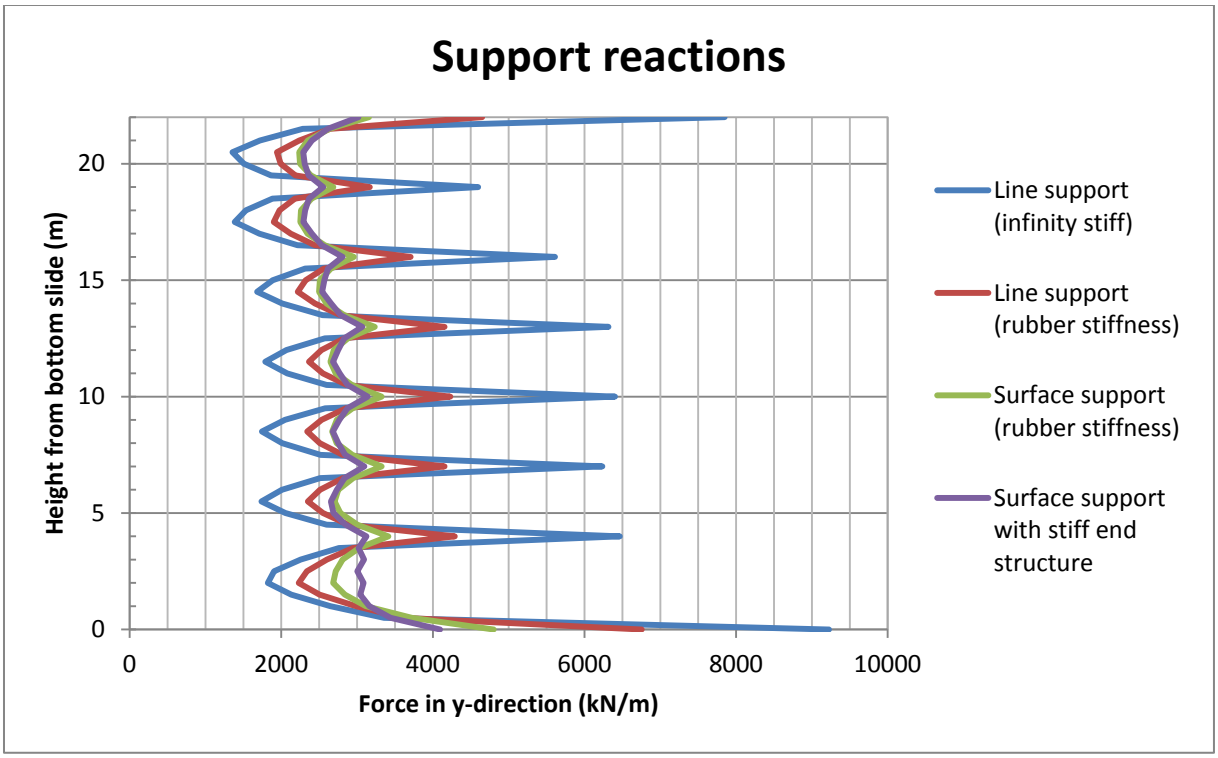


Figure 10.2 Support reactions in different FEA models

In the first three models only the side supports of the slide (green in Figure 10.12) were adapted. Thereafter, the sides of the structure were stiffened with some extra horizontal plates and an extra vertical plate at the bottom, see Figure 10.3. The support reactions of this model are shown in Figure 10.2. The support reactions are in particularly changed at the bottom of the slide. The extra horizontal plates cause a more uniform distribution of the support reaction at the bottom of the slide. This causes a reduction in the strain ε_{xy} , as shown in Table 10.3.

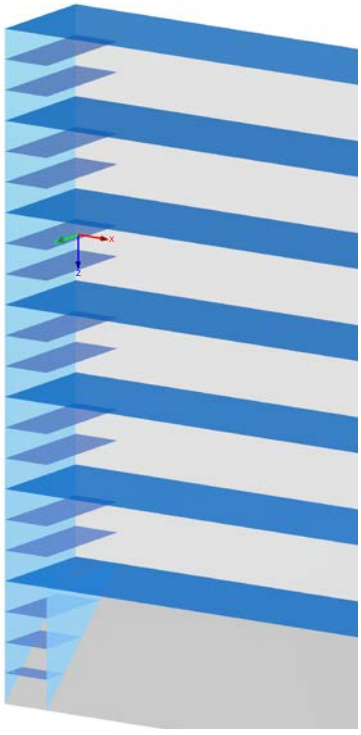


Figure 10.3 Stiffened end structure

The sides are now modeled in reasonable detail. Therefore, other improvements were carried out to reduce the strain peaks. The support at the bottom of the slide (blue in Figure 10.12) was until now modeled as an infinity stiff line support. This support is adapted to a line support with a finite stiffness of 10^6 kN/m^2. The maximum strains in the structure are reduced, see Table 10.3.

The left surface support was fixing also the translations in longitudinal direction. This longitudinal support is replaced by a nodal support at the top of the slide.

10.3.2 Addition of gaps in horizontal plates

Since the strain peaks are reduced a lot now, the gaps in the horizontal plates should be added to the structure. Initially, there were 7 gaps added to each plate with a radius of 1m. The gaps were positioned in the center of the slide with a spacing of 4m. The middle part of the slide takes the bending moment, therefore some material close to the neutral axis could be removed. The results of this addition are shown in Table 10.4. During optimization of the amount of fibers and the fiber direction the strains ε_x and ε_{xy} do not meet the strain criterion, see Figure 10.5 and Figure 10.6. Therefore, there is chosen to decrease the radius of the gaps to 0.75 m, since more material should be present to meet the strain criterion. The outer gaps are adjusted to a radius of 0.5 m, see Figure 10.4. These situations are shown in Table 10.4.

Table 10.4 Maximum strains in the FEA models (not corresponding to one special point)

Model	Gaps	Radius	ε_x (%)	ε_y (%)	ε_{xy} (%)
Large gaps	Situation 1	R=1.0m	-0,52	-0,39	0,57
Adjustment on fibers with large gaps	Situation 1	R=1.0m	-0,54	-0,37	0,65
Adjustments on fibres with smaller gaps	Situation 2	R_1=0.75m, R_2=0.5m	-0,52	-0,37	0,51

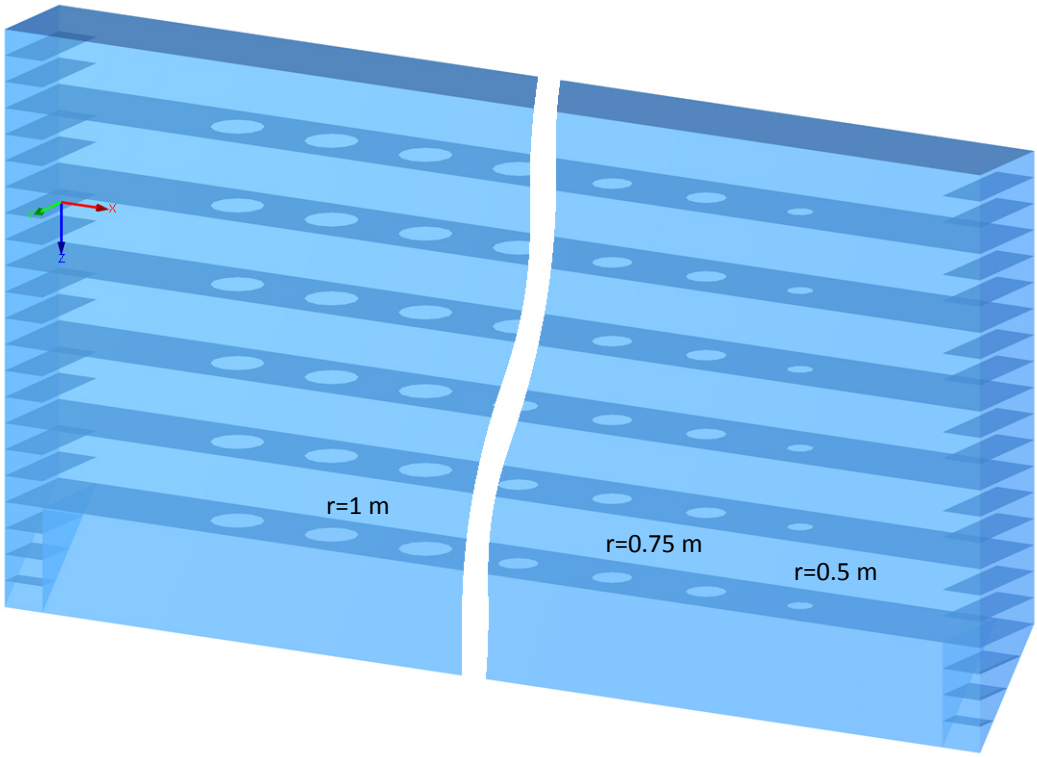


Figure 10.4 Structure with gaps (left: 1st situation, right: 2nd situation)

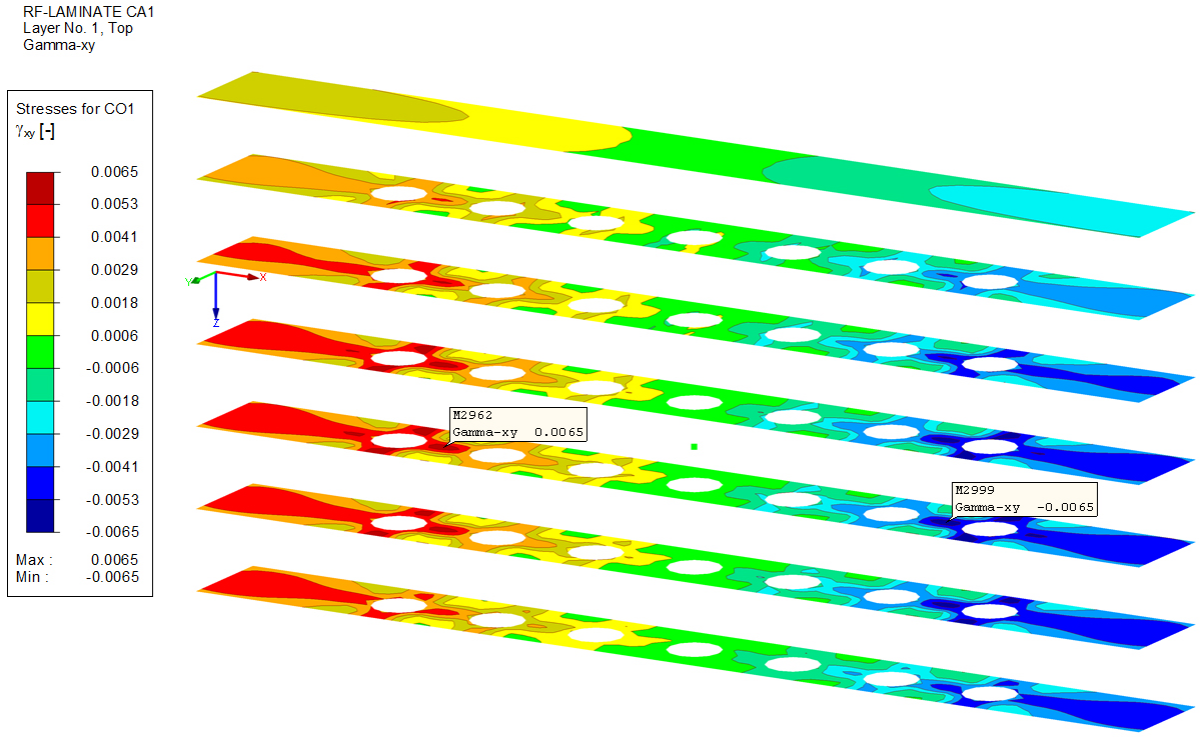


Figure 10.5 Strain ε_{xy} in optimized model in situation 1

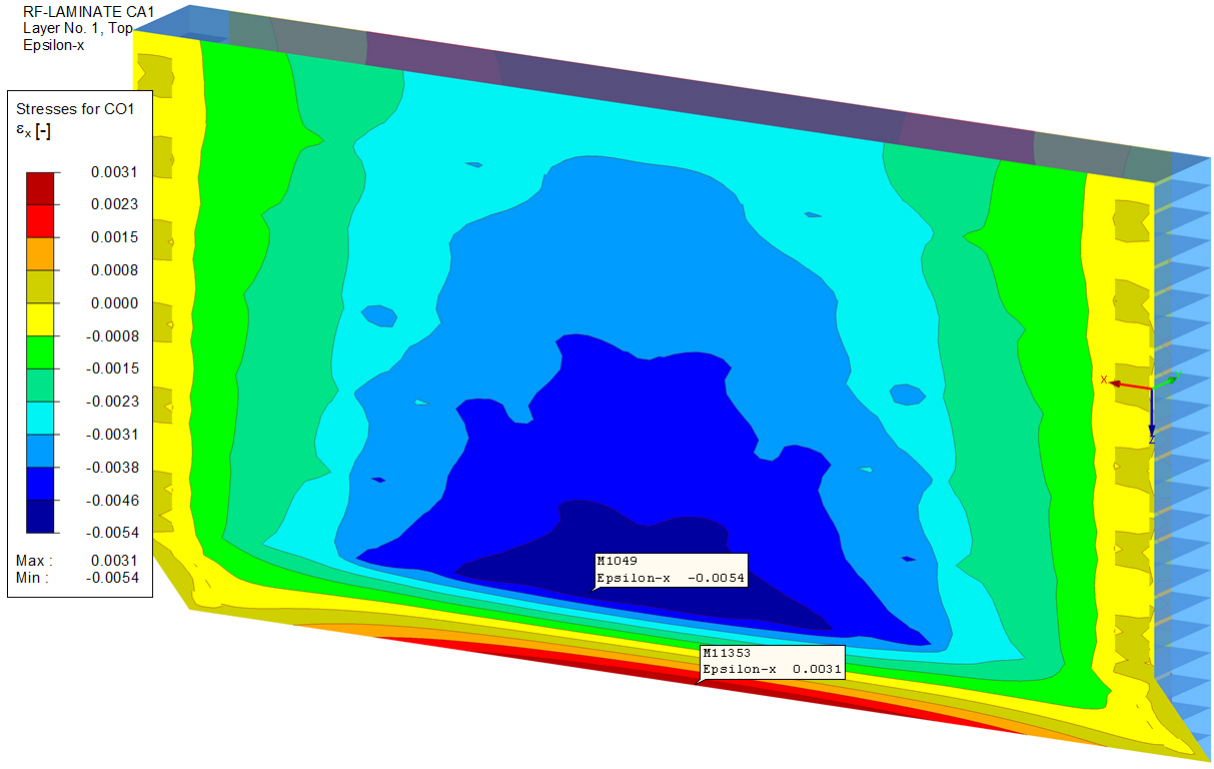


Figure 10.6 Strain ε_x in optimized model in situation 1

10.3.3 Optimizing the laminates

Since the structure is finalized by modeling the stiff end structure and adding the gaps in the horizontal plates, the laminates could be optimized further. The skin thickness of the outer sandwiches is initially estimated with a hand calculation. This calculation was based on the normal forces in these sandwiches, which were calculated with: (f = total slide thickness)

$$N = \frac{\frac{1}{8} \cdot \gamma_Q \cdot q \cdot l^2}{f} = \frac{\frac{1}{8} \cdot 1.5 \cdot 100 \cdot 41.3^2}{4} = 8000\ kN/m \tag{10.2}$$

The total skin thickness is calculated with:

$$t = \frac{N}{\sigma_{max}} = \frac{8000 \cdot 10^3}{150 \cdot 10^3} = 53\ mm \quad \rightarrow \quad h_s = \frac{t}{2} = 26.5\ mm \tag{10.3}$$

The final skin thickness used in the final design is 34 mm. The maximum normal force in the structure for the load case positive drop (ULS) was 10800 kN/m. Therefore the skin thickness is somewhat bigger than the hand calculation (of course the estimation of the maximum stress of 150 N/mm^2 is also a cause for that).

The thickness of the core material is also estimated with a hand calculation. First of all, the bending moment M_y is calculated. The length l is assumed to be equal to 4 m.

$$M_y = \frac{1}{12} \cdot \gamma_Q \cdot q \cdot l^2 = \frac{1}{12} \cdot 1.5 \cdot 100 \cdot 3^2 = 113\ kNm/m \tag{10.4}$$

The moment of inertia can be calculated as:

$$I_{yy} = \frac{1}{2} \cdot h_s \cdot b \cdot (h_c + h_s)^2 \tag{10.5}$$

From the following equation the unknown parameter h_c can be calculated:

$$\sigma_{max} = \frac{M_y \cdot (h_c + h_s)}{I_y} \tag{10.6}$$

Solving this equation, results in $h_c \geq 19\ mm$.

Finally, the core thickness is chosen equal to 50 mm, to meet the strain criterion according to the FEA model. The maximum moment M_y in the outer sandwiches was somewhat bigger in the FEA model than the value estimated with a hand calculation. To lower the moment M_y in the inclined plate at the bottom of the slide, there is an extra horizontal plate added. The strain ε_y of the model without that extra horizontal plate is shown in Figure 10.7 and of the model with an extra horizontal plate in Figure 10.8. The strain is decreased a lot due to the addition of the extra horizontal plate.

10.3.4 Adding some additional load cases

To finalize the design the number of load cases was extended. Also ice loading, collision loading and vertical wave impact loading is considered in the final design. That means, that the results mentioned in the previous subsections were based on the load cases positive drop en negative drop only.

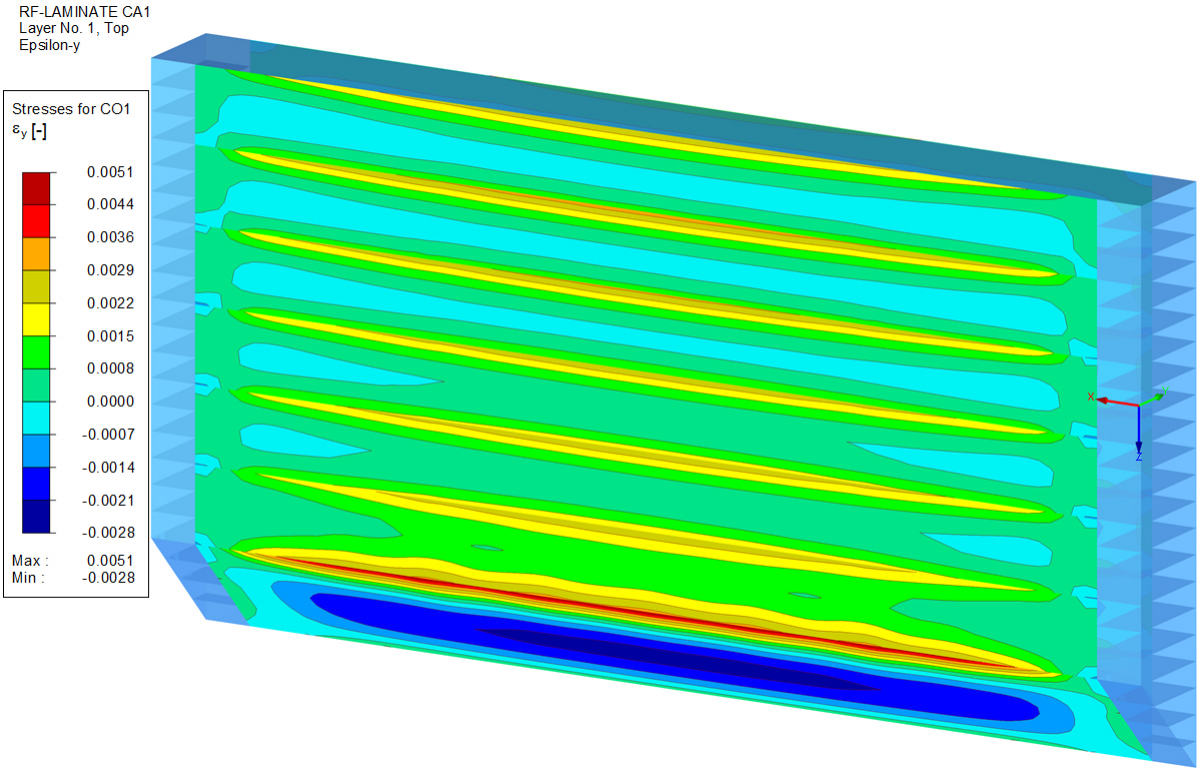


Figure 10.7 Strain ε_y in model without extra horizontal plate

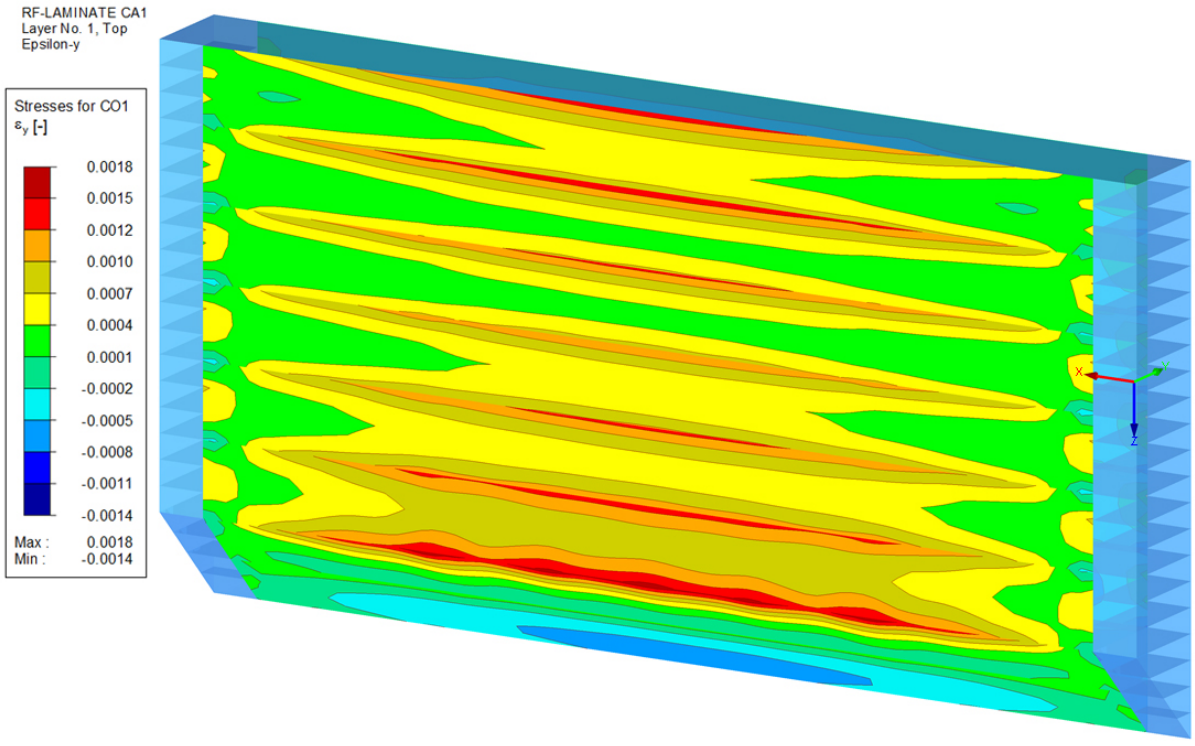


Figure 10.8 Strain ε_y in model with extra horizontal plate

10.4 Final FEA model

The final FEA model is described in this section, the results are described in the next section. The dimensions, constraints, load cases, load combinations and laminate surfaces are mentioned in the next subsections.

10.4.1 Dimensions

The dimensions of the structure are mentioned in Figure 10.9 to Figure 10.11. The theoretical span length of the slide is 41.3m, which is the length between the mid points of the surface supports at both sides. The full width of the slide is 41.5m.

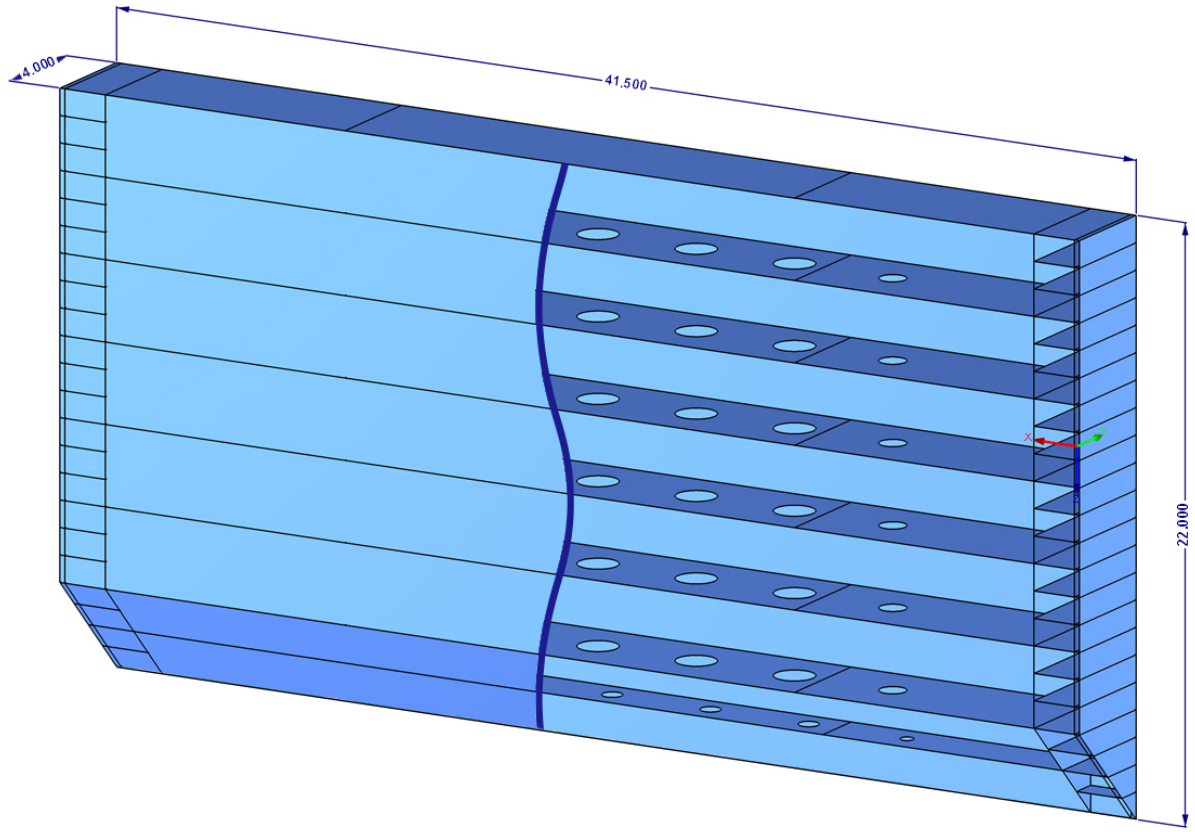


Figure 10.9 3D view of the FEA model of the structure with dimensions

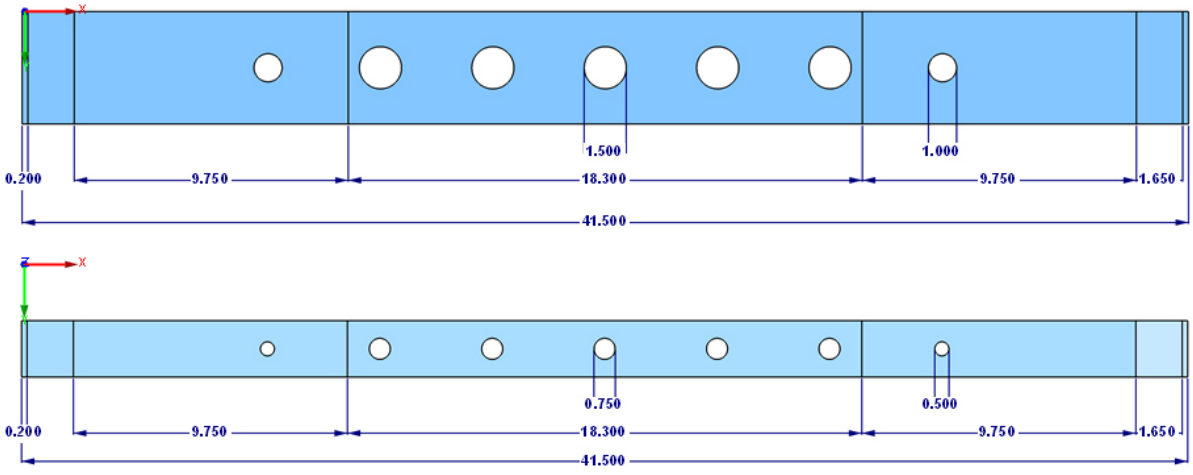


Figure 10.10 Top views of the horizontal plates with gaps

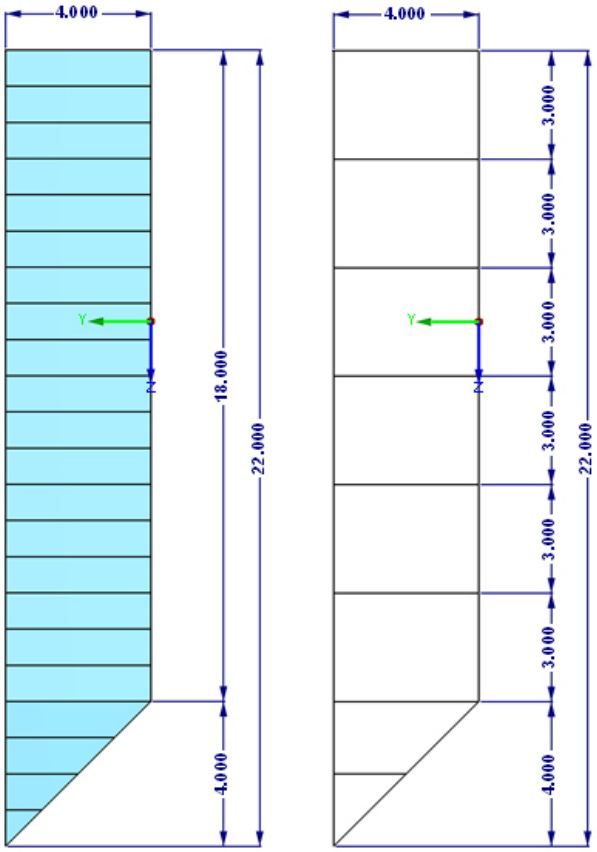


Figure 10.11 Cross-sections of the slide with dimensions

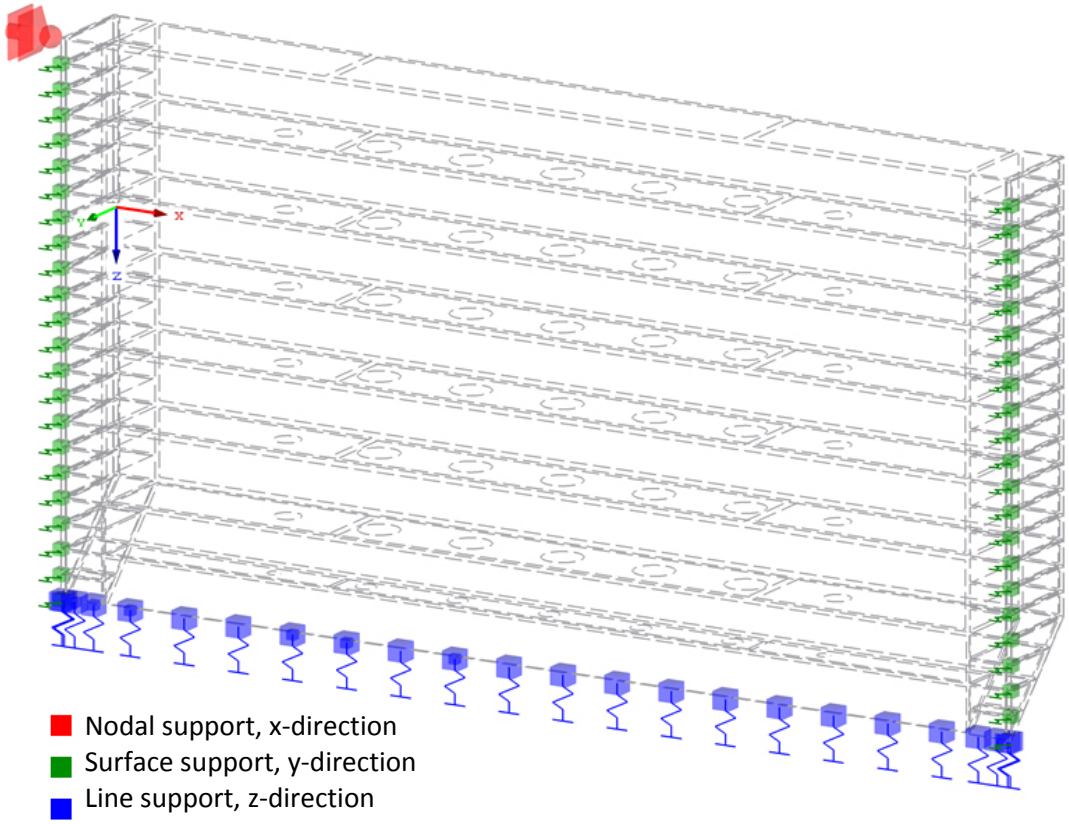


Figure 10.12 Constraints of the final structure

10.4.2 Constraints

The constraints which are used in the final model are shown in Figure 10.12. There is one nodal support (red) present to prevent translations in x-direction. Both surface supports (green) prevent the translations in y-direction and a line support (blue) is placed to prevent translations in z-direction. The width of the surface support is 200 mm.

10.4.3 Load cases

The load cases which are considered in the final design are shown in Table 10.5. These loads are visualized in Figure 10.13 to Figure 10.16. These loads are further specified in appendix E.

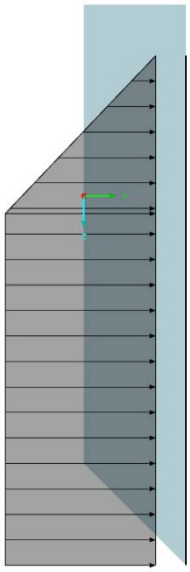


Figure 10.13a Water pressure load positive drop (LC1)

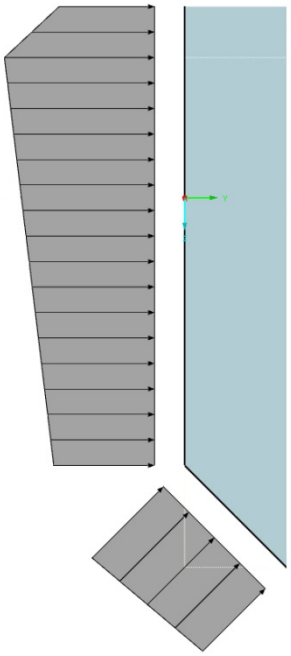


Figure 10.13b Wave pressure load positive drop (LC2)

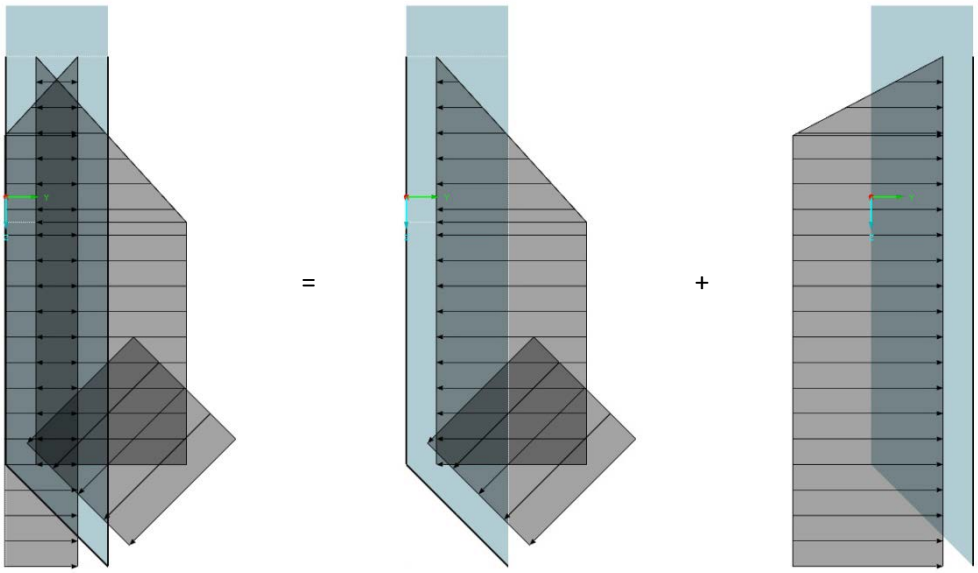


Figure 10.14 Water pressure load negative drop (LC2) Left: total loading, middle: water pressure on outer wall, right: water pressure on inner wall

Table 10.5 Overview of load cases

Load nr	Description
LC1	Water pressure difference positive drop
LC2	Wave pressure positive drop (wave crest)
LC3	Self weight
LC4	Water pressure difference negative drop
LC5	Water pressure negative drop (wave trough)
LC6	Ice
LC7	Collision
LC8	Wave impact

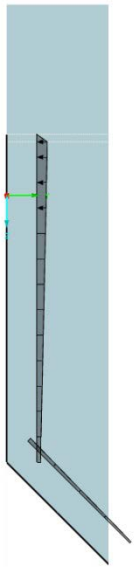


Figure 10.15a Wave pressure load negative drop (LC5)

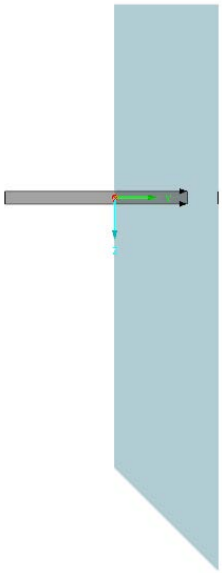


Figure 10.15b Ice load (LC6)

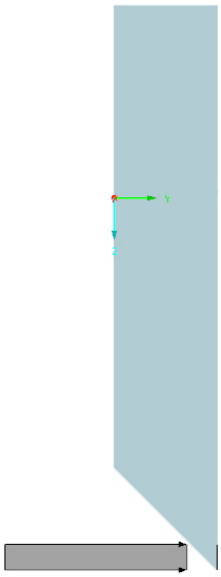


Figure 10.16a Collision load (LC7)



Figure 10.16b Wave impact load (LC8)

10.4.4 Load combinations

The load combinations which are considered are shown in Table 10.6. This table shows which loads are combined and which safety factors are used. The most important load combinations for the design are positive and negative drop (ULS).

Table 10.6 Overview of load combinations

Comb nr.	Description	Type	Loads
CO1	Positive drop	ULS	1.25 LC1+1.65 LC2+1.25 LC3
CO2	Positive drop	SLS	LC1+LC2+LC3
CO3	Negative drop	ULS	1.25 LC4+1.65 LC5+ 1.25LC3
CO4	Negative drop	SLS	LC4+LC5+LC3
CO5	Ice	ACC	LC1+LC6
CO6	Collision	ACC	LC1+LC7
CO7	Wave impact	ULS	1.25 LC1+1.65 LC8

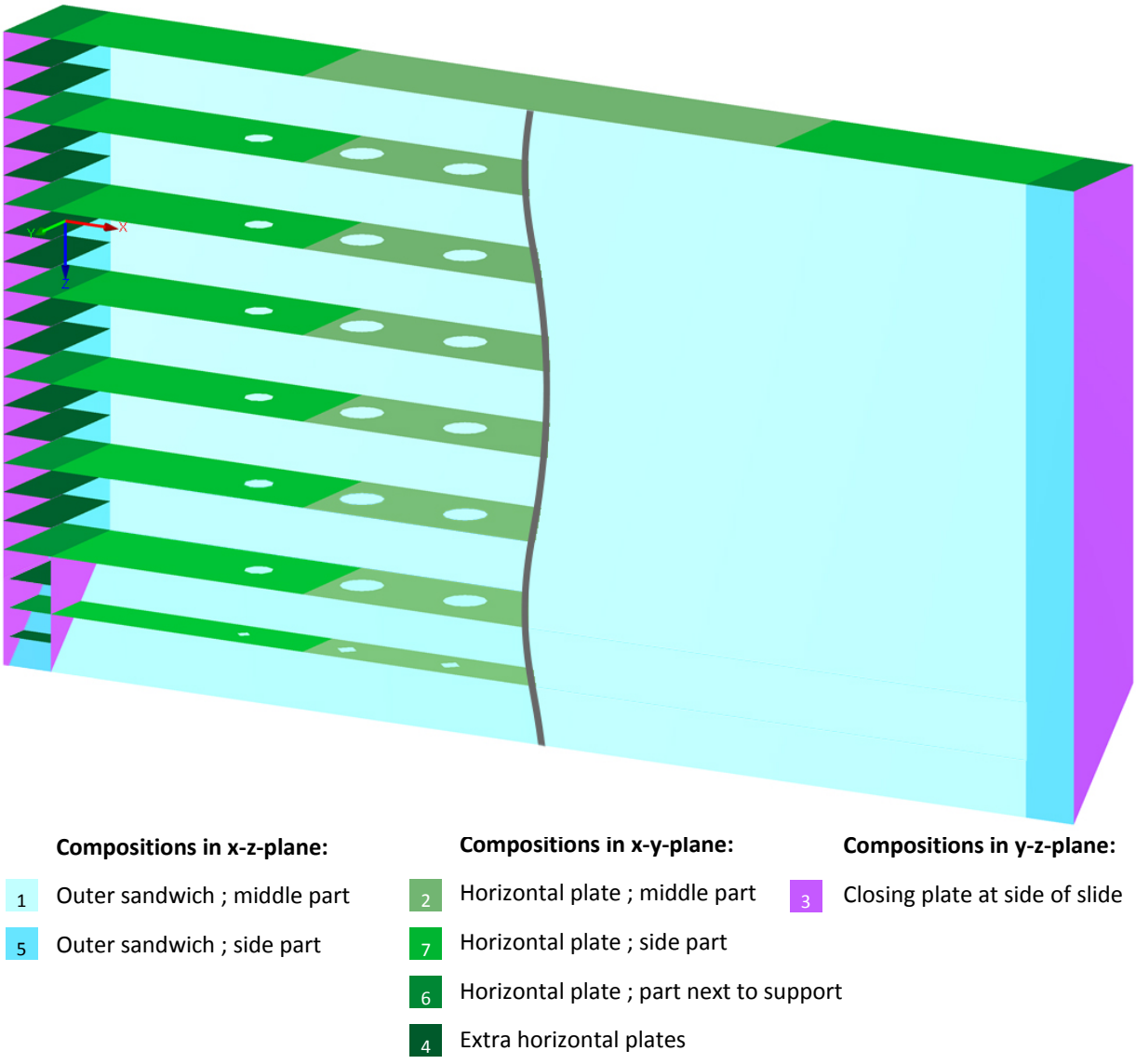


Figure 10.17 Overview of compositions in structure (composition number is shown in legend)

10.4.5 Laminate surfaces

The FEA model consists of different surfaces which form together the total structure. All these surfaces are assigned to a composition (stacking of lamellas). The different compositions are shown in Figure 10.17.

The layers of each composition are shown in Table 10.7. For each layer it's mentioned whether this layer has the properties of the core material or of a lamella. For each composition the thickness and direction of each layer are mentioned.

Table 10.7 Layers of each composition (L=laminate nr., t=thickness,d=direction)

Composition no.		1		2		3		4		5		6		7	
L	Properties	t	d	t	d	t	d	t	d	t	d	t	d	t	d
1	Lamella	18.7	0	6.0	0	7.0	45	5.0	0	5.1	0	3.6	0	3.6	0
2	Lamella	5.1	90	6.0	45	7.0	-45	5.0	90	5.1	90	13.2	-45	8.4	45
3	Lamella	5.1	-45	6.0	-45	3.0	0	5.0	-45	11.9	-45	3.6	45	8.4	-45
4	Lamella	5.1	45	6.0	90	3.0	90	5.0	45	11.9	45	3.6	90	3.6	90
5	Core	50.0	0	50.0	0	50.0	0	50.0	0	50.0	0	50.0	0	50.0	0
6	Lamella	5.1	45	6.0	90	3.0	90	5.0	45	11.9	45	3.6	90	3.6	90
7	Lamella	5.1	-45	6.0	-45	3.0	0	5.0	-45	11.9	-45	3.6	45	8.4	-45
8	Lamella	5.1	90	6.0	45	7.0	-45	5.0	90	5.1	90	13.2	-45	8.4	45
9	Lamella	18.7	0	6.0	0	7.0	45	5.0	0	5.1	0	3.6	0	3.6	0

10.5 FEA Analysis

The results of the FEA analysis are described in this section. First of all the force distribution in the slide is mentioned, where after the deformations and strains in the structure are mentioned.

10.5.1 Force distribution

The force distribution is only mentioned for the load combination positive drop (ULS). This load combination is decisive above the other load combinations, therefore the other ones are not mentioned here. The results of the other load combinations can be found in appendix F. The force distributions in the outer walls are shown in Figure 10.18 to Figure 10.22. The force distribution of the horizontal plates and the vertical end plates are shown in Figure 10.23 to Figure 10.25.

The maximum normal force in x-direction (N_x) in the outer walls in compression is 10800 kN/m (see Figure 10.18). This value is somewhat higher than the value calculated with a hand calculation in subsection 10.3.3. This is probably caused by the inclined bottom of the slide. The bottom of the outer wall at North Sea side is therefore loaded heavier.

The maximum normal force in x-direction (N_x) in the outer walls in tension is 7110 kN/m. The Eastern Scheldt side of the slide is in tension. This tensile force is quite equally distributed over the height of the slide. The upper part is somewhat lower loaded, since the water pressure load doesn't start at the top of the slide, since the current decisive water levels were used and not updated to cope with the sea level rise.

The final moments M_y in the outer wall (see Figure 10.22) are comparable with the hand calculation in subsection 10.3.3.

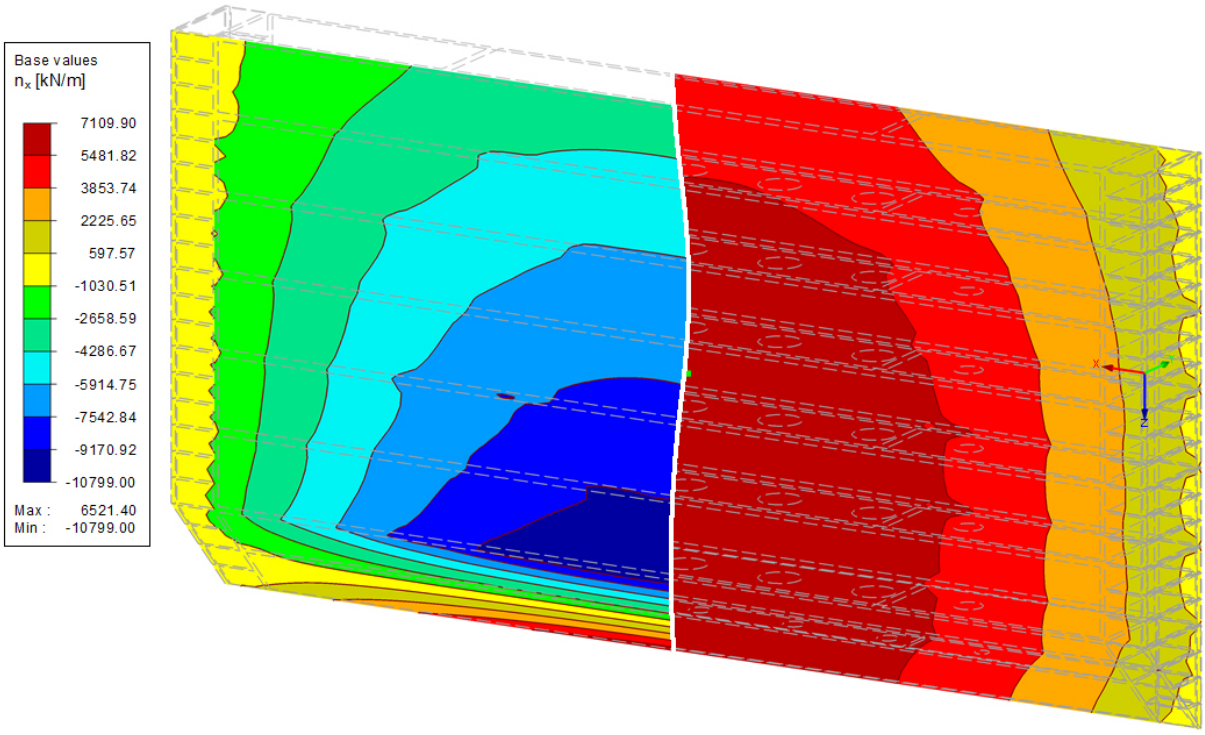


Figure 10.18 N_x in outer walls (ULS positive drop)

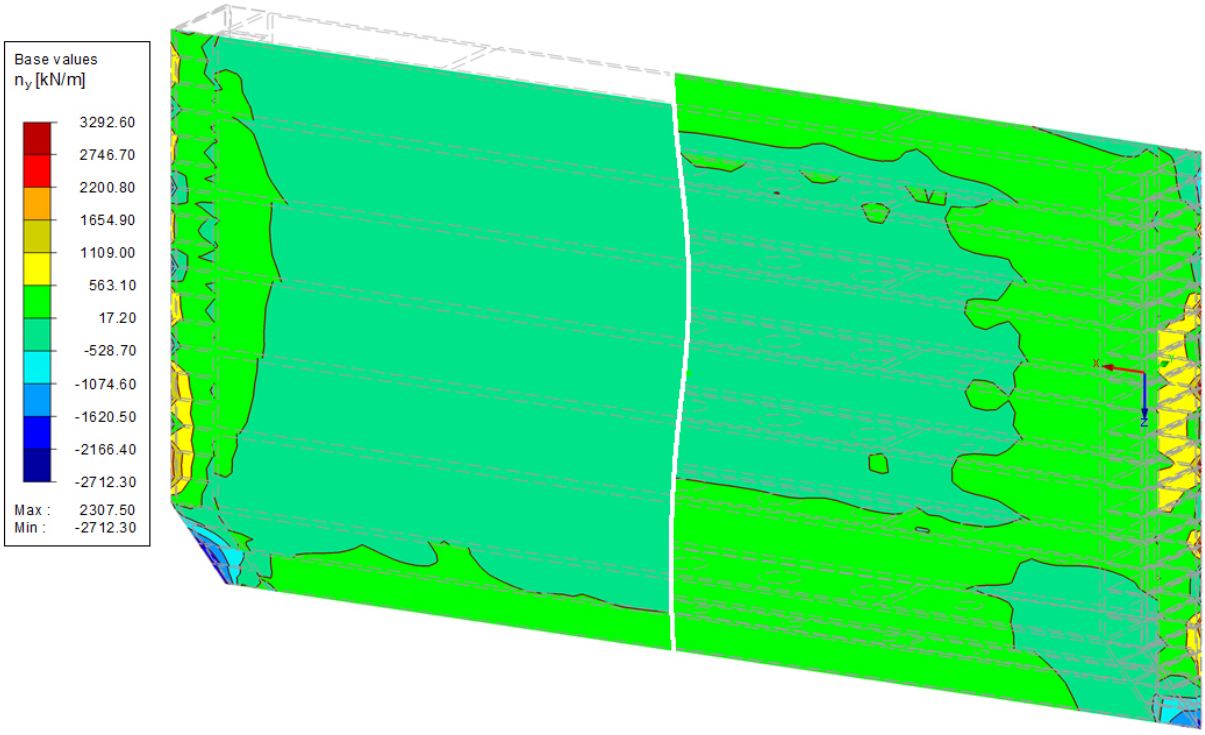


Figure 10.19 N_y in outer walls (ULS positive drop)

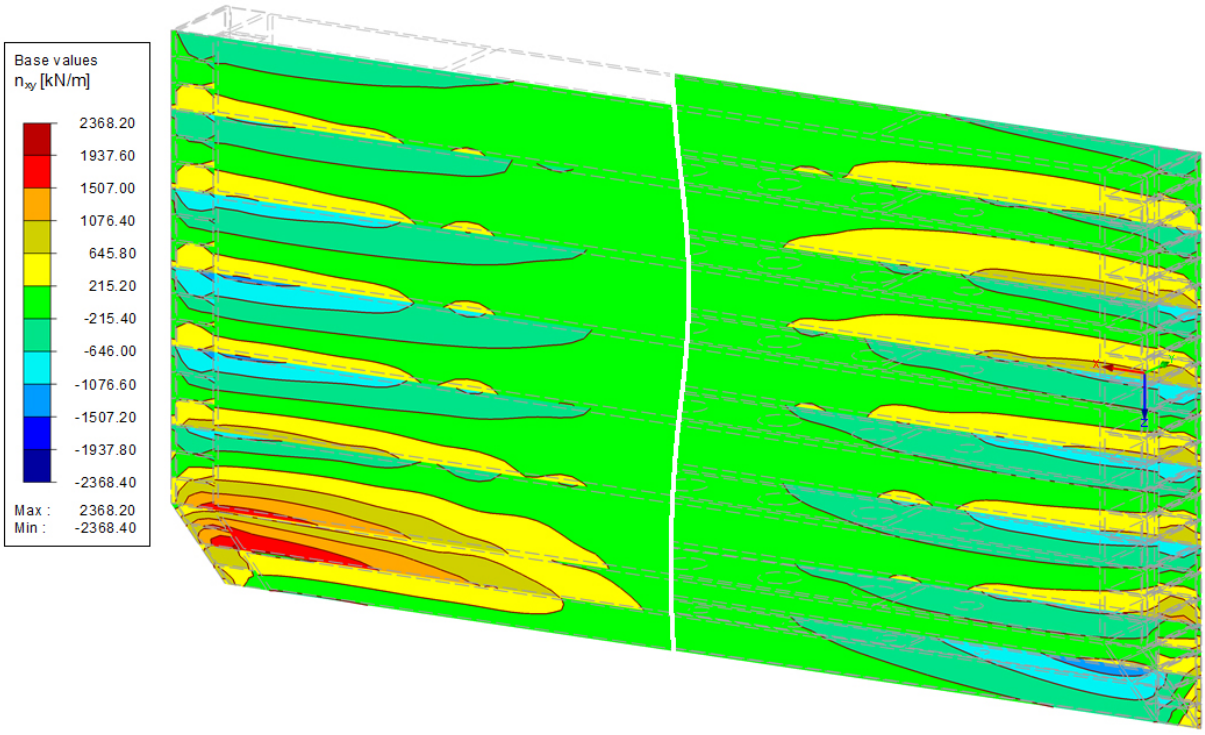


Figure 10.20 N_{xy} in outer walls (ULS positive drop)

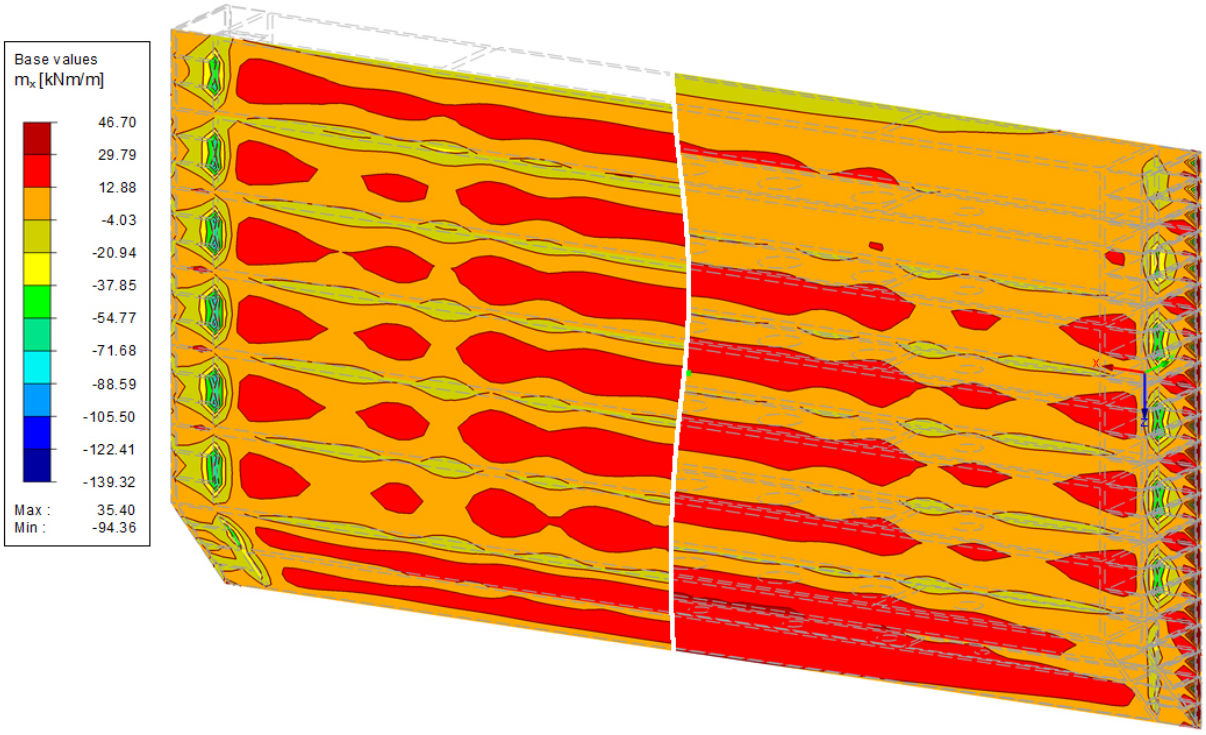


Figure 10.21 M_x in outer walls (ULS positive drop)

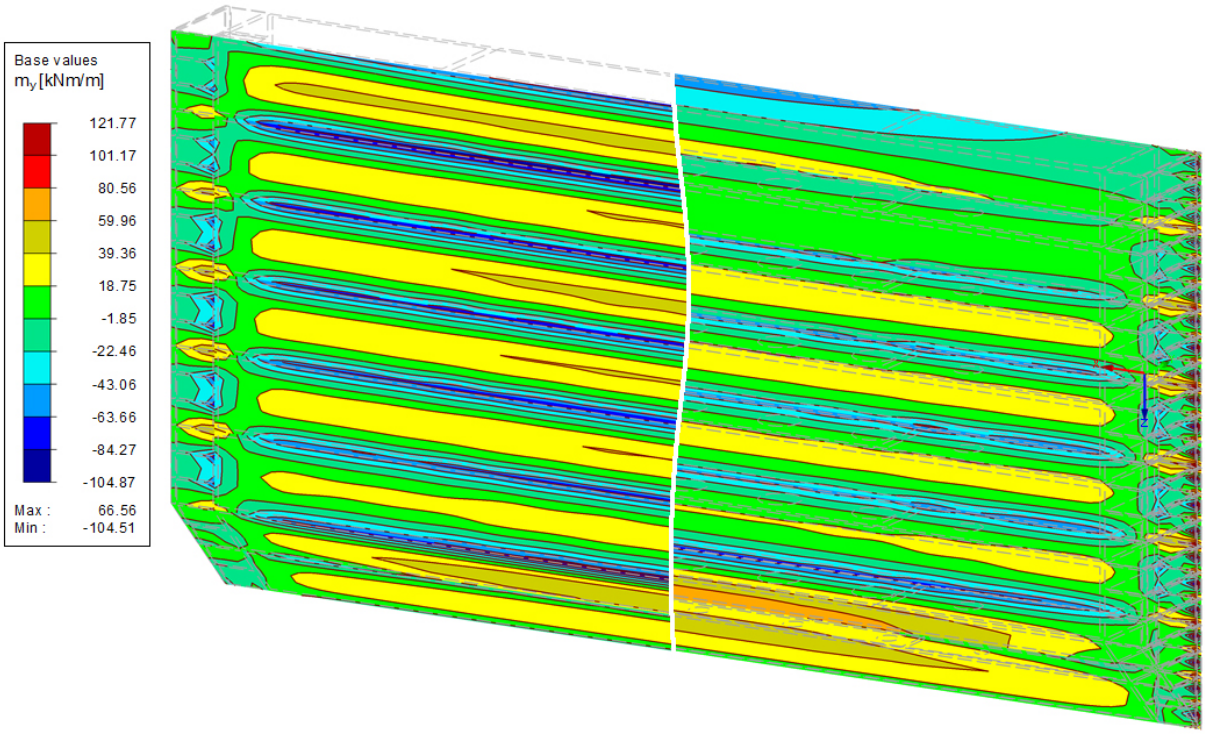


Figure 10.22 M_y in outer walls (ULS positive drop)

The normal force in x-direction (N_x) in the horizontal plates reach a maximum value of 3850 kN/m in tension and 5750 kN/m in compression. The bottom of the outer wall at North Sea side is also here loaded heavier (see Figure 10.23).

In Figure 10.25 some peaks are visible close to the gaps in the horizontal plates. Possibly the shape of the gaps could be optimized to lower these peaks, but that isn't carried out in the research.

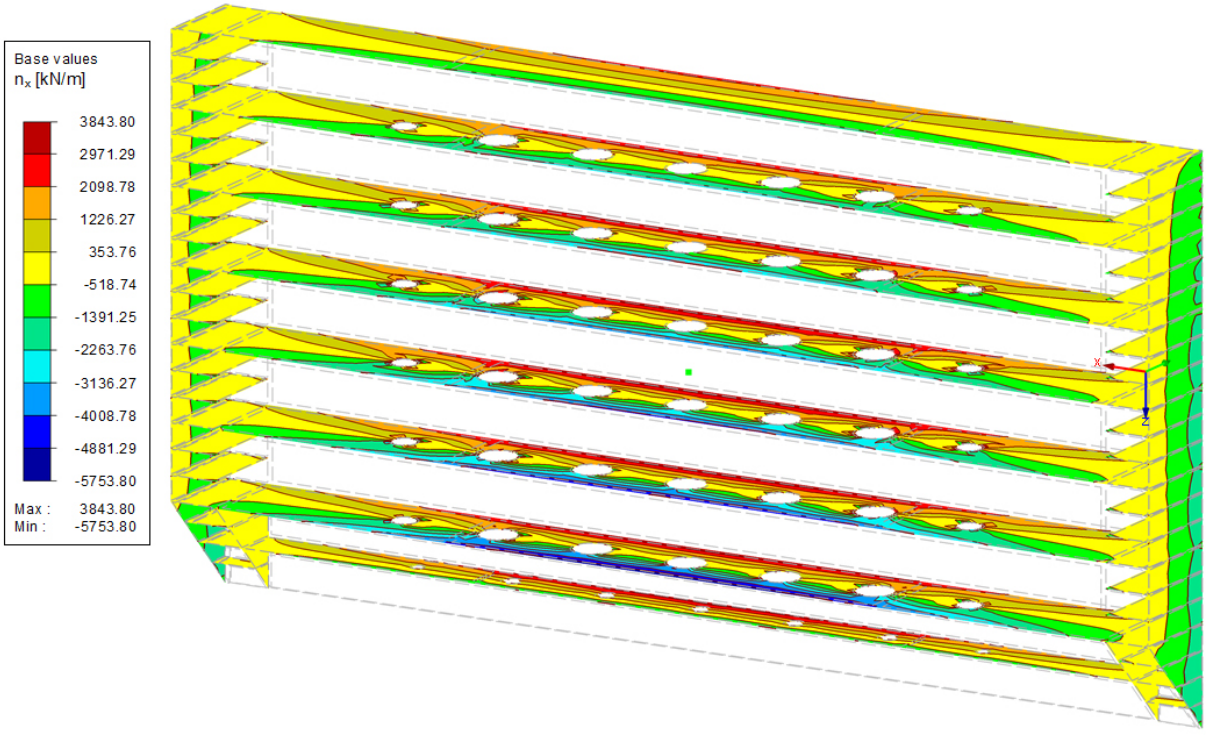


Figure 10.23 N_x in horizontal plates and vertical end plates (ULS positive drop)

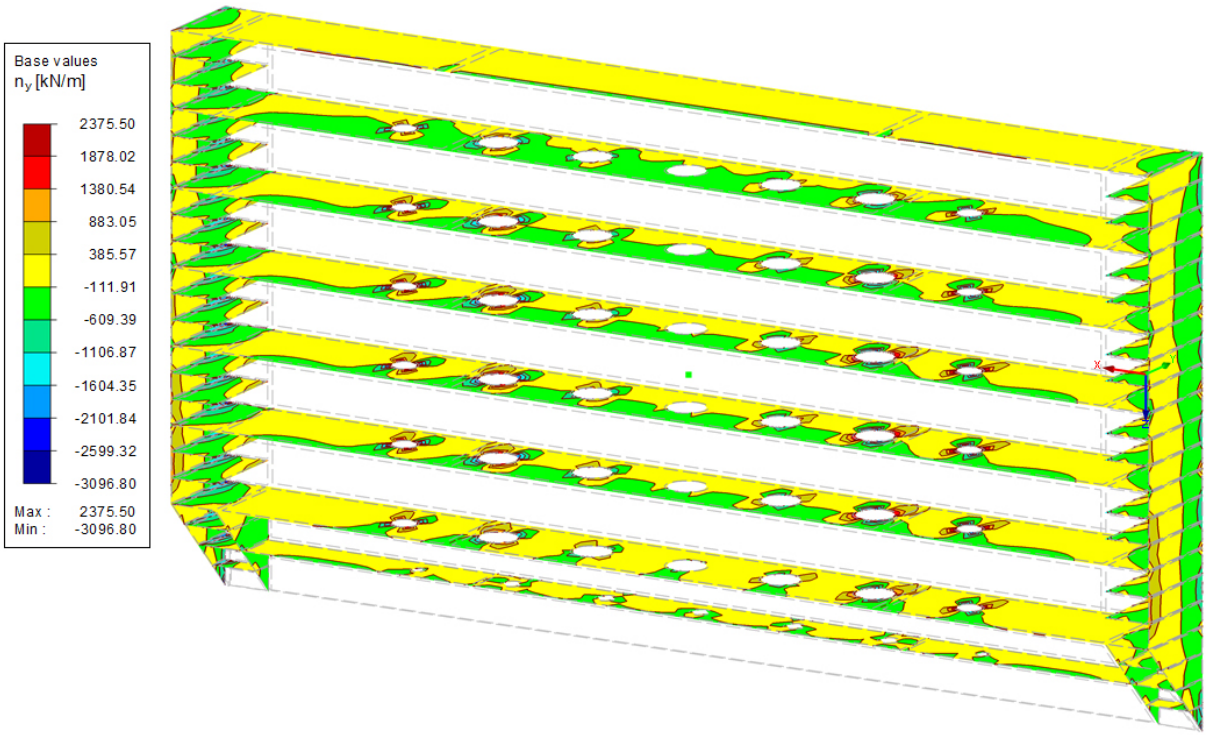


Figure 10.24 N_y in horizontal plates and vertical end plates (ULS positive drop)

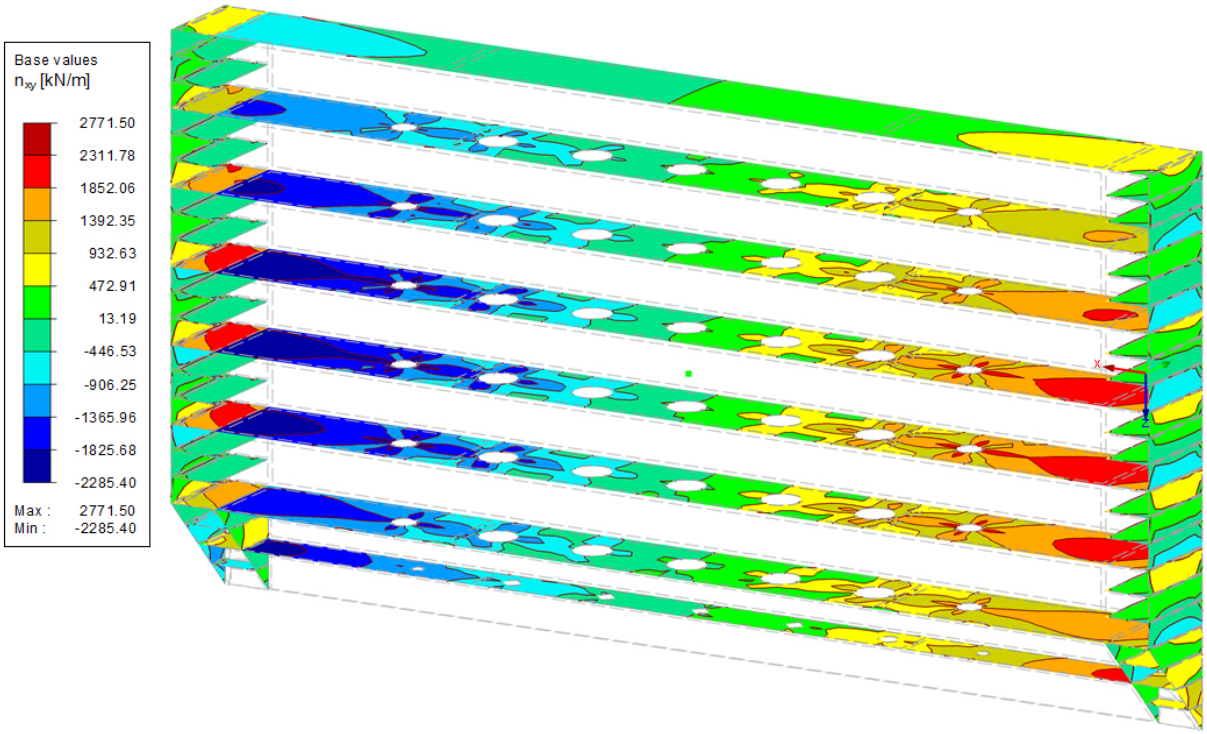


Figure 10.25 N_{xy} in horizontal plates and vertical end plates (ULS positive drop)

10.5.2 Deformations

The deformations for the load combinations positive drop and negative drop are shown in Figure 10.26 and Figure 10.27. The maximum deformation during positive drop is 422 mm in the direction of the Eastern Scheldt. The maximum deformation during negative drop is 177 mm in the direction of the North Sea.

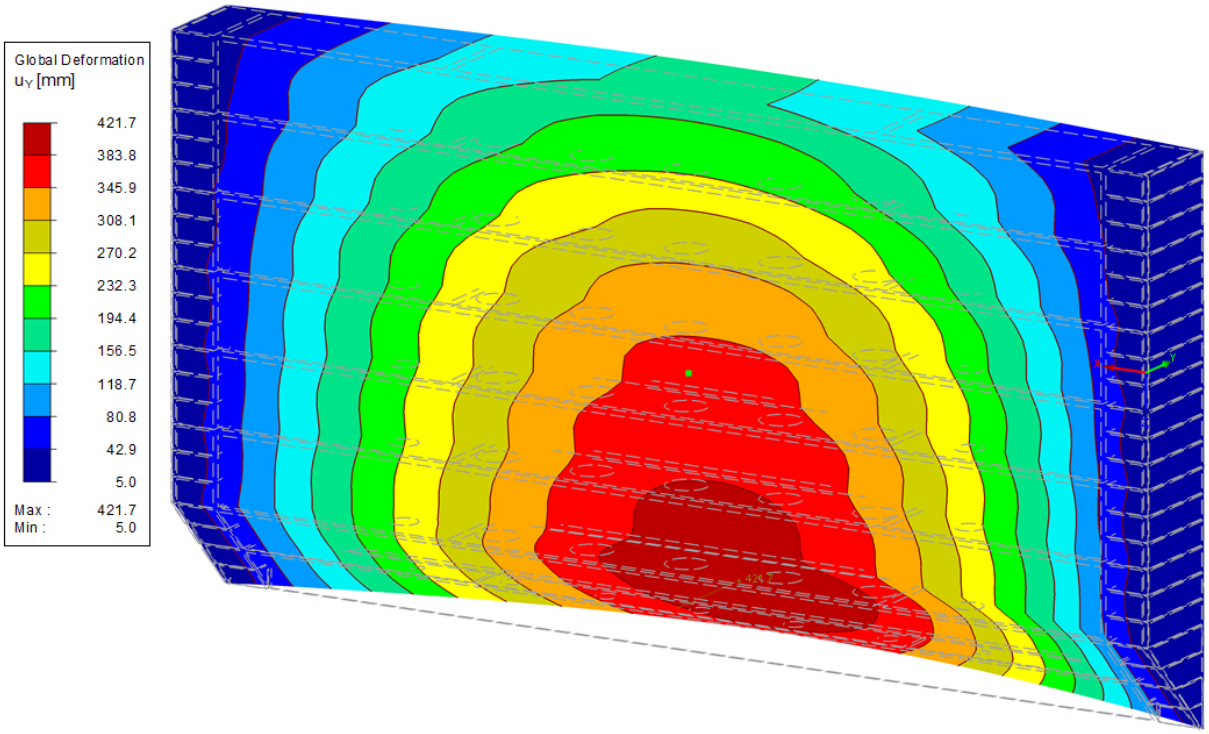


Figure 10.26 Deformation in y-direction (SLS positive drop)

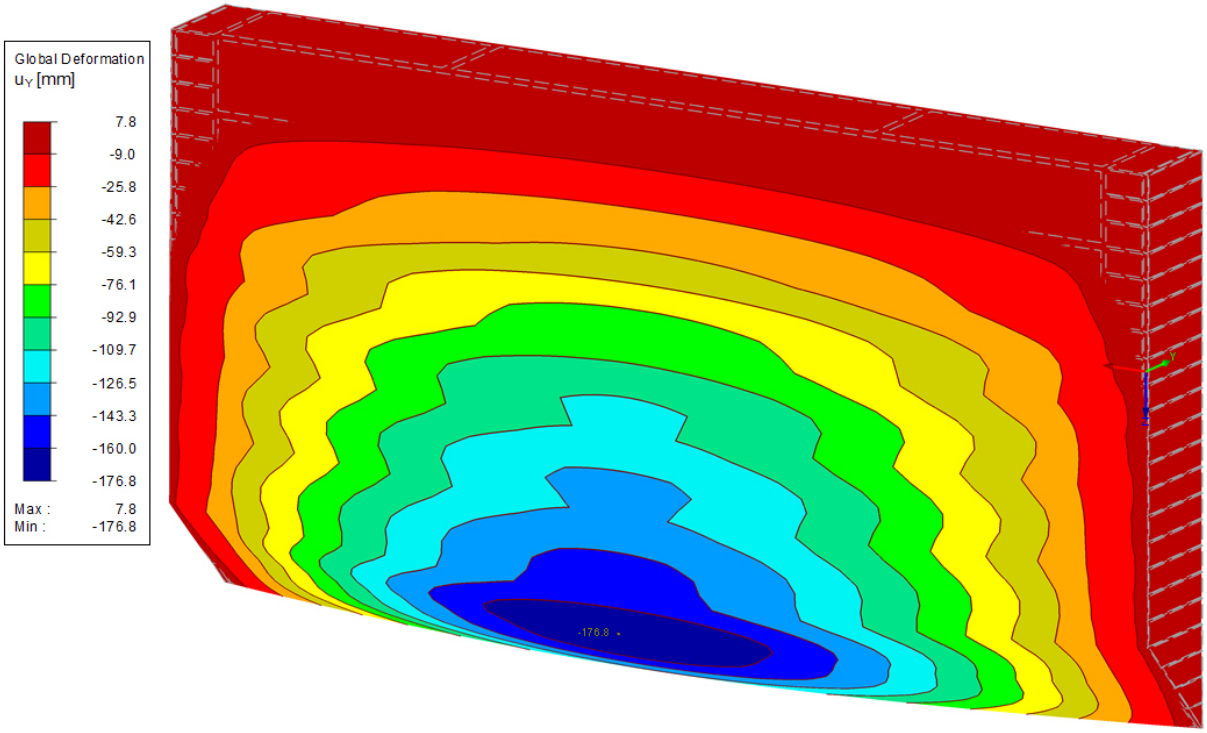


Figure 10.27 Deformation in y-direction (SLS negative drop)

The deflection during positive drop exceeds the deflection requirement of 200 mm. Therefore, it was necessary to remove the current sill beam and upper beam. Thereby, the deflection requirement doesn't hold anymore. Therefore, it isn't a problem that the slide has a maximum deformation of 422 mm, since nobody has to walk over or is hampered by this deformation.

10.5.3 Strains

The strain criterion is used to design the slide in ULS. Therefore, it is important to have a look at the maximum strains which occur in the structure. The maximum strains per load combination are shown in Table 10.8. This table shows that the decisive load combination is positive drop, since all the maximum strains of this combination are higher than for the other load combinations. All the strains do not exceed the strain criterion of 0,52%, thereby the structure should withstand the loads of each combination. Since the strain limit of the core material was much higher than 0,52% (see subsection 10.1.4), the core material should withstand the loads too. Thereby the structure is checked in ULS.

The strains mentioned in Table 10.8 are visualized in Figure 10.28 to Figure 10.42. These figures show where the maximum strains are positioned in the structure.

Table 10.8 Maximum strains per load combination (do not correspond to one point in the structure)

Comb nr.	Description	ε_x (%)	ε_y (%)	ε_{xy} (%)
CO1	Positive drop	-0,52	0,39	0,52
CO3	Negative drop	0,18	0,29	0,28
CO5	Ice	-0,08	0,26	0,16
CO6	Collision	0,02	-0,07	0,05
CO7	Wave impact	-0,07	0,30	0,16

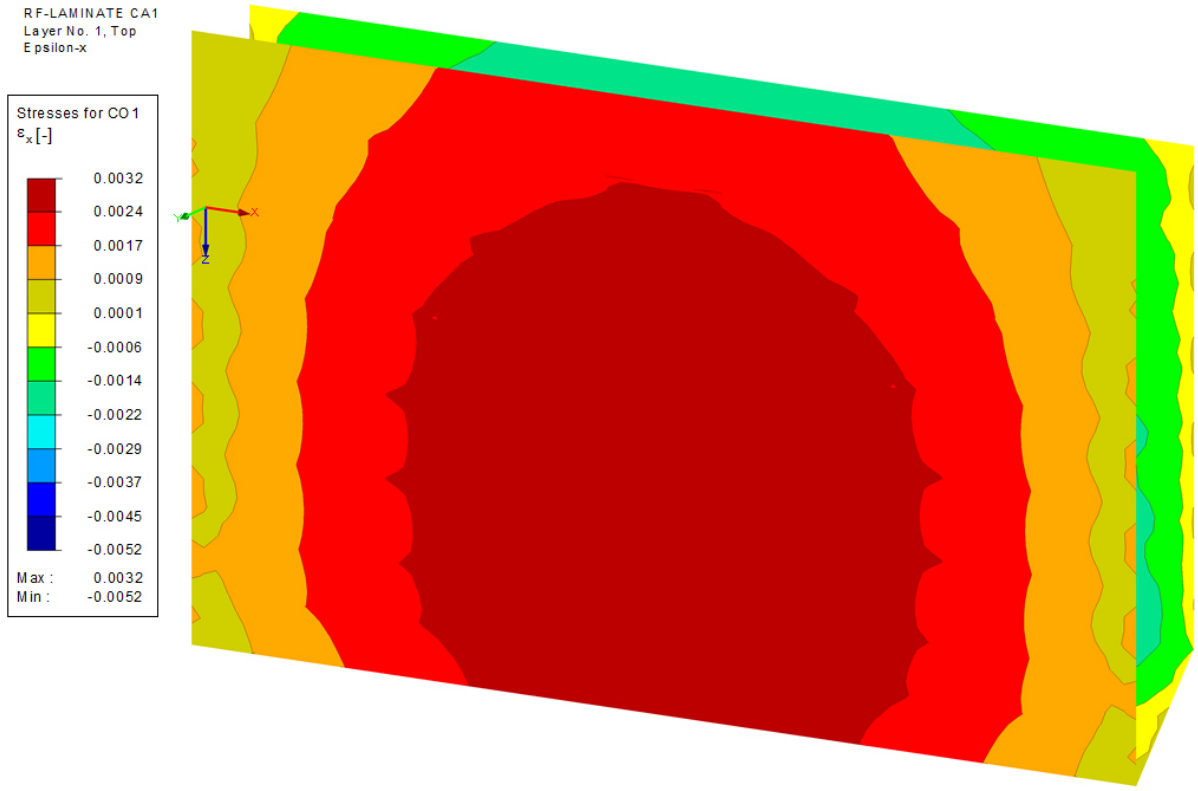


Figure 10.28 Strain ε_x at the top of layer 1 in comp. nr 1 for positive drop (CO1)

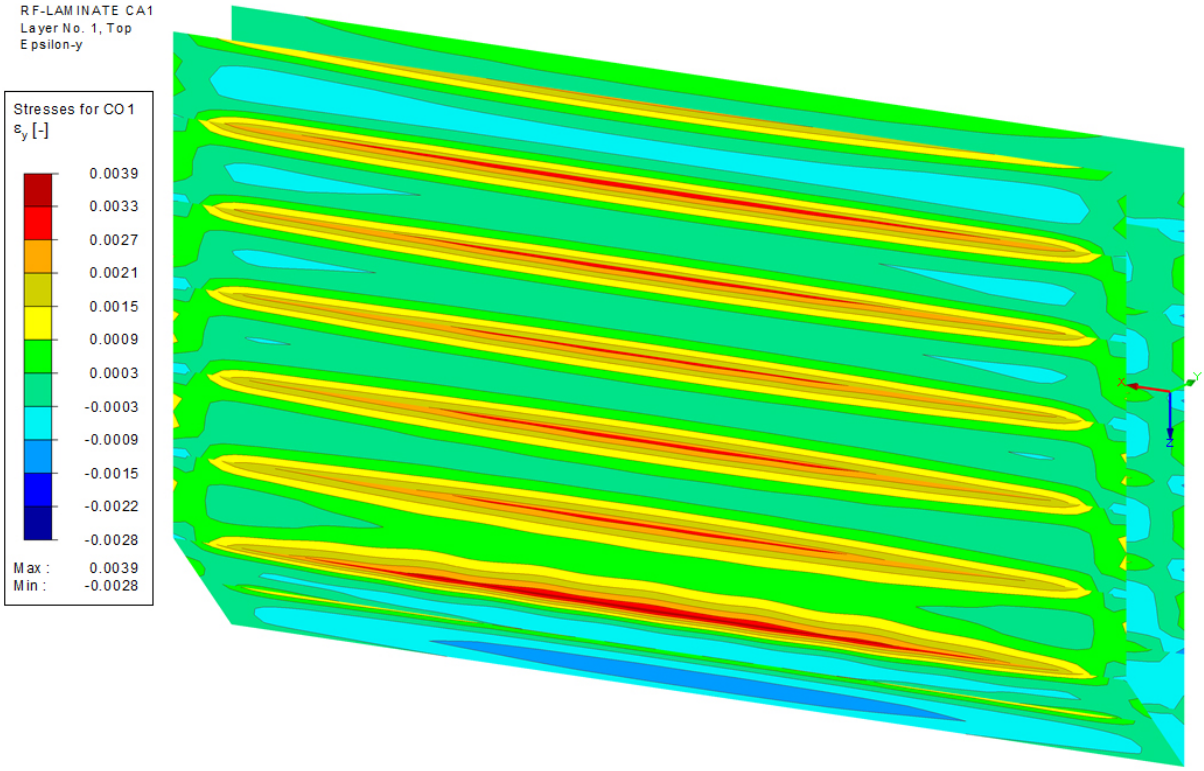


Figure 10.29 Strain ε_y at the top of layer 1 in comp. nr 1 for positive drop (CO1)

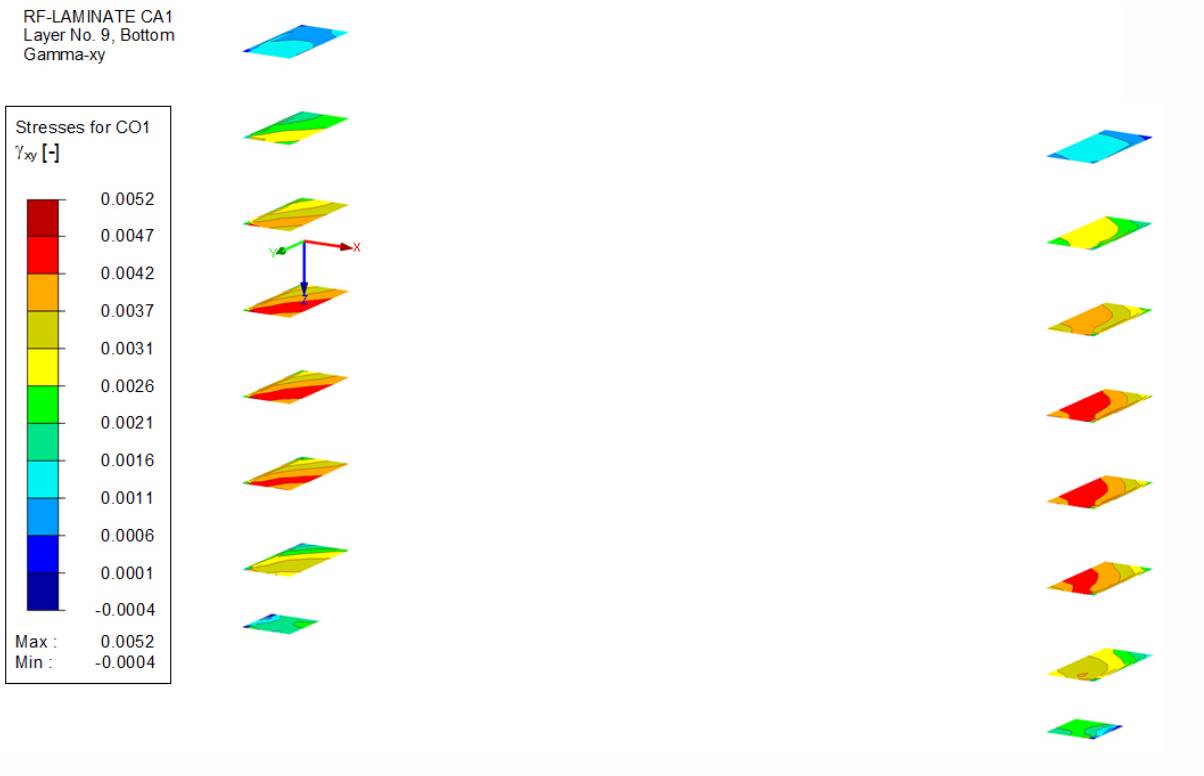


Figure 10.30 Strain ε_{xy} at the bottom of layer 9 in comp. nr 6 for positive drop (CO1)

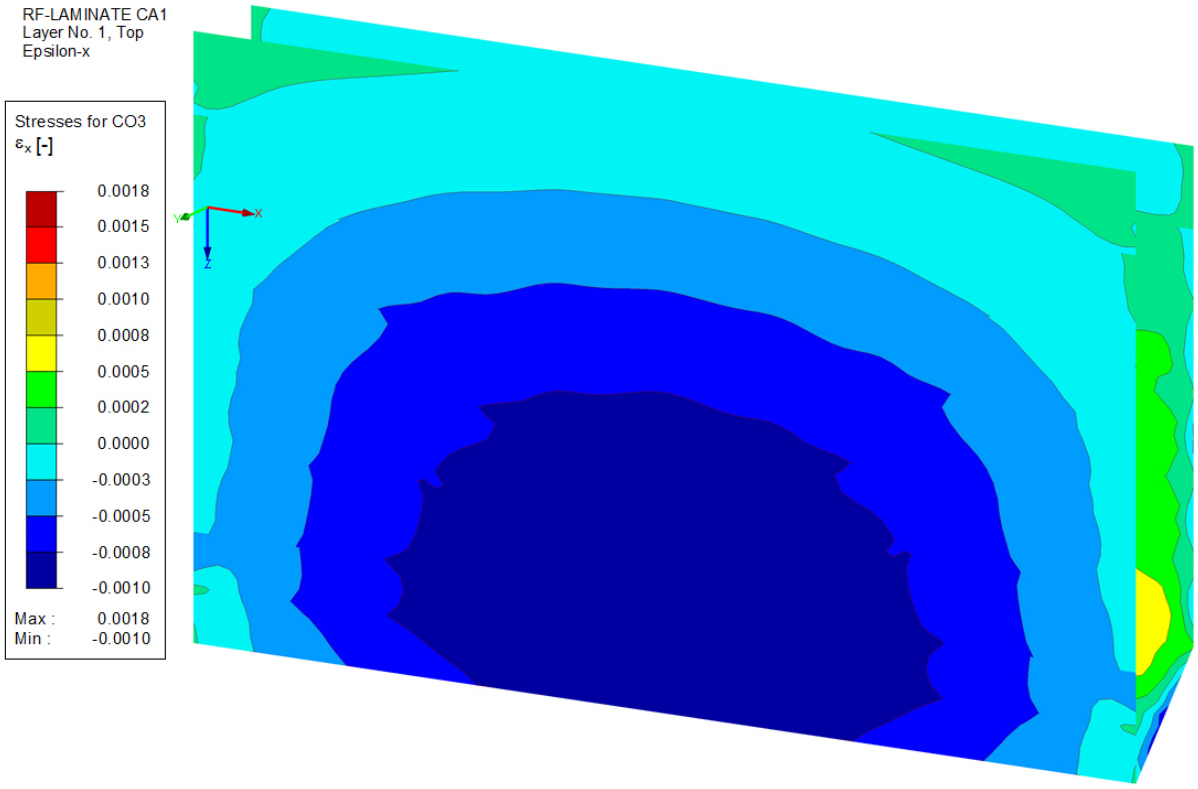


Figure 10.31 Strain ε_x at the top of layer 1 in comp. nr 1 for negative drop (CO3)

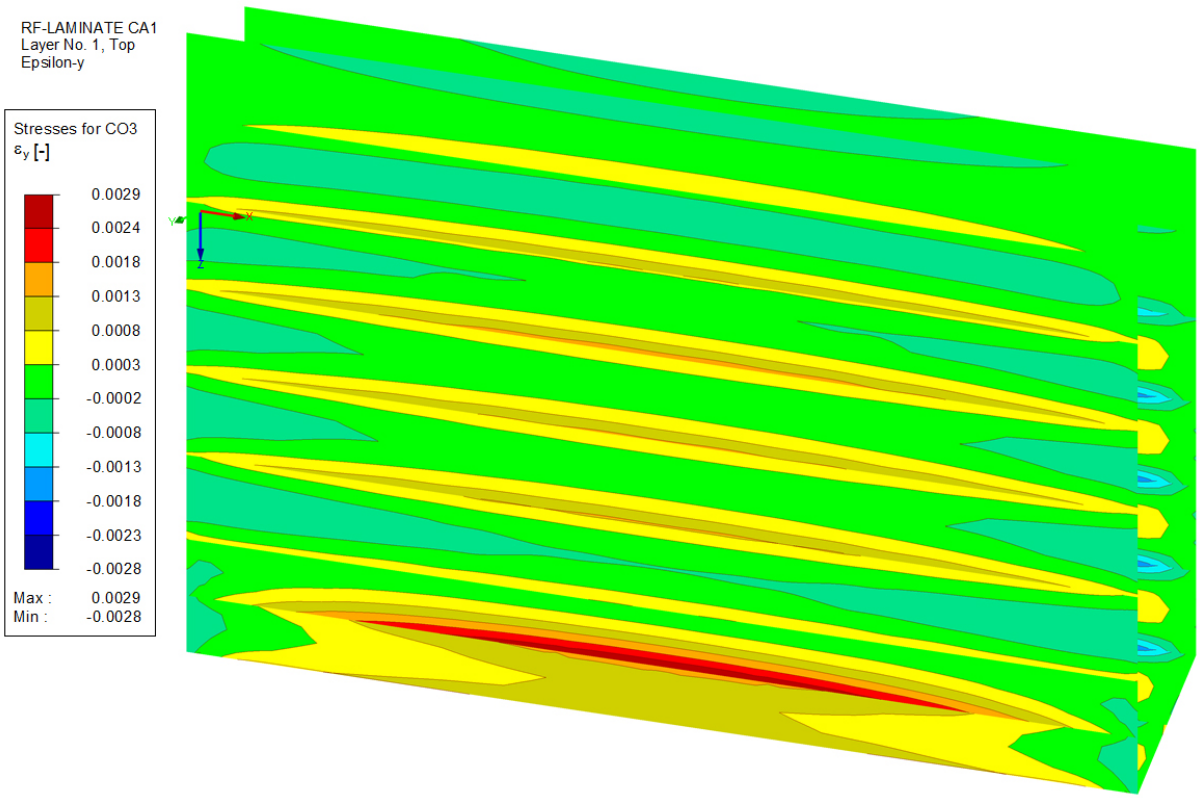


Figure 10.32 Strain ε_y at the top of layer 1 in comp. nr 1 for negative drop (CO3)

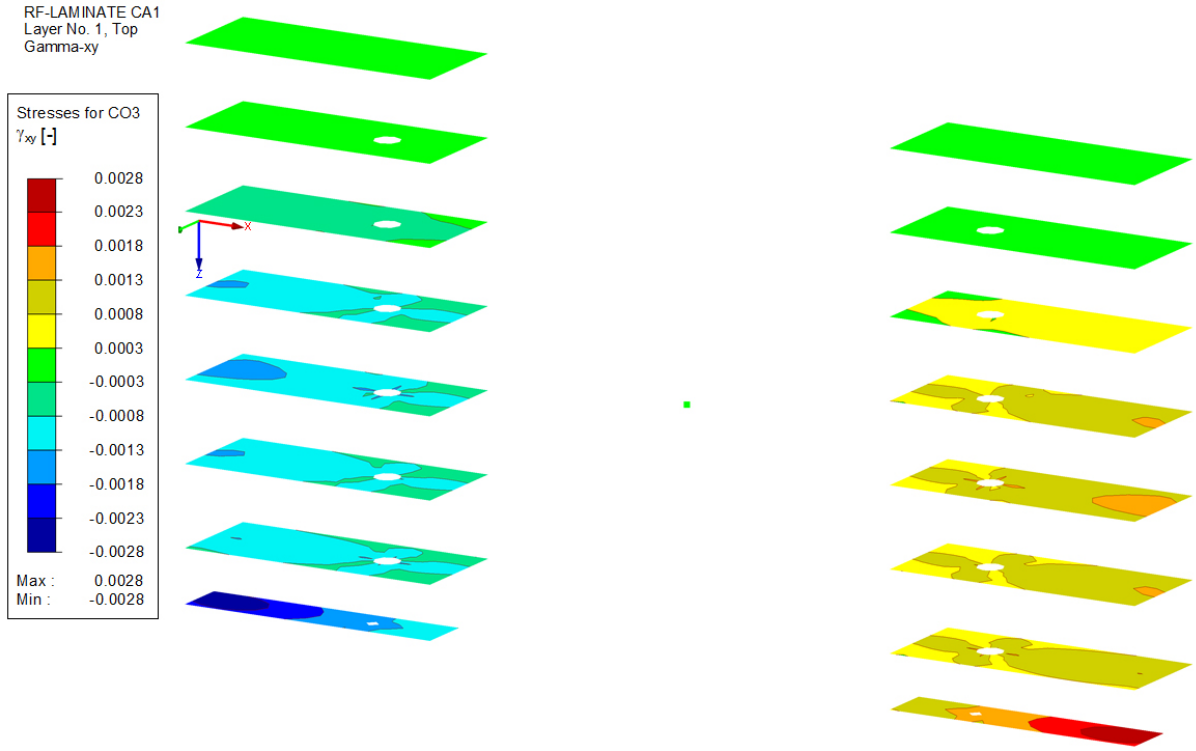


Figure 10.33 Strain ε_{xy} at the top of layer 1 in comp. nr 7 for negative drop (CO3)

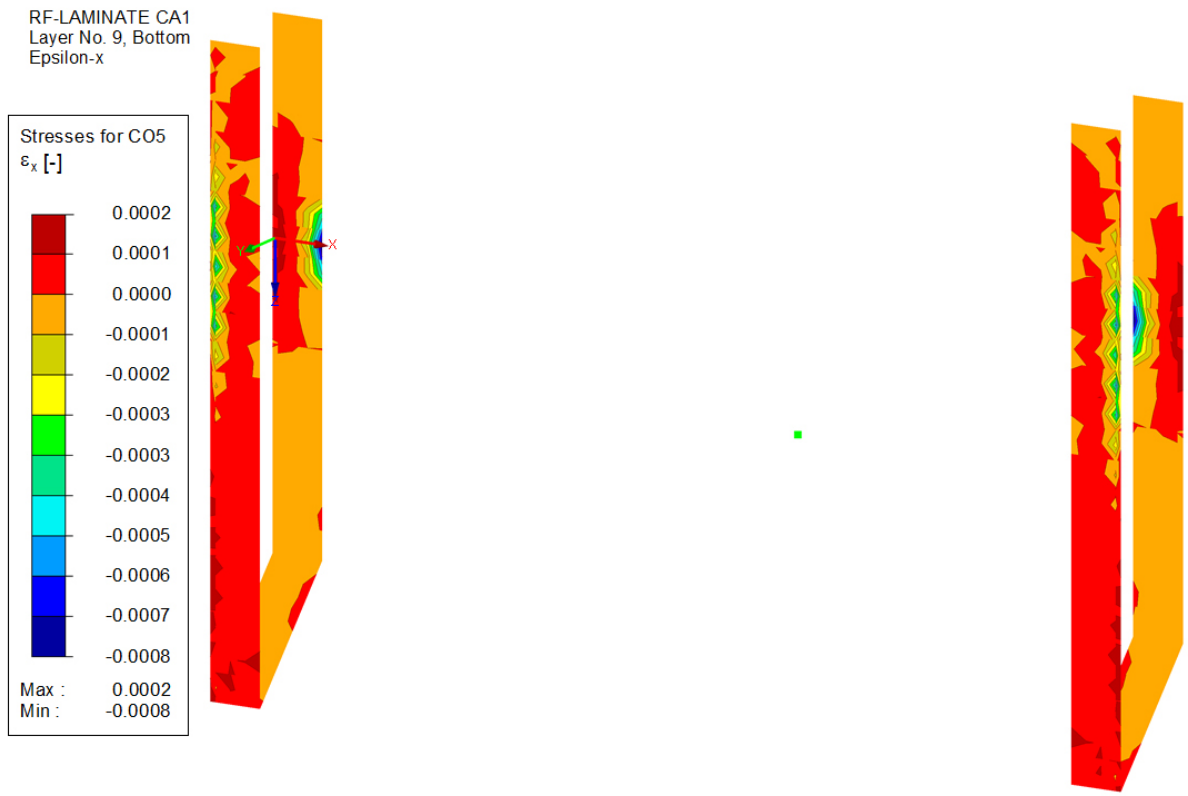


Figure 10.34 Strain ε_x at the bottom of layer 9 in comp. nr 5 for ice load (CO5)

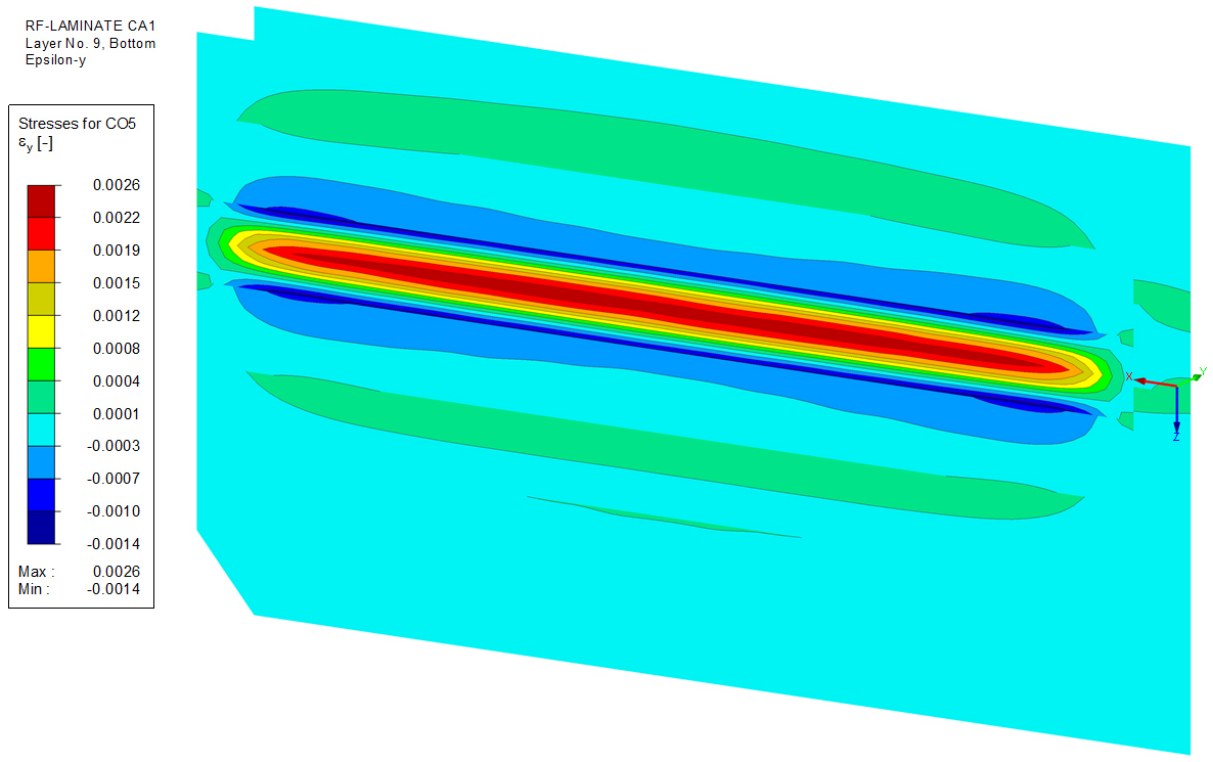


Figure 10.35 Strain ε_y at the bottom of layer 9 in comp. nr 1 for ice load (CO5)

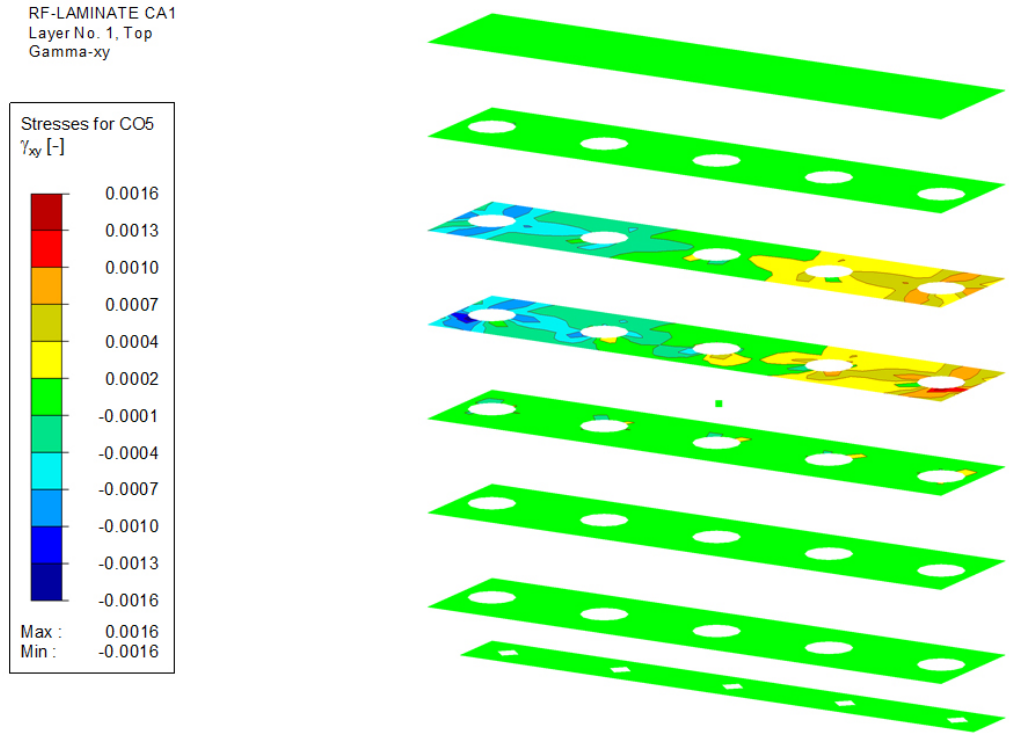


Figure 10.36 Strain ε_{xy} at the top of layer 1 in comp. nr 2 for ice load (CO5)

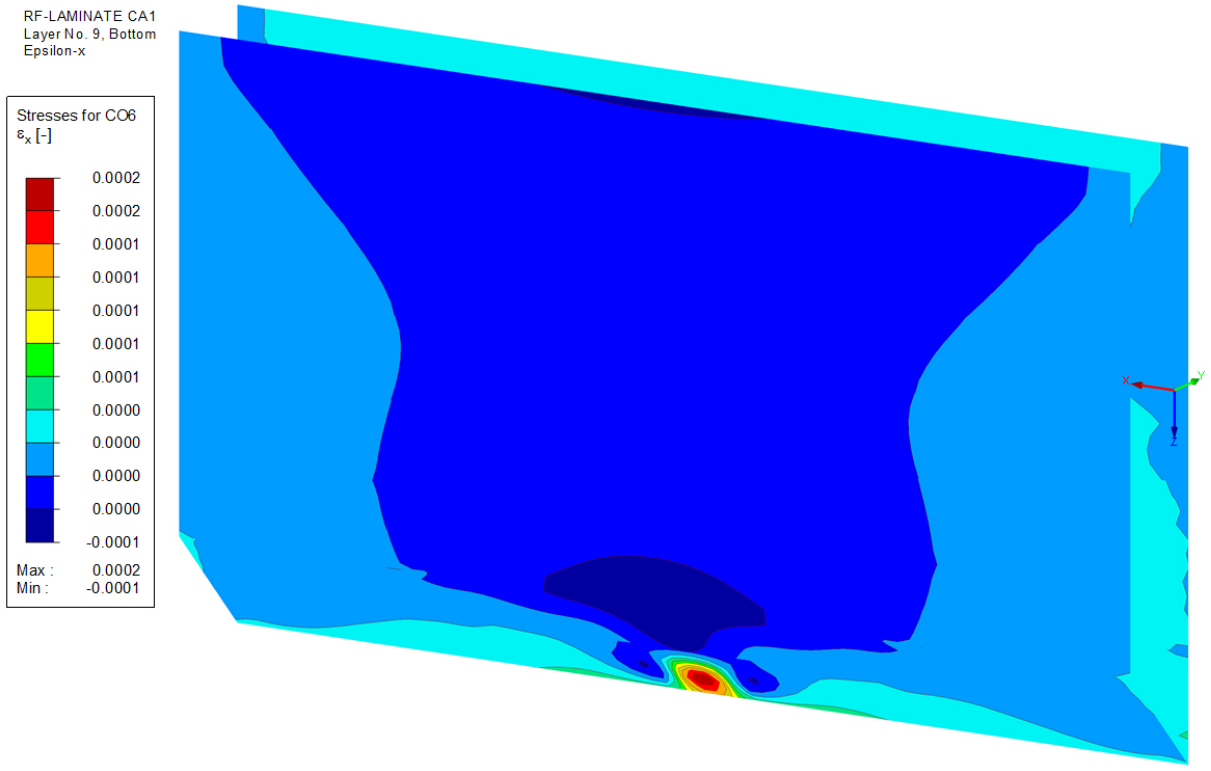


Figure 10.37 Strain ε_x at the bottom of layer 9 in comp. nr 1 for collision load (CO6)

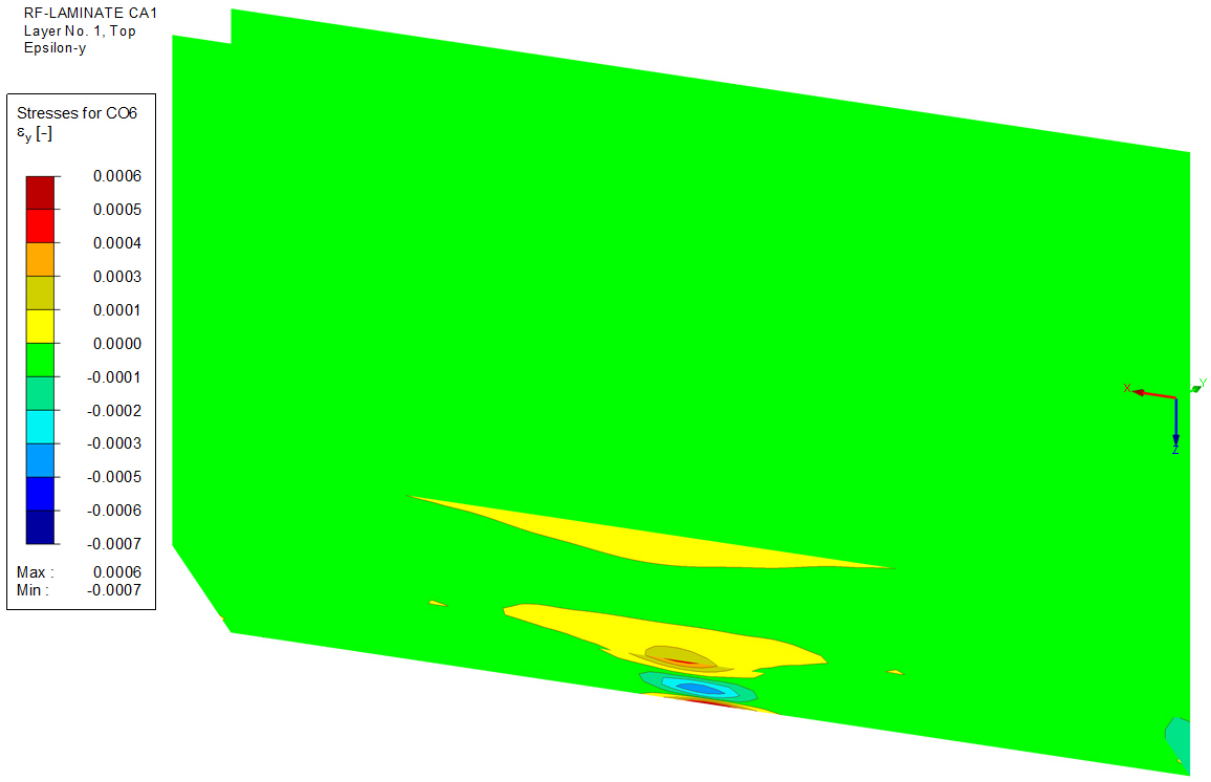


Figure 10.38 Strain ε_y at the top of layer 1 in comp. nr 1 for collision load (CO6)

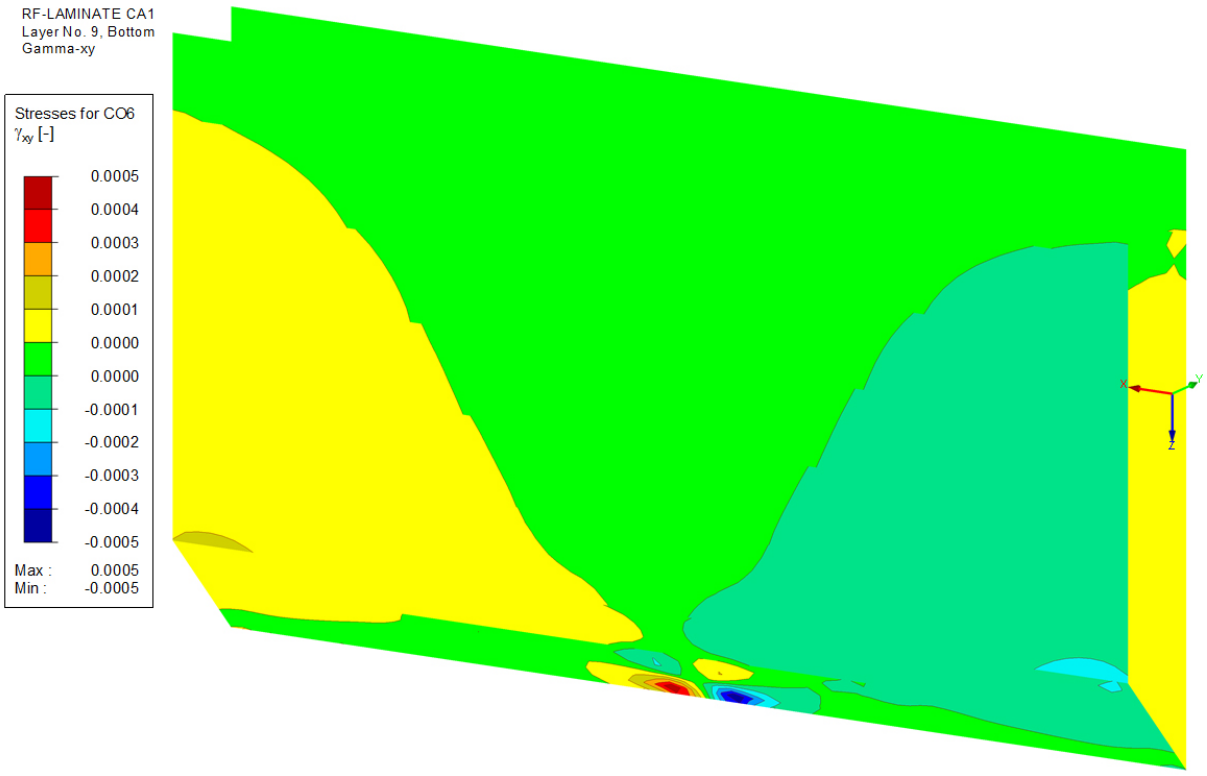


Figure 10.39 Strain ε_{xy} at the bottom of layer 9 in comp. nr 1 for collision load (CO6)

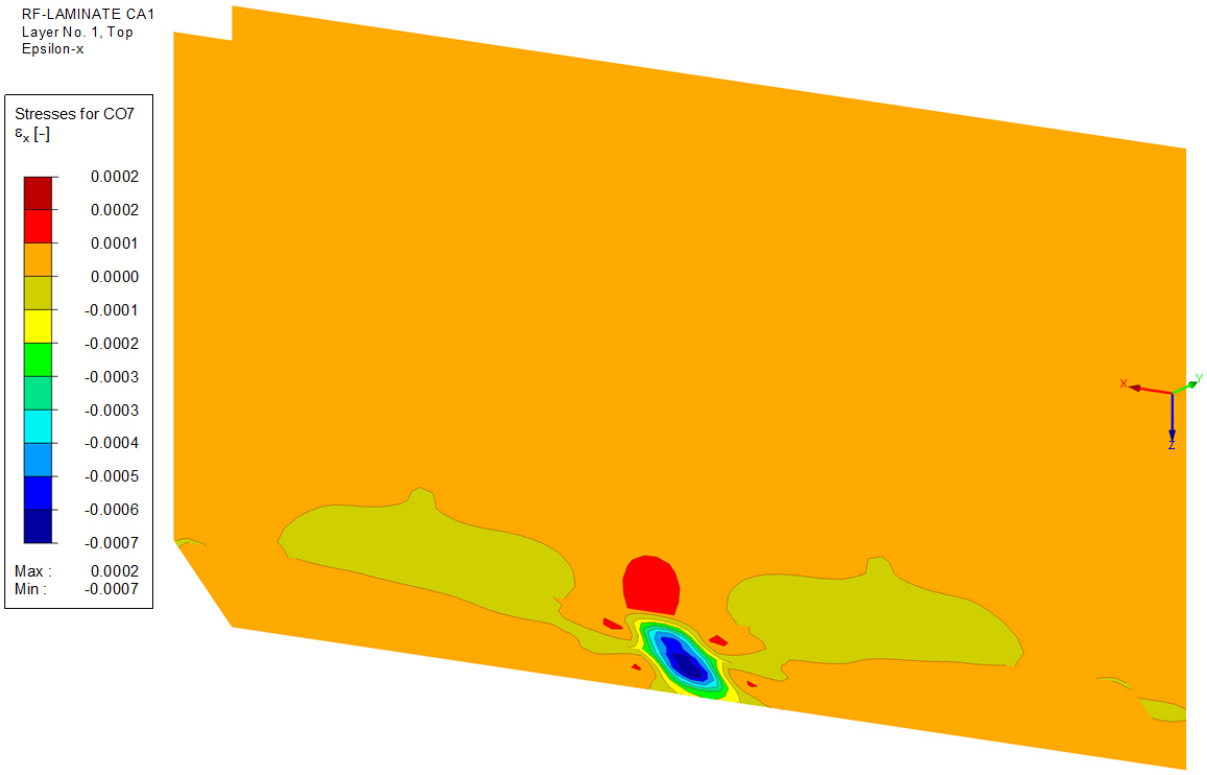


Figure 10.40 Strain ε_x at the top of layer 1 in comp. nr 1 for wave impact load (CO7)

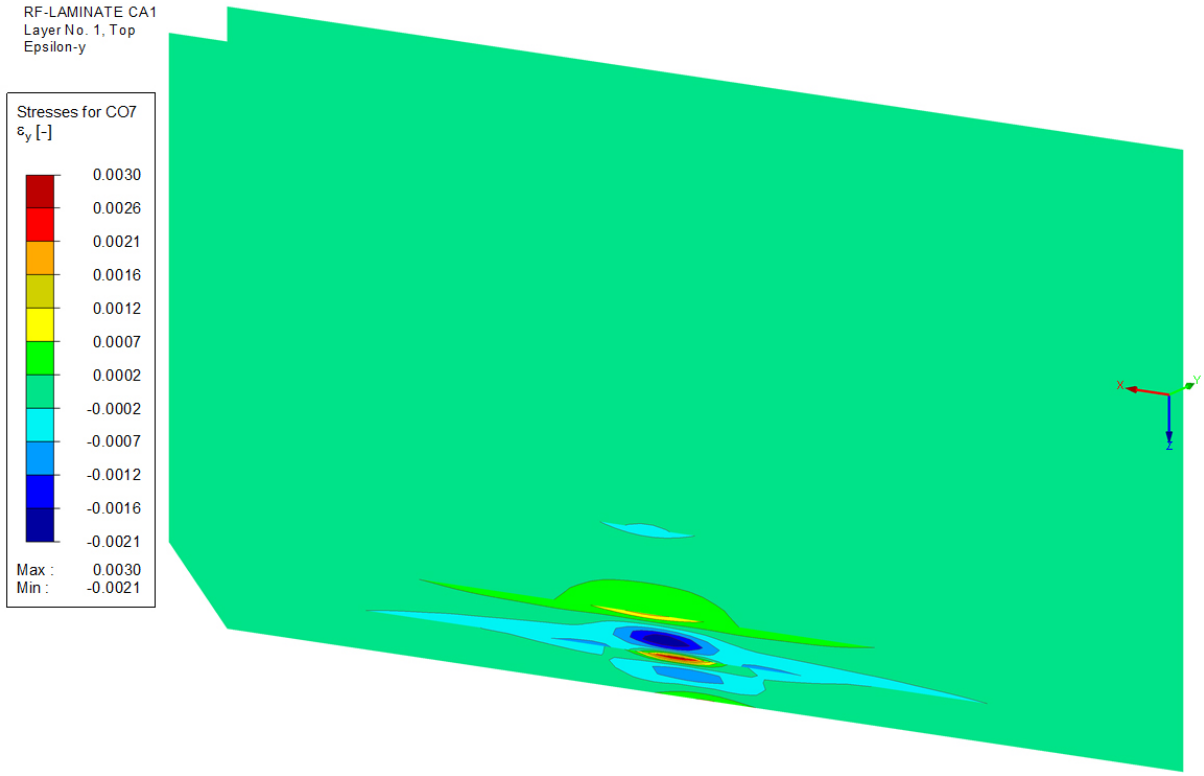


Figure 10.41 Strain ε_y at the top of layer 1 in comp. nr 1 for wave impact load (CO7)

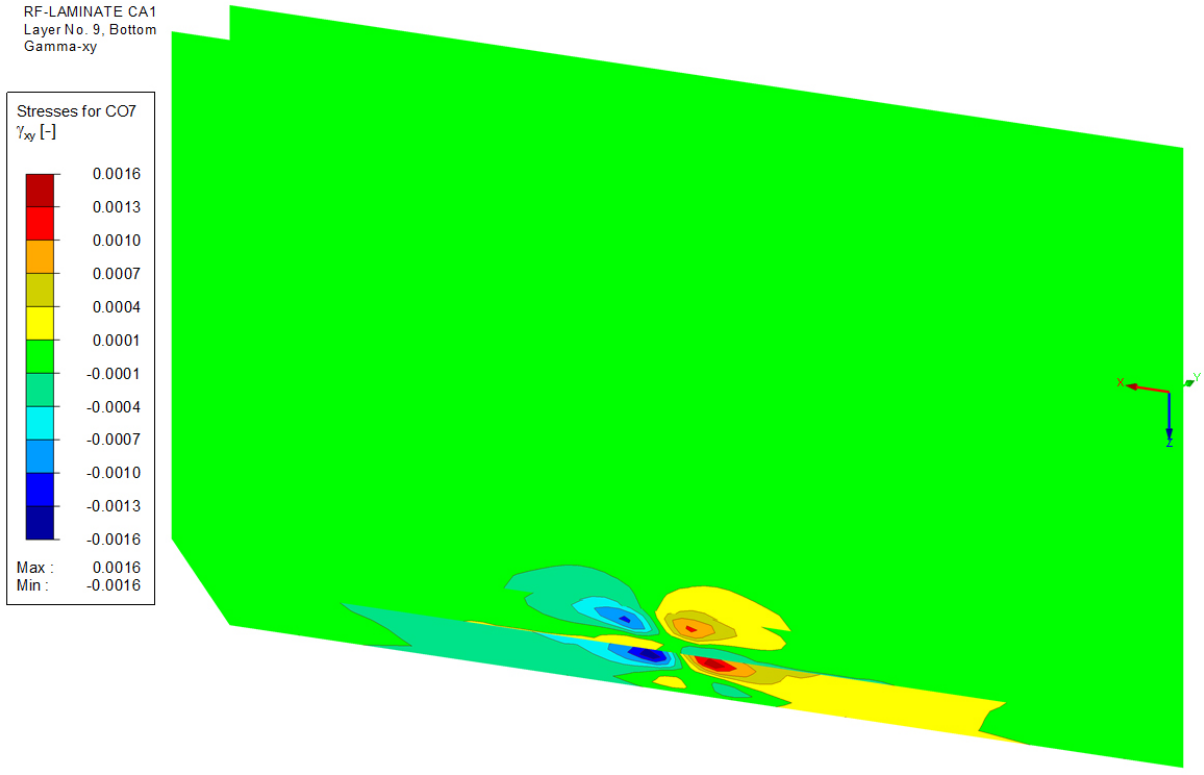


Figure 10.42 Strain ε_{xy} at the bottom of layer 9 in comp. nr 1 for wave impact load (CO7)

10.6 Buckling of horizontal plates

The stability of the horizontal plates between the two outer walls is checked according to [19]. The stability is checked for a pure bending load for the situation shown in Figure 10.43.

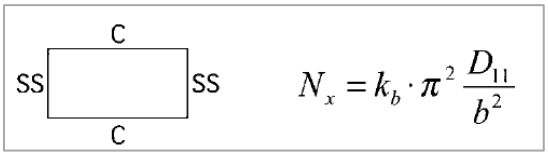
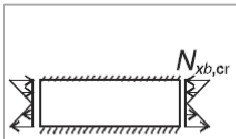


Figure 10.43 Way of supporting and associated stability formula [19]

A conservative value of k_b is 23.9 provided that $D_{22} \geq D_{11}$.The stiffness value $D_{11} = 1960\ kNm$, thereby the critical normal force is:

$$N_x = k_b \cdot \pi^2 \cdot \frac{D_{11}}{b^2} = 23.9 \cdot \pi^2 \cdot \frac{1960}{4^2} = 28896\ kN/m \tag{10.7}$$

Unfortunately the stiffness value $D_{22} = 1483\ kNm$, therefore $D_{22} < D_{11}$ and it isn't sure whether the value for k_b is still conservative or not. Therefore, the stability of the horizontal plates is checked with the revised CUR Recommendation 96 [31]. This recommendation gives more formula's to check the stability of plates. For a pure bending load and a plate which is clamped at both edges, the formulas are given in Figure 10.44.



$N_{xb,cr} = \frac{\pi^2}{L_y^2}\left[26.8\sqrt{D_{11}D_{22}} + 12.9\left(D_{12} + 2D_{66}\right)\right]$	$K \leq 3$
$N_{xb,cr} = \frac{\pi^2}{L_y^2}\left[30.1\sqrt{D_{11}D_{22}} + 11.5\left(D_{12} + 2D_{66}\right)\right]$	$3 \leq K$

Figure 10.44 Stability formulas for pure bending load [31]

The K-value is determined with:

$$K = \frac{2D_{66} + D_{12}}{\sqrt{D_{11}D_{22}}} = \frac{2 \cdot 574 + 543}{\sqrt{1960 \cdot 1483}} = 0.99 \tag{10.8}$$

The stiffness value D_{66} is in Dlubal RFEM defined as D_{33}. The other stiffness values are defined the same as in the classical lamination theory. Since $K \leq 3$, the upper formula can be used to check the stability of the plate. The critical normal force will be:

$$\begin{aligned} N_{xb,cr} &= \frac{\pi^2}{L_y^2}\left[26.8\sqrt{D_{11}D_{22}} + 12.9(D_{12} + 2D_{66})\right] \\ &= \frac{\pi^2}{4^2}\left[26.8\sqrt{1960 \cdot 1483} + 12.9(543 + 2 \cdot 574)\right] \\ &= 41641\ kN/m \end{aligned} \tag{10.9}$$

The maximum resistance (according to [31]) is:

$$Q_{Rd,b} = \frac{N_{xb,cr}}{\gamma_{mD}} = \frac{41641}{1.25} = 33312\ kN/m \tag{10.10}$$

The maximum peak in the normal force per meter width is: $Q_{Ed,b} = 5750\ kN/m$ (see Figure 10.23), therefore $UC = 0.17$. The stability of the horizontal plates will be ok.

10.7 Manufacturability

The final design will be manufactured with the vacuum-assisted resin injection method as mentioned in section 10.1.1. The two outer sandwiches could be made separately, where after these walls could be connected with the horizontal plates (as was mentioned in Figure 8.25). These horizontal plates can be connected with a T-joint with epoxy adhesive and should probably be bolted as well, since a glued joint isn't yet familiar to apply at FRP in civil engineering industry. The disadvantage of this option is that the fracture paths are probably resin-dominated, which means that the connection between the outer sandwiched and the horizontal plates isn't very robust. In the next paragraph an idea is mentioned to solve this problem.

Instead of making a glued connection between the outer sandwiches and the horizontal plates, it would be more robust to integrate this connection in the total structure. The fibercore-principle (as mentioned in Figure 8.1b) uses fibres which are positioned in a Z-shape. These fibres connect the outer skins of the sandwiches via the stiffeners, which prevent delamination of the skins. This principle could be used to connect the outer sandwiches via the horizontal plates as well. On macro level this idea is shown in Figure 10.45. This integration of the horizontal plates into the total structure should still be elaborated into more detail, but offers the opportunity to manufacture a very robust structure.

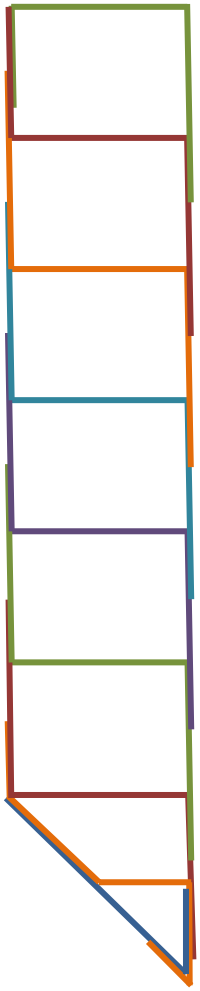


Figure 10.45 Idea to integrate the connection of the outer sandwiches in the total structure

11 Cost comparison

In this chapter the fifth sub-research question will be answered: 'Is it financially attractive to replace the current slides by slides made of FRP over the total life of the barrier? In this chapter a comparison is made between different variants which can withstand the sea level rise and/or help to solve the problem of the disappearing intertidal zones. A decision for one of the variants will not be made here, since not only the costs should be considered when this decision is made. There are a lot of factors which are influencing this decision, such as the effect on the disappearing intertidal zones, the length of the water barrier and the way that sea level rise can be resisted. This cost comparison helps to compare the long term solution with other solution which can be chosen on the long term.

Finally a life cycle analysis is carried out to compare the costs of the long term solution with the maintenance costs of the current steel slides.

11.1 Costs of variants

The following variants can offer a solution against flooding of the land around the Eastern Scheldt:

1. Raising dikes
2. Dam
3. Rigorously FRP solution

The direct investment costs of each variant are estimated in the next subsections.

11.1.1 Raising dikes

Instead of the current closable storm surge barrier, it's possible to raise the dikes around the Eastern Scheldt. So the closable barrier is no longer used. The dikes should be increased over 150 km length in that case. This solution has already been investigated before the current barrier was build. To make a rough calculation of the costs, that previous research is used to estimate the costs of raising the dikes. The most important costs are the costs for increasing the dikes, prank protection and secondary dikes, which are mentioned in Table 11.1. The total costs were estimated on 1405 million gulden (price level 1976).

Table 11.1 Costs of increasing the dikes [32]

Description	Million gulden (price level 1976)
Increase dikes (failure probability: 1/4000)	655
Foreshore protection (after C3)	510
Secondary dikes	240
	1405

The costs mentioned, hold for increasing the dikes to a height which was considered necessary in 1976. In the future the dikes should be increased probably even more, due to the sea level rise. The costs for extra adjustments on harbors and sluices due to a higher water level at the Eastern Scheldt in case of an open sea arm and costs for expropriating are not considered. Probably there are still some other indirect costs which are not considered here.

The costs mentioned do not consider demolishing the current storm surge barrier. If the current barrier stays intact, the current road between Schouwen-Duiveland and Noord-Beveland can remain. In that case, the trough flow opening is not as large as the trough flow opening which can be reached

by the rigorously solution, since the threshold of stones near the piers will remain. Another solution is to demolish the current barrier, which will increase the trough flow opening. If desirable, a new traffic bridge should be built than. But this will increase the costs.

The solution of raising the dikes coincides with the future vision of the WWF (Word Wide Fund for Nature). WWF mentioned in [33] that the Eastern Scheldt should be open in the future and that only modern storm surge barriers (like the Maeslantkering) should be built in the Grevelingen and the Haringvliet.

11.1.2 Dam

Another variant is closing the Eastern Scheldt completely with a dam. Approximately 3 kilometers of dam should be built to close the Eastern Scheldt. The costs for construction of a dam were investigated before the current barrier was constructed (but the artificial islands Neeltje Jans, Roggenplaat, Noordland and Damvak Geul were already constructed) and are shown in Table 11.2. The present value of the loss of income of oister- and mussel farmers was also mentioned in [32]. The total costs are approximately 995 million gulden.

Table 11.2 Costs of a dam [32]

Description	Million gulden (price level 1976)
Oosterscheldedam	600
Present value loss of future income oister- and mussel farmers	395
	995

These costs are valid for constructing a new dam and consider the loss of income of oister and mussel farmers. A dam will block the trough-flow opening of the barrier, this fact will be considered in the comparison of all variants in section 11.2.

11.1.3 Rigorously solution

The costs of the rigorous solution are separated in the cost of the FRP slide and the extra costs for the adjustments on the current barrier. The costs of an FRP slide will be based on the FRP construction costs which were mentioned in Table 4.7 of the literature study. The construction costs of a glass fibre/polymer FRP construction are approximately between 4 and 7 euro per kg. A value of 7 €/kg will be used.

The final slide has a total weight of 418.000 kg. Therefore the total costs will be approximately 2.9 million euro per slide (for the highest slide). The average height of the current slides is 8.64 m, therefore the average height of the final slide design will be $8.64 + 10.1 = 18.74\ m$. The average costs for a slide are estimated on: $2.9 \cdot \frac{18.74}{22} = 2.5$ million euro. The total costs of replacement become approximately 155 million euro.

This rigorously solution requires also removal of the upper beams, the adaption of the sill beams and increasing the height of the slide rabbets. These costs are estimated with unit prices from a cost expert of Witteveen+Bos.

The total extra costs for adjustments on the current barrier are estimated on 70 million euro and are further specified in appendix G. Thereby, the total cost of the rigorously solution are 225 million euro, which is shown in Table 11.3.

Table 11.3 Costs of rigorously solution

Description	Price (in million euro)
FRP slide	155
Extra adjustments on barrier (see appendix G)	70
	225

11.2 Comparison of variants

A comparison of the costs of each variant in million euros is shown in Table 11.4. The costs of dike raising and constructing a dam are converted to euro's and are updated to the present price level. Since 1976 the prices are increased by a factor: $1.02^{(2013-1976)} = 2.1$, assuming a constant inflation of 2%. The conversion factor to euros is 0.4538.

*Table 11.4 Comparison of investment costs of different variants *) Price level 1976*

Variant	Price (million euro)
Dike raising	1340
Dam	995
Rigorously solution	225

The dam variant looks not very logic in the opinion of the author, since in 1976 the decision is made to build a closeable storm surge barrier, and not to build a dam. A dam would interfere with the nature in the Eastern Scheldt, which is a disadvantage in comparison with the other two variants. The costs of the dam variant are also much higher than the costs of the rigorously solution. Therefore the dam variant is not preferable.

The two other variants, dike raising and the rigorously solution, can withstand the sea level rise and help to solve the problem with the disappearing intertidal zones and are therefore good alternatives. The rigorously solution will probably strengthen the position of the storm surge barrier as an exemplary project for the Dutch hydraulic engineering industry, dike raising will possibly weaken this position. Both variants still have some uncertainties which should be further analyzed:

- It should be checked what the effect of the increasing through flow opening is on the disappearing intertidal zones. The original trough flow opening of the Eastern Scheldt was 80.000 m^2, the trough flow opening will increase from 18,000 m^2 to 28,000 m^2 due to the rigorously solution. Depending on the elaboration of dike raising the trough flow opening will increase to minimal 28,000 m^2.
- The costs of dike raising are based on considerations made in 1976, the dike height should possibly be increased more, due to sea level rise.

Without analyzing these uncertainties further, the costs between both variants will be compared here. The rigorously solution looks much more attractive in terms of costs than raising the dikes. It should be mentioned that the trough flow opening can be increased more when the dikes are raised and the current barrier is demolished. Hydraulic research to the effect of the increasing through flow opening on the disappearing intertidal zones should prove what the minimum trough flow opening is to save the intertidal zones.

11.3 Life cycle analysis

In this section a LCA is carried out to compare the costs of the rigorously solution with the maintenance costs of the current steel slides. The maintenance costs of the rigorously solution and the steel slides are estimated in the next paragraphs.

The FRP slide does have to be inspected to detect local failures. In accordance with [18] it is assumed that these inspections are carried out every 10 years and that also some small maintenance is carried out during these inspections. The costs are estimated on 5% of the construction costs of the FRP slide, which is shown in Table 11.5.

The maintenance costs of the current barrier were mentioned in section 2.5 of the literature study. The total maintenance costs for the barrier are 17 million euro per year. During a year maximum 4 slides are maintained. It's assumed that 40% of the maintenance costs of the barrier are necessary to maintain the 4 slides. Therefore the total maintenance costs per slide are estimated on $\frac{0.4 \cdot 17}{4} = 1.7$ million euro. It is assumed that all the slides can be maintained in 15 years (actually 15,5 years). Thereby the total costs in 15 years become 105 million euro. These costs are converted to maintenance costs in every 10 year, which become $\frac{10}{15} \cdot 105 = 70$ million euro.

The LCA is carried out over a lifetime of 100 years. The present value is calculated with the following equation by considering a market rent of 1%:

$$PV = \sum \frac{C_i}{(1+r)^i} \tag{10.11}$$

Table 11.5 Calculation of present values

		Rigorously solution		Current steel slides	
Time (years)	$\frac{1}{(1+r)^i}$	Costs	Present value	Costs	Present value
0	1,00	225	225,00	0	
10	0,91	7,8	7,02	70	63,37
20	0,82	7,8	6,35	70	57,37
30	0,74	7,8	5,75	70	51,93
40	0,67	7,8	5,21	70	47,02
50	0,61	7,8	4,71	70	42,56
60	0,55	7,8	4,27	70	38,53
70	0,50	7,8	3,86	70	34,88
80	0,45	7,8	3,50	70	31,58
90	0,41	7,8	3,17	70	28,59
100	0,37	7,8	2,87	70	25,88
			272		**422**

The present value calculation of the costs is shown in Table 11.5. The present value of the rigorously solution is much lower than for the current steel slides. The payback time is between 40 and 50 years.

This comparison does not take into account that the rigorously solution can withstand the sea level rise and helps to solve the problem with the intertidal zones and the current steel slides not. Bearing in mind that the knowledge on and experience with FRP structures will increase in the future, the

costs will probably decrease too. Therefore, the rigorously solution is an financially attractive alternative in comparison with the current steel slides.

12 Conclusions and recommendations

The conclusions and recommendations of this research are presented in this chapter. First of all, the conclusions of the literature study are mentioned, where after the conclusions of the main research are mentioned. Thereafter, the main research question will be answered. Finally, some recommendations which follow from his research are mentioned.

12.1 Conclusions of literature study

The first three sub-research questions were (mainly) answered in the literature study. These sub-questions are answered in the next paragraphs.

1. How is the current barrier designed?

This question is answered in chapters 2 and 5. The current barrier is designed as closeable storm surge barrier, which can be closed at expected high sea levels. The barrier consists of concrete piers, between which steel lifting slides were placed. The water retaining part of the barrier consists of a permanent concrete sill beam, the moveable steel slide and a permanent concrete upper beam. The slide is placed before the sill beam and the upper beam with a space of 0.15 m. These steel slides corrode rapidly and need to be coated at least every 15 years.

2. Which structural designs are feasible for lifting slides in the Eastern Scheldt barrier?

This question is answered in chapter 3. All structural concepts which take into account the following considerations are in general feasible for lifting slides in the Eastern Scheldt barrier:

- No horizontal plates at North Sea side or second vertical wall to prevent wave impact loads on horizontal plates
- Inclined underside to prevent vibrations by flow
- Reasonable equal support reactions over the height

The structural designs which take these considerations into account and proved to be feasible in chapter 8 are:

- Straight box-girder
- Box-girder with thickening in the middle

These structural concepts were all made of FRP, therefore other structural designs could be feasible as well when e.g. steel or concrete is considered (provided that the considerations above are taken into account).

3. Which reinforcement, resins and manufacturing methods are suitable to apply for the slides and what are the characteristics of fibre reinforced polymers?

This question is answered in chapter 4. The reinforcements which can be used are glass fibres, aramid fibres or carbon fibres. These reinforcements are listed in order of increasing stiffness and price. If a high stiffness isn't necessary, glass fibres are the most attractive reinforcement.

The resins which could be applied are polyester resins of the type ISO or ISO-NPG and vinyl esters. These resins are suitable for use in a wet environment, as applicable on the slides. The choice between these suitable resins is particularly based on the price. Polyester resins have a much lower price.

The manufacturing methods which are suitable for the slides were mentioned in Table 7.2. The vacuum-assisted resin injection process is the most used process in the civil engineering industry. For other applications, other manufacturing processes could be beneficial as well.

The characteristics of fibre reinforced polymers are not fixed, since the reinforcement, resin and manufacturing process influence these characteristics highly. The mechanical properties which are in general achievable were mentioned in Table 4.3. Also other characteristics, such as e.g. the fire resistance, are dependable on the material choice.

12.2 Conclusions of the main research

The last two sub-research questions were answered in the main research. These sub-questions are answered in the next paragraphs.

4. What is technically the most promising design for the slide made of FRP?

This question is answered in the chapters 6, 7, 8, 9 and 10. The most promising design for the slide made of FRP is a slide of 22 m high, which is leaning on a new concrete sill beam. The current upper beam and sill beam should both be removed. The rabbets of the slide should be increased.

The increased slide height had the following advantages in comparison to the current slide:

- The top of the slide has increased to cope with the sea level rise in the future. The extra height in comparison to the top of the current upper beam is 1.7 m.
- The sill beam height is halved (to 4 m) to increase the trough-flow opening of the barrier. This can contribute to solve the problem of disappearing intertidal zones.

The new slide is also higher, since the upper beam (4.8 m) is removed.

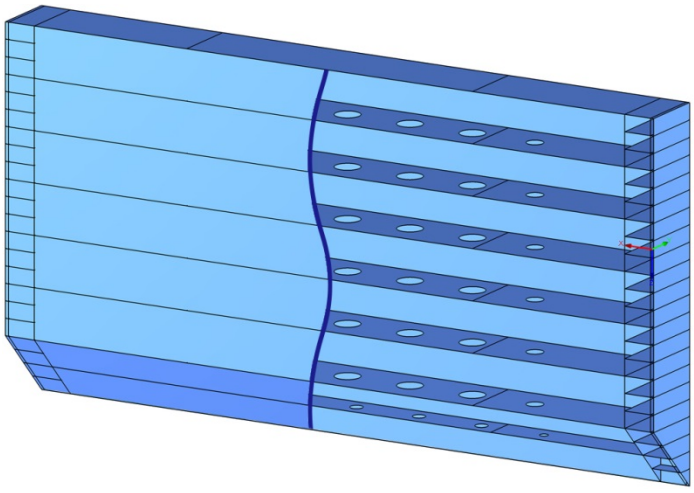


Figure 12.1 Final FRP slide design

The final design (see Figure 12.1), in the report called ‘long term solution’, has also some other advantages above the ‘short or medium term solution’, which is equal to a slide of 11.9 m high and which does not need extra adjustments on the current barrier. These advantages are:

- The deflection requirement is vanished since the sill beam is replaced and the upper beam is removed. Therefore, the slide is dimensioned on strength instead of deformation.
- Glass fibers are now used, since the stiffness wasn’t decisive. Otherwise, more expensive carbon fibers should be used to increase the stiffness.

5. **Is it financially attractive to replace the current slides by slides made of FRP over the total life of the barrier?**

This question is answered in chapter 11. The costs of the final FRP design, including the extra adjustment on the current barrier which are necessary, are estimated on 225 million euro. These investments are much less than the costs of dike raising, which could form another alternative on the long run. Next to that, a life cycle analysis (LCA) has been carried out to compare the life cycle costs of the final design with the maintenance costs of the current steel slides. This LCA showed that the payback time of the long term solution is between 40 and 50 years. Therefore the long term solution (final design) is an financially attractive alternative in comparison with the current steel slides.

12.3 Final conclusion

In this section a final answer is given on the main research question: 'Is it feasible to replace the current steel slides in the Eastern Scheldt barrier by slides made of FRP?'. This research showed that it is technically feasible to make the largest slide of the 62 slides of the Eastern Scheldt barrier in FRP. The most promising design is an FRP slide which is much higher than the current steel slides and which requires some adjustments on the current barrier. For this slide the deflection requirement has vanished. On the long term this slide can cope with the sea level rise and can help to solve the problem with the intertidal zones in the Eastern Scheldt.

Next to that, this research showed that an FRP slide is financially an attractive alternative of the current steel slides. Thereby, the main research question is answered: it is feasible to replace the current steel slides in the Eastern Scheldt barrier by slides made of FRP.

12.4 Recommendations

The recommendations which follow from this research are listed below:

- Hydraulic research should be carried out into the effect of the increasing trough-flow opening on the disappearing intertidal zones.
- The technical feasibility of the adjustments on the current barrier is not elaborated in detail. Therefore, it is recommended that the new concrete sill beam and the increment of the rabbets are elaborated into a greater detail.
- The pumping system for the new slides should be elaborated.
- The height of the new sill beam could be optimized further if the effect of the increasing trough-flow opening on the disappearing intertidal zones is known. Possibly, the height could be decreased further, to increase the trough-flow opening even more.
- A hydraulic research to the vibrations by flow of the bottom of the slide could improve the cross-section of the bottom possibly to a more structural efficient shape.
- The effect of the hybrid system, which consists of the pumping system and the current movement works, on the failure probability of the barrier should be investigated. The increased slide height could be an important parameter for this study, since a failed slide could have more consequences.
- The dynamic behavior of the slide due to waves or wind has to be investigated. Thereby a fatigue analysis should be carried out.
- New decisive water levels with a probability of occurrence of 1 in 4000 year should be determined to model the water pressure loads with more certainty.

- The strain criterion used should be replaced by a combined stress criterion to investigate the influence of the criterion on the material usage.
- The first ply failure theory which was used could be replaced by a last ply failure theory. Since it could be accepted that some damage on the slides occurs during a storm with a probability of occurrence of 1 in 4000 years. It's recommended to check the influence of such a design parameter on the material usage.
- The effective stiffness of the core material including the vertical stiffeners which are present between the outer skins should be calculated to check the influence of this on the final design.

References

[1] A. Keuzekamp, Hoge sterkte betonnen schuiven in de Stormvloedkering Oosterschelde, Delft, 1998.

[2] C. Cheung, C. v. d. Veen, D. Ros, N. Kaptijn en J. Pover, B200-hefschuiven Stormvloedkering Oosterschelde, Cement, 2002.

[3] J. Veraart, Glasvezelversterkte kunststof schuiven als alternatief voor de schuiven in de Oosterscheldekering, Delft, 1998.

[4] S. v. d. Laken, Ontwerp van schuiven van de Oosterscheldekering in vezelversterkte kunststoffen, 1999.

[5] S. D. Online, „Deltawerken.com," 2004. [Online]. Available: http://www.deltawerken.com/. [Geopend 11 2012].

[6] K. Steenepoorte, „De Stormvloedkering in de Oosterschelde," 2009.

[7] Rijkswaterstaat, Ontwerpnota stormvloedkering Oosterschelde - Boek 1: Totaalontwerp en ontwerpfilosofie, 2003.

[8] F. Biesboer, „25 Jaar Oosterscheldekering," *De Ingenieur,* 2011.

[9] D. N. Jans, „www.neeltjejans.nl," [Online]. Available: www.neeltjejans.nl. [Geopend 12 2012].

[10] Deltacommissie, „Samen werken met water," 2008.

[11] P. Z. Delta, Lange termijn verkenning Zuidwestelijke Delta, 2011.

[12] F. Bockhoudt, „Betonnen schuif Oosterschelde," [Online]. Available: http://www.dianausers.nl/pub/bockhoudt_schuif.pdf. [Geopend 19 12 2012].

[13] P. Kolkman en T. Jongeling, „Dynamisch gedrag van wouterbouwkundige constructies - Deel A constructies in stroming," NKB Offset, Bleiswijk, 1996.

[14] P. Kolkman en T. Jongeling, „Dynamisch gedrag van waterbouwkundige constructies - Deel B constructies in golven," NKB Offset, Bleiswijk, 1996.

[15] M. Kolstein, CT5128 Fibre reinforced polymer (FRP) structures, Delft, 2008.

[16] M. Chlosta, Feasibility study on fiber reinforced polymer cylindrical truss bridges for heavy traffic, Den Haag, 2012.

[17] A. Nijhof, Vezelversterkte kunststoffen, Mechanica en ontwerp, Delft: VSSD, 2004.

[18] L. Kok, Feasibility study for FRP in large hydraulic structures, Delft, 2013.

[19] Stichting CUR, Aanbeveling 96: Vezelversterkte kunststoffen in civiele draagconstructies, Gouda, 2003.

[20] G. Haverkamp, „Kunststof schuif in de kreekraksluizen," [Online]. Available: http://www.vkcn.nl/over-composieten/toepassingen/civiele-constructies-en-infrastructuur/kunststof-schuif-in-de-kreekraksluizen. [Geopend 19 12 2012].

[21] „Marineschepen.nl," [Online]. Available: http://www.marineschepen.nl/marschepen/alkmaar.html. [Geopend 12 4 2013].

[22] Rijkswaterstaat, Ontwerpnota stormvloedkering Oosterschelde - Boek 4: De sluitingsmiddelen, 2003.

[23] E. Ypey, „Het ontwerp van de schuifconstructies," *Cement,* 1982.

[24] Stichting CUR, Vezelversterkte kunststoffen in civiele draagconstructies - Achtergrondrapport bij CUR-Aanbeveling 96, Gouda, 2003.

[25] FiberCore Europe, „Kennismeeting Rotterdam Fiber Reinforced Polymers," 2013.

[26] C. Hartsuijker en H. Welleman, CT3109 Module niet-symetrische en inhomogene doorsneden, Delft, 2012.

[27] Rijkswaterstaat, Ontwerpnota stormvloedkering Oosterschelde - Boek 3: De betonwerken, 2003.

[28] P. Lievense, MEMO ZLMD-07N.17: Implic berekeningen prestatiepeilen Oosterschelde, Middelburg, 2007.

[29] Rijkswaterstaat, Deltaprogramma 2013 - Mogelijke strategieën (Zuidwestelijke Delta), 2013.

[30] Code, „FEA analyse FiberCore Oosterwolde brug," 2010.

[31] Stichting CUR, „CUR Recommendation 96 1st revised edition," 2013.

[32] Rijkswaterstaat, Analyse Oosterschelde Alternatieven, 1976.

[33] Wereld Natuur Fonds, Hoogtij voor Laag Nederland, Zeist, 2008.

[34] Ing.-Software Dlubal, RF-LAMINATE Program Description, Tiefenbach, 2012.

[35] Technische adviescommissie voor de waterkeringen, Leidraad kunstwerken, 2003.

[36] S. Bruneau, „Coastal Structures: Wave Loads," [Online]. Available: http://www.engr.mun.ca/~sbruneau/teaching/8751ocean/8751_13.pdf. [Geopend 4 2 2013].

[37] C. Honselaar, M. Kolstein, W. v. Leeuwen, H. Mullder, G. Nagtegaal, G. v. d. Weijde en S. d. Winter, Vezelversterkte kunststoffen in civiele toepassingen, Leidschendam, 1999.

[38] A. Vrijburcht, Hydraulische aspecten van stroomsluizen en hoogwaterkeringen, Delft: TU Delft, 2000.

[39] O. Zeeland, „Omroep Zeeland," 1 7 2011. [Online]. Available: http://www.omroepzeeland.nl/node/45489. [Geopend 28 1 2013].

[40] VKCN, „VKCN," [Online]. Available: http://www.vkcn.nl/. [Geopend 28 01 2013].

[41] BouwOnline, „Verzinkt staal maakt plaats voor kunststof,” [Online]. Available: http://www.bouwonline.nl/4/pdcnewsitem/00/44/27/index_4.html. [Geopend 10 4 2013].

[42] K. Snijder, „Presentatie FiberCore Europe,” Rotterdam, 2012.

[43] Bouwdienst Rijkswaterstaat, Kunststof loopbrug in Harlingen, Den Haag, 2000.

[44] Bouwdienst Rijkswaterstaat, Kunststof schuif in kreekraksluizen, Den Haag, 2000.

[45] P. Hoogenboom, „Piekspanningen in eindige-elementenberekeningen,” Delft, 2007.

[46] Rijkswaterstaat, Veilig getij - Beheer en gebruik Stormvloedkering Oosterschelde, ervaring en bijstelling, Middelburg, 1991.

[47] Rijkswaterstaat, Hydraulische Randvoorwaarden 2001, Delft, 2001.

[48] R. v. Straten, Werkboek inleiding Civiele Techniek: De Oosterscheldekering, Delft, 2008.

[49] Rijkswaterstaat, Onderzoek naar de mogelijke afsluiting van de Oosterschelde met een gedeeltelijk geprefabriceerde stormvloedkering - Deelrapport 8, 's-Gravenhage, 1988.

[50] Rijkswaterstaat, „Waarom vezelversterkte kunststof?,” [Online]. Available: http://www.rijkswaterstaat.nl/rws/e-zine/vezelversterktekunststof/index.php. [Geopend 17 05 2013].

[51] FiberCore Europe, „FiberCore Europe,” [Online]. Available: http://www.fibercore-europe.com/. [Geopend 17 05 2013].

[52] Rijkswaterstaat, „Waterstanden Roompot buiten”.

Appendices:

A	CALCULATION OF LAMELLA PROPERTIES
B	CALCULATION OF SANDWICH VARIANT
C	COMPARISON LAMINATE STIFFNESS MATRIX
D	DISTRIBUTION OF SUPPORT REACTIONS
E	LOADS SPECIFICATION
F	FINAL DESIGN DLUBAL RFEM
G	EXTRA COSTS RIGOROUSLY SOLUTION
H	INFORMATION PROVIDED ON DVD

Table of contents

APENDIX A: CALCULATION OF LAMELLA PROPERTIES 132

APENDIX B: CALCULATION OF SANDWICH VARIANT 134

APENDIX C: COMPARISON LAMINATE STIFFNESS MATRIX 136

APENDIX D: DISTRIBUTION OF SUPPORT REACTIONS 138

APENDIX E: LOADS SPECIFICATION 139

1 SAFETY FACTORS 139
1.1 Consequence class 139
1.2 Load factors 139
2 WATER AND WAVE LOADS 140
2.1 Water pressure positive drop 140
2.2 Water pressure negative drop 141
2.3 Wave pressures theory 142
2.4 Wave pressure positive drop 143
2.5 Wave pressure negative drop 145
3 COLLISION LOAD 145
4 LOAD COMBINATIONS 145
5 MAPLE SCRIPTS 146
5.1 Positive drop 146
5.2 Negative drop 156

APENDIX F: FINAL DESIGN DLUBAL RFEM 166

APENDIX G: EXTRA COSTS RIGOROUSLY SOLUTION 299

1 COSTS NEW SILL BEAM 299
2 INCREASING A RABBET 300

APENDIX H: INFORMATION PROVIDED ON DVD 302

Appendix A: Calculation of lamella properties

restart;

Resin and fibre properties

$E[R] := 3.4$:
$G[R] := 1.3$:
$\mathrm{nu}[R] := 0.35$:
$E[F] := 72$:
$G[F] := 30$:
$\mathrm{nu}[F] := 0.22$:
$V[f] := 0.6$:
$\mathrm{phi}[UD] := 0.97$:

Halpin and Tsai

$$E[1] := (E[R] + (E[F] - E[R]) \cdot V[f]) \cdot \mathrm{phi}[UD];$$

$$43.2232 \tag{2.1}$$

$$E[2] := \left(E[R] \cdot \left(\frac{1 + \mathrm{xi}[1] \cdot \mathrm{eta}[1] \cdot V[f]}{1 - \mathrm{eta}[1] \cdot V[f]}\right)\right) \cdot \mathrm{phi}[UD];$$

$$\frac{3.298\,(1 + 0.6\,\xi_1\,\eta_1)}{1 - 0.6\,\eta_1} \tag{2.2}$$

$$\mathrm{eta}[1] := \frac{\frac{E[F]}{E[R]} - 1}{\frac{E[F]}{E[R]} + \mathrm{xi}[1]} : \mathrm{xi}[1] := 2 :$$

$$G[12] := \left(G[R] \cdot \left(\frac{1 + \mathrm{xi}[2] \cdot \mathrm{eta}[2] \cdot V[f]}{1 - \mathrm{eta}[2] \cdot V[f]}\right)\right) \cdot \mathrm{phi}[UD];$$

$$\frac{1.261\,(1 + 0.6\,\xi_2\,\eta_2)}{1 - 0.6\,\eta_2} \tag{2.3}$$

$$\mathrm{eta}[2] := \frac{\frac{G[F]}{G[R]} - 1}{\frac{G[F]}{G[R]} + \mathrm{xi}[2]} : \mathrm{xi}[2] := 1 :$$

$$\mathrm{nu}[12] := \mathrm{nu}[R] - (\mathrm{nu}[R] - \mathrm{nu}[F]) \cdot V[f];$$

$$0.272 \tag{2.4}$$

$$data['HalpinTsai'] := [E[1], E[2], G[12], \mathrm{nu}[12]];$$

$$[43.2232,\ 14.11726249,\ 4.345434657,\ 0.272] \tag{2.5}$$

Output

model ≔'*HalpinTsai*';

HalpinTsai **(3.1)**

printf("E[1]= %g\nE[2]= %g\nG[12]= %g\nnu[12]= %g", *data*[*model*][1], *data*[*model*][2], *data*[*model*][3], *data*[*model*][4]);

```
E[1]=   43.2232
E[2]=   14.1173
G[12]=  4.34543
nu[12]= 0.272
```

Appendix B: Calculation of sandwich variant

restart;

Parameters

$E[s] := 15000$: #N/mm^2
$E[c] := 32.9$:#N/mm^2
$b := 1000$:
q := 0.100·b;#N/mm

$$100.000 \quad \textbf{(1.1)}$$

γq := 1.5 :#[-]
$L := 41300$:#*mm*
sigma[s] := 150 : #*caused by an assumed strain limit of 1%*
sigma[c] := 0.69 :
$h[c] := h[tot] - 2 \cdot h[s]$;#*total height is equal to core height +two times skin height*

$$h_{tot} - 2\,h_s \quad \textbf{(1.2)}$$

$t := 17$;

$$17 \quad \textbf{(1.3)}$$

$a := 100$:
$aantal := \frac{1000}{a}$;

$$10 \quad \textbf{(1.4)}$$

Determine stiffnesses

$$EI := 0.5 \cdot E[s] \cdot h[s] \cdot b \cdot (h[c] + h[s])^2 + E[s] \cdot \frac{aantal}{12} \cdot t \cdot (h[c])^3 + E[c] \cdot \frac{1}{12} \cdot (b - aantal \cdot t) \cdot (h[c])^3;$$

$$7.5000000\ 10^6\, h_s\, (h_{tot} - h_s)^2 + 2.147755833\ 10^5\, (h_{tot} - 2\,h_s)^3 \quad \textbf{(2.1)}$$

$$GA := 1950 \cdot 2 \cdot h[s] \cdot b + 26.1 \cdot h[c] \cdot (b - aantal \cdot t) + 1950 \cdot h[c] \cdot aantal \cdot t;$$

$$3.1936740\ 10^6\, h_s + 3.531630\ 10^5\, h_{tot} \quad \textbf{(2.2)}$$

Maximum moment (M[RD])

#Failing of skin:

$$M[s] := \frac{EI \cdot \text{sigma}[s]}{\frac{h[tot]}{2} \cdot E[s]} :$$

#Failing of core:

$$M[c] := \frac{EI \cdot \text{sigma}[c]}{\frac{h[c]}{2} \cdot E[c]} :$$

$M[Rd] := \min(M[s], M[c])$:

Determine design bending moment and thickness of skin (H[s]) when h[tot]=2500

$M[Ed] := \frac{1}{8} \cdot \gamma q \cdot q \cdot L^2;$

$$3.198168750\ 10^{10} \quad \textbf{(4.1)}$$

$solve(subs(h[tot] = 2500, M[Rd] = M[Ed]), h[s]);$

$$16.75736522 \quad \textbf{(4.2)}$$

$h[sn] := \%:$

Determine deflection when h[tot]=2500 and calculated h[s]

$w := \frac{5}{384} \cdot \frac{q \cdot L^4}{EI} + \frac{1}{8} \frac{q \cdot L^2}{GA};$

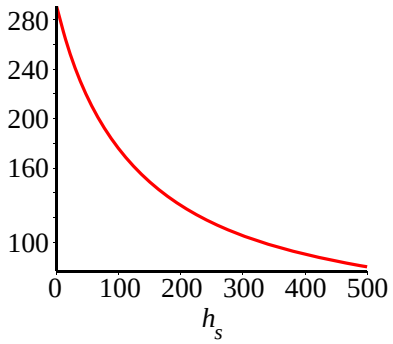
$$\frac{3.788253094\ 10^{18}}{7.5000000\ 10^6\ h_s\ (h_{tot} - h_s)^2 + 2.147755833\ 10^5\ (h_{tot} - 2\ h_s)^3} + \frac{2.132112500\ 10^{10}}{3.1936740\ 10^6\ h_s + 3.531630\ 10^5\ h_{tot}} \quad \textbf{(5.1)}$$

$subs(\{h[s] = h[sn], h[tot] = 2500\}, w);$

$$970.3741950 \quad \textbf{(5.2)}$$

Determine thickness when deflection requirement=250mm and h[tot]=4000

$plot(subs(h[tot] = 4000, w), h[s] = 0..500);$



$solve(\{subs(h[tot] = 4000, w = 250), h[s] > 0, h[s] < 500\}, h[s]);$

$$\{h_s = 23.70946537\} \quad \textbf{(6.1)}$$

Apendix C: Comparison laminate stiffness matrix

In order to check whether the lamella stiffness matrix and the laminate stiffness matrix of the module RF-Laminate in DLUBAL RFEM correspond to the stiffness matrices of the laminate design tool Kolibri (developed at Delft University of Technology), a certain stacking of lamellas was used as input. The used stacking of lamellas is shown in Table C.1. The properties of a lamella which has been used are:

$$E_1 = 19{,}48\ GPa \quad E_2 = 6{,}36\ GPa \quad G_{12} = 1{,}95\ GPa \quad \nu_{12} = 0{,}27\ GPa$$

Table C.1 Lamella stacking

Layer	Thickness (mm)	Direction (°)
1	11.0	0.00
2	3.0	90.00
3	3.0	-45.00
4	6.0	45.00
5	3.0	-45.00
6	3.0	90.00
7	11.0	0.00

The 2D stiffness matrix of a lamella (when the fibre orientation corresponds to the first principal direction) can be calculated with (according to [34]):

$$\mathrm{d_i} = \begin{pmatrix} d_{i,11} & d_{i,12} & 0 \\ & d_{i,22} & 0 \\ sym & & d_{i,33} \end{pmatrix} = \begin{pmatrix} \dfrac{E_x}{1-\upsilon_{xy}^2\dfrac{E_y}{E_x}} & \dfrac{\upsilon_{xy}E_y}{1-\upsilon_{xy}^2\dfrac{E_y}{E_x}} & 0 \\ & \dfrac{E_y}{1-\upsilon_{xy}^2\dfrac{E_y}{E_x}} & 0 \\ sym & & \dfrac{E_i}{2(1+\upsilon_i)} \end{pmatrix}$$

By filling in the properties of the lamella, the stiffness matrix corresponds to the stiffness matrix which is calculated by RFEM, see Figure C.1. When this matrix is compared with the stiffness matrix which is obtained with Kolibri, these matrices correspond very well with each other.

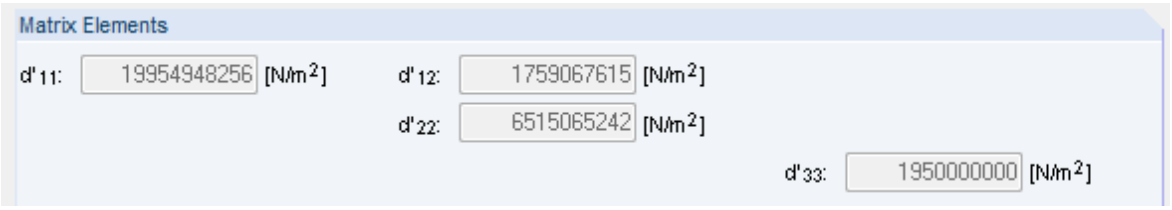


Figure C.1 Lamella stiffness matrix from DLUBAL RFEM

Stiffness Matrix 2D

$$[S] = \begin{bmatrix} 1{,}9955 \cdot 10^{10} & 1{,}7591 \cdot 10^{9} & 0 \\ 1{,}7591 \cdot 10^{9} & 6{,}5151 \cdot 10^{9} & 0 \\ 0 & 0 & 1{,}9500 \cdot 10^{9} \end{bmatrix} \text{N/m}^2$$

Figure C.2 Lamella stiffness matrix from Kolibri

The laminate stiffness matrices (ABD-matrix) of both programs are also compared with each other. The matrix which is obtained by DLUBAL RFEM is shown in Figure C.3 and the matrix which is obtained with Kolibri is shown in Figure C.4. Both matrices correspond very well to each other. That means that both programs have integrated the classical lamination theory in the same way. Since the laminate design tool Kolibri was developed at TU Delft, it can be assumed that the integration of the classical lamination theory was done correct. This is not checked anymore.

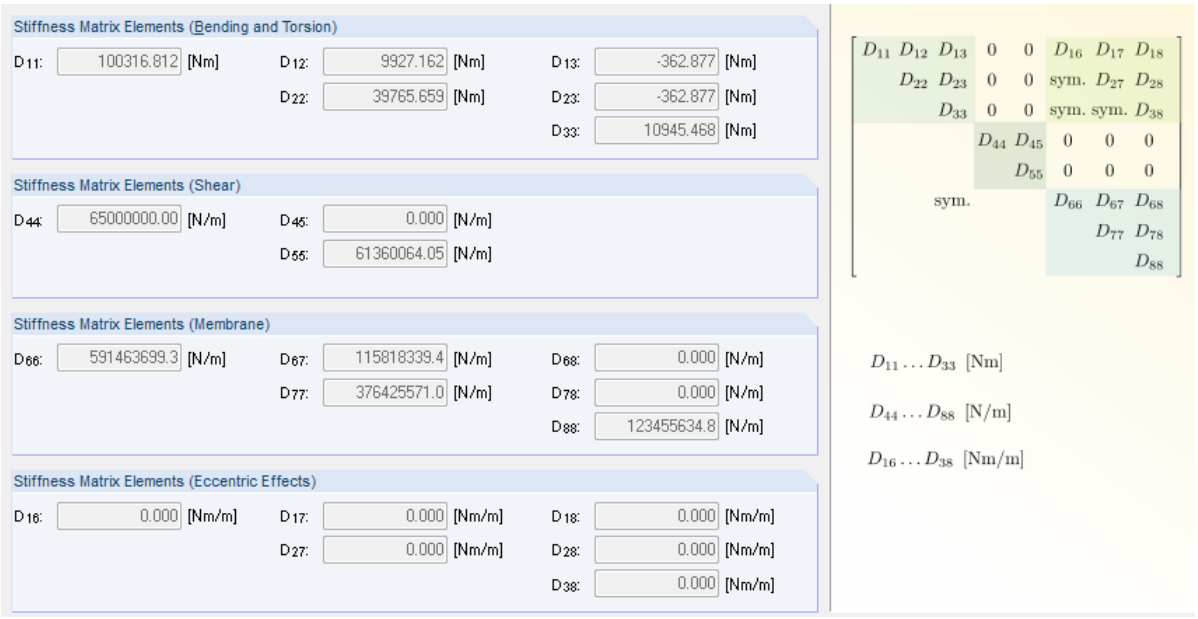


Figure C.3 Laminate stiffness matrix from DLUBAL RFEM

Laminate Stiffness Matrix

$$[ABD] = \begin{bmatrix} 5{,}9146 \cdot 10^{8} & 1{,}1582 \cdot 10^{8} & 0 & 0 & 0 & 0 \\ 1{,}1582 \cdot 10^{8} & 3{,}7643 \cdot 10^{8} & 0 & 0 & 0 & 0 \\ 0 & 0 & 1{,}2346 \cdot 10^{8} & 0 & 0 & 0 \\ 0 & 0 & 0 & 1{,}0032 \cdot 10^{5} & 9927{,}2 & -362{,}88 \\ 0 & 0 & 0 & 9927{,}2 & 39766 & -362{,}88 \\ 0 & 0 & 0 & -362{,}88 & -362{,}88 & 10945 \end{bmatrix} \text{N, m}$$

Figure C.4 Laminate stiffness matrix from Kolibri

Apendix D: Distribution of support reactions

The distribution of support forces over the height in Figure 8.10 and Figure 8.17 looks strange, since it is expected that the horizontal plates at the top and bottom carry half of the load of the other horizontal plates. Therefore these support forces are investigated into more detail.

When the support was modeled as an infinity stiff line support, the distribution of reaction forces is as shown on the left of Figure D.1. When the line support is replaced with infinity stiff nodal support at the position of the horizontal plates, the distribution of reaction forces is as expected, as shown in the middle of Figure D.1. The horizontal plates at the top and bottom carry approximately half of the load of the other horizontal plates.

To check the distribution of support reactions for the line support, the surfaces of the diagram per horizontal plate are calculated and shown on the right of Figure D.1. These values are similar to the values of the nodal support. Therefore, the horizontal plates at the top and bottom do not carry more load than the other plates. That's just a visual misunderstanding, since the surfaces near the top and bottom are much smaller than the surfaces for the other plates.

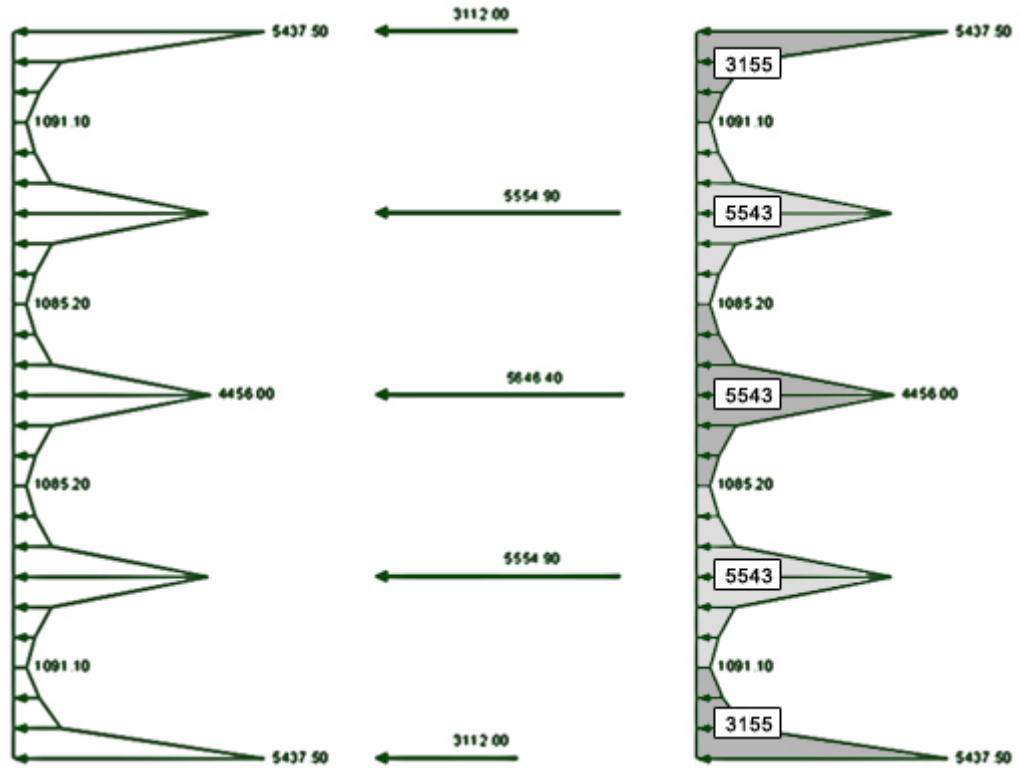


Figure D.1 Distribution of reaction forces over the height (left: line support, middle: nodal supports, right: surface calculation of line support)

Apendix E: Loads specification

1 Safety factors

1.1 Consequence class

The slide structure belongs to consequence class 3, which corresponds according to NEN-EN 1990 table NB.20-B1 with: *high consequence for loss of human life, or economic, social or environmental consequences very great.* For a primary flood barrier as the Eastern Scheldt barrier, this is definitely the case. Consequence class 3 is in comparison to the consequence classes in NEN 6700 an extra consequence class above the classes 1, 2 and 3 which were present in the NEN 6700.

1.2 Load factors

Water pressures due to decisive water levels should be interpreted as permanent loads according to NEN-EN 1990. In [35] is mentioned that these loads shouldn't be interpreted as permanent load for flood defenses, but as variable loads with specified load factors. The load factors according to NEN-EN 1990 consequence class 3 are shown in Table E.1.

Table E.1 Load factors according to NEN-EN 1990 CC3
**) could be reduced since the water level at North Sea side is physically limited (for the positive drop case).*

	Buildings		Bridges	
	6.10a	*6.10b*	*6.10a*	*6.10b*
Permanent load	1.50*/0.9	1.30/0.9	1.40*/0.9	1.25/0.9
Variable load	1.65	1.65	1.65	1.65

Since the water pressure from the North Sea side is correlated with the water pressure at the Eastern Scheldt side the sum of these loadings, the water pressure difference, is used as load for the slides. Therefore, favorable and unfavorable loadings effects doesn't have to be taken into account, which is in accordance with 'Leidraad kunstwerken' [35]. The load factors are taken from NEN-EN 1900 table NB.13-A2.4(B), load factors for bridges, since bridges are to a greater extend civil engineering structures than buildings. In general, the loadings for civil engineering structures are to a certain extend determined more precisely, which has effect on the load factors.

The load factors according to 'Leidraad kunstwerken' are determined for use in combination with NEN 6700 and are shown in Table E.2. The pressure differences due to water levels or waves should be interpreted as variable loads for which a load factor of 1.25 is determined.

Table E.2 Load factors according to Leidraad Kunstwerken

Load	Load type	Load factor
Pressure difference due to water levels	Variable load	1.25
Pressure difference due to waves	Variable load	1.25

Table E.3 Load factors per load
**) could be reduced since the water level at North Sea side is physically limited (for the positive drop case).*

	Eurocode		Leidraad
	6.10a	*6.10b*	kunstwerken
Water pressure difference	1.40*	1.25	1.25
Wave load	1.65	1.65	1.25

Since the 'Leidraad kunstwerken' is based on the expired norm NEN 6700, it is advised by the 'Helpdesk water' to take the Eurocode and the 'Leidraad water' both into account. The most unfavorable method will be decisive. The load factors per load are shown in Table E.3. The safety factors of the Eurocode are higher than the 'Leidraad kunstwerken' and will be decisive. It was assumed that equation 6.10b was decisive, therefore equation 6.10a has not been considered. During this graduation project a new document of the ROK (Richtlijnen ontwerpen kunstwerken) came out. In this document higher safety factors are defined for water pressure difference loads. It wasn't possible anymore to use these new safety factors in the final design of the slide.

2 Water and wave loads

In the initial design stage the water and wave loads could be modeled as a constant load over the height of 100 kN/m^2 (according to [1]). These loads were derived from the decisive water levels and wave conditions for the current slides. But the rigorously solution differs in such a way from the current slides that the water and wave loads should be determined again. The height of the slide is changed and the position of the bottom is also changed. The top of the slide is now positioned at N.A.P. + 7.5 m and the bottom of the slide at N.A.P. – 14.5 m. Next to that, the new slide is filled with water when the slide is in closed position. Therefore, the water pressure from inside the slide should be considered too.

2.1 Water pressure positive drop

The water pressures difference loads on the vertical walls will be determined in this section. It is assumed that the water level inside the slide is equal to the decisive water level of positive drop at North Sea side. The water pressure difference loads will be determined for the outer wall (at North Sea side) and for the inner wall (at Eastern Scheldt side), for the situations with and without holes in the horizontal plates. On the basis of the water pressure difference loads the most favorable situation will be chosen.

The water pressure difference loads for the situation without holes in the horizontal plates are shown in Figure E.1. The water pressure inside the slide increases linear from each horizontal plate to the next one and begins after that plate on zero again. Therefore the water pressure difference loads reach very high values at the bottom of the slide, which is very unfavorable.

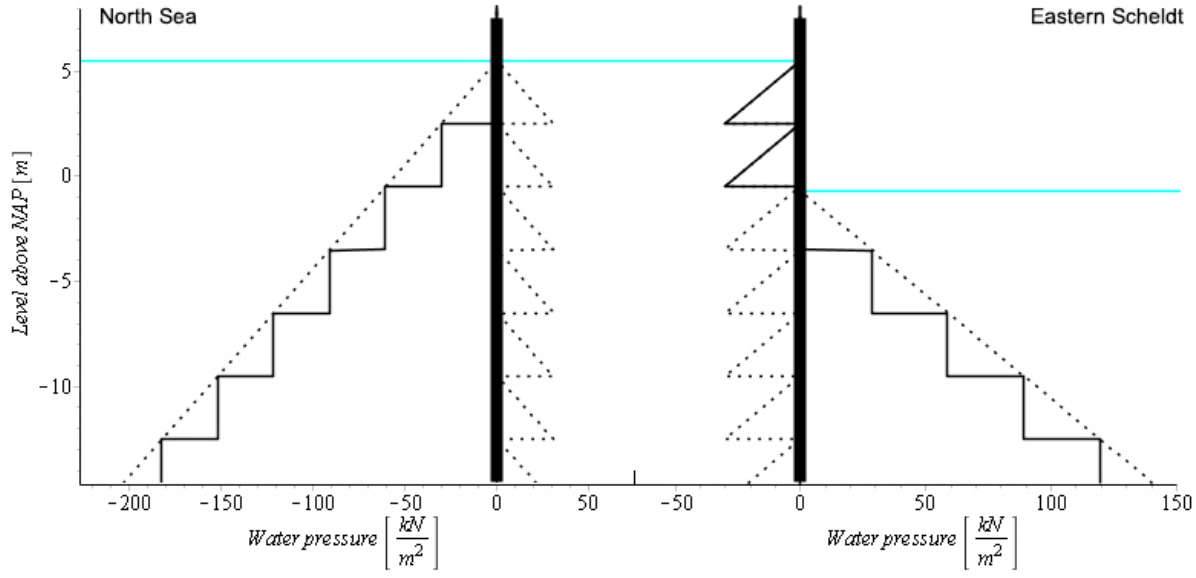


Figure E.1 Water pressure difference loads due to positive drop (situation without holes)

The water pressure difference loads for the situation with holes in the horizontal plates are shown in Figure E.2. Over the outer wall there is no water pressure difference, since the water levels on both sides are equal. The first part of the water pressure difference over the inner wall increases linearly to a value of 63 kN/m^2, where after it is constant.

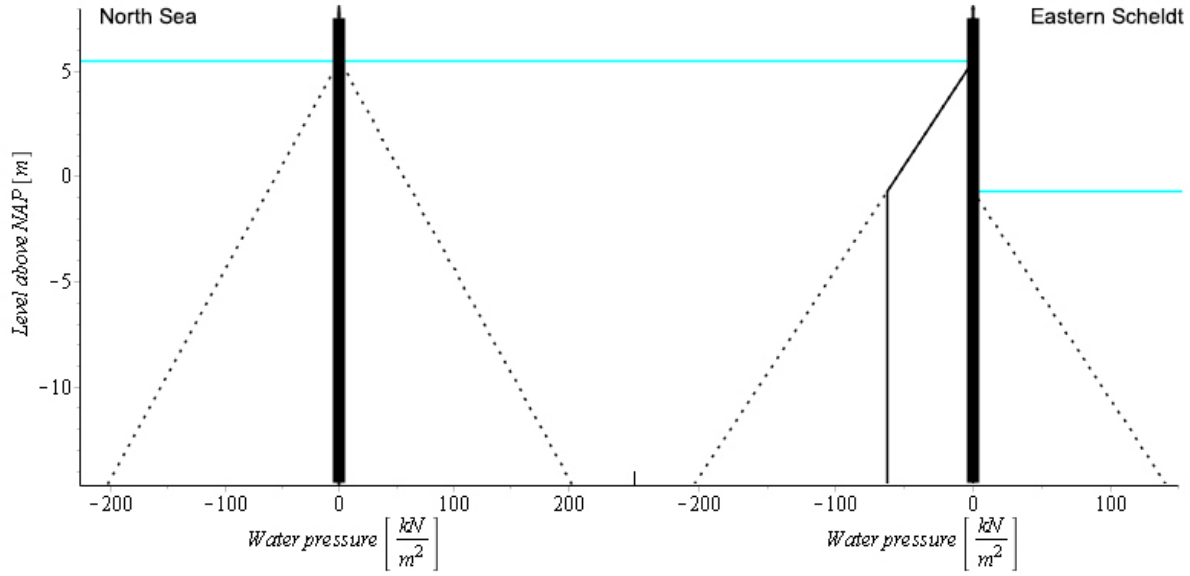


Figure E.2 Water pressure difference loads due to positive drop (situation with holes)

Since the water pressure difference loads for the situation without holes reach very high values at the bottom of the slide, it is the most favorable to make holes in the horizontal plates. This gives a much better and more constant load on the slide, as shown in Figure E.2.

2.2 Water pressure negative drop

The water pressure difference loads due to the decisive water levels during negative drop will be calculated in this section. Since the negative drop case takes place when the slides fail to be lifted up after a storm, it is assumed that the water level inside the slide is still the same as during the storm (during the positive drop case).

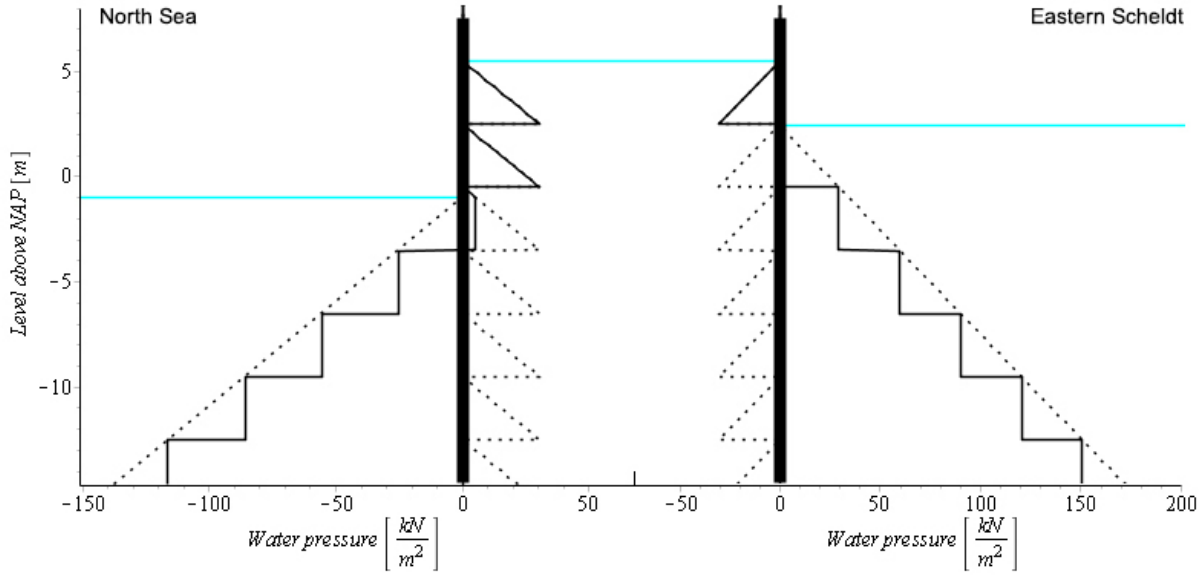


Figure E.3 Water pressure difference loads due to negative drop (situation without holes)

That will give the most unfavorable situation for negative drop. Although it is already clear that holes in the horizontal plates are favorable, the water pressure difference loads for both situations will be shown here to be complete.

The water pressure difference loads for the situation without holes in the horizontal plates are shown in Figure E.3. Also here the loads reach very high values towards the bottom of the slide. The water pressure difference loads for the situation with holes in the horizontal plates are shown in Figure E.4. The loads are also for the negative drop case much more favorable than in the situation without holes. After a first part which is linear ascending, the maximum value is reached and the load is further constant. The load at the outer wall reaches a maximum value of 66 kN/m^2 and the load on the inner wall reaches a maximum value of 32 kN/m^2.

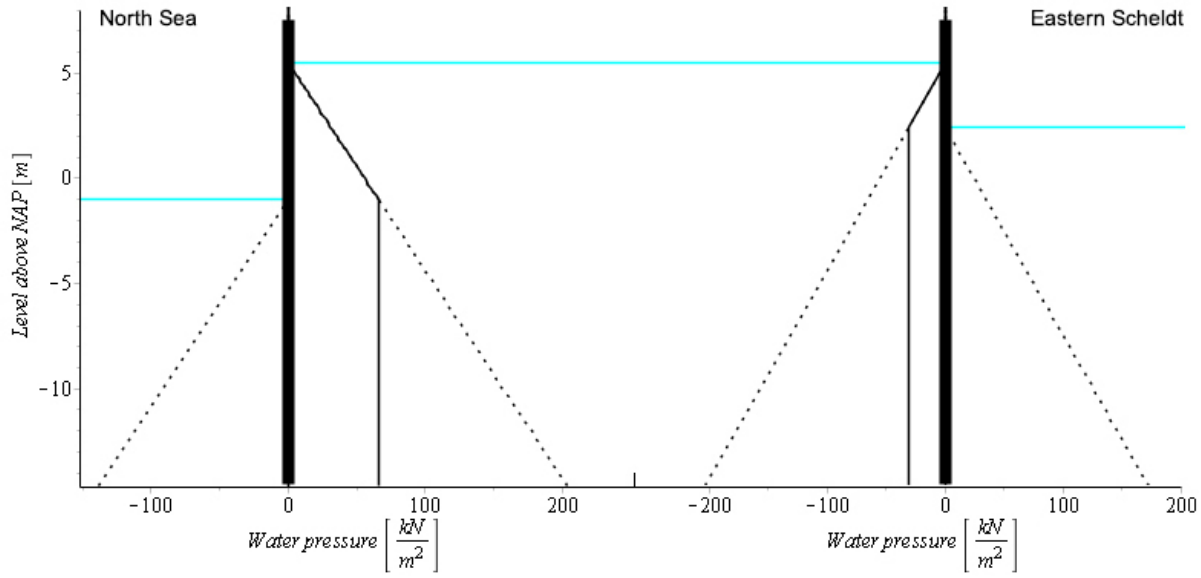


Figure E.4 Water pressure difference loads due to negative drop (situation with holes)

2.3 Wave pressures theory

The wave pressures on a vertical wall can be calculated with the model of Sainflou. To use this model the reflected design wave height for the structure and the wave length should be known, which are calculated according to 'leidraad kunstwerken' [35].

The design wave height is chosen there on the basis of a probability of exceedance during a storm peak of 10%. And can be calculated, for average Dutch circumstances along the North Sea coast, by using a Rayleigh-distribution of wave heights, with:

$$H_d = 2.2 \cdot H_s$$

The significant wave height (H_s) is known for the Eastern Scheldt barrier. The waves are reflected by the barrier, which can increase the wave height and the wave loads. The reflected design wave height for the barrier can be calculated with:

$$H_{d,refl} = (1 + \chi) \cdot H_d$$

The reflection coefficient χ is determined for the Eastern Scheldt barrier as 0.7. The wave length can be calculated with:

$$L = \frac{gT^2}{2\pi}\tanh(kh) \qquad with: k = \frac{2\pi}{L}$$

k Wave number
T Wave period

Since the reflected design wave height is known, the wave loads can be calculated with the model of Sainflou, which is schematized in Figure E.5.

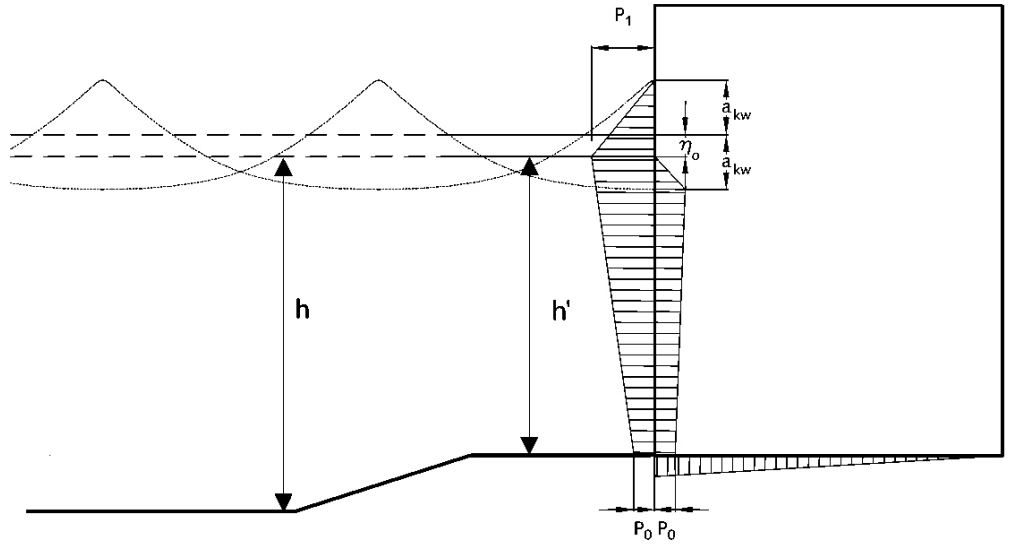


Figure E.5 Wave loads according to model of Sainflou [35]

The increase of the mean water level can be calculated with:

$$\eta_0 = \frac{1}{2} k a_{kw}^2 \coth(kh)$$

η_0 Increase of mean water level [m]
a_{kw} Half wave height before the structure $= H_{d,refl}/2$ [m]
k Wave number [m^{-1}]
h Water depth [m]

The maximum pressure at the bottom of the structure is according to Sainflou:

$$p_0 = \frac{\rho g a_{kw}}{\cosh(kh')}$$

h' Water depth above the foundation level of the structure [m]

The maximum pressure at the mean water level is assumed to be:

$$p_1 = \rho g (a_{kw} + \eta_0)$$

The water pressure gradient is assumed to be linear between p_0 and p_1. The maximum pressure caused by a wave trough is assumed to be: [36]

$$p_3 = \rho g (a_{kw} - \eta_0)$$

2.4 Wave pressure positive drop

By following the procedure of the previous section the following pressures are calculated for the wave crest: $p_0 = 72\ N/mm^2$, $p_1 = 138\ N/mm^2$. These pressures are much higher than the wave loadings which were calculated in [1] and [22]. This is caused by the fact that the significant wave

height which was given for the Eastern Scheldt barrier was already calculated using a Rayleigh-distribution with a probability of exceedance of 13.5%. Therefore it is assumed that the design wave height can be taken equal to the significant wave height which was known, so $H_d = H_s$. The loads calculated with this assumption are much more like the wave loads which were calculated in [1] and [22] , and are shown in Figure E.6. The maximum wave pressure at the slide during a wave crest is 56 kN/m^2 and at the bottom of the slide 33 kN/m^2.

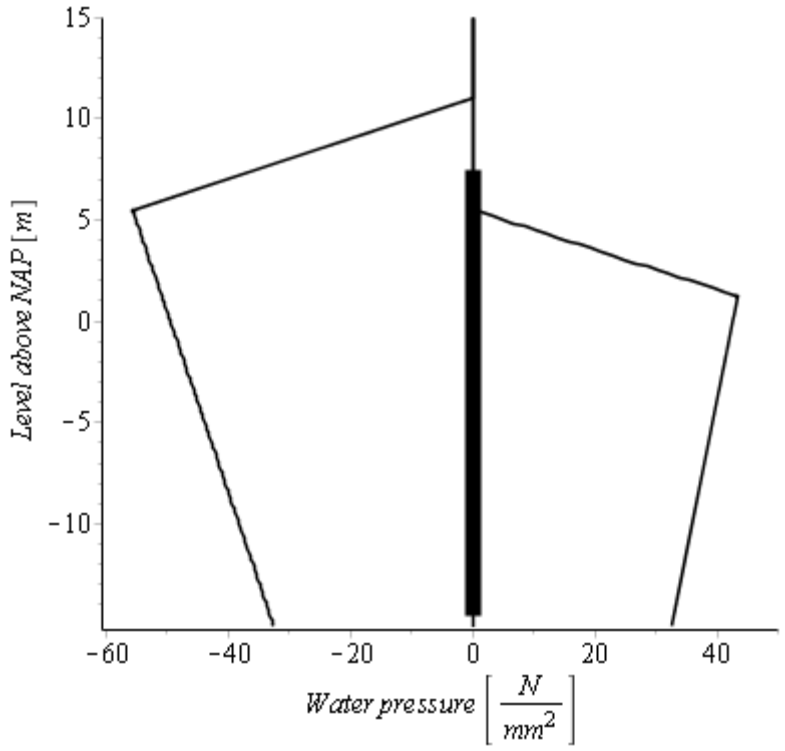


Figure E.6 Wave pressures due to positive drop (left: wave crest, right: wave trough)

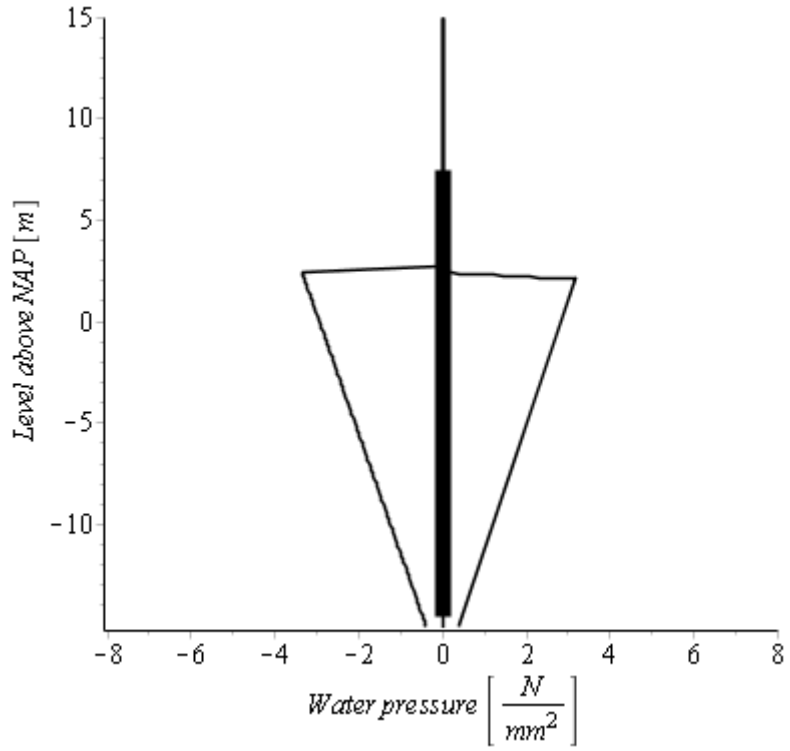


Figure E.7 Wave pressures due to negative drop (left: wave crest, right: wave trough)

2.5 Wave pressure negative drop

For the calculation of the wave pressure for negative drop it is also assumed that $H_d = H_s$. The maximum water pressure is 3.2 kN/m^2 and at the bottom of the slide the water pressure is 0.5 kN/m^2 as shown in Figure E.7.

3 Collision load

Since a collision of a ship occurred already in the current lifetime of the Eastern Scheldt barrier, a collision load has to be taken into account. The collision surfaces according to NEN-EN 1991-1-7 NB are shown in Figure E.8. The barrier is not located along a commercial shipping route, therefore only tourist boating traffic is taken into account. The total collision load for tourist boating traffic is 500 kN.

The most unfavorable situation is a collision towards the bottom of the slide, when the slide is in open position. The collision surface below the water level is therefore not present. Considering a boat length of 20 m, the load is spread over 2 m width and 1 m height. Therefore, a horizontal load of 250 kN/m^2 is modeled onto the bottom of the slide (in top view: in the middle), see Figure 10.16a.

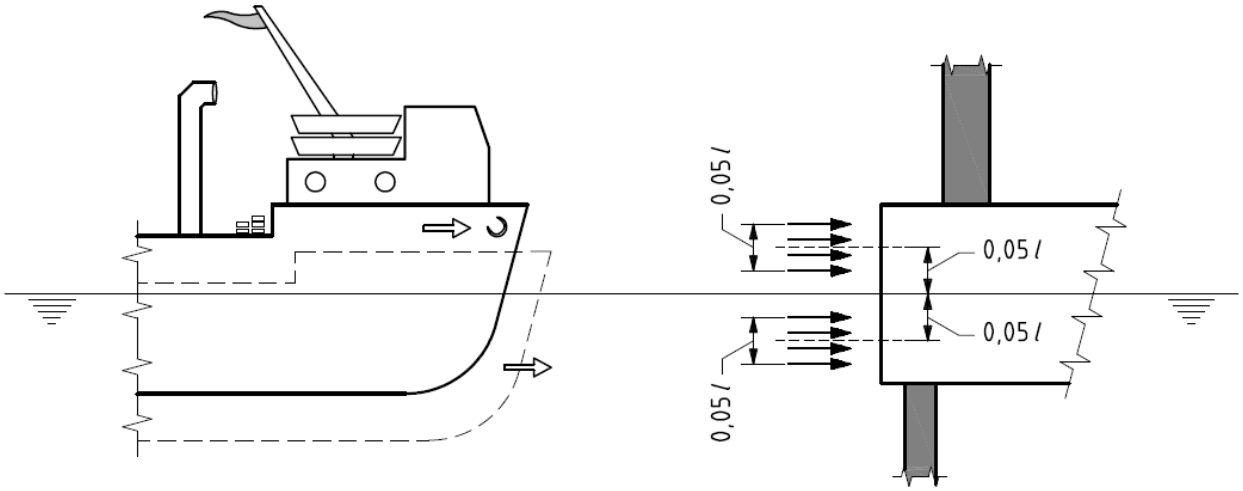


Figure E.8 Colisision surface according to NEN-EN 1991-1-7 NB

4 Load combinations

The load combinations which will be taken into account are given in Table E.4. The ψ-factors will be taken equal to 1. Therefore the load factors from the Eurocode are higher than the factors according to 'leidraad kunstwerken' and should be used as safety factors.

Table E.4 Load combinations

Load combinations →	Positive drop	Negative drop	Ice	Collision	Water impact
Dead load	x	x	x	x	X
Water pressure pos drop	x				
Waves pos drop	x				
Water pressure neg drop		x			
Waves neg drop		x			
Ice load			x		
Collision load				X	
Vertical water impact					X

5 Maple scripts

The maple scripts which were used to calculate the loads and generate the figures in this appendix are shown in the next paragraphs.

5.1 Positive drop

restart;

Parameters

Situatie 1: positief verval

waterstand[*nz*] := 5.5 : waterstand[*oz*] := −0.7 : Hs := 5.75 : T := 9.5 :

Determine waterdepth, design wave height and other definitions

rho := 1030 : g := 9.81 : alpha := 0.7 : $k := \frac{2 \cdot \mathrm{Pi}}{L}$:

htot := 30 + max(waterstand[*nz*], waterstand[*oz*]);

35.5 **(2.1)**

h := 15 + max(waterstand[*nz*], waterstand[*oz*]);

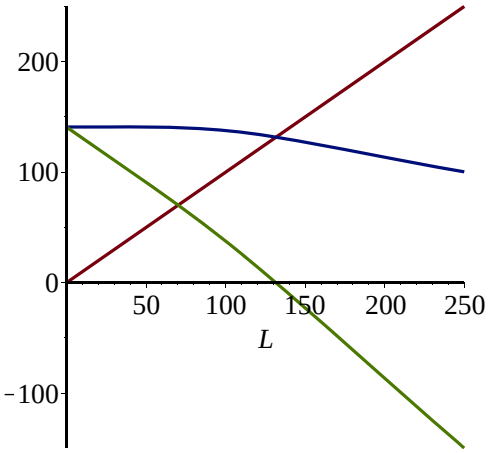
20.5 **(2.2)**

H := (1 + alpha) · *Hs*;

9.775 **(2.3)**

Determine wave length

plot$\left(\left\{ \frac{g \cdot T^2}{2 \cdot \mathrm{Pi}} \cdot \tanh(k \cdot \mathrm{htot}),\ L,\ \frac{g \cdot T^2}{2 \cdot \mathrm{Pi}} \cdot \tanh(k \cdot \mathrm{htot}) - L \right\},\ L = 0..250 \right)$;



with(*Student*[*NumericalAnalysis*]) :

$L := Bisection\left(\frac{g \cdot T^2}{2 \cdot \mathrm{Pi}} \cdot \tanh(k \cdot \mathrm{htot}) - L,\ L = [0, 250],\ tolerance = 10^{-5} \right)$;

131.6957474 **(3.1)**

Determine water pressures and wave pressures

$\text{delta} := evalf(0.5 \cdot k \cdot (0.5 \cdot H)^2 \cdot \coth(k \cdot \text{htot}))$;

$$0.6097026179 \tag{4.1}$$

$p[2] := evalf\left(\frac{\text{rho} \cdot g \cdot 0.5 \cdot H}{\cosh(\text{k} \cdot h)}\right)$;

$$32540.13651 \tag{4.2}$$

$p[1] := \text{rho} \cdot g \cdot (0.5 \cdot H + \text{delta})$;

$$55545.38441 \tag{4.3}$$

$p[3] := evalf(\text{rho} \cdot g \cdot (0.5 \cdot H - \text{delta}))$;

$$43224.14809 \tag{4.4}$$

if waterstand[nz] > waterstand[oz] **then** $z1 := 0 : z2 := -\text{waterstand}[nz] + \text{waterstand}[oz] : \text{b1} := 1 : \text{b2} := 0$: **else** $\text{z1} := -waterstand[oz] + \text{waterstand}[nz] : z2 := 0 : \text{b1} := 0 : \text{b2} := 1$: **end if**

$$0$$

$$-6.2$$

$$1$$

$$0 \tag{4.5}$$

$$0 \tag{4.6}$$

$load[nz] := piecewise(z < z1 \text{ and } z > -h, -\text{rho} \cdot g \cdot (z - z1))$;

$$1. \left(\begin{cases} -10104.30\, z & z < 0 \text{ and } -20.5 < z \\ 0 & otherwise \end{cases}\right) \tag{4.7}$$

$load[oz] := piecewise(z < z2 \text{ and } z > -h, \text{rho} \cdot g \cdot (z - z2))$;

$$1. \left(\begin{cases} 62646.660 + 10104.30\, z & z < -6.2 \text{ and } -20.5 < z \\ 0 & otherwise \end{cases}\right) \tag{4.8}$$

$load[crest] := piecewise\left(z > 0 \text{ and } z < 0.5 \cdot H + \text{delta}, p[1] - \frac{p[1]}{0.5 \cdot H + \text{delta}} \cdot z, z \le 0 \text{ and } z \ge -h, p[1] + \frac{p[1] - p[2]}{h} \cdot z\right)$;

$$1. \left(\begin{cases} 55545.38441 - 10104.30000\, z & 0 < z \text{ and } z < 5.497202618 \\ 55545.38441 + 1122.207215\, z & z \le 0 \text{ and } -20.5 \le z \end{cases}\right)$$

$$1. \left(\begin{cases} 55545.38441 - 10104.30000\, z & 0 < z \text{ and } z < 5.497202618 \\ 55545.38441 + 1122.207215\, z & z \le 0 \text{ and } -20.5 \le z \end{cases}\right) \tag{4.10}$$

$load[trough] := piecewise\left(z < 0 \text{ and } z > -0.5 \cdot H + \text{delta}, \frac{p[3]}{0.5 \cdot H - \text{delta}} \cdot z, z \le -0.5 \cdot H + \text{delta} \text{ and } z \ge -h, -p[3] - \frac{p[3] - p[2]}{h - 0.5 \cdot H + \text{delta}} \cdot (z + 0.5 \cdot H - \text{delta})\right)$;

$$1. \left(\begin{cases} 10104.30000\, z & z < 0 \text{ and } -4.277797382 < z \\ -46041.52362 - 658.6042494\, z & z \le -4.277797382 \text{ and } -20.5 \le z \end{cases}\right) \tag{4.11}$$

$z3 := 5.5 - \max(\text{waterstand}[nz], \text{waterstand}[oz])$:

$$load[situation1] := piecewise(z < z3 \text{ and } z > -h, -rho \cdot g \cdot (z - z3));$$

$$\begin{cases} -10104.30\, z & z < 0. \text{ and } -20.5 < z \\ 0 & otherwise \end{cases} \tag{4.12}$$

$$load[situation2] := piecewise(z < z3 \text{ and } z > z3 - 3, -rho \cdot g \cdot (z - z3), z < z3 - 3 \text{ and } z > z3 - 6, -rho \cdot g \cdot (z - z3 + 3), z < z3 - 6 \text{ and } z > z3 - 9, -rho \cdot g \cdot (z - z3 + 6), z < z3 - 9 \text{ and } z > z3 - 12, -rho \cdot g \cdot (z - z3 + 9), z < z3 - 12 \text{ and } z > z3 - 15, -rho \cdot g \cdot (z - z3 + 12), z < z3 - 15 \text{ and } z > z3 - 18, -rho \cdot g \cdot (z - z3 + 15), z < z3 - 18 \text{ and } z > z3 - 22, -rho \cdot g \cdot (z - z3 + 18));$$

$$\begin{cases} -10104.30\, z & z < 0. \text{ and } -3. < z \\ -10104.30\, z - 30312.90 & z < -3. \text{ and } -6. < z \\ -10104.30\, z - 60625.80 & z < -6. \text{ and } -9. < z \\ -10104.30\, z - 90938.70 & z < -9. \text{ and } -12. < z \\ -10104.30\, z - 1.2125160\, 10^5 & z < -12. \text{ and } -15. < z \\ -10104.30\, z - 1.5156450\, 10^5 & z < -15. \text{ and } -18. < z \\ -10104.30\, z - 1.8187740\, 10^5 & z < -18. \text{ and } -22. < z \end{cases} \tag{4.13}$$

Presenting loads on slide

$with(plottools):$
$with(plots):$

$$PL1 := plot\left(subs\left(z = z - \max(\text{waterstand}[nz], \text{waterstand}[oz]), \frac{load[nz]}{1000} \right), z = -h..15, color = \right.$$
$$\left. 'black', linestyle = 'dot', labeldirections = [horizontal, vertical], labels = ['x','y'] \right):$$

$$PL2 := plot\left(subs\left(z = z - \max(\text{waterstand}[nz], \text{waterstand}[oz]), \frac{load[oz]}{1000} \right), z = -h..15, color = \right.$$
$$\left. 'black', linestyle = 'dot', labeldirections = [horizontal, vertical], labels = ['x','y'] \right):$$

$$PL13 := plot\left(subs\left(z = z - \max(\text{waterstand}[nz], \text{waterstand}[oz]), \frac{-load[situation1]}{1000} \right), z = -h..15, \right.$$
$$\left. color = 'black', linestyle = 'dot', labeldirections = [horizontal, vertical], labels = ['x','y'] \right):$$

$$PL14 := plot\left(subs\left(z = z - \max(\text{waterstand}[nz], \text{waterstand}[oz]), \frac{load[nz]}{1000} - \frac{load[situation1]}{1000} \right), \right.$$
$$\left. z = -h..15, color = 'black' \right):$$

$$PL15 := plot\left(subs\left(z = z - \max(\text{waterstand}[nz], \text{waterstand}[oz]), \frac{load[situation1]}{1000} \right), z = -h..15, \right.$$
$$\left. color = 'black', linestyle = 'dot', labeldirections = [horizontal, vertical], labels = ['x','y'] \right):$$

$$PL16 := plot\left(subs\left(z = z - \max(\text{waterstand}[nz], \text{waterstand}[oz]), \frac{load[oz]}{1000} \right.\right.$$
$$\left.\left. + \frac{load[situation1]}{1000} \right), z = -h..15, color = 'black' \right):$$

$$PL17 := plot\left(subs\left(z = z - \max(\text{waterstand}[nz], \text{waterstand}[oz]), -\frac{load[situation2]}{1000} \right), z = -h..15, \right.$$
$$\left. color = 'black', linestyle = 'dot', labeldirections = [horizontal, vertical], labels = ['x','y'] \right):$$

$$PL18 := plot\left(subs\left(z = z - \max(\text{waterstand}[nz], \text{waterstand}[oz]), \frac{load[nz]}{1000} - \frac{load[situation2]}{1000} \right), \right.$$
$$\left. z = -h..15, color = 'black' \right):$$

$$PL19 := plot\left(subs\left(z = z - \max(\text{waterstand}[nz], \text{waterstand}[oz]), \frac{load[situation2]}{1000} \right), z = -h..15, \right.$$
$$\left. color = 'black', linestyle = 'dot', labeldirections = [horizontal, vertical], labels = ['x','y'] \right):$$

$$PL20 := plot\left(subs\left(z = z - \max(\text{waterstand}[nz], \text{waterstand}[oz]), \frac{load[oz]}{1000} \right.\right.$$
$$\left.\left. + \frac{load[situation2]}{1000} \right), z = -h..15, color = 'black' \right):$$

```
PL3 := plot( subs( z = z − max(waterstand[nz], waterstand[oz]), load[crest]/1000 ), z = −h..15, color = 'black' ) :

PL4 := plot( subs( z = z − max(waterstand[nz], waterstand[oz]), load[trough]/1000 ), z = −h..15, color = 'black' ) :

PL5 := plot( subs( z = z − max(waterstand[nz], waterstand[oz]), load[nz]/1000 + load[oz]/1000 ), z = −h..15, color = 'black' ) :

PL6 := plot( subs( z = z − max(waterstand[nz], waterstand[oz]), load[nz]/1000 + load[oz]/1000 + load[crest]/1000 ), z = −h..15, color = 'green' ) :

PL7 := plot( subs( z = z − max(waterstand[nz], waterstand[oz]), load[nz]/1000 + load[oz]/1000 + load[trough]/1000 ), z = −h..15, color = 'blue' ) :

PL8 := pointplot( [ [ −500, waterstand[nz] ], [ 0, waterstand[nz] ] ], connect = true, thickness = 1, color = 'cyan' ) :

PL21 := pointplot( [ [ 0, waterstand[nz] ], [ 500, waterstand[nz] ] ], connect = true, thickness = 1, color = 'cyan' ) :

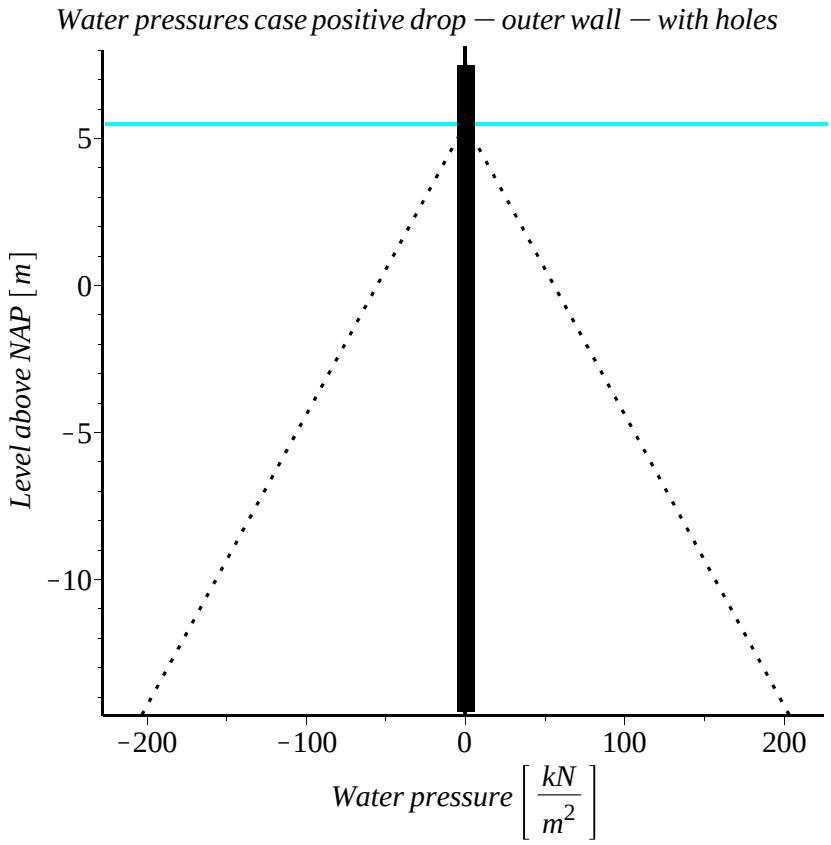
PL9 := pointplot( [ [ 0, waterstand[oz] ], [ 500, waterstand[oz] ] ], connect = true, thickness = 1, color = 'cyan' ) :

PL10 := pointplot( [ [ 0, 7.5 ], [ 0, −14.5 ] ], connect = true, thickness = 8 ) :

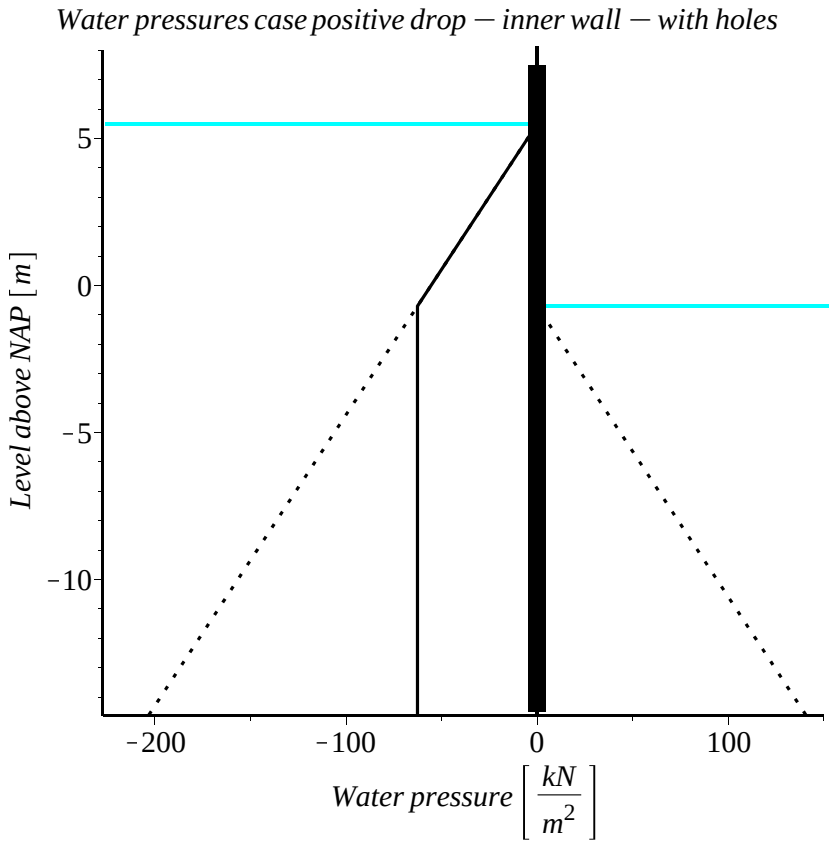
PL11 := pointplot( [ [ 0, 15 ], [ 0, −h ] ], connect = true, thickness = 1, color = 'black', labeldirections = [ horizontal, vertical ], labels = [ 'Water pressure [ kN / m^2 ]', 'Level above NAP [ m ]' ], axes = 'frame', title = 'Water pressures case positive drop', axesfont = [ arial, 11 ], font = [ arial, 11 ] ) :

PL12 := pointplot( [ [ 0, 15 ], [ 0, −h ] ], connect = true, thickness = 1, color = 'black', labeldirections = [ horizontal, vertical ], labels = [ 'Water pressure [ kN / m^2 ]', 'Level above NAP [ m ]' ], axes = 'frame', title = 'Wave pressures case positive drop', axesfont = [ arial, 11 ], font = [ arial, 11 ] ) :

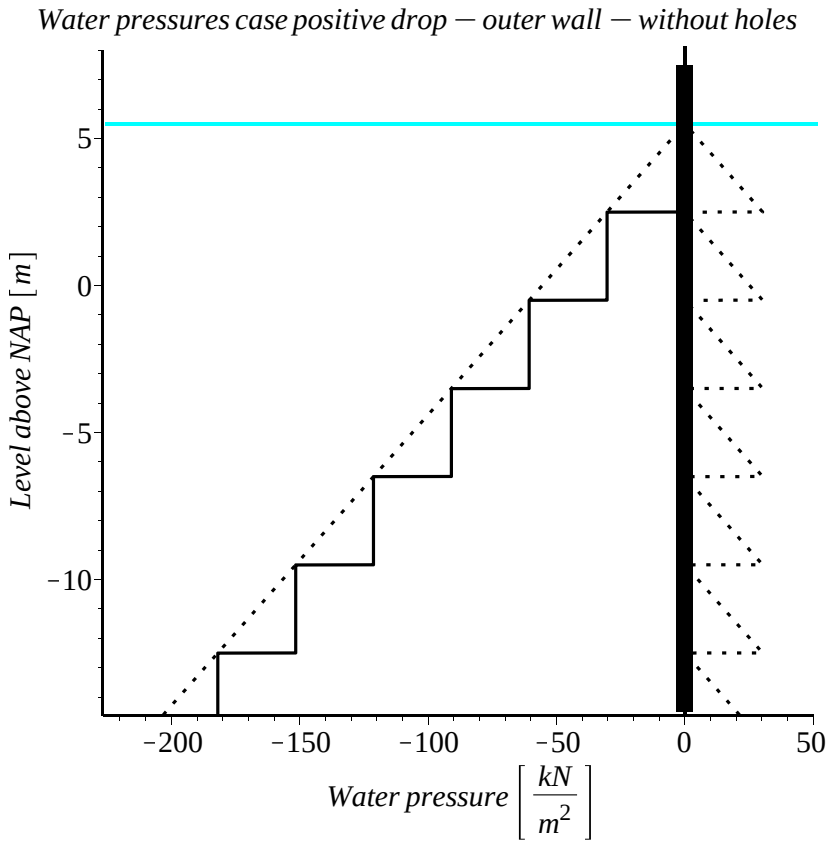
display( rotate( PL1, Pi/2 ), rotate( PL13, Pi/2 ), rotate( PL14, Pi/2 ), PL21, PL8, PL10, PL11, view = [ −225..225, −14.5..8 ], title = 'Water pressures case positive drop - outer wall - with holes' );
```



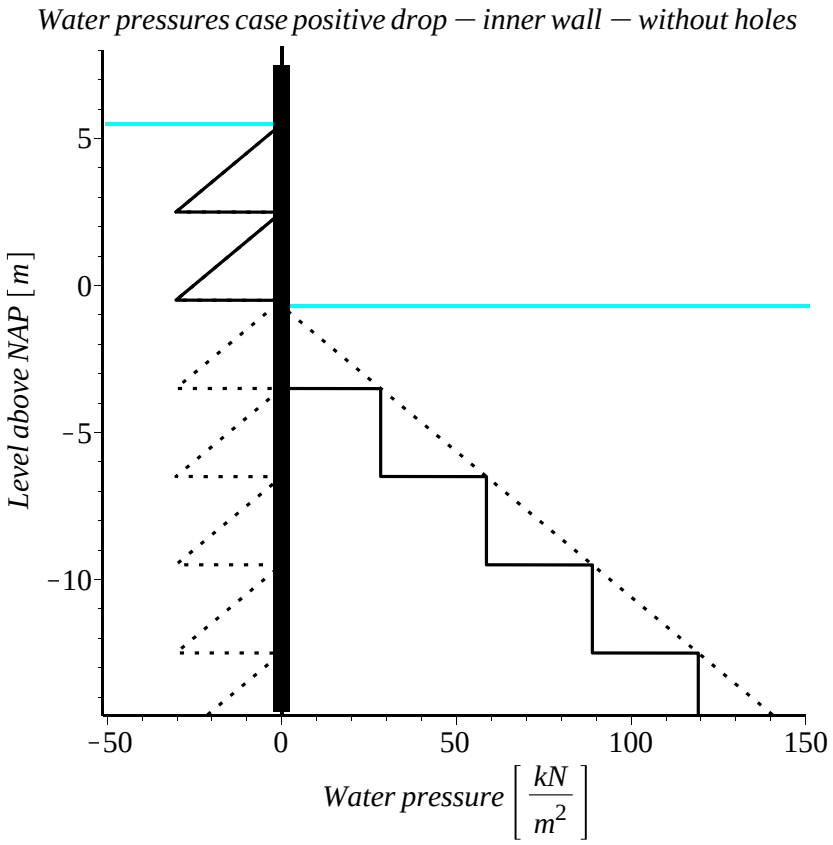

```
display( rotate( PL2, Pi/2 ), rotate( PL15, Pi/2 ), rotate( PL16, Pi/2 ), PL8, PL9, PL10, PL11, view = [
    -225..150, -14.5..8 ], title = 'Water pressures case positive drop - inner wall - with holes' );
```



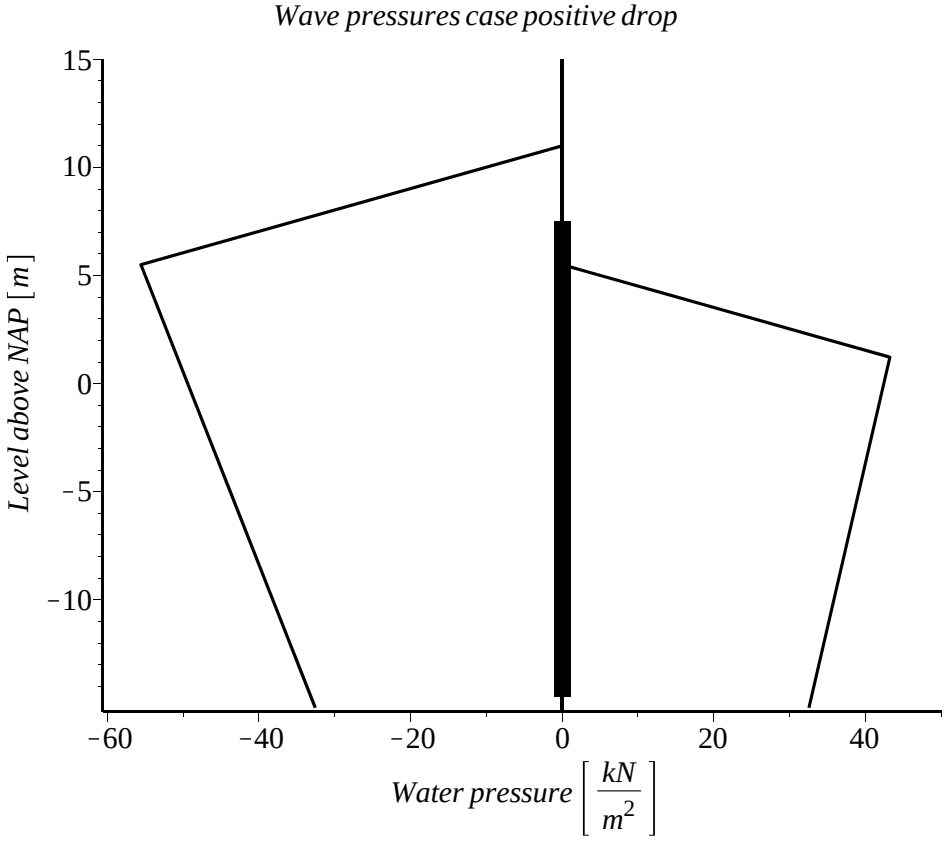
$$display\left(rotate\left(PL1, \frac{Pi}{2} \right), rotate\left(PL17, \frac{Pi}{2} \right), rotate\left(PL18, \frac{Pi}{2} \right), PL8, PL21, PL10, PL11, view = [-225..50, -14.5..8], title = 'Water\ pressures\ case\ positive\ drop - outer\ wall - without\ holes' \right);$$




```
display( rotate( PL2, Pi/2 ), rotate( PL19, Pi/2 ), rotate( PL20, Pi/2 ), PL8, PL9, PL10, PL11, view = [
    -50 ..150, -14.5 ..8 ], title = 'Water pressures case positive drop - inner wall - without holes' );
```



$$display\left(rotate\left(PL3, \frac{Pi}{2} \right), rotate\left(PL4, \frac{Pi}{2} \right), PL10, PL12, view = [\,-60..50, -14.99..15\,] \right);$$


Wave pressures case positive drop
15
10
5
0
-5
-10
Level above NAP [m]
-60
-40
-20
0
20
40
Water pressure [kN/m^2]

5.2 Positive drop

restart;

Parameters

Situatie 2: negatief verval

waterstand[*nz*] := −1 : waterstand[*oz*] := 2.4 : Hs := 0.38 : T := 5 :

Determine waterdepth, design wave height and other definitions

rho := 1030 : g := 9.81 : alpha := 0.7 : $k := \frac{2 \cdot \mathrm{Pi}}{L}$:

htot := 30 + max(waterstand[*nz*], waterstand[*oz*]);

32.4 **(7.1)**

$h := 15 + \max(\text{waterstand}[\,nz\,], \text{waterstand}[\,oz\,])$;

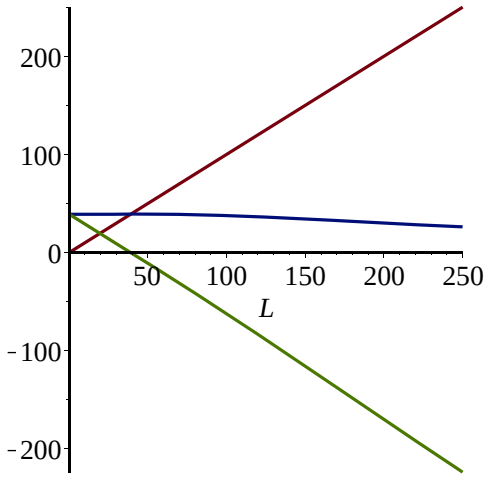
17.4 **(7.2)**

H := (1 + alpha) · *Hs*;

0.646 **(7.3)**

Determine wave length

$plot\left(\left\{ \frac{g \cdot T^2}{2 \cdot \mathrm{Pi}} \cdot \tanh(k \cdot \mathrm{htot}),\ L,\ \frac{g \cdot T^2}{2 \cdot \mathrm{Pi}} \cdot \tanh(k \cdot \mathrm{htot}) - L \right\},\ L = 0..250 \right)$;



with(*Student*[*NumericalAnalysis*]) :

$L := Bisection\left(\frac{g \cdot T^2}{2 \cdot \mathrm{Pi}} \cdot \tanh(k \cdot \mathrm{htot}) - L,\ L = [0, 250],\ tolerance = 10^{-5} \right)$;

39.03031350 **(8.1)**

Determine water pressures and wave pressures

$\text{delta} := evalf(0.5 \cdot k \cdot (0.5 \cdot H)^2 \cdot \coth(k \cdot \text{htot}))$;

$$0.008398050615 \tag{9.1}$$

$p[2] := evalf\left(\frac{\text{rho} \cdot g \cdot 0.5 \cdot H}{\cosh(\text{k} \cdot h)}\right)$;

$$395.0401753 \tag{9.2}$$

$\#p[1] := evalf\left((p[2] + \text{rho} \cdot g \cdot h) \cdot \frac{0.5 \cdot H + \text{delta}}{h + 0.5 \cdot H + \text{delta}}\right)$;

$$3293.344609 \tag{9.3}$$

$p[1] := \text{rho} \cdot g \cdot (0.5 \cdot H + \text{delta})$;

$$3348.545323 \tag{9.4}$$

$p[3] := evalf(\text{rho} \cdot g \cdot (0.5 \cdot H - \text{delta}))$;

$$3178.832477 \tag{9.5}$$

if waterstand[nz] > waterstand[oz] **then** $z1 := 0 : z2 := -\text{waterstand}[nz] + \text{waterstand}[oz] : \text{b1} := 1 : \text{b2} := 0$ **:else** $\text{z1} := -waterstand[oz] + \text{waterstand}[nz] : z2 := 0 : \text{b1} := 0 : \text{b2} := 1$ **:end if**

$$\begin{gathered} -3.4 \\ 0 \\ 0 \\ 1 \end{gathered} \tag{9.6}$$

$$1 \tag{9.7}$$

$load[nz] := piecewise(z < z1 \text{ and } z > -h, -\text{rho} \cdot g \cdot (z - z1))$;

$$1. \left(\begin{cases} -34354.620 - 10104.30\, z & z < -3.4 \text{ and } -17.4 < z \\ 0 & otherwise \end{cases}\right) \tag{9.8}$$

$load[oz] := piecewise(z < z2 \text{ and } z > -h, \text{rho} \cdot g \cdot (z - z2))$;

$$1. \left(\begin{cases} 10104.30\, z & z < 0 \text{ and } -17.4 < z \\ 0 & otherwise \end{cases}\right) \tag{9.9}$$

$load[crest] := piecewise\left(z > 0 \text{ and } z < 0.5 \cdot H + \text{delta}, p[1] - \frac{p[1]}{0.5 \cdot H + \text{delta}} \cdot z, z \le 0 \text{ and } z \ge -h, p[1] + \frac{p[1] - p[2]}{h} \cdot z\right)$;

$$1. \left(\begin{cases} 3348.545323 - 10104.30000\, z & 0 < z \text{ and } z < 0.3313980506 \\ 3348.545323 + 169.7416752\, z & z \le 0 \text{ and } -17.4 \le z \end{cases}\right)$$

$$1. \left(\begin{cases} 3348.545323 - 10104.30000\, z & 0 < z \text{ and } z < 0.3313980506 \\ 3348.545323 + 169.7416752\, z & z \le 0 \text{ and } -17.4 \le z \end{cases}\right) \tag{9.11}$$

$load[trough] := piecewise\left(z < 0 \text{ and } z > -0.5 \cdot H + \text{delta}, \frac{p[3]}{0.5 \cdot H - \text{delta}} \cdot z, z \le -0.5 \cdot H + \text{delta} \text{ and } z \ge -h, -p[3] - \frac{p[3] - p[2]}{h - 0.5 \cdot H + \text{delta}} \cdot (z + 0.5 \cdot H - \text{delta})\right)$;

$$1.\ \begin{pmatrix} \begin{cases} 10104.30000\,z & z < 0 \ \textbf{and}\ -0.3146019494 < z \\ -3230.091832 - 162.9340033\,z & z \le -0.3146019494 \ \textbf{and}\ -17.4 \le z \end{cases} \end{pmatrix} \tag{9.12}$$

$z3 := 5.5 - \max(\text{waterstand}[nz], \text{waterstand}[oz])$:

$load[situation1] := piecewise(z < z3 \ \textbf{and}\ z > -h, -\text{rho}\cdot g\cdot(z - z3))$;

$$\begin{cases} 31323.330 - 10104.30\,z & z < 3.1 \ \textbf{and}\ -17.4 < z \\ 0 & otherwise \end{cases} \tag{9.13}$$

$load[situation2] := piecewise(z < z3 \ \textbf{and}\ z > z3 - 3, -\text{rho}\cdot g\cdot(z - z3), z < z3 - 3 \ \textbf{and}\ z > z3 - 6, -\text{rho}\cdot g \cdot(z - z3 + 3), z < z3 - 6 \ \textbf{and}\ z > z3 - 9, -\text{rho}\cdot g\cdot(z - z3 + 6), z < z3 - 9 \ \textbf{and}\ z > z3 - 12, -\text{rho}\cdot g \cdot(z - z3 + 9), z < z3 - 12 \ \textbf{and}\ z > z3 - 15, -\text{rho}\cdot g\cdot(z - z3 + 12), z < z3 - 15 \ \textbf{and}\ z > z3 - 18, -\text{rho}\cdot g\cdot(z - z3 + 15), z < z3 - 18 \ \textbf{and}\ z > z3 - 22, -\text{rho}\cdot g\cdot(z - z3 + 18))$;

$$\begin{cases} 31323.330 - 10104.30\,z & z < 3.1 \ \textbf{and}\ 0.1 < z \\ -10104.30\,z + 1010.430 & z < 0.1 \ \textbf{and}\ -2.9 < z \\ -10104.30\,z - 29302.470 & z < -2.9 \ \textbf{and}\ -5.9 < z \\ -10104.30\,z - 59615.370 & z < -5.9 \ \textbf{and}\ -8.9 < z \\ -10104.30\,z - 89928.270 & z < -8.9 \ \textbf{and}\ -11.9 < z \\ -10104.30\,z - 1.20241170\,10^5 & z < -11.9 \ \textbf{and}\ -14.9 < z \\ -10104.30\,z - 1.50554070\,10^5 & z < -14.9 \ \textbf{and}\ -18.9 < z \end{cases} \tag{9.14}$$

Presenting loads on slide

```
with(plottools):
with(plots):
PL1 := plot(subs(z = z - max(waterstand[nz], waterstand[oz]), load[nz]/1000), z = -h..15, color =
    'black', linestyle='dot', labeldirections=[horizontal, vertical], labels=['x','y']):
PL2 := plot(subs(z = z - max(waterstand[nz], waterstand[oz]), load[oz]/1000), z = -h..15, color =
    'black', linestyle='dot', labeldirections=[horizontal, vertical], labels=['x','y']):
PL13 := plot(subs(z = z - max(waterstand[nz], waterstand[oz]), -load[situation1]/1000), z = -h..15,
    color='black', linestyle='dot', labeldirections=[horizontal, vertical], labels=['x','y']):

PL14 := plot(subs(z = z - max(waterstand[nz], waterstand[oz]), load[nz]/1000 - load[situation1]/1000),
    z = -h..15, color='black'):

PL15 := plot(subs(z = z - max(waterstand[nz], waterstand[oz]), load[situation1]/1000), z = -h..15,
    color='black', linestyle='dot', labeldirections=[horizontal, vertical], labels=['x','y']):
PL16 := plot(subs(z = z - max(waterstand[nz], waterstand[oz]), load[oz]/1000
    + load[situation1]/1000), z = -h..15, color='black'):

PL17 := plot(subs(z = z - max(waterstand[nz], waterstand[oz]), -load[situation2]/1000), z = -h..15,
    color='black', linestyle='dot', labeldirections=[horizontal, vertical], labels=['x','y']):
PL18 := plot(subs(z = z - max(waterstand[nz], waterstand[oz]), load[nz]/1000 - load[situation2]/1000),
    z = -h..15, color='black'):
PL19 := plot(subs(z = z - max(waterstand[nz], waterstand[oz]), load[situation2]/1000), z = -h..15,
    color='black', linestyle='dot', labeldirections=[horizontal, vertical], labels=['x','y']):
PL20 := plot(subs(z = z - max(waterstand[nz], waterstand[oz]), load[oz]/1000
    + load[situation2]/1000), z = -h..15, color='black'):
```

$$PL3 := plot\left(subs\left(z = z - \max(\text{waterstand}[nz], \text{waterstand}[oz]),\ \frac{load[crest]}{1000} \right), z = -h..15, color = \text{'black'} \right):$$

$$PL4 := plot\left(subs\left(z = z - \max(\text{waterstand}[nz], \text{waterstand}[oz]),\ \frac{load[trough]}{1000} \right), z = -h..15, color = \text{'black'} \right):$$

$$PL5 := plot\left(subs\left(z = z - \max(\text{waterstand}[nz], \text{waterstand}[oz]),\ \frac{load[nz]}{1000} + \frac{load[oz]}{1000} \right), z = -h..15, color = \text{'black'} \right):$$

$$PL6 := plot\left(subs\left(z = z - \max(\text{waterstand}[nz], \text{waterstand}[oz]),\ \frac{load[nz]}{1000} + \frac{load[oz]}{1000} + \frac{load[crest]}{1000} \right), z = -h..15, color = \text{'green'} \right):$$

$$PL7 := plot\left(subs\left(z = z - \max(\text{waterstand}[nz], \text{waterstand}[oz]),\ \frac{load[nz]}{1000} + \frac{load[oz]}{1000} + \frac{load[trough]}{1000} \right), z = -h..15, color = \text{'blue'} \right):$$

$$PL8 := pointplot([[-500, waterstand[nz]], [0, waterstand[nz]]], connect = true, thickness = 1, color = \text{'cyan'}):$$

$$PL21 := pointplot([[0, 5.5], [500, 5.5]], connect = true, thickness = 1, color = \text{'cyan'}):$$

$$PL22 := pointplot([[-500, 5.5], [0, 5.5]], connect = true, thickness = 1, color = \text{'cyan'}):$$

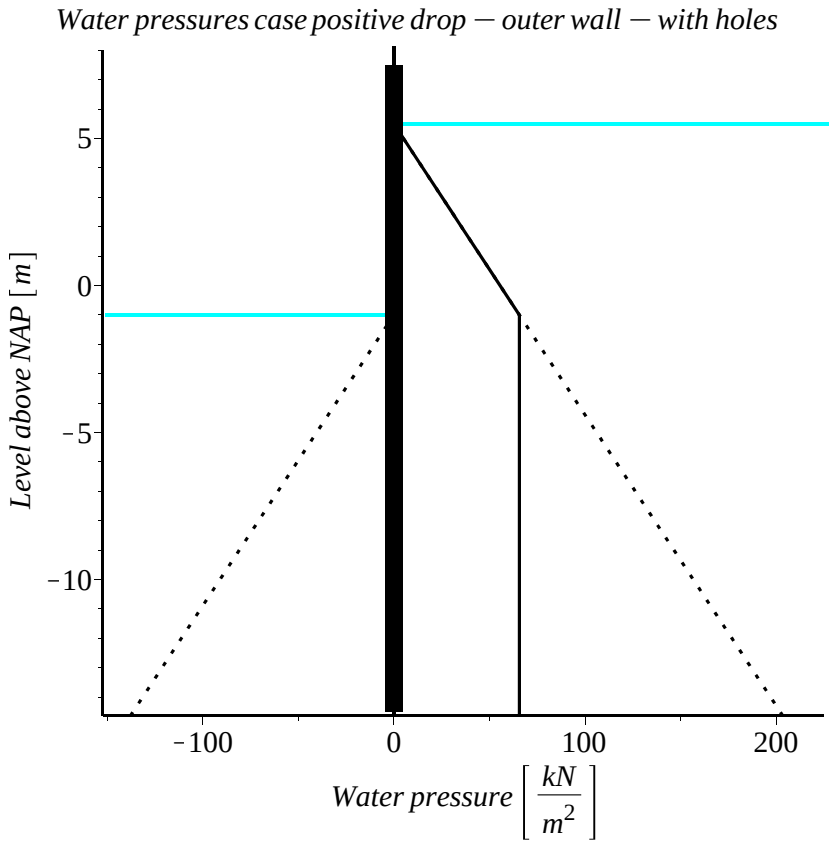
$$PL9 := pointplot([[0, waterstand[oz]], [500, waterstand[oz]]], connect = true, thickness = 1, color = \text{'cyan'}):$$

$$PL10 := pointplot([[0, 7.5], [0, -14.5]], connect = true, thickness = 8):$$

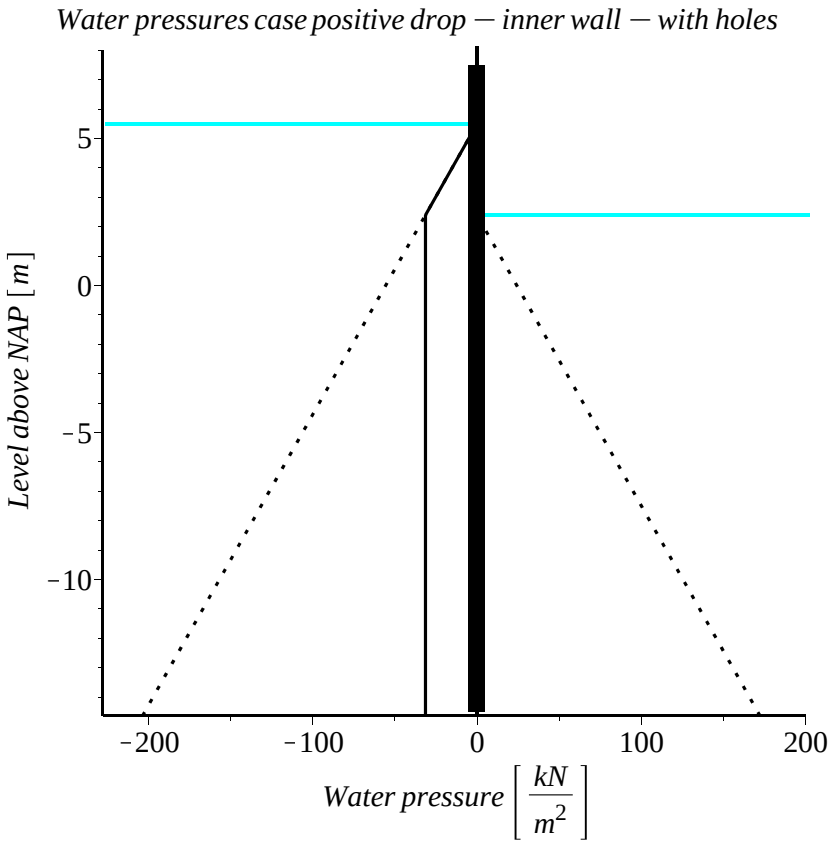
$$PL11 := pointplot([[0, 15], [0, -h]], connect = true, thickness = 1, color = \text{'black'}, labeldirections = [horizontal, vertical], labels = [\text{'Water pressure}[kN/m^2]\text{'}, \text{'Level above NAP}[m]\text{'}], axes = \text{'frame'}, title = \text{'Water pressures case positive drop'}, axesfont = [\text{arial}, 11], font = [\text{arial}, 11]):$$

$$PL12 := pointplot([[0, 15], [0, -h]], connect = true, thickness = 1, color = \text{'black'}, labeldirections = [horizontal, vertical], labels = [\text{'Water pressure}[kN/m^2]\text{'}, \text{'Level above NAP}[m]\text{'}], axes = \text{'frame'}, title = \text{'Wave pressures case positive drop'}, axesfont = [\text{arial}, 11], font = [\text{arial}, 11]):$$

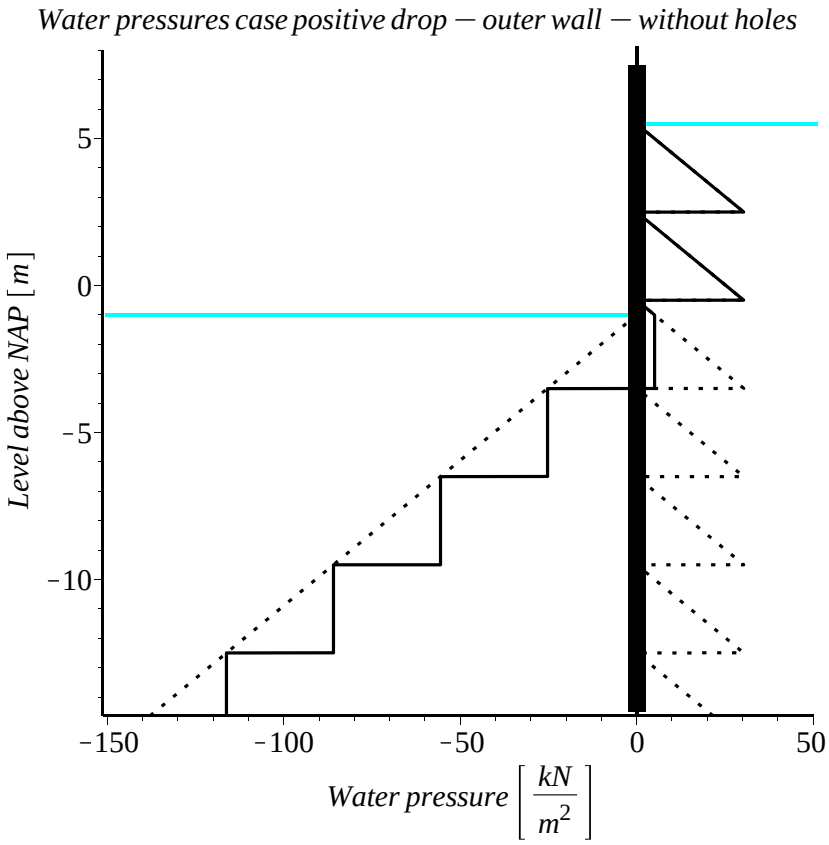
$$display\left(rotate\left(PL1, \frac{\text{Pi}}{2} \right), rotate\left(PL13, \frac{\text{Pi}}{2} \right), rotate\left(PL14, \frac{\text{Pi}}{2} \right), PL21, PL8, PL10, PL11, view = [-150..225, -14.5..8], title = \text{'Water pressures case positive drop - outer wall - with holes'} \right);$$



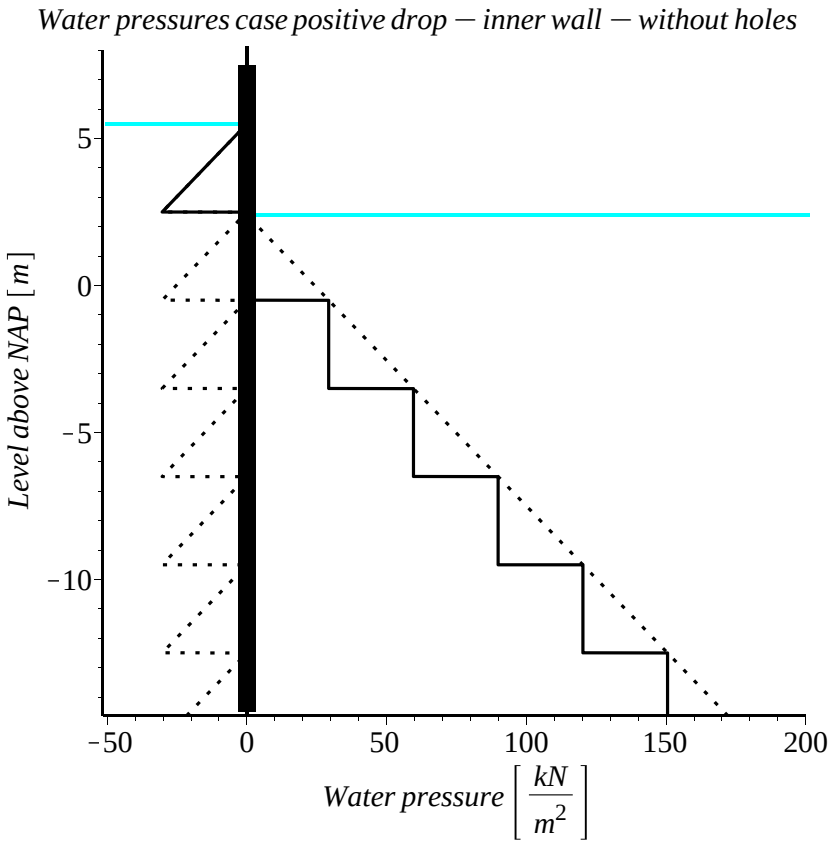

```
display( rotate( PL2, Pi/2 ), rotate( PL15, Pi/2 ), rotate( PL16, Pi/2 ), PL22, PL9, PL10, PL11, view = [
    -225 ..200, -14.5 ..8 ], title = 'Water pressures case positive drop - inner wall - with holes' );
```



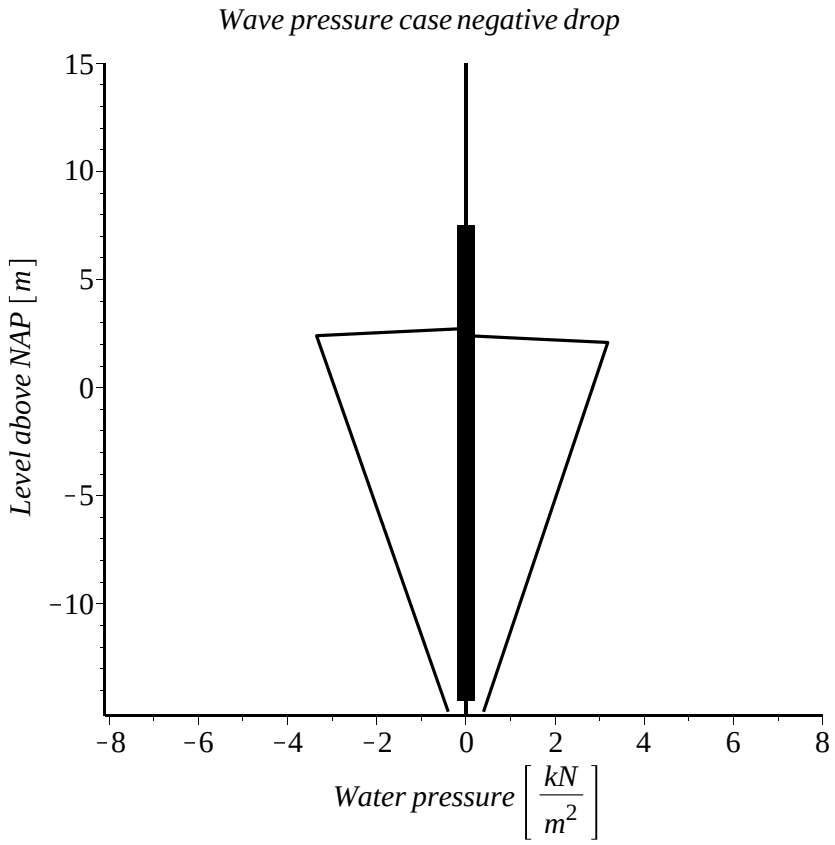
$$display\left(rotate\left(PL1, \frac{Pi}{2} \right), rotate\left(PL17, \frac{Pi}{2} \right), rotate\left(PL18, \frac{Pi}{2} \right), PL8, PL21, PL10, PL11, view = [-150..50, -14.5..8], title = \text{'Water pressures case positive drop - outer wall - without holes'} \right);$$




```
display( rotate( PL2, Pi/2 ), rotate( PL19, Pi/2 ), rotate( PL20, Pi/2 ), PL22, PL9, PL10, PL11, view = [
    -50 ..200, -14.5 ..8 ], title = 'Water pressures case positive drop - inner wall - without holes' );
```



$$display\left(rotate\left(PL3, \frac{Pi}{2}\right), rotate\left(PL4, \frac{Pi}{2}\right), PL10, PL12, view = [-8..8, -14.99..15], title = \text{'Wave pressures case negative drop'}\right);$$


Wave pressure case negative drop
15
10
5
0
−5
−10
Level above NAP [m]
−8
−6
−4
−2
0
2
4
6
8
Water pressure [kN/m^2]

Project: CIE5060 Model: V26
Graduation Project

STRUCTURAL ANALYSIS

PROJECT

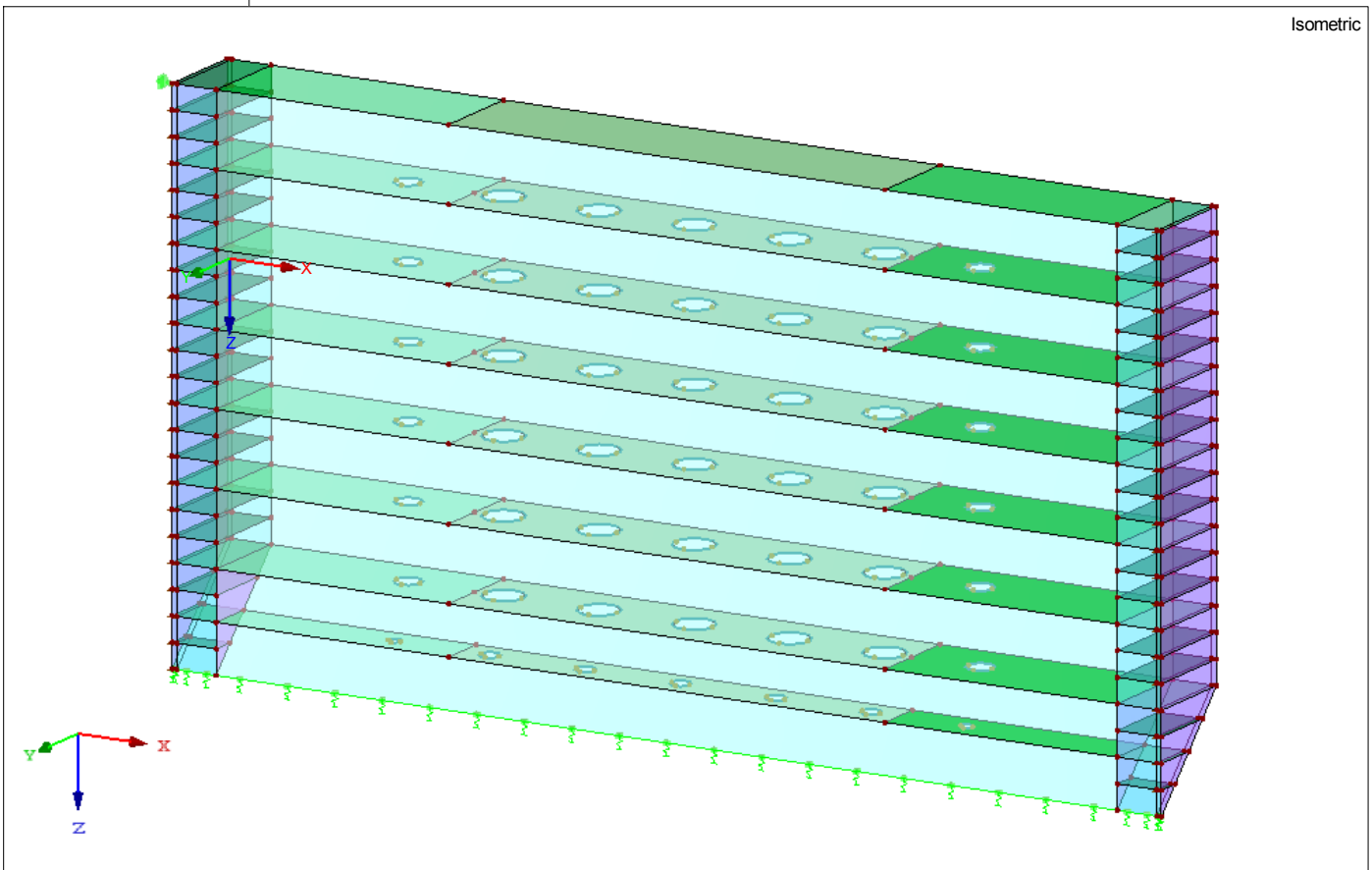
APPENDIX F:
Final design Dlubal RFEM

CLIENT

Fur the purpose of this graduation project at Delft University of Technology, carried out at the engineering office Witteveen+Bos.

CREATED BY

R.W. van Straten



Project: CIE5060 Model: V26
Graduation Project

CONTENTS

	FE Mesh Settings	3
1	**Model**	
1.1	Nodes	3
1.2	Lines	8
1.3	Materials	16
1.4	Surfaces	16
1.6	Openings	20
1.7	Nodal Supports	21
1.8	Line Supports	21
1.8.2	Line Supports - Springs	21
1.9	Surface Supports	21
	Model, In X-direction	22
	Model, In Y-direction	22
	Model, In Z-direction	23
	Model, Isometric	23
2	**Load Cases and Combinations**	
2.1	Load Cases	24
2.1.1	Load Cases - Calculation Parameters	24
2.5	Load Combinations	24
2.5.2	Load Combinations - Calculation Parameters	25
3	**Loads**	
3.8	Free Rectangular Loads	25
	LC1: Water pressure difference (positive drop), Against X-direction	26
3.8	Free Rectangular Loads	26
	LC2: Wave pressure (positive drop, wave crest), Against X-direction	27
3.8	Free Rectangular Loads	27
	LC4: Water pressure difference (negative drop), Against X-direction	29
3.8	Free Rectangular Loads	29
	LC5: Wave pressure (negative drop, wave trough), Against X-direction	30
3.8	Free Rectangular Loads	30
	LC6: Ice, Against X-direction	31
3.8	Free Rectangular Loads	31
	LC7: Collision, Against X-direction	32
3.8	Free Rectangular Loads	32
	LC8: Water impact, Against X-direction	33
4	**Results - Load Cases, Load Combinations**	
4.0	Results - Summary	33
	Base values m_x, CO1: Positive drop ULS, Isometric	34
	Base values m_y, CO1: Positive drop ULS, Isometric	34
	Base values m_{xy}, CO1: Positive drop ULS, Isometric	35
	Base values v_x, CO1: Positive drop ULS, Isometric	35
	Base values v_y, CO1: Positive drop ULS, Isometric	36
	Base values n_x, CO1: Positive drop ULS, Isometric	36
	Base values n_y, CO1: Positive drop ULS, Isometric	37
	Base values n_{xy}, CO1: Positive drop ULS, Isometric	37
	Base values m_x, CO1: Positive drop ULS, Isometric	38
	Base values m_y, CO1: Positive drop ULS, Isometric	38
	Base values m_{xy}, CO1: Positive drop ULS, Isometric	39
	Base values v_x, CO1: Positive drop ULS, Isometric	39
	Base values v_y, CO1: Positive drop ULS, Isometric	40
	Base values n_x, CO1: Positive drop ULS, Isometric	40
	Base values n_y, CO1: Positive drop ULS, Isometric	41
	Base values n_{xy}, CO1: Positive drop ULS, Isometric	41
	Base values m_x, CO1: Positive drop ULS, Isometric	42
	Base values m_y, CO1: Positive drop ULS, Isometric	42
	Base values m_{xy}, CO1: Positive drop ULS, Isometric	43
	Base values v_x, CO1: Positive drop ULS, Isometric	43
	Base values v_y, CO1: Positive drop ULS, Isometric	44
	Base values n_x, CO1: Positive drop ULS,	44
	Base values m_y, CO3: Negative drop ULS, Isometric	55
	Base values m_{xy}, CO3: Negative drop ULS, Isometric	55
	Base values v_x, CO3: Negative drop ULS, Isometric	56
	Base values v_y, CO3: Negative drop ULS, Isometric	56
	Base values n_x, CO3: Negative drop ULS, Isometric	57
	Base values n_y, CO3: Negative drop ULS, Isometric	57
	Base values n_{xy}, CO3: Negative drop ULS, Isometric	58
	Global Deformation u_Y, CO4: Negative drop SLS, Isometric	58
	Base values m_x, CO5: Ice, Isometric	59
	Base values m_y, CO5: Ice, Isometric	59
	Base values m_{xy}, CO5: Ice, Isometric	60
	Base values v_x, CO5: Ice, Isometric	60
	Base values v_y, CO5: Ice, Isometric	61
	Base values n_x, CO5: Ice, Isometric	61
	Base values n_y, CO5: Ice, Isometric	62
	Base values n_{xy}, CO5: Ice, Isometric	62
	Base values m_x, CO5: Ice, Isometric	63
	Base values m_y, CO5: Ice, Isometric	63
	Base values m_{xy}, CO5: Ice, Isometric	64
	Base values v_x, CO5: Ice, Isometric	64
	Base values v_y, CO5: Ice, Isometric	65
	Base values n_x, CO5: Ice, Isometric	65
	Base values n_y, CO5: Ice, Isometric	66
	Base values n_{xy}, CO5: Ice, Isometric	66
	Base values m_x, CO5: Ice, Isometric	67
	Base values m_y, CO5: Ice, Isometric	67
	Base values m_{xy}, CO5: Ice, Isometric	68
	Base values v_x, CO5: Ice, Isometric	68
	Base values v_y, CO5: Ice, Isometric	69
	Base values n_x, CO5: Ice, Isometric	69
	Base values n_y, CO5: Ice, Isometric	70
	Base values n_{xy}, CO5: Ice, Isometric	70
	Base values m_x, CO6: Collision, Isometric	71
	Base values m_y, CO6: Collision, Isometric	71
	Base values m_{xy}, CO6: Collision, Isometric	72
	Base values v_x, CO6: Collision, Isometric	72
	Base values v_y, CO6: Collision, Isometric	73
	Base values n_x, CO6: Collision, Isometric	73
	Base values n_y, CO6: Collision, Isometric	74
	Base values n_{xy}, CO6: Collision, Isometric	74
	Base values m_x, CO6: Collision, Isometric	75
	Base values m_y, CO6: Collision, Isometric	75
	Base values m_{xy}, CO6: Collision, Isometric	76
	Base values v_x, CO6: Collision, Isometric	76
	Base values v_y, CO6: Collision, Isometric	77
	Base values n_x, CO6: Collision, Isometric	77
	Base values n_y, CO6: Collision, Isometric	78
	Base values n_{xy}, CO6: Collision, Isometric	78
	Base values m_x, CO6: Collision, Isometric	79
	Base values m_y, CO6: Collision, Isometric	79
	Base values m_{xy}, CO6: Collision, Isometric	80
	Base values v_y, CO6: Collision, Isometric	80
	Base values v_x, CO6: Collision, Isometric	81
	Base values n_x, CO6: Collision, Isometric	81
	Base values n_y, CO6: Collision, Isometric	82
	Base values n_{xy}, CO6: Collision, Isometric	82
	Base values m_x, CO7: Water impact, Isometric	83
	Base values m_y, CO7: Water impact, Isometric	83
	Base values m_{xy}, CO7: Water impact, Isometric	84
	Base values v_x, CO7: Water impact, Isometric	84
	Base values v_y, CO7: Water impact, Isometric	85
	Base values n_x, CO7: Water impact, Isometric	85

Project: CIE5060 Model: V26
Graduation Project

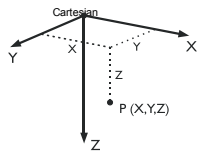
CONTENTS

	Isometric				
	Base values n_y, CO1: Positive drop ULS, Isometric	45		Base values n_y, CO7: Water impact, Isometric	86
	Base values n_{xy}, CO1: Positive drop ULS, Isometric	45		Base values n_{xy}, CO7: Water impact, Isometric	86
	Global Deformation u_Y, CO2: Positive drop SLS, Isometric	46		Base values m_x, CO7: Water impact, Isometric	87
	Base values m_x, CO3: Negative drop ULS, Isometric	46		Base values m_y, CO7: Water impact, Isometric	87
	Base values m_y, CO3: Negative drop ULS, Isometric	47		Base values m_{xy}, CO7: Water impact, Isometric	88
	Base values m_{xy}, CO3: Negative drop ULS, Isometric	47		Base values v_x, CO7: Water impact, Isometric	88
	Base values v_x, CO3: Negative drop ULS, Isometric	48		Base values v_y, CO7: Water impact, Isometric	89
	Base values v_y, CO3: Negative drop ULS, Isometric	48		Base values n_x, CO7: Water impact, Isometric	89
	Base values n_x, CO3: Negative drop ULS, Isometric	49		Base values n_y, CO7: Water impact, Isometric	90
	Base values n_y, CO3: Negative drop ULS, Isometric	49		Base values n_{xy}, CO7: Water impact, Isometric	90
	Base values n_{xy}, CO3: Negative drop ULS, Isometric	50		Base values m_x, CO7: Water impact, Isometric	91
	Base values m_x, CO3: Negative drop ULS, Isometric	50		Base values m_y, CO7: Water impact, Isometric	91
	Base values m_y, CO3: Negative drop ULS, Isometric	51		Base values m_{xy}, CO7: Water impact, Isometric	92
	Base values m_{xy}, CO3: Negative drop ULS, Isometric	51		Base values v_x, CO7: Water impact, Isometric	92
	Base values v_x, CO3: Negative drop ULS, Isometric	52		Base values v_y, CO7: Water impact, Isometric	93
	Base values v_y, CO3: Negative drop ULS, Isometric	52		Base values n_x, CO7: Water impact, Isometric	93
	Base values n_x, CO3: Negative drop ULS, Isometric	53		Base values n_y, CO7: Water impact, Isometric	94
	Base values n_y, CO3: Negative drop ULS, Isometric	53		Base values n_{xy}, CO7: Water impact, Isometric	94
	Base values n_{xy}, CO3: Negative drop ULS, Isometric	54		**RF-LAMINATE**	
	Base values m_x, CO3: Negative drop ULS, Isometric	54	1.1.1	General Data	95
			1.2	Material Characteristics - A	95
			1.2	Material Characteristics - B	96
			2.1	Max Stress Ratio by Loading	96
			2.2	Max Stress Ratio by Surface	97
			4.1	Parts List	113

FE MESH SETTINGS

	General	Target length of finite elements	l_{FE}	:	0.500 m
		Maximum distance between a node and a line to integrate it into the line	ε	:	0.001 m
		Maximum number of mesh nodes (in thousands)		:	500
	Members	Number of divisions of members with cable, elastic foundation, taper, or plastic characteristic		:	10
		☒ Activate member divisions for large deformation or post-critical analysis			
		☒ Use division for members with node lying on them			
	Surfaces	Maximum ratio of FE rectangle diagonals	Δ_D	:	1.800
		Maximum out-of-plane inclination of two finite elements	α	:	0.50 °
		Shape direction of finite elements		:	Triangles and quadrangles ☒ Same squares where possible

1.1 NODES



Node No.	Node Type	Reference Node	Coordinate System	Node Coordinates X [m]	Y [m]	Z [m]	Comment
1	Standard	-	Cartesian	21.400	2.000	-4.500	Generated
2	Standard	-	Cartesian	1.750	4.000	14.500	
3	Standard	-	Cartesian	39.550	4.000	14.500	
4	Standard	-	Cartesian	20.650	2.750	-4.500	Generated
5	Standard	-	Cartesian	1.750	0.000	10.500	
6	Standard	-	Cartesian	19.900	2.000	-4.500	Generated
7	Standard	-	Cartesian	25.400	2.000	-4.500	Generated
8	Standard	-	Cartesian	39.550	0.000	10.500	
9	Standard	-	Cartesian	24.650	2.750	-4.500	Generated
10	Standard	-	Cartesian	23.900	2.000	-4.500	Generated
11	Standard	-	Cartesian	39.550	4.000	10.500	
12	Standard	-	Cartesian	1.750	4.000	10.500	
13	Standard	-	Cartesian	29.400	2.000	-4.500	Generated
14	Standard	-	Cartesian	1.750	4.000	7.500	
15	Standard	-	Cartesian	1.750	0.000	7.500	
16	Standard	-	Cartesian	28.650	2.750	-4.500	Generated
17	Standard	-	Cartesian	39.550	4.000	7.500	
18	Standard	-	Cartesian	39.550	0.000	7.500	
19	Standard	-	Cartesian	41.200	4.000	14.500	
20	Standard	-	Cartesian	41.400	4.000	14.500	
21	Standard	-	Cartesian	1.750	4.000	4.500	
22	Standard	-	Cartesian	1.750	0.000	4.500	
23	Standard	-	Cartesian	39.550	4.000	4.500	

Project: CIE5060 Model: V26
Graduation Project

1.1 NODES

Node No.	Node Type	Reference Node	Coordinate System	Node Coordinates X [m]	Y [m]	Z [m]	Comment
24	Standard	-	Cartesian	39.550	0.000	4.500	
25	Standard	-	Cartesian	41.200	4.000	-5.500	
26	Standard	-	Cartesian	27.900	2.000	-4.500	Generated
27	Standard	-	Cartesian	41.200	0.000	10.500	
28	Standard	-	Cartesian	33.150	2.000	-4.500	Generated
29	Standard	-	Cartesian	1.750	4.000	1.500	
30	Standard	-	Cartesian	1.750	0.000	1.500	
31	Standard	-	Cartesian	39.550	4.000	1.500	
32	Standard	-	Cartesian	39.550	0.000	1.500	
33	Standard	-	Cartesian	41.200	4.000	-6.500	
34	Standard	-	Cartesian	41.200	4.000	10.500	
35	Standard	-	Cartesian	0.100	4.000	14.500	
36	Standard	-	Cartesian	41.200	0.000	-6.500	
37	Standard	-	Cartesian	1.750	4.000	-1.500	
38	Standard	-	Cartesian	1.750	0.000	-1.500	
39	Standard	-	Cartesian	39.550	4.000	-1.500	
40	Standard	-	Cartesian	39.550	0.000	-1.500	
41	Standard	-	Cartesian	41.200	0.000	-5.500	
42	Standard	-	Cartesian	41.200	4.000	-2.500	
43	Standard	-	Cartesian	41.200	4.000	7.500	
44	Standard	-	Cartesian	41.200	0.000	7.500	
45	Standard	-	Cartesian	1.750	4.000	-4.500	
46	Standard	-	Cartesian	1.750	0.000	-4.500	
47	Standard	-	Cartesian	39.550	4.000	-4.500	
48	Standard	-	Cartesian	39.550	0.000	-4.500	
49	Standard	-	Cartesian	-0.100	4.000	14.500	
50	Standard	-	Cartesian	41.200	4.000	-3.500	
51	Standard	-	Cartesian	41.200	4.000	4.500	
52	Standard	-	Cartesian	41.200	0.000	4.500	
53	Standard	-	Cartesian	1.750	4.000	-7.500	
54	Standard	-	Cartesian	1.750	0.000	-7.500	
55	Standard	-	Cartesian	39.550	4.000	-7.500	
56	Standard	-	Cartesian	39.550	0.000	-7.500	
57	Standard	-	Cartesian	32.650	2.500	-4.500	Generated
58	Standard	-	Cartesian	32.150	2.000	-4.500	Generated
59	Standard	-	Cartesian	41.200	4.000	1.500	
60	Standard	-	Cartesian	41.200	0.000	1.500	
61	Standard	-	Cartesian	0.100	4.000	-5.500	
62	Standard	-	Cartesian	0.100	0.000	10.500	
63	Standard	-	Cartesian	41.200	4.000	-1.500	
64	Standard	-	Cartesian	41.200	0.000	-1.500	
65	Standard	-	Cartesian	41.200	0.000	-3.500	
66	Standard	-	Cartesian	41.200	0.000	-2.500	
67	Standard	-	Cartesian	41.200	4.000	-4.500	
68	Standard	-	Cartesian	41.200	0.000	-4.500	
69	Standard	-	Cartesian	17.400	2.000	-4.500	Generated
70	Standard	-	Cartesian	16.650	2.750	-4.500	Generated
71	Standard	-	Cartesian	41.200	4.000	-7.500	
72	Standard	-	Cartesian	41.200	0.000	-7.500	
73	Standard	-	Cartesian	41.200	4.000	0.500	
74	Standard	-	Cartesian	41.200	4.000	-0.500	
75	Standard	-	Cartesian	0.100	4.000	-6.500	
76	Standard	-	Cartesian	0.100	4.000	10.500	
77	Standard	-	Cartesian	41.200	0.000	-0.500	
78	Standard	-	Cartesian	41.200	0.000	0.500	
79	Standard	-	Cartesian	0.100	0.000	-6.500	
80	Standard	-	Cartesian	15.900	2.000	-4.500	Generated
81	Standard	-	Cartesian	41.200	4.000	3.500	
82	Standard	-	Cartesian	41.200	4.000	2.500	
83	Standard	-	Cartesian	13.400	2.000	-4.500	Generated
84	Standard	-	Cartesian	0.100	0.000	-5.500	
85	Standard	-	Cartesian	41.200	0.000	2.500	
86	Standard	-	Cartesian	41.200	0.000	3.500	
87	Standard	-	Cartesian	0.100	4.000	-2.500	
88	Standard	-	Cartesian	0.100	4.000	7.500	
89	Standard	-	Cartesian	41.200	4.000	6.500	
90	Standard	-	Cartesian	41.200	4.000	5.500	
91	Standard	-	Cartesian	41.200	0.000	5.500	
92	Standard	-	Cartesian	41.200	0.000	6.500	
93	Standard	-	Cartesian	41.200	4.000	9.500	
94	Standard	-	Cartesian	41.200	4.000	8.500	
95	Standard	-	Cartesian	41.200	0.000	8.500	
96	Standard	-	Cartesian	41.200	0.000	9.500	
97	Standard	-	Cartesian	39.550	4.000	-2.500	
98	Standard	-	Cartesian	39.550	4.000	-3.500	
99	Standard	-	Cartesian	39.550	4.000	-5.500	
100	Standard	-	Cartesian	39.550	4.000	-6.500	
101	Standard	-	Cartesian	39.550	0.000	8.500	
102	Standard	-	Cartesian	39.550	0.000	9.500	
103	Standard	-	Cartesian	39.550	0.000	5.500	
104	Standard	-	Cartesian	39.550	0.000	6.500	
105	Standard	-	Cartesian	39.550	0.000	2.500	
106	Standard	-	Cartesian	39.550	0.000	3.500	
107	Standard	-	Cartesian	39.550	0.000	-0.500	
108	Standard	-	Cartesian	39.550	0.000	0.500	
109	Standard	-	Cartesian	39.550	0.000	-3.500	
110	Standard	-	Cartesian	39.550	0.000	-2.500	
111	Standard	-	Cartesian	39.550	0.000	-6.500	
112	Standard	-	Cartesian	39.550	0.000	-5.500	
113	Standard	-	Cartesian	39.550	4.000	9.500	
114	Standard	-	Cartesian	39.550	4.000	8.500	
115	Standard	-	Cartesian	39.550	4.000	6.500	

Project: CIE5060 Model: V26
Graduation Project

1.1 NODES

Node No.	Node Type	Reference Node	Coordinate System	Node Coordinates X [m]	Y [m]	Z [m]	Comment
116	Standard	-	Cartesian	39.550	4.000	5.500	
117	Standard	-	Cartesian	39.550	4.000	3.500	
118	Standard	-	Cartesian	39.550	4.000	2.500	
119	Standard	-	Cartesian	39.550	4.000	0.500	
120	Standard	-	Cartesian	39.550	4.000	-0.500	
121	Standard	-	Cartesian	0.100	0.000	7.500	
122	Standard	-	Cartesian	12.650	2.750	-4.500	Generated
123	Standard	-	Cartesian	11.900	2.000	-4.500	Generated
124	Standard	-	Cartesian	0.100	4.000	-3.500	
125	Standard	-	Cartesian	0.100	4.000	4.500	
126	Standard	-	Cartesian	0.100	0.000	4.500	
127	Standard	-	Cartesian	9.150	2.000	-4.500	Generated
128	Standard	-	Cartesian	41.400	4.000	-5.500	
129	Standard	-	Cartesian	8.650	2.500	-4.500	Generated
130	Standard	-	Cartesian	41.400	0.000	10.500	
131	Standard	-	Cartesian	0.100	4.000	1.500	
132	Standard	-	Cartesian	0.100	0.000	1.500	
133	Standard	-	Cartesian	41.400	4.000	-6.500	
134	Standard	-	Cartesian	41.400	4.000	10.500	
135	Standard	-	Cartesian	41.400	0.000	-6.500	
136	Standard	-	Cartesian	0.100	4.000	-1.500	
137	Standard	-	Cartesian	0.100	0.000	-1.500	
138	Standard	-	Cartesian	41.400	0.000	-5.500	
139	Standard	-	Cartesian	41.400	4.000	-2.500	
140	Standard	-	Cartesian	41.400	4.000	7.500	
141	Standard	-	Cartesian	41.400	0.000	7.500	
142	Standard	-	Cartesian	0.100	0.000	-3.500	
143	Standard	-	Cartesian	0.100	0.000	-2.500	
144	Standard	-	Cartesian	41.400	4.000	-3.500	
145	Standard	-	Cartesian	41.400	4.000	4.500	
146	Standard	-	Cartesian	41.400	0.000	4.500	
147	Standard	-	Cartesian	0.100	4.000	-4.500	
148	Standard	-	Cartesian	0.100	0.000	-4.500	
149	Standard	-	Cartesian	41.400	4.000	1.500	
150	Standard	-	Cartesian	41.400	0.000	1.500	
151	Standard	-	Cartesian	41.400	4.000	-1.500	
152	Standard	-	Cartesian	41.400	0.000	-1.500	
153	Standard	-	Cartesian	41.400	0.000	-3.500	
154	Standard	-	Cartesian	41.400	0.000	-2.500	
155	Standard	-	Cartesian	41.400	4.000	-4.500	
156	Standard	-	Cartesian	41.400	0.000	-4.500	
157	Standard	-	Cartesian	41.400	4.000	-7.500	
158	Standard	-	Cartesian	41.400	0.000	-7.500	
159	Standard	-	Cartesian	41.400	4.000	0.500	
160	Standard	-	Cartesian	41.400	4.000	-0.500	
161	Standard	-	Cartesian	41.400	0.000	-0.500	
162	Standard	-	Cartesian	41.400	0.000	0.500	
163	Standard	-	Cartesian	41.400	4.000	3.500	
164	Standard	-	Cartesian	41.400	4.000	2.500	
165	Standard	-	Cartesian	41.400	0.000	2.500	
166	Standard	-	Cartesian	41.400	0.000	3.500	
167	Standard	-	Cartesian	41.400	4.000	6.500	
168	Standard	-	Cartesian	41.400	4.000	5.500	
169	Standard	-	Cartesian	41.400	0.000	5.500	
170	Standard	-	Cartesian	41.400	0.000	6.500	
171	Standard	-	Cartesian	41.400	4.000	9.500	
172	Standard	-	Cartesian	41.400	4.000	8.500	
173	Standard	-	Cartesian	41.400	0.000	8.500	
174	Standard	-	Cartesian	41.400	0.000	9.500	
175	Standard	-	Cartesian	39.550	4.000	11.500	
176	Standard	-	Cartesian	39.550	4.000	12.500	
177	Standard	-	Cartesian	39.550	4.000	13.500	
178	Standard	-	Cartesian	41.200	4.000	13.500	
179	Standard	-	Cartesian	41.200	4.000	12.500	
180	Standard	-	Cartesian	41.200	4.000	11.500	
181	Standard	-	Cartesian	39.550	1.000	11.500	
182	Standard	-	Cartesian	39.550	2.000	12.500	
183	Standard	-	Cartesian	39.550	3.000	13.500	
184	Standard	-	Cartesian	41.200	1.000	11.500	
185	Standard	-	Cartesian	41.200	2.000	12.500	
186	Standard	-	Cartesian	41.200	3.000	13.500	
187	Standard	-	Cartesian	41.400	4.000	13.500	
188	Standard	-	Cartesian	41.400	4.000	12.500	
189	Standard	-	Cartesian	41.400	4.000	11.500	
190	Standard	-	Cartesian	41.400	1.000	11.500	
191	Standard	-	Cartesian	41.400	2.000	12.500	
192	Standard	-	Cartesian	41.400	3.000	13.500	
193	Standard	-	Cartesian	0.100	4.000	-7.500	
194	Standard	-	Cartesian	0.100	0.000	-7.500	
195	Standard	-	Cartesian	0.100	4.000	0.500	
196	Standard	-	Cartesian	0.100	4.000	-0.500	
197	Standard	-	Cartesian	0.100	0.000	-0.500	
198	Standard	-	Cartesian	0.100	0.000	0.500	
199	Standard	-	Cartesian	0.100	4.000	3.500	
200	Standard	-	Cartesian	0.100	4.000	2.500	
201	Standard	-	Cartesian	0.100	0.000	2.500	
202	Standard	-	Cartesian	0.100	0.000	3.500	
203	Standard	-	Cartesian	0.100	4.000	6.500	
204	Standard	-	Cartesian	0.100	4.000	5.500	
205	Standard	-	Cartesian	0.100	0.000	5.500	
206	Standard	-	Cartesian	0.100	0.000	6.500	
207	Standard	-	Cartesian	0.100	4.000	9.500	

Project: CIE5060 Model: V26
Graduation Project

1.1 NODES

Node No.	Node Type	Reference Node	Coordinate System	Node Coordinates X [m]	Y [m]	Z [m]	Comment
208	Standard	-	Cartesian	0.100	4.000	8.500	
209	Standard	-	Cartesian	0.100	0.000	8.500	
210	Standard	-	Cartesian	0.100	0.000	9.500	
211	Standard	-	Cartesian	1.750	4.000	-2.500	
212	Standard	-	Cartesian	1.750	4.000	-3.500	
213	Standard	-	Cartesian	1.750	4.000	-5.500	
214	Standard	-	Cartesian	1.750	4.000	-6.500	
215	Standard	-	Cartesian	1.750	0.000	8.500	
216	Standard	-	Cartesian	1.750	0.000	9.500	
217	Standard	-	Cartesian	1.750	0.000	5.500	
218	Standard	-	Cartesian	1.750	0.000	6.500	
219	Standard	-	Cartesian	1.750	0.000	2.500	
220	Standard	-	Cartesian	1.750	0.000	3.500	
221	Standard	-	Cartesian	1.750	0.000	-0.500	
222	Standard	-	Cartesian	1.750	0.000	0.500	
223	Standard	-	Cartesian	1.750	0.000	-3.500	
224	Standard	-	Cartesian	1.750	0.000	-2.500	
225	Standard	-	Cartesian	1.750	0.000	-6.500	
226	Standard	-	Cartesian	1.750	0.000	-5.500	
227	Standard	-	Cartesian	1.750	4.000	9.500	
228	Standard	-	Cartesian	1.750	4.000	8.500	
229	Standard	-	Cartesian	1.750	4.000	6.500	
230	Standard	-	Cartesian	1.750	4.000	5.500	
231	Standard	-	Cartesian	1.750	4.000	3.500	
232	Standard	-	Cartesian	1.750	4.000	2.500	
233	Standard	-	Cartesian	1.750	4.000	0.500	
234	Standard	-	Cartesian	1.750	4.000	-0.500	
235	Standard	-	Cartesian	-0.100	4.000	-5.500	
236	Standard	-	Cartesian	-0.100	0.000	10.500	
237	Standard	-	Cartesian	-0.100	4.000	-6.500	
238	Standard	-	Cartesian	-0.100	4.000	10.500	
239	Standard	-	Cartesian	-0.100	0.000	-6.500	
240	Standard	-	Cartesian	-0.100	0.000	-5.500	
241	Standard	-	Cartesian	-0.100	4.000	-2.500	
242	Standard	-	Cartesian	-0.100	4.000	7.500	
243	Standard	-	Cartesian	-0.100	0.000	7.500	
244	Standard	-	Cartesian	-0.100	4.000	-3.500	
245	Standard	-	Cartesian	-0.100	4.000	4.500	
246	Standard	-	Cartesian	-0.100	0.000	4.500	
247	Standard	-	Cartesian	-0.100	4.000	1.500	
248	Standard	-	Cartesian	-0.100	0.000	1.500	
249	Standard	-	Cartesian	-0.100	4.000	-1.500	
250	Standard	-	Cartesian	-0.100	0.000	-1.500	
251	Standard	-	Cartesian	-0.100	0.000	-3.500	
252	Standard	-	Cartesian	-0.100	0.000	-2.500	
253	Standard	-	Cartesian	-0.100	4.000	-4.500	
254	Standard	-	Cartesian	-0.100	0.000	-4.500	
255	Standard	-	Cartesian	-0.100	4.000	-7.500	
256	Standard	-	Cartesian	-0.100	0.000	-7.500	
257	Standard	-	Cartesian	-0.100	4.000	0.500	
258	Standard	-	Cartesian	-0.100	4.000	-0.500	
259	Standard	-	Cartesian	-0.100	0.000	-0.500	
260	Standard	-	Cartesian	-0.100	0.000	0.500	
261	Standard	-	Cartesian	-0.100	4.000	3.500	
262	Standard	-	Cartesian	-0.100	4.000	2.500	
263	Standard	-	Cartesian	-0.100	0.000	2.500	
264	Standard	-	Cartesian	-0.100	0.000	3.500	
265	Standard	-	Cartesian	-0.100	4.000	6.500	
266	Standard	-	Cartesian	-0.100	4.000	5.500	
267	Standard	-	Cartesian	-0.100	0.000	5.500	
268	Standard	-	Cartesian	-0.100	0.000	6.500	
269	Standard	-	Cartesian	-0.100	4.000	9.500	
270	Standard	-	Cartesian	-0.100	4.000	8.500	
271	Standard	-	Cartesian	-0.100	0.000	8.500	
272	Standard	-	Cartesian	-0.100	0.000	9.500	
273	Standard	-	Cartesian	1.750	4.000	11.500	
274	Standard	-	Cartesian	1.750	4.000	12.500	
275	Standard	-	Cartesian	1.750	4.000	13.500	
276	Standard	-	Cartesian	0.100	4.000	13.500	
277	Standard	-	Cartesian	0.100	4.000	12.500	
278	Standard	-	Cartesian	0.100	4.000	11.500	
279	Standard	-	Cartesian	1.750	1.000	11.500	
280	Standard	-	Cartesian	1.750	2.000	12.500	
281	Standard	-	Cartesian	1.750	3.000	13.500	
282	Standard	-	Cartesian	0.100	1.000	11.500	
283	Standard	-	Cartesian	0.100	2.000	12.500	
284	Standard	-	Cartesian	0.100	3.000	13.500	
285	Standard	-	Cartesian	-0.100	4.000	13.500	
286	Standard	-	Cartesian	-0.100	4.000	12.500	
287	Standard	-	Cartesian	-0.100	4.000	11.500	
288	Standard	-	Cartesian	-0.100	1.000	11.500	
289	Standard	-	Cartesian	-0.100	2.000	12.500	
290	Standard	-	Cartesian	-0.100	3.000	13.500	
291	Standard	-	Cartesian	8.150	2.000	-4.500	Generated
292	Standard	-	Cartesian	21.400	2.000	-1.500	Generated
293	Standard	-	Cartesian	20.650	2.750	-1.500	Generated
294	Standard	-	Cartesian	19.900	2.000	-1.500	Generated
295	Standard	-	Cartesian	25.400	2.000	-1.500	Generated
296	Standard	-	Cartesian	24.650	2.750	-1.500	Generated
297	Standard	-	Cartesian	23.900	2.000	-1.500	Generated
298	Standard	-	Cartesian	29.400	2.000	-1.500	Generated
299	Standard	-	Cartesian	28.650	2.750	-1.500	Generated

Project: CIE5060 Model: V26
Graduation Project

1.1 NODES

Node No.	Node Type	Reference Node	Coordinate System	Node Coordinates X [m]	Y [m]	Z [m]	Comment
300	Standard	-	Cartesian	27.900	2.000	-1.500	Generated
301	Standard	-	Cartesian	33.150	2.000	-1.500	Generated
302	Standard	-	Cartesian	32.650	2.500	-1.500	Generated
303	Standard	-	Cartesian	32.150	2.000	-1.500	Generated
304	Standard	-	Cartesian	17.400	2.000	-1.500	Generated
305	Standard	-	Cartesian	16.650	2.750	-1.500	Generated
306	Standard	-	Cartesian	15.900	2.000	-1.500	Generated
307	Standard	-	Cartesian	13.400	2.000	-1.500	Generated
308	Standard	-	Cartesian	12.650	2.750	-1.500	Generated
309	Standard	-	Cartesian	11.900	2.000	-1.500	Generated
310	Standard	-	Cartesian	9.150	2.000	-1.500	Generated
311	Standard	-	Cartesian	8.650	2.500	-1.500	Generated
312	Standard	-	Cartesian	8.150	2.000	-1.500	Generated
313	Standard	-	Cartesian	21.400	2.000	1.500	Generated
314	Standard	-	Cartesian	20.650	2.750	1.500	Generated
315	Standard	-	Cartesian	19.900	2.000	1.500	Generated
316	Standard	-	Cartesian	25.400	2.000	1.500	Generated
317	Standard	-	Cartesian	24.650	2.750	1.500	Generated
318	Standard	-	Cartesian	23.900	2.000	1.500	Generated
319	Standard	-	Cartesian	29.400	2.000	1.500	Generated
320	Standard	-	Cartesian	28.650	2.750	1.500	Generated
321	Standard	-	Cartesian	27.900	2.000	1.500	Generated
322	Standard	-	Cartesian	33.150	2.000	1.500	Generated
323	Standard	-	Cartesian	32.650	2.500	1.500	Generated
324	Standard	-	Cartesian	32.150	2.000	1.500	Generated
325	Standard	-	Cartesian	17.400	2.000	1.500	Generated
326	Standard	-	Cartesian	16.650	2.750	1.500	Generated
327	Standard	-	Cartesian	15.900	2.000	1.500	Generated
328	Standard	-	Cartesian	13.400	2.000	1.500	Generated
329	Standard	-	Cartesian	12.650	2.750	1.500	Generated
330	Standard	-	Cartesian	11.900	2.000	1.500	Generated
331	Standard	-	Cartesian	9.150	2.000	1.500	Generated
332	Standard	-	Cartesian	8.650	2.500	1.500	Generated
333	Standard	-	Cartesian	8.150	2.000	1.500	Generated
334	Standard	-	Cartesian	21.400	2.000	4.500	Generated
335	Standard	-	Cartesian	20.650	2.750	4.500	Generated
336	Standard	-	Cartesian	19.900	2.000	4.500	Generated
337	Standard	-	Cartesian	25.400	2.000	4.500	Generated
338	Standard	-	Cartesian	24.650	2.750	4.500	Generated
339	Standard	-	Cartesian	23.900	2.000	4.500	Generated
340	Standard	-	Cartesian	29.400	2.000	4.500	Generated
341	Standard	-	Cartesian	28.650	2.750	4.500	Generated
342	Standard	-	Cartesian	27.900	2.000	4.500	Generated
343	Standard	-	Cartesian	33.150	2.000	4.500	Generated
344	Standard	-	Cartesian	32.650	2.500	4.500	Generated
345	Standard	-	Cartesian	32.150	2.000	4.500	Generated
346	Standard	-	Cartesian	17.400	2.000	4.500	Generated
347	Standard	-	Cartesian	16.650	2.750	4.500	Generated
348	Standard	-	Cartesian	15.900	2.000	4.500	Generated
349	Standard	-	Cartesian	13.400	2.000	4.500	Generated
350	Standard	-	Cartesian	12.650	2.750	4.500	Generated
351	Standard	-	Cartesian	11.900	2.000	4.500	Generated
352	Standard	-	Cartesian	9.150	2.000	4.500	Generated
353	Standard	-	Cartesian	8.650	2.500	4.500	Generated
354	Standard	-	Cartesian	8.150	2.000	4.500	Generated
355	Standard	-	Cartesian	21.400	2.000	7.500	Generated
356	Standard	-	Cartesian	20.650	2.750	7.500	Generated
357	Standard	-	Cartesian	19.900	2.000	7.500	Generated
358	Standard	-	Cartesian	25.400	2.000	7.500	Generated
359	Standard	-	Cartesian	24.650	2.750	7.500	Generated
360	Standard	-	Cartesian	23.900	2.000	7.500	Generated
361	Standard	-	Cartesian	29.400	2.000	7.500	Generated
362	Standard	-	Cartesian	28.650	2.750	7.500	Generated
363	Standard	-	Cartesian	27.900	2.000	7.500	Generated
364	Standard	-	Cartesian	33.150	2.000	7.500	Generated
365	Standard	-	Cartesian	32.650	2.500	7.500	Generated
366	Standard	-	Cartesian	32.150	2.000	7.500	Generated
367	Standard	-	Cartesian	17.400	2.000	7.500	Generated
368	Standard	-	Cartesian	16.650	2.750	7.500	Generated
369	Standard	-	Cartesian	15.900	2.000	7.500	Generated
370	Standard	-	Cartesian	13.400	2.000	7.500	Generated
371	Standard	-	Cartesian	12.650	2.750	7.500	Generated
372	Standard	-	Cartesian	11.900	2.000	7.500	Generated
373	Standard	-	Cartesian	9.150	2.000	7.500	Generated
374	Standard	-	Cartesian	8.650	2.500	7.500	Generated
375	Standard	-	Cartesian	8.150	2.000	7.500	Generated
376	Standard	-	Cartesian	21.400	2.000	10.500	Generated
377	Standard	-	Cartesian	20.650	2.750	10.500	Generated
378	Standard	-	Cartesian	19.900	2.000	10.500	Generated
379	Standard	-	Cartesian	25.400	2.000	10.500	Generated
380	Standard	-	Cartesian	24.650	2.750	10.500	Generated
381	Standard	-	Cartesian	23.900	2.000	10.500	Generated
382	Standard	-	Cartesian	29.400	2.000	10.500	Generated
383	Standard	-	Cartesian	28.650	2.750	10.500	Generated
384	Standard	-	Cartesian	27.900	2.000	10.500	Generated
385	Standard	-	Cartesian	33.150	2.000	10.500	Generated
386	Standard	-	Cartesian	32.650	2.500	10.500	Generated
387	Standard	-	Cartesian	32.150	2.000	10.500	Generated
388	Standard	-	Cartesian	17.400	2.000	10.500	Generated
389	Standard	-	Cartesian	16.650	2.750	10.500	Generated
390	Standard	-	Cartesian	15.900	2.000	10.500	Generated
391	Standard	-	Cartesian	13.400	2.000	10.500	Generated

Project: CIE5060 Model: V26
Graduation Project

1.1 NODES

Node No.	Node Type	Reference Node	Coordinate System	Node Coordinates X [m]	Y [m]	Z [m]	Comment
392	Standard	-	Cartesian	12.650	2.750	10.500	Generated
393	Standard	-	Cartesian	11.900	2.000	10.500	Generated
394	Standard	-	Cartesian	9.150	2.000	10.500	Generated
395	Standard	-	Cartesian	8.650	2.500	10.500	Generated
396	Standard	-	Cartesian	8.150	2.000	10.500	Generated
397	Standard	-	Cartesian	11.500	0.000	7.500	
398	Standard	-	Cartesian	29.800	0.000	7.500	
399	Standard	-	Cartesian	11.500	4.000	7.500	
400	Standard	-	Cartesian	29.800	4.000	7.500	
401	Standard	-	Cartesian	11.500	0.000	4.500	
402	Standard	-	Cartesian	29.800	0.000	4.500	
403	Standard	-	Cartesian	11.500	4.000	4.500	
404	Standard	-	Cartesian	29.800	4.000	4.500	
405	Standard	-	Cartesian	11.500	0.000	1.500	
406	Standard	-	Cartesian	29.800	0.000	1.500	
407	Standard	-	Cartesian	11.500	4.000	1.500	
408	Standard	-	Cartesian	29.800	4.000	1.500	
409	Standard	-	Cartesian	11.500	0.000	-1.500	
410	Standard	-	Cartesian	29.800	0.000	-1.500	
411	Standard	-	Cartesian	11.500	4.000	-1.500	
412	Standard	-	Cartesian	29.800	4.000	-1.500	
413	Standard	-	Cartesian	11.500	0.000	-4.500	
414	Standard	-	Cartesian	29.800	0.000	-4.500	
415	Standard	-	Cartesian	11.500	4.000	-4.500	
416	Standard	-	Cartesian	29.800	4.000	-4.500	
417	Standard	-	Cartesian	11.500	0.000	-7.500	
418	Standard	-	Cartesian	29.800	0.000	-7.500	
419	Standard	-	Cartesian	11.500	4.000	-7.500	
420	Standard	-	Cartesian	29.800	4.000	-7.500	
421	Standard	-	Cartesian	11.500	0.000	10.500	
422	Standard	-	Cartesian	29.800	0.000	10.500	
423	Standard	-	Cartesian	11.500	4.000	10.500	
424	Standard	-	Cartesian	29.800	4.000	10.500	
425	Standard	-	Cartesian	11.490	2.100	-4.500	
426	Standard	-	Cartesian	11.490	2.100	-1.500	
427	Standard	-	Cartesian	11.490	2.100	1.500	
428	Standard	-	Cartesian	11.490	2.100	4.500	
429	Standard	-	Cartesian	11.490	2.100	7.500	
430	Standard	-	Cartesian	11.490	2.100	10.500	
431	Standard	-	Cartesian	29.810	2.100	-4.500	
432	Standard	-	Cartesian	29.810	2.100	-1.500	
433	Standard	-	Cartesian	29.810	2.100	1.500	
434	Standard	-	Cartesian	29.810	2.100	4.500	
435	Standard	-	Cartesian	29.810	2.100	7.500	
436	Standard	-	Cartesian	29.810	2.100	10.500	
437	Standard	-	Cartesian	29.800	4.000	12.500	
438	Standard	-	Cartesian	11.500	4.000	12.500	
439	Standard	-	Cartesian	11.500	2.000	12.500	
440	Standard	-	Cartesian	29.800	2.000	12.500	
441	Standard	-	Cartesian	21.025	3.000	12.500	Generated
442	Standard	-	Cartesian	20.650	3.375	12.500	Generated
443	Standard	-	Cartesian	20.275	3.000	12.500	Generated
444	Standard	-	Cartesian	25.025	3.000	12.500	Generated
445	Standard	-	Cartesian	24.650	3.375	12.500	Generated
446	Standard	-	Cartesian	24.275	3.000	12.500	Generated
447	Standard	-	Cartesian	29.025	3.000	12.500	Generated
448	Standard	-	Cartesian	28.650	3.375	12.500	Generated
449	Standard	-	Cartesian	28.275	3.000	12.500	Generated
450	Standard	-	Cartesian	32.900	3.000	12.500	Generated
451	Standard	-	Cartesian	32.650	3.250	12.500	Generated
452	Standard	-	Cartesian	32.400	3.000	12.500	Generated
453	Standard	-	Cartesian	17.025	3.000	12.500	Generated
454	Standard	-	Cartesian	16.650	3.375	12.500	Generated
455	Standard	-	Cartesian	16.275	3.000	12.500	Generated
456	Standard	-	Cartesian	13.025	3.000	12.500	Generated
457	Standard	-	Cartesian	12.650	3.375	12.500	Generated
458	Standard	-	Cartesian	12.275	3.000	12.500	Generated
459	Standard	-	Cartesian	8.900	3.000	12.500	Generated
460	Standard	-	Cartesian	8.650	3.250	12.500	Generated
461	Standard	-	Cartesian	8.400	3.000	12.500	Generated

1.2 LINES

Line No.	Line Type	Nodes No.	Line Length L [m]		Comment
1	Polyline	11,8	4.000	Y	
2	Polyline	2,3	37.800	X	
3	Polyline	11,175	1.000	Z	
4	Polyline	19,178	1.000	Z	
5	Polyline	34,27	4.000	Y	
6	Polyline	8,181	1.414	YZ	
7	Polyline	27,184	1.414	YZ	
8	Polyline	5,421	9.750	X	
9	Polyline	5,12	4.000	Y	
10	Circle	1,4,6	4.712	XY	
11	Polyline	20,187	1.000	Z	
12	Polyline	130,190	1.414	YZ	
13	Polyline	273,12	1.000	Z	
14	Polyline	12,423	9.750	X	
15	Polyline	20,19	0.200	X	

Project: CIE5060 Model: V26
Graduation Project

1.2 LINES

Line No.	Line Type	Nodes No.	Line Length L [m]		Comment
16	Polyline	180,184	3.000	Y	
17	Polyline	276,35	1.000	Z	
18	Polyline	184,181	1.650	X	
19	Polyline	12,14	3.000	Z	
20	Polyline	14,15	4.000	Y	
21	Polyline	15,5	3.000	Z	
22	Polyline	11,113	1.000	Z	
23	Polyline	17,18	4.000	Y	
24	Polyline	18,101	1.000	Z	
25	Polyline	14,399	9.750	X	
26	Polyline	15,397	9.750	X	
27	Polyline	62,76	4.000	Y	
28	Polyline	3,19	1.650	X	
29	Polyline	14,21	3.000	Z	
30	Polyline	21,22	4.000	Y	
31	Polyline	22,15	3.000	Z	
32	Polyline	17,115	1.000	Z	
33	Polyline	23,24	4.000	Y	
34	Polyline	24,103	1.000	Z	
35	Polyline	21,403	9.750	X	
36	Polyline	22,401	9.750	X	
37	Polyline	181,175	3.000	Y	
38	Polyline	175,180	1.650	X	
39	Polyline	21,29	3.000	Z	
40	Polyline	29,30	4.000	Y	
41	Polyline	30,22	3.000	Z	
42	Polyline	23,117	1.000	Z	
43	Polyline	31,32	4.000	Y	
44	Polyline	32,105	1.000	Z	
45	Polyline	29,407	9.750	X	
46	Polyline	30,405	9.750	X	
47	Polyline	279,5	1.414	YZ	
48	Polyline	180,189	0.200	X	
49	Polyline	29,37	3.000	Z	
50	Polyline	37,38	4.000	Y	
51	Polyline	38,30	3.000	Z	
52	Polyline	31,119	1.000	Z	
53	Polyline	39,40	4.000	Y	
54	Polyline	40,107	1.000	Z	
55	Polyline	37,411	9.750	X	
56	Polyline	38,409	9.750	X	
57	Polyline	189,190	3.000	Y	
58	Polyline	8,27	1.650	X	
59	Polyline	37,45	3.000	Z	
60	Polyline	45,46	4.000	Y	
61	Polyline	46,38	3.000	Z	
62	Polyline	39,97	1.000	Z	
63	Polyline	47,48	4.000	Y	
64	Polyline	48,109	1.000	Z	
65	Polyline	45,415	9.750	X	
66	Polyline	46,413	9.750	X	
67	Polyline	25,33	1.000	Z	
68	Polyline	282,62	1.414	YZ	
69	Polyline	45,53	3.000	Z	
70	Polyline	53,54	4.000	Y	
71	Polyline	54,46	3.000	Z	
72	Polyline	47,99	1.000	Z	
73	Polyline	55,56	4.000	Y	
74	Polyline	56,111	1.000	Z	
75	Polyline	53,419	9.750	X	
76	Polyline	54,417	9.750	X	
77	Polyline	190,184	0.200	X	
78	Polyline	179,185	2.000	Y	
79	Polyline	285,49	1.000	Z	
80	Polyline	11,34	1.650	X	
81	Polyline	185,182	1.650	X	
82	Polyline	182,176	2.000	Y	
83	Polyline	33,71	1.000	Z	
84	Polyline	176,179	1.650	X	
85	Polyline	36,41	1.000	Z	
86	Polyline	288,236	1.414	YZ	
87	Polyline	35,49	0.200	X	
88	Polyline	34,93	1.000	Z	
89	Polyline	43,44	4.000	Y	
90	Polyline	44,95	1.000	Z	
91	Polyline	17,43	1.650	X	
92	Polyline	18,44	1.650	X	
93	Polyline	282,278	3.000	Y	
94	Polyline	41,68	1.000	Z	
95	Polyline	279,282	1.650	X	
96	Polyline	43,89	1.000	Z	
97	Polyline	51,52	4.000	Y	
98	Polyline	52,91	1.000	Z	
99	Polyline	23,51	1.650	X	
100	Polyline	24,52	1.650	X	
101	Polyline	227,12	1.000	Z	
102	Circle	7,9,10	4.712	XY	
103	Polyline	36,33	4.000	Y	
104	Polyline	51,81	1.000	Z	
105	Polyline	59,60	4.000	Y	
106	Polyline	60,85	1.000	Z	
107	Polyline	31,59	1.650	X	

Project: CIE5060 Model: V26
Graduation Project

1.2 LINES

Line No.	Line Type	Nodes No.	Line Length L [m]		Comment
108	Polyline	32,60	1.650	X	
109	Polyline	41,25	4.000	Y	
110	Polyline	215,15	1.000	Z	
111	Polyline	35,2	1.650	X	
112	Polyline	59,73	1.000	Z	
113	Polyline	63,64	4.000	Y	
114	Polyline	64,77	1.000	Z	
115	Polyline	39,63	1.650	X	
116	Polyline	40,64	1.650	X	
117	Polyline	229,14	1.000	Z	
118	Circle	13,16,26	4.712	XY	
119	Polyline	217,22	1.000	Z	
120	Polyline	63,42	1.000	Z	
121	Polyline	67,68	4.000	Y	
122	Polyline	68,65	1.000	Z	
123	Polyline	47,67	1.650	X	
124	Polyline	48,68	1.650	X	
125	Polyline	42,50	1.000	Z	
126	Polyline	50,67	1.000	Z	
127	Polyline	65,66	1.000	Z	
128	Polyline	67,25	1.000	Z	
129	Polyline	71,72	4.000	Y	
130	Polyline	72,36	1.000	Z	
131	Polyline	55,71	1.650	X	
132	Polyline	56,72	1.650	X	
133	Polyline	273,279	3.000	Y	
134	Polyline	278,273	1.650	X	
135	Polyline	231,21	1.000	Z	
136	Circle	28,57,58	3.142	XY	
137	Polyline	219,30	1.000	Z	
138	Polyline	66,64	1.000	Z	
139	Polyline	66,42	4.000	Y	
140	Polyline	65,50	4.000	Y	
141	Polyline	287,278	0.200	X	
142	Polyline	233,29	1.000	Z	
143	Circle	69,70,80	4.712	XY	
144	Polyline	221,38	1.000	Z	
145	Polyline	288,287	3.000	Y	
146	Polyline	73,74	1.000	Z	
147	Polyline	74,63	1.000	Z	
148	Polyline	77,78	1.000	Z	
149	Polyline	62,5	1.650	X	
150	Polyline	211,37	1.000	Z	
151	Circle	83,122,123	4.712	XY	
152	Polyline	223,46	1.000	Z	
153	Polyline	75,61	1.000	Z	
154	Polyline	78,60	1.000	Z	
155	Polyline	78,73	4.000	Y	
156	Polyline	77,74	4.000	Y	
157	Polyline	213,45	1.000	Z	
158	Circle	127,129,291	3.142	XY	
159	Polyline	225,54	1.000	Z	
160	Polyline	282,288	0.200	X	
161	Polyline	283,277	2.000	Y	
162	Polyline	81,82	1.000	Z	
163	Polyline	82,59	1.000	Z	
164	Polyline	85,86	1.000	Z	
165	Polyline	76,12	1.650	X	
166	Polyline	280,283	1.650	X	
167	Polyline	274,280	2.000	Y	
168	Polyline	193,75	1.000	Z	
169	Polyline	277,274	1.650	X	
170	Polyline	86,52	1.000	Z	
171	Polyline	86,81	4.000	Y	
172	Polyline	85,82	4.000	Y	
173	Polyline	84,79	1.000	Z	
174	Polyline	207,76	1.000	Z	
175	Polyline	89,90	1.000	Z	
176	Polyline	90,51	1.000	Z	
177	Polyline	91,92	1.000	Z	
178	Polyline	92,44	1.000	Z	
179	Polyline	92,89	4.000	Y	
180	Polyline	91,90	4.000	Y	
181	Polyline	93,94	1.000	Z	
182	Polyline	94,43	1.000	Z	
183	Polyline	95,96	1.000	Z	
184	Polyline	96,27	1.000	Z	
185	Polyline	97,98	1.000	Z	
186	Polyline	98,47	1.000	Z	
187	Polyline	99,100	1.000	Z	
188	Polyline	100,55	1.000	Z	
189	Polyline	101,102	1.000	Z	
190	Polyline	102,8	1.000	Z	
191	Polyline	103,104	1.000	Z	
192	Polyline	104,18	1.000	Z	
193	Polyline	105,106	1.000	Z	
194	Polyline	106,24	1.000	Z	
195	Polyline	107,108	1.000	Z	
196	Polyline	108,32	1.000	Z	
197	Polyline	109,110	1.000	Z	
198	Polyline	110,40	1.000	Z	
199	Polyline	111,112	1.000	Z	

Project: CIE5060 Model: V26
Graduation Project

1.2 LINES

Line No.	Line Type	Nodes No.	Line Length L [m]		Comment
200	Polyline	112,48	1.000	Z	
201	Polyline	113,114	1.000	Z	
202	Polyline	114,17	1.000	Z	
203	Polyline	115,116	1.000	Z	
204	Polyline	116,23	1.000	Z	
205	Polyline	117,118	1.000	Z	
206	Polyline	118,31	1.000	Z	
207	Polyline	119,120	1.000	Z	
208	Polyline	120,39	1.000	Z	
209	Polyline	100,111	4.000	Y	
210	Polyline	112,99	4.000	Y	
211	Polyline	98,109	4.000	Y	
212	Polyline	110,97	4.000	Y	
213	Polyline	33,100	1.650	X	
214	Polyline	107,120	4.000	Y	
215	Polyline	108,119	4.000	Y	
216	Polyline	118,105	4.000	Y	
217	Polyline	117,106	4.000	Y	
218	Polyline	116,103	4.000	Y	
219	Polyline	104,115	4.000	Y	
220	Polyline	101,114	4.000	Y	
221	Polyline	113,102	4.000	Y	
222	Polyline	95,94	4.000	Y	
223	Polyline	93,96	4.000	Y	
224	Polyline	36,111	1.650	X	
225	Polyline	112,41	1.650	X	
226	Polyline	25,99	1.650	X	
227	Polyline	50,98	1.650	X	
228	Polyline	42,97	1.650	X	
229	Polyline	179,188	0.200	X	
230	Polyline	188,191	2.000	Y	
231	Polyline	109,65	1.650	X	
232	Polyline	191,185	0.200	X	
233	Polyline	110,66	1.650	X	
234	Polyline	177,183	1.000	Y	
235	Polyline	74,120	1.650	X	
236	Polyline	73,119	1.650	X	
237	Polyline	107,77	1.650	X	
238	Polyline	108,78	1.650	X	
239	Polyline	82,118	1.650	X	
240	Polyline	81,117	1.650	X	
241	Polyline	105,85	1.650	X	
242	Polyline	106,86	1.650	X	
243	Polyline	183,186	1.650	X	
244	Polyline	186,178	1.000	Y	
245	Polyline	178,177	1.650	X	
246	Polyline	178,187	0.200	X	
247	Polyline	90,116	1.650	X	
248	Polyline	89,115	1.650	X	
249	Polyline	103,91	1.650	X	
250	Polyline	104,92	1.650	X	
251	Polyline	187,192	1.000	Y	
252	Polyline	192,186	0.200	X	
253	Polyline	121,88	4.000	Y	
254	Polyline	209,121	1.000	Z	
255	Polyline	94,114	1.650	X	
256	Polyline	93,113	1.650	X	
257	Polyline	101,95	1.650	X	
258	Polyline	102,96	1.650	X	
259	Polyline	88,14	1.650	X	
260	Polyline	121,15	1.650	X	
261	Polyline	27,130	0.200	X	
262	Polyline	148,84	1.000	Z	
263	Polyline	203,88	1.000	Z	
264	Polyline	126,125	4.000	Y	
265	Polyline	128,133	1.000	Z	
266	Polyline	205,126	1.000	Z	
267	Polyline	125,21	1.650	X	
268	Polyline	126,22	1.650	X	
269	Polyline	34,134	0.200	X	
270	Polyline	75,79	4.000	Y	
271	Polyline	199,125	1.000	Z	
272	Polyline	133,157	1.000	Z	
273	Polyline	132,131	4.000	Y	
274	Polyline	135,138	1.000	Z	
275	Polyline	134,171	1.000	Z	
276	Polyline	140,141	4.000	Y	
277	Polyline	141,173	1.000	Z	
278	Polyline	43,140	0.200	X	
279	Polyline	44,141	0.200	X	
280	Polyline	138,156	1.000	Z	
281	Polyline	140,167	1.000	Z	
282	Polyline	145,146	4.000	Y	
283	Polyline	146,169	1.000	Z	
284	Polyline	51,145	0.200	X	
285	Polyline	52,146	0.200	X	
286	Polyline	135,133	4.000	Y	
287	Polyline	145,163	1.000	Z	
288	Polyline	149,150	4.000	Y	
289	Polyline	150,165	1.000	Z	
290	Polyline	59,149	0.200	X	
291	Polyline	60,150	0.200	X	

Project: CIE5060 Model: V26
Graduation Project

1.2 LINES

Line No.	Line Type	Nodes No.	Line Length L [m]		Comment
292	Polyline	138,128	4.000	Y	
293	Polyline	149,159	1.000	Z	
294	Polyline	151,152	4.000	Y	
295	Polyline	152,161	1.000	Z	
296	Polyline	63,151	0.200	X	
297	Polyline	64,152	0.200	X	
298	Polyline	151,139	1.000	Z	
299	Polyline	155,156	4.000	Y	
300	Polyline	156,153	1.000	Z	
301	Polyline	67,155	0.200	X	
302	Polyline	68,156	0.200	X	
303	Polyline	139,144	1.000	Z	
304	Polyline	144,155	1.000	Z	
305	Polyline	153,154	1.000	Z	
306	Polyline	155,128	1.000	Z	
307	Polyline	157,158	4.000	Y	
308	Polyline	158,135	1.000	Z	
309	Polyline	71,157	0.200	X	
310	Polyline	72,158	0.200	X	
311	Polyline	154,152	1.000	Z	
312	Polyline	154,139	4.000	Y	
313	Polyline	153,144	4.000	Y	
314	Polyline	159,160	1.000	Z	
315	Polyline	160,151	1.000	Z	
316	Polyline	161,162	1.000	Z	
317	Polyline	162,150	1.000	Z	
318	Polyline	162,159	4.000	Y	
319	Polyline	161,160	4.000	Y	
320	Polyline	163,164	1.000	Z	
321	Polyline	164,149	1.000	Z	
322	Polyline	165,166	1.000	Z	
323	Polyline	166,146	1.000	Z	
324	Polyline	166,163	4.000	Y	
325	Polyline	165,164	4.000	Y	
326	Polyline	167,168	1.000	Z	
327	Polyline	168,145	1.000	Z	
328	Polyline	169,170	1.000	Z	
329	Polyline	170,141	1.000	Z	
330	Polyline	170,167	4.000	Y	
331	Polyline	169,168	4.000	Y	
332	Polyline	171,172	1.000	Z	
333	Polyline	172,140	1.000	Z	
334	Polyline	173,174	1.000	Z	
335	Polyline	174,130	1.000	Z	
336	Polyline	201,132	1.000	Z	
337	Polyline	131,29	1.650	X	
338	Polyline	132,30	1.650	X	
339	Polyline	61,84	4.000	Y	
340	Polyline	195,131	1.000	Z	
341	Polyline	137,136	4.000	Y	
342	Polyline	197,137	1.000	Z	
343	Polyline	136,37	1.650	X	
344	Polyline	137,38	1.650	X	
345	Polyline	87,136	1.000	Z	
346	Polyline	148,147	4.000	Y	
347	Polyline	142,148	1.000	Z	
348	Polyline	147,45	1.650	X	
349	Polyline	148,46	1.650	X	
350	Polyline	124,87	1.000	Z	
351	Polyline	147,124	1.000	Z	
352	Polyline	143,142	1.000	Z	
353	Polyline	61,147	1.000	Z	
354	Polyline	194,193	4.000	Y	
355	Polyline	79,194	1.000	Z	
356	Polyline	193,53	1.650	X	
357	Polyline	194,54	1.650	X	
358	Polyline	137,143	1.000	Z	
359	Polyline	87,143	4.000	Y	
360	Polyline	124,142	4.000	Y	
361	Polyline	196,195	1.000	Z	
362	Polyline	136,196	1.000	Z	
363	Polyline	198,197	1.000	Z	
364	Polyline	133,33	0.200	X	
365	Polyline	132,198	1.000	Z	
366	Polyline	195,198	4.000	Y	
367	Polyline	196,197	4.000	Y	
368	Polyline	200,199	1.000	Z	
369	Polyline	131,200	1.000	Z	
370	Polyline	202,201	1.000	Z	
371	Polyline	126,202	1.000	Z	
372	Polyline	199,202	4.000	Y	
373	Polyline	173,172	4.000	Y	
374	Polyline	171,174	4.000	Y	
375	Polyline	135,36	0.200	X	
376	Polyline	41,138	0.200	X	
377	Polyline	128,25	0.200	X	
378	Polyline	144,50	0.200	X	
379	Polyline	139,42	0.200	X	
380	Polyline	65,153	0.200	X	
381	Polyline	66,154	0.200	X	
382	Polyline	160,74	0.200	X	
383	Polyline	159,73	0.200	X	

Project: CIE5060 Model: V26
Graduation Project

1.2 LINES

Line No.	Line Type	Nodes No.	Line Length L [m]		Comment
384	Polyline	77,161	0.200	X	
385	Polyline	78,162	0.200	X	
386	Polyline	164,82	0.200	X	
387	Polyline	163,81	0.200	X	
388	Polyline	85,165	0.200	X	
389	Polyline	86,166	0.200	X	
390	Polyline	168,90	0.200	X	
391	Polyline	167,89	0.200	X	
392	Polyline	91,169	0.200	X	
393	Polyline	92,170	0.200	X	
394	Polyline	172,94	0.200	X	
395	Polyline	171,93	0.200	X	
396	Polyline	95,173	0.200	X	
397	Polyline	96,174	0.200	X	
398	Polyline	200,201	4.000	Y	
399	Polyline	204,203	1.000	Z	
400	Polyline	125,204	1.000	Z	
401	Polyline	206,205	1.000	Z	
402	Polyline	121,206	1.000	Z	
403	Polyline	203,206	4.000	Y	
404	Polyline	204,205	4.000	Y	
405	Polyline	208,207	1.000	Z	
406	Polyline	88,208	1.000	Z	
407	Polyline	210,209	1.000	Z	
408	Polyline	62,210	1.000	Z	
409	Polyline	212,211	1.000	Z	
410	Polyline	45,212	1.000	Z	
411	Polyline	214,213	1.000	Z	
412	Polyline	53,214	1.000	Z	
413	Polyline	216,215	1.000	Z	
414	Polyline	5,216	1.000	Z	
415	Polyline	218,217	1.000	Z	
416	Polyline	15,218	1.000	Z	
417	Polyline	220,219	1.000	Z	
418	Polyline	22,220	1.000	Z	
419	Polyline	222,221	1.000	Z	
420	Polyline	30,222	1.000	Z	
421	Polyline	224,223	1.000	Z	
422	Polyline	38,224	1.000	Z	
423	Polyline	226,225	1.000	Z	
424	Polyline	46,226	1.000	Z	
425	Polyline	228,227	1.000	Z	
426	Polyline	14,228	1.000	Z	
427	Polyline	130,134	4.000	Y	
428	Polyline	175,176	1.000	Z	
429	Polyline	176,177	1.000	Z	
430	Polyline	177,3	1.000	Z	
431	Polyline	178,179	1.000	Z	
432	Polyline	179,180	1.000	Z	
433	Polyline	180,34	1.000	Z	
434	Polyline	181,182	1.414	YZ	
435	Polyline	182,183	1.414	YZ	
436	Polyline	183,3	1.414	YZ	
437	Polyline	184,185	1.414	YZ	
438	Polyline	185,186	1.414	YZ	
439	Polyline	186,19	1.414	YZ	
440	Polyline	187,188	1.000	Z	
441	Polyline	188,189	1.000	Z	
442	Polyline	189,134	1.000	Z	
443	Polyline	190,191	1.414	YZ	
444	Polyline	191,192	1.414	YZ	
445	Polyline	192,20	1.414	YZ	
446	Polyline	230,229	1.000	Z	
447	Polyline	21,230	1.000	Z	
448	Polyline	232,231	1.000	Z	
449	Polyline	29,232	1.000	Z	
450	Polyline	234,233	1.000	Z	
451	Polyline	37,234	1.000	Z	
452	Polyline	225,214	4.000	Y	
453	Polyline	213,226	4.000	Y	
454	Polyline	223,212	4.000	Y	
455	Polyline	211,224	4.000	Y	
456	Polyline	214,75	1.650	X	
457	Polyline	234,221	4.000	Y	
458	Polyline	233,222	4.000	Y	
459	Polyline	219,232	4.000	Y	
460	Polyline	220,231	4.000	Y	
461	Polyline	217,230	4.000	Y	
462	Polyline	229,218	4.000	Y	
463	Polyline	228,215	4.000	Y	
464	Polyline	216,227	4.000	Y	
465	Polyline	208,209	4.000	Y	
466	Polyline	210,207	4.000	Y	
467	Polyline	225,79	1.650	X	
468	Polyline	84,226	1.650	X	
469	Polyline	213,61	1.650	X	
470	Polyline	212,124	1.650	X	
471	Polyline	211,87	1.650	X	
472	Polyline	286,277	0.200	X	
473	Polyline	289,286	2.000	Y	
474	Polyline	142,223	1.650	X	
475	Polyline	283,289	0.200	X	

Project: CIE5060 Model: V26
Graduation Project

1.2 LINES

Line No.	Line Type	Nodes No.	Line Length L [m]		Comment
476	Polyline	143,224	1.650	X	
477	Polyline	281,275	1.000	Y	
478	Polyline	234,196	1.650	X	
479	Polyline	233,195	1.650	X	
480	Polyline	197,221	1.650	X	
481	Polyline	198,222	1.650	X	
482	Polyline	232,200	1.650	X	
483	Polyline	231,199	1.650	X	
484	Polyline	201,219	1.650	X	
485	Polyline	202,220	1.650	X	
486	Polyline	284,281	1.650	X	
487	Polyline	276,284	1.000	Y	
488	Polyline	275,276	1.650	X	
489	Polyline	285,276	0.200	X	
490	Polyline	230,204	1.650	X	
491	Polyline	229,203	1.650	X	
492	Polyline	205,217	1.650	X	
493	Polyline	206,218	1.650	X	
494	Polyline	290,285	1.000	Y	
495	Polyline	284,290	0.200	X	
496	Polyline	228,208	1.650	X	
497	Polyline	227,207	1.650	X	
498	Polyline	209,215	1.650	X	
499	Polyline	210,216	1.650	X	
500	Polyline	236,62	0.200	X	
501	Polyline	237,235	1.000	Z	
502	Polyline	238,76	0.200	X	
503	Polyline	255,237	1.000	Z	
504	Polyline	240,239	1.000	Z	
505	Polyline	269,238	1.000	Z	
506	Polyline	243,242	4.000	Y	
507	Polyline	271,243	1.000	Z	
508	Polyline	242,88	0.200	X	
509	Polyline	243,121	0.200	X	
510	Polyline	254,240	1.000	Z	
511	Polyline	265,242	1.000	Z	
512	Polyline	246,245	4.000	Y	
513	Polyline	267,246	1.000	Z	
514	Polyline	245,125	0.200	X	
515	Polyline	246,126	0.200	X	
516	Polyline	237,239	4.000	Y	
517	Polyline	261,245	1.000	Z	
518	Polyline	248,247	4.000	Y	
519	Polyline	263,248	1.000	Z	
520	Polyline	247,131	0.200	X	
521	Polyline	248,132	0.200	X	
522	Polyline	235,240	4.000	Y	
523	Polyline	257,247	1.000	Z	
524	Polyline	250,249	4.000	Y	
525	Polyline	259,250	1.000	Z	
526	Polyline	249,136	0.200	X	
527	Polyline	250,137	0.200	X	
528	Polyline	241,249	1.000	Z	
529	Polyline	254,253	4.000	Y	
530	Polyline	251,254	1.000	Z	
531	Polyline	253,147	0.200	X	
532	Polyline	254,148	0.200	X	
533	Polyline	244,241	1.000	Z	
534	Polyline	253,244	1.000	Z	
535	Polyline	252,251	1.000	Z	
536	Polyline	235,253	1.000	Z	
537	Polyline	256,255	4.000	Y	
538	Polyline	239,256	1.000	Z	
539	Polyline	255,193	0.200	X	
540	Polyline	256,194	0.200	X	
541	Polyline	250,252	1.000	Z	
542	Polyline	241,252	4.000	Y	
543	Polyline	244,251	4.000	Y	
544	Polyline	258,257	1.000	Z	
545	Polyline	249,258	1.000	Z	
546	Polyline	260,259	1.000	Z	
547	Polyline	248,260	1.000	Z	
548	Polyline	257,260	4.000	Y	
549	Polyline	258,259	4.000	Y	
550	Polyline	262,261	1.000	Z	
551	Polyline	247,262	1.000	Z	
552	Polyline	264,263	1.000	Z	
553	Polyline	246,264	1.000	Z	
554	Polyline	261,264	4.000	Y	
555	Polyline	262,263	4.000	Y	
556	Polyline	266,265	1.000	Z	
557	Polyline	245,266	1.000	Z	
558	Polyline	268,267	1.000	Z	
559	Polyline	243,268	1.000	Z	
560	Polyline	265,268	4.000	Y	
561	Polyline	266,267	4.000	Y	
562	Polyline	270,269	1.000	Z	
563	Polyline	242,270	1.000	Z	
564	Polyline	272,271	1.000	Z	
565	Polyline	236,272	1.000	Z	
566	Polyline	75,237	0.200	X	
567	Polyline	270,271	4.000	Y	

Project: CIE5060 Model: V26
Graduation Project

1.2 LINES

Line No.	Line Type	Nodes No.	Line Length L [m]		Comment
568	Polyline	272,269	4.000	Y	
569	Polyline	79,239	0.200	X	
570	Polyline	240,84	0.200	X	
571	Polyline	61,235	0.200	X	
572	Polyline	124,244	0.200	X	
573	Polyline	87,241	0.200	X	
574	Polyline	251,142	0.200	X	
575	Polyline	252,143	0.200	X	
576	Polyline	196,258	0.200	X	
577	Polyline	195,257	0.200	X	
578	Polyline	259,197	0.200	X	
579	Polyline	260,198	0.200	X	
580	Polyline	200,262	0.200	X	
581	Polyline	199,261	0.200	X	
582	Polyline	263,201	0.200	X	
583	Polyline	264,202	0.200	X	
584	Polyline	204,266	0.200	X	
585	Polyline	203,265	0.200	X	
586	Polyline	267,205	0.200	X	
587	Polyline	268,206	0.200	X	
588	Polyline	208,270	0.200	X	
589	Polyline	207,269	0.200	X	
590	Polyline	271,209	0.200	X	
591	Polyline	272,210	0.200	X	
592	Polyline	238,236	4.000	Y	
593	Polyline	274,273	1.000	Z	
594	Polyline	275,274	1.000	Z	
595	Polyline	2,275	1.000	Z	
596	Polyline	277,276	1.000	Z	
597	Polyline	278,277	1.000	Z	
598	Polyline	76,278	1.000	Z	
599	Polyline	280,279	1.414	YZ	
600	Polyline	281,280	1.414	YZ	
601	Polyline	2,281	1.414	YZ	
602	Polyline	283,282	1.414	YZ	
603	Polyline	284,283	1.414	YZ	
604	Polyline	35,284	1.414	YZ	
605	Polyline	286,285	1.000	Z	
606	Polyline	287,286	1.000	Z	
607	Polyline	238,287	1.000	Z	
608	Polyline	289,288	1.414	YZ	
609	Polyline	290,289	1.414	YZ	
610	Polyline	49,290	1.414	YZ	
611	Circle	292-294	4.712	XY	
612	Circle	295-297	4.712	XY	
613	Circle	298-300	4.712	XY	
614	Circle	301-303	3.142	XY	
615	Circle	304-306	4.712	XY	
616	Circle	307-309	4.712	XY	
617	Circle	310-312	3.142	XY	
618	Circle	313-315	4.712	XY	
619	Circle	316-318	4.712	XY	
620	Circle	319-321	4.712	XY	
621	Circle	322-324	3.142	XY	
622	Circle	325-327	4.712	XY	
623	Circle	328-330	4.712	XY	
624	Circle	331-333	3.142	XY	
625	Circle	334-336	4.712	XY	
626	Circle	337-339	4.712	XY	
627	Circle	340-342	4.712	XY	
628	Circle	343-345	3.142	XY	
629	Circle	346-348	4.712	XY	
630	Circle	349-351	4.712	XY	
631	Circle	352-354	3.142	XY	
632	Circle	355-357	4.712	XY	
633	Circle	358-360	4.712	XY	
634	Circle	361-363	4.712	XY	
635	Circle	364-366	3.142	XY	
636	Circle	367-369	4.712	XY	
637	Circle	370-372	4.712	XY	
638	Circle	373-375	3.142	XY	
639	Circle	376-378	4.712	XY	
640	Circle	379-381	4.712	XY	
641	Circle	382-384	4.712	XY	
642	Circle	385-387	3.142	XY	
643	Circle	388-390	4.712	XY	
644	Circle	391-393	4.712	XY	
645	Circle	394-396	3.142	XY	
646	Polyline	397,398	18.300	X	
647	Polyline	398,18	9.750	X	
648	Polyline	399,400	18.300	X	
649	Polyline	400,17	9.750	X	
650	Polyline	399,397	4.000	Y	
651	Polyline	400,398	4.000	Y	
652	Polyline	401,402	18.300	X	
653	Polyline	402,24	9.750	X	
654	Polyline	403,404	18.300	X	
655	Polyline	404,23	9.750	X	
656	Polyline	403,401	4.000	Y	
657	Polyline	404,402	4.000	Y	
658	Polyline	405,406	18.300	X	
659	Polyline	406,32	9.750	X	

Project: CIE5060 Model: V26
Graduation Project

1.2 LINES

Line No.	Line Type	Nodes No.	Line Length L [m]		Comment
660	Polyline	407,408	18.300	X	
661	Polyline	408,31	9.750	X	
662	Polyline	407,405	4.000	Y	
663	Polyline	408,406	4.000	Y	
664	Polyline	409,410	18.300	X	
665	Polyline	410,40	9.750	X	
666	Polyline	411,412	18.300	X	
667	Polyline	412,39	9.750	X	
668	Polyline	411,409	4.000	Y	
669	Polyline	412,410	4.000	Y	
670	Polyline	413,414	18.300	X	
671	Polyline	414,48	9.750	X	
672	Polyline	415,416	18.300	X	
673	Polyline	416,47	9.750	X	
674	Polyline	415,413	4.000	Y	
675	Polyline	416,414	4.000	Y	
676	Polyline	417,418	18.300	X	
677	Polyline	418,56	9.750	X	
678	Polyline	419,420	18.300	X	
679	Polyline	420,55	9.750	X	
680	Polyline	419,417	4.000	Y	
681	Polyline	420,418	4.000	Y	
682	Polyline	421,422	18.300	X	
683	Polyline	422,8	9.750	X	
684	Polyline	423,424	18.300	X	
685	Polyline	424,11	9.750	X	
686	Polyline	424,422	4.000	Y	
687	Polyline	423,421	4.000	Y	
688	Polyline	280,439	9.750	X	
689	Polyline	176,437	9.750	X	
690	Polyline	437,438	18.301	X	
691	Polyline	438,274	9.750	X	
692	Polyline	439,440	18.301	X	
693	Polyline	440,182	9.750	X	
694	Polyline	440,437	2.000	Y	
695	Polyline	439,438	2.000	Y	
696	Circle	441-443	2.356	XY	
697	Circle	444-446	2.356	XY	
698	Circle	447-449	2.356	XY	
699	Circle	450-452	1.571	XY	
700	Circle	453-455	2.356	XY	
701	Circle	456-458	2.356	XY	
702	Circle	459-461	1.571	XY	

1.3 MATERIALS

Matl. No.	Modulus E [kN/cm²]	Modulus G [kN/cm²]	Poisson's Ratio ν [-]	Spec. Weight γ [kN/m³]	Therm. Coeff. α [1/°C]	Partial Factor γ_M [-]	Material Model
1	Concrete C30/37 | EN 1992-1-1:2004/AC:2010						
	3300.00	1375.00	0.200	25.00	1.00E-05	1.00	Isotropic Linear Elastic
2	Steel S 235 | EN 10025-2:2004-11						
	21000.00	8076.92	0.300	78.50	1.20E-05	1.00	Isotropic Linear Elastic
3	RF-LAMINATE Comp. 1						
	0.00	0.00	0.000	11.96	0.00E+00	1.00	Isotropic Linear Elastic
	Created by RF-LAMINATE module						
4	RF-LAMINATE Comp. 2						
	0.00	0.00	0.000	10.28	0.00E+00	1.00	Isotropic Linear Elastic
	Created by RF-LAMINATE module						
5	kern						
	32.90	26.10	-0.370	0.00E+00	0.00E+00	1.00	Isotropic Linear Elastic
6	RF-LAMINATE Comp. 3						
	0.00	0.00	0.000	9.40	0.00E+00	1.00	Isotropic Linear Elastic
	Created by RF-LAMINATE module						
7	RF-LAMINATE Comp. 4						
	0.00	0.00	0.000	9.40	0.00E+00	1.00	Isotropic Linear Elastic
	Created by RF-LAMINATE module						
8	RF-LAMINATE Comp. 5						
	0.00	0.00	0.000	11.96	0.00E+00	1.00	Isotropic Linear Elastic
	Created by RF-LAMINATE module						
9	RF-LAMINATE Comp. 6						
	0.00	0.00	0.000	10.28	0.00E+00	1.00	Isotropic Linear Elastic
	Created by RF-LAMINATE module						
10	RF-LAMINATE Comp. 7						
	0.00	0.00	0.000	10.28	0.00E+00	1.00	Isotropic Linear Elastic
	Created by RF-LAMINATE module						
11	RF-LAMINATE Comp. 8						
	0.00	0.00	0.000	10.28	0.00E+00	1.00	Isotropic Linear Elastic
	Created by RF-LAMINATE module						
12	RF-LAMINATE Comp. 9						
	0.00	0.00	0.000	9.40	0.00E+00	1.00	Isotropic Linear Elastic
	Created by RF-LAMINATE module						
13	RF-LAMINATE Comp. 10						
	0.00	0.00	0.000	9.40	0.00E+00	1.00	Isotropic Linear Elastic
	Created by RF-LAMINATE module						

Project: CIE5060 Model: V26
Graduation Project

1.4 SURFACES

Surface No.	Surface Type Geometry	Stiffness	Boundary Lines No.	Matl. No.	Thickness Type	d [mm]	Area A [m²]	Weight W [kg]
1	Quadrangle	Laminate	650,646,651,648	4	Constant	98.0	64.763	6523.92
2	Quadrangle	Laminate	651,647,23,649	11	Constant	98.0	38.293	3857.47
3	Quadrangle	Laminate	656,652,657,654	4	Constant	98.0	64.763	6523.92
4	Quadrangle	Laminate	657,653,33,655	11	Constant	98.0	38.293	3857.47
5	Quadrangle	Laminate	662,658,663,660	4	Constant	98.0	64.763	6523.92
6	Quadrangle	Laminate	663,659,43,661	11	Constant	98.0	38.293	3857.47
7	Plane	Laminate	19,14,684,685,22,201,202, 649,648,25	3	Constant	118.0	113.400	16009.40
8	Plane	Laminate	647,646,26,21,8,682,683, 190,189,24	3	Constant	118.0	113.400	16009.40
9	Quadrangle	Laminate	20,26,650,25	11	Constant	98.0	38.293	3857.47
10	Plane	Laminate	29,25,648,649,32,203,204, 655,654,35	3	Constant	118.0	113.400	16009.40
11	Plane	Laminate	653,652,36,31,26,646,647, 192,191,34	3	Constant	118.0	113.400	16009.40
12	Quadrangle	Laminate	30,36,656,35	11	Constant	98.0	38.293	3857.47
13	Plane	Laminate	39,35,654,655,42,205,206, 661,660,45	3	Constant	118.0	113.400	16009.40
14	Plane	Laminate	659,658,46,41,36,652,653, 194,193,44	3	Constant	118.0	113.400	16009.40
15	Quadrangle	Laminate	40,46,662,45	11	Constant	98.0	38.293	3857.47
16	Plane	Laminate	49,45,660,661,52,207,208, 667,666,55	3	Constant	118.0	113.400	16009.40
17	Plane	Laminate	665,664,56,51,46,658,659, 196,195,54	3	Constant	118.0	113.400	16009.40
18	Quadrangle	Laminate	50,56,668,55	11	Constant	98.0	38.293	3857.47
19	Plane	Laminate	59,55,666,667,62,185,186, 673,672,65	3	Constant	118.0	113.400	16009.40
20	Plane	Laminate	671,670,66,61,56,664,665, 198,197,64	3	Constant	118.0	113.400	16009.40
21	Quadrangle	Laminate	60,66,674,65	11	Constant	98.0	38.293	3857.47
22	Plane	Laminate	69,65,672,673,72,187,188, 679,678,75	3	Constant	118.0	113.400	16009.40
23	Plane	Laminate	677,676,76,71,66,670,671, 200,199,74	3	Constant	118.0	113.400	16009.40
24	Quadrangle	Laminate	70,76,680,75	11	Constant	98.0	39.000	3928.70
25	Quadrangle	Laminate	668,664,669,666	4	Constant	98.0	64.763	6523.92
26	Quadrangle	Laminate	669,665,53,667	11	Constant	98.0	38.293	3857.47
27	Quadrangle	Laminate	674,670,675,672	4	Constant	98.0	64.763	6523.92
28	Quadrangle	Laminate	675,671,63,673	11	Constant	98.0	38.293	3857.47
29	Quadrangle	Laminate	680,676,681,678	4	Constant	98.0	73.200	7373.88
30	Quadrangle	Laminate	681,677,73,679	11	Constant	98.0	39.000	3928.70
31	Quadrangle	Laminate	686,682,687,684	4	Constant	98.0	64.763	6523.92
32	Quadrangle	Laminate	687,8,9,14	11	Constant	98.0	38.293	3857.47
33	Quadrangle	Laminate	694,690,695,692	4	Constant	98.0	35.195	3545.38
34	Quadrangle	Laminate	695,691,167,688	11	Constant	98.0	19.374	1951.71
47	Plane	Laminate	23,92,89,91	9	Constant	98.0	6.600	664.86
48	Plane	Laminate	89,279,276,278	9	Constant	98.0	0.800	80.59
49	Plane	Laminate	20,260,253,259	9	Constant	98.0	6.600	664.86
50	Plane	Laminate	33,100,97,99	9	Constant	98.0	6.600	664.86
51	Plane	Laminate	97,285,282,284	9	Constant	98.0	0.800	80.59
52	Plane	Laminate	253,509,506,508	9	Constant	98.0	0.800	80.59
53	Plane	Laminate	43,108,105,107	9	Constant	98.0	6.600	664.86
54	Plane	Laminate	105,291,288,290	9	Constant	98.0	0.800	80.59
55	Plane	Laminate	30,268,264,267	9	Constant	98.0	6.600	664.86
56	Plane	Laminate	53,116,113,115	9	Constant	98.0	6.600	664.86
57	Plane	Laminate	113,297,294,296	9	Constant	98.0	0.800	80.59
58	Plane	Laminate	264,515,512,514	9	Constant	98.0	0.800	80.59
59	Plane	Laminate	63,124,121,123	9	Constant	98.0	6.600	664.86
60	Plane	Laminate	121,302,299,301	9	Constant	98.0	0.800	80.59
61	Plane	Laminate	40,338,273,337	9	Constant	98.0	6.600	664.86
62	Plane	Laminate	273,521,518,520	9	Constant	98.0	0.800	80.59
63	Plane	Laminate	50,344,341,343	9	Constant	98.0	6.600	664.86
64	Plane	Laminate	341,527,524,526	9	Constant	98.0	0.800	80.59
65	Plane	Laminate	60,349,346,348	9	Constant	98.0	6.600	664.86
66	Plane	Laminate	346,532,529,531	9	Constant	98.0	0.800	80.59
101	Plane	Laminate	73,132,129,131	9	Constant	98.0	6.600	664.86
102	Plane	Laminate	103,213,209,224	7	Constant	90.0	6.600	558.10
103	Plane	Laminate	109,226,210,225	7	Constant	90.0	6.600	558.10
104	Plane	Laminate	140,227,211,231	7	Constant	90.0	6.600	558.10
105	Plane	Laminate	139,228,212,233	7	Constant	90.0	6.600	558.10
106	Plane	Laminate	156,235,214,237	7	Constant	90.0	6.600	558.10
107	Plane	Laminate	155,236,215,238	7	Constant	90.0	6.600	558.10
108	Plane	Laminate	172,239,216,241	7	Constant	90.0	6.600	558.10
109	Plane	Laminate	171,240,217,242	7	Constant	90.0	6.600	558.10
110	Plane	Laminate	180,247,218,249	7	Constant	90.0	6.600	558.10
111	Plane	Laminate	179,248,219,250	7	Constant	90.0	6.600	558.10
112	Plane	Laminate	222,255,220,257	7	Constant	90.0	6.600	558.10
113	Plane	Laminate	223,256,221,258	7	Constant	90.0	6.600	558.10
114	Plane	Laminate	83,131,188,213	8	Constant	118.0	1.650	232.93
115	Plane	Laminate	74,224,130,132	8	Constant	118.0	1.650	232.93
116	Plane	Laminate	67,213,187,226	8	Constant	118.0	1.650	232.96
117	Plane	Laminate	199,225,85,224	8	Constant	118.0	1.650	232.96
118	Plane	Laminate	128,226,72,123	8	Constant	118.0	1.650	232.93
119	Plane	Laminate	200,124,94,225	8	Constant	118.0	1.650	232.93
120	Plane	Laminate	126,123,186,227	8	Constant	118.0	1.650	232.93
121	Plane	Laminate	64,231,122,124	8	Constant	118.0	1.650	232.93
122	Plane	Laminate	125,227,185,228	8	Constant	118.0	1.650	232.96
123	Plane	Laminate	197,233,127,231	8	Constant	118.0	1.650	232.96
124	Plane	Laminate	120,228,62,115	8	Constant	118.0	1.650	232.93
125	Plane	Laminate	198,116,138,233	8	Constant	118.0	1.650	232.93
126	Plane	Laminate	147,115,208,235	8	Constant	118.0	1.650	232.93

Project: CIE5060 Model: V26
Graduation Project

1.4 SURFACES

Surface No.	Surface Type Geometry	Stiffness	Boundary Lines No.	Matl. No.	Thickness Type	d [mm]	Area A [m²]	Weight W [kg]
127	Plane	Laminate	54,237,114,116	8	Constant	118.0	1.650	232.93
128	Plane	Laminate	146,235,207,236	8	Constant	118.0	1.650	232.96
129	Plane	Laminate	195,238,148,237	8	Constant	118.0	1.650	232.96
130	Plane	Laminate	112,236,52,107	8	Constant	118.0	1.650	232.93
131	Plane	Laminate	196,108,154,238	8	Constant	118.0	1.650	232.93
132	Plane	Laminate	163,107,206,239	8	Constant	118.0	1.650	232.93
133	Plane	Laminate	44,241,106,108	8	Constant	118.0	1.650	232.93
134	Plane	Laminate	162,239,205,240	8	Constant	118.0	1.650	232.96
135	Plane	Laminate	193,242,164,241	8	Constant	118.0	1.650	232.96
136	Plane	Laminate	104,240,42,99	8	Constant	118.0	1.650	232.93
137	Plane	Laminate	194,100,170,242	8	Constant	118.0	1.650	232.93
138	Plane	Laminate	176,99,204,247	8	Constant	118.0	1.650	232.93
139	Plane	Laminate	34,249,98,100	8	Constant	118.0	1.650	232.93
140	Plane	Laminate	175,247,203,248	8	Constant	118.0	1.650	232.96
141	Plane	Laminate	191,250,177,249	8	Constant	118.0	1.650	232.96
142	Plane	Laminate	96,248,32,91	8	Constant	118.0	1.650	232.93
143	Plane	Laminate	192,92,178,250	8	Constant	118.0	1.650	232.93
144	Plane	Laminate	182,91,202,255	8	Constant	118.0	1.650	232.94
145	Plane	Laminate	24,257,90,92	8	Constant	118.0	1.650	232.94
146	Plane	Laminate	181,255,201,256	8	Constant	118.0	1.650	232.94
147	Plane	Laminate	189,258,183,257	8	Constant	118.0	1.650	232.94
148	Plane	Laminate	88,256,22,80	8	Constant	118.0	1.650	232.94
149	Plane	Laminate	190,58,184,258	8	Constant	118.0	1.650	232.94
150	Plane	Laminate	129,310,307,309	9	Constant	98.0	0.800	80.59
151	Plane	Laminate	286,364,103,375	7	Constant	90.0	0.800	67.65
152	Plane	Laminate	292,377,109,376	7	Constant	90.0	0.800	67.65
153	Plane	Laminate	313,378,140,380	7	Constant	90.0	0.800	67.65
154	Plane	Laminate	312,379,139,381	7	Constant	90.0	0.800	67.65
155	Plane	Laminate	319,382,156,384	7	Constant	90.0	0.800	67.65
156	Plane	Laminate	318,383,155,385	7	Constant	90.0	0.800	67.65
157	Plane	Laminate	325,386,172,388	7	Constant	90.0	0.800	67.65
158	Plane	Laminate	324,387,171,389	7	Constant	90.0	0.800	67.65
159	Plane	Laminate	331,390,180,392	7	Constant	90.0	0.800	67.65
160	Plane	Laminate	330,391,179,393	7	Constant	90.0	0.800	67.65
161	Plane	Laminate	373,394,222,396	7	Constant	90.0	0.800	67.65
162	Plane	Laminate	374,395,223,397	7	Constant	90.0	0.800	67.65
163	Plane	Laminate	272,309,83,364	8	Constant	118.0	0.200	28.23
164	Plane	Laminate	130,375,308,310	8	Constant	118.0	0.200	28.23
165	Plane	Laminate	265,364,67,377	8	Constant	118.0	0.200	28.24
166	Plane	Laminate	85,376,274,375	8	Constant	118.0	0.200	28.24
167	Plane	Laminate	306,377,128,301	8	Constant	118.0	0.200	28.23
168	Plane	Laminate	94,302,280,376	8	Constant	118.0	0.200	28.23
169	Plane	Laminate	304,301,126,378	8	Constant	118.0	0.200	28.23
170	Plane	Laminate	122,380,300,302	8	Constant	118.0	0.200	28.23
171	Plane	Laminate	303,378,125,379	8	Constant	118.0	0.200	28.24
172	Plane	Laminate	127,381,305,380	8	Constant	118.0	0.200	28.24
173	Plane	Laminate	298,379,120,296	8	Constant	118.0	0.200	28.23
174	Plane	Laminate	138,297,311,381	8	Constant	118.0	0.200	28.23
175	Plane	Laminate	315,296,147,382	8	Constant	118.0	0.200	28.23
176	Plane	Laminate	114,384,295,297	8	Constant	118.0	0.200	28.23
177	Plane	Laminate	314,382,146,383	8	Constant	118.0	0.200	28.24
178	Plane	Laminate	148,385,316,384	8	Constant	118.0	0.200	28.24
179	Plane	Laminate	293,383,112,290	8	Constant	118.0	0.200	28.23
180	Plane	Laminate	154,291,317,385	8	Constant	118.0	0.200	28.23
181	Plane	Laminate	321,290,163,386	8	Constant	118.0	0.200	28.23
182	Plane	Laminate	106,388,289,291	8	Constant	118.0	0.200	28.23
183	Plane	Laminate	320,386,162,387	8	Constant	118.0	0.200	28.24
184	Plane	Laminate	164,389,322,388	8	Constant	118.0	0.200	28.24
185	Plane	Laminate	287,387,104,284	8	Constant	118.0	0.200	28.23
186	Plane	Laminate	170,285,323,389	8	Constant	118.0	0.200	28.23
187	Plane	Laminate	327,284,176,390	8	Constant	118.0	0.200	28.23
188	Plane	Laminate	98,392,283,285	8	Constant	118.0	0.200	28.23
189	Plane	Laminate	326,390,175,391	8	Constant	118.0	0.200	28.24
190	Plane	Laminate	177,393,328,392	8	Constant	118.0	0.200	28.24
191	Plane	Laminate	281,391,96,278	8	Constant	118.0	0.200	28.23
192	Plane	Laminate	178,279,329,393	8	Constant	118.0	0.200	28.23
193	Plane	Laminate	333,278,182,394	8	Constant	118.0	0.200	28.24
194	Plane	Laminate	90,396,277,279	8	Constant	118.0	0.200	28.24
195	Plane	Laminate	332,394,181,395	8	Constant	118.0	0.200	28.24
196	Plane	Laminate	183,397,334,396	8	Constant	118.0	0.200	28.24
197	Plane	Laminate	275,395,88,269	8	Constant	118.0	0.200	28.24
198	Plane	Laminate	184,261,335,397	8	Constant	118.0	0.200	28.24
199	Plane	Laminate	272,286,308,307	6	Constant	90.0	4.000	338.21
200	Plane	Laminate	265,292,274,286	6	Constant	90.0	4.001	338.31
201	Plane	Laminate	306,299,280,292	6	Constant	90.0	4.000	338.21
202	Plane	Laminate	304,313,300,299	6	Constant	90.0	4.000	338.21
203	Plane	Laminate	303,312,305,313	6	Constant	90.0	4.001	338.31
204	Plane	Laminate	298,294,311,312	6	Constant	90.0	4.000	338.21
205	Plane	Laminate	315,319,295,294	6	Constant	90.0	4.000	338.21
206	Plane	Laminate	314,318,316,319	6	Constant	90.0	4.001	338.31
207	Plane	Laminate	293,288,317,318	6	Constant	90.0	4.000	338.21
208	Plane	Laminate	321,325,289,288	6	Constant	90.0	4.000	338.21
209	Plane	Laminate	320,324,322,325	6	Constant	90.0	4.001	338.31
210	Plane	Laminate	287,282,323,324	6	Constant	90.0	4.000	338.21
211	Plane	Laminate	327,331,283,282	6	Constant	90.0	4.000	338.21
212	Plane	Laminate	326,330,328,331	6	Constant	90.0	4.001	338.31
213	Plane	Laminate	281,276,329,330	6	Constant	90.0	4.000	338.21
214	Plane	Laminate	333,373,277,276	6	Constant	90.0	4.000	338.24
215	Plane	Laminate	332,374,334,373	6	Constant	90.0	4.000	338.24
216	Plane	Laminate	275,427,335,374	6	Constant	90.0	4.000	338.24
217	Plane	Laminate	5,80,1,58	9	Constant	98.0	6.600	664.86
218	Plane	Laminate	427,269,5,261	9	Constant	98.0	0.800	80.59

Project: CIE5060 Model: V26
Graduation Project

1.4 SURFACES

Surface No.	Surface Type Geometry	Stiffness	Boundary Lines No.	Matl. No.	Thickness Type	d [mm]	Area A [m²]	Weight W [kg]
219	Plane	Laminate	1,3,37,6	6	Constant	90.0	3.500	295.96
220	Plane	Laminate	37,428,82,434	6	Constant	90.0	2.500	211.40
221	Plane	Laminate	82,429,234,435	6	Constant	90.0	1.500	126.84
222	Plane	Laminate	234,430,436	6	Constant	90.0	0.500	42.28
223	Plane	Laminate	16,18,37,38	7	Constant	90.0	4.950	418.57
224	Plane	Laminate	16,48,57,77	7	Constant	90.0	0.600	50.74
225	Plane	Laminate	78,81,82,84	9	Constant	98.0	3.300	332.43
226	Plane	Laminate	78,229,230,232	9	Constant	98.0	0.400	40.29
227	Plane	Laminate	234,243-245	7	Constant	90.0	1.650	139.52
228	Plane	Laminate	244,246,251,252	7	Constant	90.0	0.200	16.91
233	Plane	Laminate	427,442,57,12	6	Constant	90.0	3.500	295.96
234	Plane	Laminate	57,441,230,443	6	Constant	90.0	2.500	211.40
235	Plane	Laminate	230,440,251,444	6	Constant	90.0	1.500	126.84
236	Plane	Laminate	251,11,445	6	Constant	90.0	0.500	42.28
237	Plane	Laminate	433,80,3,38	8	Constant	118.0	1.650	232.94
238	Plane	Laminate	442,269,433,48	8	Constant	118.0	0.200	28.24
239	Plane	Laminate	432,38,428,84	8	Constant	118.0	1.650	232.94
240	Plane	Laminate	441,48,432,229	8	Constant	118.0	0.200	28.24
241	Plane	Laminate	431,84,429,245	8	Constant	118.0	1.650	232.94
242	Plane	Laminate	440,229,431,246	8	Constant	118.0	0.200	28.24
243	Plane	Laminate	4,245,430,28	8	Constant	118.0	1.650	232.94
244	Plane	Laminate	11,246,4,15	8	Constant	118.0	0.200	28.24
245	Plane	Laminate	6,18,7,58	8	Constant	118.0	2.333	329.43
246	Plane	Laminate	7,77,12,261	8	Constant	118.0	0.283	39.93
247	Plane	Laminate	434,81,437,18	8	Constant	118.0	2.333	329.43
248	Plane	Laminate	437,232,443,77	8	Constant	118.0	0.283	39.93
249	Plane	Laminate	435,243,438,81	8	Constant	118.0	2.333	329.43
250	Plane	Laminate	438,252,444,232	8	Constant	118.0	0.283	39.93
251	Plane	Laminate	436,28,439,243	8	Constant	118.0	2.333	329.43
252	Plane	Laminate	439,15,445,252	8	Constant	118.0	0.283	39.93
253	Plane	Laminate	70,357,354,356	9	Constant	98.0	6.600	664.86
254	Plane	Laminate	270,456,452,467	7	Constant	90.0	6.600	558.10
255	Plane	Laminate	339,469,453,468	7	Constant	90.0	6.600	558.10
256	Plane	Laminate	360,470,454,474	7	Constant	90.0	6.600	558.10
257	Plane	Laminate	359,471,455,476	7	Constant	90.0	6.600	558.10
258	Plane	Laminate	367,478,457,480	7	Constant	90.0	6.600	558.10
259	Plane	Laminate	366,479,458,481	7	Constant	90.0	6.600	558.10
260	Plane	Laminate	398,482,459,484	7	Constant	90.0	6.600	558.10
261	Plane	Laminate	372,483,460,485	7	Constant	90.0	6.600	558.10
262	Plane	Laminate	404,490,461,492	7	Constant	90.0	6.600	558.10
263	Plane	Laminate	403,491,462,493	7	Constant	90.0	6.600	558.10
264	Plane	Laminate	465,496,463,498	7	Constant	90.0	6.600	558.10
265	Plane	Laminate	466,497,464,499	7	Constant	90.0	6.600	558.10
266	Plane	Laminate	168,356,412,456	8	Constant	118.0	1.650	232.93
267	Plane	Laminate	159,467,355,357	8	Constant	118.0	1.650	232.93
268	Plane	Laminate	153,456,411,469	8	Constant	118.0	1.650	232.96
269	Plane	Laminate	423,468,173,467	8	Constant	118.0	1.650	232.96
270	Plane	Laminate	353,469,157,348	8	Constant	118.0	1.650	232.93
271	Plane	Laminate	424,349,262,468	8	Constant	118.0	1.650	232.93
272	Plane	Laminate	351,348,410,470	8	Constant	118.0	1.650	232.93
273	Plane	Laminate	152,474,347,349	8	Constant	118.0	1.650	232.93
274	Plane	Laminate	350,470,409,471	8	Constant	118.0	1.650	232.96
275	Plane	Laminate	421,476,352,474	8	Constant	118.0	1.650	232.96
276	Plane	Laminate	345,471,150,343	8	Constant	118.0	1.650	232.93
277	Plane	Laminate	422,344,358,476	8	Constant	118.0	1.650	232.93
278	Plane	Laminate	362,343,451,478	8	Constant	118.0	1.650	232.93
279	Plane	Laminate	144,480,342,344	8	Constant	118.0	1.650	232.93
280	Plane	Laminate	361,478,450,479	8	Constant	118.0	1.650	232.96
281	Plane	Laminate	419,481,363,480	8	Constant	118.0	1.650	232.96
282	Plane	Laminate	340,479,142,337	8	Constant	118.0	1.650	232.93
283	Plane	Laminate	420,338,365,481	8	Constant	118.0	1.650	232.93
284	Plane	Laminate	369,337,449,482	8	Constant	118.0	1.650	232.93
285	Plane	Laminate	137,484,336,338	8	Constant	118.0	1.650	232.93
286	Plane	Laminate	368,482,448,483	8	Constant	118.0	1.650	232.96
287	Plane	Laminate	417,485,370,484	8	Constant	118.0	1.650	232.96
288	Plane	Laminate	271,483,135,267	8	Constant	118.0	1.650	232.93
289	Plane	Laminate	418,268,371,485	8	Constant	118.0	1.650	232.93
290	Plane	Laminate	400,267,447,490	8	Constant	118.0	1.650	232.93
291	Plane	Laminate	119,492,266,268	8	Constant	118.0	1.650	232.93
292	Plane	Laminate	399,490,446,491	8	Constant	118.0	1.650	232.96
293	Plane	Laminate	415,493,401,492	8	Constant	118.0	1.650	232.96
294	Plane	Laminate	263,491,117,259	8	Constant	118.0	1.650	232.93
295	Plane	Laminate	416,260,402,493	8	Constant	118.0	1.650	232.93
296	Plane	Laminate	406,259,426,496	8	Constant	118.0	1.650	232.94
297	Plane	Laminate	110,498,254,260	8	Constant	118.0	1.650	232.94
298	Plane	Laminate	405,496,425,497	8	Constant	118.0	1.650	232.94
299	Plane	Laminate	413,499,407,498	8	Constant	118.0	1.650	232.94
300	Plane	Laminate	174,497,101,165	8	Constant	118.0	1.650	232.94
301	Plane	Laminate	414,149,408,499	8	Constant	118.0	1.650	232.94
302	Plane	Laminate	354,540,537,539	9	Constant	98.0	0.800	80.59
303	Plane	Laminate	516,566,270,569	7	Constant	90.0	0.800	67.65
304	Plane	Laminate	522,571,339,570	7	Constant	90.0	0.800	67.65
305	Plane	Laminate	543,572,360,574	7	Constant	90.0	0.800	67.65
306	Plane	Laminate	542,573,359,575	7	Constant	90.0	0.800	67.65
307	Plane	Laminate	549,576,367,578	7	Constant	90.0	0.800	67.65
308	Plane	Laminate	548,577,366,579	7	Constant	90.0	0.800	67.65
309	Plane	Laminate	555,580,398,582	7	Constant	90.0	0.800	67.65
310	Plane	Laminate	554,581,372,583	7	Constant	90.0	0.800	67.65
311	Plane	Laminate	561,584,404,586	7	Constant	90.0	0.800	67.65
312	Plane	Laminate	560,585,403,587	7	Constant	90.0	0.800	67.65
313	Plane	Laminate	567,588,465,590	7	Constant	90.0	0.800	67.65
314	Plane	Laminate	568,589,466,591	7	Constant	90.0	0.800	67.65

Project: CIE5060 Model: V26
Graduation Project

1.4 SURFACES

Surface No.	Surface Type Geometry	Stiffness	Boundary Lines No.	Matl. No.	Thickness Type	d [mm]	Area A [m²]	Weight W [kg]
315	Plane	Laminate	503,539,168,566	8	Constant	118.0	0.200	28.23
316	Plane	Laminate	355,569,538,540	8	Constant	118.0	0.200	28.23
317	Plane	Laminate	501,566,153,571	8	Constant	118.0	0.200	28.24
318	Plane	Laminate	173,570,504,569	8	Constant	118.0	0.200	28.24
319	Plane	Laminate	536,571,353,531	8	Constant	118.0	0.200	28.23
320	Plane	Laminate	262,532,510,570	8	Constant	118.0	0.200	28.23
321	Plane	Laminate	534,531,351,572	8	Constant	118.0	0.200	28.23
322	Plane	Laminate	347,574,530,532	8	Constant	118.0	0.200	28.23
323	Plane	Laminate	533,572,350,573	8	Constant	118.0	0.200	28.24
324	Plane	Laminate	352,575,535,574	8	Constant	118.0	0.200	28.24
325	Plane	Laminate	528,573,345,526	8	Constant	118.0	0.200	28.23
326	Plane	Laminate	358,527,541,575	8	Constant	118.0	0.200	28.23
327	Plane	Laminate	545,526,362,576	8	Constant	118.0	0.200	28.23
328	Plane	Laminate	342,578,525,527	8	Constant	118.0	0.200	28.23
329	Plane	Laminate	544,576,361,577	8	Constant	118.0	0.200	28.24
330	Plane	Laminate	363,579,546,578	8	Constant	118.0	0.200	28.24
331	Plane	Laminate	523,577,340,520	8	Constant	118.0	0.200	28.23
332	Plane	Laminate	365,521,547,579	8	Constant	118.0	0.200	28.23
333	Plane	Laminate	551,520,369,580	8	Constant	118.0	0.200	28.23
334	Plane	Laminate	336,582,519,521	8	Constant	118.0	0.200	28.23
335	Plane	Laminate	550,580,368,581	8	Constant	118.0	0.200	28.24
336	Plane	Laminate	370,583,552,582	8	Constant	118.0	0.200	28.24
337	Plane	Laminate	517,581,271,514	8	Constant	118.0	0.200	28.23
338	Plane	Laminate	371,515,553,583	8	Constant	118.0	0.200	28.23
339	Plane	Laminate	557,514,400,584	8	Constant	118.0	0.200	28.23
340	Plane	Laminate	266,586,513,515	8	Constant	118.0	0.200	28.23
341	Plane	Laminate	556,584,399,585	8	Constant	118.0	0.200	28.24
342	Plane	Laminate	401,587,558,586	8	Constant	118.0	0.200	28.24
343	Plane	Laminate	511,585,263,508	8	Constant	118.0	0.200	28.23
344	Plane	Laminate	402,509,559,587	8	Constant	118.0	0.200	28.23
345	Plane	Laminate	563,508,406,588	8	Constant	118.0	0.200	28.24
346	Plane	Laminate	254,590,507,509	8	Constant	118.0	0.200	28.24
347	Plane	Laminate	562,588,405,589	8	Constant	118.0	0.200	28.24
348	Plane	Laminate	407,591,564,590	8	Constant	118.0	0.200	28.24
349	Plane	Laminate	505,589,174,502	8	Constant	118.0	0.200	28.24
350	Plane	Laminate	408,500,565,591	8	Constant	118.0	0.200	28.24
351	Plane	Laminate	503,516,538,537	6	Constant	90.0	4.000	338.21
352	Plane	Laminate	501,522,504,516	6	Constant	90.0	4.001	338.31
353	Plane	Laminate	536,529,510,522	6	Constant	90.0	4.000	338.21
354	Plane	Laminate	534,543,530,529	6	Constant	90.0	4.000	338.21
355	Plane	Laminate	533,542,535,543	6	Constant	90.0	4.001	338.31
356	Plane	Laminate	528,524,541,542	6	Constant	90.0	4.000	338.21
357	Plane	Laminate	545,549,525,524	6	Constant	90.0	4.000	338.21
358	Plane	Laminate	544,548,546,549	6	Constant	90.0	4.001	338.31
359	Plane	Laminate	523,518,547,548	6	Constant	90.0	4.000	338.21
360	Plane	Laminate	551,555,519,518	6	Constant	90.0	4.000	338.21
361	Plane	Laminate	550,554,552,555	6	Constant	90.0	4.001	338.31
362	Plane	Laminate	517,512,553,554	6	Constant	90.0	4.000	338.21
363	Plane	Laminate	557,561,513,512	6	Constant	90.0	4.000	338.21
364	Plane	Laminate	556,560,558,561	6	Constant	90.0	4.001	338.31
365	Plane	Laminate	511,506,559,560	6	Constant	90.0	4.000	338.21
366	Plane	Laminate	563,567,507,506	6	Constant	90.0	4.000	338.24
367	Plane	Laminate	562,568,564,567	6	Constant	90.0	4.000	338.24
368	Plane	Laminate	505,592,565,568	6	Constant	90.0	4.000	338.24
369	Plane	Laminate	27,165,9,149	9	Constant	98.0	6.600	664.86
370	Plane	Laminate	592,502,27,500	9	Constant	98.0	0.800	80.59
371	Plane	Laminate	9,13,133,47	6	Constant	90.0	3.500	295.96
372	Plane	Laminate	133,593,167,599	6	Constant	90.0	2.500	211.40
373	Plane	Laminate	167,594,477,600	6	Constant	90.0	1.500	126.84
374	Plane	Laminate	477,595,601	6	Constant	90.0	0.500	42.28
375	Plane	Laminate	93,95,133,134	7	Constant	90.0	4.950	418.57
376	Plane	Laminate	93,141,145,160	7	Constant	90.0	0.600	50.74
377	Plane	Laminate	161,166,167,169	9	Constant	98.0	3.300	332.43
378	Plane	Laminate	161,472,473,475	9	Constant	98.0	0.400	40.29
379	Plane	Laminate	477,486-488	7	Constant	90.0	1.650	139.52
380	Plane	Laminate	487,489,494,495	7	Constant	90.0	0.200	16.91
385	Plane	Laminate	592,607,145,86	6	Constant	90.0	3.500	295.96
386	Plane	Laminate	145,606,473,608	6	Constant	90.0	2.500	211.40
387	Plane	Laminate	473,605,494,609	6	Constant	90.0	1.500	126.84
388	Plane	Laminate	494,79,610	6	Constant	90.0	0.500	42.28
389	Plane	Laminate	598,165,13,134	8	Constant	118.0	1.650	232.94
390	Plane	Laminate	607,502,598,141	8	Constant	118.0	0.200	28.24
391	Plane	Laminate	597,134,593,169	8	Constant	118.0	1.650	232.94
392	Plane	Laminate	606,141,597,472	8	Constant	118.0	0.200	28.24
393	Plane	Laminate	596,169,594,488	8	Constant	118.0	1.650	232.94
394	Plane	Laminate	605,472,596,489	8	Constant	118.0	0.200	28.24
395	Plane	Laminate	17,488,595,111	8	Constant	118.0	1.650	232.94
396	Plane	Laminate	79,489,17,87	8	Constant	118.0	0.200	28.24
397	Plane	Laminate	47,95,68,149	8	Constant	118.0	2.333	329.43
398	Plane	Laminate	68,160,86,500	8	Constant	118.0	0.283	39.93
399	Plane	Laminate	599,166,602,95	8	Constant	118.0	2.333	329.43
400	Plane	Laminate	602,475,608,160	8	Constant	118.0	0.283	39.93
401	Plane	Laminate	600,486,603,166	8	Constant	118.0	2.333	329.43
402	Plane	Laminate	603,495,609,475	8	Constant	118.0	0.283	39.93
403	Plane	Laminate	601,111,604,486	8	Constant	118.0	2.333	329.43
404	Plane	Laminate	604,87,610,495	8	Constant	118.0	0.283	39.93
406	Quadrangle	Laminate	1,683,686,685	11	Constant	98.0	38.293	3857.47
407	Quadrangle	Laminate	82,689,694,693	11	Constant	98.0	19.374	1951.71
408	Plane	Laminate	3,428,689-691,593,13,14,684, 685	3	Constant	118.0	75.600	10672.90
409	Plane	Laminate	2,430,429,689-691,594,595	3	Constant	118.0	75.600	10672.90
410	Plane	Laminate	6,434,693,692,688,599,47,8,	3	Constant	118.0	106.915	15093.80

Project: CIE5060 Model: V26
Graduation Project

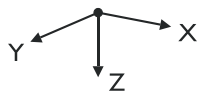
1.4 SURFACES

Surface No.	Surface Type Geometry	Stiffness	Boundary Lines No.	Matl. No.	Thickness Type	d [mm]	Area A [m²]	Weight W [kg]
411	Plane	Laminate	682,683 2,436,435,693,692,688,600, 601	3	Constant	118.0	106.915	15093.80

1.6 OPENINGS

Opening No.	Boundary Lines No.	In Surface No.	Area A [m²]	Comment
1	158	21	0.784	
2	151	27	1.764	
3	143	27	1.764	
4	10	27	1.764	
5	102	27	1.764	
6	118	27	1.764	
7	136	28	0.784	
8	617	18	0.784	
9	616	25	1.764	
10	615	25	1.764	
11	611	25	1.764	
12	612	25	1.764	
13	613	25	1.764	
14	614	26	0.784	
15	624	15	0.784	
16	623	5	1.764	
17	622	5	1.764	
18	618	5	1.764	
19	619	5	1.764	
20	620	5	1.764	
21	621	6	0.784	
22	631	12	0.784	
23	630	3	1.764	
24	629	3	1.764	
25	625	3	1.764	
26	626	3	1.764	
27	627	3	1.764	
28	628	4	0.784	
29	638	9	0.784	
30	637	1	1.764	
31	636	1	1.764	
32	632	1	1.764	
33	633	1	1.764	
34	634	1	1.764	
35	635	2	0.784	
36	645	32	0.784	
37	644	31	1.764	
38	643	31	1.764	
39	639	31	1.764	
40	640	31	1.764	
41	641	31	1.764	
42	642	406	0.784	
43	702	34	0.196	
44	701	33	0.441	
45	700	33	0.441	
46	696	33	0.441	
47	697	33	0.441	
48	698	33	0.441	
49	699	407	0.196	

1.7 NODAL SUPPORTS



Support No.	Nodes No.	Sequen.	Rotation [°] about X	about Y	about Z	Colum in Z	Support Conditions $u_{X'}$	$u_{Y'}$	$u_{Z'}$	$\varphi_{X'}$	$\varphi_{Y'}$	$\varphi_{Z'}$
1	255	XYZ	0.00	0.00	0.00	☐	☒	☐	☐	☐	☐	☐

1.8 LINE SUPPORTS

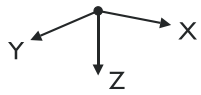
Support No.	Lines No.	Reference System	Rotation β [°]	Wall in Z	Support Conditions u_X	u_Y	u_Z	φ_X	φ_Y	φ_Z
3	2,15,28,87,111	Global		☐	☐	☐	Spring	☐	☐	☐

1.8.2 LINE SUPPORTS - SPRINGS

Support No.	Lines No.	Translation Spring [kN/m²] $C_{u,X'}$	$C_{u,Y'}$	$C_{u,Z'}$	Rotation Spring [kNm/rad/m] $C_{\varphi,X'}$	$C_{\varphi,Y'}$	$C_{\varphi,Z'}$
3	2,15,28,87,111	-	-	1000000.000	-	-	-

Project: CIE5060 Model: V26
Graduation Project

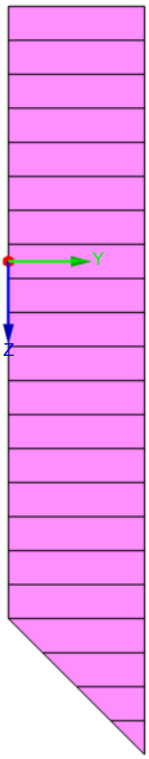
1.9 SURFACE SUPPORTS

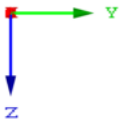


Found. No.	On Surfaces No.	Spring Constants RF-SOILIN	Translation Support or Spring [kN/m³] u_x	u_y	u_z	Shear Spring [kN/m] v_{xz}	v_{yz}
2	163,165,167,169, 171,173,175,177, 179,181,183,185, 187,189,191,193, 195,197,238,240, 242,244,315,317, 319,321,323,325, 327,329,331,333, 335,337,339,341, 343,345,347,349, 390,392,394,396	-	☐	☐	1000000.000	☐	☐

MODEL, IN X-DIRECTION

In X-direction





4.447 m

Project: CIE5060 Model: V26
Graduation Project

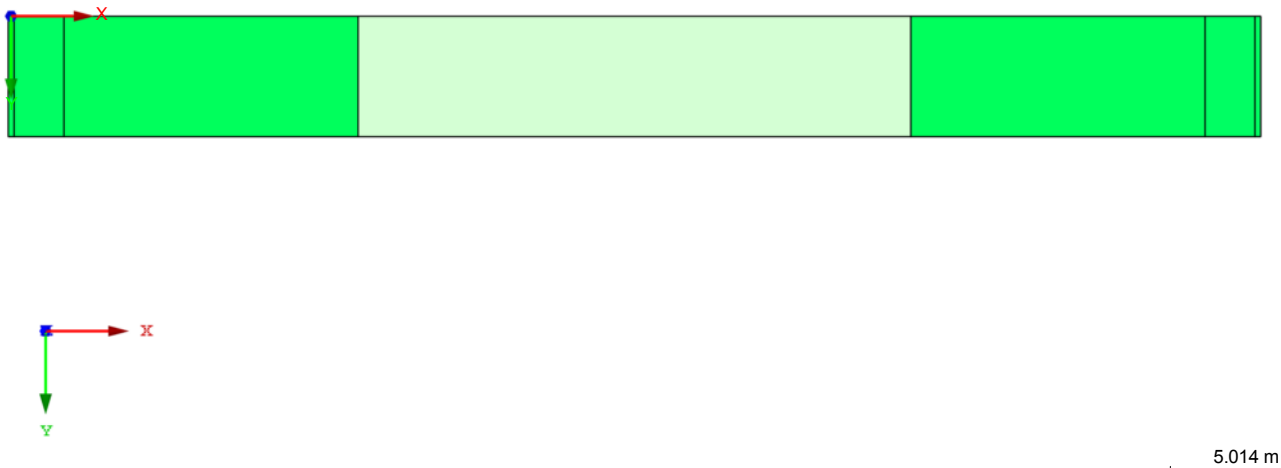
MODEL, IN Y-DIRECTION

In Y-direction



MODEL, IN Z-DIRECTION

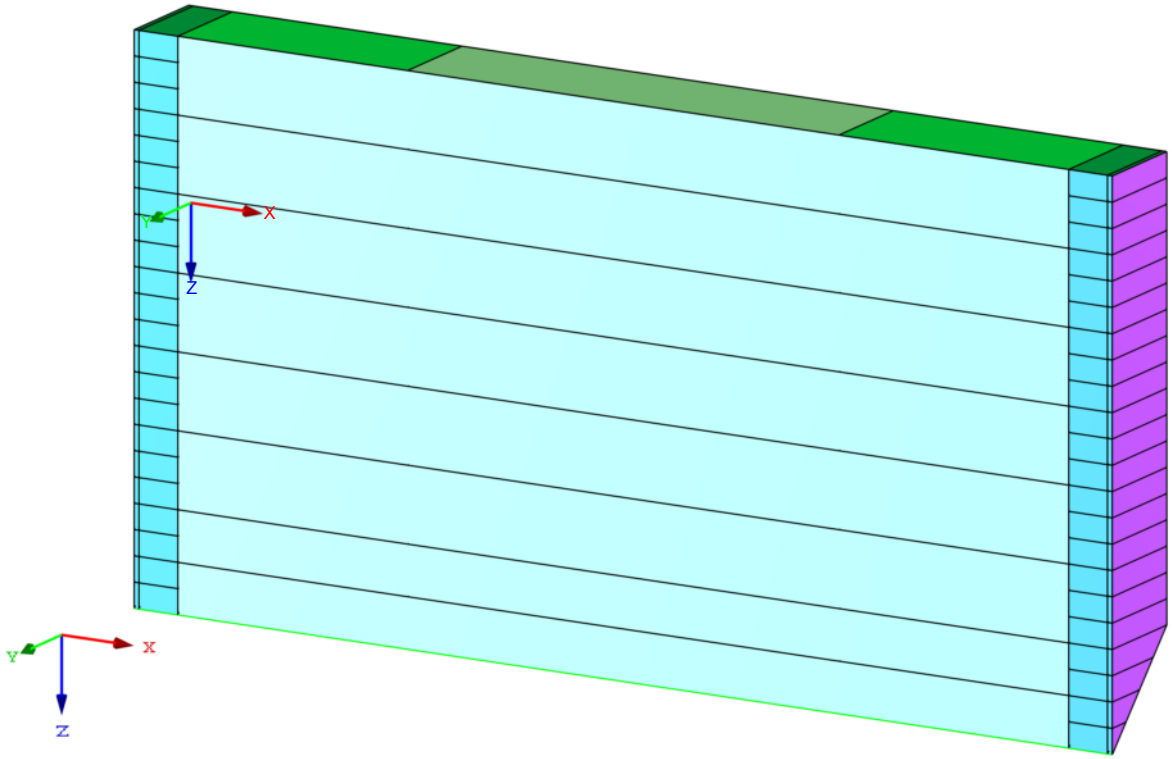
In Z-direction



Project: CIE5060 Model: V26
Graduation Project

MODEL, ISOMETRIC

Isometric



2.1 LOAD CASES

Load Case	Load Case Description	No Standard Action Category	Self-Weight - Factor in Direction			
			Active	X	Y	Z
LC1	Water pressure difference (positive drop)	Imposed	☐			
LC2	Wave pressure (positive drop, wave crest)	Imposed	☐			
LC3	Self weight	Permanent	☒	0.000	0.000	1.000
LC4	Water pressure difference (negative drop)	Imposed	☐			
LC5	Wave pressure (negative drop, wave trough)	Imposed	☐			
LC6	Ice	Snow / ice	☐			
LC7	Collision	Accidental	☐			
LC8	Water impact	Imposed	☐			

2.1.1 LOAD CASES - CALCULATION PARAMETERS

Load Case	Load Case Description	Calculation parameters		
LC1	Water pressure difference (positive drop)	Method of analysis	: ◉	Geometrically linear static analysis
		Method for solving system of nonlinear algebraic equations	: ◉	Newton-Raphson
			: ☐	Activate extra options
LC2	Wave pressure (positive drop, wave crest)	Method of analysis	: ◉	Geometrically linear static analysis
		Method for solving system of nonlinear algebraic equations	: ◉	Newton-Raphson
			: ☐	Activate extra options
LC3	Self weight	Method of analysis	: ◉	Geometrically linear static analysis
		Method for solving system of nonlinear algebraic equations	: ◉	Newton-Raphson
			: ☐	Activate extra options
LC4	Water pressure difference (negative drop)	Method of analysis	: ◉	Geometrically linear static analysis
		Method for solving system of nonlinear algebraic equations	: ◉	Newton-Raphson
			: ☐	Activate extra options
LC5	Wave pressure (negative drop, wave trough)	Method of analysis	: ◉	Geometrically linear static analysis
		Method for solving system of nonlinear algebraic equations	: ◉	Newton-Raphson
			: ☐	Activate extra options

Project: CIE5060 Model: V26
Graduation Project

2.1.1 LOAD CASES - CALCULATION PARAMETERS

Load Case	Load Case Description	Calculation parameters
LC6	Ice	Method of analysis : ⊙ Geometrically linear static analysis Method for solving system of nonlinear algebraic equations : ⊙ Newton-Raphson : ☐ Activate extra options
LC7	Collision	Method of analysis : ⊙ Geometrically linear static analysis Method for solving system of nonlinear algebraic equations : ⊙ Newton-Raphson : ☐ Activate extra options
LC8	Water impact	Method of analysis : ⊙ Geometrically linear static analysis Method for solving system of nonlinear algebraic equations : ⊙ Newton-Raphson : ☐ Activate extra options

2.5 LOAD COMBINATIONS

Load Combin.	DS	Load Combination Description	No.	Factor	Load Case	
CO1	ULS	Positive drop ULS	1	1.25	LC1	Water pressure difference (positive drop)
			2	1.65	LC2	Wave pressure (positive drop, wave crest)
			3	1.25	LC3	Self weight
CO2	SLS	Positive drop SLS	1	1.00	LC1	Water pressure difference (positive drop)
			2	1.00	LC2	Wave pressure (positive drop, wave crest)
			3	1.00	LC3	Self weight
CO3	ULS	Negative drop ULS	1	1.65	LC5	Wave pressure (negative drop, wave trough)
			2	1.25	LC4	Water pressure difference (negative drop)
			3	1.25	LC3	Self weight
CO4	SLS	Negative drop SLS	1	1.00	LC3	Self weight
			2	1.00	LC5	Wave pressure (negative drop, wave trough)
			3	1.00	LC4	Water pressure difference (negative drop)
CO5	ACC	Ice	1	1.00	LC6	Ice
			2	1.00	LC3	Self weight
CO6	ACC	Collision	1	1.00	LC7	Collision
			2	1.00	LC3	Self weight
CO7	ULS	Water impact	1	1.65	LC8	Water impact
			2	1.25	LC3	Self weight

2.5.2 LOAD COMBINATIONS - CALCULATION PARAMETERS

Load Combin.	Description	Calculation parameters
CO1	Positive drop ULS	Method of analysis : ⊙ Second order analysis (P-Delta) Method for solving system of nonlinear algebraic equations : ⊙ Picard Options : ☒ Consider favorable effects due to tension : ☒ Refer internal forces to deformed system for: ☒ Normal forces N ☒ Shear forces V_y and V_z ☒ Moments M_y, M_z and M_T
CO2	Positive drop SLS	Method of analysis : ⊙ Second order analysis (P-Delta) Method for solving system of nonlinear algebraic equations : ⊙ Picard Options : ☒ Consider favorable effects due to tension : ☒ Refer internal forces to deformed system for: ☒ Normal forces N ☒ Shear forces V_y and V_z ☒ Moments M_y, M_z and M_T : ☒ Divide stiffness (E,G) by partial factor γ_M from Table 1.3
CO3	Negative drop ULS	Method of analysis : ⊙ Second order analysis (P-Delta) Method for solving system of nonlinear algebraic equations : ⊙ Picard Options : ☒ Consider favorable effects due to tension : ☒ Refer internal forces to deformed system for: ☒ Normal forces N ☒ Shear forces V_y and V_z ☒ Moments M_y, M_z and M_T
CO4	Negative drop SLS	Method of analysis : ⊙ Second order analysis (P-Delta) Method for solving system of nonlinear algebraic equations : ⊙ Picard Options : ☒ Consider favorable effects due to tension : ☒ Refer internal forces to deformed system for: ☒ Normal forces N ☒ Shear forces V_y and V_z ☒ Moments M_y, M_z and M_T : ☒ Divide stiffness (E,G) by partial factor γ_M from Table 1.3
CO5	Ice	Method of analysis : ⊙ Second order analysis (P-Delta) Method for solving system of nonlinear algebraic equations : ⊙ Picard Options : ☒ Consider favorable effects due to tension : ☒ Refer internal forces to deformed system for: ☒ Normal forces N ☒ Shear forces V_y and V_z

Project: CIE5060 Model: V26
Graduation Project

2.5.2 LOAD COMBINATIONS - CALCULATION PARAMETERS

Load Combin.	Description	Calculation parameters		
				☒ Moments M_y, M_z and M_T
CO6	Collision	Method of analysis	: ⊙	Second order analysis (P-Delta)
		Method for solving system of nonlinear algebraic equations	: ⊙	Picard
		Options	: ☒	Consider favorable effects due to tension
			: ☒	Refer internal forces to deformed system for:
				☒ Normal forces N
				☒ Shear forces V_y and V_z
				☒ Moments M_y, M_z and M_T
CO7	Water impact	Method of analysis	: ⊙	Second order analysis (P-Delta)
		Method for solving system of nonlinear algebraic equations	: ⊙	Picard
		Options	: ☒	Consider favorable effects due to tension
			: ☒	Refer internal forces to deformed system for:
				☒ Normal forces N
				☒ Shear forces V_y and V_z
				☒ Moments M_y, M_z and M_T

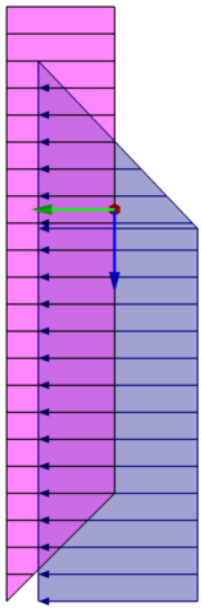
3.8 FREE RECTANGULAR LOADS

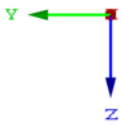
LC1: Water pressure difference (positive drop)

No.	On Surfaces No.	Project.	Load Distribution	Load Direction	Magnitude Symbol	Magnitude Value	Magnitude Unit	Load Position X [m]	Load Position Y [m]	Load Position Z [m]
1	7,10,13,16,19,22, 114,116,118,120, 122,124,126,128, 130,132,134,136, 138,140,142,144, 146,148,163,165, 167,169,171,173, 175,177,179,181, 183,185,187,189, 191,193,195,197, 237-244,266,268, 270,272,274,276, 278,280,282,284, 286,288,290,292, 294,296,298,300, 315,317,319,321, 323,325,327,329, 331,333,335,337, 339,341,343,345, 347,349,389-396, 408,409	XZ	Linear Z	z	p_1	0.000	kN/m²	0.000		-5.500
					p_2	63.000	kN/m²	41.300		0.700
2	7,10,13,16,19,22, 114,116,118,120, 122,124,126,128, 130,132,134,136, 138,140,142,144, 146,148,163,165, 167,169,171,173, 175,177,179,181, 183,185,187,189, 191,193,195,197, 237-244,266,268, 270,272,274,276, 278,280,282,284, 286,288,290,292, 294,296,298,300, 315,317,319,321, 323,325,327,329, 331,333,335,337, 339,341,343,345, 347,349,389-396, 408,409	XZ	Uniform	z	p	63.000	kN/m²	0.000		0.700
								41.300		14.500

LC1: WATER PRESSURE DIFFERENCE (POSITIVE DROP), AGAINST X-DIRECTION

LC1: Water pressure difference (positive drop) Against X-direction





5.604 m

3.8 FREE RECTANGULAR LOADS

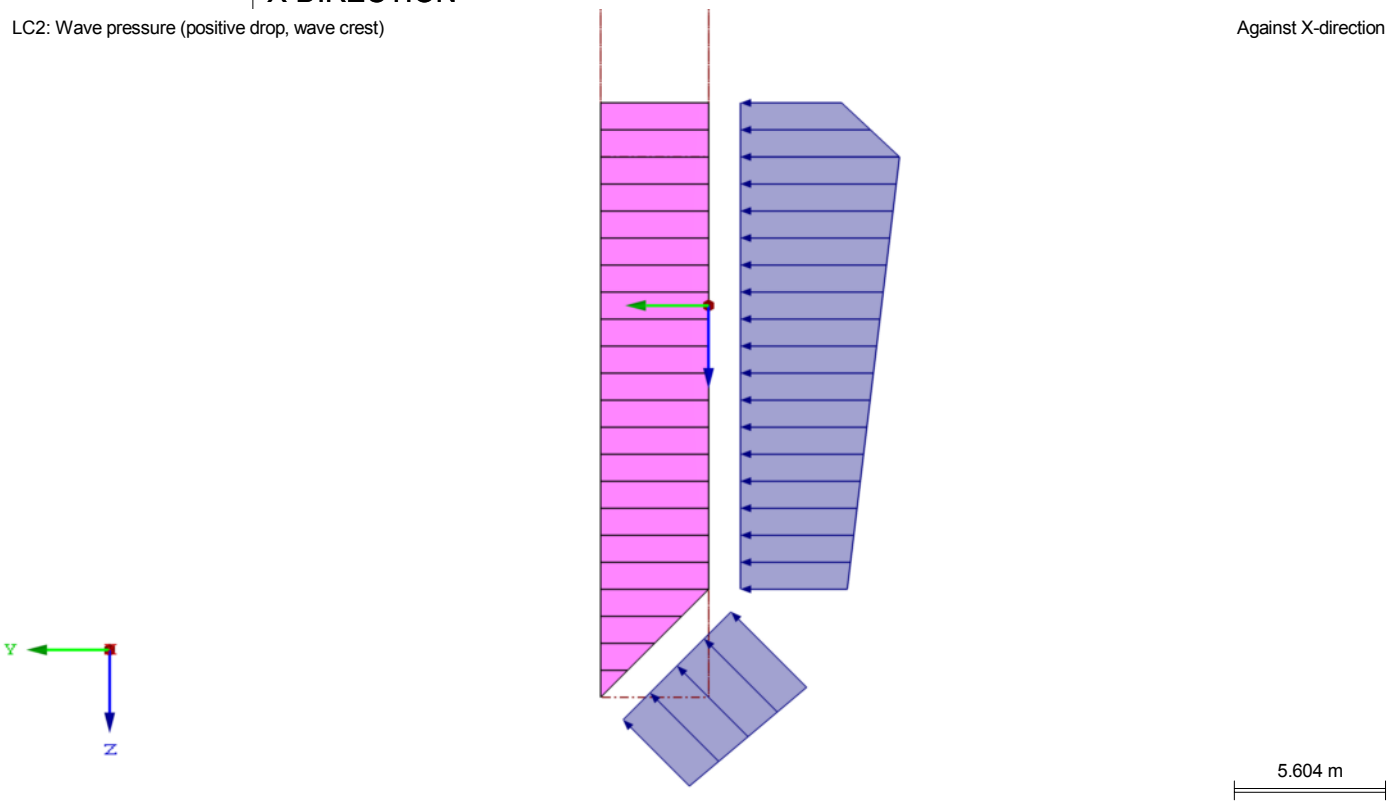
LC2: Wave pressure (positive drop, wave crest)

No.	On Surfaces No.	Project.	Load Distribution	Load Direction	Magnitude Symbol	Magnitude Value	Magnitude Unit	Load Position X [m]	Load Position Y [m]	Load Position Z [m]
1	8,11,14,17,20,23, 115,117,119,121, 123,125,127,129, 131,133,135,137, 139,141,143,145, 147,149,164,166, 168,170,172,174, 176,178,180,182, 184,186,188,190, 192,194,196,198, 245-252,267,269, 271,273,275,277, 279,281,283,285, 287,289,291,293, 295,297,299,301, 316,318,320,322, 324,326,328,330, 332,334,336,338, 340,342,344,346, 348,350,397-404, 410,411	XZ	Linear Z	z	p_1	0.000	kN/m²	0.000		-11.000
					p_2	56.000	kN/m²	41.300		-5.500
2	8,11,14,17,20,23, 115,117,119,121, 123,125,127,129, 131,133,135,137, 139,141,143,145, 147,149,164,166, 168,170,172,174, 176,178,180,182, 184,186,188,190, 192,194,196,198, 245-252,267,269, 271,273,275,277, 279,281,283,285, 287,289,291,293, 295,297,299,301, 316,318,320,322, 324,326,328,330, 332,334,336,338, 340,342,344,346, 348,350,397-404, 410,411	XZ	Linear Z	z	p_1	56.000	kN/m²	0.000		-5.500
					p_2	33.000	kN/m²	41.300		14.500

LC2: WAVE PRESSURE (POSITIVE DROP, WAVE CREST), AGAINST X-DIRECTION

LC2: Wave pressure (positive drop, wave crest)

Against X-direction



3.8 FREE RECTANGULAR LOADS

LC4: Water pressure difference (negative drop)

No.	On Surfaces No.	Project.	Load Distribution	Load Direction	Magnitude Symbol	Magnitude Value	Magnitude Unit	Load Position X [m]	Load Position Y [m]	Load Position Z [m]
1	7,10,13,16,19,22, 114,116,118,120, 122,124,126,128, 130,132,134,136, 138,140,142,144, 146,148,163,165, 167,169,171,173, 175,177,179,181, 183,185,187,189, 191,193,195,197, 237-244,266,268, 270,272,274,276, 278,280,282,284, 286,288,290,292, 294,296,298,300, 315,317,319,321, 323,325,327,329, 331,333,335,337, 339,341,343,345, 347,349,389-396, 408,409	XZ	Linear Z	z	p_1	0.000	kN/m²	0.000		-5.500
					p_2	32.000	kN/m²	41.300		-2.400
2	7,10,13,16,19,22, 114,116,118,120, 122,124,126,128, 130,132,134,136, 138,140,142,144, 146,148,163,165, 167,169,171,173, 175,177,179,181, 183,185,187,189, 191,193,195,197, 237-244,266,268, 270,272,274,276, 278,280,282,284, 286,288,290,292, 294,296,298,300, 315,317,319,321, 323,325,327,329, 331,333,335,337, 339,341,343,345, 347,349,389-396, 408,409	XZ	Uniform	z	p	32.000	kN/m²	0.000		-2.400
								41.300		14.500
3	8,11,14,17,20,23,	XZ	Linear Z	z	p_1	0.000	kN/m²	0.000		-5.500

Project: CIE5060 Model: V26
Graduation Project

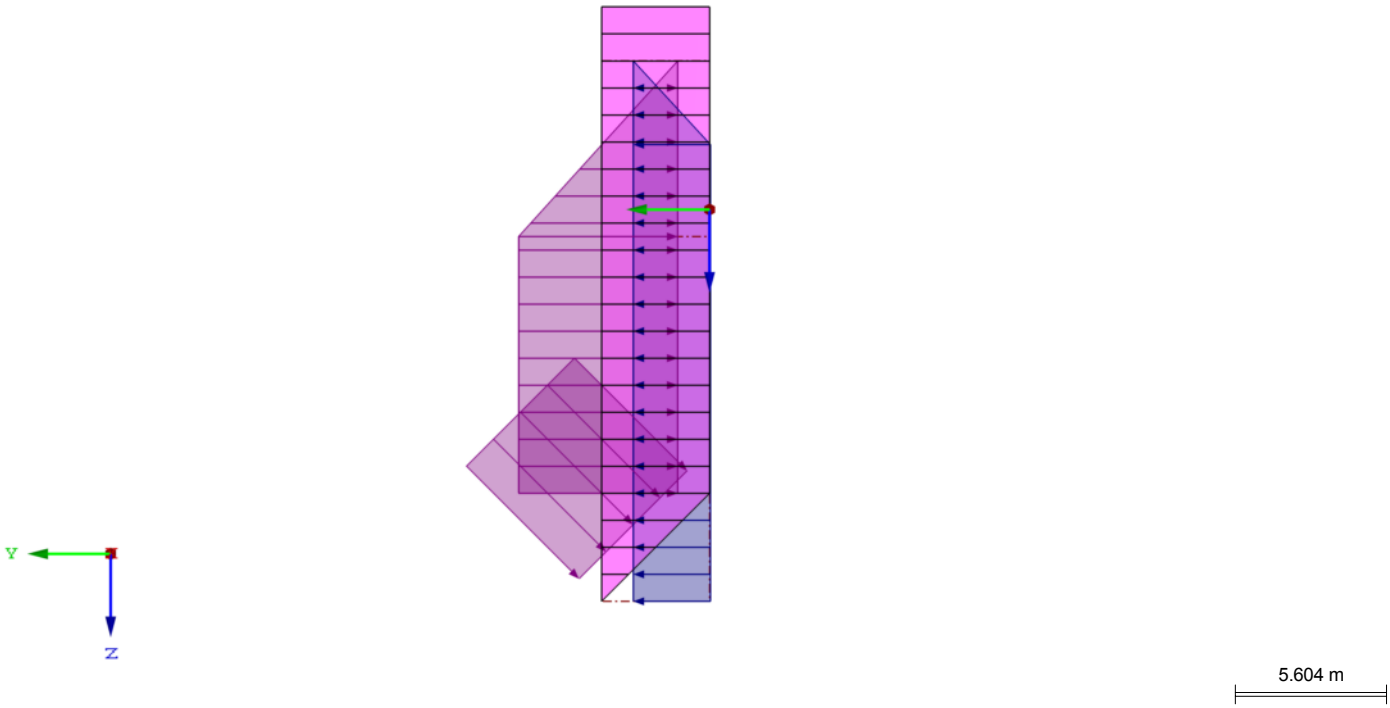
3.8 FREE RECTANGULAR LOADS

LC4: Water pressure difference (negative drop)

No.	On Surfaces No.	Project.	Load Distribution	Load Direction	Magnitude Symbol	Magnitude Value	Magnitude Unit	Load Position X [m]	Load Position Y [m]	Load Position Z [m]
	115,117,119,121, 123,125,127,129, 131,133,135,137, 139,141,143,145, 147,149,164,166, 168,170,172,174, 176,178,180,182, 184,186,188,190, 192,194,196,198, 245-252,267,269, 271,273,275,277, 279,281,283,285, 287,289,291,293, 295,297,299,301, 316,318,320,322, 324,326,328,330, 332,334,336,338, 340,342,344,346, 348,350,397-404, 410,411									
					p_2	-66.000	kN/m²	41.300		1.000
4	8,11,14,17,20,23, 115,117,119,121, 123,125,127,129, 131,133,135,137, 139,141,143,145, 147,149,164,166, 168,170,172,174, 176,178,180,182, 184,186,188,190, 192,194,196,198, 245-252,267,269, 271,273,275,277, 279,281,283,285, 287,289,291,293, 295,297,299,301, 316,318,320,322, 324,326,328,330, 332,334,336,338, 340,342,344,346, 348,350,397-404, 410,411	XZ	Uniform	z	p	-66.000	kN/m²	0.000		1.000
								41.300		14.500

LC4: WATER PRESSURE DIFFERENCE (NEGATIVE DROP), AGAINST X-DIRECTION

LC4: Water pressure difference (negative drop) Against X-direction



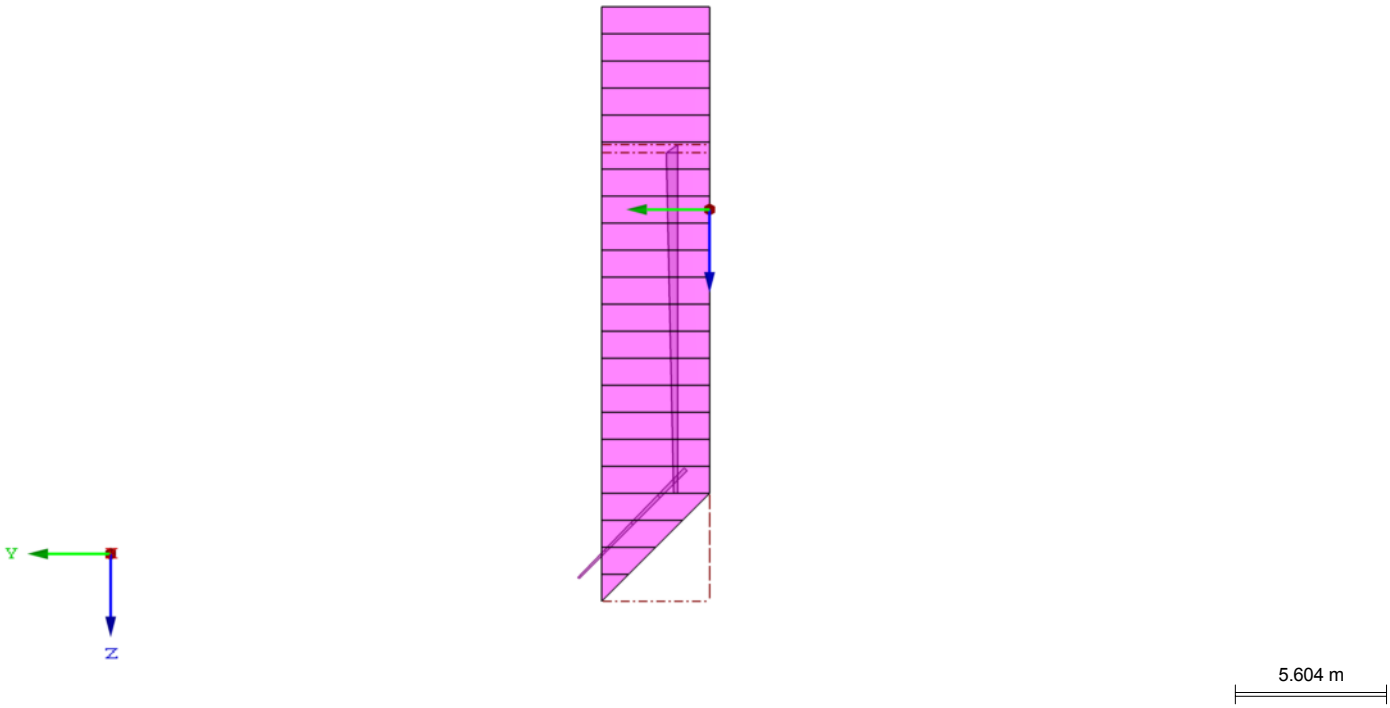
3.8 FREE RECTANGULAR LOADS

LC5: Wave pressure (negative drop, wave trough)

No.	On Surfaces No.	Project.	Load Distribution	Load Direction	Magnitude Symbol	Magnitude Value	Magnitude Unit	Load Position X [m]	Load Position Y [m]	Load Position Z [m]
1	8,11,14,17,20,23, 115,117,119,121, 123,125,127,129, 131,133,135,137, 139,141,143,145, 147,149,164,166, 168,170,172,174, 176,178,180,182, 184,186,188,190, 192,194,196,198, 245-252,267,269, 271,273,275,277, 279,281,283,285, 287,289,291,293, 295,297,299,301, 316,318,320,322, 324,326,328,330, 332,334,336,338, 340,342,344,346, 348,350,397-404, 410,411	XZ	Linear Z	z	p_1	0.000	kN/m²	0.000		-2.400
					p_2	-3.200	kN/m²	41.300		-2.100
2	8,11,14,17,20,23, 115,117,119,121, 123,125,127,129, 131,133,135,137, 139,141,143,145, 147,149,164,166, 168,170,172,174, 176,178,180,182, 184,186,188,190, 192,194,196,198, 245-252,267,269, 271,273,275,277, 279,281,283,285, 287,289,291,293, 295,297,299,301, 316,318,320,322, 324,326,328,330, 332,334,336,338, 340,342,344,346, 348,350,397-404, 410,411	XZ	Linear Z	z	p_1	-3.200	kN/m²	0.000		-2.100
					p_2	-0.500	kN/m²	41.300		14.500

LC5: WAVE PRESSURE (NEGATIVE DROP, WAVE TROUGH), AGAINST X-DIRECTION

LC5: Wave pressure (negative drop, wave trough) Against X-direction



3.8 FREE RECTANGULAR LOADS

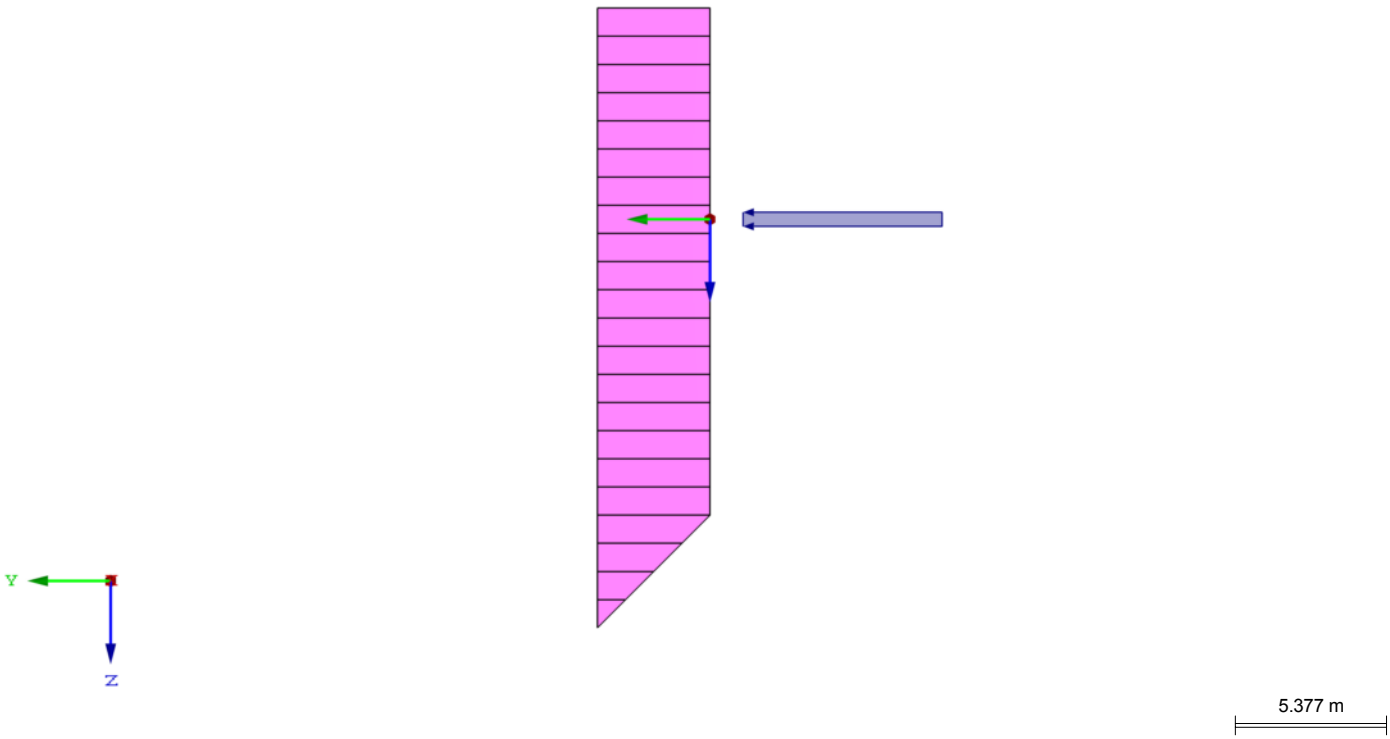
LC6: Ice

No.	On Surfaces No.	Project.	Load Distribution	Load Direction	Magnitude Symbol	Magnitude Value	Magnitude Unit	Load Position X [m]	Load Position Y [m]	Load Position Z [m]
1	8,11,14,17,20,23, 115,117,119,121, 123,125,127,129, 131,133,135,137, 139,141,143,145, 147,149,164,166, 168,170,172,174, 176,178,180,182, 184,186,188,190, 192,194,196,198, 267,269,271,273, 275,277,279,281, 283,285,287,289, 291,293,295,297, 299,301,316,318, 320,322,324,326, 328,330,332,334, 336,338,340,342, 344,346,348,350	XZ	Uniform	YL	p	457.000	kN/m²	3.150		0.250
								38.150		-0.250

LC6: ICE, AGAINST X-DIRECTION

LC6: Ice

Against X-direction



3.8 FREE RECTANGULAR LOADS

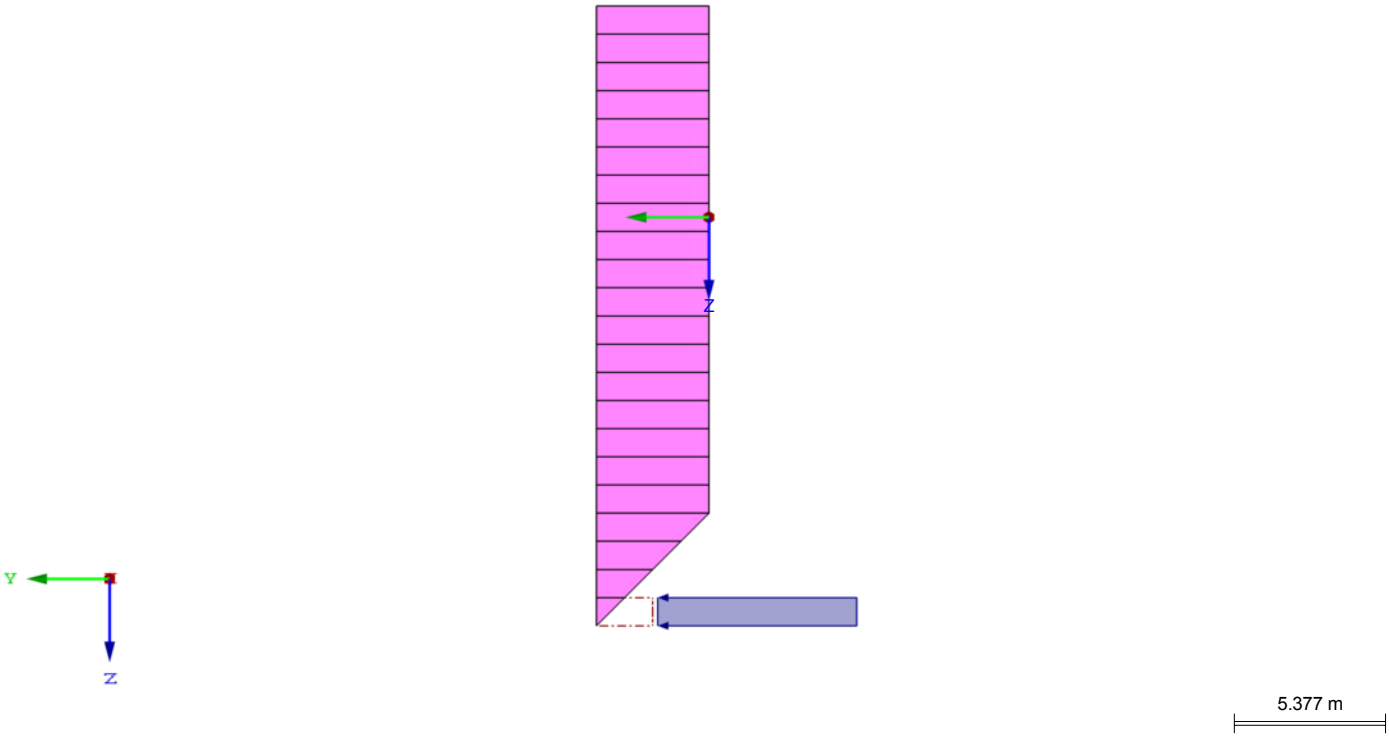
LC7: Collision

No.	On Surfaces No.	Project.	Load Distribution	Load Direction	Magnitude Symbol	Magnitude Value	Magnitude Unit	Load Position X [m]	Load Position Y [m]	Load Position Z [m]
1	411	XZ	Uniform	YP	p	250.000	kN/m²	19.650		14.500
								21.650		13.500

LC7: COLLISION, AGAINST X-DIRECTION

LC7: Collision

Against X-direction



3.8 FREE RECTANGULAR LOADS

LC8: Water impact

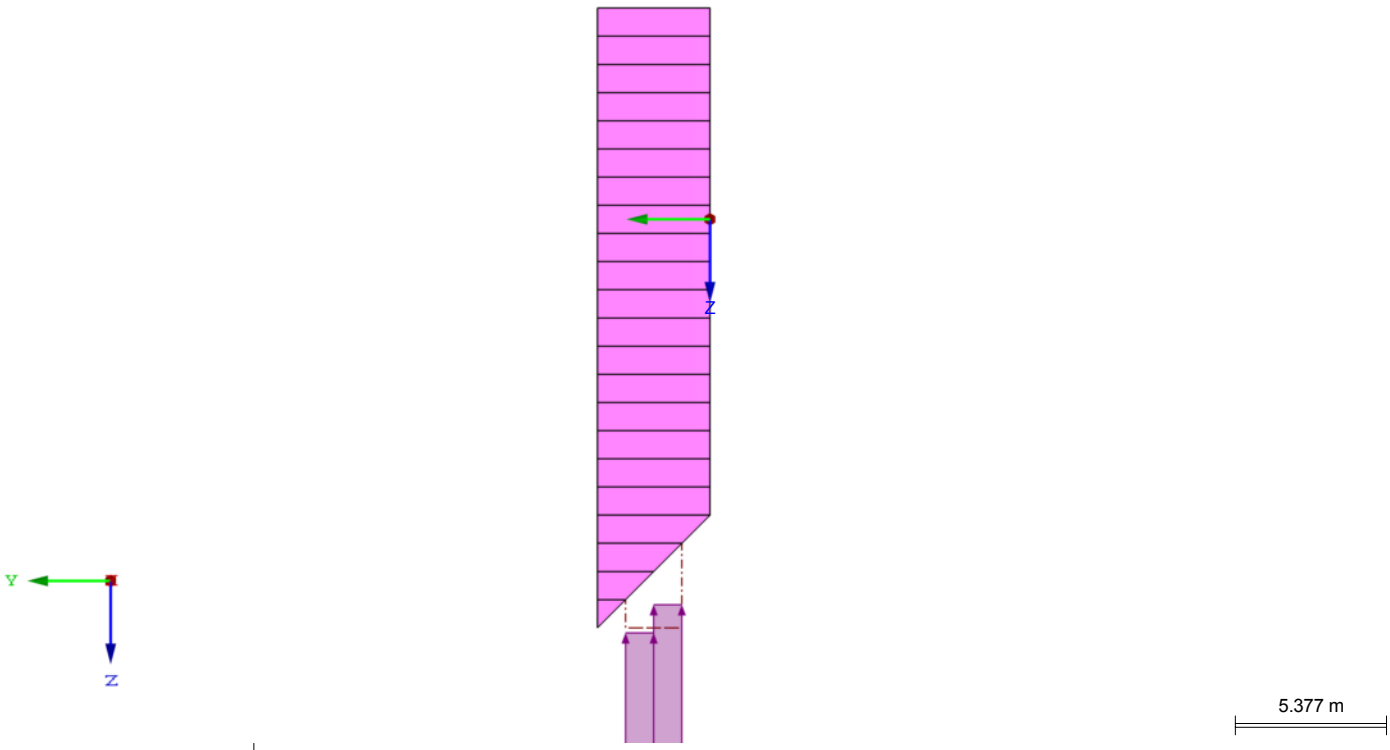
No.	On Surfaces No.	Project.	Load Distribution	Load Direction	Magnitude Symbol	Magnitude Value	Magnitude Unit	Load Position X [m]	Load Position Y [m]	Load Position Z [m]
1	410,411	XY	Uniform	ZP	p	-440.000	kN/m²	19.650	1.000	
								21.650	3.000	

Project: CIE5060 Model: V26
Graduation Project

LC8: WATER IMPACT, AGAINST X-DIRECTION

LC8: Water impact

Against X-direction



4.0 RESULTS - SUMMARY

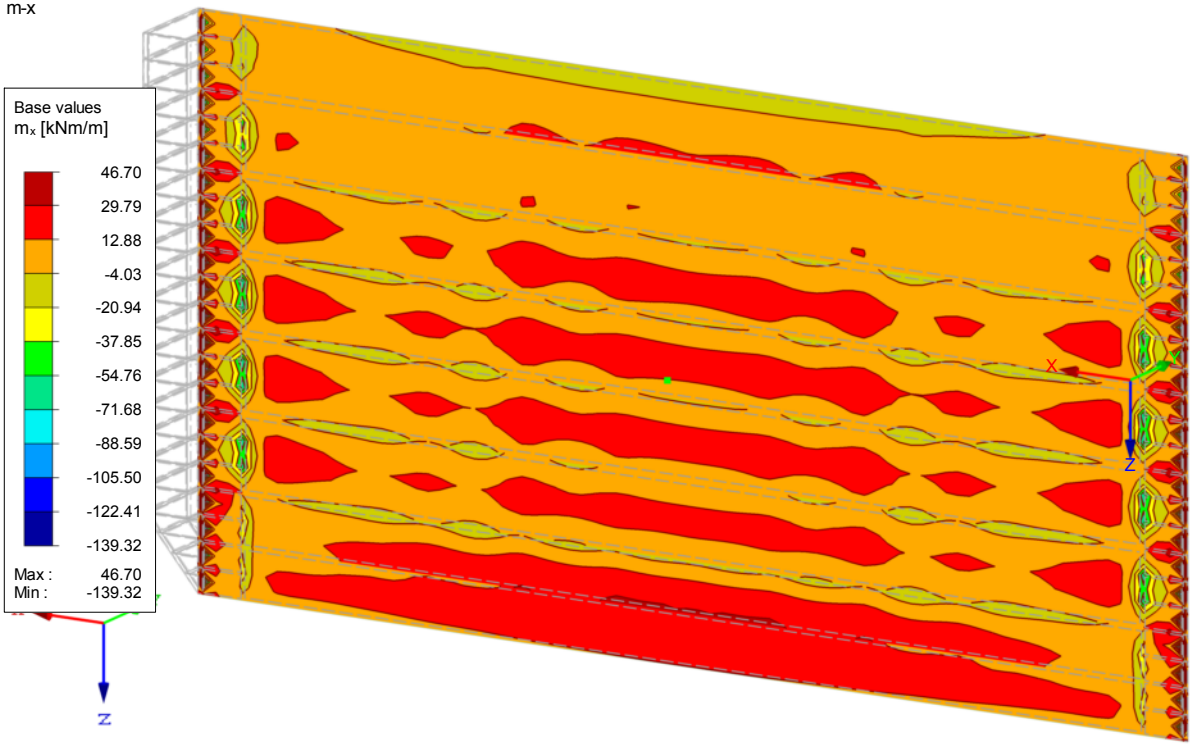
Summary			
Other Settings	Number of 1D finite elements	:	0
	Number of 2D finite elements	:	14290
	Number of 3D finite elements	:	0
	Number of FE mesh nodes	:	13540
	Number of equations	:	81240
	Max. number of iterations	:	100
	Number of divisions for member results	:	10
	Division of cable/foundation/tapered members	:	10
	Number of member divisions for searching maximum values	:	10
	Subdivisions of FE mesh for graphical results	:	0
	Percentage of iterations according to Picard method in combination with Newton-Raphson method	:	5 %
Options	☒ Activate shear stiffness of members (Ay, Az)		
	☒ Activate member divisions for large deformation or post-critical analysis		
	☒ Activate entered stiffness modifications		
	☐ Ignore rotational degrees of freedom		
	☒ Check of critical forces of members		
	Method for the system of equations	◉ Direct ○ Iteration	
	Plate bending theory	◉ Mindlin ○ Kirchhoff	
	Solver version	◉ 32-bit ○ 64-bit	
Precision and Tolerance	☐ Change default setting		

Project: CIE5060 Model: V26
Graduation Project

BASE VALUES M_x, CO1: POSITIVE DROP ULS, ISOMETRIC

CO1: Positive drop ULS
m-x

Isometric

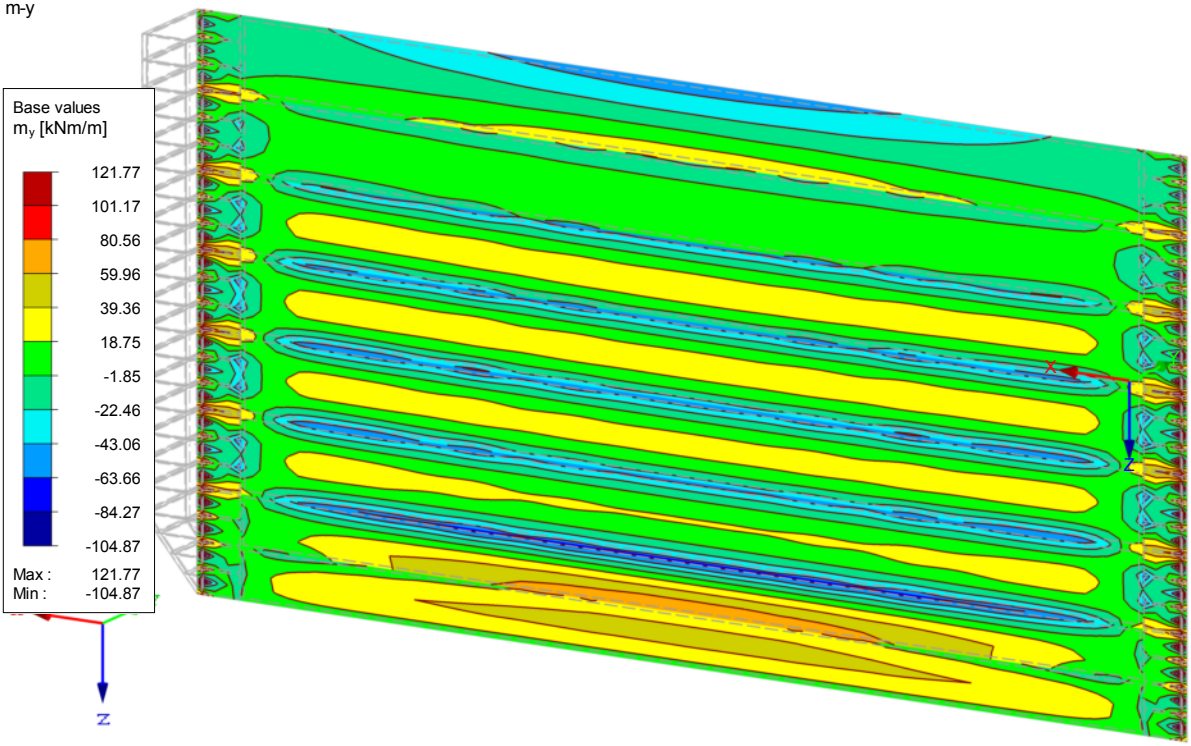


Max m-x: 46.70, Min m-x: -139.32 [kNm/m]

BASE VALUES M_y, CO1: POSITIVE DROP ULS, ISOMETRIC

CO1: Positive drop ULS
m-y

Isometric

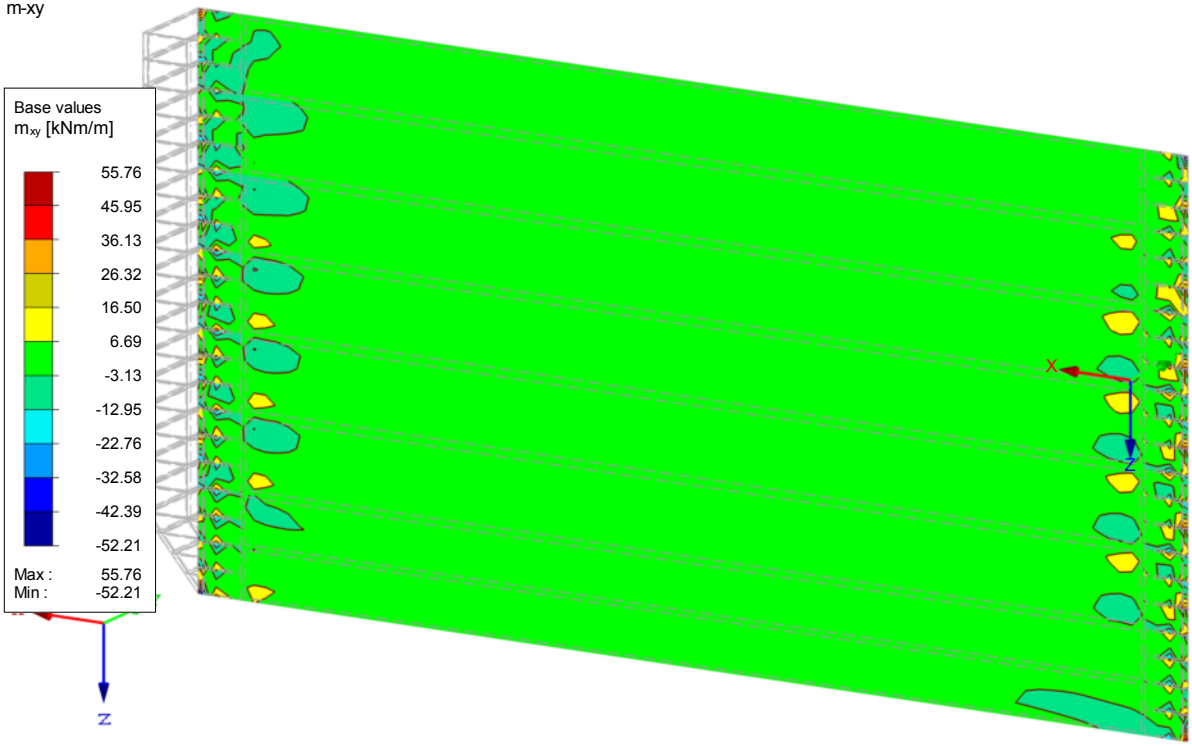


Max m-y: 121.77, Min m-y: -104.87 [kNm/m]

BASE VALUES M_{xy}, CO1: POSITIVE DROP ULS, ISOMETRIC

CO1: Positive drop ULS
m-xy

Isometric

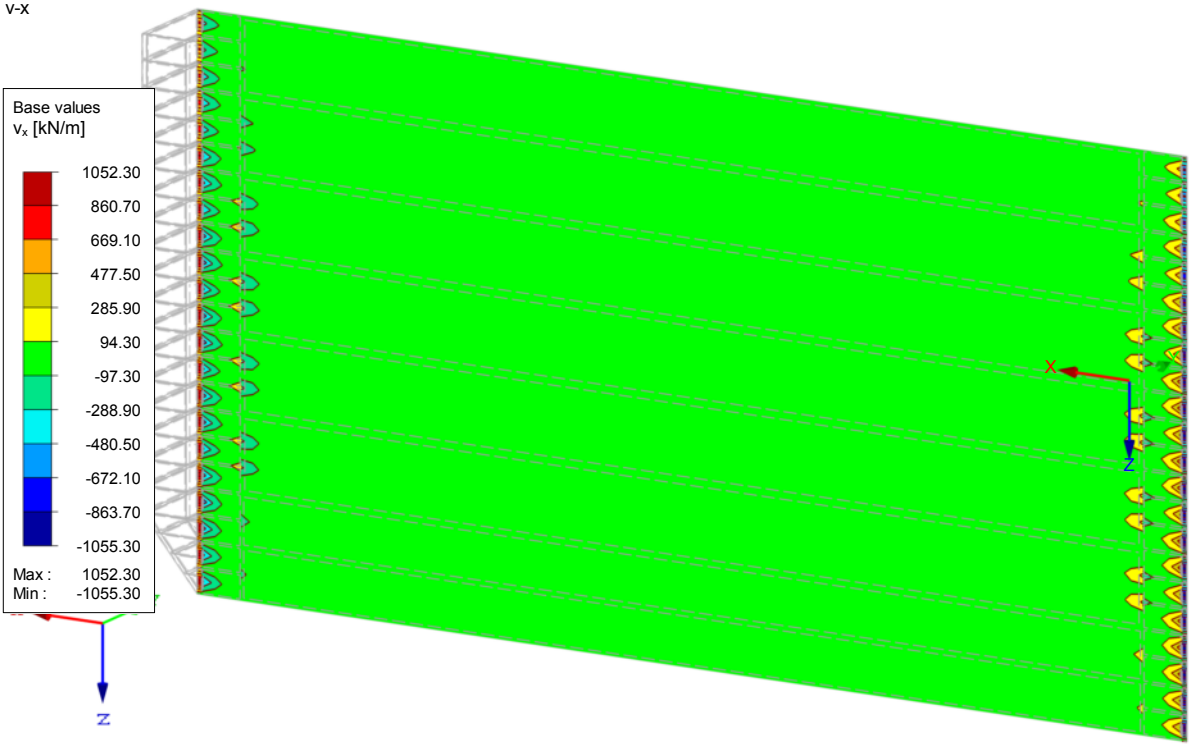


Max m-xy: 55.76, Min m-xy: -52.21 [kNm/m]

BASE VALUES V_x, CO1: POSITIVE DROP ULS, ISOMETRIC

CO1: Positive drop ULS
v-x

Isometric

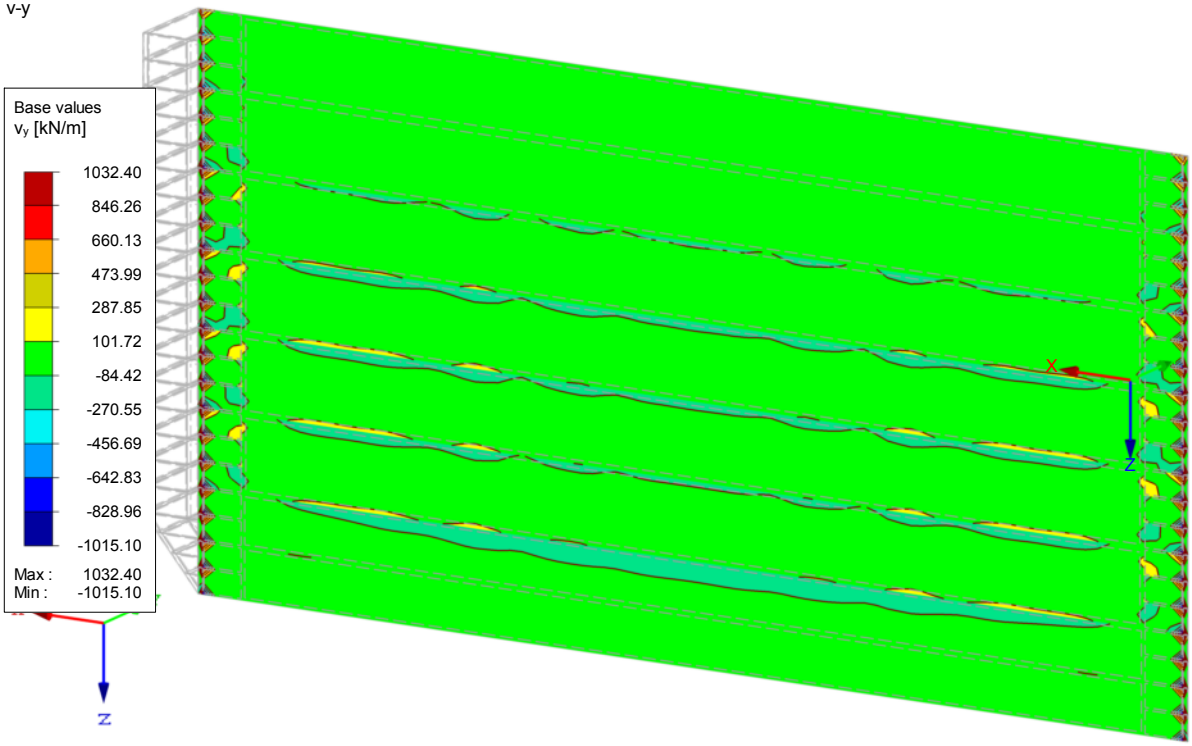


Max v-x: 1052.30, Min v-x: -1055.30 [kN/m]

BASE VALUES V_y, CO1: POSITIVE DROP ULS, ISOMETRIC

CO1: Positive drop ULS
v-y

Isometric

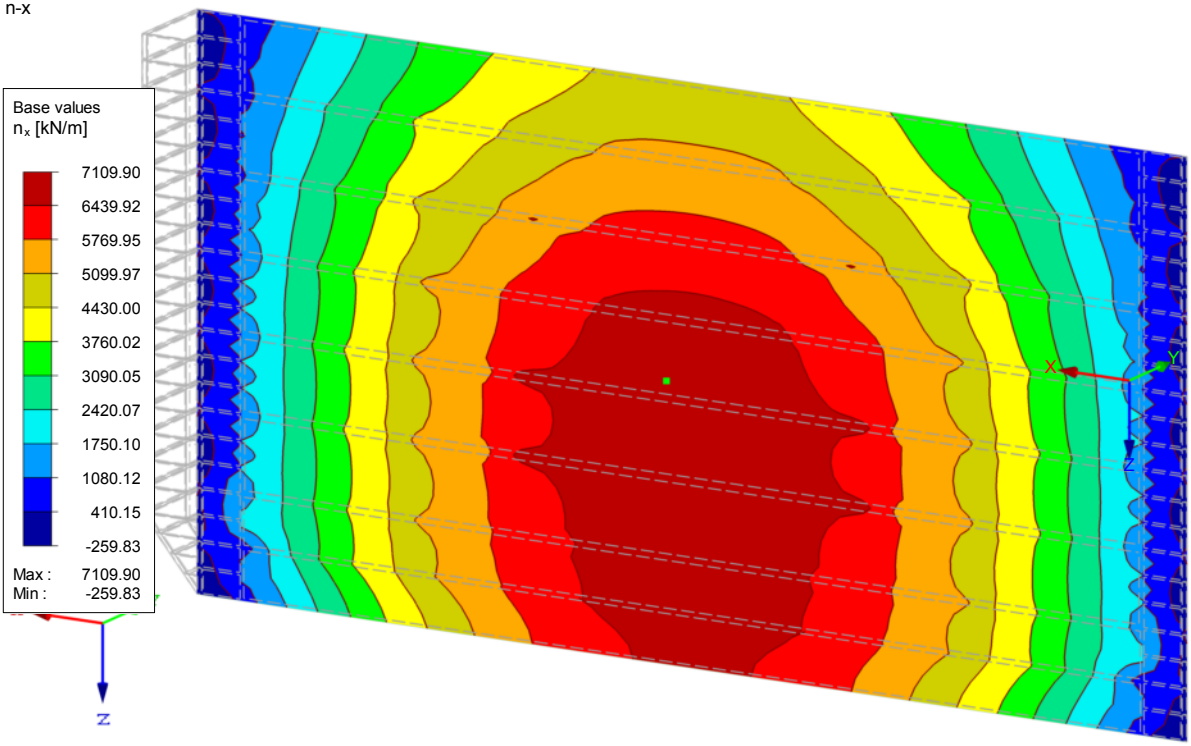


Max v-y: 1032.40, Min v-y: -1015.10 [kN/m]

BASE VALUES N_x, CO1: POSITIVE DROP ULS, ISOMETRIC

CO1: Positive drop ULS
n-x

Isometric



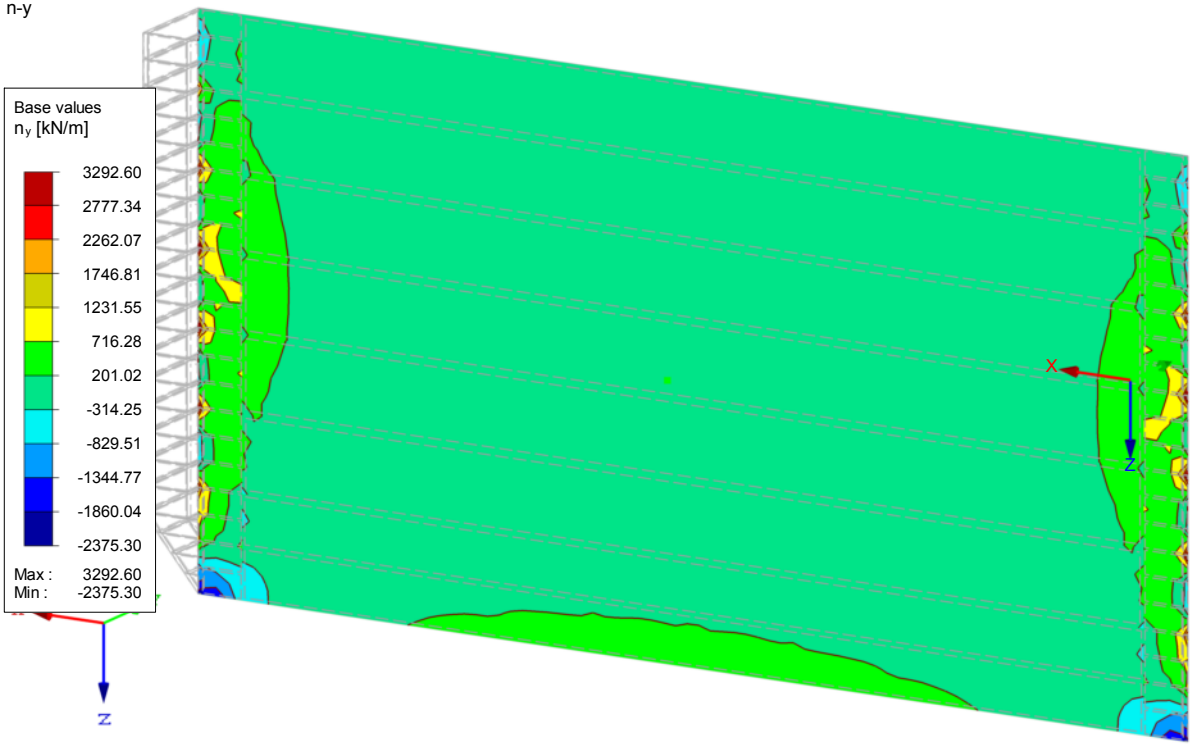
Max n-x: 7109.90, Min n-x: -259.83 [kN/m]

Project: CIE5060 Model: V26
Graduation Project

BASE VALUES N_y, CO1: POSITIVE DROP ULS, ISOMETRIC

CO1: Positive drop ULS
n-y

Isometric

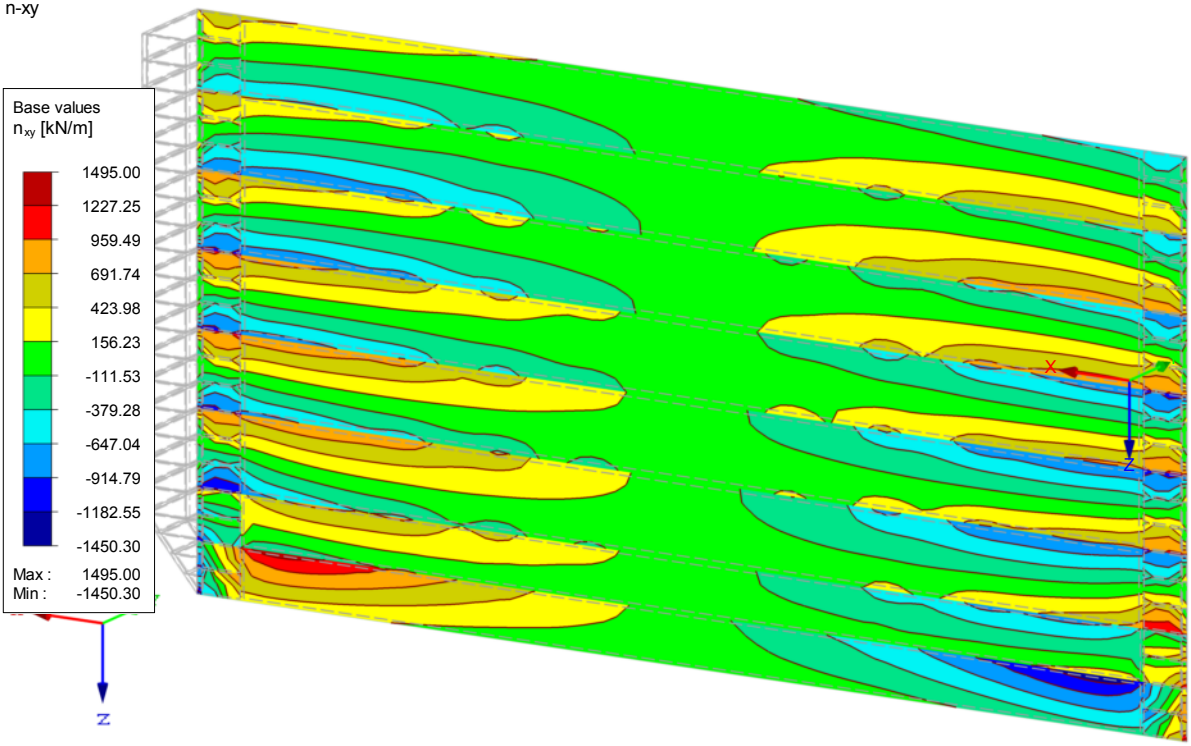


Max n-y: 3292.60, Min n-y: -2375.30 [kN/m]

BASE VALUES N_{xy}, CO1: POSITIVE DROP ULS, ISOMETRIC

CO1: Positive drop ULS
n-xy

Isometric

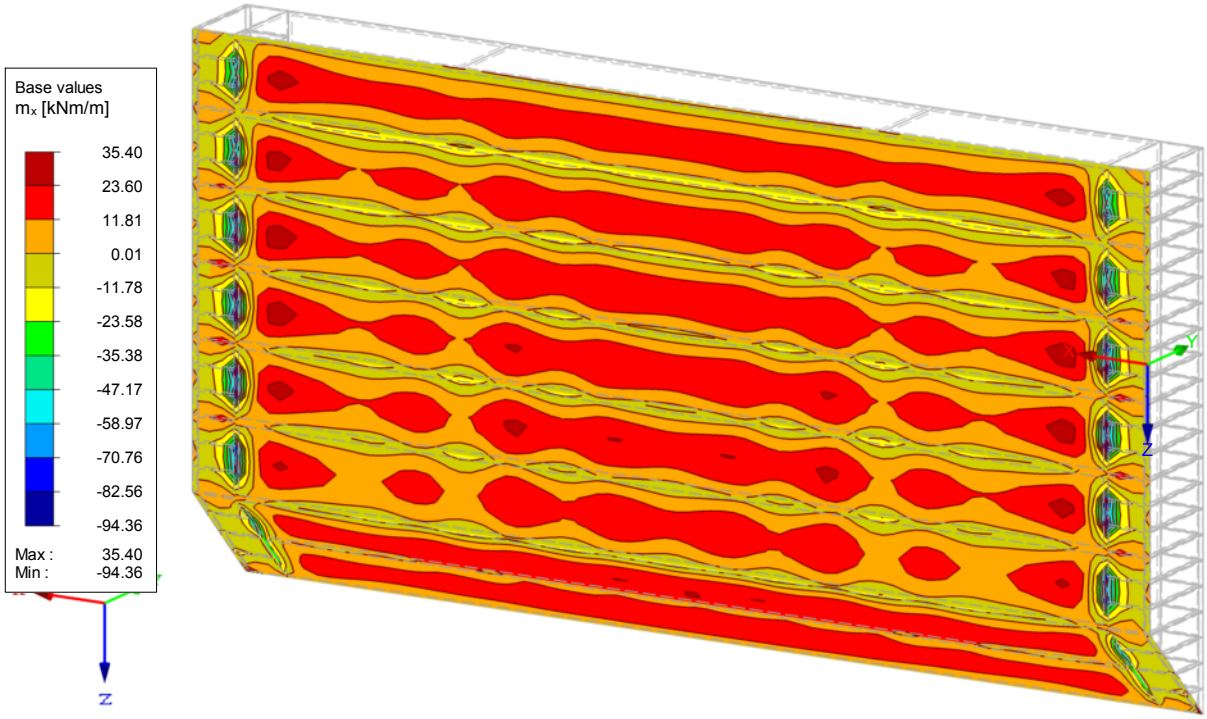


Max n-xy: 1495.00, Min n-xy: -1450.30 [kN/m]

BASE VALUES M_x, CO1: POSITIVE DROP ULS, ISOMETRIC

CO1: Positive drop ULS
m-x

Isometric

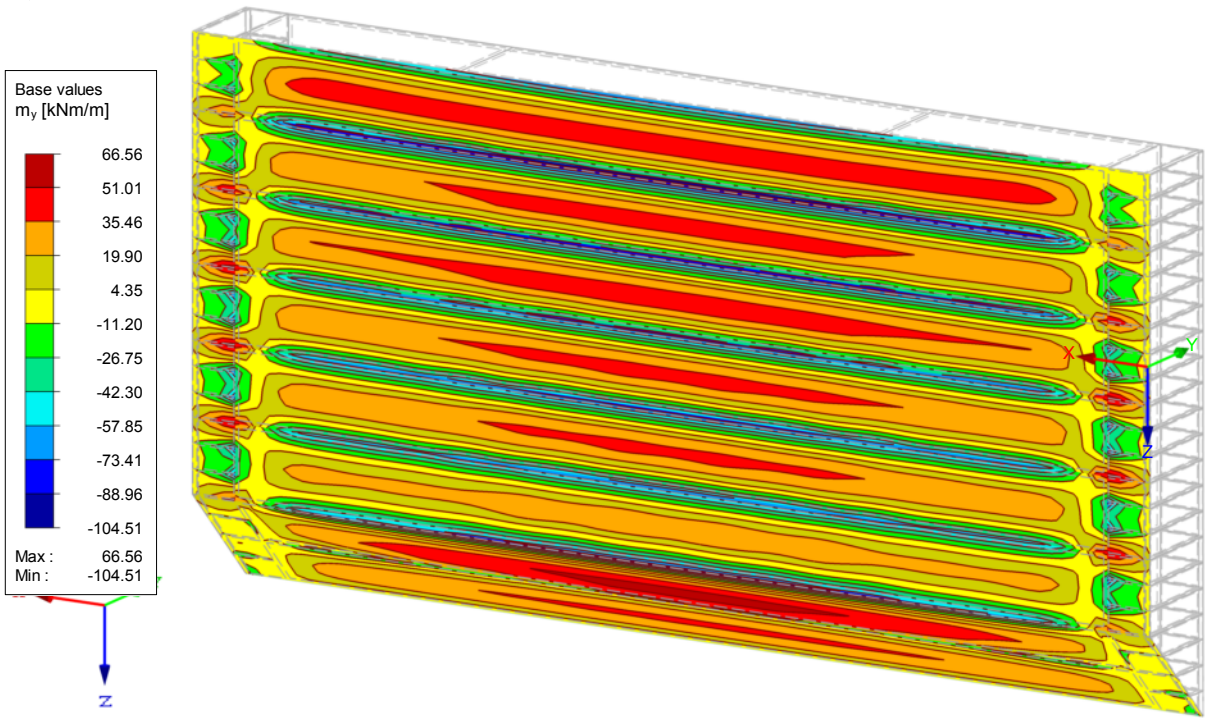


Max m-x: 35.40, Min m-x: -94.36 [kNm/m]

BASE VALUES M_y, CO1: POSITIVE DROP ULS, ISOMETRIC

CO1: Positive drop ULS
m-y

Isometric

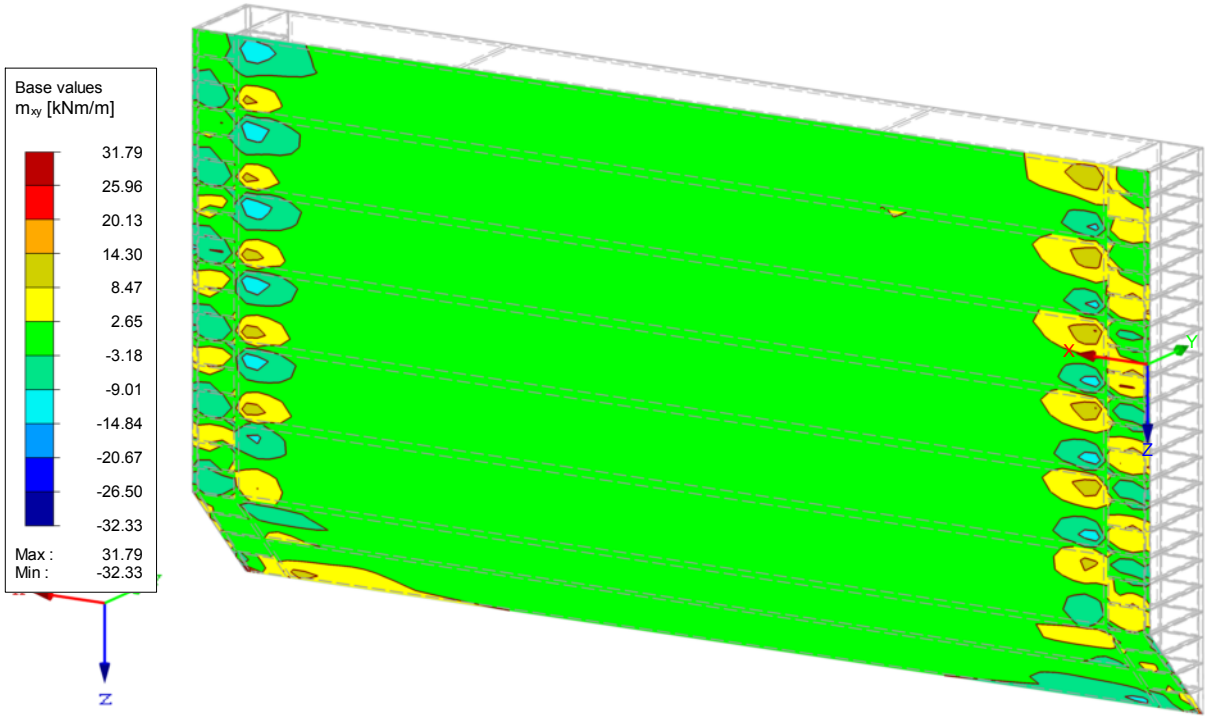


Max m-y: 66.56, Min m-y: -104.51 [kNm/m]

BASE VALUES M_{xy}, CO1: POSITIVE DROP ULS, ISOMETRIC

CO1: Positive drop ULS
m-xy

Isometric

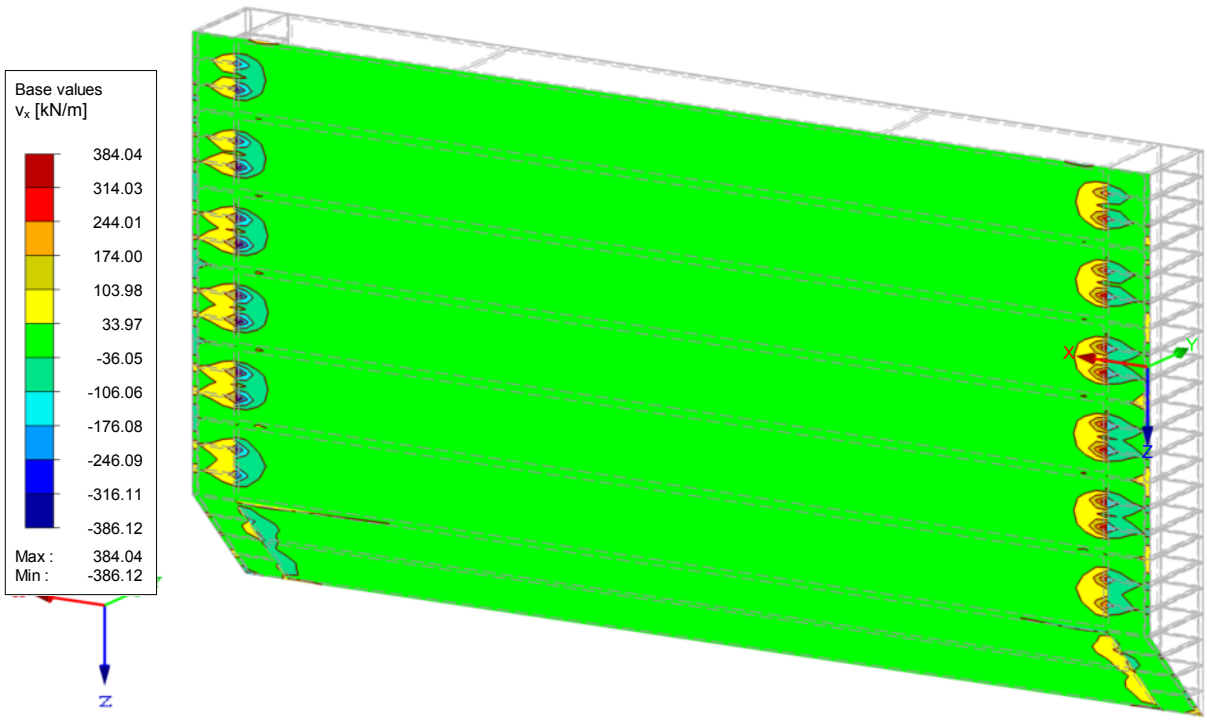


Max m-xy: 31.79, Min m-xy: -32.33 [kNm/m]

BASE VALUES V_x, CO1: POSITIVE DROP ULS, ISOMETRIC

CO1: Positive drop ULS
v-x

Isometric

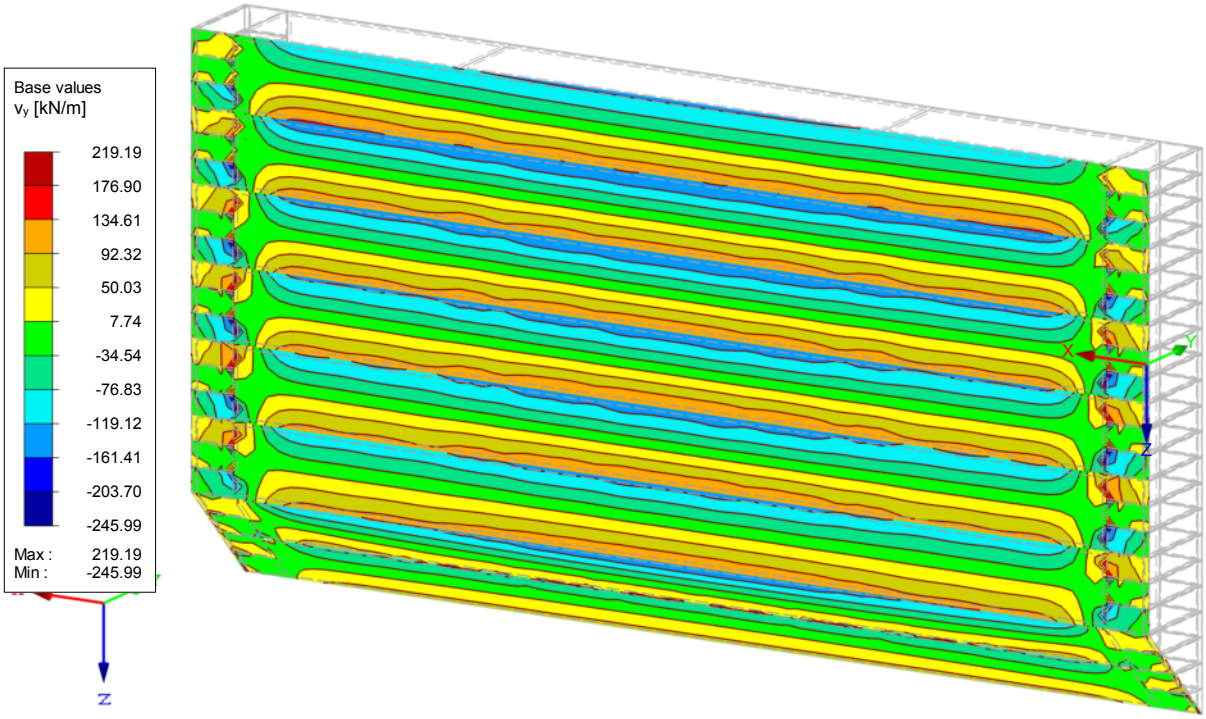


Max v-x: 384.04, Min v-x: -386.12 [kN/m]

BASE VALUES V_y, CO1: POSITIVE DROP ULS, ISOMETRIC

CO1: Positive drop ULS
v-y

Isometric

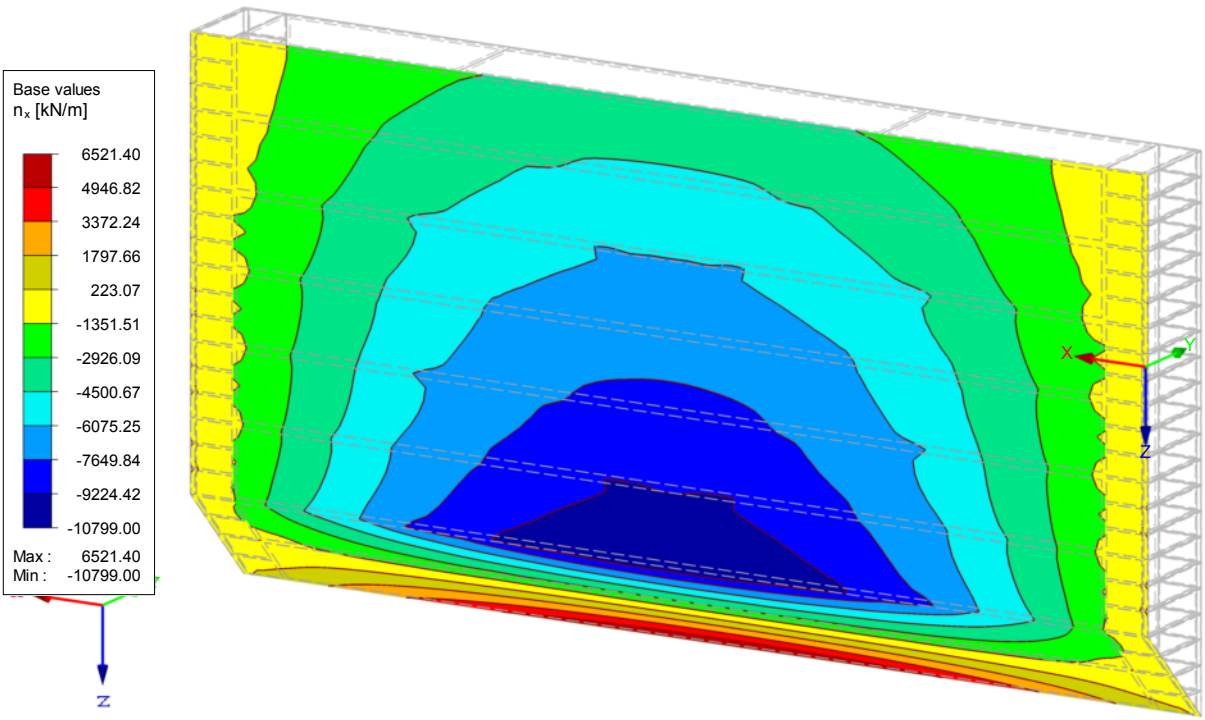


Max v-y: 219.19, Min v-y: -245.99 [kN/m]

BASE VALUES N_x, CO1: POSITIVE DROP ULS, ISOMETRIC

CO1: Positive drop ULS
n-x

Isometric

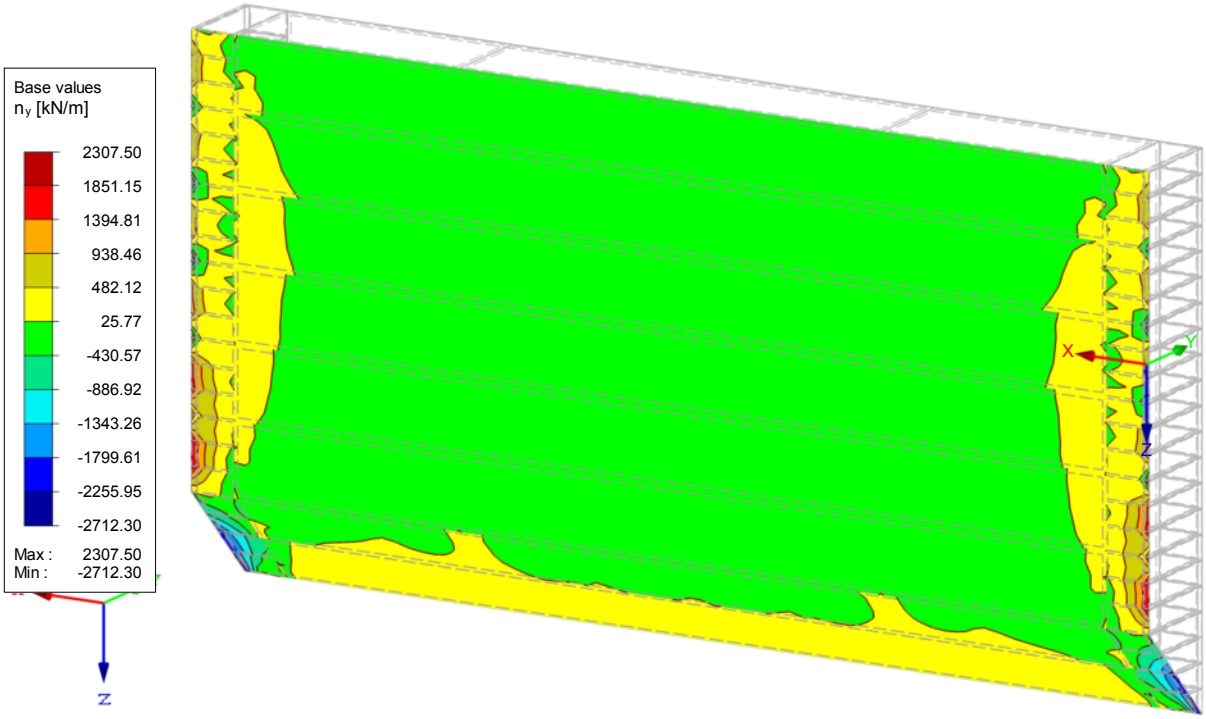


Max n-x: 6521.40, Min n-x: -10799.00 [kN/m]

BASE VALUES N_y, CO1: POSITIVE DROP ULS, ISOMETRIC

CO1: Positive drop ULS
n-y

Isometric

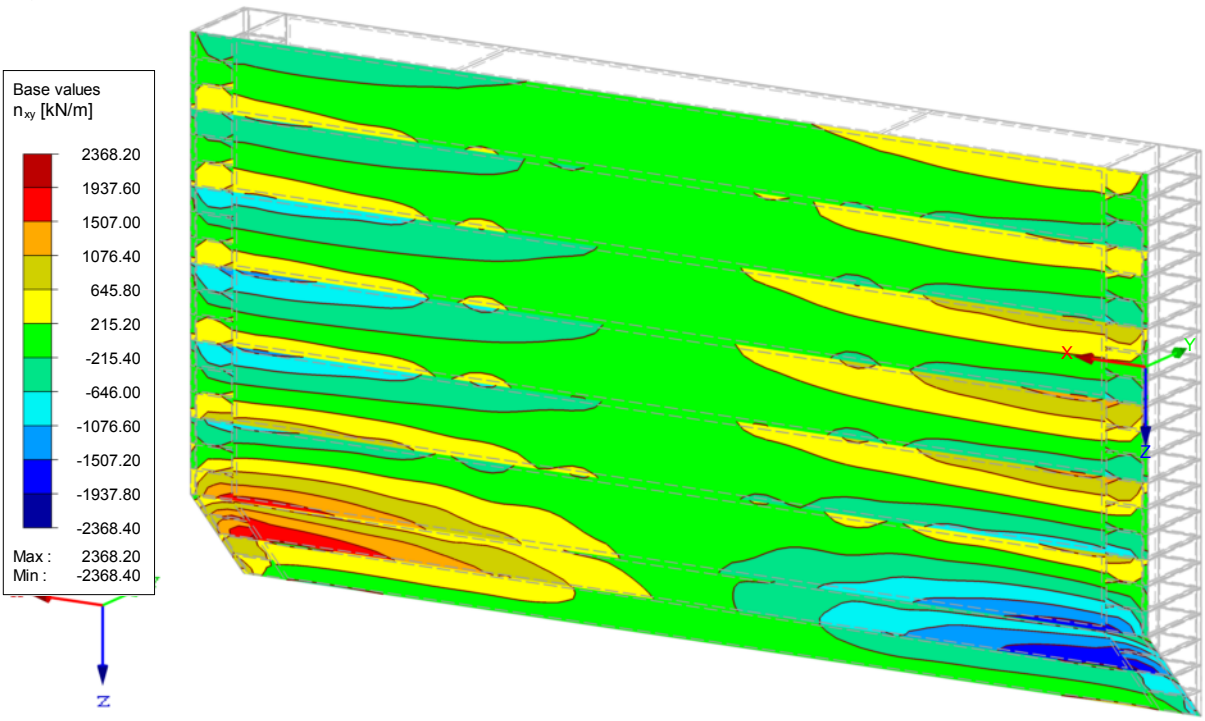


Max n-y: 2307.50, Min n-y: -2712.30 [kN/m]

BASE VALUES N_{xy}, CO1: POSITIVE DROP ULS, ISOMETRIC

CO1: Positive drop ULS
n-xy

Isometric



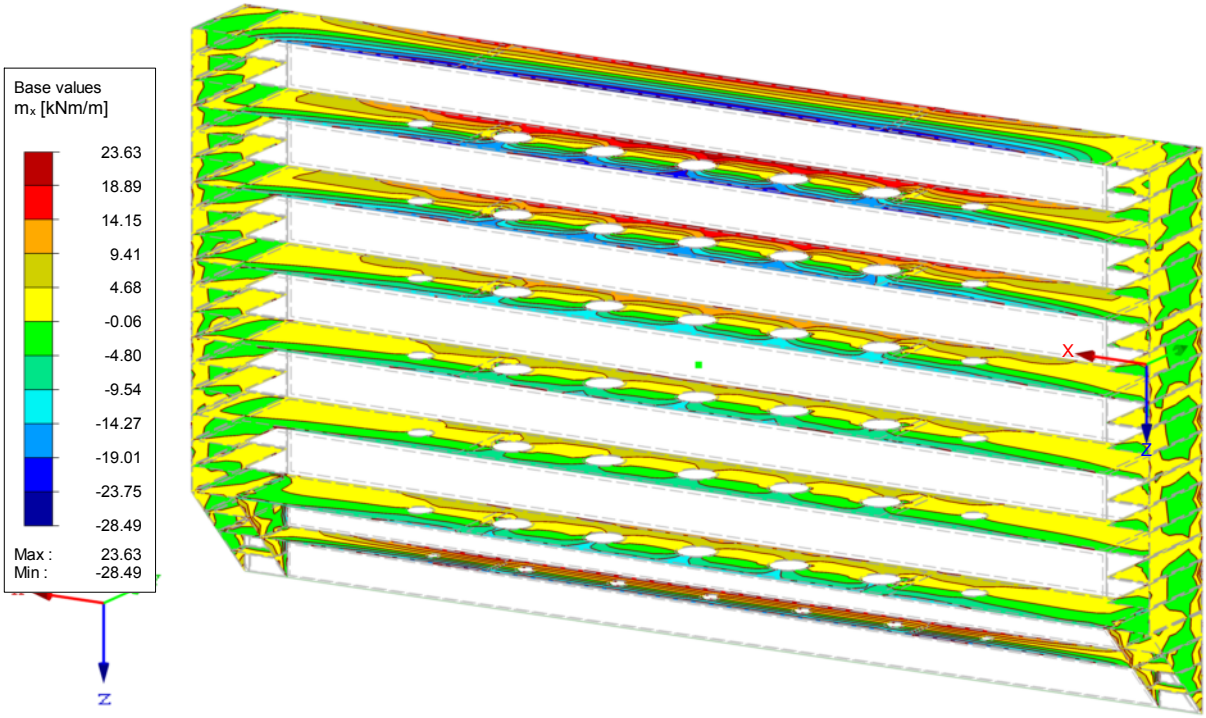
Max n-xy: 2368.20, Min n-xy: -2368.40 [kN/m]

Project: CIE5060 Model: V26
Graduation Project

BASE VALUES M_x, CO1: POSITIVE DROP ULS, ISOMETRIC

CO1: Positive drop ULS
m-x

Isometric

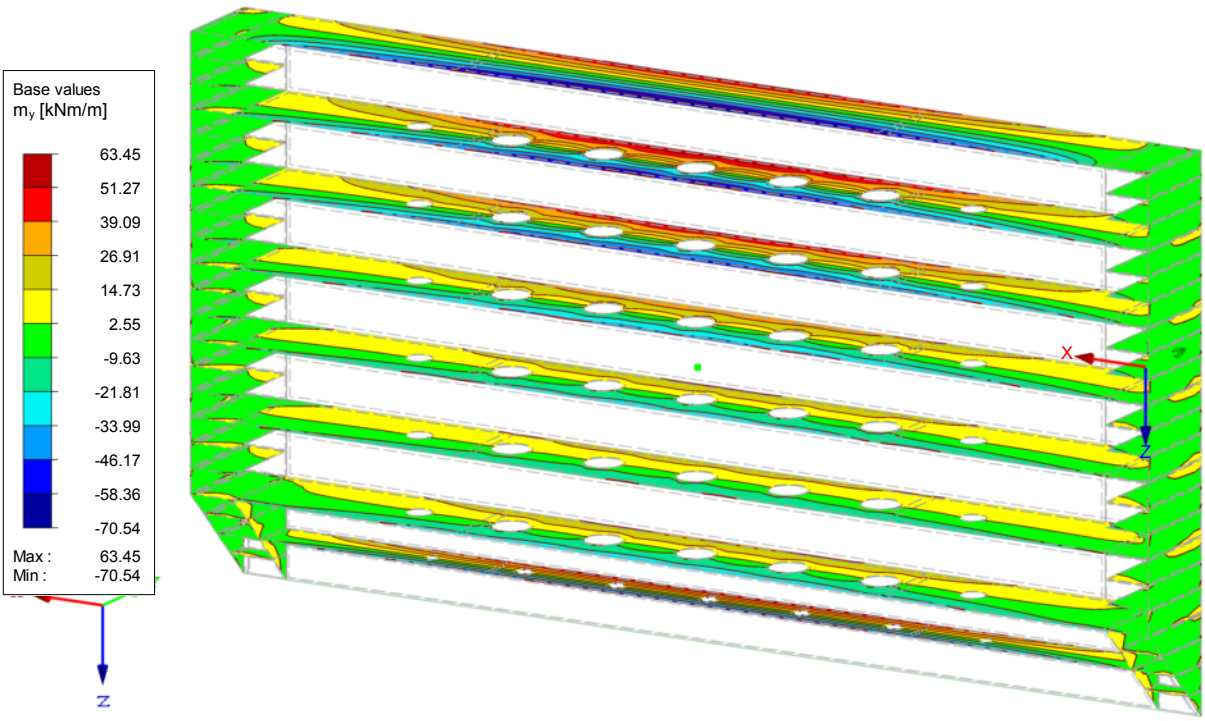


Max m-x: 23.63, Min m-x: -28.49 [kNm/m]

BASE VALUES M_y, CO1: POSITIVE DROP ULS, ISOMETRIC

CO1: Positive drop ULS
m-y

Isometric

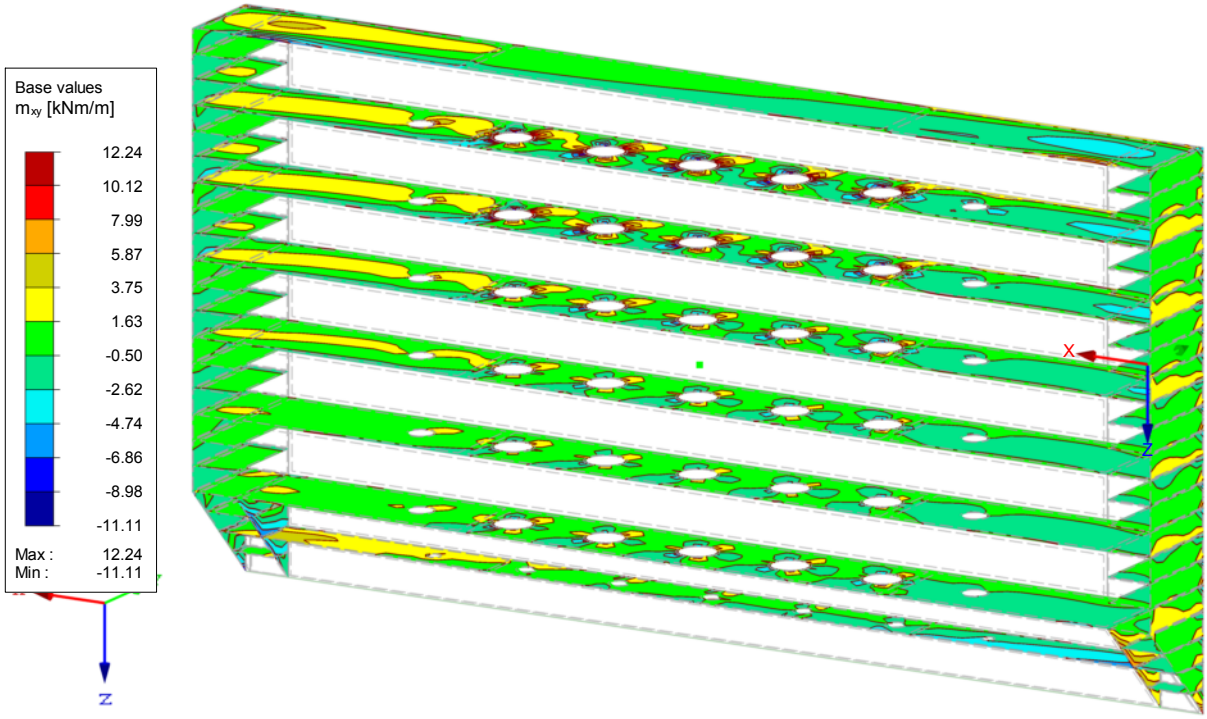


Max m-y: 63.45, Min m-y: -70.54 [kNm/m]

BASE VALUES M_{xy}, CO1: POSITIVE DROP ULS, ISOMETRIC

CO1: Positive drop ULS
m-xy

Isometric

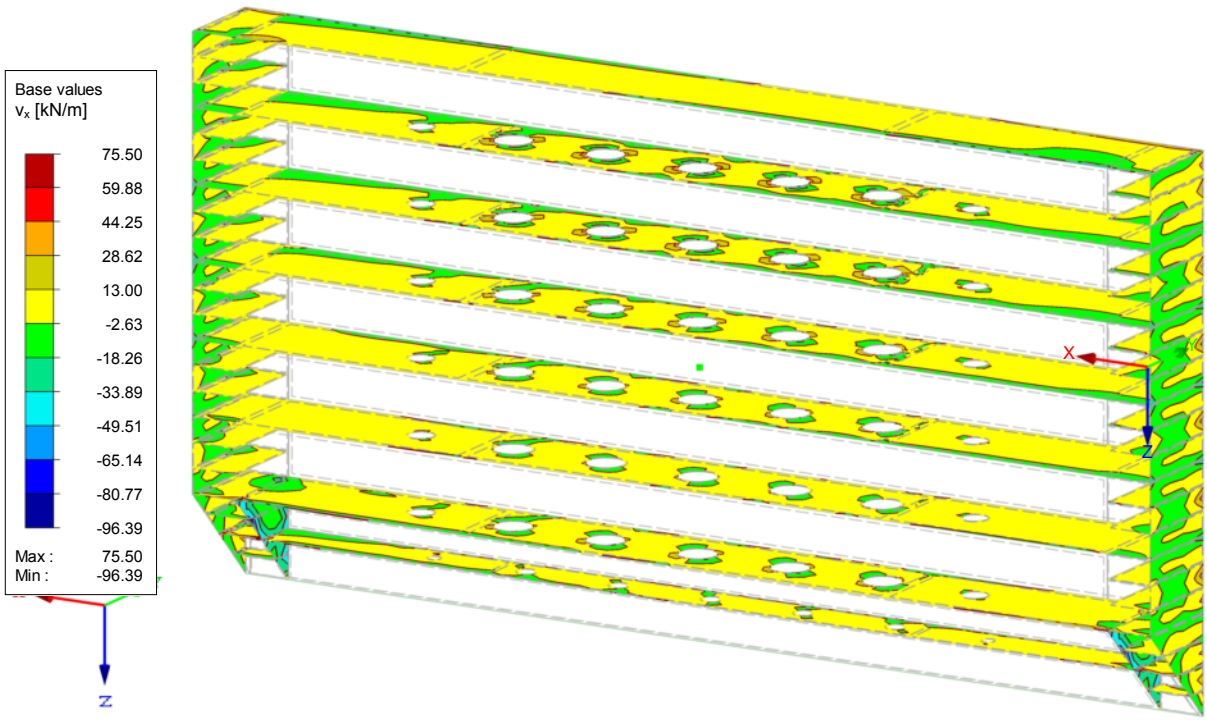


Max m-xy: 12.24, Min m-xy: -11.11 [kNm/m]

BASE VALUES V_x, CO1: POSITIVE DROP ULS, ISOMETRIC

CO1: Positive drop ULS
v-x

Isometric



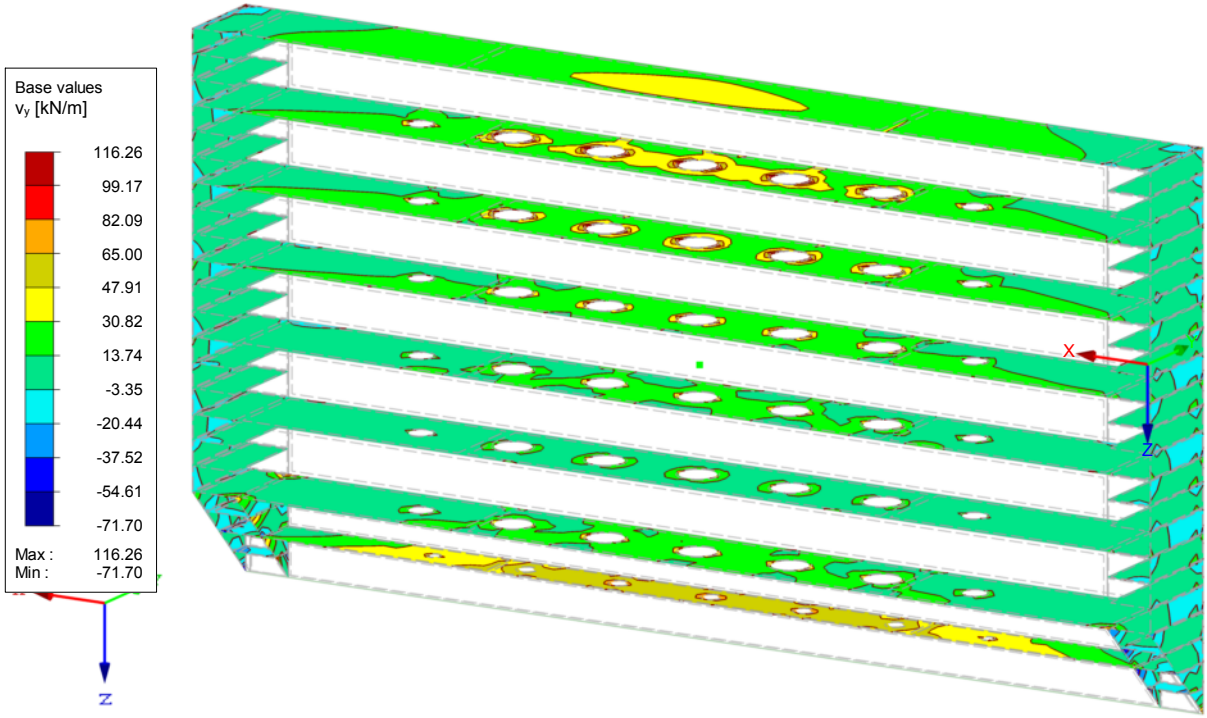
Max v-x: 75.50, Min v-x: -96.39 [kN/m]

Project: CIE5060 Model: V26
Graduation Project

BASE VALUES V_y, CO1: POSITIVE DROP ULS, ISOMETRIC

CO1: Positive drop ULS
v-y

Isometric

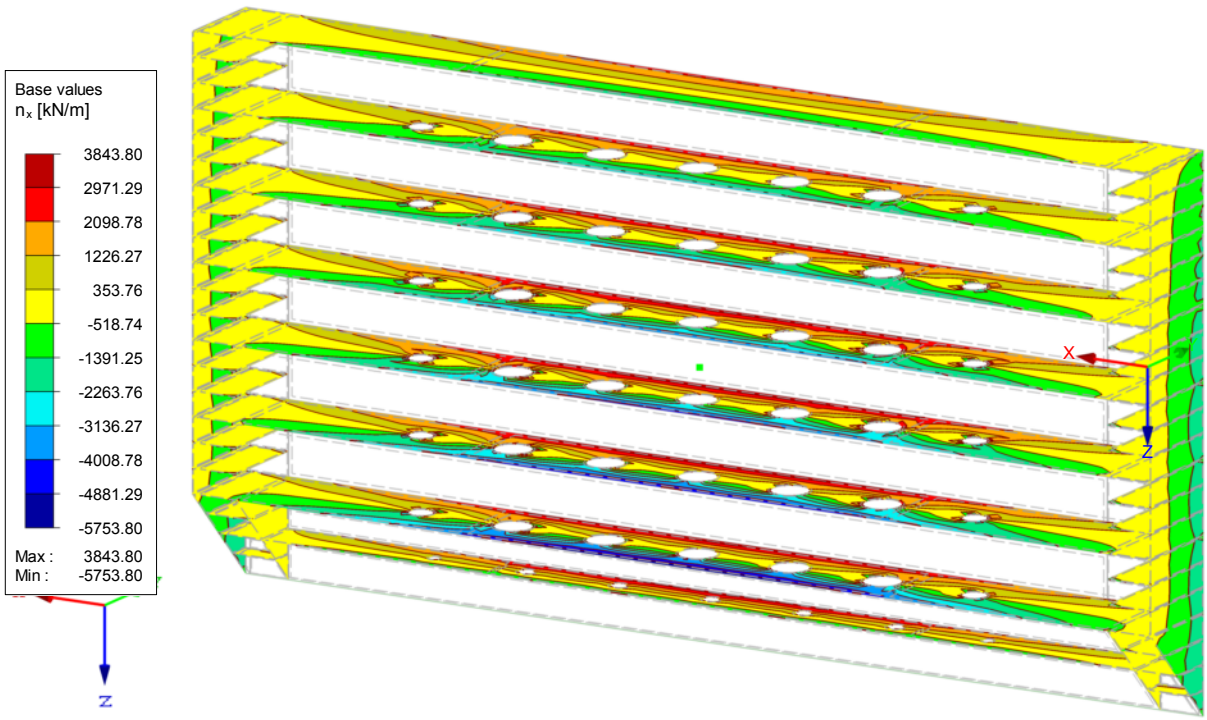


Max v-y: 116.26, Min v-y: -71.70 [kN/m]

BASE VALUES N_x, CO1: POSITIVE DROP ULS, ISOMETRIC

CO1: Positive drop ULS
n-x

Isometric

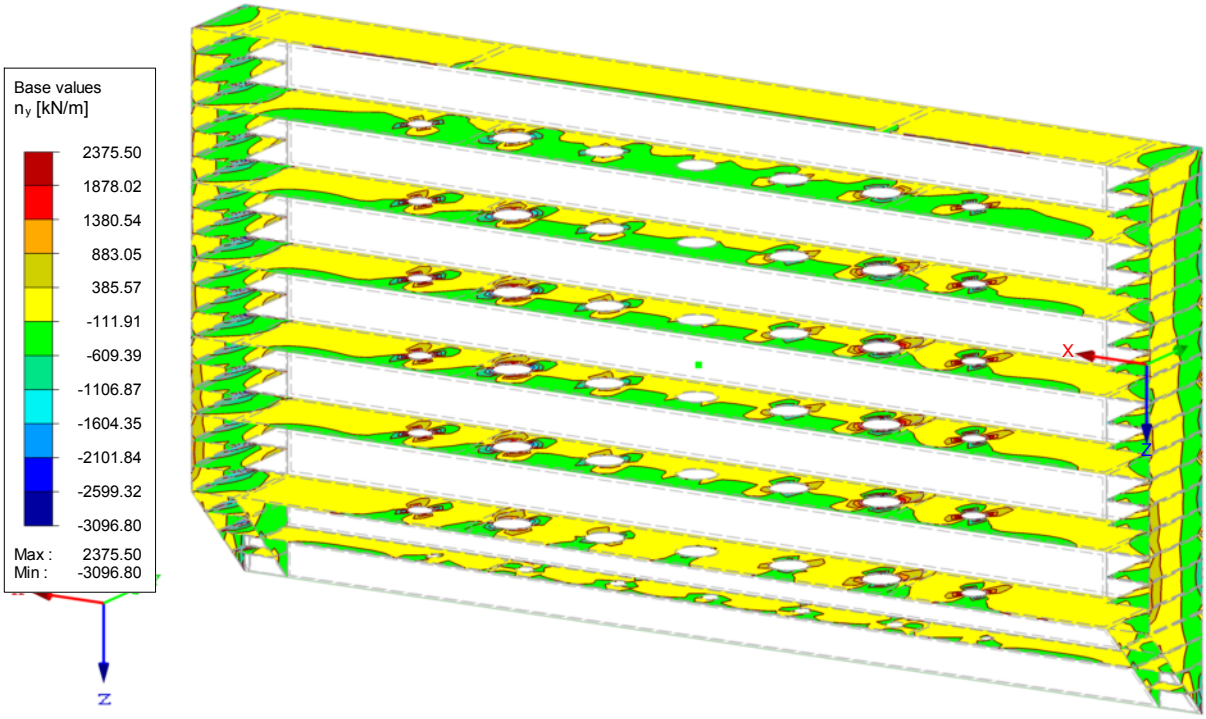


Max n-x: 3843.80, Min n-x: -5753.80 [kN/m]

BASE VALUES N_y, CO1: POSITIVE DROP ULS, ISOMETRIC

CO1: Positive drop ULS
n-y

Isometric

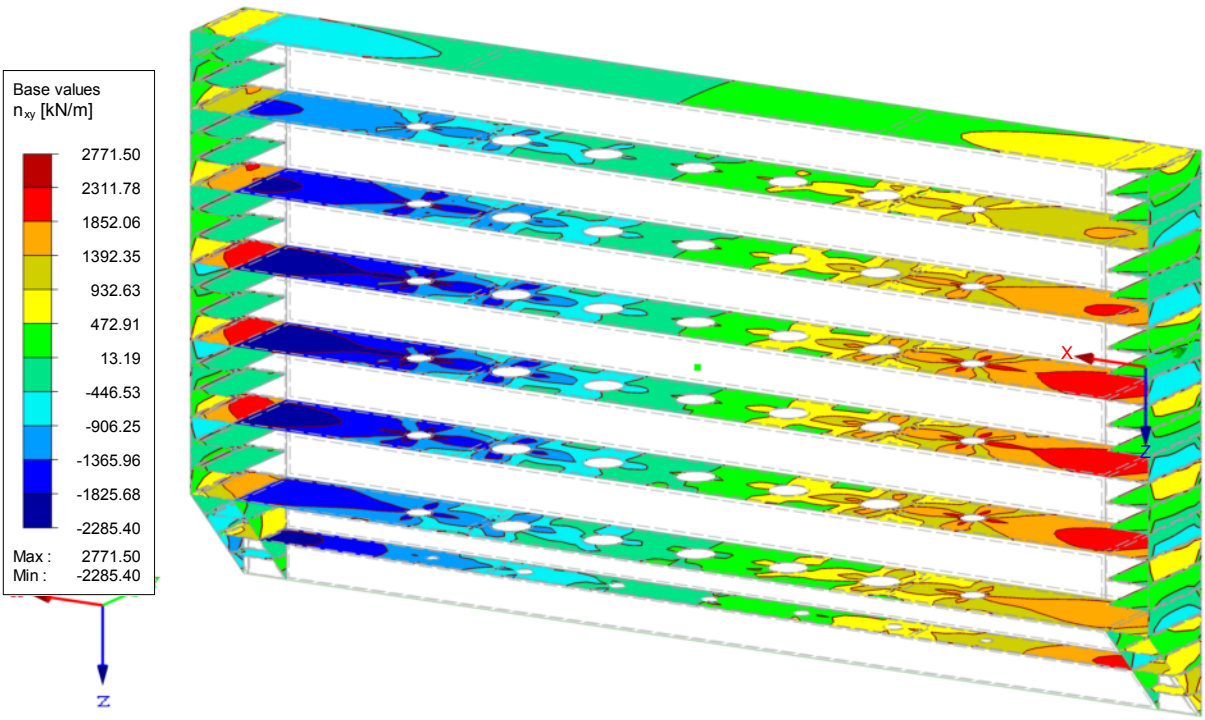


Max n-y: 2375.50, Min n-y: -3096.80 [kN/m]

BASE VALUES N_{xy}, CO1: POSITIVE DROP ULS, ISOMETRIC

CO1: Positive drop ULS
n-xy

Isometric

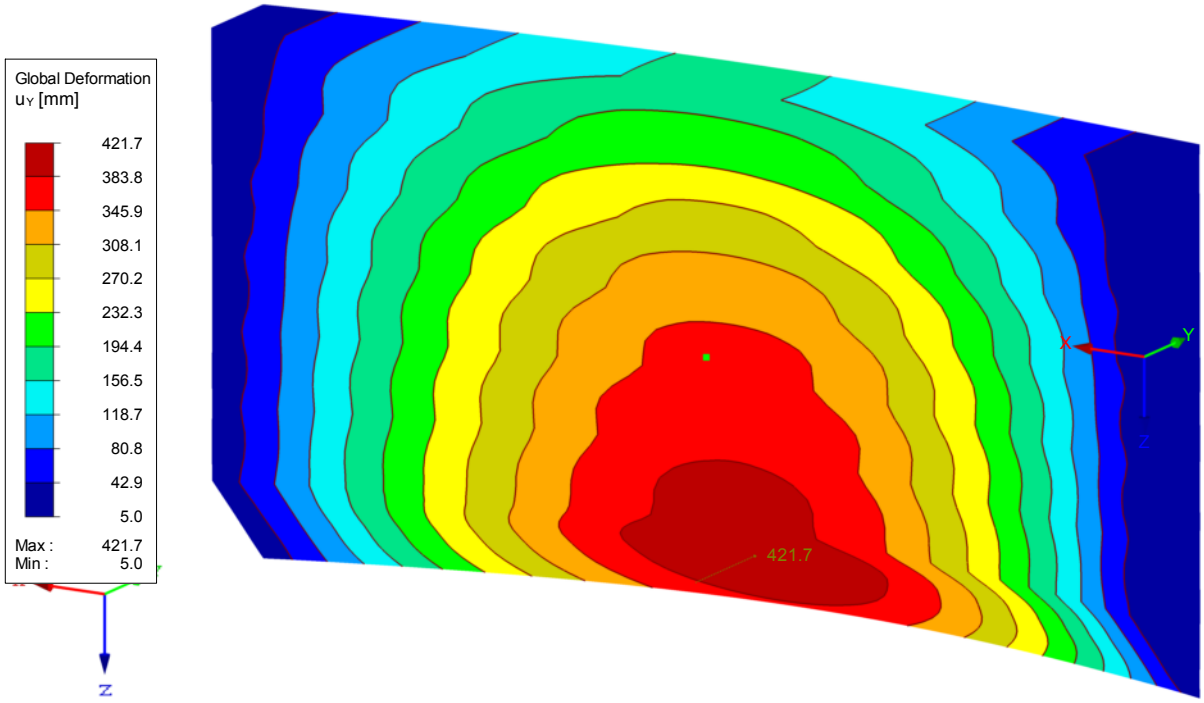


Max n-xy: 2771.50, Min n-xy: -2285.40 [kN/m]

GLOBAL DEFORMATION U_Y, CO2: POSITIVE DROP SLS, ISOMETRIC

CO2: Positive drop SLS
u-Y

Isometric

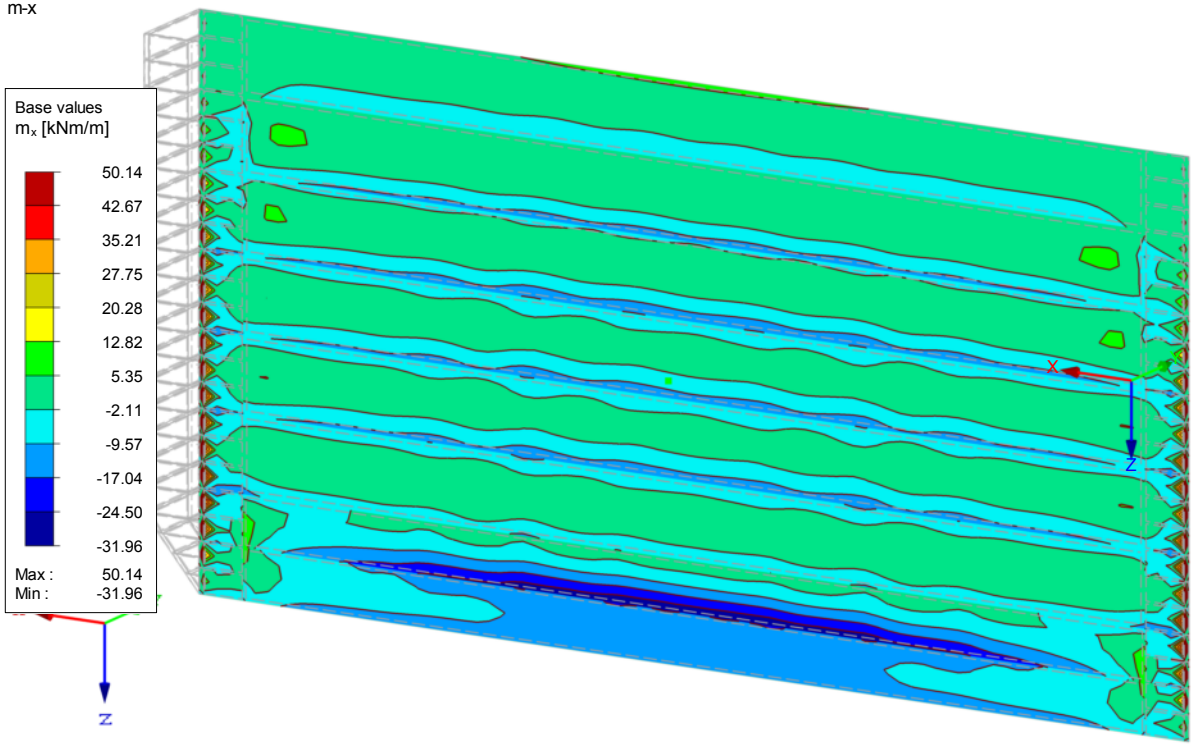


Max u-Y: 421.7, Min u-Y: 5.0 [mm]
Factor of deformations: 11.00

BASE VALUES M_x, CO3: NEGATIVE DROP ULS, ISOMETRIC

CO3: Negative drop ULS
m-x

Isometric

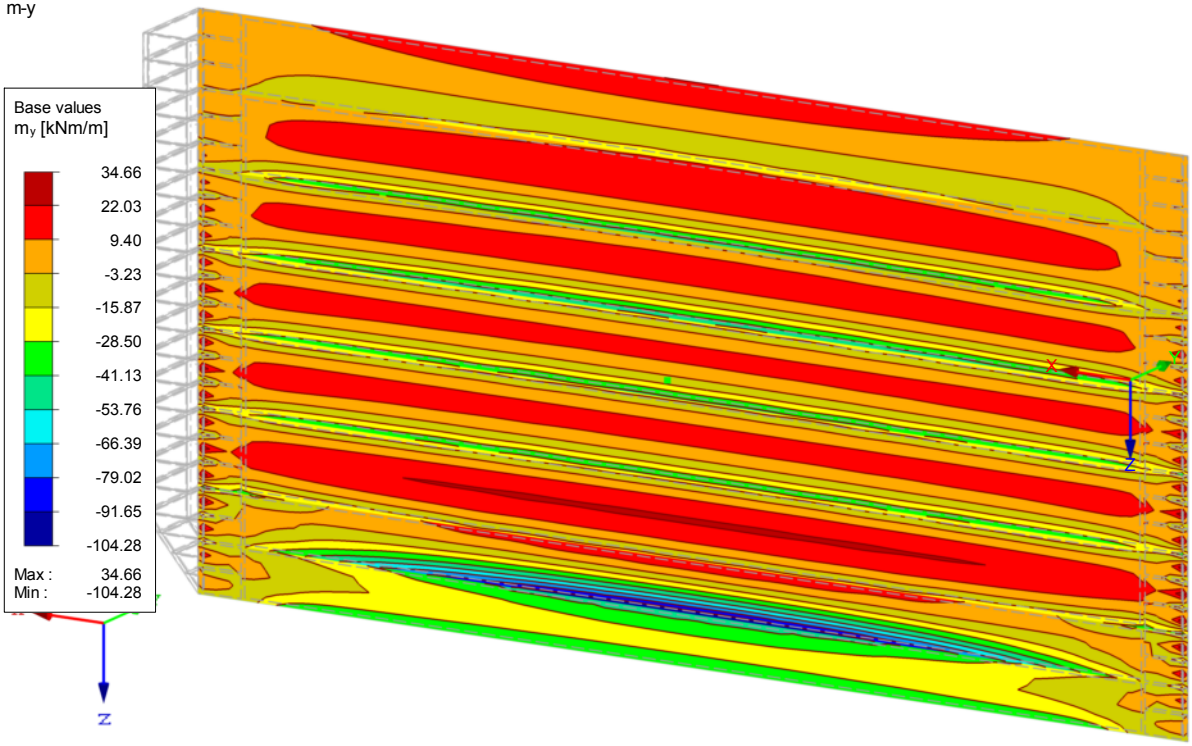


Max m-x: 50.14, Min m-x: -31.96 [kNm/m]

BASE VALUES M_y, CO3: NEGATIVE DROP ULS, ISOMETRIC

CO3: Negative drop ULS
m-y

Isometric

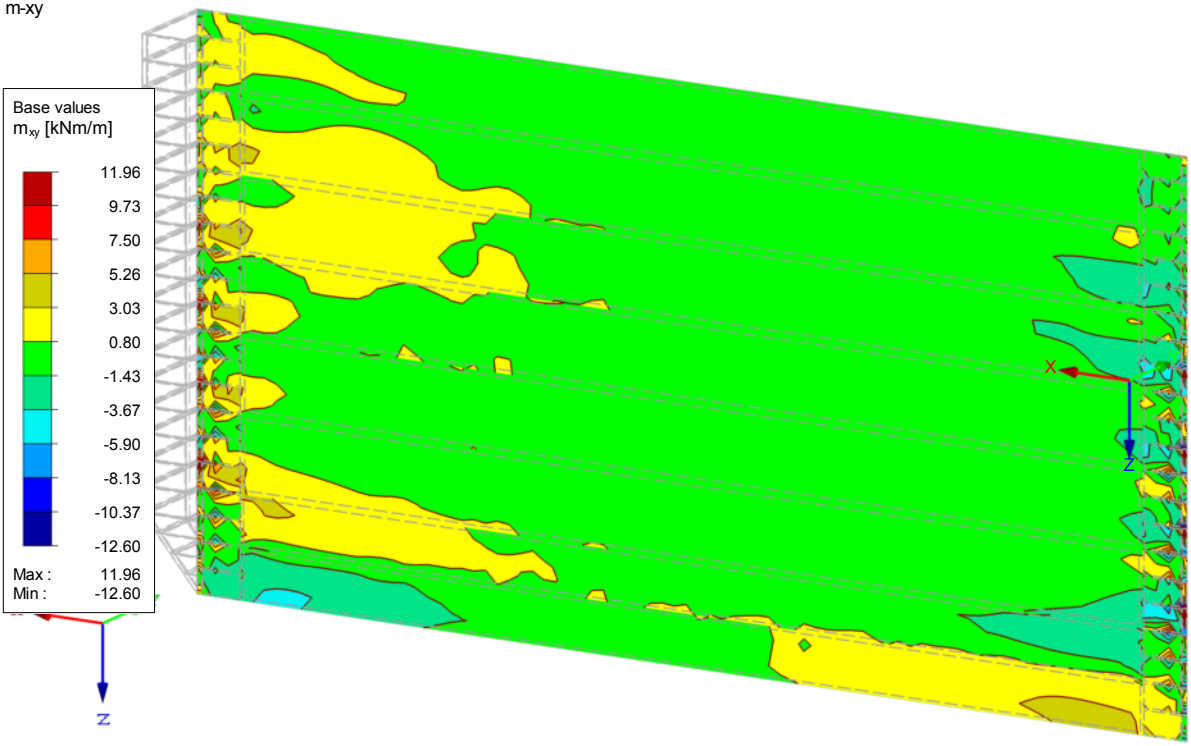


Max m-y: 34.66, Min m-y: -104.28 [kNm/m]

BASE VALUES M_{xy}, CO3: NEGATIVE DROP ULS, ISOMETRIC

CO3: Negative drop ULS
m-xy

Isometric



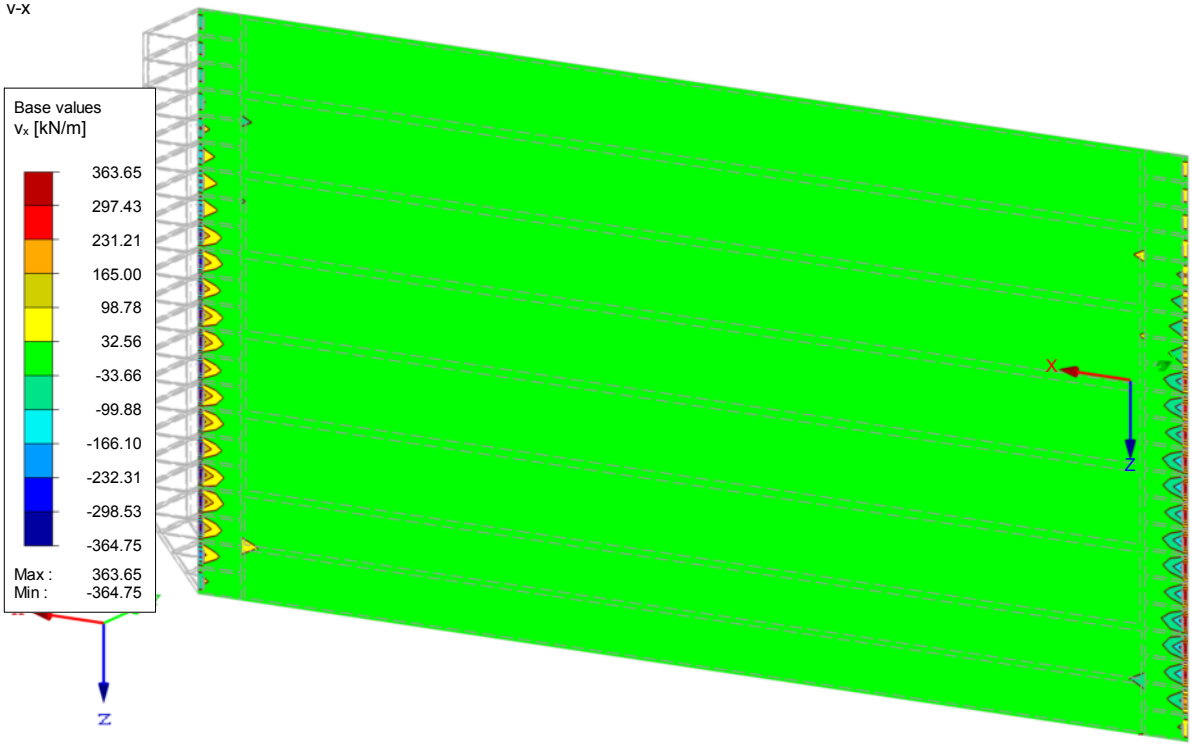
Max m-xy: 11.96, Min m-xy: -12.60 [kNm/m]

Project: CIE5060 Model: V26
Graduation Project

BASE VALUES V_x, CO3: NEGATIVE DROP ULS, ISOMETRIC

CO3: Negative drop ULS
v-x

Isometric

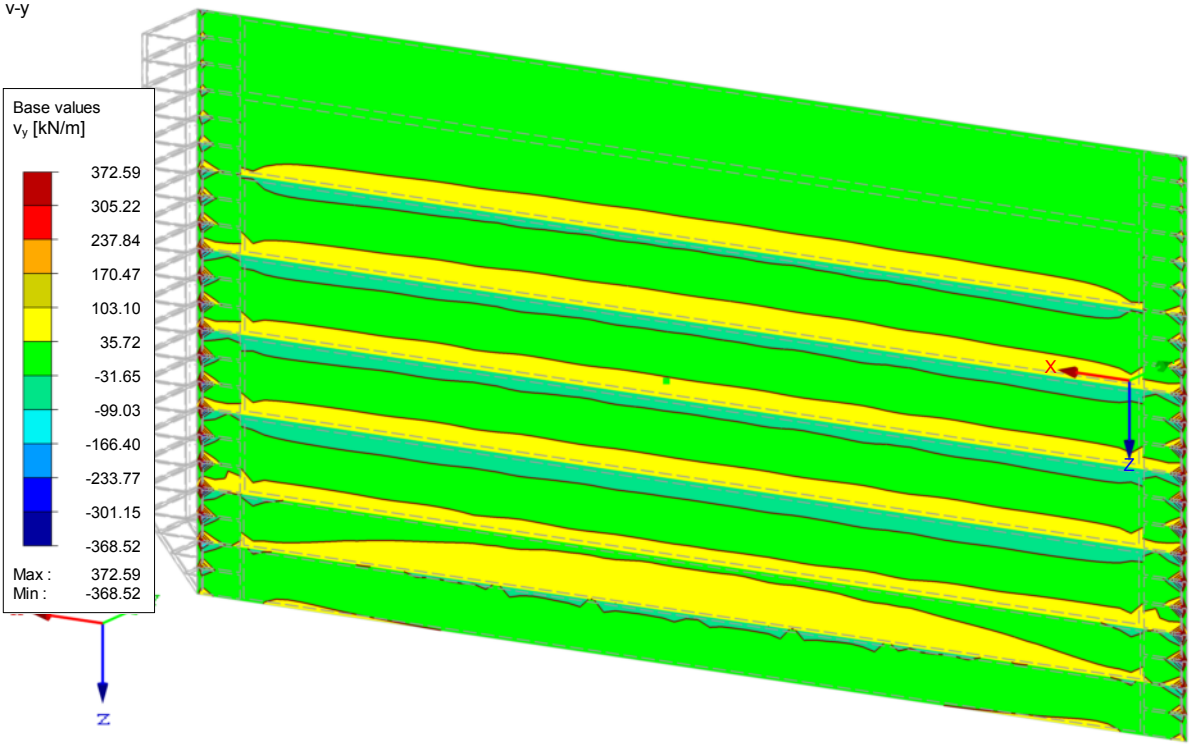


Max v-x: 363.65, Min v-x: -364.75 [kN/m]

BASE VALUES V_y, CO3: NEGATIVE DROP ULS, ISOMETRIC

CO3: Negative drop ULS
v-y

Isometric



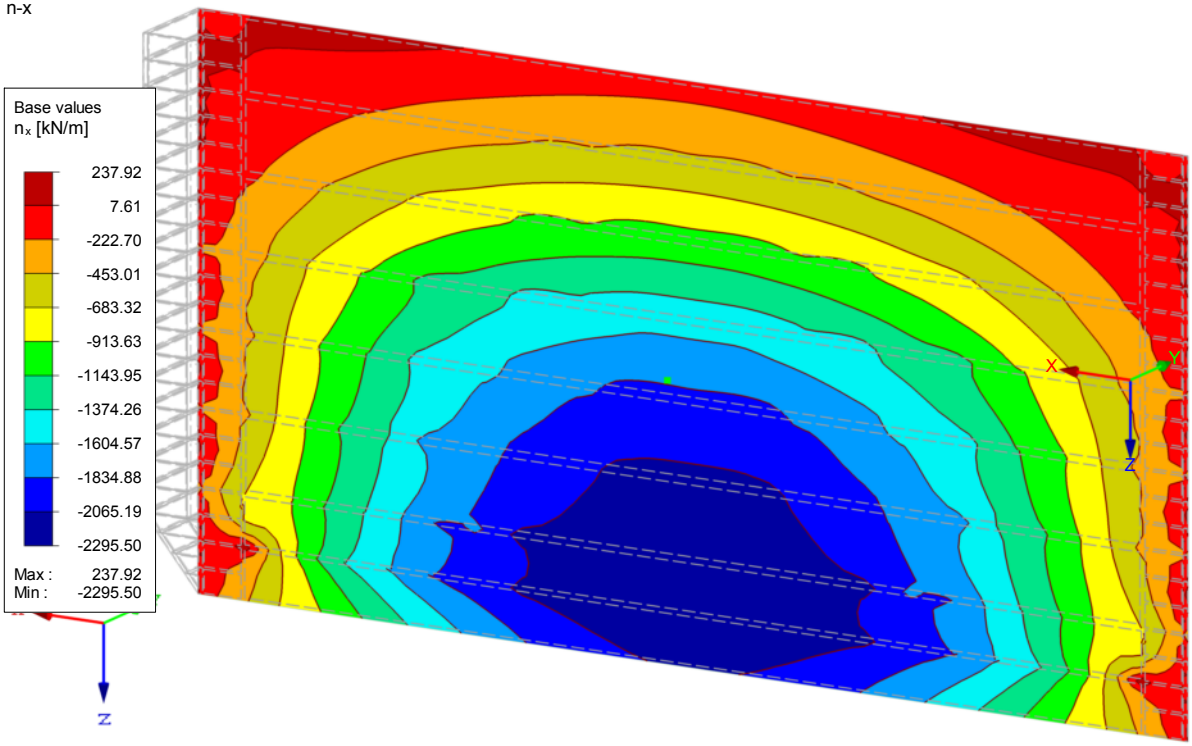
Max v-y: 372.59, Min v-y: -368.52 [kN/m]

Project: CIE5060 Model: V26
Graduation Project

BASE VALUES N_x, CO3: NEGATIVE DROP ULS, ISOMETRIC

CO3: Negative drop ULS
n-x

Isometric

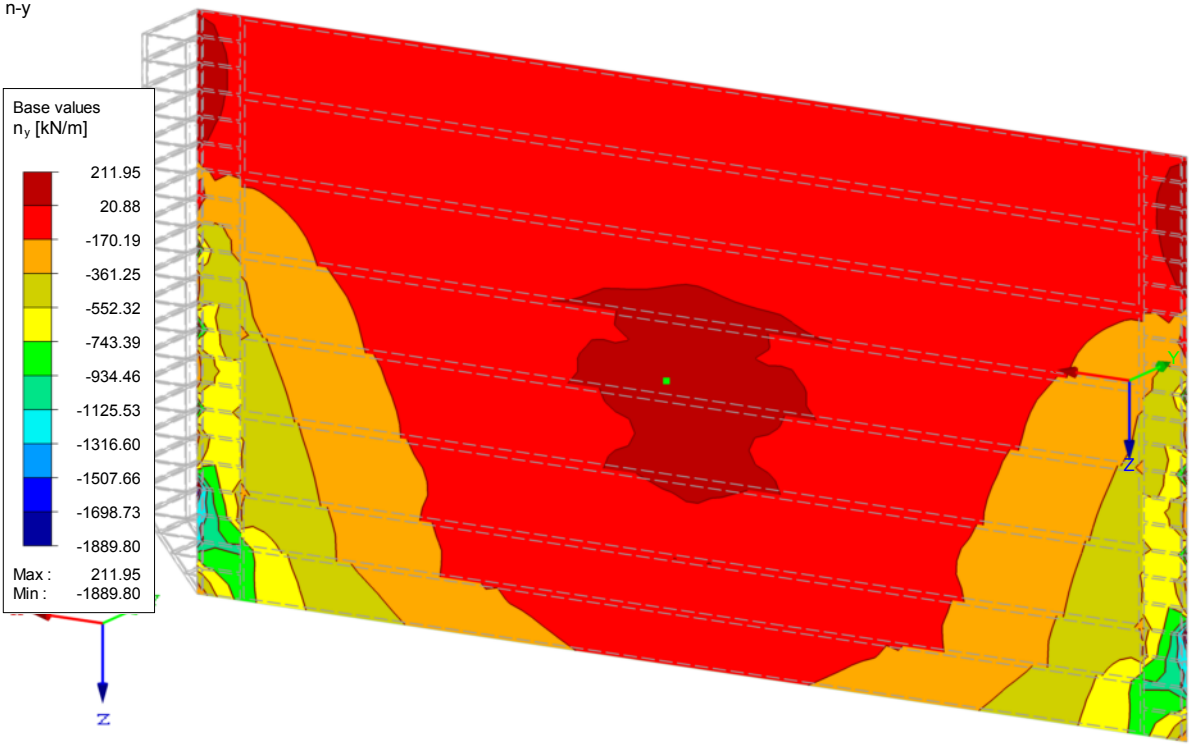


Max n-x: 237.92, Min n-x: -2295.50 [kN/m]

BASE VALUES N_y, CO3: NEGATIVE DROP ULS, ISOMETRIC

CO3: Negative drop ULS
n-y

Isometric



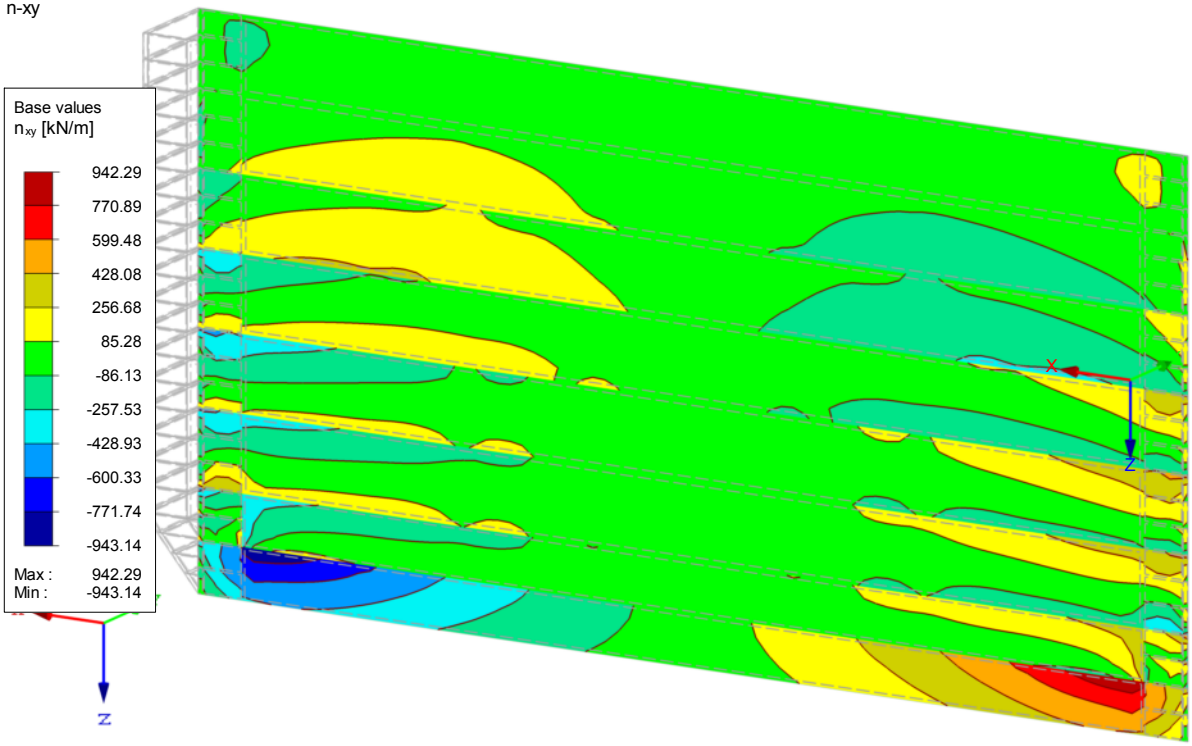
Max n-y: 211.95, Min n-y: -1889.80 [kN/m]

Project: CIE5060 Model: V26
Graduation Project

BASE VALUES N_{xy}, CO3: NEGATIVE DROP ULS, ISOMETRIC

CO3: Negative drop ULS
n-xy

Isometric

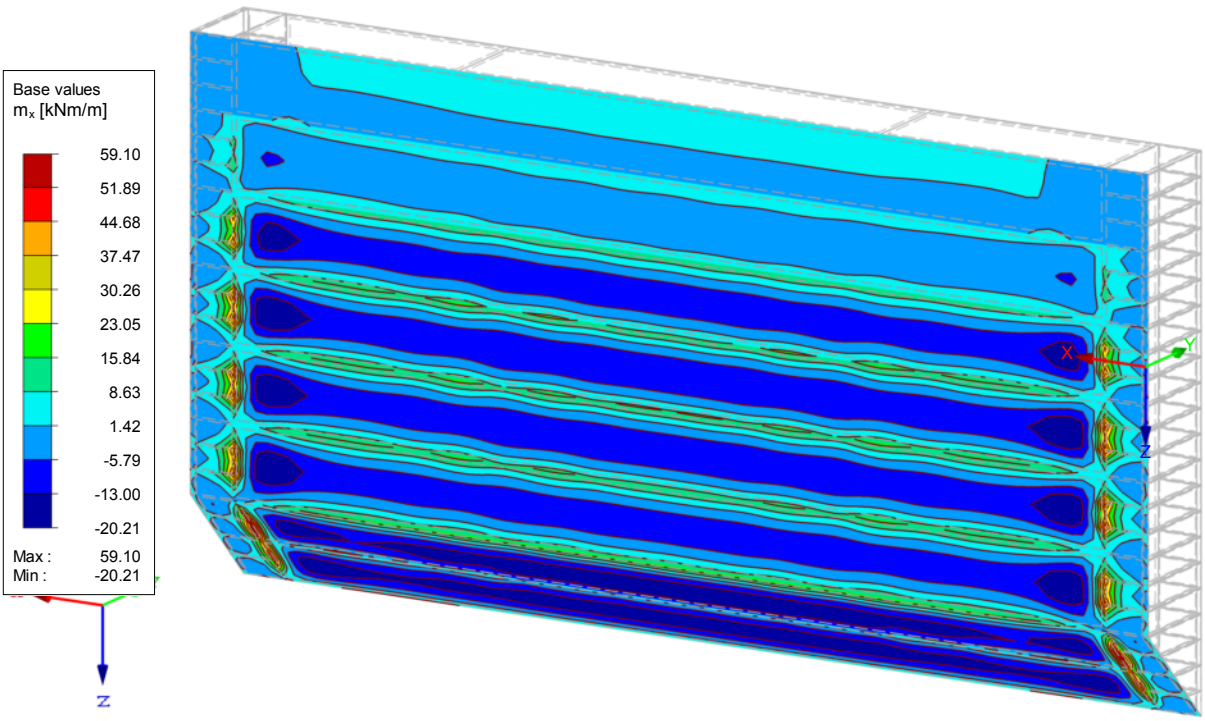


Max n-xy: 942.29, Min n-xy: -943.14 [kN/m]

BASE VALUES M_x, CO3: NEGATIVE DROP ULS, ISOMETRIC

CO3: Negative drop ULS
m-x

Isometric

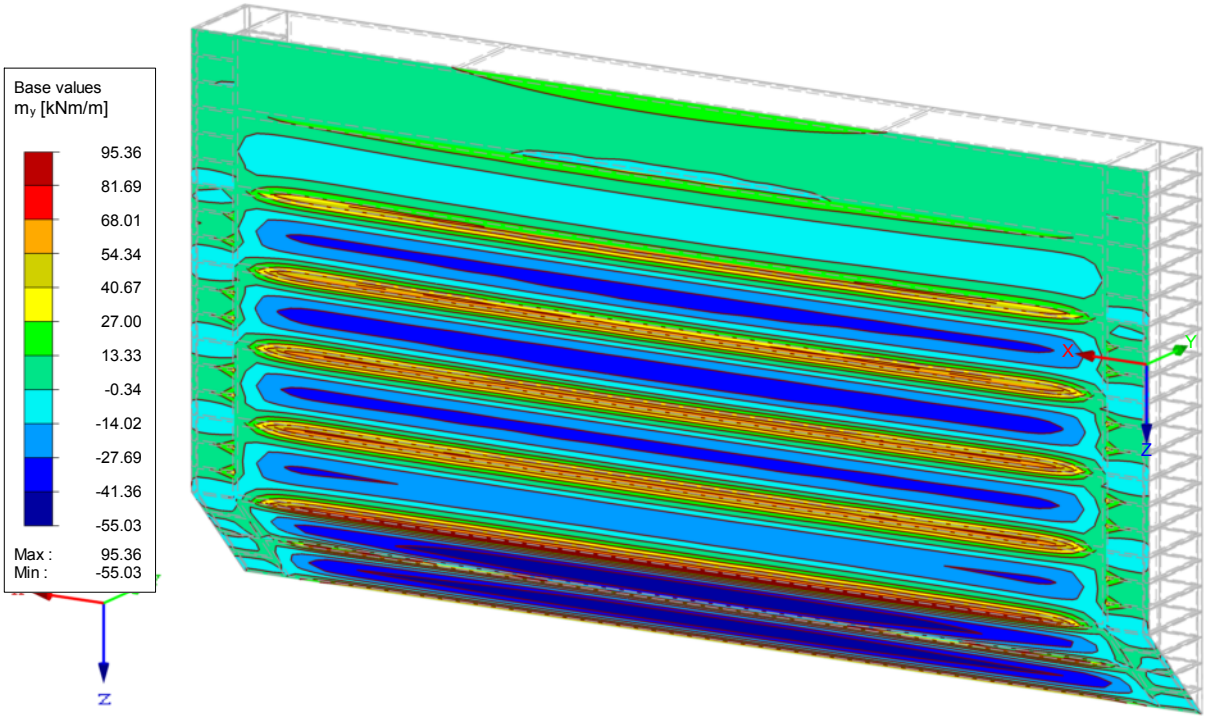


Max m-x: 59.10, Min m-x: -20.21 [kNm/m]

BASE VALUES M_y, CO3: NEGATIVE DROP ULS, ISOMETRIC

CO3: Negative drop ULS
m-y

Isometric

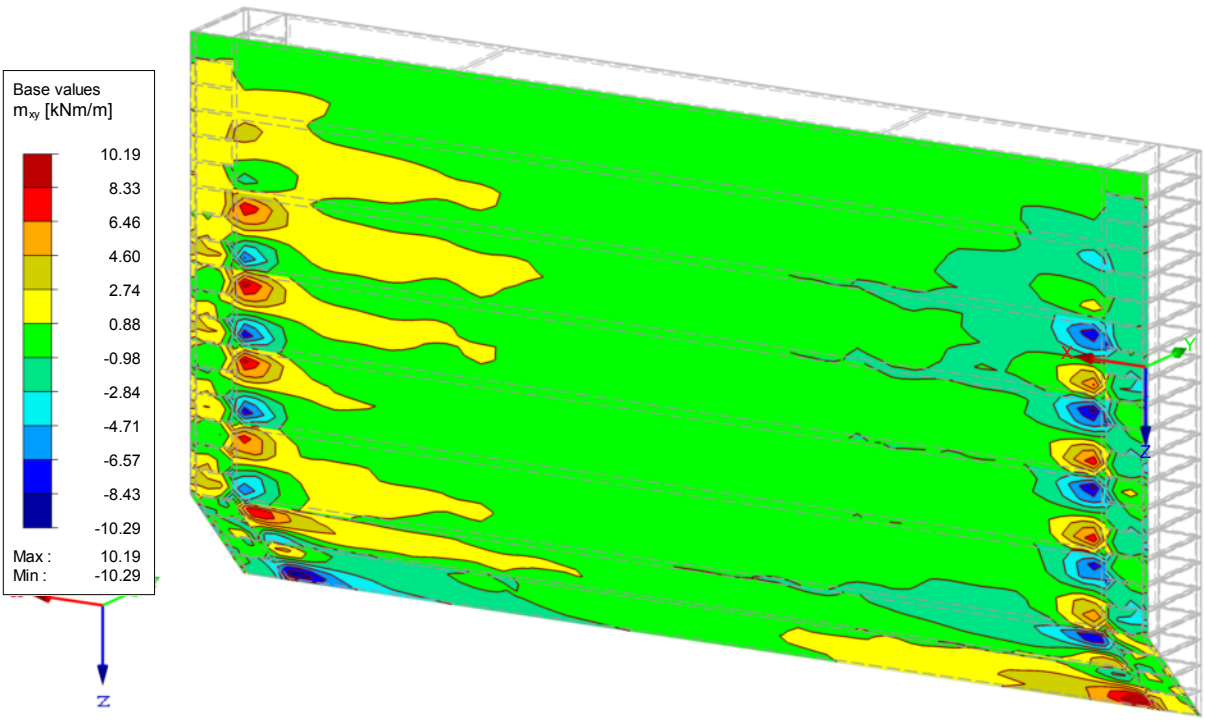


Max m-y: 95.36, Min m-y: -55.03 [kNm/m]

BASE VALUES M_{xy}, CO3: NEGATIVE DROP ULS, ISOMETRIC

CO3: Negative drop ULS
m-xy

Isometric



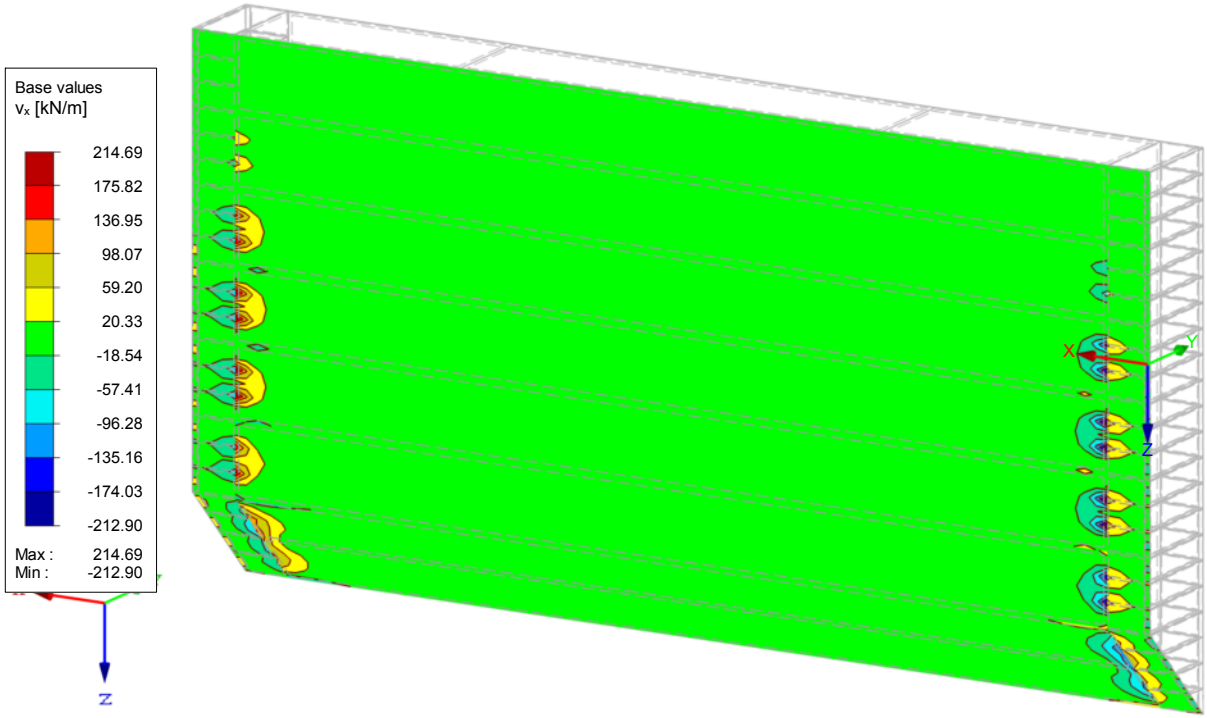
Max m-xy: 10.19, Min m-xy: -10.29 [kNm/m]

Project: CIE5060 Model: V26
Graduation Project

BASE VALUES V_x, CO3: NEGATIVE DROP ULS, ISOMETRIC

CO3: Negative drop ULS
v-x

Isometric

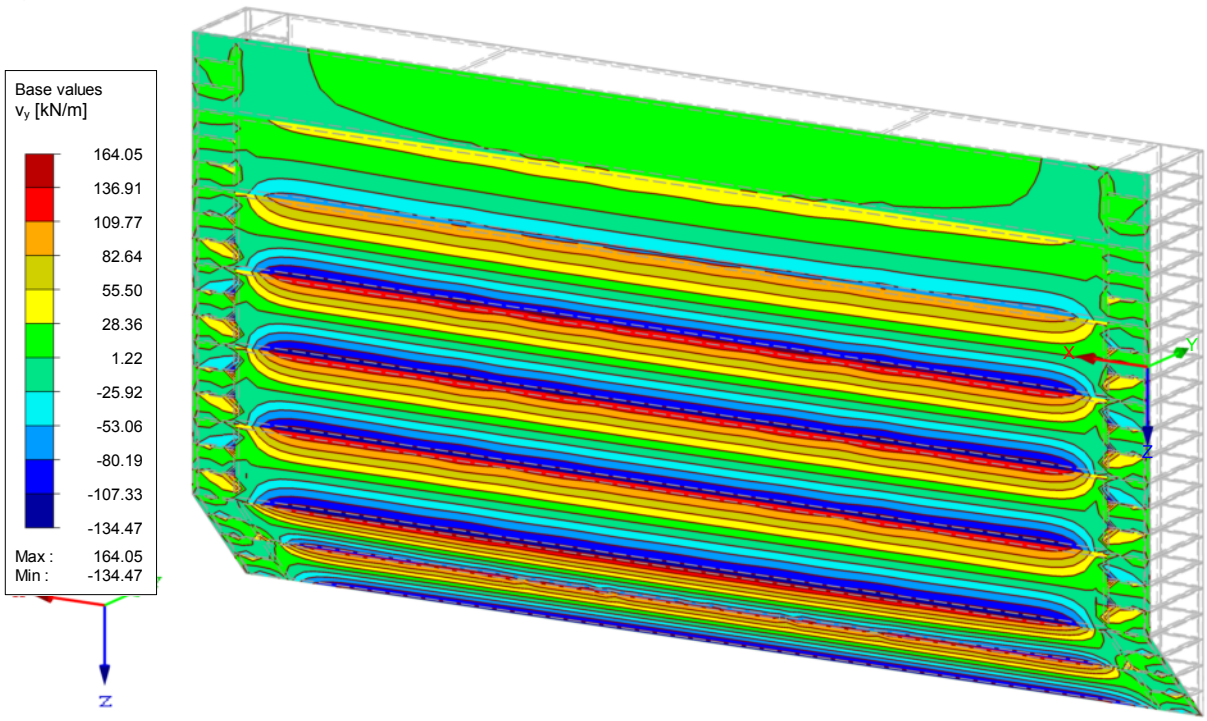


Max v-x: 214.69, Min v-x: -212.90 [kN/m]

BASE VALUES V_y, CO3: NEGATIVE DROP ULS, ISOMETRIC

CO3: Negative drop ULS
v-y

Isometric

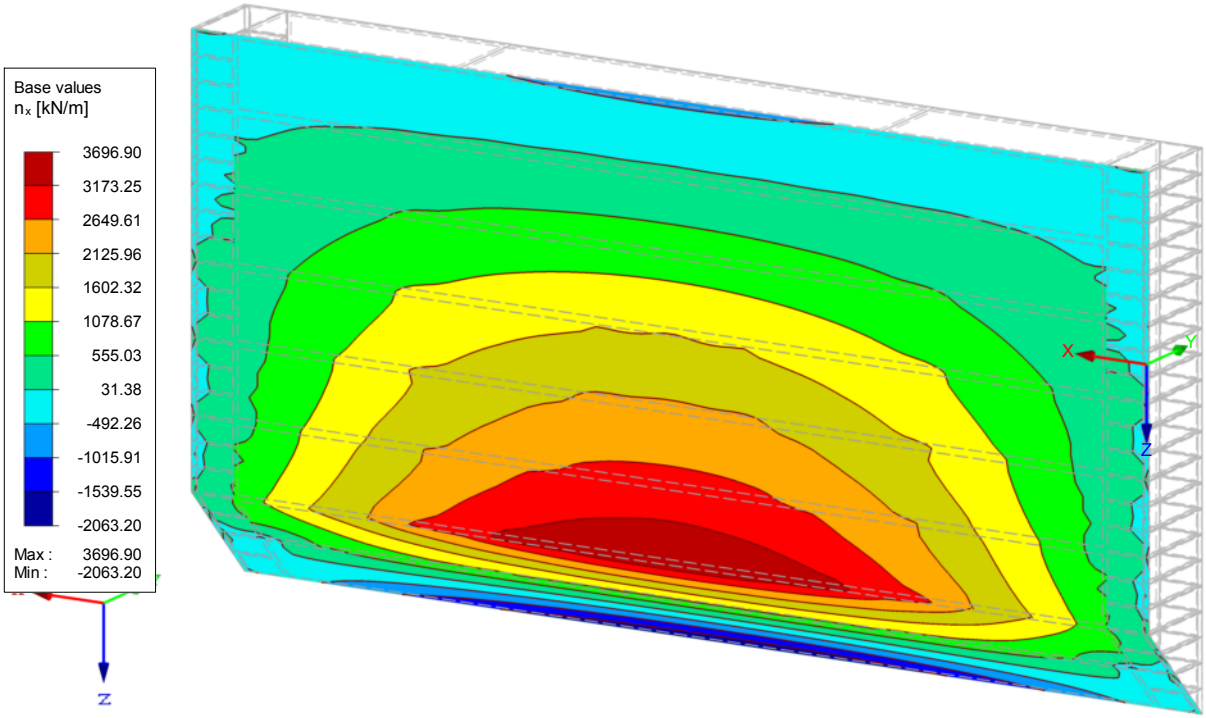


Max v-y: 164.05, Min v-y: -134.47 [kN/m]

BASE VALUES N_x, CO3: NEGATIVE DROP ULS, ISOMETRIC

CO3: Negative drop ULS
n-x

Isometric

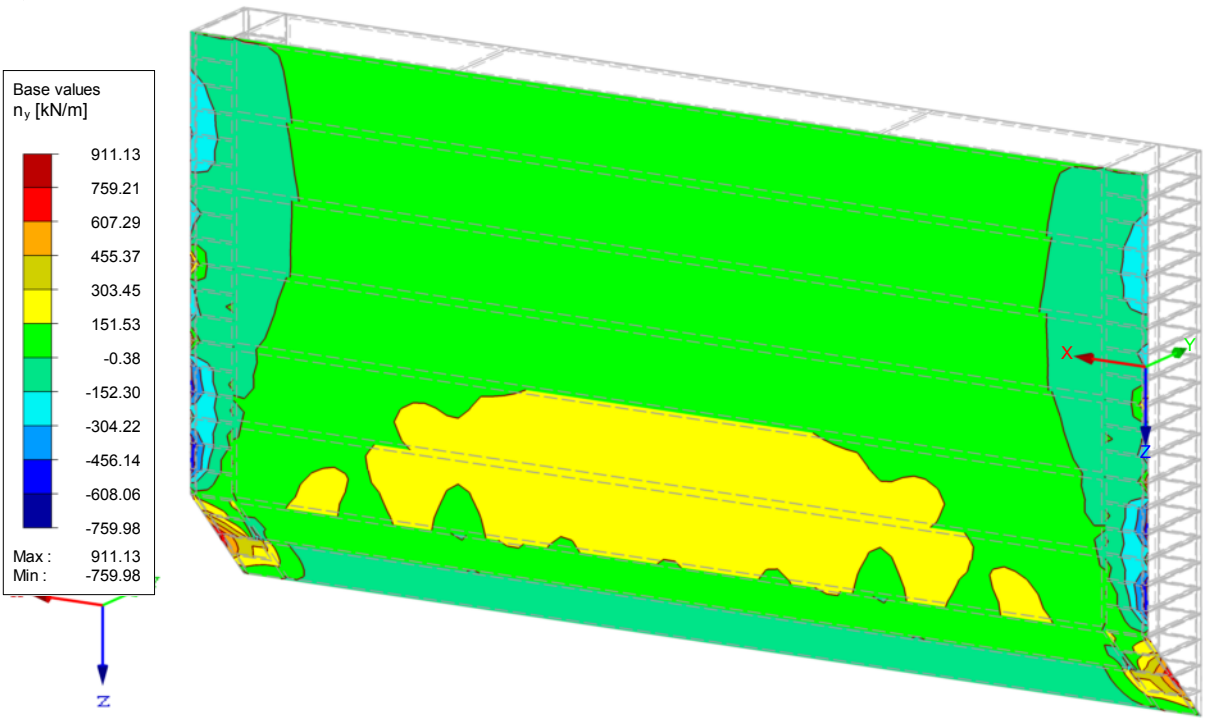


Max n-x: 3696.90, Min n-x: -2063.20 [kN/m]

BASE VALUES N_y, CO3: NEGATIVE DROP ULS, ISOMETRIC

CO3: Negative drop ULS
n-y

Isometric

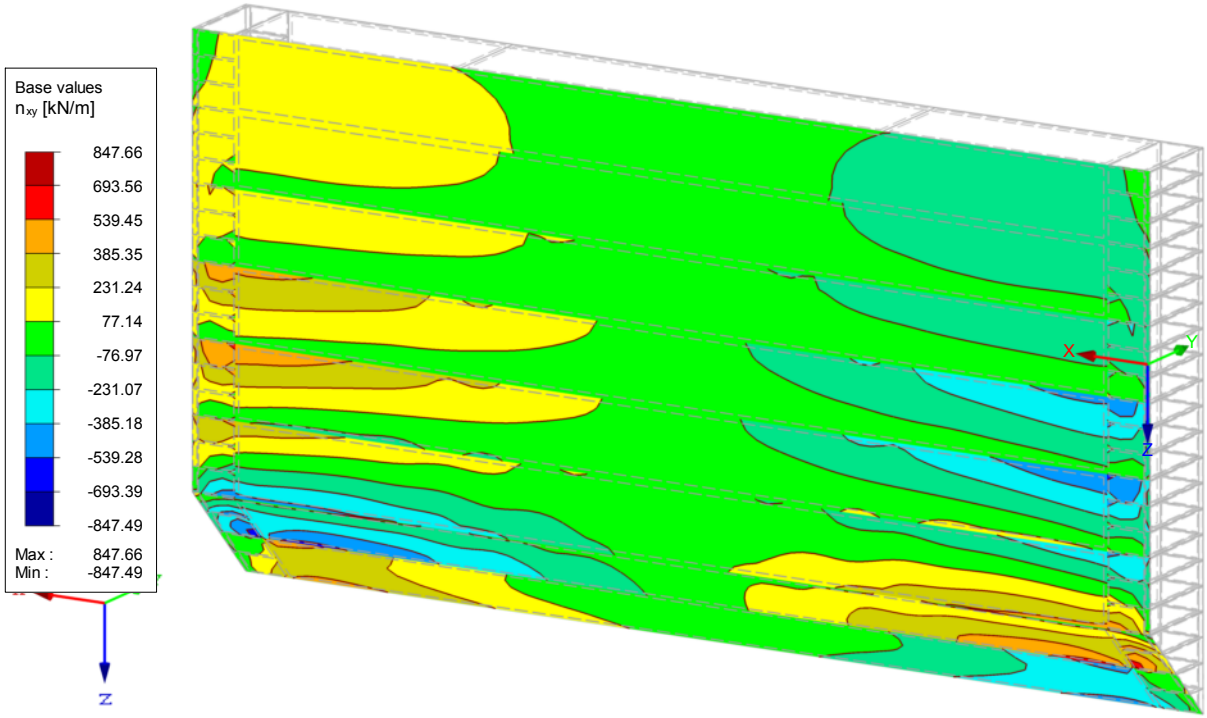


Max n-y: 911.13, Min n-y: -759.98 [kN/m]

BASE VALUES N_{xy}, CO3: NEGATIVE DROP ULS, ISOMETRIC

CO3: Negative drop ULS
n-xy

Isometric

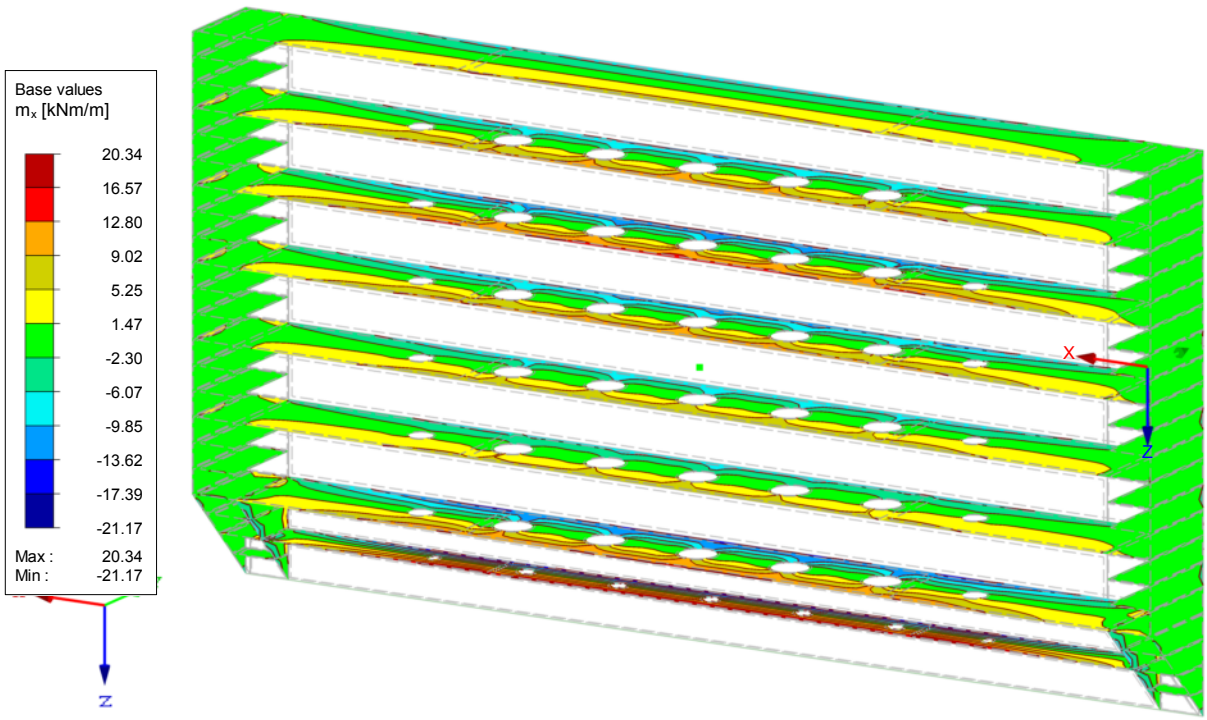


Max n-xy: 847.66, Min n-xy: -847.49 [kN/m]

BASE VALUES M_x, CO3: NEGATIVE DROP ULS, ISOMETRIC

CO3: Negative drop ULS
m-x

Isometric

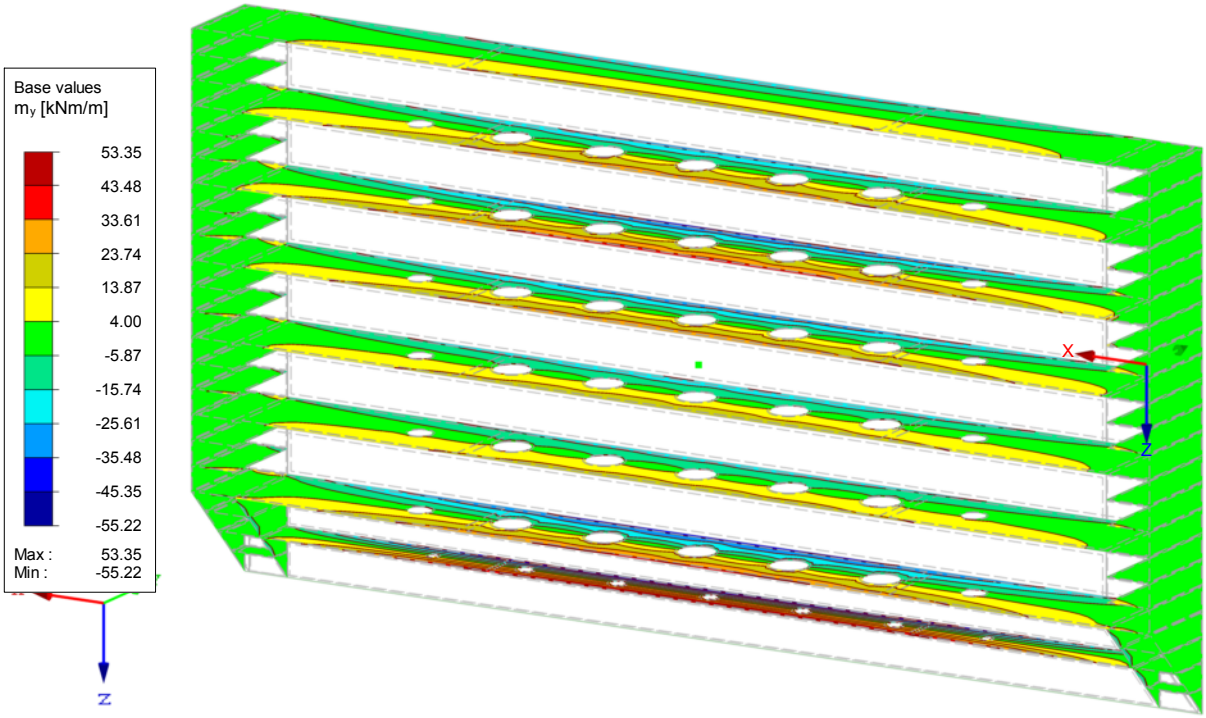


Max m-x: 20.34, Min m-x: -21.17 [kNm/m]

BASE VALUES M_y, CO3: NEGATIVE DROP ULS, ISOMETRIC

CO3: Negative drop ULS
m-y

Isometric

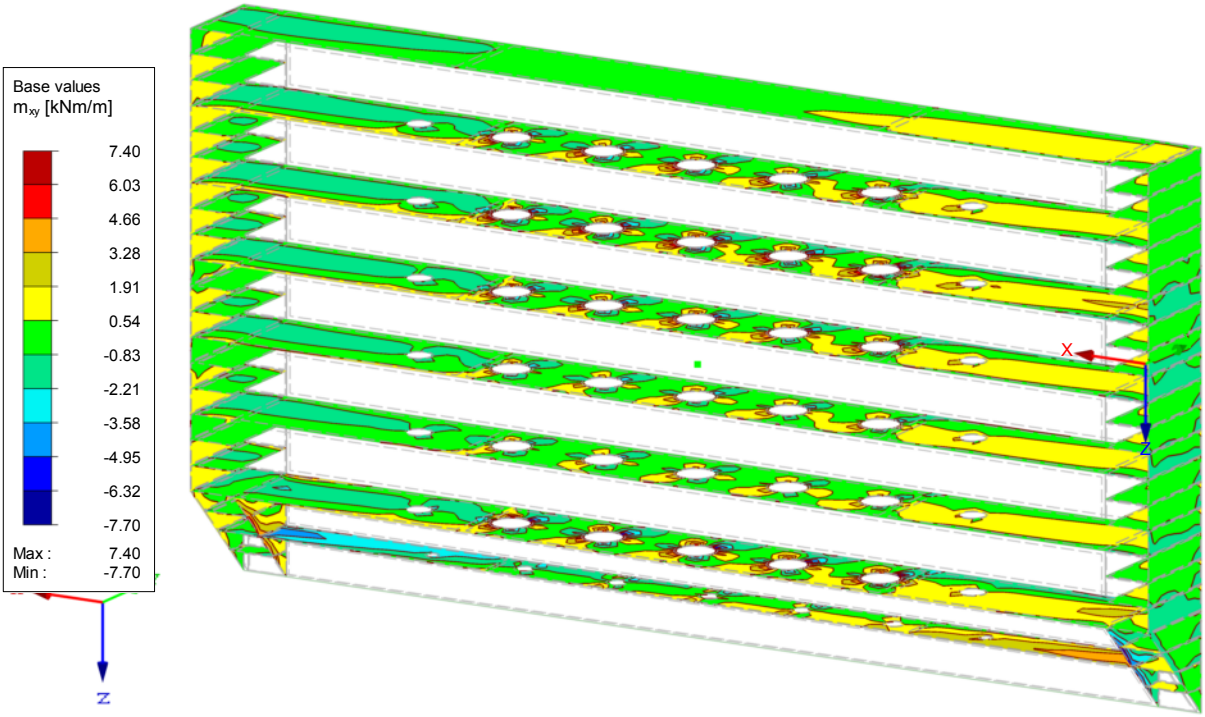


Max m-y: 53.35, Min m-y: -55.22 [kNm/m]

BASE VALUES M_{xy}, CO3: NEGATIVE DROP ULS, ISOMETRIC

CO3: Negative drop ULS
m-xy

Isometric

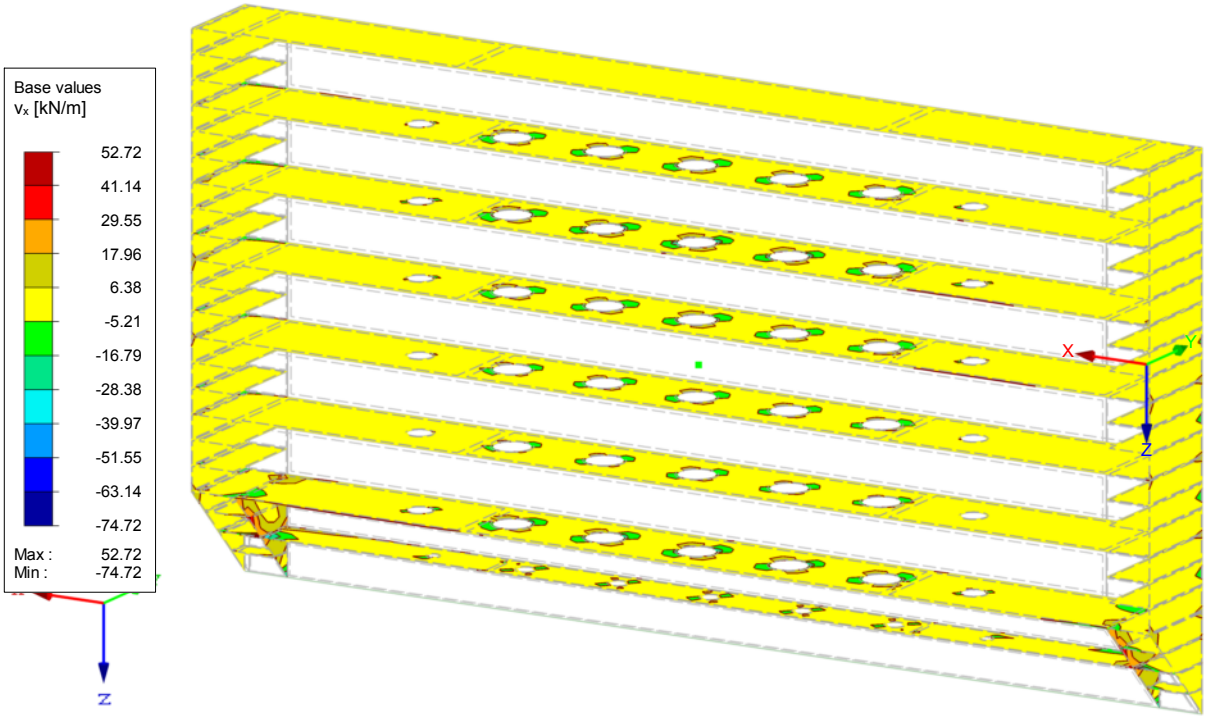


Max m-xy: 7.40, Min m-xy: -7.70 [kNm/m]

BASE VALUES V_x, CO3: NEGATIVE DROP ULS, ISOMETRIC

CO3: Negative drop ULS
v-x

Isometric

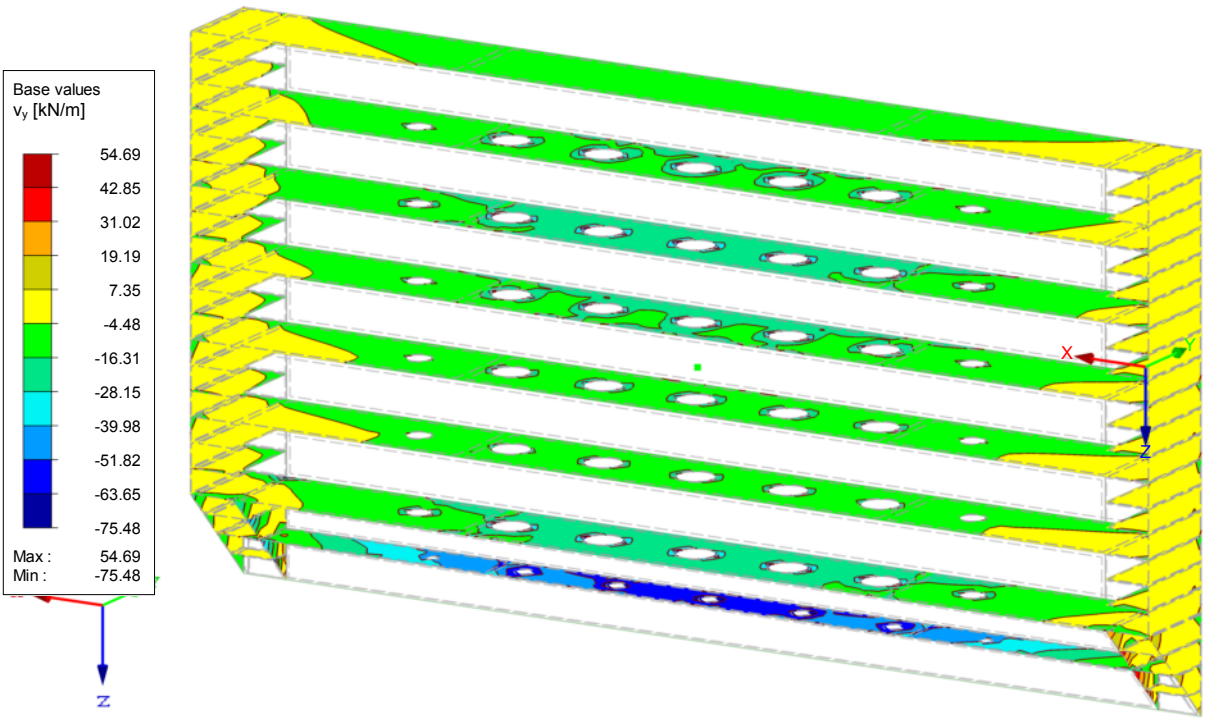


Max v-x: 52.72, Min v-x: -74.72 [kN/m]

BASE VALUES V_y, CO3: NEGATIVE DROP ULS, ISOMETRIC

CO3: Negative drop ULS
v-y

Isometric

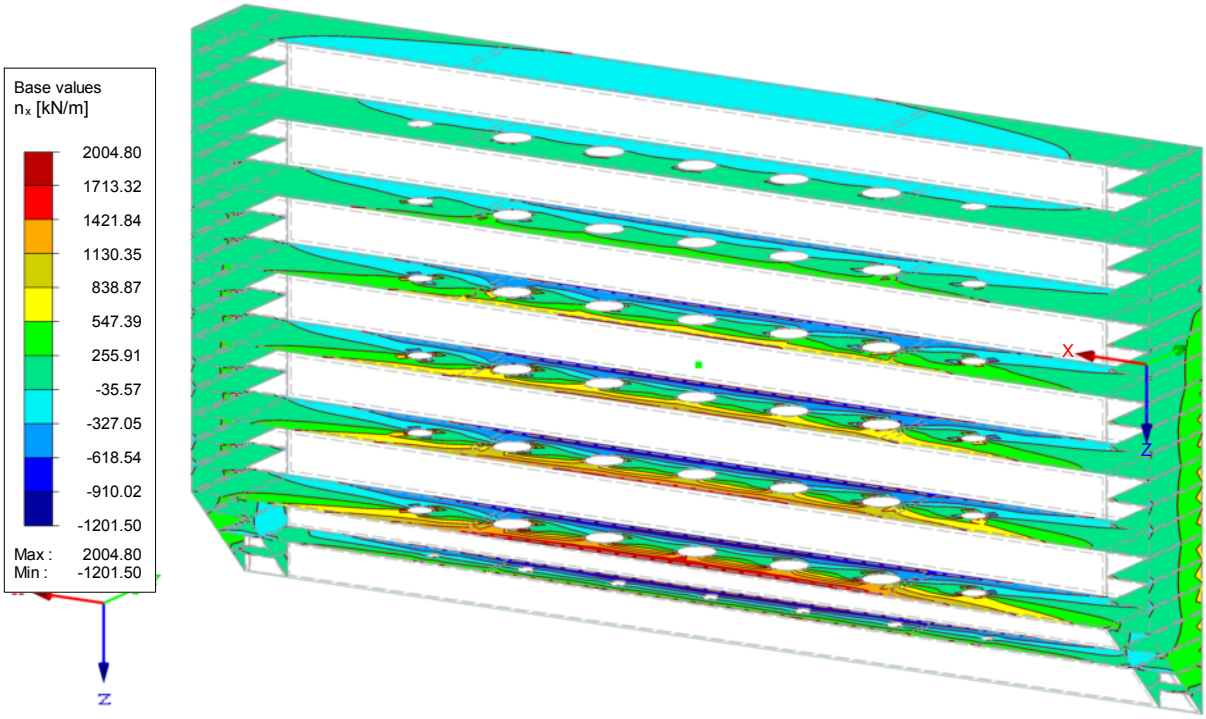


Max v-y: 54.69, Min v-y: -75.48 [kN/m]

BASE VALUES N_x, CO3: NEGATIVE DROP ULS, ISOMETRIC

CO3: Negative drop ULS
n-x

Isometric

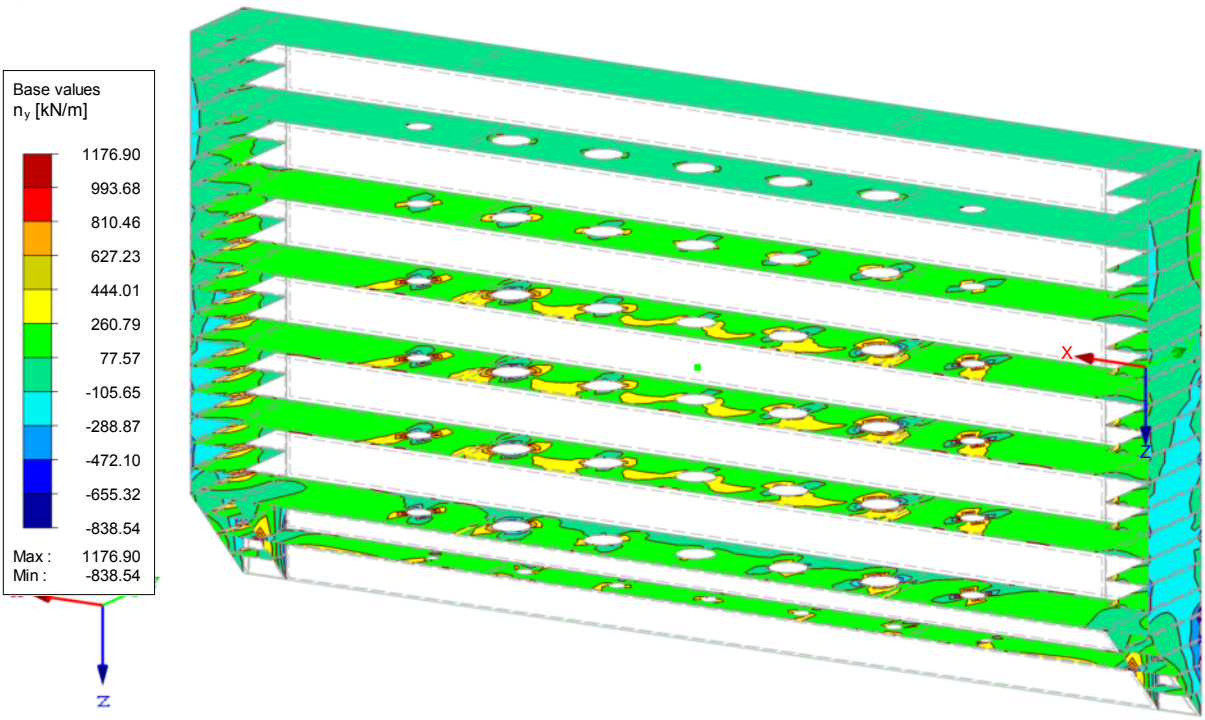


Max n-x: 2004.80, Min n-x: -1201.50 [kN/m]

BASE VALUES N_y, CO3: NEGATIVE DROP ULS, ISOMETRIC

CO3: Negative drop ULS
n-y

Isometric



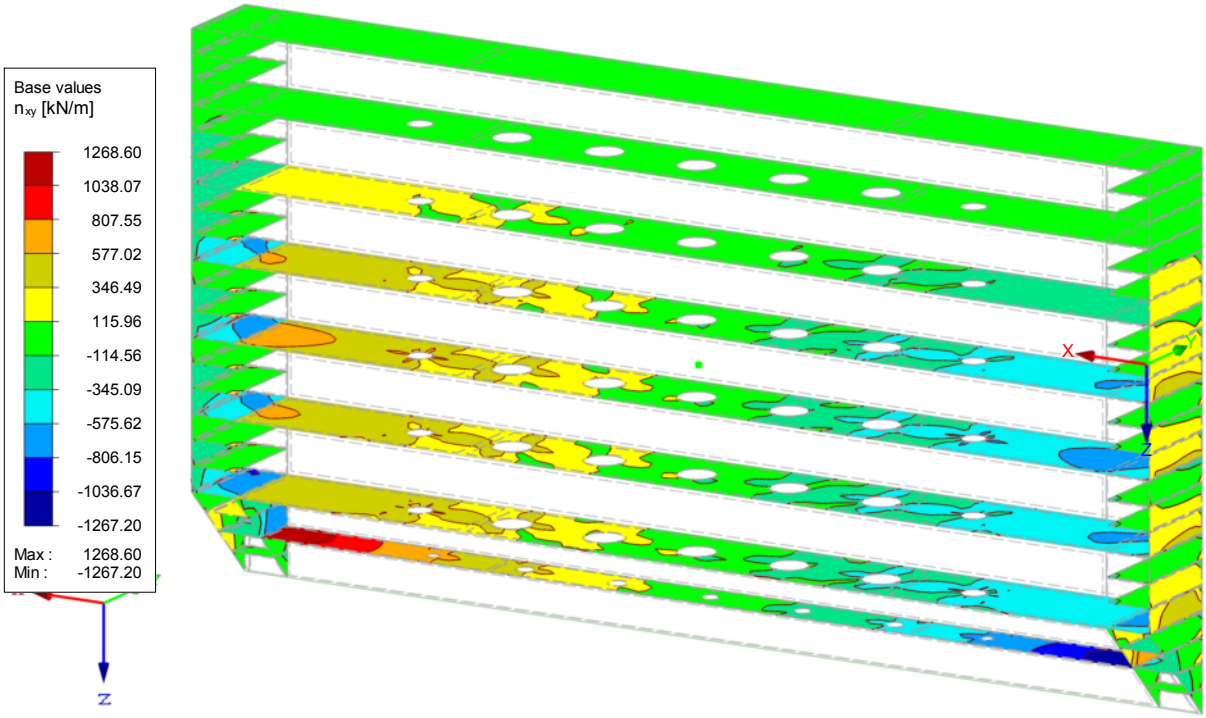
Max n-y: 1176.90, Min n-y: -838.54 [kN/m]

Project: CIE5060 Model: V26
Graduation Project

BASE VALUES N_{xy}, CO3: NEGATIVE DROP ULS, ISOMETRIC

CO3: Negative drop ULS
n-xy

Isometric

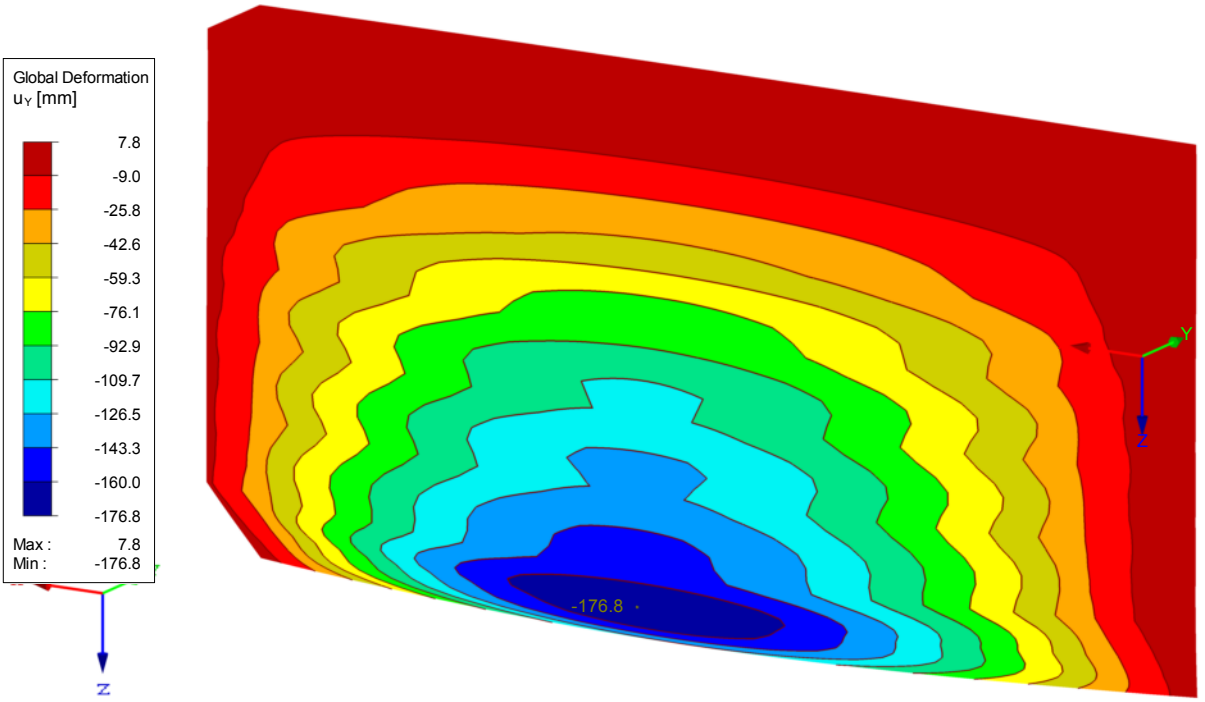


Max n-xy: 1268.60, Min n-xy: -1267.20 [kN/m]

GLOBAL DEFORMATION U_Y, CO4: NEGATIVE DROP SLS, ISOMETRIC

CO4: Negative drop SLS
u-Y

Isometric

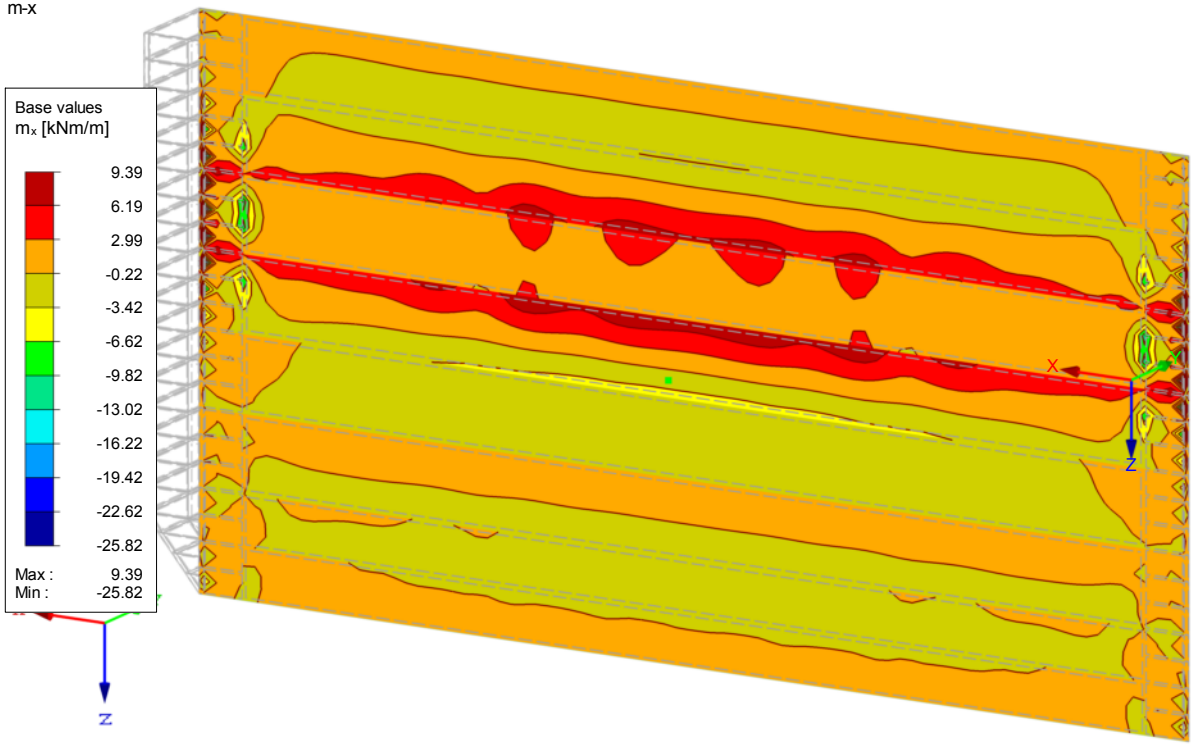


Max u-Y: 7.8, Min u-Y: -176.8 [mm]
Factor of deformations: 24.00

BASE VALUES M_x, CO5: ICE, ISOMETRIC

CO5: Ice
m-x

Isometric

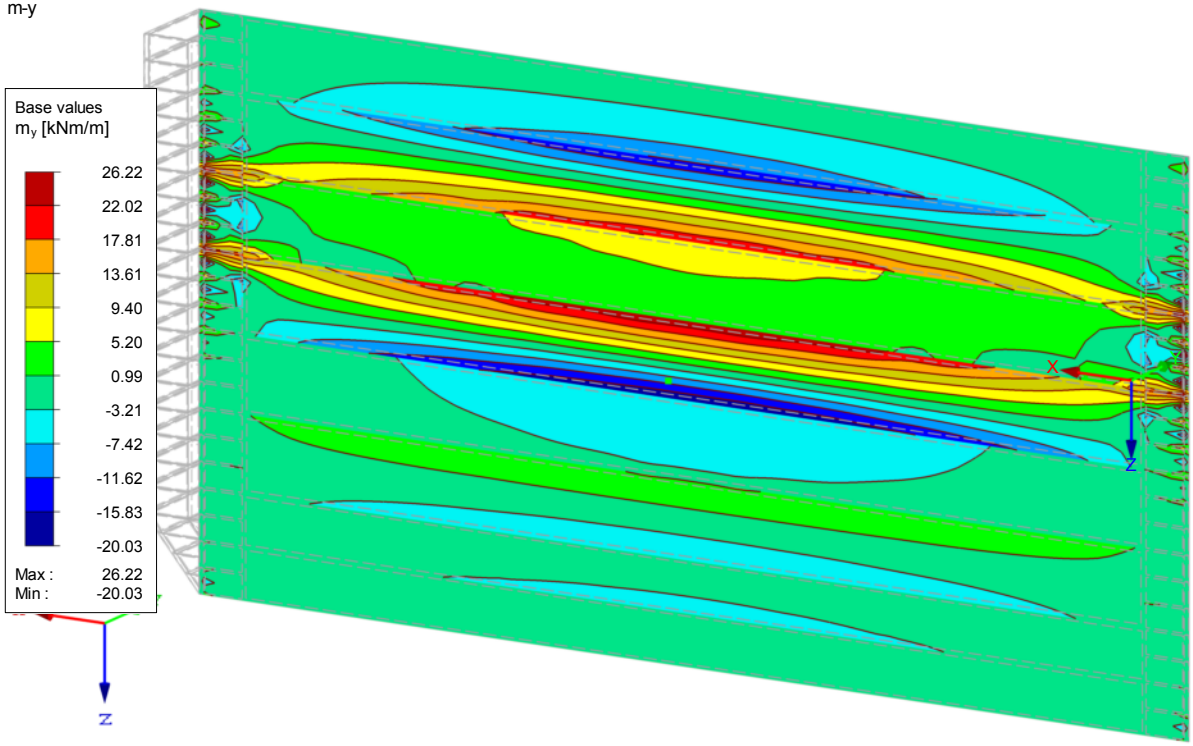


Max m-x: 9.39, Min m-x: -25.82 [kNm/m]

BASE VALUES M_y, CO5: ICE, ISOMETRIC

CO5: Ice
m-y

Isometric

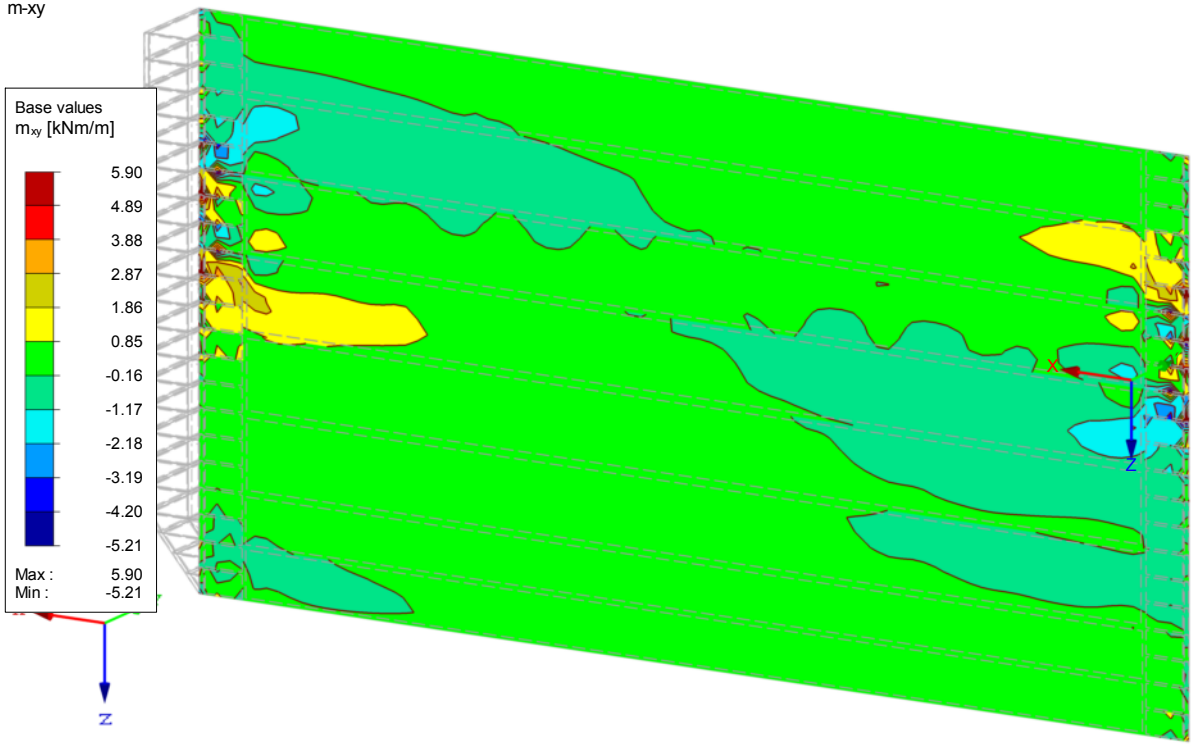


Max m-y: 26.22, Min m-y: -20.03 [kNm/m]

BASE VALUES M_{xy}, CO5: ICE, ISOMETRIC

CO5: Ice
m-xy

Isometric

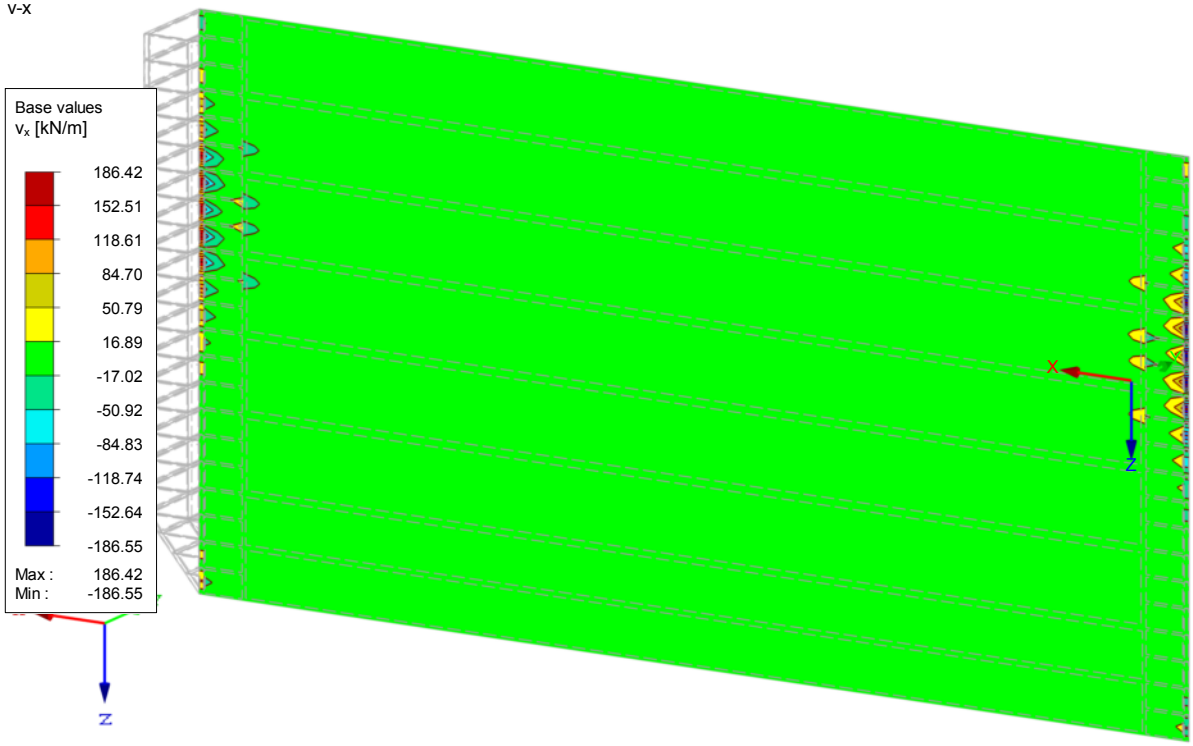


Max m-xy: 5.90, Min m-xy: -5.21 [kNm/m]

BASE VALUES V_x, CO5: ICE, ISOMETRIC

CO5: Ice
v-x

Isometric



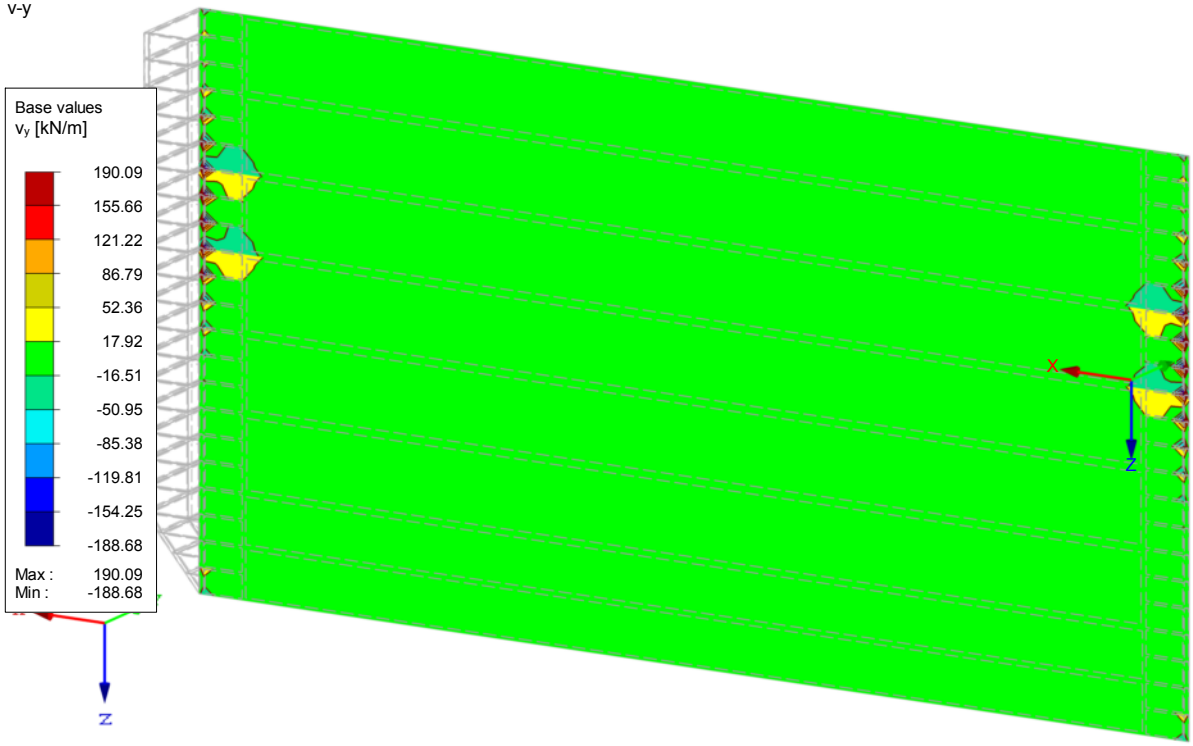
Max v-x: 186.42, Min v-x: -186.55 [kN/m]

Project: CIE5060 Model: V26
Graduation Project

BASE VALUES V_y, CO5: ICE, ISOMETRIC

CO5: Ice
v-y

Isometric

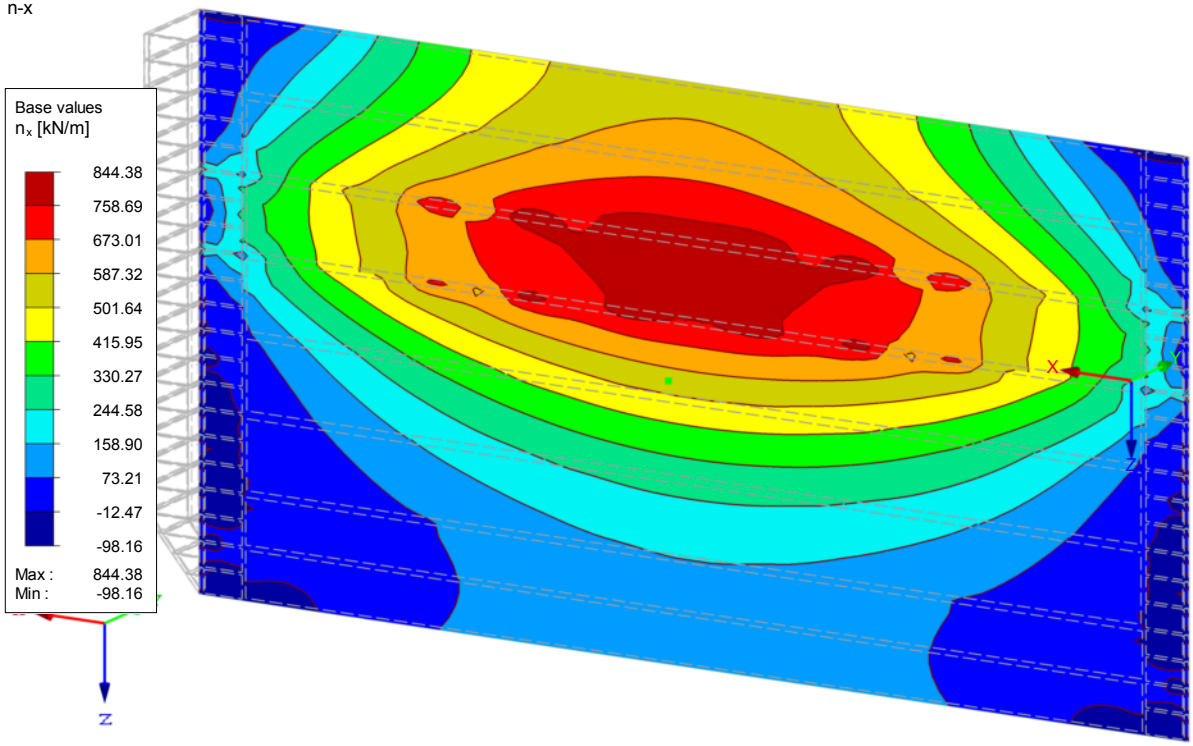


Max v-y: 190.09, Min v-y: -188.68 [kN/m]

BASE VALUES N_x, CO5: ICE, ISOMETRIC

CO5: Ice
n-x

Isometric

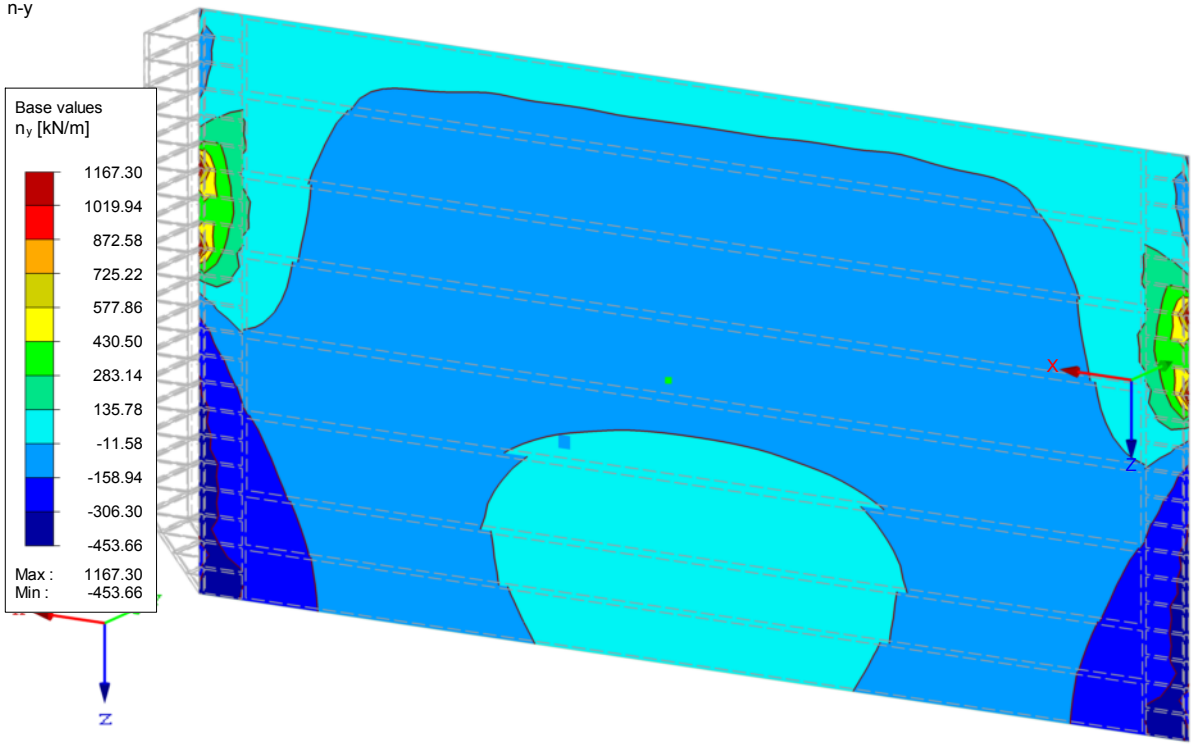


Max n-x: 844.38, Min n-x: -98.16 [kN/m]

BASE VALUES N_y, CO5: ICE, ISOMETRIC

CO5: Ice
n-y

Isometric

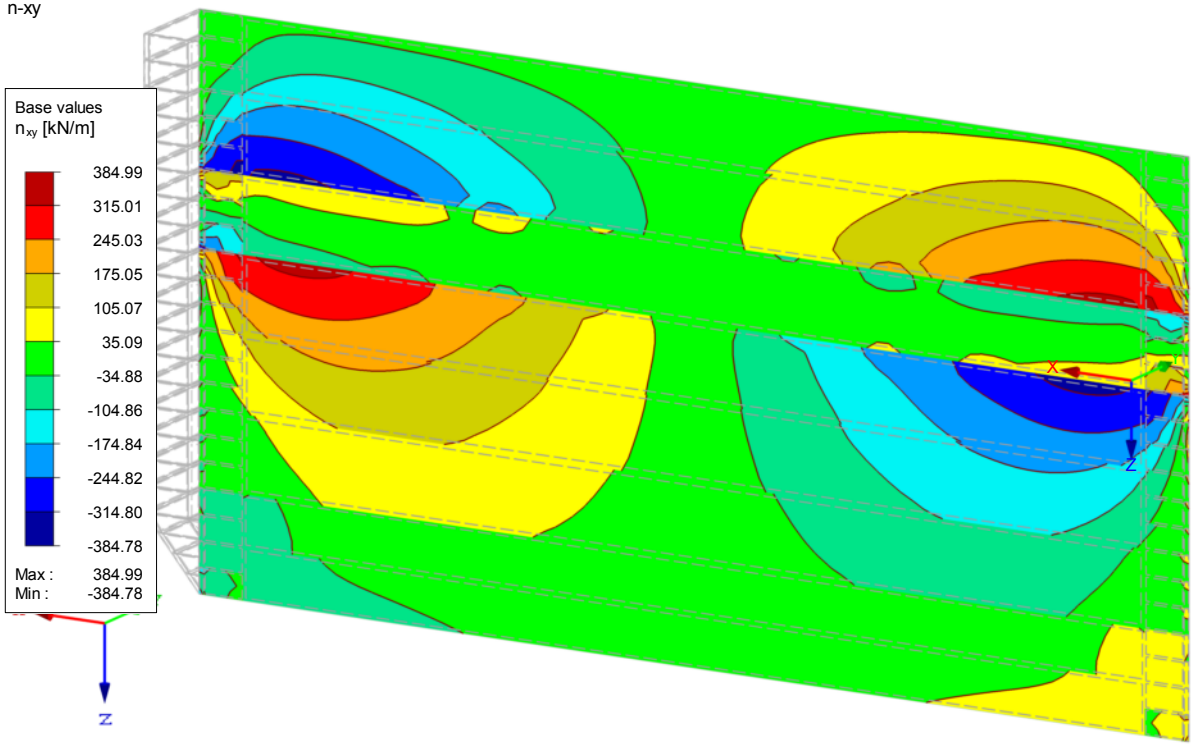


Max n-y: 1167.30, Min n-y: -453.66 [kN/m]

BASE VALUES N_{xy}, CO5: ICE, ISOMETRIC

CO5: Ice
n-xy

Isometric

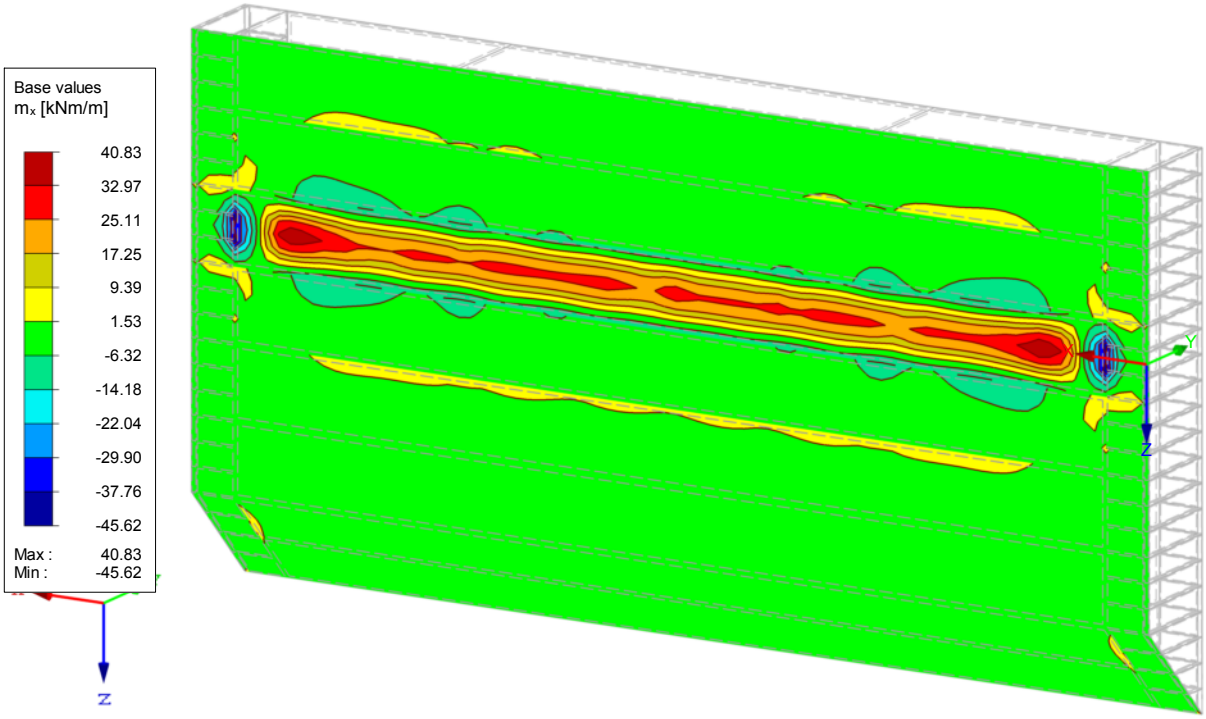


Max n-xy: 384.99, Min n-xy: -384.78 [kN/m]

BASE VALUES M_x, CO5: ICE, ISOMETRIC

CO5: Ice
m-x

Isometric

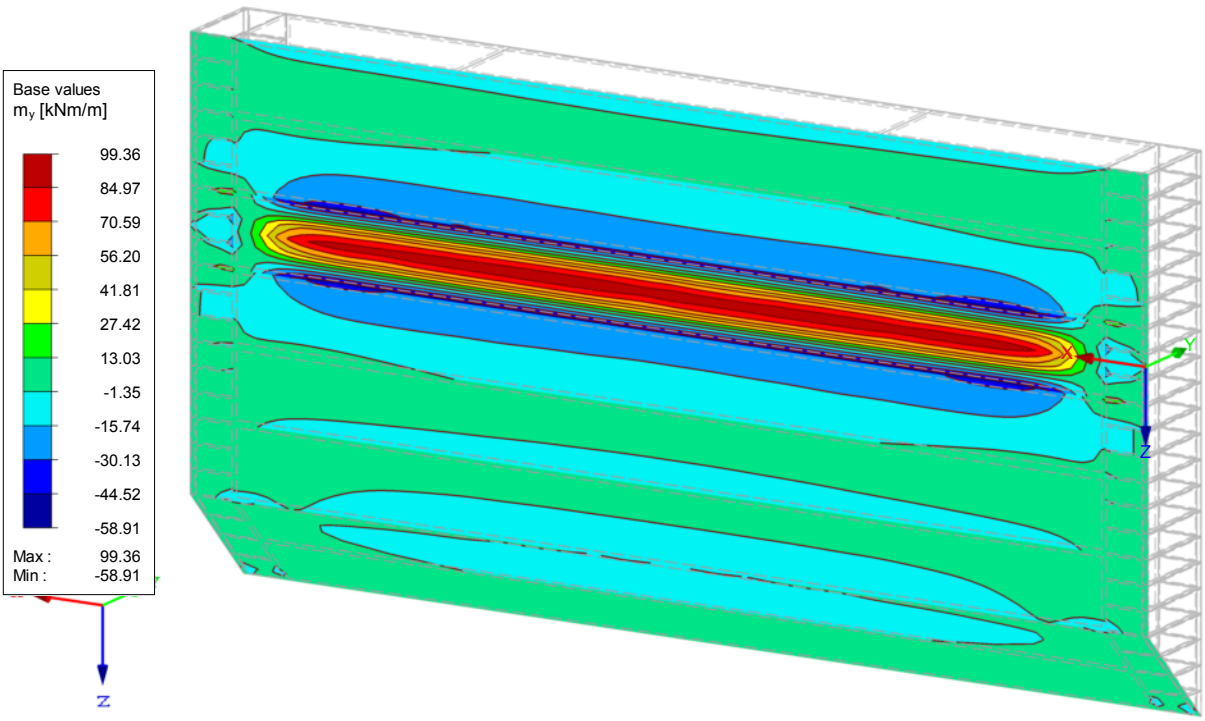


Max m-x: 40.83, Min m-x: -45.62 [kNm/m]

BASE VALUES M_y, CO5: ICE, ISOMETRIC

CO5: Ice
m-y

Isometric

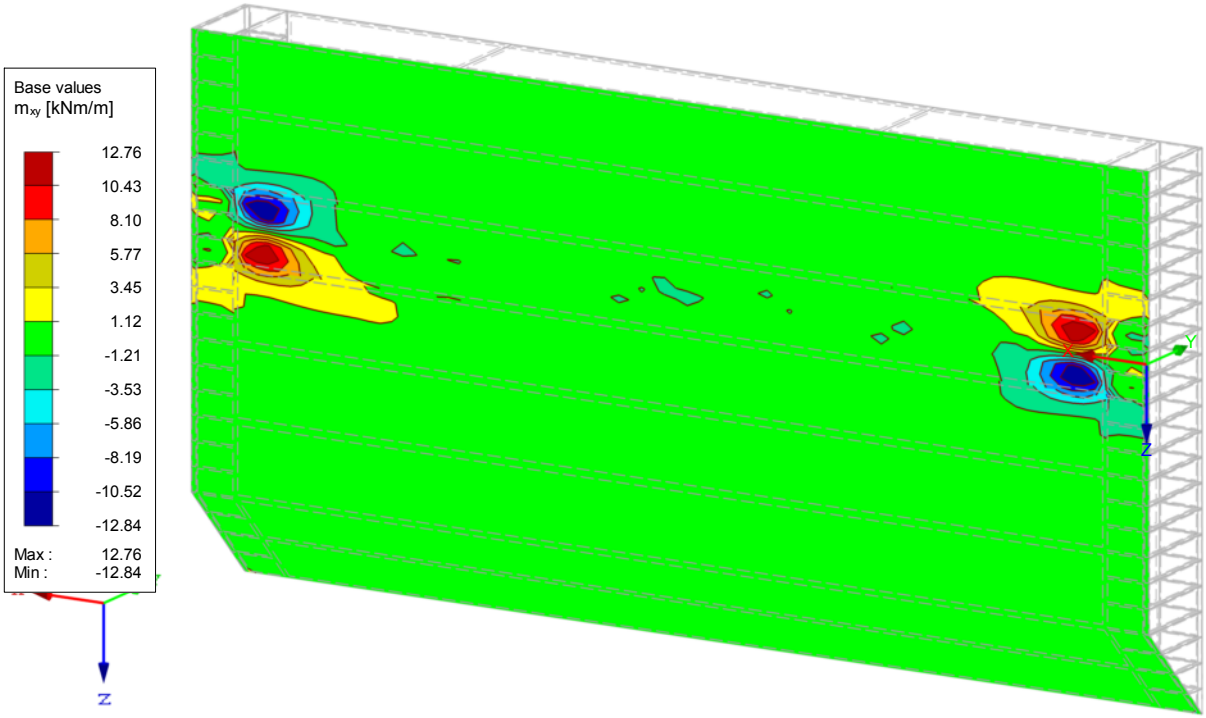


Max m-y: 99.36, Min m-y: -58.91 [kNm/m]

BASE VALUES M_{xy}, CO5: ICE, ISOMETRIC

CO5: Ice
m-xy

Isometric

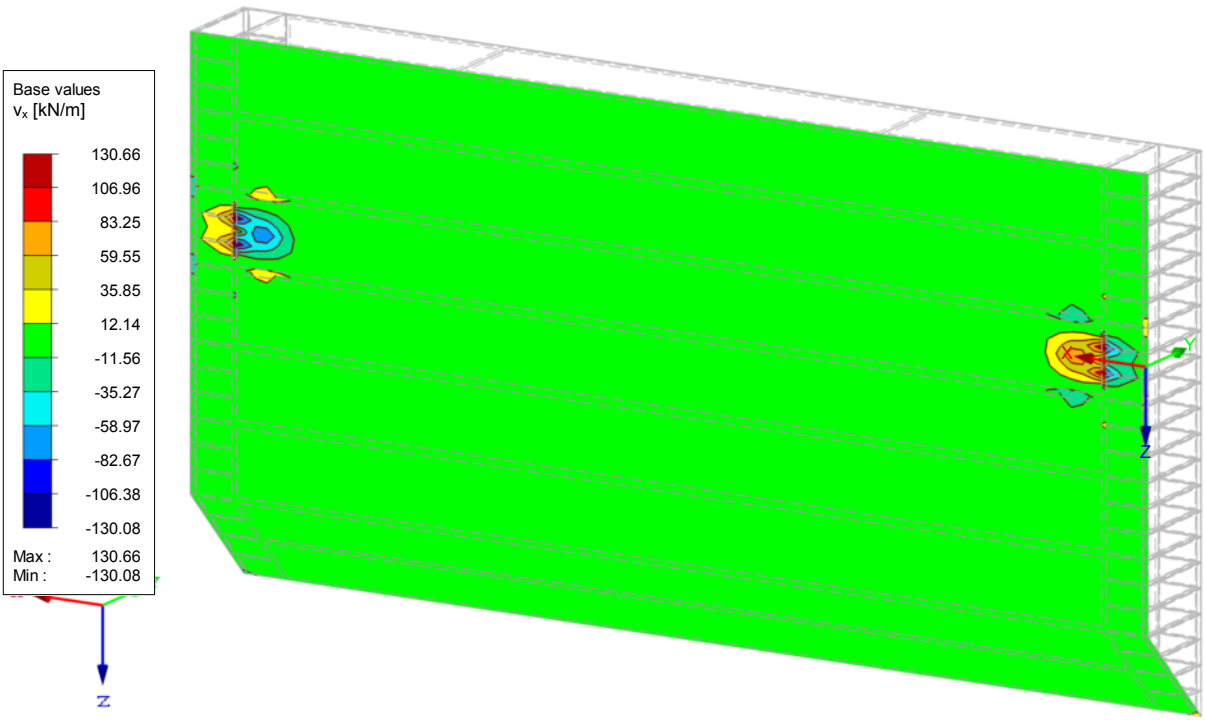


Max m-xy: 12.76, Min m-xy: -12.84 [kNm/m]

BASE VALUES V_x, CO5: ICE, ISOMETRIC

CO5: Ice
v-x

Isometric

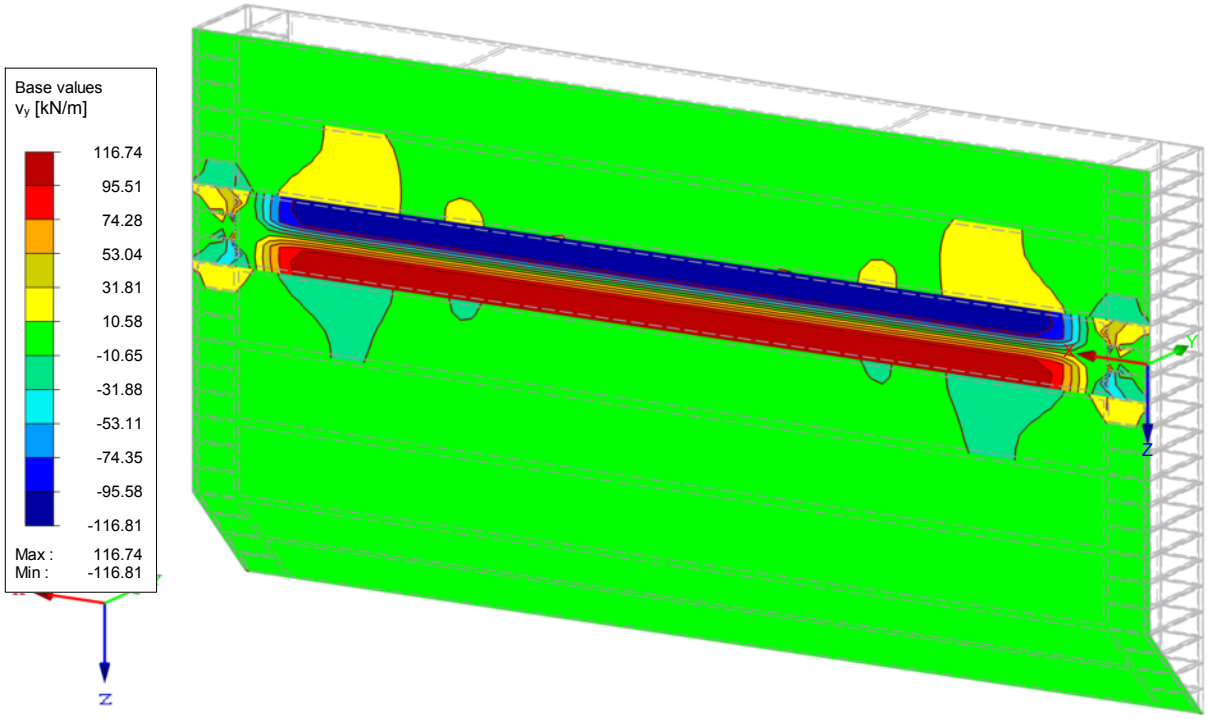


Max v-x: 130.66, Min v-x: -130.08 [kN/m]

BASE VALUES V_y, CO5: ICE, ISOMETRIC

CO5: Ice
v-y

Isometric

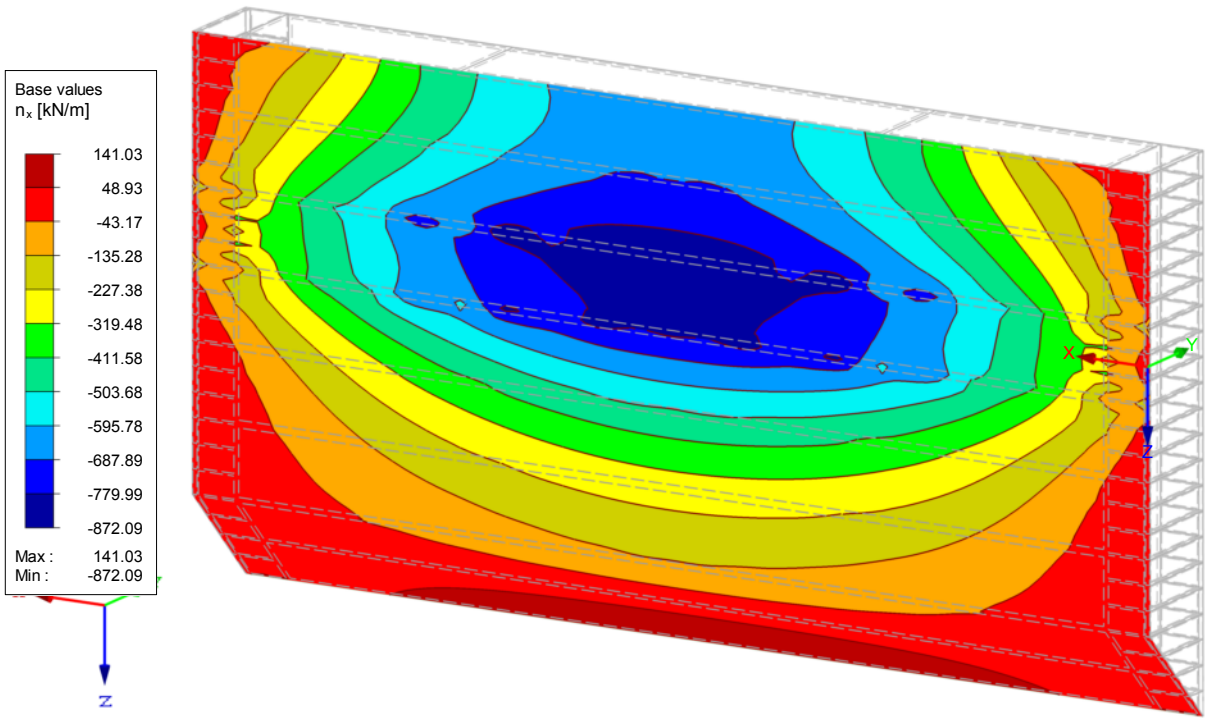


Max v-y: 116.74, Min v-y: -116.81 [kN/m]

BASE VALUES N_x, CO5: ICE, ISOMETRIC

CO5: Ice
n-x

Isometric



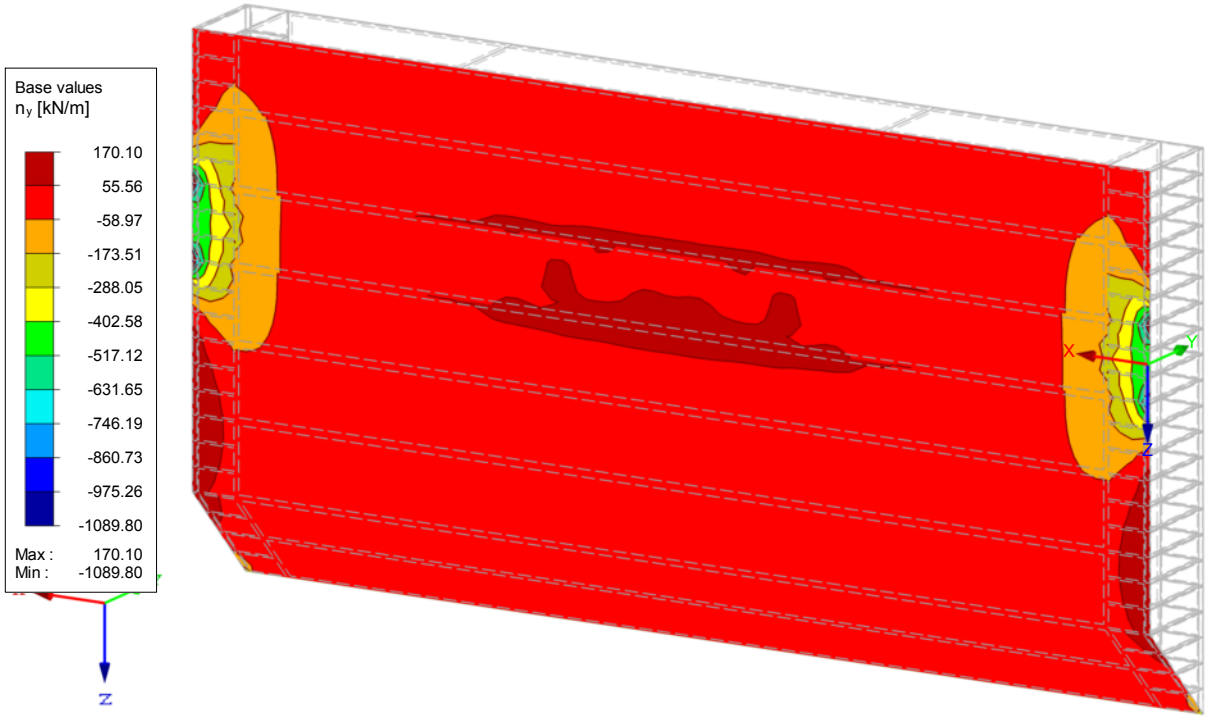
Max n-x: 141.03, Min n-x: -872.09 [kN/m]

Project: CIE5060 Model: V26
Graduation Project

BASE VALUES N_y, CO5: ICE, ISOMETRIC

CO5: Ice
n-y

Isometric

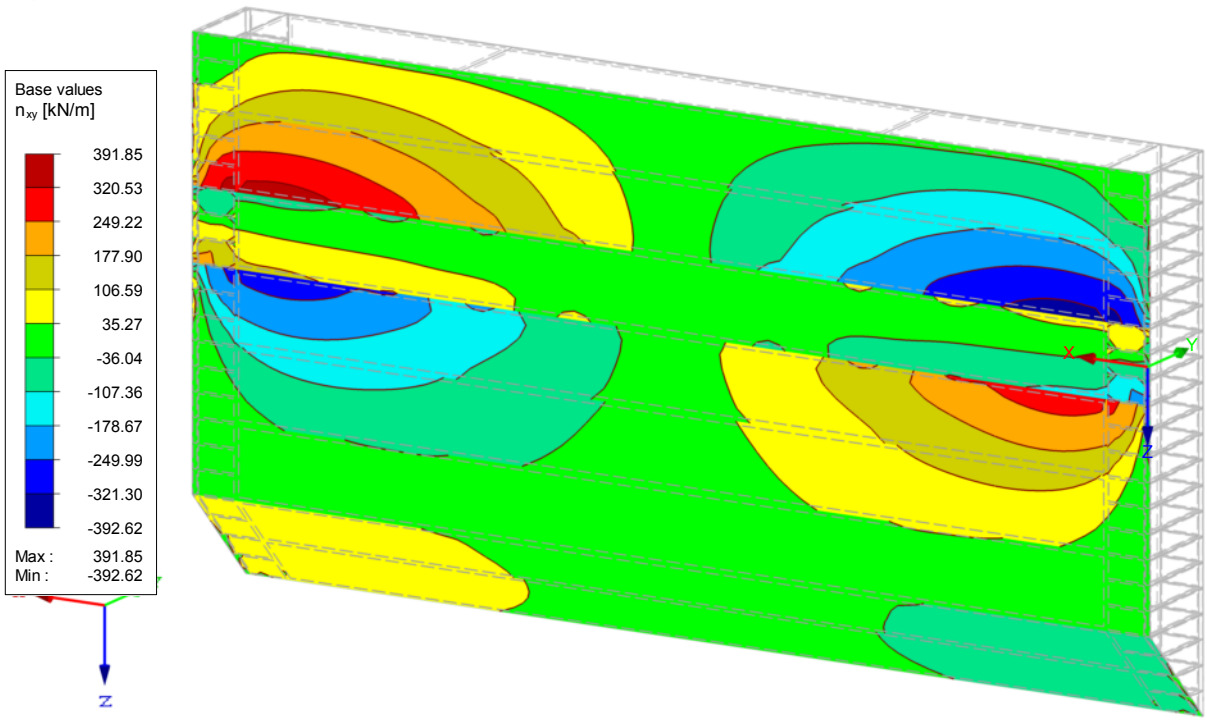


Max n-y: 170.10, Min n-y: -1089.80 [kN/m]

BASE VALUES N_{xy}, CO5: ICE, ISOMETRIC

CO5: Ice
n-xy

Isometric

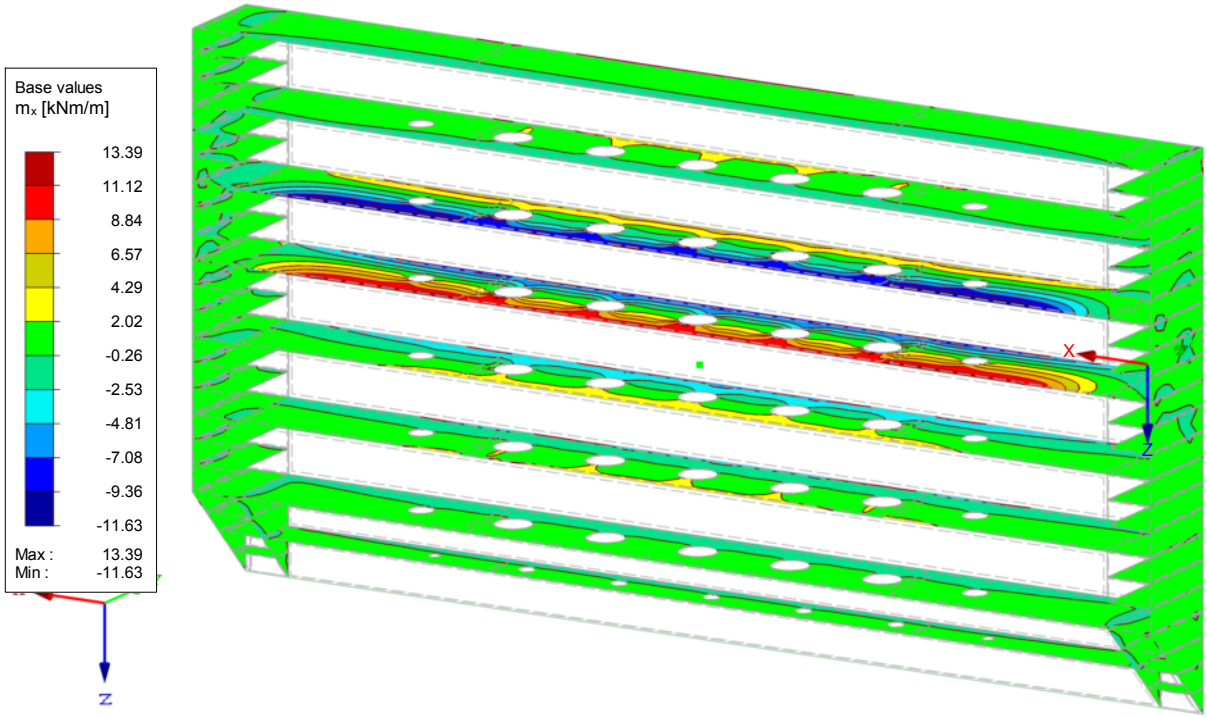


Max n-xy: 391.85, Min n-xy: -392.62 [kN/m]

BASE VALUES M_x, CO5: ICE, ISOMETRIC

CO5: Ice
m-x

Isometric

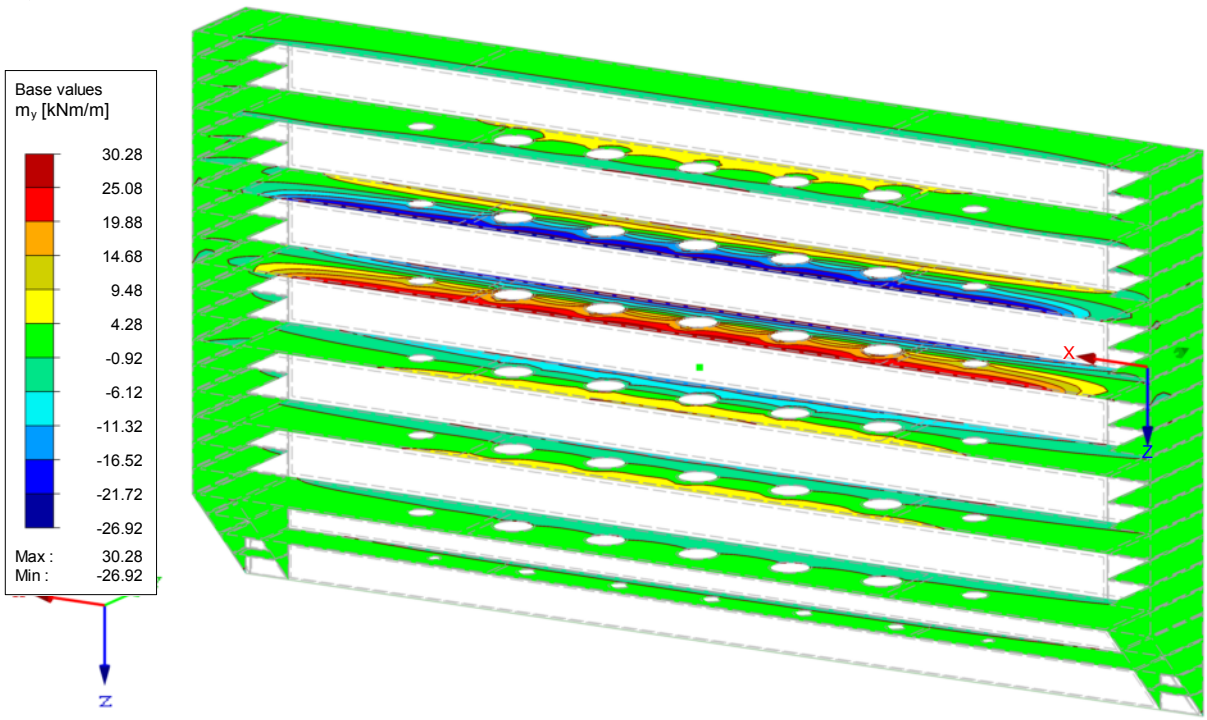


Max m-x: 13.39, Min m-x: -11.63 [kNm/m]

BASE VALUES M_y, CO5: ICE, ISOMETRIC

CO5: Ice
m-y

Isometric

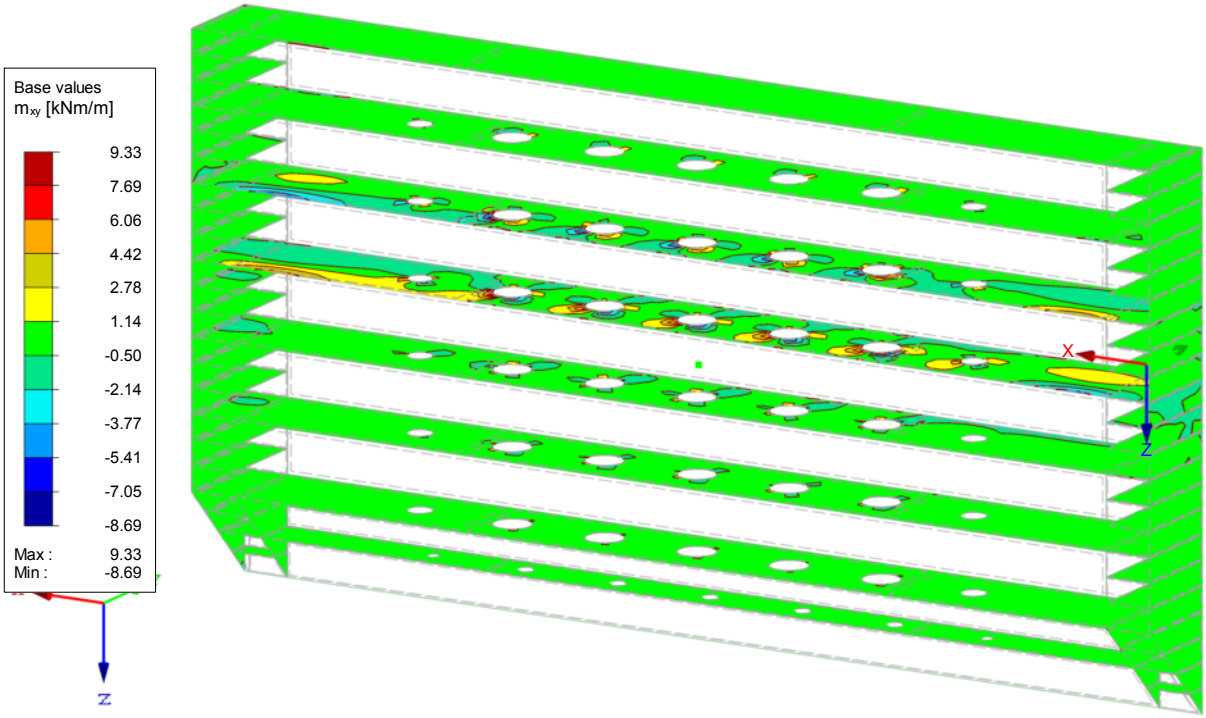


Max m-y: 30.28, Min m-y: -26.92 [kNm/m]

BASE VALUES M_{xy}, CO5: ICE, ISOMETRIC

CO5: Ice
m-xy

Isometric

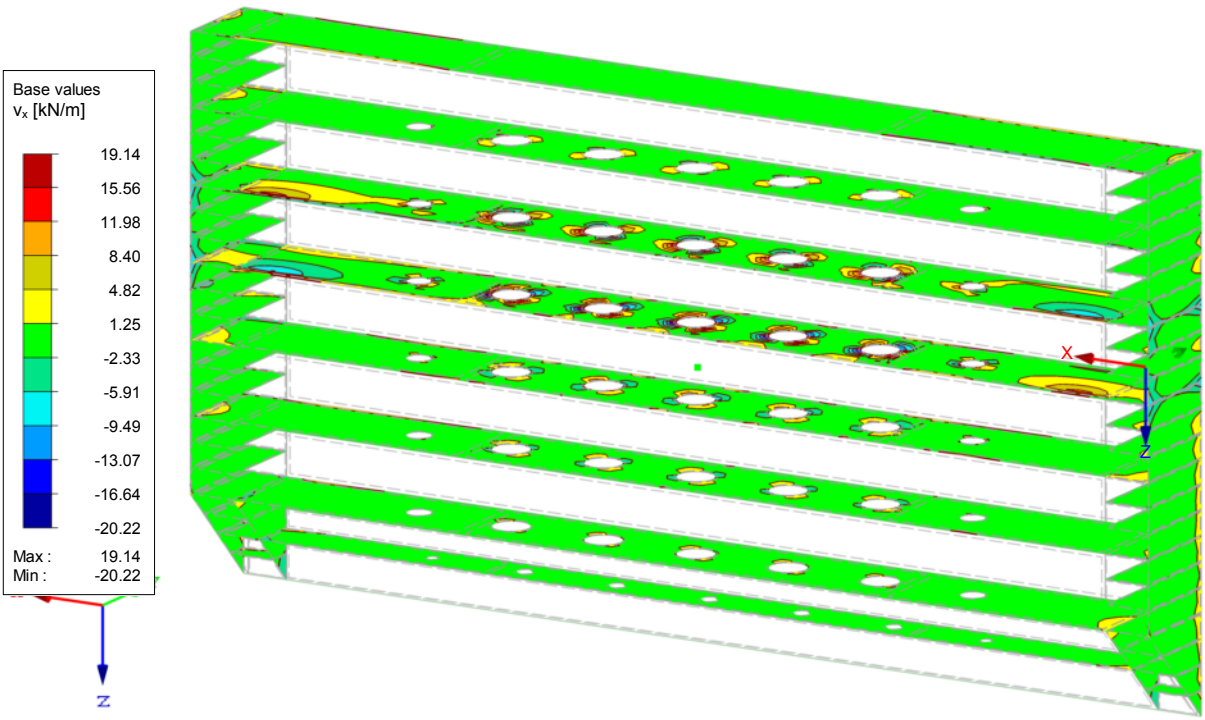


Max m-xy: 9.33, Min m-xy: -8.69 [kNm/m]

BASE VALUES V_x, CO5: ICE, ISOMETRIC

CO5: Ice
v-x

Isometric

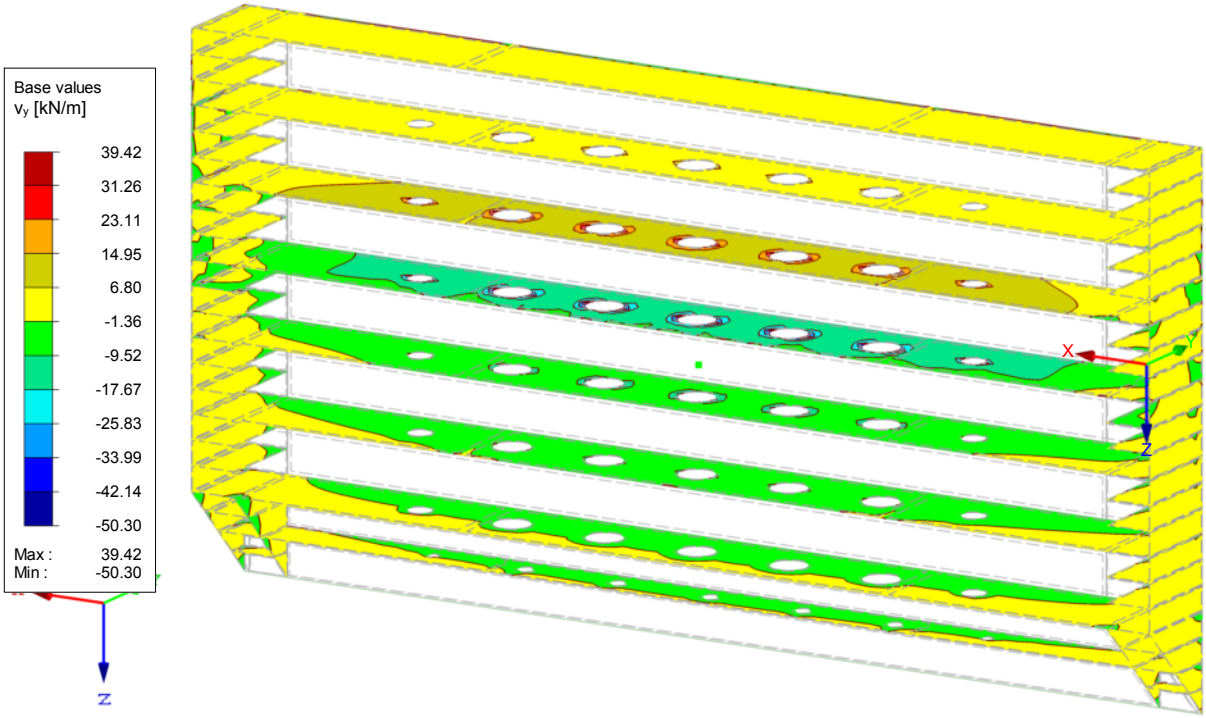


Max v-x: 19.14, Min v-x: -20.22 [kN/m]

BASE VALUES V_y, CO5: ICE, ISOMETRIC

CO5: Ice
v-y

Isometric

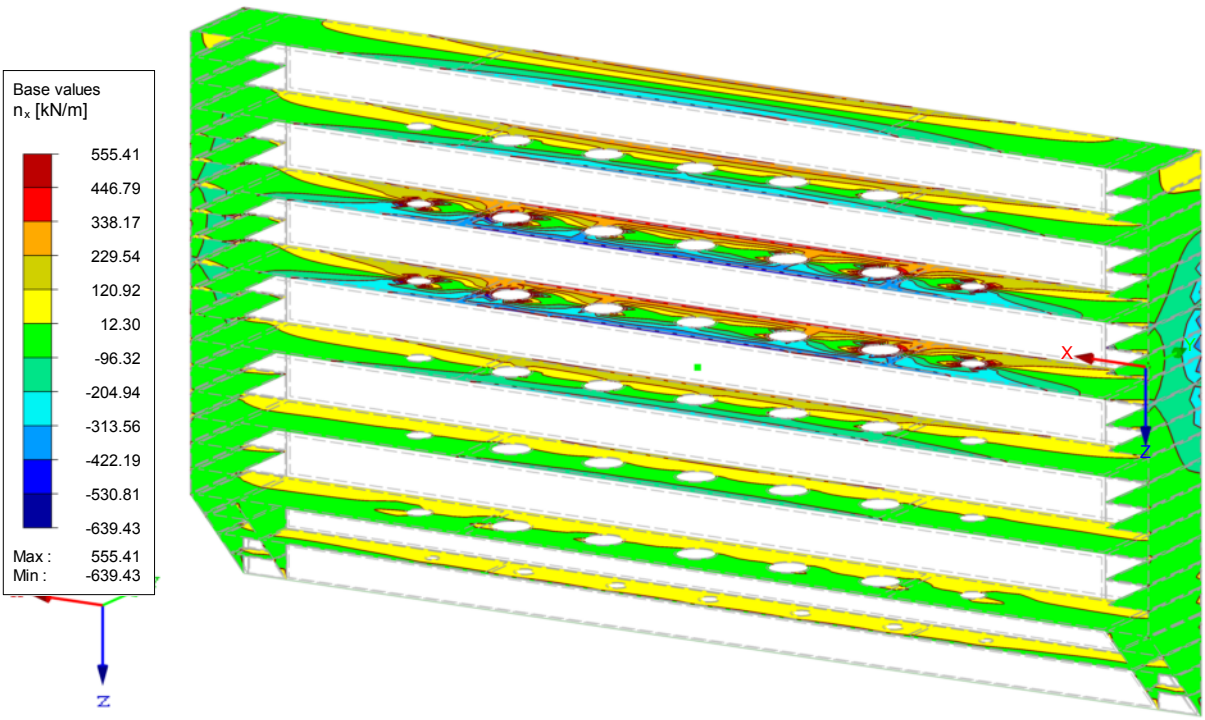


Max v-y: 39.42, Min v-y: -50.30 [kN/m]

BASE VALUES N_x, CO5: ICE, ISOMETRIC

CO5: Ice
n-x

Isometric

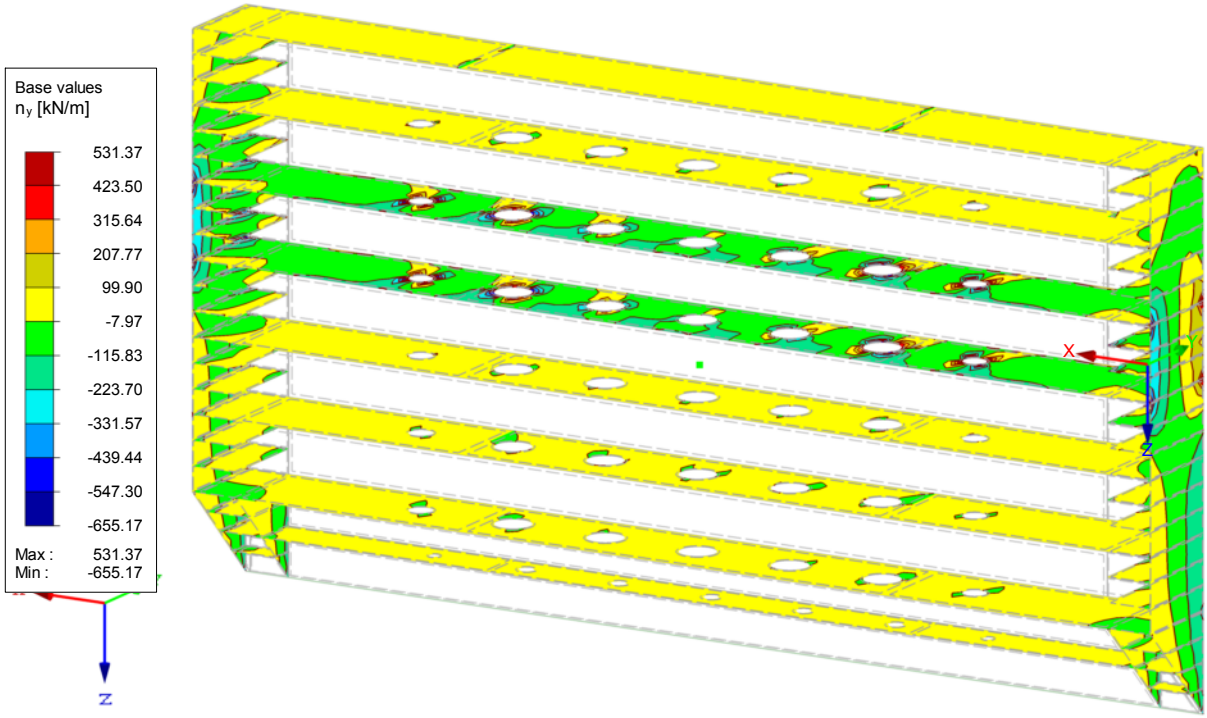


Max n-x: 555.41, Min n-x: -639.43 [kN/m]

BASE VALUES N_y, CO5: ICE, ISOMETRIC

CO5: Ice
n-y

Isometric

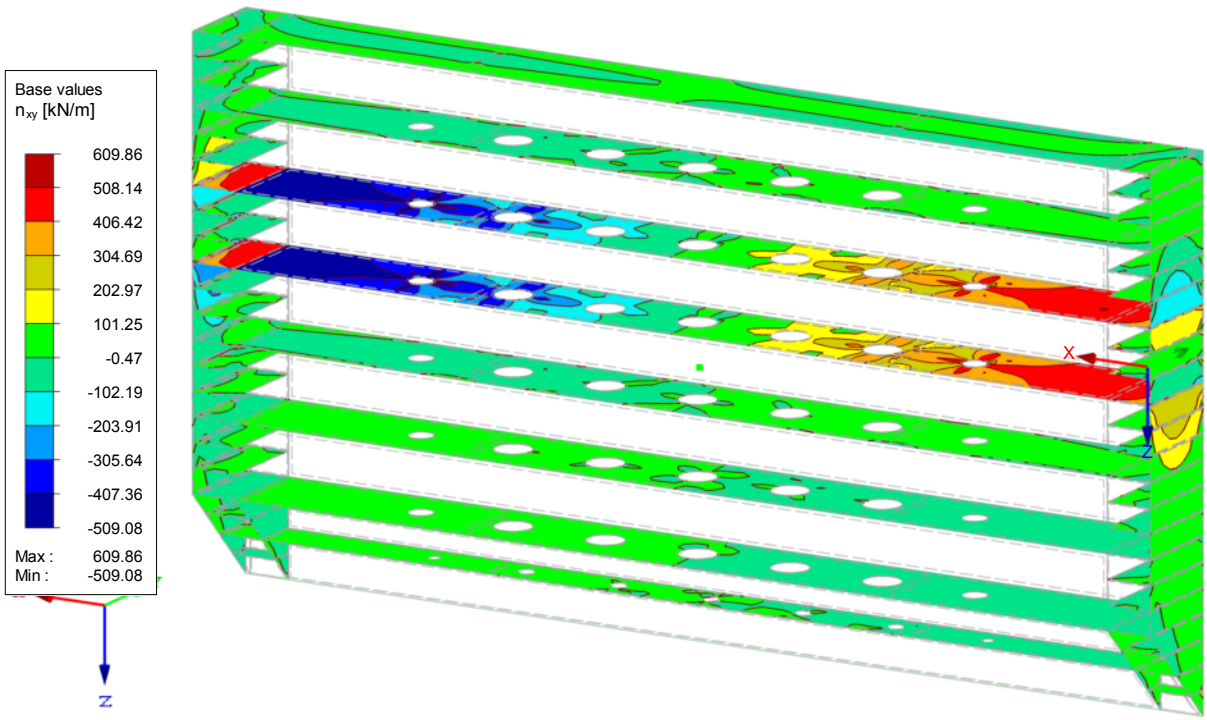


Max n-y: 531.37, Min n-y: -655.17 [kN/m]

BASE VALUES N_{xy}, CO5: ICE, ISOMETRIC

CO5: Ice
n-xy

Isometric



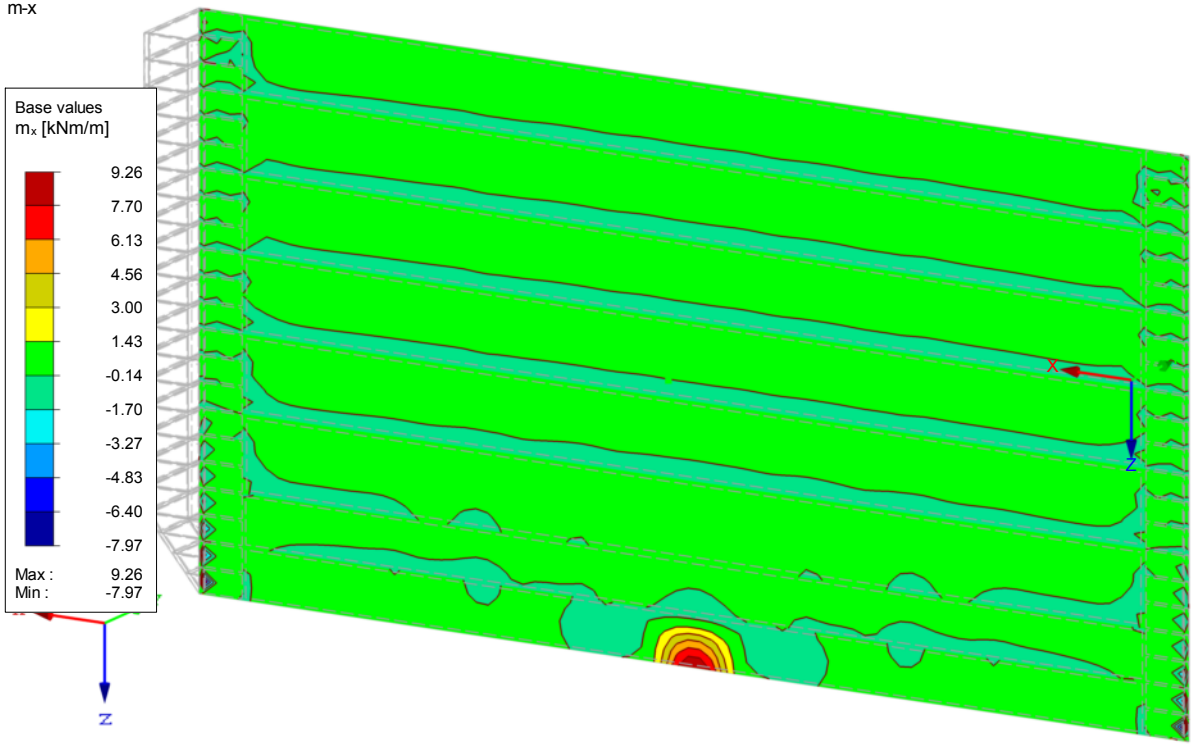
Max n-xy: 609.86, Min n-xy: -509.08 [kN/m]

Project: CIE5060 Model: V26
Graduation Project

BASE VALUES M_x, CO6: COLLISION, ISOMETRIC

CO6: Collision
m-x

Isometric

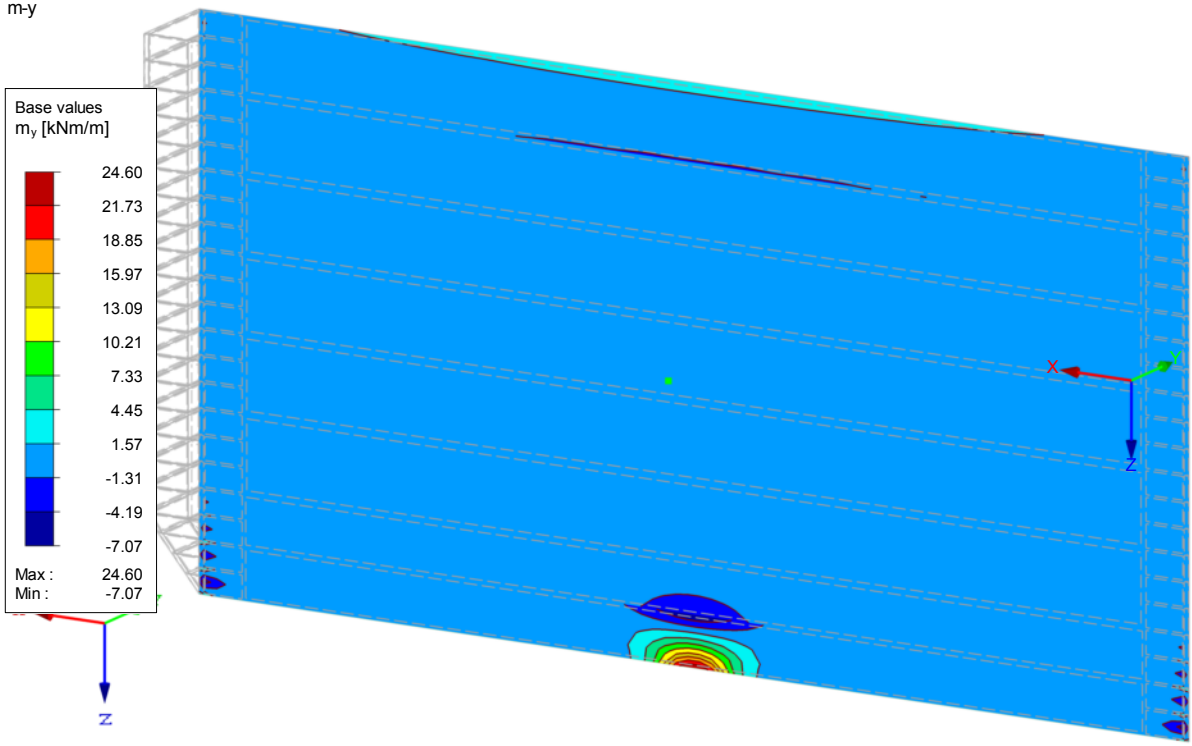


Max m-x: 9.26, Min m-x: -7.97 [kNm/m]

BASE VALUES M_y, CO6: COLLISION, ISOMETRIC

CO6: Collision
m-y

Isometric



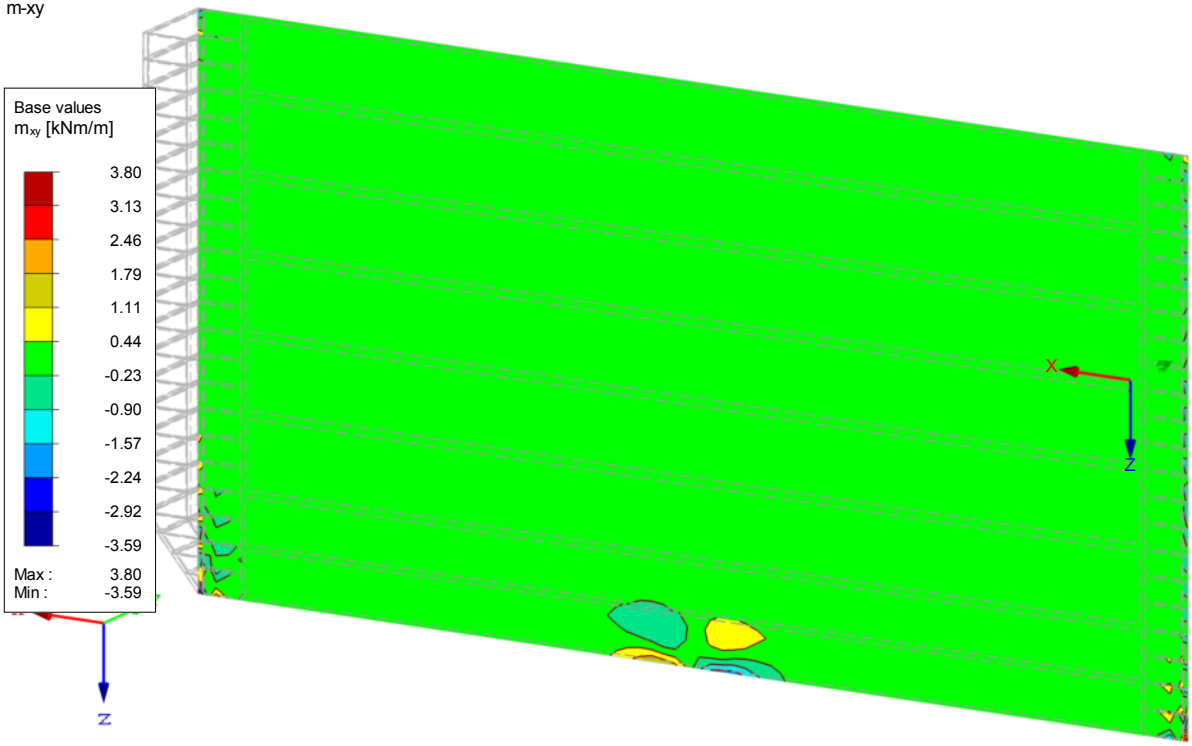
Max m-y: 24.60, Min m-y: -7.07 [kNm/m]

Project: CIE5060 Model: V26
Graduation Project

BASE VALUES M_{xy}, CO6: COLLISION, ISOMETRIC

CO6: Collision
m-xy

Isometric

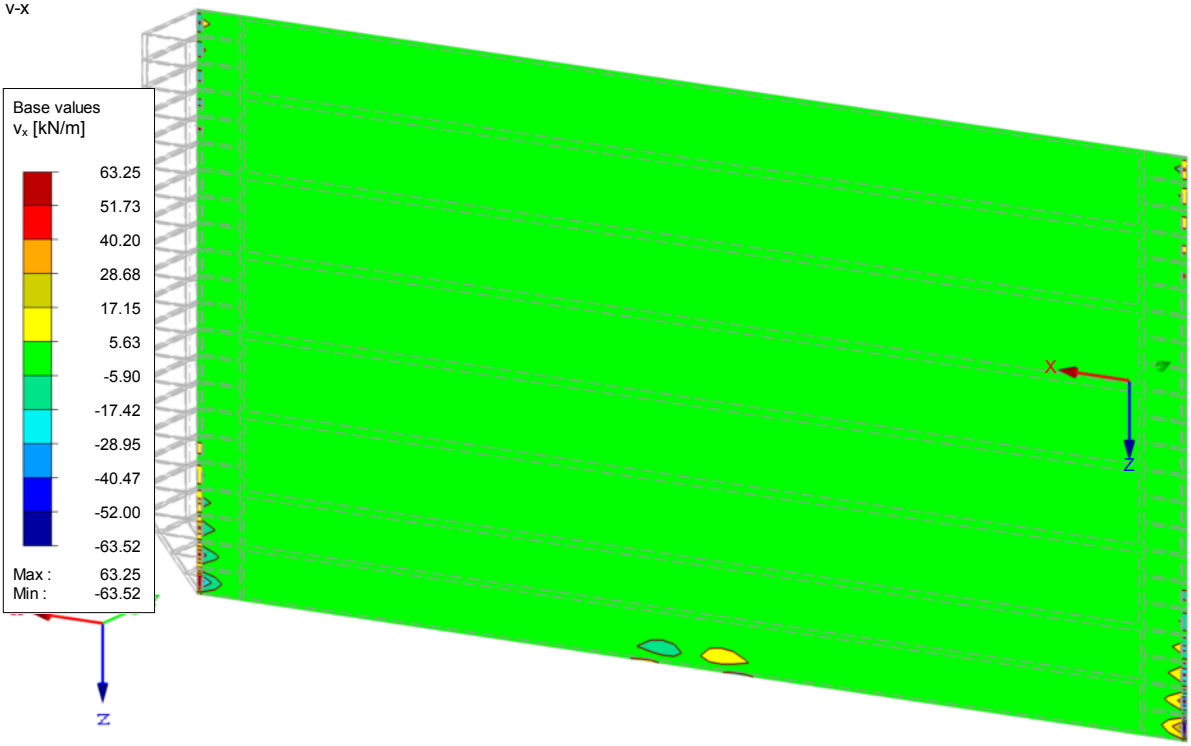


Max m-xy: 3.80, Min m-xy: -3.59 [kNm/m]

BASE VALUES V_x, CO6: COLLISION, ISOMETRIC

CO6: Collision
v-x

Isometric

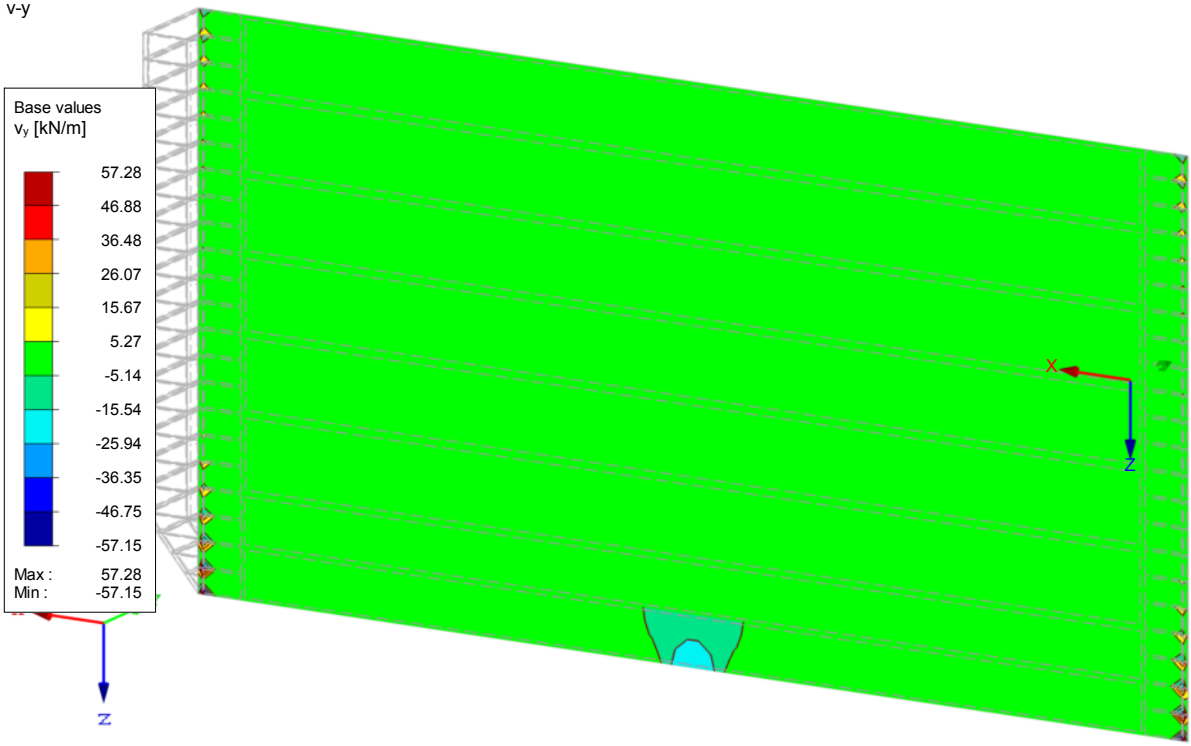


Max v-x: 63.25, Min v-x: -63.52 [kN/m]

BASE VALUES V_y, CO6: COLLISION, ISOMETRIC

CO6: Collision
v-y

Isometric

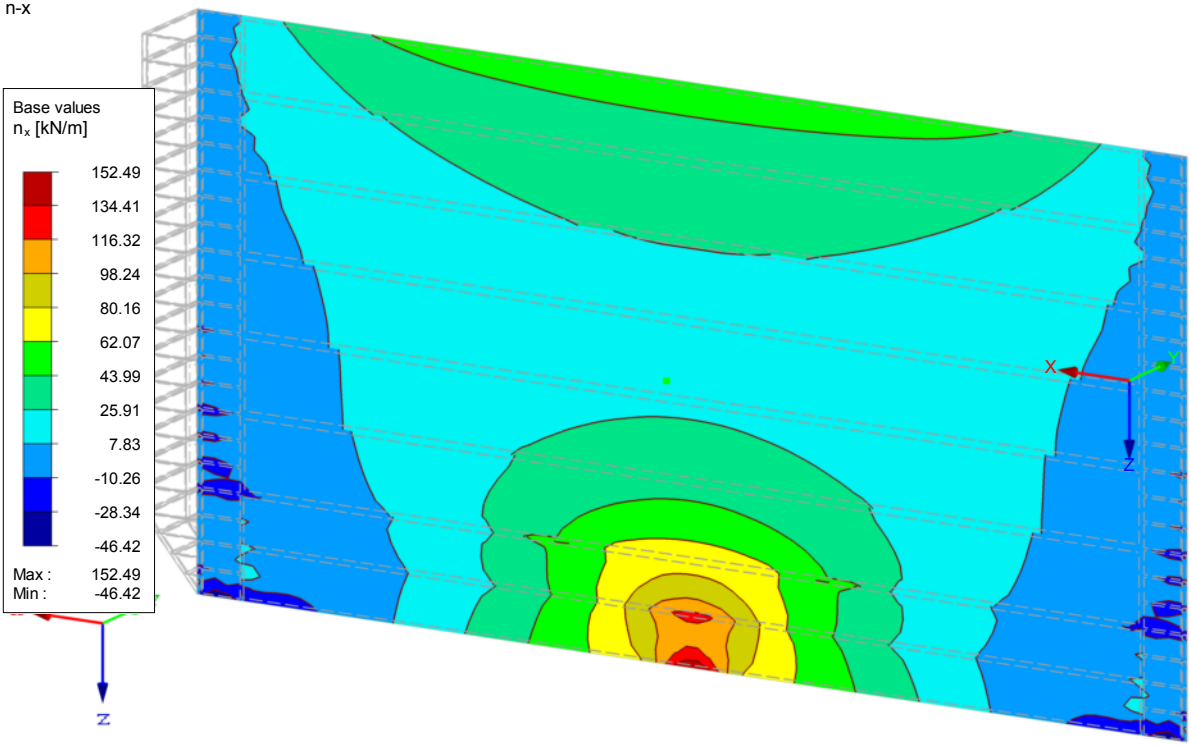


Max v-y: 57.28, Min v-y: -57.15 [kN/m]

BASE VALUES N_x, CO6: COLLISION, ISOMETRIC

CO6: Collision
n-x

Isometric



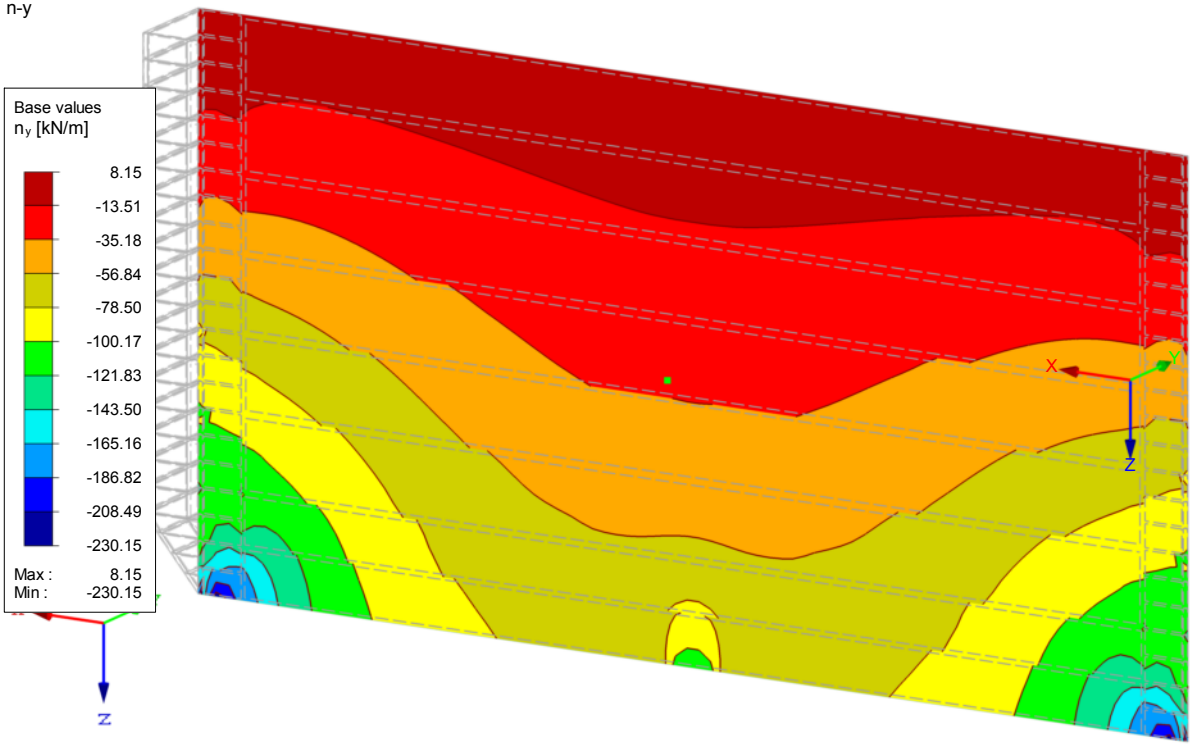
Max n-x: 152.49, Min n-x: -46.42 [kN/m]

Project: CIE5060 Model: V26
Graduation Project

BASE VALUES N_y, CO6: COLLISION, ISOMETRIC

CO6: Collision
n-y

Isometric

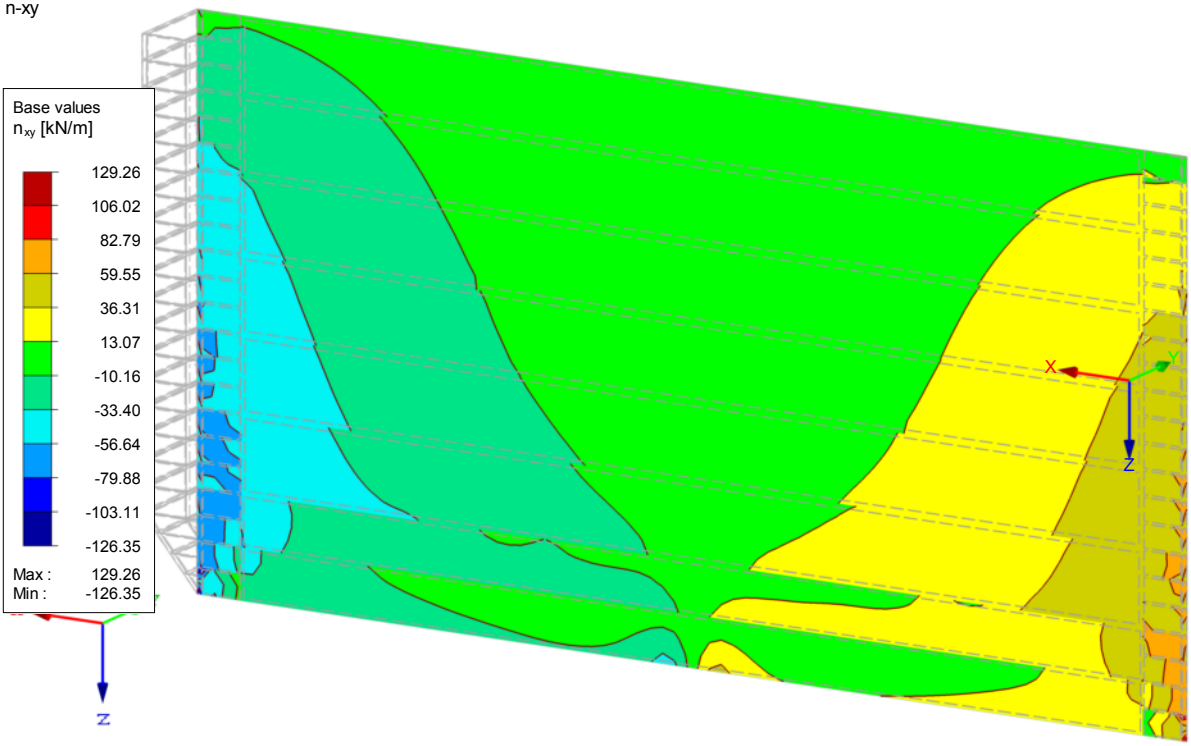


Max n-y: 8.15, Min n-y: -230.15 [kN/m]

BASE VALUES N_{xy}, CO6: COLLISION, ISOMETRIC

CO6: Collision
n-xy

Isometric

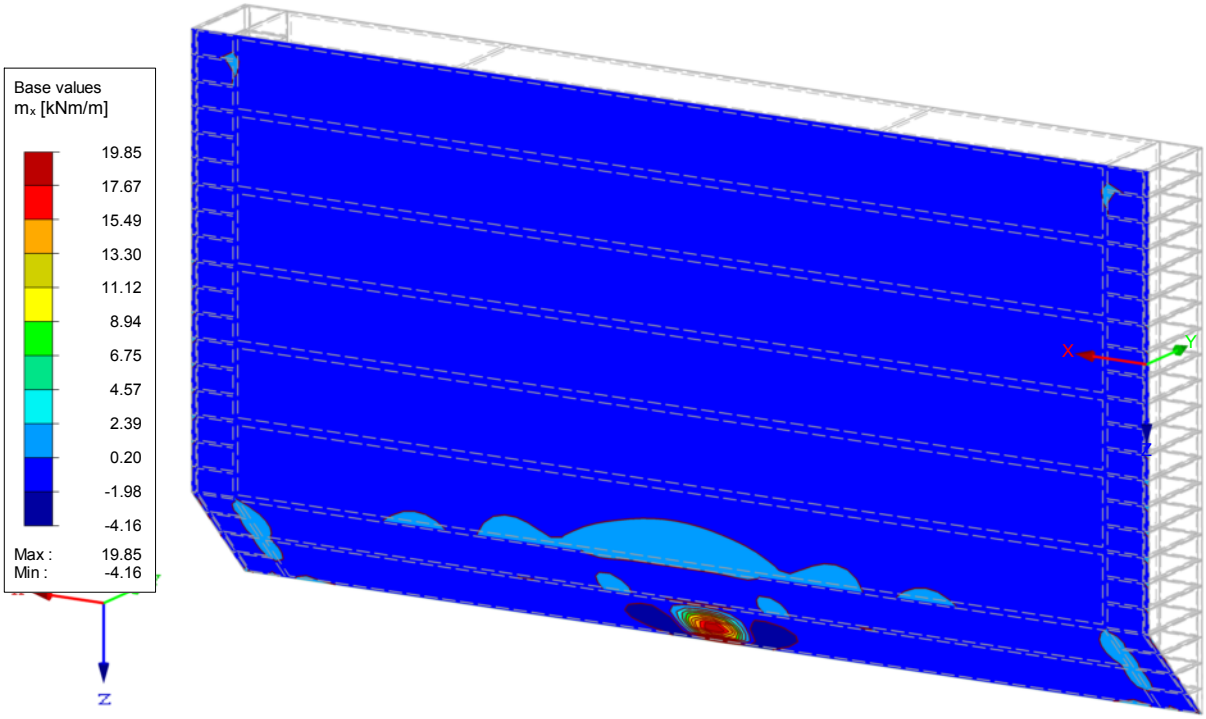


Max n-xy: 129.26, Min n-xy: -126.35 [kN/m]

BASE VALUES M_x, CO6: COLLISION, ISOMETRIC

CO6: Collision
m-x

Isometric

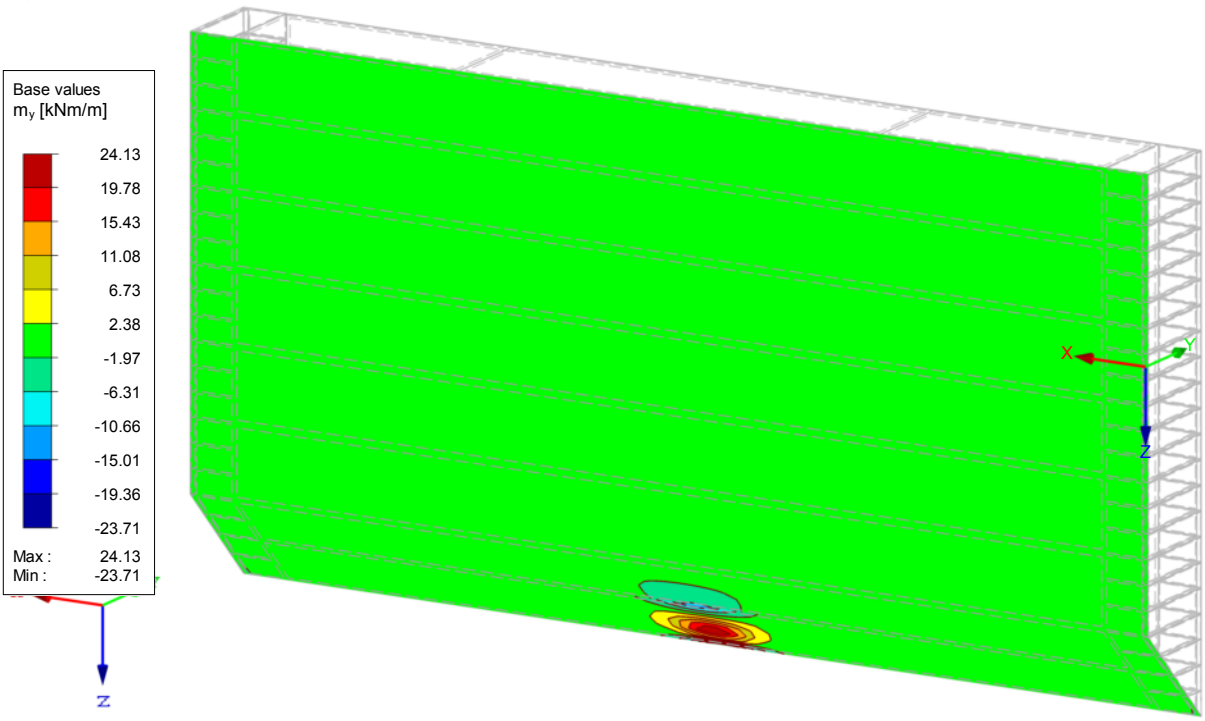


Max m-x: 19.85, Min m-x: -4.16 [kNm/m]

BASE VALUES M_y, CO6: COLLISION, ISOMETRIC

CO6: Collision
m-y

Isometric



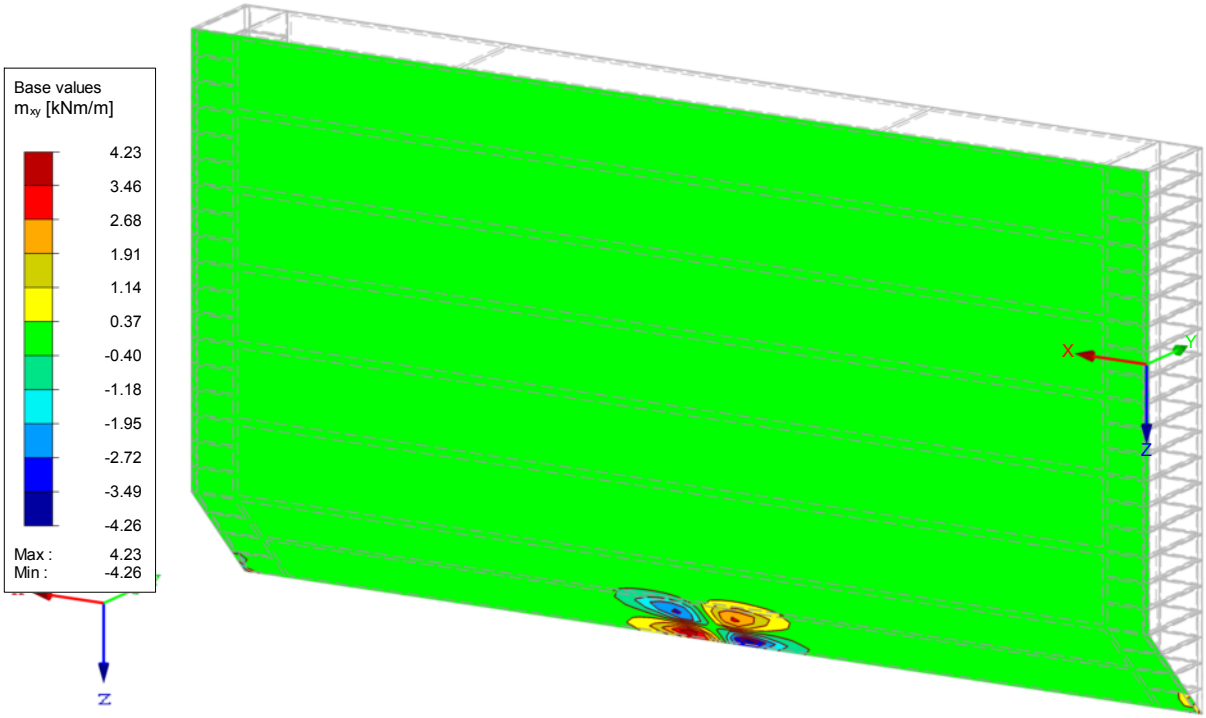
Max m-y: 24.13, Min m-y: -23.71 [kNm/m]

Project: CIE5060 Model: V26
Graduation Project

BASE VALUES M_{xy}, CO6: COLLISION, ISOMETRIC

CO6: Collision
m-xy

Isometric

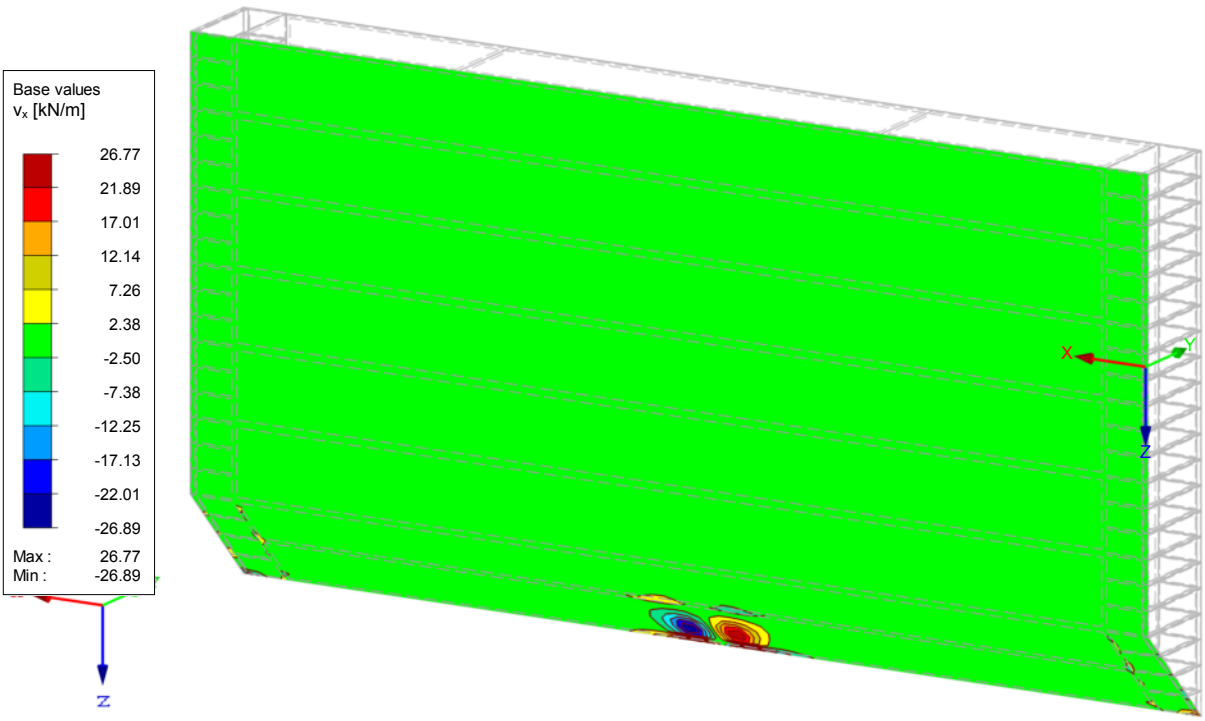


Max m-xy: 4.23, Min m-xy: -4.26 [kNm/m]

BASE VALUES V_x, CO6: COLLISION, ISOMETRIC

CO6: Collision
v-x

Isometric

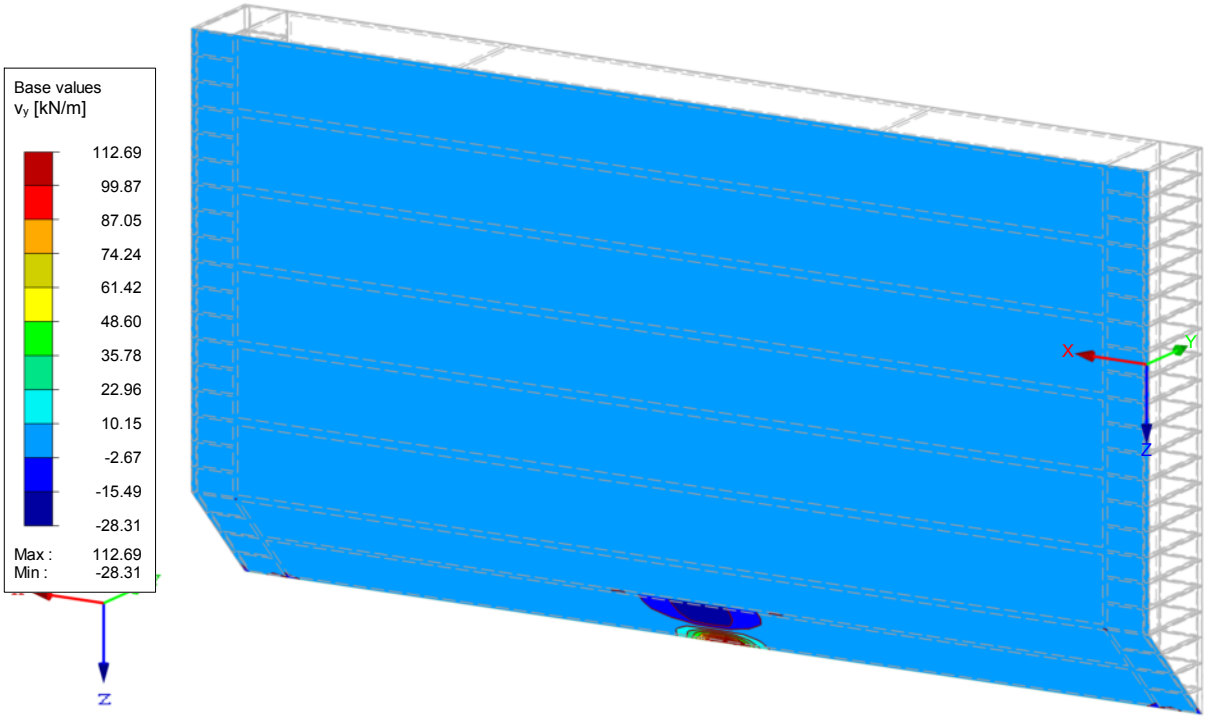


Max v-x: 26.77, Min v-x: -26.89 [kN/m]

BASE VALUES V_y, CO6: COLLISION, ISOMETRIC

CO6: Collision
v-y

Isometric

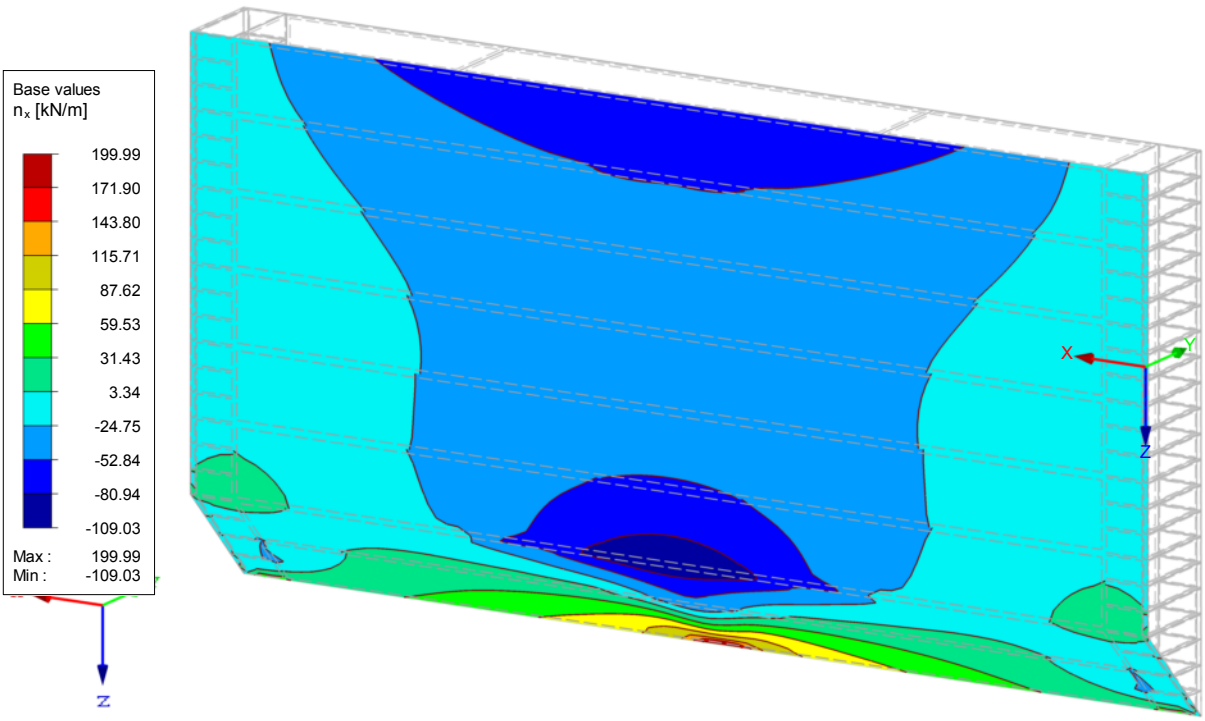


Max v-y: 112.69, Min v-y: -28.31 [kN/m]

BASE VALUES N_x, CO6: COLLISION, ISOMETRIC

CO6: Collision
n-x

Isometric



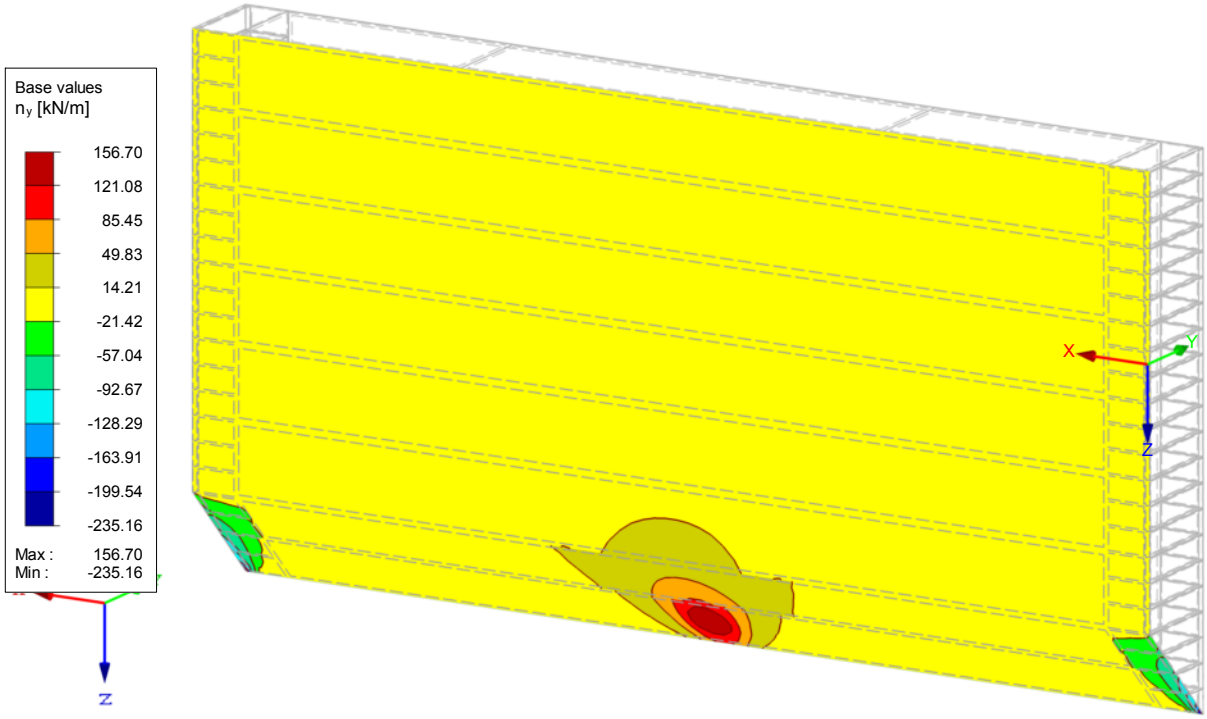
Max n-x: 199.99, Min n-x: -109.03 [kN/m]

Project: CIE5060 Model: V26
Graduation Project

BASE VALUES N_y, CO6: COLLISION, ISOMETRIC

CO6: Collision
n-y

Isometric

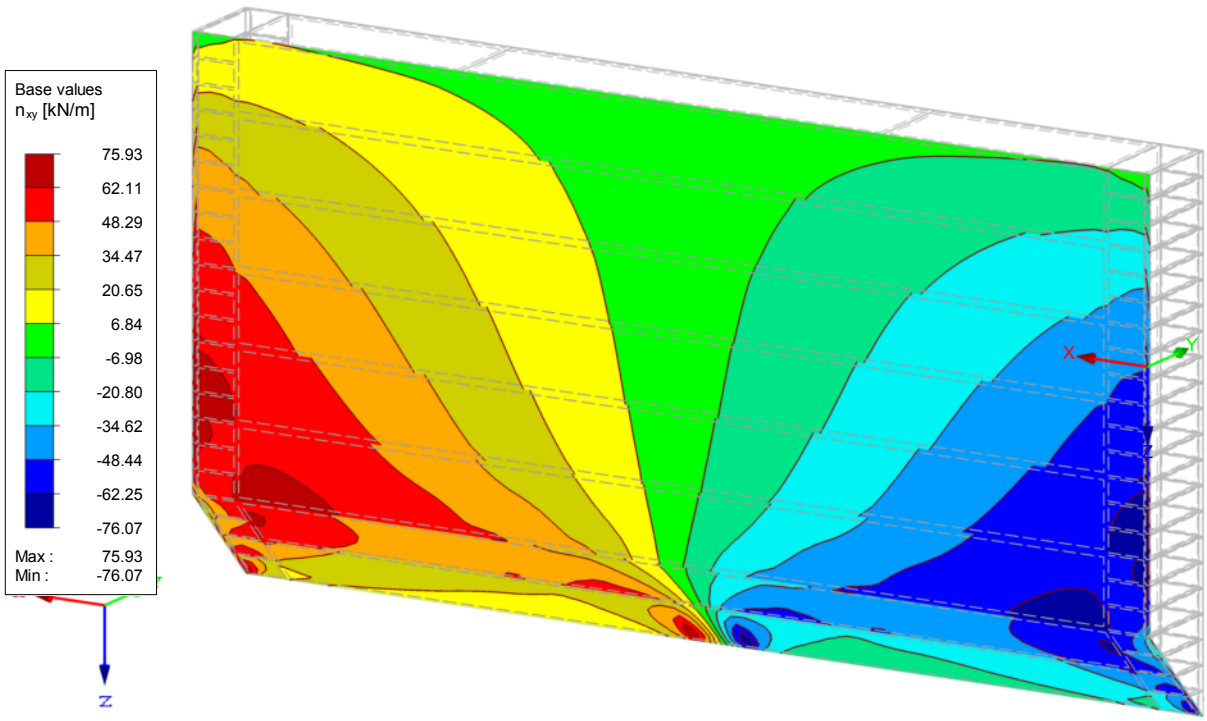


Max n-y: 156.70, Min n-y: -235.16 [kN/m]

BASE VALUES N_{xy}, CO6: COLLISION, ISOMETRIC

CO6: Collision
n-xy

Isometric

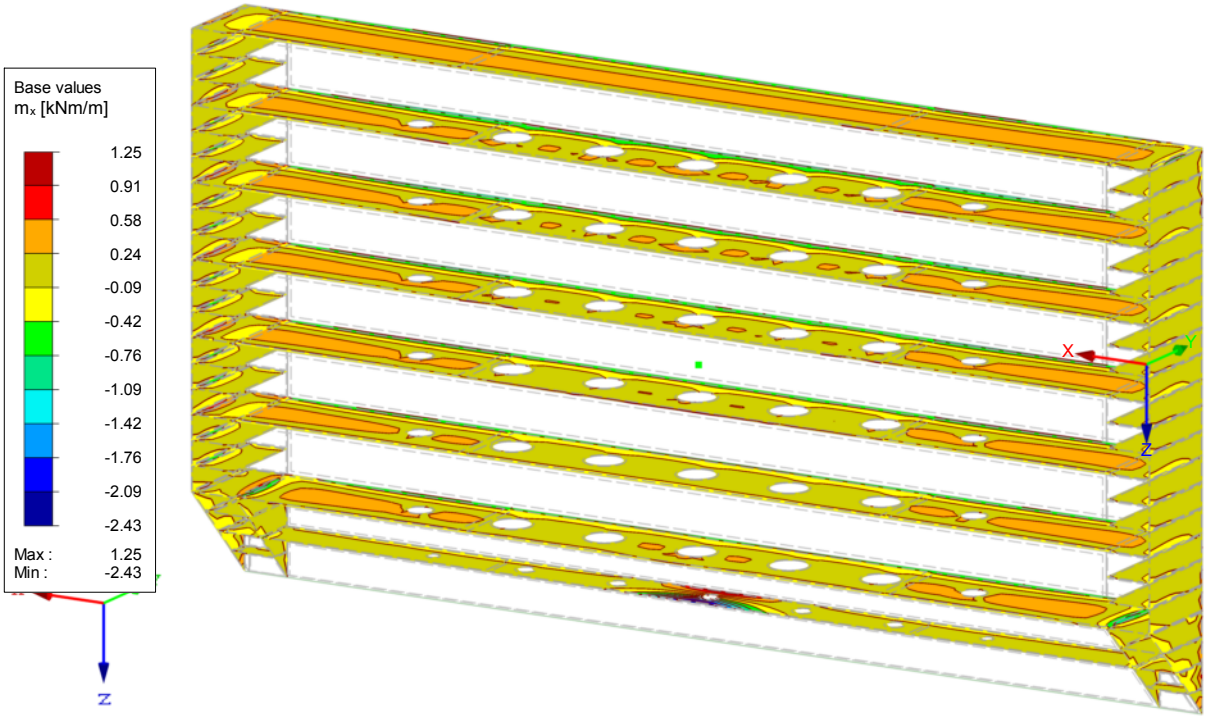


Max n-xy: 75.93, Min n-xy: -76.07 [kN/m]

BASE VALUES M_x, CO6: COLLISION, ISOMETRIC

CO6: Collision
m-x

Isometric

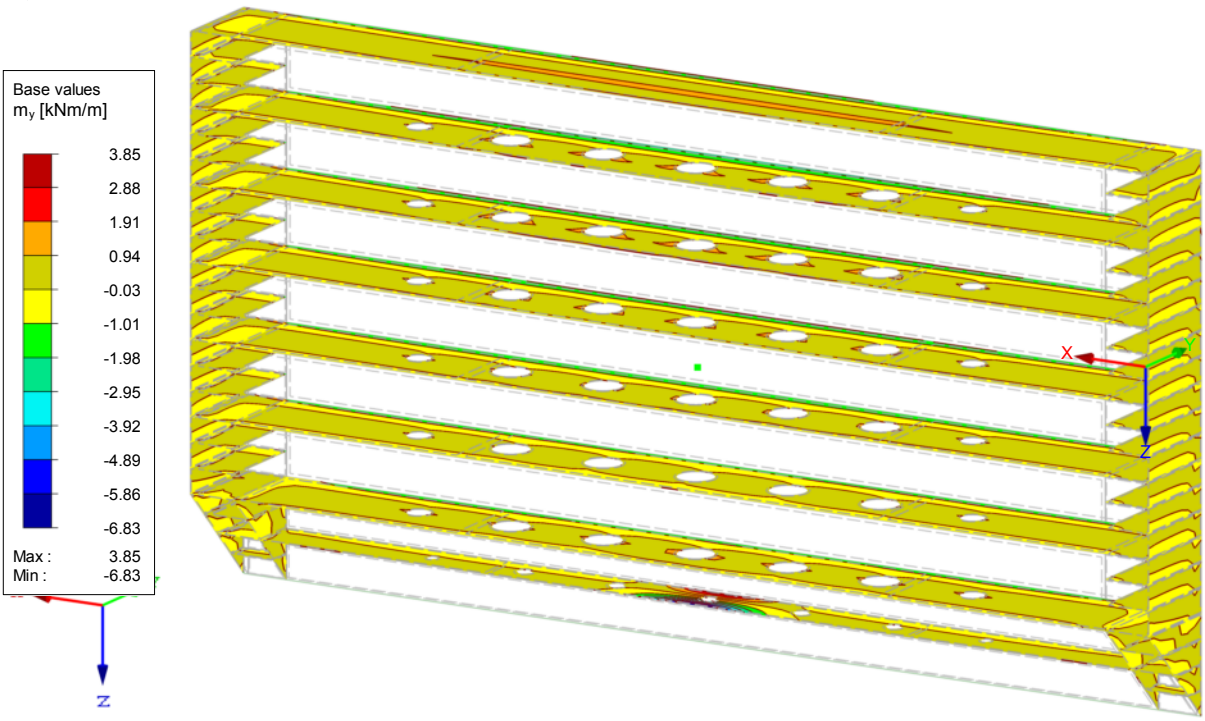


Max m-x: 1.25, Min m-x: -2.43 [kNm/m]

BASE VALUES M_y, CO6: COLLISION, ISOMETRIC

CO6: Collision
m-y

Isometric

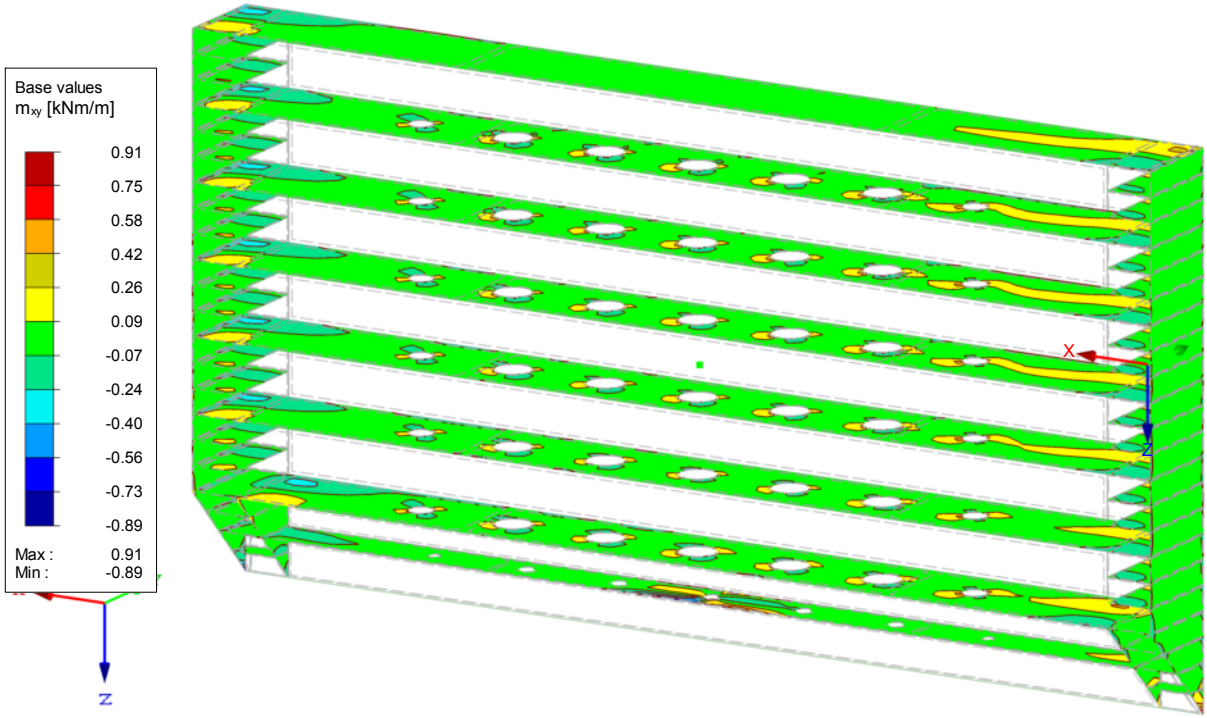


Max m-y: 3.85, Min m-y: -6.83 [kNm/m]

BASE VALUES M_{xy}, CO6: COLLISION, ISOMETRIC

CO6: Collision
m-xy

Isometric

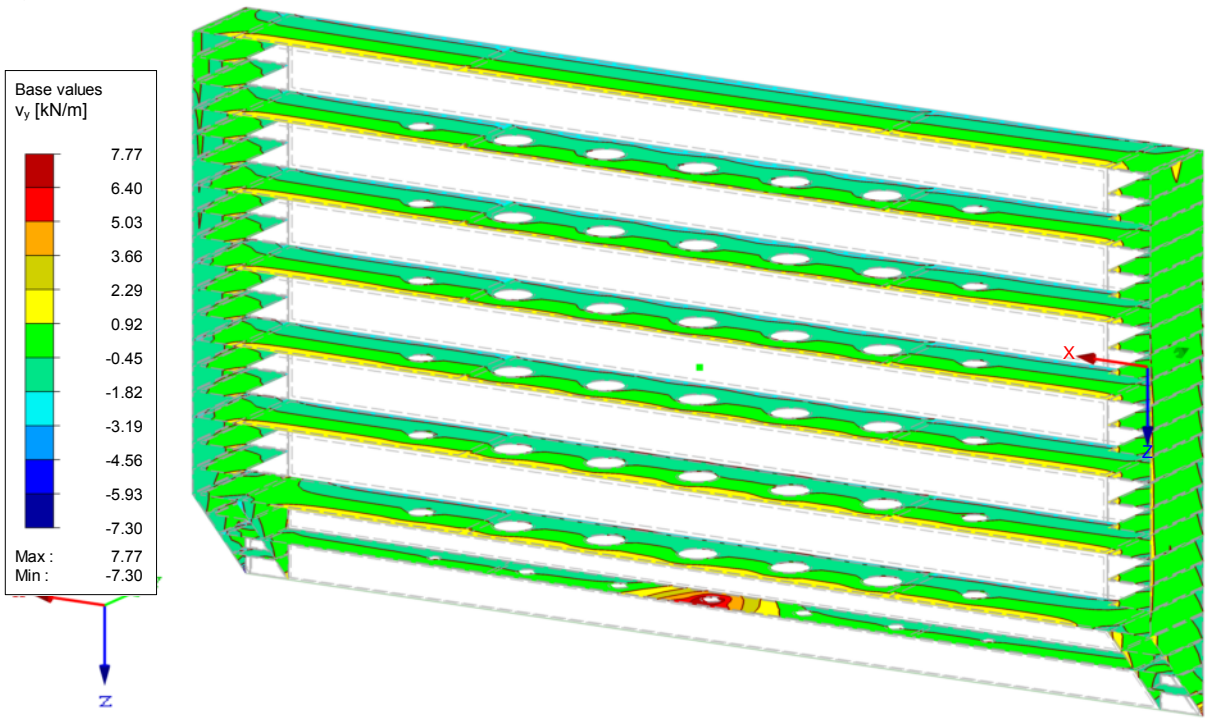


Max m-xy: 0.91, Min m-xy: -0.89 [kNm/m]

BASE VALUES V_y, CO6: COLLISION, ISOMETRIC

CO6: Collision
v-y

Isometric

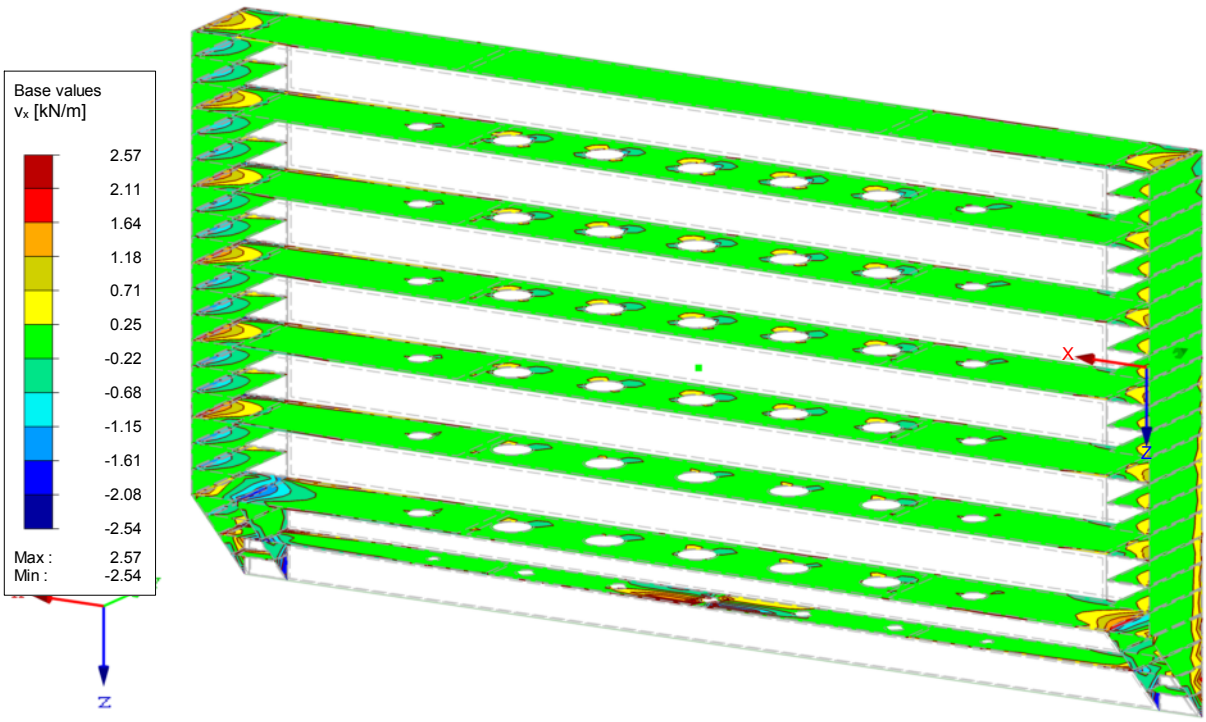


Max v-y: 7.77, Min v-y: -7.30 [kN/m]

BASE VALUES V_x, CO6: COLLISION, ISOMETRIC

CO6: Collision
v-x

Isometric

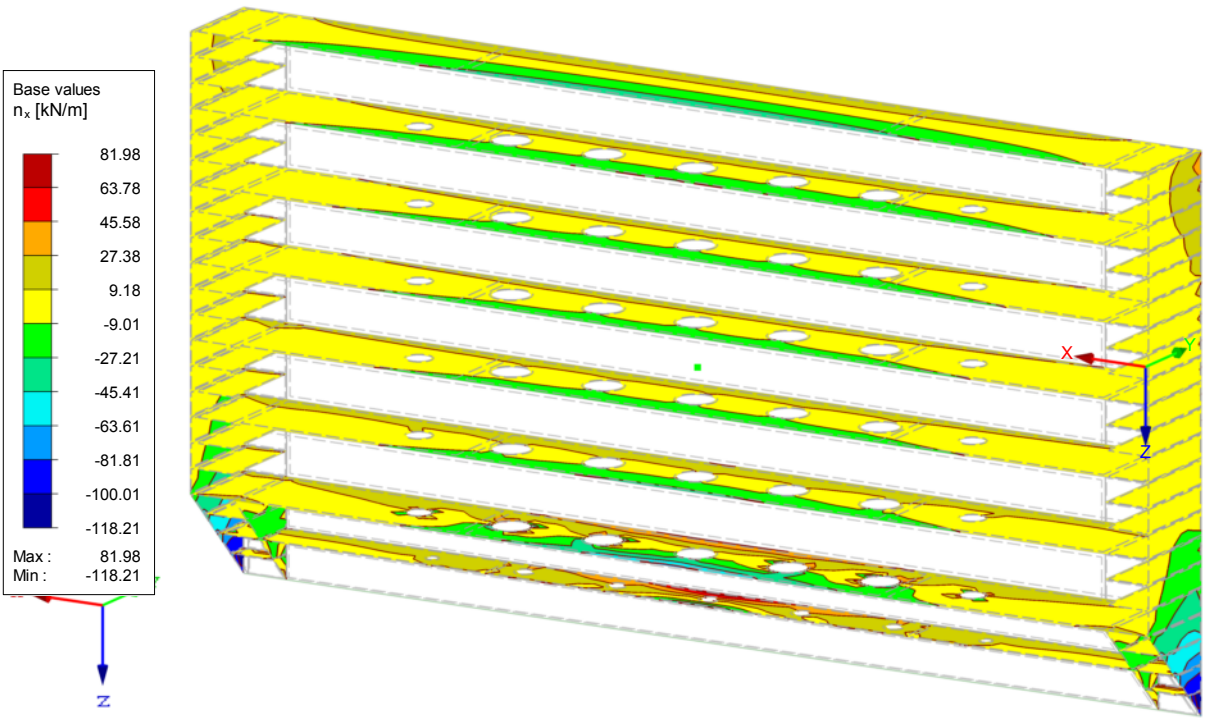


Max v-x: 2.57, Min v-x: -2.54 [kN/m]

BASE VALUES N_x, CO6: COLLISION, ISOMETRIC

CO6: Collision
n-x

Isometric

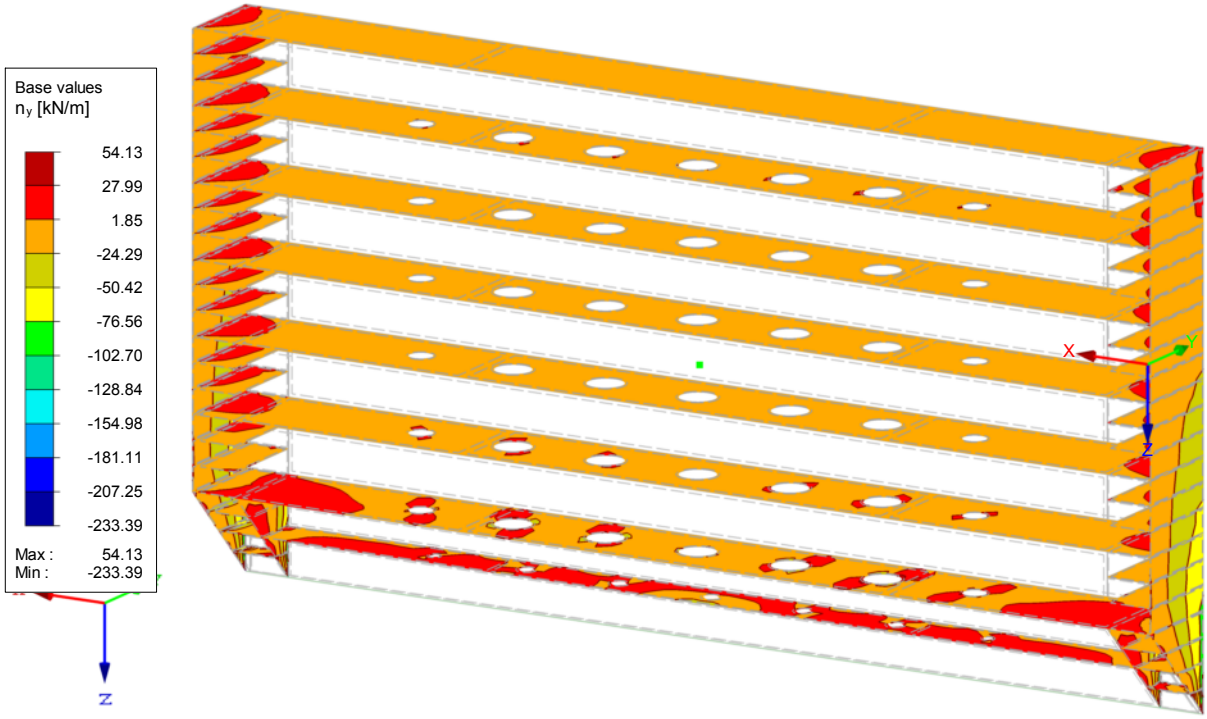


Max n-x: 81.98, Min n-x: -118.21 [kN/m]

BASE VALUES N_y, CO6: COLLISION, ISOMETRIC

CO6: Collision
n-y

Isometric

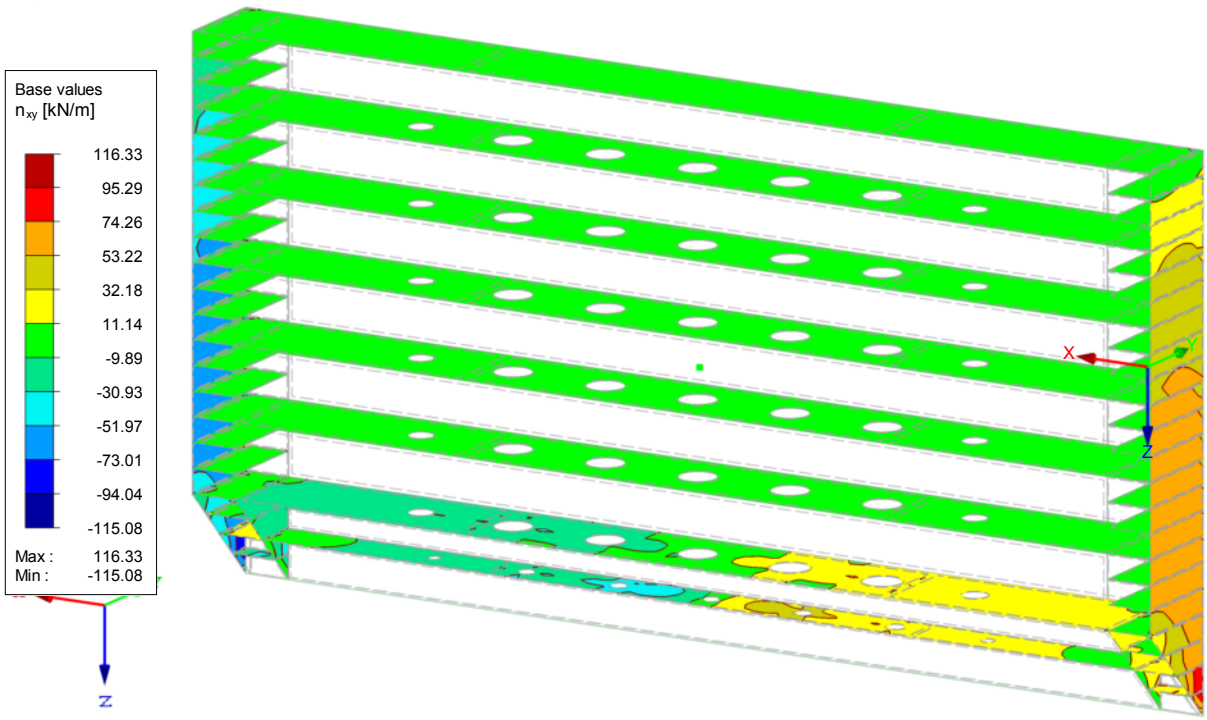


Max n-y: 54.13, Min n-y: -233.39 [kN/m]

BASE VALUES N_{xy}, CO6: COLLISION, ISOMETRIC

CO6: Collision
n-xy

Isometric

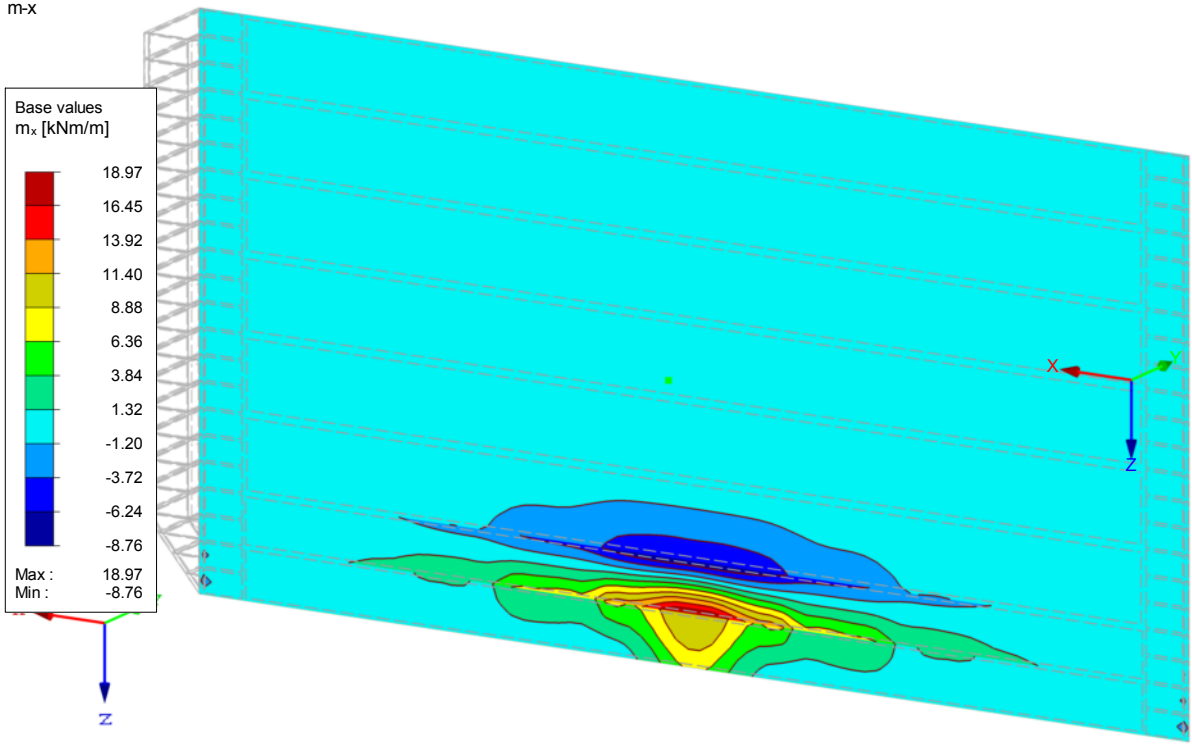


Max n-xy: 116.33, Min n-xy: -115.08 [kN/m]

BASE VALUES M_x, CO7: WATER IMPACT, ISOMETRIC

CO7: Water impact
m-x

Isometric

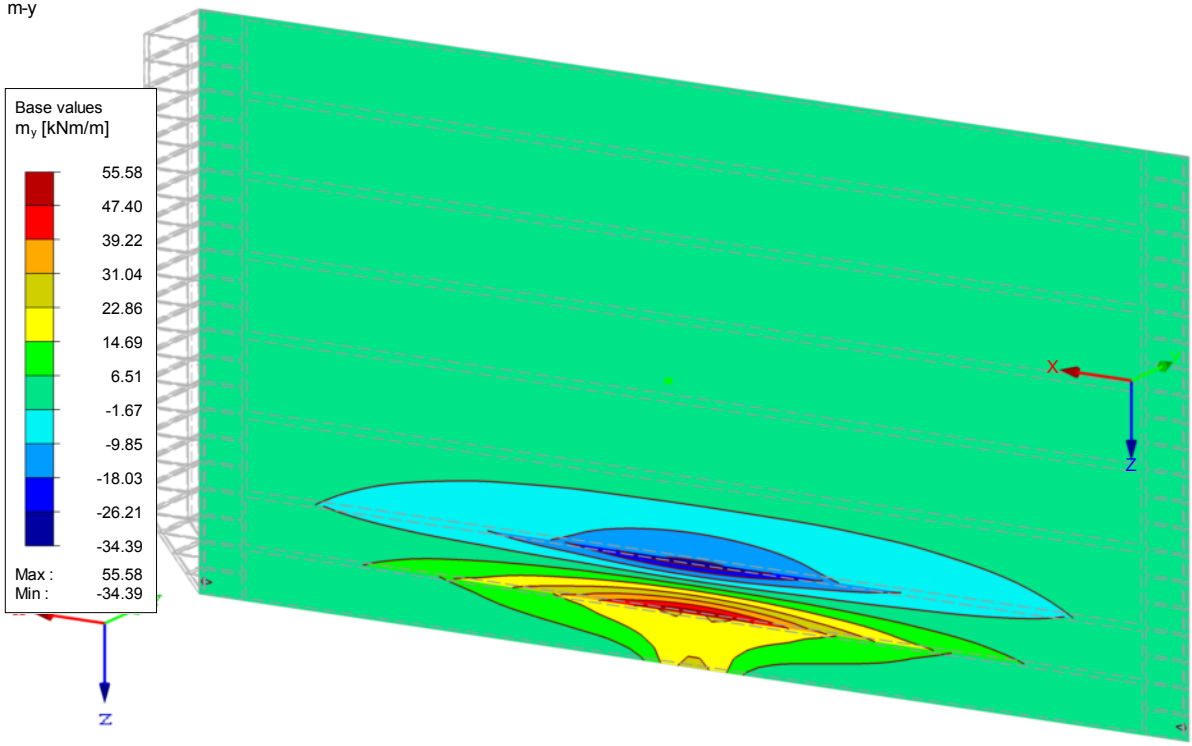


Max m-x: 18.97, Min m-x: -8.76 [kNm/m]

BASE VALUES M_y, CO7: WATER IMPACT, ISOMETRIC

CO7: Water impact
m-y

Isometric



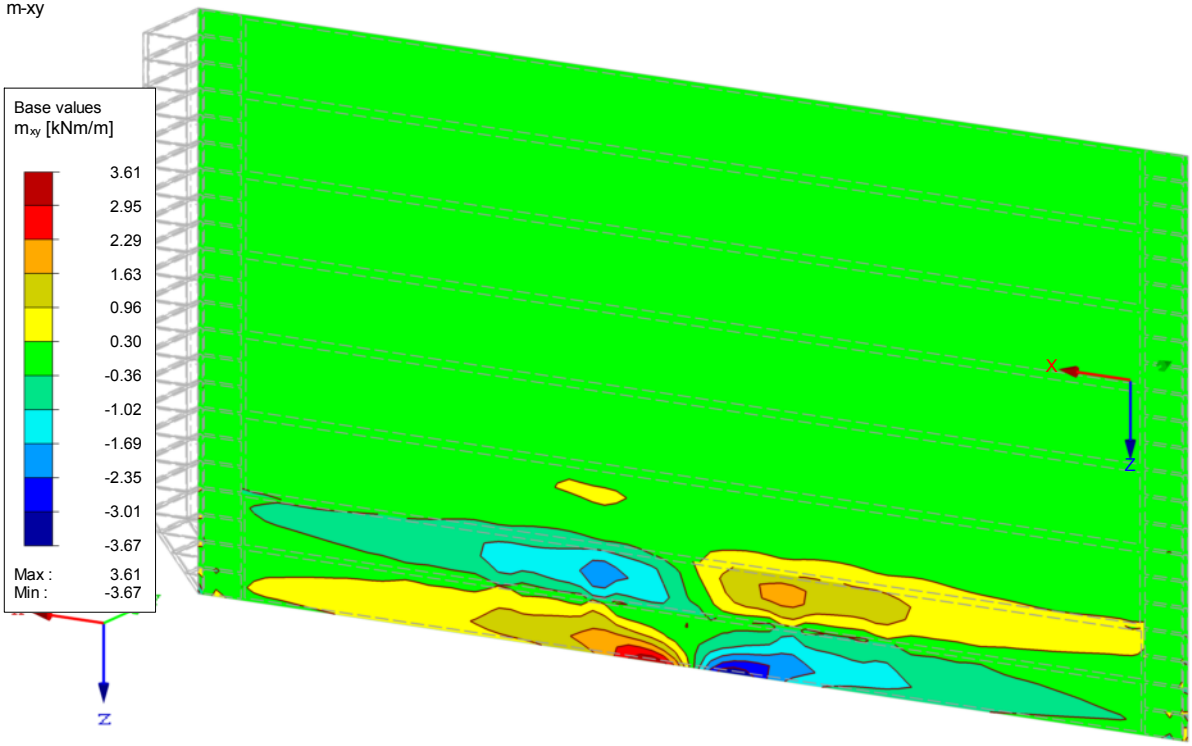
Max m-y: 55.58, Min m-y: -34.39 [kNm/m]

Project: CIE5060 Model: V26
Graduation Project

BASE VALUES M_{xy}, CO7: WATER IMPACT, ISOMETRIC

CO7: Water impact
m-xy

Isometric

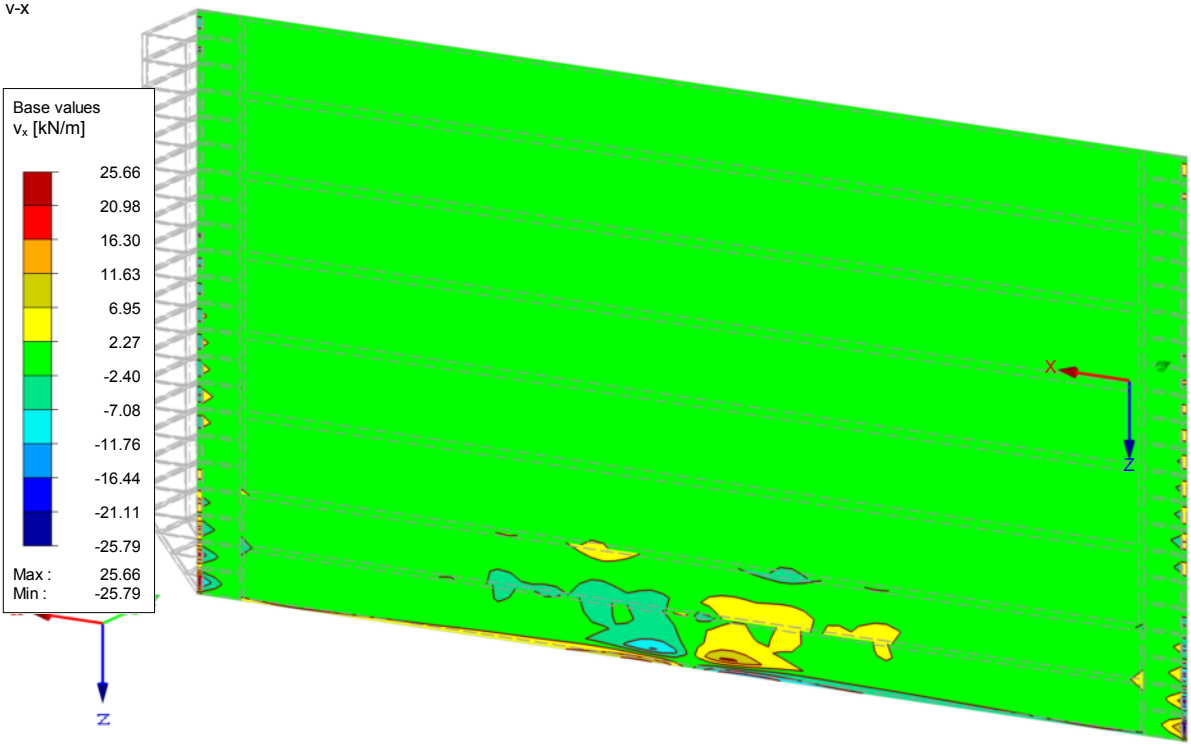


Max m-xy: 3.61, Min m-xy: -3.67 [kNm/m]

BASE VALUES V_x, CO7: WATER IMPACT, ISOMETRIC

CO7: Water impact
v-x

Isometric

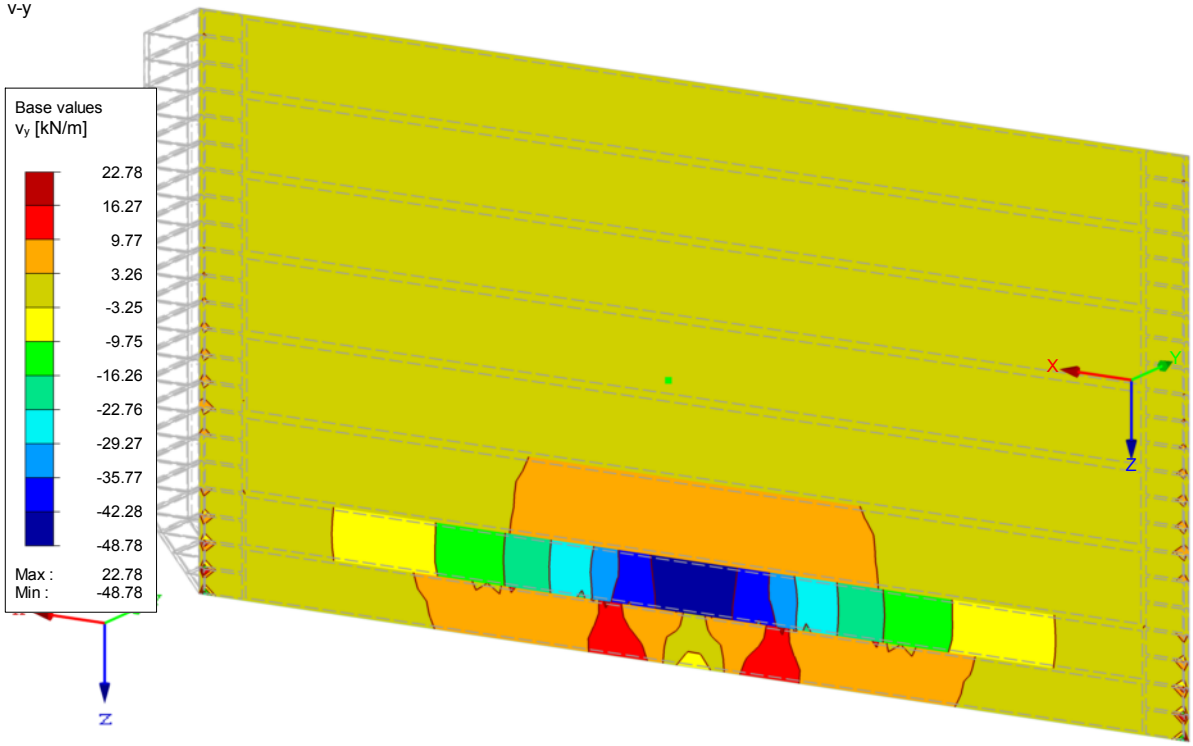


Max v-x: 25.66, Min v-x: -25.79 [kN/m]

BASE VALUES V_y, CO7: WATER IMPACT, ISOMETRIC

CO7: Water impact
v-y

Isometric

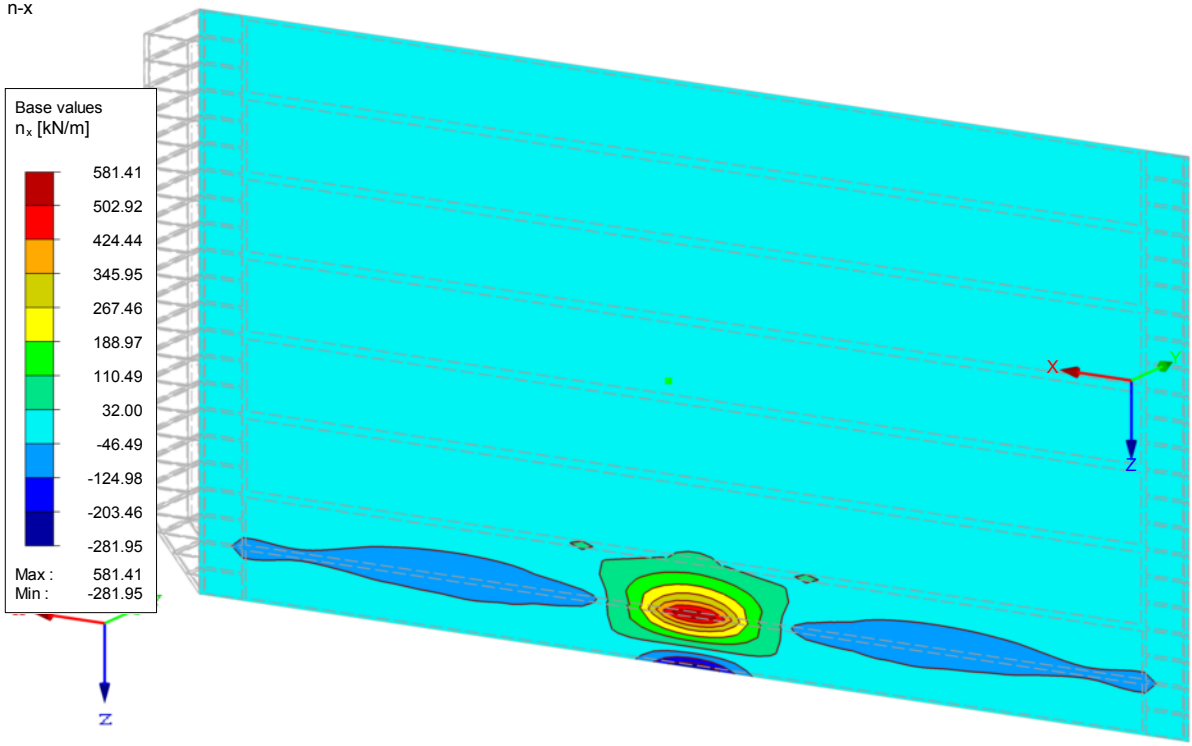


Max v-y: 22.78, Min v-y: -48.78 [kN/m]

BASE VALUES N_x, CO7: WATER IMPACT, ISOMETRIC

CO7: Water impact
n-x

Isometric

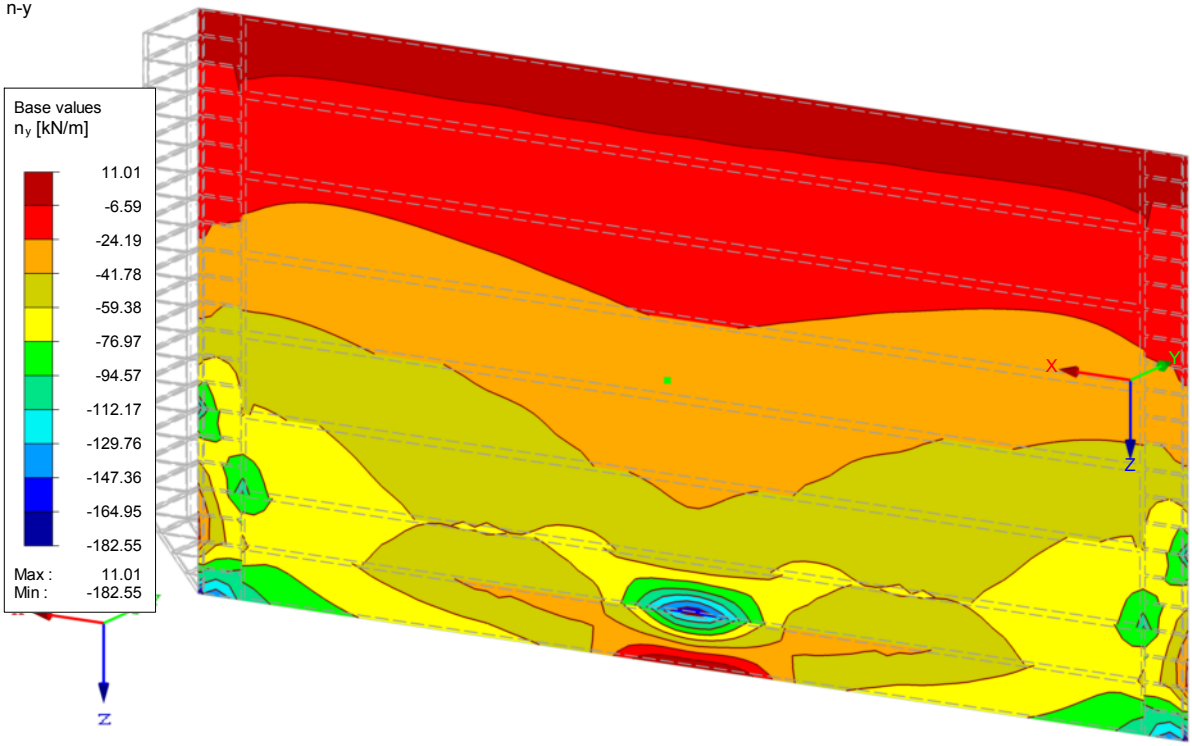


Max n-x: 581.41, Min n-x: -281.95 [kN/m]

BASE VALUES N_y, CO7: WATER IMPACT, ISOMETRIC

CO7: Water impact
n-y

Isometric

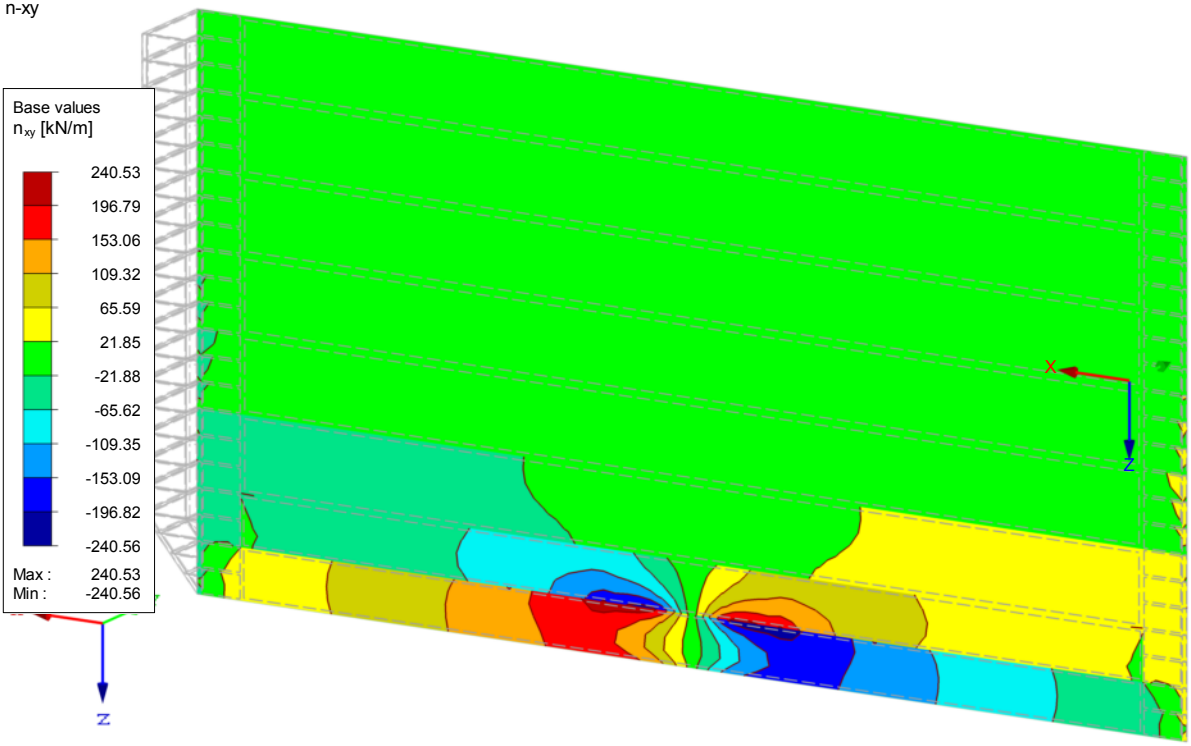


Max n-y: 11.01, Min n-y: -182.55 [kN/m]

BASE VALUES N_{xy}, CO7: WATER IMPACT, ISOMETRIC

CO7: Water impact
n-xy

Isometric



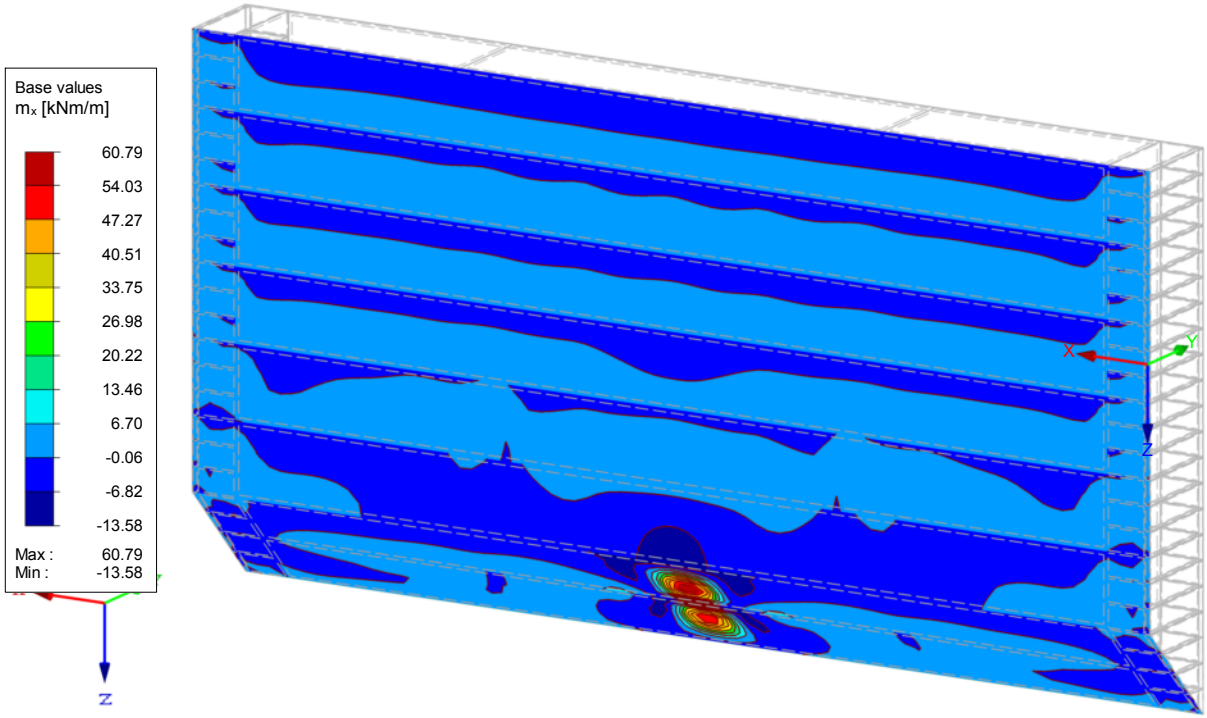
Max n-xy: 240.53, Min n-xy: -240.56 [kN/m]

Project: CIE5060 Model: V26
Graduation Project

BASE VALUES M_x, CO7: WATER IMPACT, ISOMETRIC

CO7: Water impact
m-x

Isometric

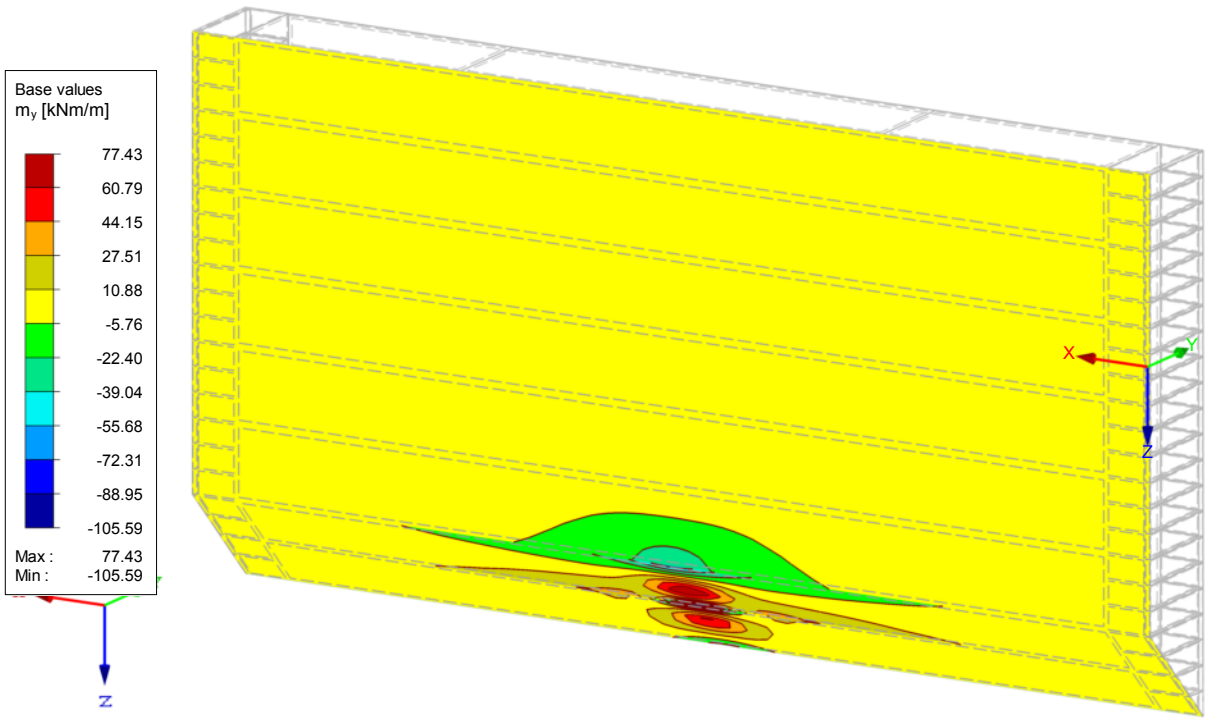


Max m-x: 60.79, Min m-x: -13.58 [kNm/m]

BASE VALUES M_y, CO7: WATER IMPACT, ISOMETRIC

CO7: Water impact
m-y

Isometric

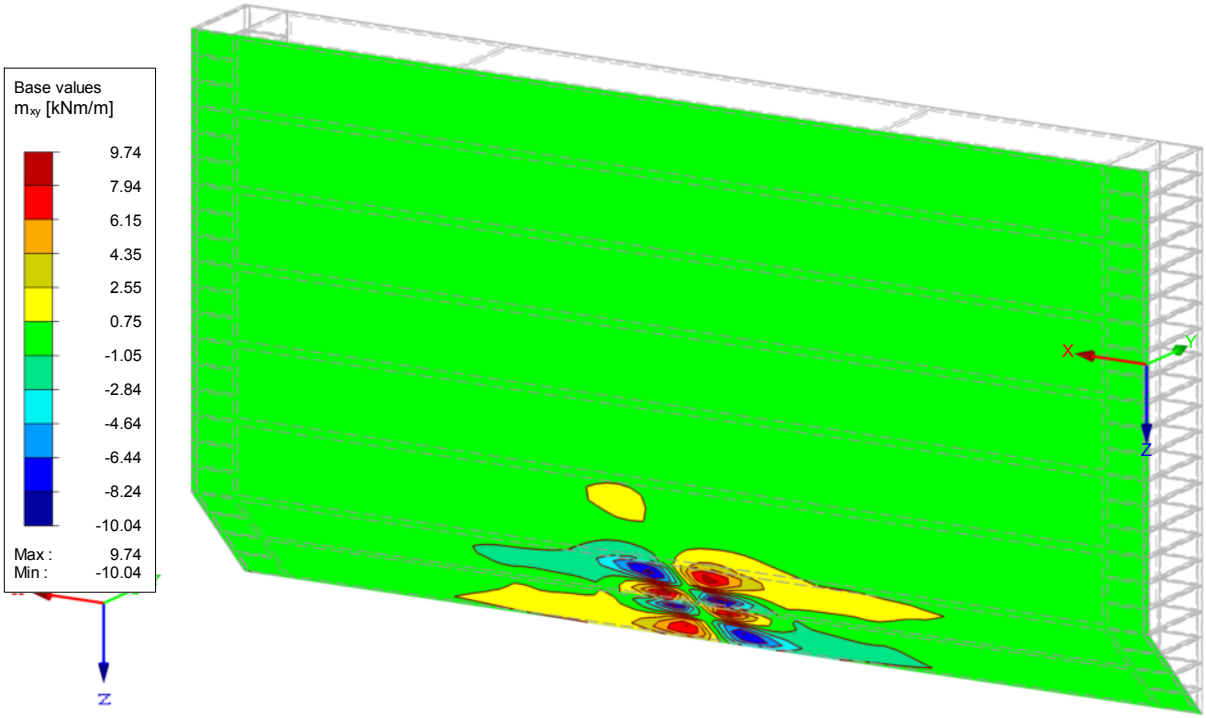


Max m-y: 77.43, Min m-y: -105.59 [kNm/m]

BASE VALUES M_{xy}, CO7: WATER IMPACT, ISOMETRIC

CO7: Water impact
m-xy

Isometric

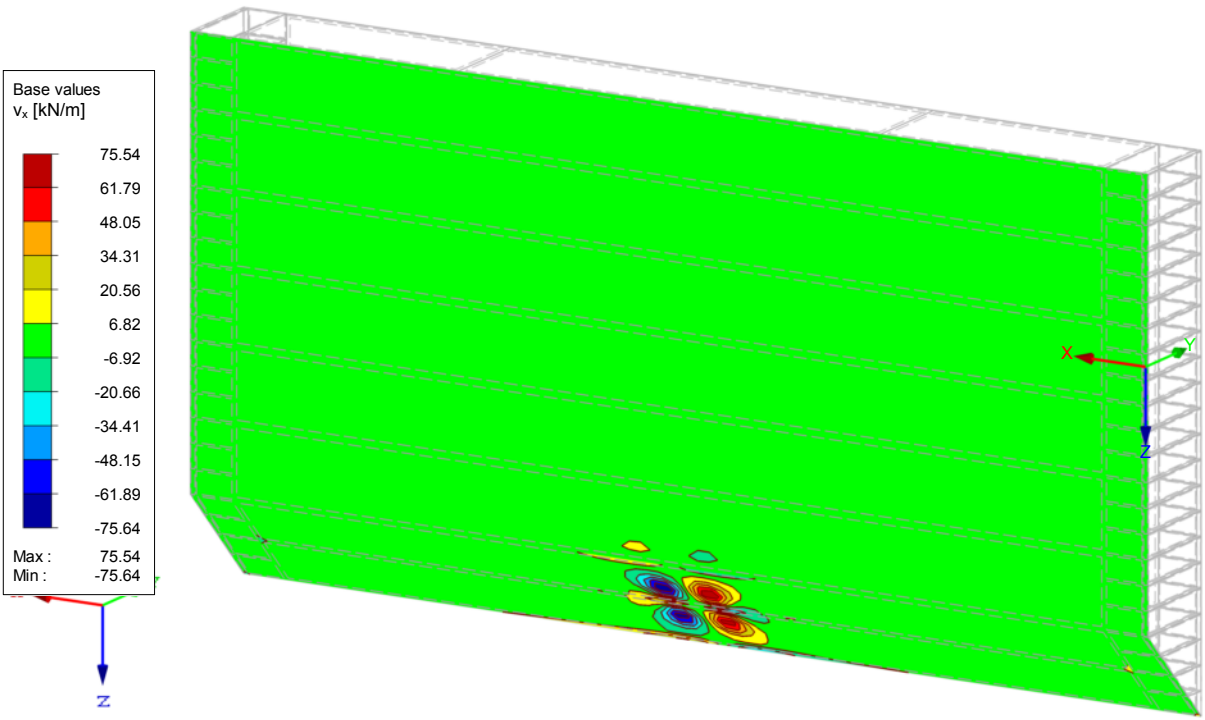


Max m-xy: 9.74, Min m-xy: -10.04 [kNm/m]

BASE VALUES V_x, CO7: WATER IMPACT, ISOMETRIC

CO7: Water impact
v-x

Isometric



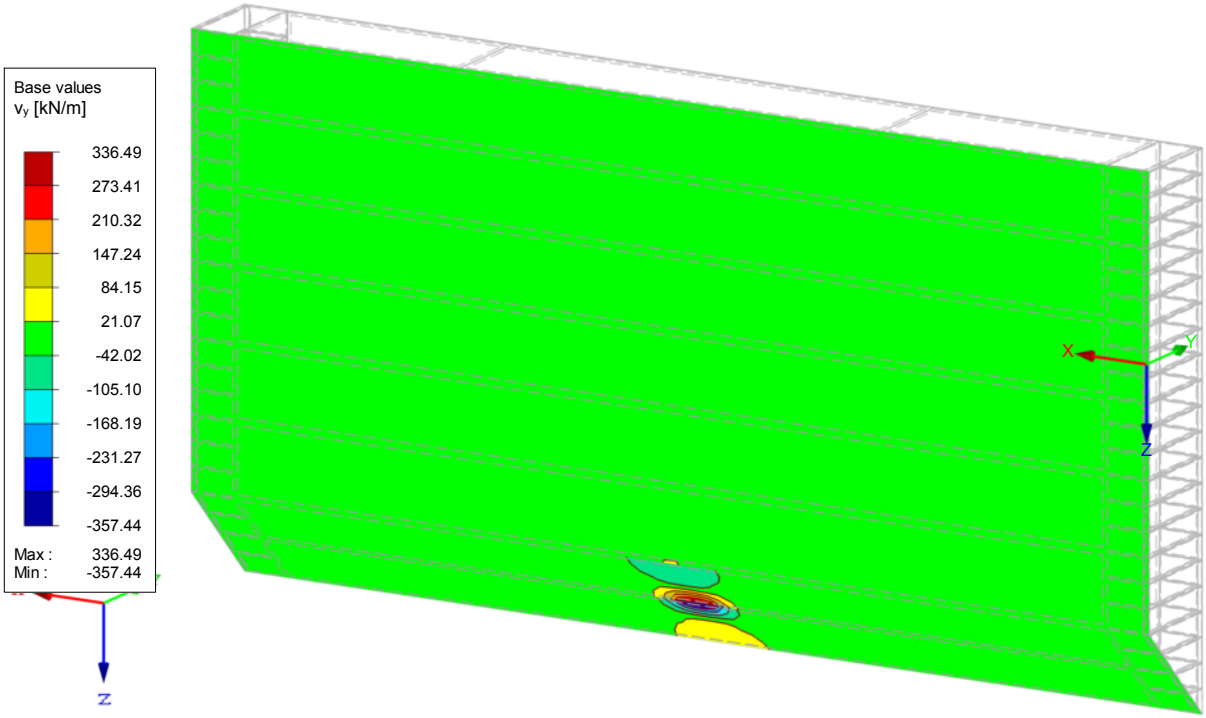
Max v-x: 75.54, Min v-x: -75.64 [kN/m]

Project: CIE5060 Model: V26
Graduation Project

BASE VALUES V_y, CO7: WATER IMPACT, ISOMETRIC

CO7: Water impact
v-y

Isometric

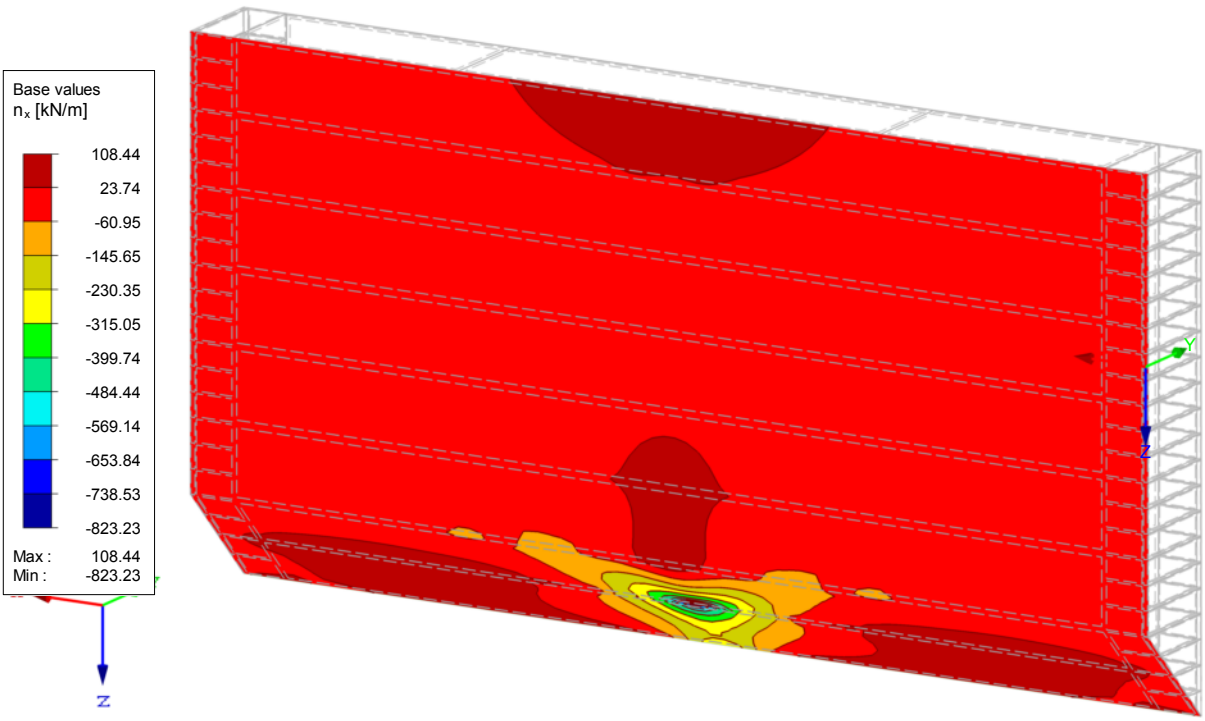


Max v-y: 336.49, Min v-y: -357.44 [kN/m]

BASE VALUES N_x, CO7: WATER IMPACT, ISOMETRIC

CO7: Water impact
n-x

Isometric

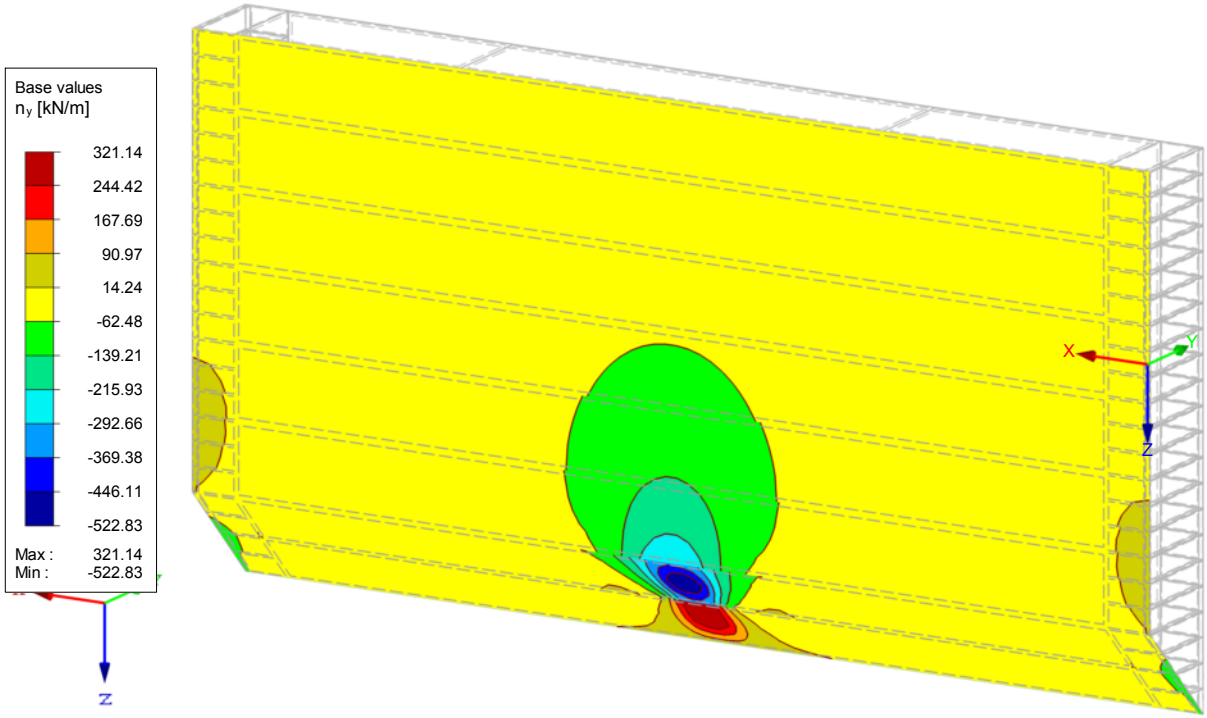


Max n-x: 108.44, Min n-x: -823.23 [kN/m]

BASE VALUES N_y, CO7: WATER IMPACT, ISOMETRIC

CO7: Water impact
n-y

Isometric

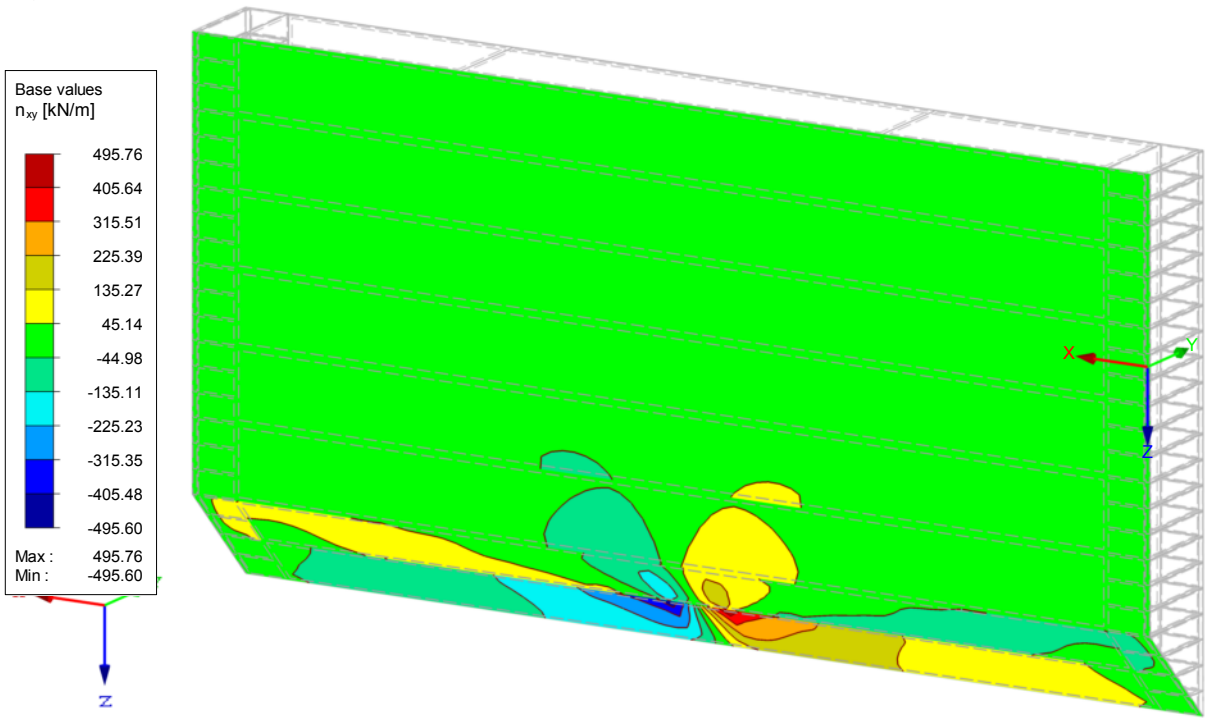


Max n-y: 321.14, Min n-y: -522.83 [kN/m]

BASE VALUES N_{xy}, CO7: WATER IMPACT, ISOMETRIC

CO7: Water impact
n-xy

Isometric



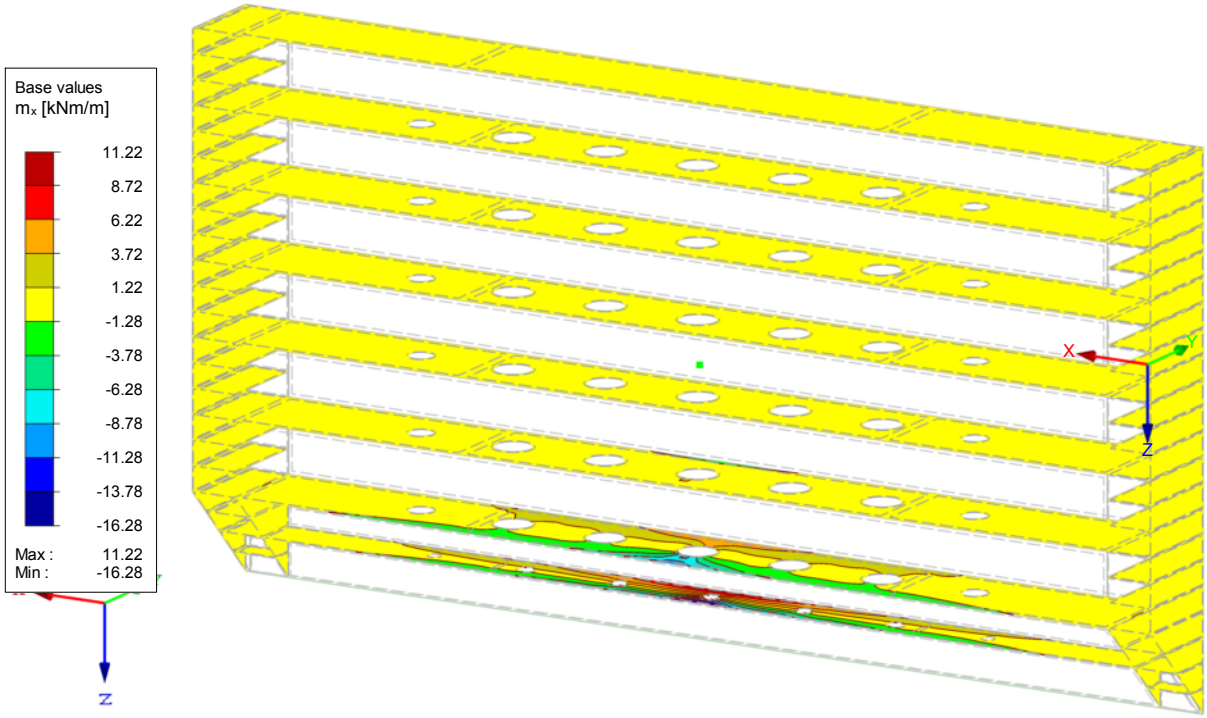
Max n-xy: 495.76, Min n-xy: -495.60 [kN/m]

Project: CIE5060 Model: V26
Graduation Project

BASE VALUES M_x, CO7: WATER IMPACT, ISOMETRIC

CO7: Water impact
m-x

Isometric

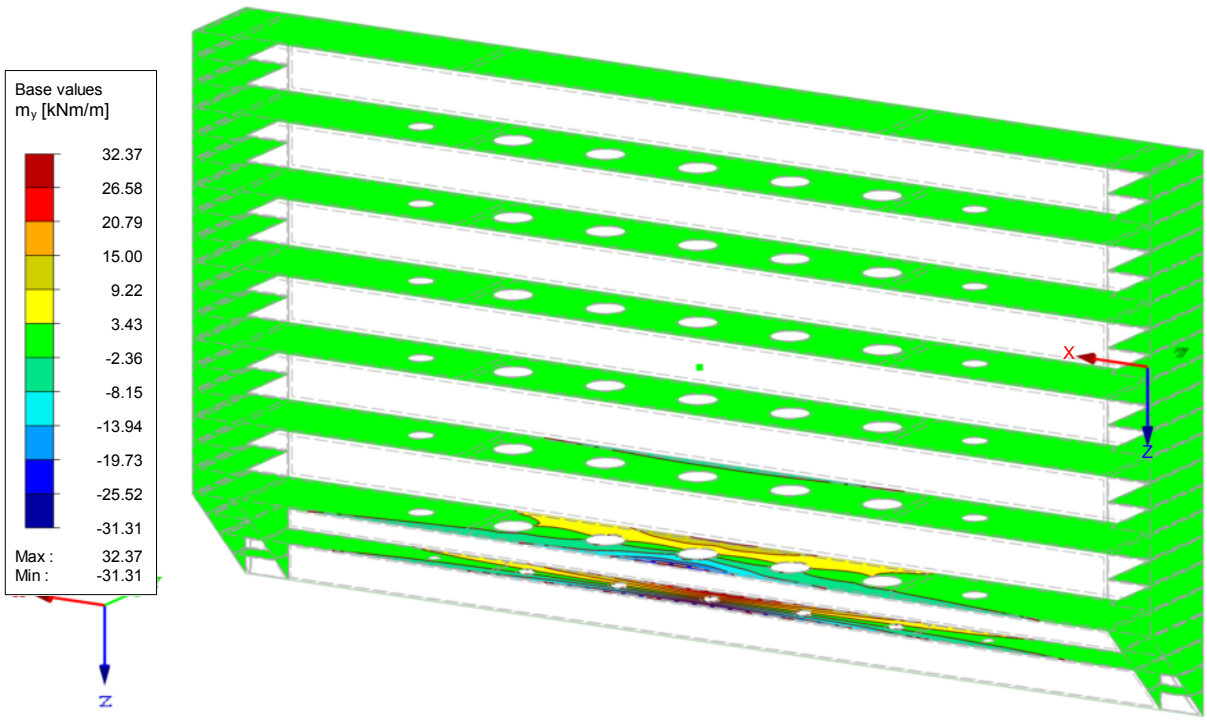


Max m-x: 11.22, Min m-x: -16.28 [kNm/m]

BASE VALUES M_y, CO7: WATER IMPACT, ISOMETRIC

CO7: Water impact
m-y

Isometric

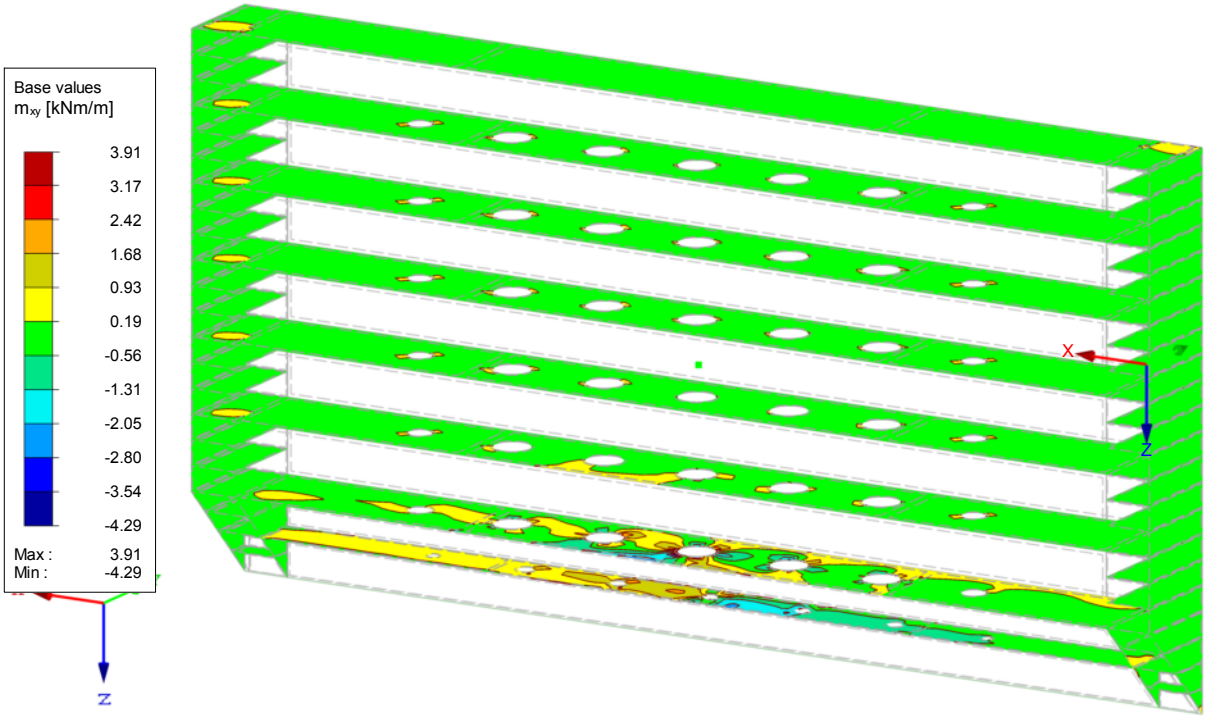


Max m-y: 32.37, Min m-y: -31.31 [kNm/m]

BASE VALUES M_{xy}, CO7: WATER IMPACT, ISOMETRIC

CO7: Water impact
m-xy

Isometric

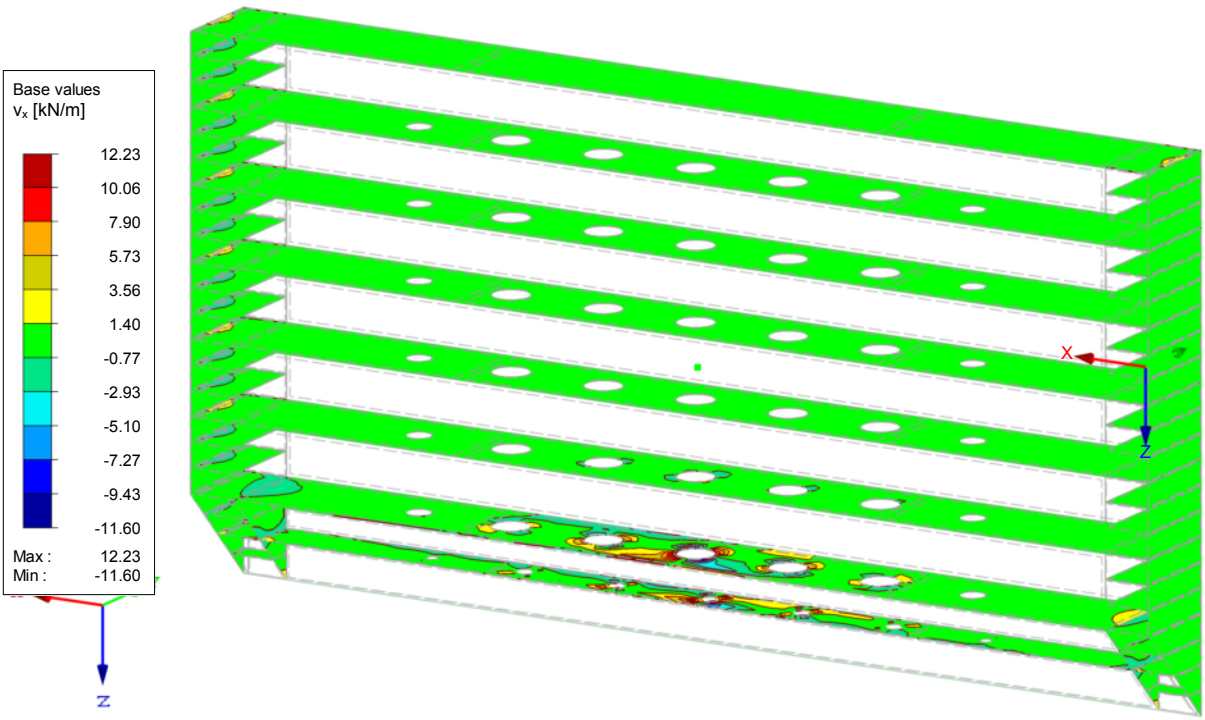


Max m-xy: 3.91, Min m-xy: -4.29 [kNm/m]

BASE VALUES V_x, CO7: WATER IMPACT, ISOMETRIC

CO7: Water impact
v-x

Isometric

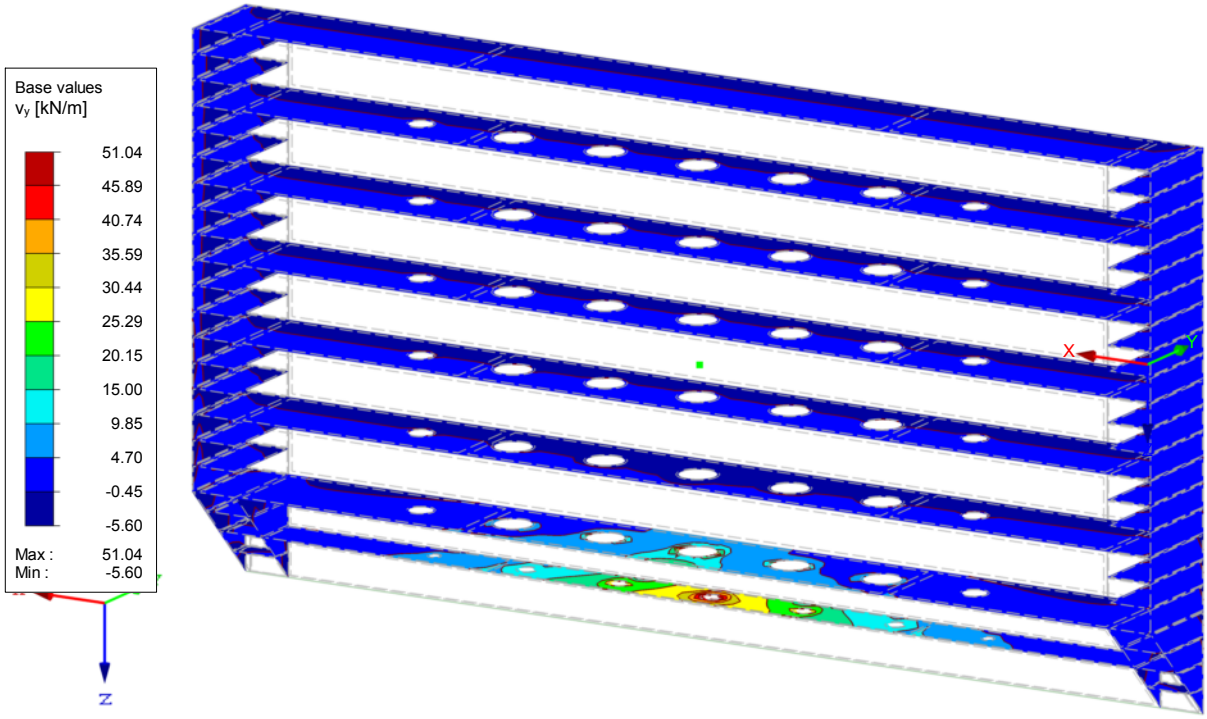


Max v-x: 12.23, Min v-x: -11.60 [kN/m]

BASE VALUES V_y, CO7: WATER IMPACT, ISOMETRIC

CO7: Water impact
v-y

Isometric

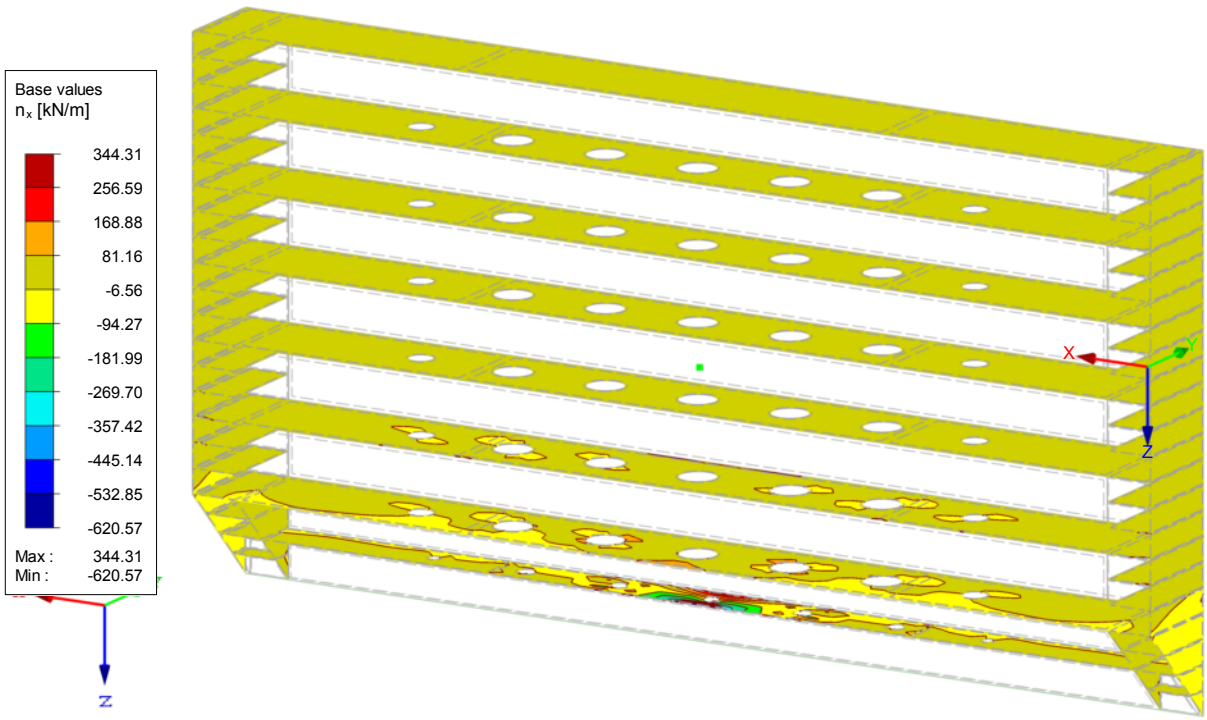


Max v-y: 51.04, Min v-y: -5.60 [kN/m]

BASE VALUES N_x, CO7: WATER IMPACT, ISOMETRIC

CO7: Water impact
n-x

Isometric



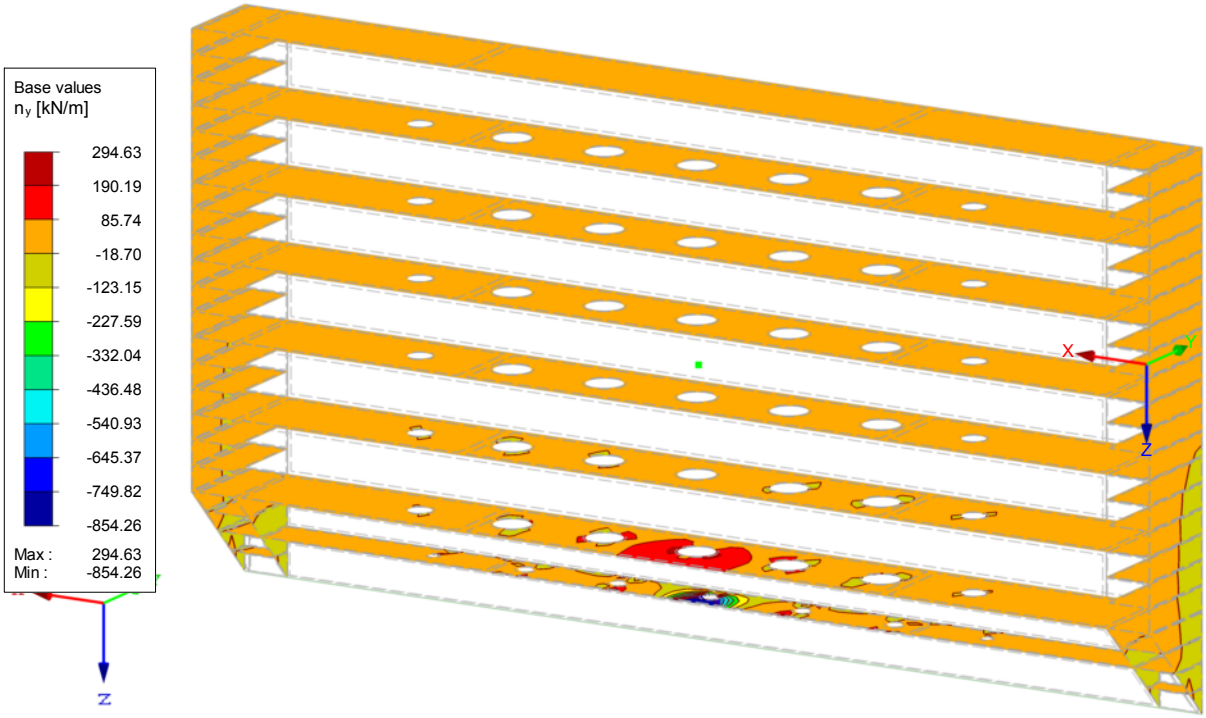
Max n-x: 344.31, Min n-x: -620.57 [kN/m]

Project: CIE5060 Model: V26
Graduation Project

BASE VALUES N_y, CO7: WATER IMPACT, ISOMETRIC

CO7: Water impact
n-y

Isometric

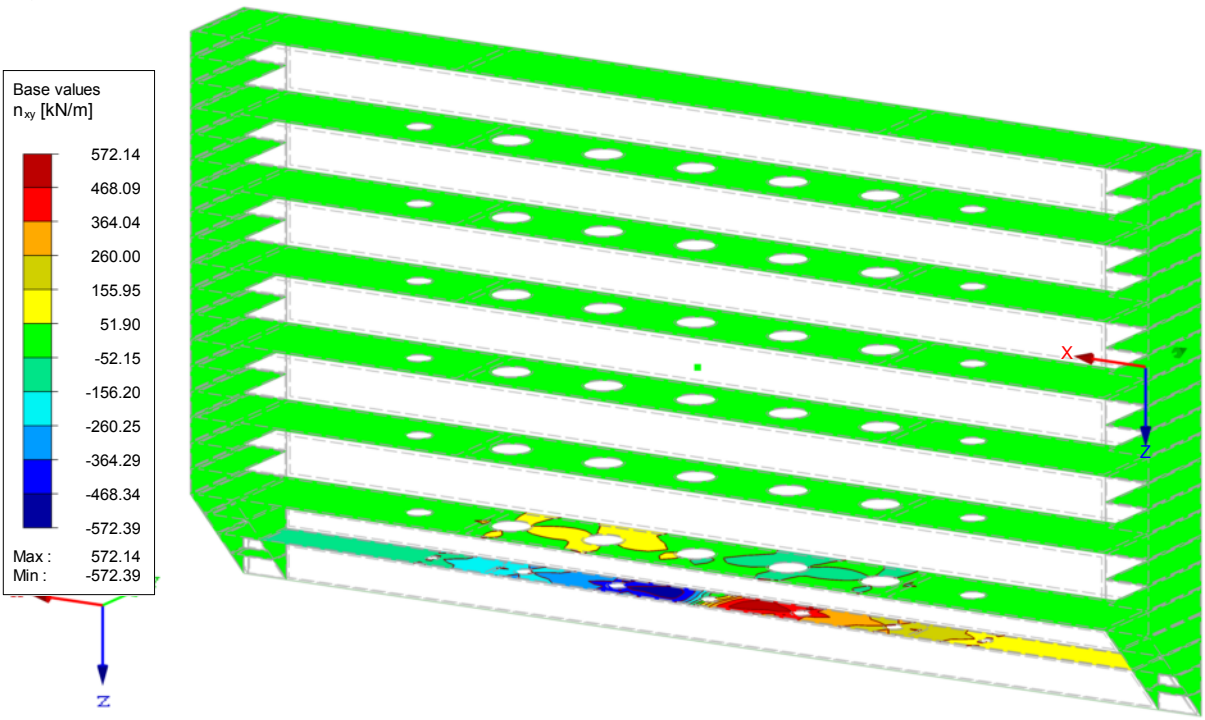


Max n-y: 294.63, Min n-y: -854.26 [kN/m]

BASE VALUES N_{xy}, CO7: WATER IMPACT, ISOMETRIC

CO7: Water impact
n-xy

Isometric



Max n-xy: 572.14, Min n-xy: -572.39 [kN/m]

Project: CIE5060 Model: V26
Graduation Project

RF-LAMINATE
Design of laminate surfaces

1.1.1 GENERAL DATA

Surfaces to design	1-34,47-66,101-228,233-380,385-404,406-411		
Material model:	Orthotropic		
Ultimate Limit State			
Load combinations to design	CO1	Positive drop ULS	Persistent/transient
	CO3	Negative drop ULS	Persistent/transient
	CO5	Ice	Persistent/transient
	CO6	Collision	Persistent/transient
	CO7	Water impact	Persistent/transient

1.2 MATERIAL CHARACTERISTICS - A

Comp. No.	Layer No.	Material Description	Thickness t [mm]	Angle β [°]	Poisson's Ratio [-] ν_{xy}	ν_{yx}	Shear Modulus [N/mm²] G_{xz}	G_{yz}	G_{xy}
1	**Outer sandwich | Middle part**								
	1	Lamina properties	18.7	0.00	0.270	0.088	4340.0	4340.0	4340.0
	2	Lamina properties	5.1	90.00	0.270	0.088	4340.0	4340.0	4340.0
	3	Lamina properties	5.1	-45.00	0.270	0.088	4340.0	4340.0	4340.0
	4	Lamina properties	5.1	45.00	0.270	0.088	4340.0	4340.0	4340.0
	5	kern	50.0	0.00	0.088	0.088	120.0	120.0	120.0
	6	Lamina properties	5.1	45.00	0.270	0.088	4340.0	4340.0	4340.0
	7	Lamina properties	5.1	-45.00	0.270	0.088	4340.0	4340.0	4340.0
	8	Lamina properties	5.1	90.00	0.270	0.088	4340.0	4340.0	4340.0
	9	Lamina properties	18.7	0.00	0.270	0.088	4340.0	4340.0	4340.0
2	**Horizontal plate | Middle part**								
	1	Lamina properties	6.0	0.00	0.269	0.088	4340.0	4340.0	4340.0
	2	Lamina properties	6.0	45.00	0.270	0.088	4340.0	4340.0	4340.0
	3	Lamina properties	6.0	-45.00	0.270	0.088	4340.0	4340.0	4340.0
	4	Lamina properties	6.0	90.00	0.270	0.088	4340.0	4340.0	4340.0
	5	kern	50.0	0.00	0.088	0.088	120.0	120.0	120.0
	6	Lamina properties	6.0	90.00	0.270	0.088	4340.0	4340.0	4340.0
	7	Lamina properties	6.0	-45.00	0.270	0.088	4340.0	4340.0	4340.0
	8	Lamina properties	6.0	45.00	0.270	0.088	4340.0	4340.0	4340.0
	9	Lamina properties	6.0	0.00	0.270	0.088	4340.0	4340.0	4340.0
3	**Closing plate at side of slide**								
	1	Lamina properties	7.0	45.00	0.269	0.088	4340.0	4340.0	4340.0
	2	Lamina properties	7.0	-45.00	0.270	0.088	4340.0	4340.0	4340.0
	3	Lamina properties	3.0	0.00	0.270	0.088	4340.0	4340.0	4340.0
	4	Lamina properties	3.0	90.00	0.270	0.088	4340.0	4340.0	4340.0
	5	kern	50.0	0.00	0.088	0.088	120.0	120.0	120.0
	6	Lamina properties	3.0	90.00	0.270	0.088	4340.0	4340.0	4340.0
	7	Lamina properties	3.0	0.00	0.270	0.088	4340.0	4340.0	4340.0
	8	Lamina properties	7.0	-45.00	0.270	0.088	4340.0	4340.0	4340.0
	9	Lamina properties	7.0	45.00	0.270	0.088	4340.0	4340.0	4340.0
4	**Extra horizontal plates**								
	1	Lamina properties	5.0	0.00	0.270	0.088	4340.0	4340.0	4340.0
	2	Lamina properties	5.0	90.00	0.270	0.088	4340.0	4340.0	4340.0
	3	Lamina properties	5.0	-45.00	0.270	0.088	4340.0	4340.0	4340.0
	4	Lamina properties	5.0	45.00	0.270	0.088	4340.0	4340.0	4340.0
	5	kern	50.0	0.00	0.088	0.088	120.0	120.0	120.0
	6	Lamina properties	5.0	45.00	0.270	0.088	4340.0	4340.0	4340.0
	7	Lamina properties	5.0	-45.00	0.270	0.088	4340.0	4340.0	4340.0
	8	Lamina properties	5.0	90.00	0.270	0.088	4340.0	4340.0	4340.0
	9	Lamina properties	5.0	0.00	0.270	0.088	4340.0	4340.0	4340.0
5	**Outer sandwich | Side part**								
	1	Lamina properties	5.1	0.00	0.270	0.088	4340.0	4340.0	4340.0
	2	Lamina properties	5.1	90.00	0.270	0.088	4340.0	4340.0	4340.0
	3	Lamina properties	11.9	-45.00	0.270	0.088	4340.0	4340.0	4340.0
	4	Lamina properties	11.9	45.00	0.270	0.088	4340.0	4340.0	4340.0
	5	kern	50.0	0.00	0.088	0.088	120.0	120.0	120.0
	6	Lamina properties	11.9	45.00	0.270	0.088	4340.0	4340.0	4340.0
	7	Lamina properties	11.9	-45.00	0.270	0.088	4340.0	4340.0	4340.0
	8	Lamina properties	5.1	90.00	0.270	0.088	4340.0	4340.0	4340.0
	9	Lamina properties	5.1	0.00	0.270	0.088	4340.0	4340.0	4340.0
6	**Horizontal plate | Part next to support**								
	1	Lamina properties	3.6	0.00	0.269	0.088	4340.0	4340.0	4340.0
	2	Lamina properties	13.2	-45.00	0.270	0.088	4340.0	4340.0	4340.0
	3	Lamina properties	3.6	45.00	0.270	0.088	4340.0	4340.0	4340.0
	4	Lamina properties	3.6	90.00	0.270	0.088	4340.0	4340.0	4340.0
	5	kern	50.0	0.00	0.088	0.088	120.0	120.0	120.0
	6	Lamina properties	3.6	90.00	0.270	0.088	4340.0	4340.0	4340.0
	7	Lamina properties	3.6	45.00	0.270	0.088	4340.0	4340.0	4340.0
	8	Lamina properties	13.2	-45.00	0.270	0.088	4340.0	4340.0	4340.0
	9	Lamina properties	3.6	0.00	0.270	0.088	4340.0	4340.0	4340.0
8	**Horizontal plate | Side part**								
	1	Lamina properties	3.6	0.00	0.269	0.088	4340.0	4340.0	4340.0
	2	Lamina properties	8.4	45.00	0.270	0.088	4340.0	4340.0	4340.0
	3	Lamina properties	8.4	-45.00	0.270	0.088	4340.0	4340.0	4340.0
	4	Lamina properties	3.6	90.00	0.270	0.088	4340.0	4340.0	4340.0
	5	kern	50.0	0.00	0.088	0.088	120.0	120.0	120.0
	6	Lamina properties	3.6	90.00	0.270	0.088	4340.0	4340.0	4340.0
	7	Lamina properties	8.4	-45.00	0.270	0.088	4340.0	4340.0	4340.0
	8	Lamina properties	8.4	45.00	0.270	0.088	4340.0	4340.0	4340.0
	9	Lamina properties	3.6	0.00	0.270	0.088	4340.0	4340.0	4340.0

Project: CIE5060 Model: V26
Graduation Project

1.2 MATERIAL CHARACTERISTICS - B

Comp. No.	Layer No.	Material Description	Modulus of Elast. [N/mm²] E_x	E_y	Sp. Weight γ [N/m³]	Coef. of Th. Exp. α_T [1/K]
1	**Outer sandwich | Middle part**					
	1	Lamina properties	43200.0	14100.0	20220.0	0.0E+00
	2	Lamina properties	43200.0	14100.0	20220.0	0.0E+00
	3	Lamina properties	43200.0	14100.0	20220.0	0.0E+00
	4	Lamina properties	43200.0	14100.0	20220.0	0.0E+00
	5	kern	310.0	310.0	736.0	0.0E+00
	6	Lamina properties	43200.0	14100.0	20220.0	0.0E+00
	7	Lamina properties	43200.0	14100.0	20220.0	0.0E+00
	8	Lamina properties	43200.0	14100.0	20220.0	0.0E+00
	9	Lamina properties	43200.0	14100.0	20220.0	0.0E+00
2	**Horizontal plate | Middle part**					
	1	Lamina properties	43200.0	14100.0	20220.0	0.0E+00
	2	Lamina properties	43200.0	14100.0	20220.0	0.0E+00
	3	Lamina properties	43200.0	14100.0	20220.0	0.0E+00
	4	Lamina properties	43200.0	14100.0	20220.0	0.0E+00
	5	kern	310.0	310.0	736.0	0.0E+00
	6	Lamina properties	43200.0	14100.0	20220.0	0.0E+00
	7	Lamina properties	43200.0	14100.0	20220.0	0.0E+00
	8	Lamina properties	43200.0	14100.0	20220.0	0.0E+00
	9	Lamina properties	43200.0	14100.0	20220.0	0.0E+00
3	**Closing plate at side of slide**					
	1	Lamina properties	43200.0	14100.0	20220.0	0.0E+00
	2	Lamina properties	43200.0	14100.0	20220.0	0.0E+00
	3	Lamina properties	43200.0	14100.0	20220.0	0.0E+00
	4	Lamina properties	43200.0	14100.0	20220.0	0.0E+00
	5	kern	310.0	310.0	736.0	0.0E+00
	6	Lamina properties	43200.0	14100.0	20220.0	0.0E+00
	7	Lamina properties	43200.0	14100.0	20220.0	0.0E+00
	8	Lamina properties	43200.0	14100.0	20220.0	0.0E+00
	9	Lamina properties	43200.0	14100.0	20220.0	0.0E+00
4	**Extra horizontal plates**					
	1	Lamina properties	43200.0	14100.0	20220.0	0.0E+00
	2	Lamina properties	43200.0	14100.0	20220.0	0.0E+00
	3	Lamina properties	43200.0	14100.0	20220.0	0.0E+00
	4	Lamina properties	43200.0	14100.0	20220.0	0.0E+00
	5	kern	310.0	310.0	736.0	0.0E+00
	6	Lamina properties	43200.0	14100.0	20220.0	0.0E+00
	7	Lamina properties	43200.0	14100.0	20220.0	0.0E+00
	8	Lamina properties	43200.0	14100.0	20220.0	0.0E+00
	9	Lamina properties	43200.0	14100.0	20220.0	0.0E+00
5	**Outer sandwich | Side part**					
	1	Lamina properties	43200.0	14100.0	20220.0	0.0E+00
	2	Lamina properties	43200.0	14100.0	20220.0	0.0E+00
	3	Lamina properties	43200.0	14100.0	20220.0	0.0E+00
	4	Lamina properties	43200.0	14100.0	20220.0	0.0E+00
	5	kern	310.0	310.0	736.0	0.0E+00
	6	Lamina properties	43200.0	14100.0	20220.0	0.0E+00
	7	Lamina properties	43200.0	14100.0	20220.0	0.0E+00
	8	Lamina properties	43200.0	14100.0	20220.0	0.0E+00
	9	Lamina properties	43200.0	14100.0	20220.0	0.0E+00
6	**Horizontal plate | Part next to support**					
	1	Lamina properties	43200.0	14100.0	20220.0	0.0E+00
	2	Lamina properties	43200.0	14100.0	20220.0	0.0E+00
	3	Lamina properties	43200.0	14100.0	20220.0	0.0E+00
	4	Lamina properties	43200.0	14100.0	20220.0	0.0E+00
	5	kern	310.0	310.0	736.0	0.0E+00
	6	Lamina properties	43200.0	14100.0	20220.0	0.0E+00
	7	Lamina properties	43200.0	14100.0	20220.0	0.0E+00
	8	Lamina properties	43200.0	14100.0	20220.0	0.0E+00
	9	Lamina properties	43200.0	14100.0	20220.0	0.0E+00
8	**Horizontal plate | Side part**					
	1	Lamina properties	43200.0	14100.0	20220.0	0.0E+00
	2	Lamina properties	43200.0	14100.0	20220.0	0.0E+00
	3	Lamina properties	43200.0	14100.0	20220.0	0.0E+00
	4	Lamina properties	43200.0	14100.0	20220.0	0.0E+00
	5	kern	310.0	310.0	736.0	0.0E+00
	6	Lamina properties	43200.0	14100.0	20220.0	0.0E+00
	7	Lamina properties	43200.0	14100.0	20220.0	0.0E+00
	8	Lamina properties	43200.0	14100.0	20220.0	0.0E+00
	9	Lamina properties	43200.0	14100.0	20220.0	0.0E+00

2.1 MAX STRESS RATIO BY LOADING

Load-ing	Surface No.	Point No.	Point Coordinates [m] X	Y	Z	Layer No.	z [mm]	Side	Stresses [-] Symbol	Existing	Limit	Ratio [-]
CO1	**Positive drop ULS**											
	8	2436	22.876	0.000	10.500	1	0.0	Top	ε_x	-0.0052		
	410	2440	20.897	0.000	10.500	1	0.0	Top	ε_y	0.0039		
	396	49	-0.100	4.000	14.500	9	118.0	Bottom	γ_{xy}	0.0052		
CO3	**Negative drop ULS**											
	8	2436	22.876	0.000	10.500	1	0.0	Top	ε_x	0.0018		
	408	9344	21.887	4.000	12.500	1	0.0	Top	ε_y	0.0029		
	407	12197	39.062	2.500	12.500	1	0.0	Top	γ_{xy}	0.0028		
CO5	**Ice**											
	281	5316	1.750	0.000	0.000	9	118.0	Bottom	ε_x	-0.0008		
	17	5268	25.349	0.000	0.000	9	118.0	Bottom	ε_y	0.0026		
	5	1101	12.275	1.350	1.500	1	0.0	Top	γ_{xy}	0.0016		

Project: CIE5060 Model: V26
Graduation Project

2.1 MAX STRESS RATIO BY LOADING

Load-ing	Surface No.	Point No.	Point Coordinates [m] X	Y	Z	Layer No.	z [mm]	Side	Stresses [-] Symbol	Existing	Limit	Ratio [-]
CO6	**Collision**											
	411	13275	20.896	3.333	13.833	9	118.0	Bottom	ε_x	0.0002		
	409	12553	20.895	4.000	14.500	1	0.0	Top	ε_y	-0.0007		
	411	13201	21.879	3.667	14.167	9	118.0	Bottom	γ_{xy}	0.0005		
CO7	**Water impact**											
	411	13426	20.403	2.667	13.167	1	0.0	Top	ε_x	-0.0007		
	411	9388	20.897	2.000	12.500	1	0.0	Top	ε_y	0.0030		
	411	13500	19.415	2.333	12.833	9	118.0	Bottom	γ_{xy}	0.0016		
-	**Maximum Stresses**											
CO1	8	2436	22.876	0.000	10.500	1	0.0	Top	ε_x	-0.0052		
CO1	410	2440	20.897	0.000	10.500	1	0.0	Top	ε_y	0.0039		
CO1	396	49	-0.100	4.000	14.500	9	118.0	Bottom	γ_{xy}	0.0052		
Maximum Ratio		**0.0000**										

2.2 MAX STRESS RATIO BY SURFACE

Surface No.	Point No.	Point Coordinates [m] X	Y	Z	Load-ing	Layer No.	z [mm]	Side	Stresses [-] Symbol	Existing	Limit	Ratio [-]
1	10525	20.403	0.000	7.500	CO1	9	98.0	Bottom	ε_x	-0.0045		
	10680	28.275	1.350	7.500	CO1	1	0.0	Top	ε_y	0.0020		
	6087	29.800	1.500	7.500	CO1	1	0.0	Top	γ_{xy}	-0.0041		
2	398	29.800	0.000	7.500	CO1	1	0.0	Top	ε_x	-0.0034		
	7794	31.263	0.000	7.500	CO1	1	0.0	Top	ε_y	0.0018		
	366	32.150	2.000	7.500	CO1	1	0.0	Top	γ_{xy}	-0.0045		
3	528	20.403	0.000	4.500	CO1	9	98.0	Bottom	ε_x	-0.0039		
	594	13.025	2.650	4.500	CO1	1	0.0	Top	ε_y	-0.0021		
	600	12.275	1.350	4.500	CO1	9	98.0	Bottom	γ_{xy}	0.0042		
4	402	29.800	0.000	4.500	CO1	1	0.0	Top	ε_x	-0.0030		
	874	32.296	2.354	4.500	CO1	1	0.0	Top	ε_y	-0.0019		
	345	32.150	2.000	4.500	CO1	1	0.0	Top	γ_{xy}	-0.0047		
5	1029	20.403	0.000	1.500	CO1	9	98.0	Bottom	ε_x	-0.0035		
	1071	22.381	4.000	1.500	CO1	1	0.0	Top	ε_y	-0.0022		
	1101	12.275	1.350	1.500	CO1	9	98.0	Bottom	γ_{xy}	0.0043		
6	406	29.800	0.000	1.500	CO1	1	0.0	Top	ε_x	-0.0026		
	1327	31.263	0.000	1.500	CO1	1	0.0	Top	ε_y	0.0020		
	324	32.150	2.000	1.500	CO1	1	0.0	Top	γ_{xy}	-0.0047		
7	9814	23.865	4.000	7.500	CO1	9	118.0	Bottom	ε_x	0.0035		
	8187	15.951	4.000	7.500	CO1	9	118.0	Bottom	ε_y	-0.0024		
	1506	2.237	4.000	8.000	CO1	1	0.0	Top	γ_{xy}	-0.0023		
8	2436	22.876	0.000	10.500	CO1	1	0.0	Top	ε_x	-0.0052		
	2441	20.403	0.000	10.500	CO1	1	0.0	Top	ε_y	0.0031		
	2477	2.725	0.000	10.500	CO1	9	118.0	Bottom	γ_{xy}	-0.0040		
9	397	11.500	0.000	7.500	CO1	9	98.0	Bottom	ε_x	-0.0034		
	2054	10.038	0.000	7.500	CO1	1	0.0	Top	ε_y	0.0019		
	373	9.150	2.000	7.500	CO1	1	0.0	Top	γ_{xy}	0.0045		
10	579	17.930	4.000	4.500	CO1	9	118.0	Bottom	ε_x	0.0035		
	574	20.403	4.000	4.500	CO1	9	118.0	Bottom	ε_y	-0.0026		
	2621	2.237	4.000	5.000	CO1	1	0.0	Top	γ_{xy}	-0.0024		
11	10020	23.370	0.000	7.500	CO1	1	0.0	Top	ε_x	-0.0045		
	524	18.424	0.000	4.500	CO1	1	0.0	Top	ε_y	0.0030		
	3124	2.237	0.000	5.000	CO1	9	118.0	Bottom	γ_{xy}	0.0028		
12	401	11.500	0.000	4.500	CO1	9	98.0	Bottom	ε_x	-0.0030		
	3447	9.004	2.354	4.500	CO1	1	0.0	Top	ε_y	-0.0019		
	352	9.150	2.000	4.500	CO1	1	0.0	Top	γ_{xy}	0.0047		
13	568	23.370	4.000	4.500	CO1	9	118.0	Bottom	ε_x	0.0035		
	1075	20.403	4.000	1.500	CO1	9	118.0	Bottom	ε_y	-0.0025		
	3580	2.237	4.000	2.000	CO1	1	0.0	Top	γ_{xy}	-0.0023		
14	534	23.370	0.000	4.500	CO1	1	0.0	Top	ε_x	-0.0040		
	1025	18.424	0.000	1.500	CO1	1	0.0	Top	ε_y	0.0029		
	4083	2.237	0.000	2.000	CO1	9	118.0	Bottom	γ_{xy}	0.0030		
15	405	11.500	0.000	1.500	CO1	9	98.0	Bottom	ε_x	-0.0027		
	4406	9.004	2.354	1.500	CO1	1	0.0	Top	ε_y	-0.0020		
	331	9.150	2.000	1.500	CO1	1	0.0	Top	γ_{xy}	0.0046		
16	1069	23.370	4.000	1.500	CO1	9	118.0	Bottom	ε_x	0.0034		
	4766	20.403	4.000	-1.500	CO1	9	118.0	Bottom	ε_y	-0.0023		
	4998	39.063	4.000	1.000	CO1	1	0.0	Top	γ_{xy}	-0.0022		

Project: CIE5060 Model: V26
Graduation Project

2.2 MAX STRESS RATIO BY SURFACE

Surface No.	Point No.	Point Coordinates [m] X	Y	Z	Load-ing	Layer No.	z [mm]	Side	Stresses [-] Symbol	Existing	Limit	Ratio [-]
17	1035	23.370	0.000	1.500	CO1	1	0.0	Top	ε_x	-0.0035		
	5075	22.381	0.000	-1.500	CO1	1	0.0	Top	ε_y	0.0031		
	5158	2.237	0.000	-1.000	CO1	9	118.0	Bottom	γ_{xy}	0.0026		
18	411	11.500	4.000	-1.500	CO1	1	0.0	Top	ε_x	0.0024		
	4652	11.012	4.000	-1.500	CO1	1	0.0	Top	ε_y	-0.0022		
	310	9.150	2.000	-1.500	CO1	1	0.0	Top	γ_{xy}	0.0041		
19	4736	17.930	4.000	-1.500	CO1	9	118.0	Bottom	ε_x	0.0031		
	5848	20.403	4.000	-4.500	CO1	9	118.0	Bottom	ε_y	-0.0014		
	4970	37.112	4.000	-1.500	CO1	9	118.0	Bottom	γ_{xy}	-0.0020		
20	5071	23.370	0.000	-1.500	CO1	1	0.0	Top	ε_x	-0.0030		
	6157	22.381	0.000	-4.500	CO1	1	0.0	Top	ε_y	0.0032		
	6240	2.237	0.000	-4.000	CO1	9	118.0	Bottom	γ_{xy}	0.0020		
21	415	11.500	4.000	-4.500	CO1	1	0.0	Top	ε_x	0.0021		
	5734	11.012	4.000	-4.500	CO1	1	0.0	Top	ε_y	-0.0024		
	6581	2.237	1.500	-4.500	CO1	1	0.0	Top	γ_{xy}	0.0031		
22	5884	23.370	4.000	-4.500	CO1	9	118.0	Bottom	ε_x	0.0026		
	6936	20.897	4.000	-7.500	CO1	9	118.0	Bottom	ε_y	-0.0020		
	5644	3.700	4.000	-4.500	CO1	9	118.0	Bottom	γ_{xy}	0.0017		
23	6151	23.865	0.000	-4.500	CO1	1	0.0	Top	ε_x	-0.0024		
	7247	20.403	0.000	-7.500	CO1	1	0.0	Top	ε_y	0.0022		
	7322	2.237	0.000	-7.000	CO1	9	118.0	Bottom	γ_{xy}	0.0019		
24	419	11.500	4.000	-7.500	CO1	1	0.0	Top	ε_x	0.0018		
	417	11.500	0.000	-7.500	CO1	1	0.0	Top	ε_y	0.0025		
	7319	2.725	0.000	-7.500	CO1	9	98.0	Bottom	γ_{xy}	0.0017		
25	4772	20.897	4.000	-1.500	CO1	9	98.0	Bottom	ε_x	0.0030		
	4790	22.381	4.000	-1.500	CO1	1	0.0	Top	ε_y	-0.0026		
	7799	12.275	1.350	-1.500	CO1	9	98.0	Bottom	γ_{xy}	0.0041		
26	412	29.800	4.000	-1.500	CO1	9	98.0	Bottom	ε_x	0.0023		
	4886	30.288	4.000	-1.500	CO1	1	0.0	Top	ε_y	-0.0022		
	303	32.150	2.000	-1.500	CO1	1	0.0	Top	γ_{xy}	-0.0041		
27	5854	20.897	4.000	-4.500	CO1	9	98.0	Bottom	ε_x	0.0026		
	5872	22.381	4.000	-4.500	CO1	1	0.0	Top	ε_y	-0.0029		
	8177	12.275	1.350	-4.500	CO1	9	98.0	Bottom	γ_{xy}	0.0033		
28	416	29.800	4.000	-4.500	CO1	9	98.0	Bottom	ε_x	0.0020		
	5968	30.288	4.000	-4.500	CO1	1	0.0	Top	ε_y	-0.0024		
	8442	39.063	1.500	-4.500	CO1	1	0.0	Top	γ_{xy}	-0.0031		
29	6930	20.403	4.000	-7.500	CO1	1	0.0	Top	ε_x	0.0022		
	7247	20.403	0.000	-7.500	CO1	1	0.0	Top	ε_y	0.0027		
	8788	29.305	2.000	-7.500	CO1	1	0.0	Top	γ_{xy}	-0.0010		
30	420	29.800	4.000	-7.500	CO1	9	98.0	Bottom	ε_x	0.0018		
	418	29.800	0.000	-7.500	CO1	1	0.0	Top	ε_y	0.0024		
	7173	38.575	0.000	-7.500	CO1	9	98.0	Bottom	γ_{xy}	-0.0016		
31	2441	20.403	0.000	10.500	CO1	9	98.0	Bottom	ε_x	-0.0052		
	2445	18.424	0.000	10.500	CO1	1	0.0	Top	ε_y	0.0027		
	8948	11.500	1.500	10.500	CO1	9	98.0	Bottom	γ_{xy}	0.0036		
32	421	11.500	0.000	10.500	CO1	1	0.0	Top	ε_x	-0.0040		
	2462	10.037	0.000	10.500	CO1	1	0.0	Top	ε_y	0.0025		
	394	9.150	2.000	10.500	CO1	1	0.0	Top	γ_{xy}	0.0038		
33	9348	19.908	4.000	12.500	CO1	1	0.0	Top	ε_x	0.0032		
	9339	24.360	4.000	12.500	CO1	1	0.0	Top	ε_y	-0.0029		
	9404	28.811	2.000	12.500	CO1	1	0.0	Top	γ_{xy}	-0.0029		
34	438	11.500	4.000	12.500	CO1	1	0.0	Top	ε_x	0.0028		
	438	11.500	4.000	12.500	CO1	1	0.0	Top	ε_y	-0.0028		
	9586	2.238	2.500	12.500	CO1	1	0.0	Top	γ_{xy}	0.0046		
47	9636	41.200	3.500	7.500	CO1	9	98.0	Bottom	ε_x	0.0012		
	43	41.200	4.000	7.500	CO1	9	98.0	Bottom	ε_y	-0.0023		
	43	41.200	4.000	7.500	CO1	1	0.0	Top	γ_{xy}	0.0049		
48	9636	41.200	3.500	7.500	CO1	9	98.0	Bottom	ε_x	0.0014		
	43	41.200	4.000	7.500	CO1	1	0.0	Top	ε_y	-0.0025		
	9638	41.200	2.500	7.500	CO1	9	98.0	Bottom	γ_{xy}	0.0042		
49	9672	0.100	3.500	7.500	CO1	1	0.0	Top	ε_x	0.0012		
	88	0.100	4.000	7.500	CO1	9	98.0	Bottom	ε_y	-0.0023		
	88	0.100	4.000	7.500	CO1	9	98.0	Bottom	γ_{xy}	0.0049		
50	9699	41.200	3.500	4.500	CO1	9	98.0	Bottom	ε_x	0.0012		

Project: CIE5060 Model: V26
Graduation Project

2.2 MAX STRESS RATIO BY SURFACE

Surface No.	Point No.	Point Coordinates [m] X	Y	Z	Load-ing	Layer No.	z [mm]	Side	Stresses [-] Symbol	Existing	Limit	Ratio [-]
	51	41.200	4.000	4.500	CO1	9	98.0	Bottom	ε_y	-0.0024		
	51	41.200	4.000	4.500	CO1	1	0.0	Top	γ_{xy}	0.0051		
51	9699	41.200	3.500	4.500	CO1	9	98.0	Bottom	ε_x	0.0014		
	51	41.200	4.000	4.500	CO1	9	98.0	Bottom	ε_y	-0.0026		
	9701	41.200	2.500	4.500	CO1	9	98.0	Bottom	γ_{xy}	0.0043		
52	9672	0.100	3.500	7.500	CO1	1	0.0	Top	ε_x	0.0014		
	88	0.100	4.000	7.500	CO1	9	98.0	Bottom	ε_y	-0.0025		
	9674	0.100	2.500	7.500	CO1	1	0.0	Top	γ_{xy}	0.0042		
53	9744	41.200	3.500	1.500	CO1	9	98.0	Bottom	ε_x	0.0012		
	59	41.200	4.000	1.500	CO1	9	98.0	Bottom	ε_y	-0.0023		
	59	41.200	4.000	1.500	CO1	1	0.0	Top	γ_{xy}	0.0051		
54	9744	41.200	3.500	1.500	CO1	9	98.0	Bottom	ε_x	0.0015		
	59	41.200	4.000	1.500	CO1	9	98.0	Bottom	ε_y	-0.0026		
	9746	41.200	2.500	1.500	CO1	9	98.0	Bottom	γ_{xy}	0.0043		
55	9780	0.100	3.500	4.500	CO1	1	0.0	Top	ε_x	0.0012		
	125	0.100	4.000	4.500	CO1	9	98.0	Bottom	ε_y	-0.0024		
	125	0.100	4.000	4.500	CO1	9	98.0	Bottom	γ_{xy}	0.0051		
56	9807	41.200	3.500	-1.500	CO1	9	98.0	Bottom	ε_x	0.0011		
	63	41.200	4.000	-1.500	CO1	9	98.0	Bottom	ε_y	-0.0021		
	63	41.200	4.000	-1.500	CO1	1	0.0	Top	γ_{xy}	0.0045		
57	9807	41.200	3.500	-1.500	CO1	9	98.0	Bottom	ε_x	0.0013		
	63	41.200	4.000	-1.500	CO1	9	98.0	Bottom	ε_y	-0.0024		
	9809	41.200	2.500	-1.500	CO1	9	98.0	Bottom	γ_{xy}	0.0038		
58	9780	0.100	3.500	4.500	CO1	1	0.0	Top	ε_x	0.0014		
	125	0.100	4.000	4.500	CO1	9	98.0	Bottom	ε_y	-0.0026		
	9782	0.100	2.500	4.500	CO1	1	0.0	Top	γ_{xy}	0.0043		
59	9852	41.200	3.500	-4.500	CO1	9	98.0	Bottom	ε_x	0.0009		
	67	41.200	4.000	-4.500	CO1	9	98.0	Bottom	ε_y	-0.0018		
	67	41.200	4.000	-4.500	CO1	1	0.0	Top	γ_{xy}	0.0035		
60	9861	41.400	3.500	-4.500	CO1	9	98.0	Bottom	ε_x	0.0010		
	67	41.200	4.000	-4.500	CO1	9	98.0	Bottom	ε_y	-0.0020		
	9854	41.200	2.500	-4.500	CO1	9	98.0	Bottom	γ_{xy}	0.0029		
61	9888	0.100	3.500	1.500	CO1	1	0.0	Top	ε_x	0.0012		
	131	0.100	4.000	1.500	CO1	9	98.0	Bottom	ε_y	-0.0023		
	131	0.100	4.000	1.500	CO1	9	98.0	Bottom	γ_{xy}	0.0052		
62	9888	0.100	3.500	1.500	CO1	1	0.0	Top	ε_x	0.0014		
	131	0.100	4.000	1.500	CO1	1	0.0	Top	ε_y	-0.0026		
	9890	0.100	2.500	1.500	CO1	1	0.0	Top	γ_{xy}	0.0043		
63	9924	0.100	3.500	-1.500	CO1	1	0.0	Top	ε_x	0.0011		
	136	0.100	4.000	-1.500	CO1	1	0.0	Top	ε_y	-0.0021		
	136	0.100	4.000	-1.500	CO1	9	98.0	Bottom	γ_{xy}	0.0045		
64	9933	-0.100	3.500	-1.500	CO1	1	0.0	Top	ε_x	0.0013		
	136	0.100	4.000	-1.500	CO1	1	0.0	Top	ε_y	-0.0023		
	9926	0.100	2.500	-1.500	CO1	1	0.0	Top	γ_{xy}	0.0038		
65	9960	0.100	3.500	-4.500	CO1	1	0.0	Top	ε_x	0.0009		
	147	0.100	4.000	-4.500	CO1	1	0.0	Top	ε_y	-0.0017		
	147	0.100	4.000	-4.500	CO1	9	98.0	Bottom	γ_{xy}	0.0035		
66	9969	-0.100	3.500	-4.500	CO1	1	0.0	Top	ε_x	0.0010		
	147	0.100	4.000	-4.500	CO1	1	0.0	Top	ε_y	-0.0020		
	9962	0.100	2.500	-4.500	CO1	1	0.0	Top	γ_{xy}	0.0029		
101	55	39.550	4.000	-7.500	CO1	1	0.0	Top	ε_x	0.0005		
	71	41.200	4.000	-7.500	CO1	1	0.0	Top	ε_y	-0.0014		
	8935	39.550	2.000	-7.500	CO1	9	98.0	Bottom	γ_{xy}	0.0016		
102	111	39.550	0.000	-6.500	CO1	1	0.0	Top	ε_x	-0.0008		
	33	41.200	4.000	-6.500	CO1	1	0.0	Top	ε_y	-0.0018		
	111	39.550	0.000	-6.500	CO1	9	90.0	Bottom	γ_{xy}	-0.0020		
103	112	39.550	0.000	-5.500	CO1	1	0.0	Top	ε_x	-0.0010		
	25	41.200	4.000	-5.500	CO1	1	0.0	Top	ε_y	-0.0020		
	112	39.550	0.000	-5.500	CO1	9	90.0	Bottom	γ_{xy}	-0.0025		
104	109	39.550	0.000	-3.500	CO1	9	90.0	Bottom	ε_x	-0.0011		
	50	41.200	4.000	-3.500	CO1	9	90.0	Bottom	ε_y	-0.0021		
	109	39.550	0.000	-3.500	CO1	9	90.0	Bottom	γ_{xy}	-0.0024		
105	110	39.550	0.000	-2.500	CO1	1	0.0	Top	ε_x	-0.0013		
	42	41.200	4.000	-2.500	CO1	1	0.0	Top	ε_y	-0.0024		
	110	39.550	0.000	-2.500	CO1	9	90.0	Bottom	γ_{xy}	-0.0030		

Project: CIE5060 Model: V26
Graduation Project

2.2 MAX STRESS RATIO BY SURFACE

Surface No.	Point No.	Point Coordinates [m] X	Y	Z	Load-ing	Layer No.	z [mm]	Side	Stresses [-] Symbol	Existing	Limit	Ratio [-]
106	107	39.550	0.000	-0.500	CO1	9	90.0	Bottom	ε_x	-0.0013		
	74	41.200	4.000	-0.500	CO1	9	90.0	Bottom	ε_y	-0.0025		
	107	39.550	0.000	-0.500	CO1	9	90.0	Bottom	γ_{xy}	-0.0027		
107	108	39.550	0.000	0.500	CO1	1	0.0	Top	ε_x	-0.0015		
	73	41.200	4.000	0.500	CO1	1	0.0	Top	ε_y	-0.0027		
	108	39.550	0.000	0.500	CO1	9	90.0	Bottom	γ_{xy}	-0.0033		
108	105	39.550	0.000	2.500	CO1	9	90.0	Bottom	ε_x	-0.0014		
	82	41.200	4.000	2.500	CO1	9	90.0	Bottom	ε_y	-0.0028		
	105	39.550	0.000	2.500	CO1	1	0.0	Top	γ_{xy}	-0.0029		
109	106	39.550	0.000	3.500	CO1	1	0.0	Top	ε_x	-0.0015		
	81	41.200	4.000	3.500	CO1	1	0.0	Top	ε_y	-0.0028		
	106	39.550	0.000	3.500	CO1	9	90.0	Bottom	γ_{xy}	-0.0033		
110	103	39.550	0.000	5.500	CO1	9	90.0	Bottom	ε_x	-0.0015		
	90	41.200	4.000	5.500	CO1	9	90.0	Bottom	ε_y	-0.0027		
	103	39.550	0.000	5.500	CO1	1	0.0	Top	γ_{xy}	-0.0030		
111	104	39.550	0.000	6.500	CO1	1	0.0	Top	ε_x	-0.0015		
	89	41.200	4.000	6.500	CO1	1	0.0	Top	ε_y	-0.0027		
	104	39.550	0.000	6.500	CO1	9	90.0	Bottom	γ_{xy}	-0.0033		
112	101	39.550	0.000	8.500	CO1	9	90.0	Bottom	ε_x	-0.0013		
	94	41.200	4.000	8.500	CO1	9	90.0	Bottom	ε_y	-0.0027		
	101	39.550	0.000	8.500	CO1	1	0.0	Top	γ_{xy}	-0.0028		
113	102	39.550	0.000	9.500	CO1	1	0.0	Top	ε_x	-0.0013		
	93	41.200	4.000	9.500	CO1	1	0.0	Top	ε_y	-0.0027		
	102	39.550	0.000	9.500	CO1	9	90.0	Bottom	γ_{xy}	-0.0028		
114	10412	41.200	4.000	-7.000	CO1	1	0.0	Top	ε_x	0.0012		
	33	41.200	4.000	-6.500	CO1	1	0.0	Top	ε_y	-0.0013		
	71	41.200	4.000	-7.500	CO1	9	118.0	Bottom	γ_{xy}	0.0017		
115	111	39.550	0.000	-6.500	CO1	9	118.0	Bottom	ε_x	-0.0010		
	36	41.200	0.000	-6.500	CO1	1	0.0	Top	ε_y	0.0006		
	56	39.550	0.000	-7.500	CO1	9	118.0	Bottom	γ_{xy}	-0.0014		
116	10418	41.200	4.000	-6.000	CO1	1	0.0	Top	ε_x	0.0012		
	25	41.200	4.000	-5.500	CO1	1	0.0	Top	ε_y	-0.0014		
	33	41.200	4.000	-6.500	CO1	9	118.0	Bottom	γ_{xy}	0.0012		
117	7404	39.550	0.000	-6.000	CO1	9	118.0	Bottom	ε_x	-0.0012		
	112	39.550	0.000	-5.500	CO1	1	0.0	Top	ε_y	0.0008		
	111	39.550	0.000	-6.500	CO1	9	118.0	Bottom	γ_{xy}	-0.0012		
118	10424	41.200	4.000	-5.000	CO1	1	0.0	Top	ε_x	0.0014		
	67	41.200	4.000	-4.500	CO1	9	118.0	Bottom	ε_y	0.0021		
	9842	40.650	4.000	-4.500	CO1	1	0.0	Top	γ_{xy}	-0.0016		
119	112	39.550	0.000	-5.500	CO1	9	118.0	Bottom	ε_x	-0.0010		
	48	39.550	0.000	-4.500	CO1	9	118.0	Bottom	ε_y	0.0010		
	48	39.550	0.000	-4.500	CO1	9	118.0	Bottom	γ_{xy}	0.0014		
120	10430	41.200	4.000	-4.000	CO1	1	0.0	Top	ε_x	0.0014		
	67	41.200	4.000	-4.500	CO1	9	118.0	Bottom	ε_y	0.0019		
	9842	40.650	4.000	-4.500	CO1	1	0.0	Top	γ_{xy}	0.0018		
121	109	39.550	0.000	-3.500	CO1	9	118.0	Bottom	ε_x	-0.0012		
	109	39.550	0.000	-3.500	CO1	1	0.0	Top	ε_y	0.0009		
	48	39.550	0.000	-4.500	CO1	9	118.0	Bottom	γ_{xy}	-0.0016		
122	10436	41.200	4.000	-3.000	CO1	1	0.0	Top	ε_x	0.0013		
	42	41.200	4.000	-2.500	CO1	1	0.0	Top	ε_y	-0.0014		
	50	41.200	4.000	-3.500	CO1	9	118.0	Bottom	γ_{xy}	0.0015		
123	6322	39.550	0.000	-3.000	CO1	9	118.0	Bottom	ε_x	-0.0015		
	109	39.550	0.000	-3.500	CO1	1	0.0	Top	ε_y	0.0011		
	109	39.550	0.000	-3.500	CO1	9	118.0	Bottom	γ_{xy}	-0.0014		
124	10442	41.200	4.000	-2.000	CO1	1	0.0	Top	ε_x	0.0016		
	63	41.200	4.000	-1.500	CO1	9	118.0	Bottom	ε_y	0.0030		
	9797	40.650	4.000	-1.500	CO1	1	0.0	Top	γ_{xy}	-0.0023		
125	110	39.550	0.000	-2.500	CO1	9	118.0	Bottom	ε_x	-0.0013		
	40	39.550	0.000	-1.500	CO1	9	118.0	Bottom	ε_y	0.0015		
	40	39.550	0.000	-1.500	CO1	9	118.0	Bottom	γ_{xy}	0.0017		
126	10448	41.200	4.000	-1.000	CO1	9	118.0	Bottom	ε_x	-0.0016		
	63	41.200	4.000	-1.500	CO1	9	118.0	Bottom	ε_y	0.0027		
	9797	40.650	4.000	-1.500	CO1	1	0.0	Top	γ_{xy}	0.0023		
127	107	39.550	0.000	-0.500	CO1	9	118.0	Bottom	ε_x	-0.0014		

Project: CIE5060 Model: V26
Graduation Project

2.2 MAX STRESS RATIO BY SURFACE

Surface No.	Point No.	Point Coordinates [m] X	Y	Z	Load-ing	Layer No.	z [mm]	Side	Stresses [-] Symbol	Existing	Limit	Ratio [-]
	107	39.550	0.000	-0.500	CO1	1	0.0	Top	ε_y	0.0012		
	40	39.550	0.000	-1.500	CO1	9	118.0	Bottom	γ_{xy}	-0.0021		
128	10454	41.200	4.000	0.000	CO1	9	118.0	Bottom	ε_x	-0.0017		
	73	41.200	4.000	0.500	CO1	9	118.0	Bottom	ε_y	0.0018		
	73	41.200	4.000	0.500	CO1	9	118.0	Bottom	γ_{xy}	-0.0016		
129	5240	39.550	0.000	0.000	CO1	9	118.0	Bottom	ε_x	-0.0018		
	107	39.550	0.000	-0.500	CO1	1	0.0	Top	ε_y	0.0012		
	107	39.550	0.000	-0.500	CO1	9	118.0	Bottom	γ_{xy}	-0.0017		
130	10460	41.200	4.000	1.000	CO1	9	118.0	Bottom	ε_x	-0.0019		
	59	41.200	4.000	1.500	CO1	9	118.0	Bottom	ε_y	0.0035		
	9734	40.650	4.000	1.500	CO1	1	0.0	Top	γ_{xy}	-0.0027		
131	108	39.550	0.000	0.500	CO1	9	118.0	Bottom	ε_x	-0.0015		
	32	39.550	0.000	1.500	CO1	9	118.0	Bottom	ε_y	0.0017		
	32	39.550	0.000	1.500	CO1	9	118.0	Bottom	γ_{xy}	0.0018		
132	10466	41.200	4.000	2.000	CO1	9	118.0	Bottom	ε_x	-0.0018		
	59	41.200	4.000	1.500	CO1	9	118.0	Bottom	ε_y	0.0033		
	9734	40.650	4.000	1.500	CO1	1	0.0	Top	γ_{xy}	0.0026		
133	105	39.550	0.000	2.500	CO1	9	118.0	Bottom	ε_x	-0.0015		
	32	39.550	0.000	1.500	CO1	9	118.0	Bottom	ε_y	0.0014		
	32	39.550	0.000	1.500	CO1	9	118.0	Bottom	γ_{xy}	-0.0025		
134	10472	41.200	4.000	3.000	CO1	9	118.0	Bottom	ε_x	-0.0021		
	81	41.200	4.000	3.500	CO1	9	118.0	Bottom	ε_y	0.0019		
	10225	40.650	4.000	2.500	CO1	1	0.0	Top	γ_{xy}	0.0016		
135	4165	39.550	0.000	3.000	CO1	9	118.0	Bottom	ε_x	-0.0019		
	106	39.550	0.000	3.500	CO1	1	0.0	Top	ε_y	0.0013		
	105	39.550	0.000	2.500	CO1	9	118.0	Bottom	γ_{xy}	-0.0018		
136	10478	41.200	4.000	4.000	CO1	9	118.0	Bottom	ε_x	-0.0019		
	51	41.200	4.000	4.500	CO1	9	118.0	Bottom	ε_y	0.0034		
	9689	40.650	4.000	4.500	CO1	1	0.0	Top	γ_{xy}	-0.0028		
137	106	39.550	0.000	3.500	CO1	9	118.0	Bottom	ε_x	-0.0016		
	24	39.550	0.000	4.500	CO1	9	118.0	Bottom	ε_y	0.0017		
	24	39.550	0.000	4.500	CO1	9	118.0	Bottom	γ_{xy}	0.0018		
138	10484	41.200	4.000	5.000	CO1	9	118.0	Bottom	ε_x	-0.0017		
	51	41.200	4.000	4.500	CO1	9	118.0	Bottom	ε_y	0.0032		
	9689	40.650	4.000	4.500	CO1	1	0.0	Top	γ_{xy}	0.0026		
139	103	39.550	0.000	5.500	CO1	9	118.0	Bottom	ε_x	-0.0015		
	24	39.550	0.000	4.500	CO1	9	118.0	Bottom	ε_y	0.0015		
	24	39.550	0.000	4.500	CO1	9	118.0	Bottom	γ_{xy}	-0.0025		
140	10490	41.200	4.000	6.000	CO1	9	118.0	Bottom	ε_x	-0.0020		
	90	41.200	4.000	5.500	CO1	9	118.0	Bottom	ε_y	0.0017		
	10327	40.650	4.000	6.500	CO1	1	0.0	Top	γ_{xy}	-0.0015		
141	3206	39.550	0.000	6.000	CO1	9	118.0	Bottom	ε_x	-0.0019		
	104	39.550	0.000	6.500	CO1	1	0.0	Top	ε_y	0.0014		
	103	39.550	0.000	5.500	CO1	9	118.0	Bottom	γ_{xy}	-0.0016		
142	10496	41.200	4.000	7.000	CO1	1	0.0	Top	ε_x	0.0018		
	43	41.200	4.000	7.500	CO1	9	118.0	Bottom	ε_y	0.0031		
	9626	40.650	4.000	7.500	CO1	1	0.0	Top	γ_{xy}	-0.0028		
143	104	39.550	0.000	6.500	CO1	9	118.0	Bottom	ε_x	-0.0016		
	18	39.550	0.000	7.500	CO1	9	118.0	Bottom	ε_y	0.0016		
	18	39.550	0.000	7.500	CO1	9	118.0	Bottom	γ_{xy}	0.0021		
144	10502	41.200	4.000	8.000	CO1	1	0.0	Top	ε_x	0.0018		
	43	41.200	4.000	7.500	CO1	9	118.0	Bottom	ε_y	0.0029		
	9626	40.650	4.000	7.500	CO1	1	0.0	Top	γ_{xy}	0.0024		
145	1993	39.550	0.000	8.000	CO1	9	118.0	Bottom	ε_x	-0.0015		
	101	39.550	0.000	8.500	CO1	1	0.0	Top	ε_y	0.0015		
	18	39.550	0.000	7.500	CO1	9	118.0	Bottom	γ_{xy}	-0.0020		
146	10508	41.200	4.000	9.000	CO1	1	0.0	Top	ε_x	0.0019		
	93	41.200	4.000	9.500	CO1	1	0.0	Top	ε_y	-0.0019		
	10395	40.650	4.000	9.500	CO1	1	0.0	Top	γ_{xy}	-0.0016		
147	2169	39.550	0.000	9.000	CO1	9	118.0	Bottom	ε_x	-0.0021		
	101	39.550	0.000	8.500	CO1	1	0.0	Top	ε_y	0.0014		
	102	39.550	0.000	9.500	CO1	9	118.0	Bottom	γ_{xy}	0.0019		
148	10515	41.200	4.000	10.000	CO1	1	0.0	Top	ε_x	0.0019		
	34	41.200	4.000	10.500	CO1	9	118.0	Bottom	ε_y	0.0029		
	10517	40.650	4.000	10.500	CO1	1	0.0	Top	γ_{xy}	-0.0031		

Project: CIE5060 Model: V26
Graduation Project

2.2 MAX STRESS RATIO BY SURFACE

Surface No.	Point No.	Point Coordinates [m] X	Y	Z	Load-ing	Layer No.	z [mm]	Side	Stresses [-] Symbol	Existing	Limit	Ratio [-]
149	2325	39.550	0.000	10.000	CO1	9	118.0	Bottom	ε_x	-0.0015		
	102	39.550	0.000	9.500	CO1	1	0.0	Top	ε_y	0.0014		
	8	39.550	0.000	10.500	CO1	9	118.0	Bottom	γ_{xy}	0.0033		
150	10527	41.400	3.500	-7.500	CO1	9	98.0	Bottom	ε_x	0.0005		
	71	41.200	4.000	-7.500	CO1	1	0.0	Top	ε_y	-0.0011		
	9997	41.200	3.000	-7.500	CO1	9	98.0	Bottom	γ_{xy}	0.0014		
151	10542	41.400	3.500	-6.500	CO1	1	0.0	Top	ε_x	0.0006		
	33	41.200	4.000	-6.500	CO1	1	0.0	Top	ε_y	-0.0017		
	33	41.200	4.000	-6.500	CO1	1	0.0	Top	γ_{xy}	0.0012		
152	10551	41.400	3.500	-5.500	CO1	1	0.0	Top	ε_x	0.0006		
	25	41.200	4.000	-5.500	CO1	1	0.0	Top	ε_y	-0.0019		
	25	41.200	4.000	-5.500	CO1	1	0.0	Top	γ_{xy}	0.0012		
153	10560	41.400	3.500	-3.500	CO1	1	0.0	Top	ε_x	0.0007		
	50	41.200	4.000	-3.500	CO1	9	90.0	Bottom	ε_y	-0.0020		
	50	41.200	4.000	-3.500	CO1	9	90.0	Bottom	γ_{xy}	0.0012		
154	10569	41.400	3.500	-2.500	CO1	1	0.0	Top	ε_x	0.0007		
	42	41.200	4.000	-2.500	CO1	1	0.0	Top	ε_y	-0.0023		
	42	41.200	4.000	-2.500	CO1	1	0.0	Top	γ_{xy}	0.0013		
155	10578	41.400	3.500	-0.500	CO1	1	0.0	Top	ε_x	0.0008		
	74	41.200	4.000	-0.500	CO1	9	90.0	Bottom	ε_y	-0.0024		
	74	41.200	4.000	-0.500	CO1	9	90.0	Bottom	γ_{xy}	0.0013		
156	10587	41.400	3.500	0.500	CO1	1	0.0	Top	ε_x	0.0008		
	73	41.200	4.000	0.500	CO1	1	0.0	Top	ε_y	-0.0026		
	73	41.200	4.000	0.500	CO1	1	0.0	Top	γ_{xy}	0.0014		
157	10222	41.200	3.500	2.500	CO1	1	0.0	Top	ε_x	0.0009		
	82	41.200	4.000	2.500	CO1	9	90.0	Bottom	ε_y	-0.0026		
	82	41.200	4.000	2.500	CO1	9	90.0	Bottom	γ_{xy}	0.0014		
158	10605	41.400	3.500	3.500	CO1	1	0.0	Top	ε_x	0.0008		
	81	41.200	4.000	3.500	CO1	1	0.0	Top	ε_y	-0.0027		
	81	41.200	4.000	3.500	CO1	1	0.0	Top	γ_{xy}	0.0015		
159	10290	41.200	3.500	5.500	CO1	1	0.0	Top	ε_x	0.0008		
	90	41.200	4.000	5.500	CO1	9	90.0	Bottom	ε_y	-0.0026		
	90	41.200	4.000	5.500	CO1	9	90.0	Bottom	γ_{xy}	0.0015		
160	10623	41.400	3.500	6.500	CO1	1	0.0	Top	ε_x	0.0008		
	89	41.200	4.000	6.500	CO1	1	0.0	Top	ε_y	-0.0026		
	89	41.200	4.000	6.500	CO1	1	0.0	Top	γ_{xy}	0.0016		
161	10358	41.200	3.500	8.500	CO1	1	0.0	Top	ε_x	0.0008		
	94	41.200	4.000	8.500	CO1	9	90.0	Bottom	ε_y	-0.0026		
	94	41.200	4.000	8.500	CO1	9	90.0	Bottom	γ_{xy}	0.0017		
162	10641	41.400	3.500	9.500	CO1	1	0.0	Top	ε_x	0.0008		
	93	41.200	4.000	9.500	CO1	1	0.0	Top	ε_y	-0.0025		
	93	41.200	4.000	9.500	CO1	1	0.0	Top	γ_{xy}	0.0017		
163	10412	41.200	4.000	-7.000	CO1	1	0.0	Top	ε_x	0.0013		
	33	41.200	4.000	-6.500	CO1	1	0.0	Top	ε_y	-0.0014		
	157	41.400	4.000	-7.500	CO1	9	118.0	Bottom	γ_{xy}	0.0031		
164	36	41.200	0.000	-6.500	CO1	9	118.0	Bottom	ε_x	-0.0003		
	135	41.400	0.000	-6.500	CO1	1	0.0	Top	ε_y	0.0008		
	72	41.200	0.000	-7.500	CO1	9	118.0	Bottom	γ_{xy}	-0.0003		
165	10418	41.200	4.000	-6.000	CO1	1	0.0	Top	ε_x	0.0012		
	33	41.200	4.000	-6.500	CO1	1	0.0	Top	ε_y	-0.0015		
	128	41.400	4.000	-5.500	CO1	1	0.0	Top	γ_{xy}	0.0013		
166	10646	41.400	0.000	-6.000	CO1	1	0.0	Top	ε_x	-0.0003		
	135	41.400	0.000	-6.500	CO1	1	0.0	Top	ε_y	0.0007		
	138	41.400	0.000	-5.500	CO1	9	118.0	Bottom	γ_{xy}	-0.0004		
167	10424	41.200	4.000	-5.000	CO1	9	118.0	Bottom	ε_x	-0.0016		
	67	41.200	4.000	-4.500	CO1	9	118.0	Bottom	ε_y	0.0019		
	155	41.400	4.000	-4.500	CO1	9	118.0	Bottom	γ_{xy}	-0.0016		
168	41	41.200	0.000	-5.500	CO1	9	118.0	Bottom	ε_x	-0.0002		
	138	41.400	0.000	-5.500	CO1	1	0.0	Top	ε_y	0.0009		
	68	41.200	0.000	-4.500	CO1	9	118.0	Bottom	γ_{xy}	0.0005		
169	10430	41.200	4.000	-4.000	CO1	9	118.0	Bottom	ε_x	-0.0016		
	67	41.200	4.000	-4.500	CO1	9	118.0	Bottom	ε_y	0.0020		
	155	41.400	4.000	-4.500	CO1	9	118.0	Bottom	γ_{xy}	0.0018		
170	65	41.200	0.000	-3.500	CO1	9	118.0	Bottom	ε_x	-0.0002		

Project: CIE5060 Model: V26
Graduation Project

2.2 MAX STRESS RATIO BY SURFACE

Surface No.	Point No.	Point Coordinates [m] X	Y	Z	Load-ing	Layer No.	z [mm]	Side	Stresses [-] Symbol	Existing	Limit	Ratio [-]
	153	41.400	0.000	-3.500	CO1	1	0.0	Top	ε_y	0.0008		
	68	41.200	0.000	-4.500	CO1	9	118.0	Bottom	γ_{xy}	-0.0008		
171	10436	41.200	4.000	-3.000	CO1	1	0.0	Top	ε_x	0.0013		
	10436	41.200	4.000	-3.000	CO1	9	118.0	Bottom	ε_y	-0.0013		
	139	41.400	4.000	-2.500	CO1	1	0.0	Top	γ_{xy}	0.0013		
172	10441	41.200	0.000	-3.000	CO1	1	0.0	Top	ε_x	-0.0003		
	153	41.400	0.000	-3.500	CO1	1	0.0	Top	ε_y	0.0007		
	66	41.200	0.000	-2.500	CO1	9	118.0	Bottom	γ_{xy}	-0.0007		
173	10442	41.200	4.000	-2.000	CO1	9	118.0	Bottom	ε_x	-0.0021		
	63	41.200	4.000	-1.500	CO1	9	118.0	Bottom	ε_y	0.0028		
	151	41.400	4.000	-1.500	CO1	9	118.0	Bottom	γ_{xy}	-0.0021		
174	10654	41.400	0.000	-2.000	CO5	1	0.0	Top	ε_x	0.0002		
	152	41.400	0.000	-1.500	CO1	1	0.0	Top	ε_y	-0.0013		
	64	41.200	0.000	-1.500	CO1	9	118.0	Bottom	γ_{xy}	0.0008		
175	10448	41.200	4.000	-1.000	CO1	9	118.0	Bottom	ε_x	-0.0022		
	63	41.200	4.000	-1.500	CO1	9	118.0	Bottom	ε_y	0.0029		
	151	41.400	4.000	-1.500	CO1	9	118.0	Bottom	γ_{xy}	0.0023		
176	10656	41.400	0.000	-1.000	CO5	1	0.0	Top	ε_x	0.0003		
	152	41.400	0.000	-1.500	CO1	1	0.0	Top	ε_y	-0.0013		
	64	41.200	0.000	-1.500	CO1	9	118.0	Bottom	γ_{xy}	-0.0012		
177	10454	41.200	4.000	0.000	CO1	1	0.0	Top	ε_x	0.0014		
	10454	41.200	4.000	0.000	CO1	1	0.0	Top	ε_y	0.0015		
	160	41.400	4.000	-0.500	CO1	9	118.0	Bottom	γ_{xy}	0.0015		
178	10459	41.200	0.000	0.000	CO1	1	0.0	Top	ε_x	-0.0003		
	10658	41.400	0.000	0.000	CO1	1	0.0	Top	ε_y	0.0006		
	78	41.200	0.000	0.500	CO1	9	118.0	Bottom	γ_{xy}	-0.0007		
179	10460	41.200	4.000	1.000	CO1	9	118.0	Bottom	ε_x	-0.0024		
	59	41.200	4.000	1.500	CO1	9	118.0	Bottom	ε_y	0.0033		
	149	41.400	4.000	1.500	CO1	9	118.0	Bottom	γ_{xy}	-0.0025		
180	10660	41.400	0.000	1.000	CO5	1	0.0	Top	ε_x	0.0003		
	150	41.400	0.000	1.500	CO1	1	0.0	Top	ε_y	-0.0015		
	60	41.200	0.000	1.500	CO1	9	118.0	Bottom	γ_{xy}	0.0009		
181	10466	41.200	4.000	2.000	CO1	9	118.0	Bottom	ε_x	-0.0025		
	59	41.200	4.000	1.500	CO1	9	118.0	Bottom	ε_y	0.0034		
	149	41.400	4.000	1.500	CO1	9	118.0	Bottom	γ_{xy}	0.0026		
182	85	41.200	0.000	2.500	CO1	9	118.0	Bottom	ε_x	-0.0003		
	150	41.400	0.000	1.500	CO1	1	0.0	Top	ε_y	-0.0014		
	60	41.200	0.000	1.500	CO1	9	118.0	Bottom	γ_{xy}	-0.0014		
183	10472	41.200	4.000	3.000	CO1	1	0.0	Top	ε_x	0.0015		
	10472	41.200	4.000	3.000	CO1	1	0.0	Top	ε_y	0.0016		
	82	41.200	4.000	2.500	CO1	9	118.0	Bottom	γ_{xy}	0.0017		
184	10664	41.400	0.000	3.000	CO1	1	0.0	Top	ε_x	-0.0004		
	166	41.400	0.000	3.500	CO1	1	0.0	Top	ε_y	0.0009		
	86	41.200	0.000	3.500	CO1	9	118.0	Bottom	γ_{xy}	-0.0007		
185	10478	41.200	4.000	4.000	CO1	9	118.0	Bottom	ε_x	-0.0024		
	51	41.200	4.000	4.500	CO1	9	118.0	Bottom	ε_y	0.0032		
	145	41.400	4.000	4.500	CO1	9	118.0	Bottom	γ_{xy}	-0.0026		
186	10666	41.400	0.000	4.000	CO1	9	118.0	Bottom	ε_x	-0.0003		
	166	41.400	0.000	3.500	CO1	1	0.0	Top	ε_y	0.0012		
	52	41.200	0.000	4.500	CO1	9	118.0	Bottom	γ_{xy}	0.0009		
187	10484	41.200	4.000	5.000	CO1	9	118.0	Bottom	ε_x	-0.0024		
	51	41.200	4.000	4.500	CO1	9	118.0	Bottom	ε_y	0.0033		
	145	41.400	4.000	4.500	CO1	9	118.0	Bottom	γ_{xy}	0.0025		
188	91	41.200	0.000	5.500	CO1	9	118.0	Bottom	ε_x	-0.0004		
	169	41.400	0.000	5.500	CO1	1	0.0	Top	ε_y	0.0014		
	52	41.200	0.000	4.500	CO1	9	118.0	Bottom	γ_{xy}	-0.0012		
189	10490	41.200	4.000	6.000	CO1	1	0.0	Top	ε_x	0.0016		
	10490	41.200	4.000	6.000	CO1	9	118.0	Bottom	ε_y	-0.0016		
	90	41.200	4.000	5.500	CO1	9	118.0	Bottom	γ_{xy}	0.0016		
190	10670	41.400	0.000	6.000	CO1	1	0.0	Top	ε_x	-0.0005		
	170	41.400	0.000	6.500	CO1	1	0.0	Top	ε_y	0.0013		
	92	41.200	0.000	6.500	CO3	9	118.0	Bottom	γ_{xy}	0.0006		
191	10496	41.200	4.000	7.000	CO1	9	118.0	Bottom	ε_x	-0.0022		
	43	41.200	4.000	7.500	CO1	9	118.0	Bottom	ε_y	0.0029		
	140	41.400	4.000	7.500	CO1	9	118.0	Bottom	γ_{xy}	-0.0025		

Project: CIE5060 Model: V26
Graduation Project

2.2 MAX STRESS RATIO BY SURFACE

Surface No.	Point No.	Point Coordinates [m] X	Y	Z	Load-ing	Layer No.	z [mm]	Side	Stresses [-] Symbol	Existing	Limit	Ratio [-]
192	10672	41.400	0.000	7.000	CO1	9	118.0	Bottom	ε_x	-0.0004		
	170	41.400	0.000	6.500	CO1	1	0.0	Top	ε_y	0.0016		
	44	41.200	0.000	7.500	CO1	9	118.0	Bottom	γ_{xy}	0.0010		
193	10502	41.200	4.000	8.000	CO1	9	118.0	Bottom	ε_x	-0.0023		
	43	41.200	4.000	7.500	CO1	9	118.0	Bottom	ε_y	0.0030		
	140	41.400	4.000	7.500	CO1	9	118.0	Bottom	γ_{xy}	0.0023		
194	10674	41.400	0.000	8.000	CO1	9	118.0	Bottom	ε_x	-0.0005		
	173	41.400	0.000	8.500	CO1	1	0.0	Top	ε_y	0.0017		
	44	41.200	0.000	7.500	CO1	9	118.0	Bottom	γ_{xy}	-0.0009		
195	10508	41.200	4.000	9.000	CO1	1	0.0	Top	ε_x	0.0016		
	10508	41.200	4.000	9.000	CO1	9	118.0	Bottom	ε_y	-0.0017		
	172	41.400	4.000	8.500	CO1	1	0.0	Top	γ_{xy}	-0.0017		
196	10676	41.400	0.000	9.000	CO1	1	0.0	Top	ε_x	-0.0006		
	174	41.400	0.000	9.500	CO1	1	0.0	Top	ε_y	0.0015		
	173	41.400	0.000	8.500	CO1	9	118.0	Bottom	γ_{xy}	0.0007		
197	10515	41.200	4.000	10.000	CO1	9	118.0	Bottom	ε_x	-0.0021		
	34	41.200	4.000	10.500	CO1	9	118.0	Bottom	ε_y	0.0026		
	134	41.400	4.000	10.500	CO1	9	118.0	Bottom	γ_{xy}	-0.0025		
198	10524	41.200	0.000	10.000	CO1	9	118.0	Bottom	ε_x	-0.0004		
	174	41.400	0.000	9.500	CO1	1	0.0	Top	ε_y	0.0016		
	27	41.200	0.000	10.500	CO1	9	118.0	Bottom	γ_{xy}	0.0009		
199	10643	41.400	4.000	-7.000	CO1	1	0.0	Top	ε_x	-0.0019		
	135	41.400	0.000	-6.500	CO1	9	90.0	Bottom	ε_y	0.0007		
	133	41.400	4.000	-6.500	CO1	1	0.0	Top	γ_{xy}	0.0018		
200	10645	41.400	4.000	-6.000	CO1	1	0.0	Top	ε_x	-0.0019		
	10645	41.400	4.000	-6.000	CO1	9	90.0	Bottom	ε_y	-0.0008		
	128	41.400	4.000	-5.500	CO1	1	0.0	Top	γ_{xy}	0.0013		
201	10647	41.400	4.000	-5.000	CO1	1	0.0	Top	ε_x	-0.0020		
	155	41.400	4.000	-4.500	CO1	9	90.0	Bottom	ε_y	0.0009		
	155	41.400	4.000	-4.500	CO1	1	0.0	Top	γ_{xy}	0.0022		
202	10649	41.400	4.000	-4.000	CO1	1	0.0	Top	ε_x	-0.0021		
	155	41.400	4.000	-4.500	CO1	9	90.0	Bottom	ε_y	0.0010		
	155	41.400	4.000	-4.500	CO1	1	0.0	Top	γ_{xy}	-0.0015		
203	10651	41.400	4.000	-3.000	CO1	1	0.0	Top	ε_x	-0.0024		
	153	41.400	0.000	-3.500	CO1	9	90.0	Bottom	ε_y	0.0006		
	139	41.400	4.000	-2.500	CO1	1	0.0	Top	γ_{xy}	0.0014		
204	10653	41.400	4.000	-2.000	CO1	1	0.0	Top	ε_x	-0.0025		
	151	41.400	4.000	-1.500	CO1	9	90.0	Bottom	ε_y	0.0016		
	151	41.400	4.000	-1.500	CO1	1	0.0	Top	γ_{xy}	0.0027		
205	10655	41.400	4.000	-1.000	CO1	1	0.0	Top	ε_x	-0.0026		
	151	41.400	4.000	-1.500	CO1	9	90.0	Bottom	ε_y	0.0016		
	151	41.400	4.000	-1.500	CO1	1	0.0	Top	γ_{xy}	-0.0022		
206	10657	41.400	4.000	0.000	CO1	1	0.0	Top	ε_x	-0.0029		
	10586	41.400	3.000	0.500	CO1	1	0.0	Top	ε_y	0.0006		
	159	41.400	4.000	0.500	CO1	1	0.0	Top	γ_{xy}	0.0015		
207	10659	41.400	4.000	1.000	CO1	1	0.0	Top	ε_x	-0.0029		
	149	41.400	4.000	1.500	CO1	9	90.0	Bottom	ε_y	0.0020		
	149	41.400	4.000	1.500	CO1	1	0.0	Top	γ_{xy}	0.0029		
208	10661	41.400	4.000	2.000	CO1	1	0.0	Top	ε_x	-0.0029		
	149	41.400	4.000	1.500	CO1	9	90.0	Bottom	ε_y	0.0020		
	149	41.400	4.000	1.500	CO1	1	0.0	Top	γ_{xy}	-0.0028		
209	10663	41.400	4.000	3.000	CO1	1	0.0	Top	ε_x	-0.0031		
	166	41.400	0.000	3.500	CO1	9	90.0	Bottom	ε_y	0.0008		
	164	41.400	4.000	2.500	CO1	1	0.0	Top	γ_{xy}	-0.0014		
210	10665	41.400	4.000	4.000	CO1	1	0.0	Top	ε_x	-0.0029		
	145	41.400	4.000	4.500	CO1	9	90.0	Bottom	ε_y	0.0019		
	145	41.400	4.000	4.500	CO1	1	0.0	Top	γ_{xy}	0.0028		
211	10667	41.400	4.000	5.000	CO1	1	0.0	Top	ε_x	-0.0029		
	145	41.400	4.000	4.500	CO1	9	90.0	Bottom	ε_y	0.0019		
	145	41.400	4.000	4.500	CO1	1	0.0	Top	γ_{xy}	-0.0029		
212	10669	41.400	4.000	6.000	CO1	1	0.0	Top	ε_x	-0.0030		
	170	41.400	0.000	6.500	CO1	9	90.0	Bottom	ε_y	0.0012		
	168	41.400	4.000	5.500	CO1	1	0.0	Top	γ_{xy}	-0.0015		
213	10671	41.400	4.000	7.000	CO1	1	0.0	Top	ε_x	-0.0028		

Project: CIE5060 Model: V26
Graduation Project

2.2 MAX STRESS RATIO BY SURFACE

Surface No.	Point No.	Point Coordinates [m] X	Y	Z	Load-ing	Layer No.	z [mm]	Side	Stresses [-] Symbol	Existing	Limit	Ratio [-]
	140	41.400	4.000	7.500	CO1	9	90.0	Bottom	ε_y	0.0016		
	140	41.400	4.000	7.500	CO1	1	0.0	Top	γ_{xy}	0.0025		
214	10673	41.400	4.000	8.000	CO1	1	0.0	Top	ε_x	-0.0027		
	140	41.400	4.000	7.500	CO1	9	90.0	Bottom	ε_y	0.0016		
	140	41.400	4.000	7.500	CO1	1	0.0	Top	γ_{xy}	-0.0028		
215	10675	41.400	4.000	9.000	CO1	1	0.0	Top	ε_x	-0.0029		
	173	41.400	0.000	8.500	CO1	9	90.0	Bottom	ε_y	0.0015		
	172	41.400	4.000	8.500	CO1	1	0.0	Top	γ_{xy}	-0.0015		
216	10678	41.400	4.000	10.000	CO1	1	0.0	Top	ε_x	-0.0028		
	174	41.400	0.000	9.500	CO1	9	90.0	Bottom	ε_y	0.0015		
	10805	41.400	2.500	10.500	CO1	1	0.0	Top	γ_{xy}	0.0020		
217	11	39.550	4.000	10.500	CO1	1	0.0	Top	ε_x	0.0013		
	34	41.200	4.000	10.500	CO1	9	98.0	Bottom	ε_y	-0.0025		
	34	41.200	4.000	10.500	CO1	1	0.0	Top	γ_{xy}	0.0041		
218	10827	41.200	3.500	10.500	CO1	1	0.0	Top	ε_x	0.0013		
	34	41.200	4.000	10.500	CO1	9	98.0	Bottom	ε_y	-0.0026		
	10825	41.200	3.000	10.500	CO1	9	98.0	Bottom	γ_{xy}	0.0033		
219	10842	39.550	4.000	11.000	CO1	1	0.0	Top	ε_x	0.0010		
	181	39.550	1.000	11.500	CO1	9	90.0	Bottom	ε_y	0.0010		
	10848	39.550	1.500	11.500	CO1	9	90.0	Bottom	γ_{xy}	-0.0013		
220	181	39.550	1.000	11.500	CO1	1	0.0	Top	ε_x	-0.0009		
	182	39.550	2.000	12.500	CO3	1	0.0	Top	ε_y	0.0014		
	10862	39.550	2.500	12.500	CO1	1	0.0	Top	γ_{xy}	0.0023		
221	10870	39.550	4.000	13.000	CO1	1	0.0	Top	ε_x	0.0008		
	182	39.550	2.000	12.500	CO3	1	0.0	Top	ε_y	0.0009		
	10872	39.550	3.500	13.500	CO1	9	90.0	Bottom	γ_{xy}	-0.0013		
222	10878	39.550	4.000	14.000	CO1	1	0.0	Top	ε_x	0.0004		
	177	39.550	4.000	13.500	CO1	9	90.0	Bottom	ε_y	-0.0007		
	183	39.550	3.000	13.500	CO1	1	0.0	Top	γ_{xy}	0.0006		
223	181	39.550	1.000	11.500	CO1	1	0.0	Top	ε_x	-0.0015		
	180	41.200	4.000	11.500	CO1	9	90.0	Bottom	ε_y	-0.0029		
	180	41.200	4.000	11.500	CO1	1	0.0	Top	γ_{xy}	-0.0040		
224	10885	41.200	3.500	11.500	CO1	1	0.0	Top	ε_x	0.0009		
	180	41.200	4.000	11.500	CO1	9	90.0	Bottom	ε_y	-0.0029		
	10887	41.200	3.000	11.500	CO1	9	90.0	Bottom	γ_{xy}	-0.0021		
225	10911	41.200	3.500	12.500	CO1	1	0.0	Top	ε_x	0.0009		
	179	41.200	4.000	12.500	CO1	1	0.0	Top	ε_y	-0.0025		
	179	41.200	4.000	12.500	CO1	9	98.0	Bottom	γ_{xy}	0.0029		
226	10928	41.400	3.500	12.500	CO1	1	0.0	Top	ε_x	0.0012		
	179	41.200	4.000	12.500	CO1	1	0.0	Top	ε_y	-0.0027		
	10914	41.200	3.000	12.500	CO1	1	0.0	Top	γ_{xy}	0.0017		
227	177	39.550	4.000	13.500	CO1	1	0.0	Top	ε_x	0.0011		
	178	41.200	4.000	13.500	CO1	9	90.0	Bottom	ε_y	-0.0028		
	178	41.200	4.000	13.500	CO1	1	0.0	Top	γ_{xy}	-0.0023		
228	187	41.400	4.000	13.500	CO1	1	0.0	Top	ε_x	0.0007		
	178	41.200	4.000	13.500	CO1	9	90.0	Bottom	ε_y	-0.0027		
	178	41.200	4.000	13.500	CO1	9	90.0	Bottom	γ_{xy}	0.0011		
233	10942	41.400	4.000	11.000	CO1	1	0.0	Top	ε_x	-0.0029		
	134	41.400	4.000	10.500	CO1	9	90.0	Bottom	ε_y	0.0013		
	134	41.400	4.000	10.500	CO1	1	0.0	Top	γ_{xy}	-0.0030		
234	10951	41.400	4.000	12.000	CO1	1	0.0	Top	ε_x	-0.0028		
	189	41.400	4.000	11.500	CO3	9	90.0	Bottom	ε_y	-0.0009		
	189	41.400	4.000	11.500	CO1	1	0.0	Top	γ_{xy}	-0.0028		
235	10958	41.400	4.000	13.000	CO1	1	0.0	Top	ε_x	-0.0025		
	10959	41.400	2.667	13.167	CO1	9	90.0	Bottom	ε_y	0.0010		
	188	41.400	4.000	12.500	CO1	1	0.0	Top	γ_{xy}	-0.0034		
236	192	41.400	3.000	13.500	CO1	9	90.0	Bottom	ε_x	-0.0022		
	20	41.400	4.000	14.500	CO1	9	90.0	Bottom	ε_y	-0.0037		
	187	41.400	4.000	13.500	CO1	1	0.0	Top	γ_{xy}	-0.0036		
237	10967	41.200	4.000	11.000	CO1	1	0.0	Top	ε_x	0.0018		
	34	41.200	4.000	10.500	CO1	9	118.0	Bottom	ε_y	0.0025		
	10883	40.650	4.000	11.500	CO1	1	0.0	Top	γ_{xy}	-0.0020		
238	10967	41.200	4.000	11.000	CO1	9	118.0	Bottom	ε_x	-0.0024		
	34	41.200	4.000	10.500	CO1	9	118.0	Bottom	ε_y	0.0029		
	189	41.400	4.000	11.500	CO1	9	118.0	Bottom	γ_{xy}	-0.0020		

Project: CIE5060 Model: V26
Graduation Project

2.2 MAX STRESS RATIO BY SURFACE

Surface No.	Point No.	Point Coordinates [m] X	Y	Z	Load-ing	Layer No.	z [mm]	Side	Stresses [-] Symbol	Existing	Limit	Ratio [-]
239	10970	41.200	4.000	12.000	CO1	1	0.0	Top	ε_x	0.0017		
	180	41.200	4.000	11.500	CO1	9	118.0	Bottom	ε_y	0.0020		
	10913	40.650	4.000	12.500	CO1	1	0.0	Top	γ_{xy}	-0.0021		
240	10970	41.200	4.000	12.000	CO1	9	118.0	Bottom	ε_x	-0.0021		
	180	41.200	4.000	11.500	CO1	9	118.0	Bottom	ε_y	0.0023		
	188	41.400	4.000	12.500	CO1	9	118.0	Bottom	γ_{xy}	-0.0025		
241	10973	41.200	4.000	13.000	CO1	1	0.0	Top	ε_x	0.0017		
	179	41.200	4.000	12.500	CO1	9	118.0	Bottom	ε_y	0.0019		
	178	41.200	4.000	13.500	CO1	9	118.0	Bottom	γ_{xy}	-0.0020		
242	10973	41.200	4.000	13.000	CO1	1	0.0	Top	ε_x	0.0019		
	179	41.200	4.000	12.500	CO1	9	118.0	Bottom	ε_y	0.0021		
	187	41.400	4.000	13.500	CO1	9	118.0	Bottom	γ_{xy}	-0.0023		
243	10977	41.200	4.000	14.000	CO1	1	0.0	Top	ε_x	0.0018		
	19	41.200	4.000	14.500	CO1	1	0.0	Top	ε_y	-0.0024		
	178	41.200	4.000	13.500	CO1	1	0.0	Top	γ_{xy}	-0.0024		
244	10977	41.200	4.000	14.000	CO1	1	0.0	Top	ε_x	0.0022		
	19	41.200	4.000	14.500	CO1	1	0.0	Top	ε_y	-0.0023		
	20	41.400	4.000	14.500	CO1	9	118.0	Bottom	γ_{xy}	-0.0047		
245	181	39.550	1.000	11.500	CO1	9	118.0	Bottom	ε_x	-0.0015		
	184	41.200	1.000	11.500	CO1	9	118.0	Bottom	ε_y	-0.0008		
	10902	40.100	1.000	11.500	CO1	1	0.0	Top	γ_{xy}	0.0026		
246	184	41.200	1.000	11.500	CO1	1	0.0	Top	ε_x	0.0005		
	184	41.200	1.000	11.500	CO1	9	118.0	Bottom	ε_y	-0.0008		
	184	41.200	1.000	11.500	CO1	9	118.0	Bottom	γ_{xy}	0.0017		
247	10865	39.550	1.333	11.833	CO1	9	118.0	Bottom	ε_x	-0.0015		
	185	41.200	2.000	12.500	CO1	9	118.0	Bottom	ε_y	-0.0016		
	182	39.550	2.000	12.500	CO1	9	118.0	Bottom	γ_{xy}	0.0034		
248	185	41.200	2.000	12.500	CO1	1	0.0	Top	ε_x	0.0009		
	191	41.400	2.000	12.500	CO1	9	118.0	Bottom	ε_y	-0.0017		
	10993	41.200	1.667	12.167	CO1	9	118.0	Bottom	γ_{xy}	0.0018		
249	186	41.200	3.000	13.500	CO1	1	0.0	Top	ε_x	0.0009		
	186	41.200	3.000	13.500	CO1	9	118.0	Bottom	ε_y	-0.0018		
	10935	40.650	3.000	13.500	CO1	1	0.0	Top	γ_{xy}	0.0017		
250	186	41.200	3.000	13.500	CO1	1	0.0	Top	ε_x	0.0010		
	192	41.400	3.000	13.500	CO1	9	118.0	Bottom	ε_y	-0.0019		
	186	41.200	3.000	13.500	CO1	1	0.0	Top	γ_{xy}	0.0020		
251	19	41.200	4.000	14.500	CO1	1	0.0	Top	ε_x	0.0010		
	11005	41.200	3.667	14.167	CO1	9	118.0	Bottom	ε_y	-0.0017		
	19	41.200	4.000	14.500	CO1	9	118.0	Bottom	γ_{xy}	0.0023		
252	19	41.200	4.000	14.500	CO1	9	118.0	Bottom	ε_x	0.0014		
	19	41.200	4.000	14.500	CO1	9	118.0	Bottom	ε_y	-0.0022		
	20	41.400	4.000	14.500	CO1	1	0.0	Top	γ_{xy}	0.0020		
253	53	1.750	4.000	-7.500	CO1	9	98.0	Bottom	ε_x	0.0005		
	193	0.100	4.000	-7.500	CO1	9	98.0	Bottom	ε_y	-0.0014		
	193	0.100	4.000	-7.500	CO1	9	98.0	Bottom	γ_{xy}	0.0016		
254	225	1.750	0.000	-6.500	CO1	9	90.0	Bottom	ε_x	-0.0008		
	75	0.100	4.000	-6.500	CO1	1	0.0	Top	ε_y	-0.0018		
	225	1.750	0.000	-6.500	CO1	9	90.0	Bottom	γ_{xy}	0.0020		
255	226	1.750	0.000	-5.500	CO1	1	0.0	Top	ε_x	-0.0010		
	61	0.100	4.000	-5.500	CO1	1	0.0	Top	ε_y	-0.0020		
	226	1.750	0.000	-5.500	CO1	9	90.0	Bottom	γ_{xy}	0.0025		
256	223	1.750	0.000	-3.500	CO1	9	90.0	Bottom	ε_x	-0.0011		
	124	0.100	4.000	-3.500	CO1	9	90.0	Bottom	ε_y	-0.0021		
	223	1.750	0.000	-3.500	CO1	9	90.0	Bottom	γ_{xy}	0.0023		
257	224	1.750	0.000	-2.500	CO1	1	0.0	Top	ε_x	-0.0013		
	87	0.100	4.000	-2.500	CO1	1	0.0	Top	ε_y	-0.0024		
	224	1.750	0.000	-2.500	CO1	9	90.0	Bottom	γ_{xy}	0.0029		
258	221	1.750	0.000	-0.500	CO1	9	90.0	Bottom	ε_x	-0.0013		
	196	0.100	4.000	-0.500	CO1	9	90.0	Bottom	ε_y	-0.0025		
	221	1.750	0.000	-0.500	CO1	9	90.0	Bottom	γ_{xy}	0.0027		
259	222	1.750	0.000	0.500	CO1	1	0.0	Top	ε_x	-0.0015		
	195	0.100	4.000	0.500	CO1	1	0.0	Top	ε_y	-0.0027		
	222	1.750	0.000	0.500	CO1	9	90.0	Bottom	γ_{xy}	0.0032		
260	219	1.750	0.000	2.500	CO1	9	90.0	Bottom	ε_x	-0.0014		

Project: CIE5060 Model: V26
Graduation Project

2.2 MAX STRESS RATIO BY SURFACE

Surface No.	Point No.	Point Coordinates [m] X	Y	Z	Load-ing	Layer No.	z [mm]	Side	Stresses [-] Symbol	Existing	Limit	Ratio [-]
	200	0.100	4.000	2.500	CO1	9	90.0	Bottom	ε_y	-0.0028		
	219	1.750	0.000	2.500	CO1	1	0.0	Top	γ_{xy}	0.0029		
261	220	1.750	0.000	3.500	CO1	1	0.0	Top	ε_x	-0.0015		
	199	0.100	4.000	3.500	CO1	1	0.0	Top	ε_y	-0.0028		
	220	1.750	0.000	3.500	CO1	9	90.0	Bottom	γ_{xy}	0.0032		
262	217	1.750	0.000	5.500	CO1	9	90.0	Bottom	ε_x	-0.0015		
	204	0.100	4.000	5.500	CO1	9	90.0	Bottom	ε_y	-0.0028		
	217	1.750	0.000	5.500	CO1	1	0.0	Top	γ_{xy}	0.0030		
263	218	1.750	0.000	6.500	CO1	1	0.0	Top	ε_x	-0.0015		
	203	0.100	4.000	6.500	CO1	1	0.0	Top	ε_y	-0.0027		
	218	1.750	0.000	6.500	CO1	9	90.0	Bottom	γ_{xy}	0.0032		
264	215	1.750	0.000	8.500	CO1	9	90.0	Bottom	ε_x	-0.0013		
	208	0.100	4.000	8.500	CO1	9	90.0	Bottom	ε_y	-0.0027		
	215	1.750	0.000	8.500	CO1	1	0.0	Top	γ_{xy}	0.0028		
265	216	1.750	0.000	9.500	CO1	1	0.0	Top	ε_x	-0.0013		
	207	0.100	4.000	9.500	CO1	1	0.0	Top	ε_y	-0.0027		
	216	1.750	0.000	9.500	CO1	9	90.0	Bottom	γ_{xy}	0.0027		
266	11442	0.100	4.000	-7.000	CO1	1	0.0	Top	ε_x	0.0012		
	75	0.100	4.000	-6.500	CO1	1	0.0	Top	ε_y	-0.0013		
	11015	0.650	4.000	-7.500	CO1	1	0.0	Top	γ_{xy}	-0.0017		
267	225	1.750	0.000	-6.500	CO1	9	118.0	Bottom	ε_x	-0.0009		
	79	0.100	0.000	-6.500	CO1	1	0.0	Top	ε_y	0.0006		
	54	1.750	0.000	-7.500	CO1	9	118.0	Bottom	γ_{xy}	0.0013		
268	11448	0.100	4.000	-6.000	CO1	1	0.0	Top	ε_x	0.0011		
	61	0.100	4.000	-5.500	CO1	1	0.0	Top	ε_y	-0.0014		
	61	0.100	4.000	-5.500	CO1	9	118.0	Bottom	γ_{xy}	0.0015		
269	7480	1.750	0.000	-6.000	CO1	9	118.0	Bottom	ε_x	-0.0012		
	225	1.750	0.000	-6.500	CO1	1	0.0	Top	ε_y	0.0008		
	225	1.750	0.000	-6.500	CO1	9	118.0	Bottom	γ_{xy}	0.0009		
270	11454	0.100	4.000	-5.000	CO1	1	0.0	Top	ε_x	0.0014		
	147	0.100	4.000	-4.500	CO1	9	118.0	Bottom	ε_y	0.0021		
	147	0.100	4.000	-4.500	CO1	9	118.0	Bottom	γ_{xy}	0.0017		
271	226	1.750	0.000	-5.500	CO1	9	118.0	Bottom	ε_x	-0.0010		
	226	1.750	0.000	-5.500	CO1	1	0.0	Top	ε_y	0.0011		
	46	1.750	0.000	-4.500	CO1	9	118.0	Bottom	γ_{xy}	-0.0014		
272	11460	0.100	4.000	-4.000	CO1	1	0.0	Top	ε_x	0.0014		
	147	0.100	4.000	-4.500	CO1	9	118.0	Bottom	ε_y	0.0019		
	9950	0.650	4.000	-4.500	CO1	1	0.0	Top	γ_{xy}	-0.0020		
273	223	1.750	0.000	-3.500	CO1	9	118.0	Bottom	ε_x	-0.0011		
	223	1.750	0.000	-3.500	CO1	1	0.0	Top	ε_y	0.0010		
	46	1.750	0.000	-4.500	CO1	9	118.0	Bottom	γ_{xy}	0.0015		
274	5625	1.750	4.000	-3.000	CO1	1	0.0	Top	ε_x	0.0013		
	87	0.100	4.000	-2.500	CO1	1	0.0	Top	ε_y	-0.0013		
	87	0.100	4.000	-2.500	CO1	9	118.0	Bottom	γ_{xy}	0.0019		
275	6398	1.750	0.000	-3.000	CO1	9	118.0	Bottom	ε_x	-0.0016		
	223	1.750	0.000	-3.500	CO1	1	0.0	Top	ε_y	0.0012		
	224	1.750	0.000	-2.500	CO1	1	0.0	Top	γ_{xy}	-0.0010		
276	11472	0.100	4.000	-2.000	CO1	1	0.0	Top	ε_x	0.0016		
	136	0.100	4.000	-1.500	CO1	9	118.0	Bottom	ε_y	0.0029		
	9914	0.650	4.000	-1.500	CO1	1	0.0	Top	γ_{xy}	0.0021		
277	224	1.750	0.000	-2.500	CO1	9	118.0	Bottom	ε_x	-0.0013		
	38	1.750	0.000	-1.500	CO1	9	118.0	Bottom	ε_y	0.0015		
	38	1.750	0.000	-1.500	CO1	9	118.0	Bottom	γ_{xy}	-0.0017		
278	11478	0.100	4.000	-1.000	CO1	9	118.0	Bottom	ε_x	-0.0016		
	136	0.100	4.000	-1.500	CO1	9	118.0	Bottom	ε_y	0.0028		
	9914	0.650	4.000	-1.500	CO1	1	0.0	Top	γ_{xy}	-0.0026		
279	221	1.750	0.000	-0.500	CO1	9	118.0	Bottom	ε_x	-0.0014		
	221	1.750	0.000	-0.500	CO1	1	0.0	Top	ε_y	0.0012		
	38	1.750	0.000	-1.500	CO1	9	118.0	Bottom	γ_{xy}	0.0021		
280	4543	1.750	4.000	0.000	CO1	1	0.0	Top	ε_x	0.0017		
	195	0.100	4.000	0.500	CO1	9	118.0	Bottom	ε_y	0.0017		
	195	0.100	4.000	0.500	CO1	9	118.0	Bottom	γ_{xy}	0.0022		
281	5316	1.750	0.000	0.000	CO1	9	118.0	Bottom	ε_x	-0.0019		
	221	1.750	0.000	-0.500	CO1	1	0.0	Top	ε_y	0.0014		
	221	1.750	0.000	-0.500	CO1	9	118.0	Bottom	γ_{xy}	0.0012		

Project: CIE5060 Model: V26
Graduation Project

2.2 MAX STRESS RATIO BY SURFACE

Surface No.	Point No.	Point Coordinates [m] X	Y	Z	Load-ing	Layer No.	z [mm]	Side	Stresses [-] Symbol	Existing	Limit	Ratio [-]
282	11490	0.100	4.000	1.000	CO1	9	118.0	Bottom	ε_x	-0.0018		
	131	0.100	4.000	1.500	CO1	9	118.0	Bottom	ε_y	0.0034		
	9878	0.650	4.000	1.500	CO1	1	0.0	Top	γ_{xy}	0.0025		
283	222	1.750	0.000	0.500	CO1	9	118.0	Bottom	ε_x	-0.0014		
	30	1.750	0.000	1.500	CO1	9	118.0	Bottom	ε_y	0.0017		
	30	1.750	0.000	1.500	CO1	9	118.0	Bottom	γ_{xy}	-0.0018		
284	11496	0.100	4.000	2.000	CO1	9	118.0	Bottom	ε_x	-0.0018		
	131	0.100	4.000	1.500	CO1	9	118.0	Bottom	ε_y	0.0034		
	9878	0.650	4.000	1.500	CO1	1	0.0	Top	γ_{xy}	-0.0029		
285	219	1.750	0.000	2.500	CO1	9	118.0	Bottom	ε_x	-0.0015		
	30	1.750	0.000	1.500	CO1	9	118.0	Bottom	ε_y	0.0014		
	30	1.750	0.000	1.500	CO1	9	118.0	Bottom	γ_{xy}	0.0025		
286	3584	1.750	4.000	3.000	CO1	1	0.0	Top	ε_x	0.0018		
	199	0.100	4.000	3.500	CO1	9	118.0	Bottom	ε_y	0.0018		
	199	0.100	4.000	3.500	CO1	9	118.0	Bottom	γ_{xy}	0.0023		
287	4241	1.750	0.000	3.000	CO1	9	118.0	Bottom	ε_x	-0.0020		
	219	1.750	0.000	2.500	CO1	1	0.0	Top	ε_y	0.0015		
	219	1.750	0.000	2.500	CO1	1	0.0	Top	γ_{xy}	0.0014		
288	11508	0.100	4.000	4.000	CO1	9	118.0	Bottom	ε_x	-0.0018		
	125	0.100	4.000	4.500	CO1	9	118.0	Bottom	ε_y	0.0033		
	9770	0.650	4.000	4.500	CO1	1	0.0	Top	γ_{xy}	0.0026		
289	220	1.750	0.000	3.500	CO1	9	118.0	Bottom	ε_x	-0.0015		
	22	1.750	0.000	4.500	CO1	9	118.0	Bottom	ε_y	0.0017		
	22	1.750	0.000	4.500	CO1	9	118.0	Bottom	γ_{xy}	-0.0018		
290	11514	0.100	4.000	5.000	CO1	9	118.0	Bottom	ε_x	-0.0018		
	125	0.100	4.000	4.500	CO1	9	118.0	Bottom	ε_y	0.0033		
	9770	0.650	4.000	4.500	CO1	1	0.0	Top	γ_{xy}	-0.0029		
291	217	1.750	0.000	5.500	CO1	9	118.0	Bottom	ε_x	-0.0016		
	22	1.750	0.000	4.500	CO1	9	118.0	Bottom	ε_y	0.0015		
	22	1.750	0.000	4.500	CO1	9	118.0	Bottom	γ_{xy}	0.0025		
292	2625	1.750	4.000	6.000	CO1	1	0.0	Top	ε_x	0.0018		
	203	0.100	4.000	6.500	CO1	1	0.0	Top	ε_y	-0.0016		
	203	0.100	4.000	6.500	CO1	9	118.0	Bottom	γ_{xy}	0.0023		
293	3282	1.750	0.000	6.000	CO1	9	118.0	Bottom	ε_x	-0.0020		
	217	1.750	0.000	5.500	CO1	1	0.0	Top	ε_y	0.0016		
	217	1.750	0.000	5.500	CO1	1	0.0	Top	γ_{xy}	0.0013		
294	11526	0.100	4.000	7.000	CO1	1	0.0	Top	ε_x	0.0018		
	88	0.100	4.000	7.500	CO1	9	118.0	Bottom	ε_y	0.0030		
	9662	0.650	4.000	7.500	CO1	1	0.0	Top	γ_{xy}	0.0026		
295	218	1.750	0.000	6.500	CO1	9	118.0	Bottom	ε_x	-0.0015		
	15	1.750	0.000	7.500	CO1	9	118.0	Bottom	ε_y	0.0017		
	15	1.750	0.000	7.500	CO1	9	118.0	Bottom	γ_{xy}	-0.0020		
296	11532	0.100	4.000	8.000	CO1	1	0.0	Top	ε_x	0.0018		
	88	0.100	4.000	7.500	CO1	9	118.0	Bottom	ε_y	0.0030		
	9662	0.650	4.000	7.500	CO1	1	0.0	Top	γ_{xy}	-0.0027		
297	2089	1.750	0.000	8.000	CO1	9	118.0	Bottom	ε_x	-0.0014		
	15	1.750	0.000	7.500	CO1	9	118.0	Bottom	ε_y	0.0015		
	15	1.750	0.000	7.500	CO1	9	118.0	Bottom	γ_{xy}	0.0020		
298	1510	1.750	4.000	9.000	CO1	1	0.0	Top	ε_x	0.0018		
	207	0.100	4.000	9.500	CO1	1	0.0	Top	ε_y	-0.0018		
	207	0.100	4.000	9.500	CO1	9	118.0	Bottom	γ_{xy}	0.0023		
299	2245	1.750	0.000	9.000	CO1	9	118.0	Bottom	ε_x	-0.0019		
	215	1.750	0.000	8.500	CO1	1	0.0	Top	ε_y	0.0015		
	216	1.750	0.000	9.500	CO1	9	118.0	Bottom	γ_{xy}	-0.0017		
300	11546	0.100	4.000	10.000	CO1	1	0.0	Top	ε_x	0.0018		
	76	0.100	4.000	10.500	CO1	9	118.0	Bottom	ε_y	0.0028		
	11544	0.650	4.000	10.500	CO1	1	0.0	Top	γ_{xy}	0.0027		
301	2401	1.750	0.000	10.000	CO1	9	118.0	Bottom	ε_x	-0.0015		
	216	1.750	0.000	9.500	CO1	1	0.0	Top	ε_y	0.0014		
	5	1.750	0.000	10.500	CO1	9	118.0	Bottom	γ_{xy}	-0.0033		
302	11556	-0.100	3.500	-7.500	CO1	1	0.0	Top	ε_x	0.0005		
	193	0.100	4.000	-7.500	CO1	9	98.0	Bottom	ε_y	-0.0011		
	11025	0.100	3.500	-7.500	CO1	1	0.0	Top	γ_{xy}	0.0014		
303	11571	-0.100	3.500	-6.500	CO1	1	0.0	Top	ε_x	0.0006		

Project: CIE5060 Model: V26
Graduation Project

2.2 MAX STRESS RATIO BY SURFACE

Surface No.	Point No.	Point Coordinates [m] X	Y	Z	Load-ing	Layer No.	z [mm]	Side	Stresses [-] Symbol	Existing	Limit	Ratio [-]
	75	0.100	4.000	-6.500	CO1	1	0.0	Top	ε_y	-0.0017		
	75	0.100	4.000	-6.500	CO1	1	0.0	Top	γ_{xy}	-0.0012		
304	11580	-0.100	3.500	-5.500	CO1	1	0.0	Top	ε_x	0.0006		
	61	0.100	4.000	-5.500	CO1	1	0.0	Top	ε_y	-0.0019		
	61	0.100	4.000	-5.500	CO1	1	0.0	Top	γ_{xy}	-0.0012		
305	11589	-0.100	3.500	-3.500	CO1	1	0.0	Top	ε_x	0.0007		
	124	0.100	4.000	-3.500	CO1	9	90.0	Bottom	ε_y	-0.0020		
	124	0.100	4.000	-3.500	CO1	9	90.0	Bottom	γ_{xy}	-0.0013		
306	11598	-0.100	3.500	-2.500	CO1	1	0.0	Top	ε_x	0.0007		
	87	0.100	4.000	-2.500	CO1	1	0.0	Top	ε_y	-0.0023		
	87	0.100	4.000	-2.500	CO1	1	0.0	Top	γ_{xy}	-0.0013		
307	11607	-0.100	3.500	-0.500	CO1	1	0.0	Top	ε_x	0.0008		
	196	0.100	4.000	-0.500	CO1	9	90.0	Bottom	ε_y	-0.0024		
	196	0.100	4.000	-0.500	CO1	9	90.0	Bottom	γ_{xy}	-0.0014		
308	11616	-0.100	3.500	0.500	CO1	1	0.0	Top	ε_x	0.0008		
	195	0.100	4.000	0.500	CO1	1	0.0	Top	ε_y	-0.0026		
	195	0.100	4.000	0.500	CO1	1	0.0	Top	γ_{xy}	-0.0014		
309	11625	-0.100	3.500	2.500	CO1	1	0.0	Top	ε_x	0.0009		
	200	0.100	4.000	2.500	CO1	9	90.0	Bottom	ε_y	-0.0026		
	200	0.100	4.000	2.500	CO1	9	90.0	Bottom	γ_{xy}	-0.0015		
310	11634	-0.100	3.500	3.500	CO1	1	0.0	Top	ε_x	0.0008		
	199	0.100	4.000	3.500	CO1	1	0.0	Top	ε_y	-0.0027		
	199	0.100	4.000	3.500	CO1	1	0.0	Top	γ_{xy}	-0.0015		
311	11320	0.100	3.500	5.500	CO1	1	0.0	Top	ε_x	0.0008		
	204	0.100	4.000	5.500	CO1	9	90.0	Bottom	ε_y	-0.0026		
	204	0.100	4.000	5.500	CO1	9	90.0	Bottom	γ_{xy}	-0.0016		
312	11652	-0.100	3.500	6.500	CO1	1	0.0	Top	ε_x	0.0008		
	203	0.100	4.000	6.500	CO1	1	0.0	Top	ε_y	-0.0026		
	203	0.100	4.000	6.500	CO1	1	0.0	Top	γ_{xy}	-0.0016		
313	11388	0.100	3.500	8.500	CO1	1	0.0	Top	ε_x	0.0008		
	208	0.100	4.000	8.500	CO1	9	90.0	Bottom	ε_y	-0.0026		
	208	0.100	4.000	8.500	CO1	9	90.0	Bottom	γ_{xy}	-0.0017		
314	11422	0.100	3.500	9.500	CO1	9	90.0	Bottom	ε_x	0.0008		
	207	0.100	4.000	9.500	CO1	1	0.0	Top	ε_y	-0.0025		
	207	0.100	4.000	9.500	CO1	1	0.0	Top	γ_{xy}	-0.0017		
315	11442	0.100	4.000	-7.000	CO1	1	0.0	Top	ε_x	0.0011		
	75	0.100	4.000	-6.500	CO1	1	0.0	Top	ε_y	-0.0014		
	255	-0.100	4.000	-7.500	CO1	9	118.0	Bottom	γ_{xy}	-0.0028		
316	79	0.100	0.000	-6.500	CO1	9	118.0	Bottom	ε_x	-0.0003		
	239	-0.100	0.000	-6.500	CO1	1	0.0	Top	ε_y	0.0008		
	194	0.100	0.000	-7.500	CO1	9	118.0	Bottom	γ_{xy}	0.0003		
317	11448	0.100	4.000	-6.000	CO1	1	0.0	Top	ε_x	0.0013		
	75	0.100	4.000	-6.500	CO1	1	0.0	Top	ε_y	-0.0014		
	235	-0.100	4.000	-5.500	CO1	1	0.0	Top	γ_{xy}	-0.0015		
318	11675	-0.100	0.000	-6.000	CO1	1	0.0	Top	ε_x	-0.0003		
	239	-0.100	0.000	-6.500	CO1	1	0.0	Top	ε_y	0.0007		
	240	-0.100	0.000	-5.500	CO1	9	118.0	Bottom	γ_{xy}	0.0004		
319	11454	0.100	4.000	-5.000	CO1	9	118.0	Bottom	ε_x	-0.0016		
	147	0.100	4.000	-4.500	CO1	9	118.0	Bottom	ε_y	0.0019		
	253	-0.100	4.000	-4.500	CO1	9	118.0	Bottom	γ_{xy}	0.0018		
320	84	0.100	0.000	-5.500	CO1	9	118.0	Bottom	ε_x	-0.0002		
	240	-0.100	0.000	-5.500	CO1	1	0.0	Top	ε_y	0.0009		
	148	0.100	0.000	-4.500	CO1	9	118.0	Bottom	γ_{xy}	-0.0006		
321	11460	0.100	4.000	-4.000	CO1	9	118.0	Bottom	ε_x	-0.0015		
	147	0.100	4.000	-4.500	CO1	9	118.0	Bottom	ε_y	0.0020		
	253	-0.100	4.000	-4.500	CO1	9	118.0	Bottom	γ_{xy}	-0.0017		
322	142	0.100	0.000	-3.500	CO1	9	118.0	Bottom	ε_x	-0.0002		
	251	-0.100	0.000	-3.500	CO1	1	0.0	Top	ε_y	0.0008		
	148	0.100	0.000	-4.500	CO1	9	118.0	Bottom	γ_{xy}	0.0008		
323	11466	0.100	4.000	-3.000	CO1	1	0.0	Top	ε_x	0.0014		
	124	0.100	4.000	-3.500	CO1	1	0.0	Top	ε_y	-0.0013		
	241	-0.100	4.000	-2.500	CO1	1	0.0	Top	γ_{xy}	-0.0016		
324	11470	0.100	0.000	-3.000	CO1	1	0.0	Top	ε_x	-0.0003		
	251	-0.100	0.000	-3.500	CO1	1	0.0	Top	ε_y	0.0007		
	252	-0.100	0.000	-2.500	CO1	9	118.0	Bottom	γ_{xy}	0.0007		

Project: CIE5060 Model: V26
Graduation Project

2.2 MAX STRESS RATIO BY SURFACE

Surface No.	Point No.	Point Coordinates [m] X	Y	Z	Load-ing	Layer No.	z [mm]	Side	Stresses [-] Symbol	Existing	Limit	Ratio [-]
325	11472	0.100	4.000	-2.000	CO1	9	118.0	Bottom	ε_x	-0.0022		
	136	0.100	4.000	-1.500	CO1	9	118.0	Bottom	ε_y	0.0028		
	249	-0.100	4.000	-1.500	CO1	9	118.0	Bottom	γ_{xy}	0.0023		
326	11683	-0.100	0.000	-2.000	CO5	1	0.0	Top	ε_x	0.0002		
	250	-0.100	0.000	-1.500	CO1	1	0.0	Top	ε_y	-0.0013		
	137	0.100	0.000	-1.500	CO1	9	118.0	Bottom	γ_{xy}	-0.0008		
327	11478	0.100	4.000	-1.000	CO1	9	118.0	Bottom	ε_x	-0.0021		
	136	0.100	4.000	-1.500	CO1	9	118.0	Bottom	ε_y	0.0029		
	249	-0.100	4.000	-1.500	CO1	9	118.0	Bottom	γ_{xy}	-0.0021		
328	11685	-0.100	0.000	-1.000	CO5	1	0.0	Top	ε_x	0.0003		
	250	-0.100	0.000	-1.500	CO1	1	0.0	Top	ε_y	-0.0013		
	137	0.100	0.000	-1.500	CO1	9	118.0	Bottom	γ_{xy}	0.0012		
329	11484	0.100	4.000	0.000	CO1	1	0.0	Top	ε_x	0.0015		
	11484	0.100	4.000	0.000	CO1	1	0.0	Top	ε_y	0.0015		
	195	0.100	4.000	0.500	CO1	9	118.0	Bottom	γ_{xy}	0.0018		
330	11488	0.100	0.000	0.000	CO1	1	0.0	Top	ε_x	-0.0002		
	11687	-0.100	0.000	0.000	CO1	1	0.0	Top	ε_y	0.0006		
	260	-0.100	0.000	0.500	CO1	9	118.0	Bottom	γ_{xy}	0.0007		
331	11490	0.100	4.000	1.000	CO1	9	118.0	Bottom	ε_x	-0.0025		
	131	0.100	4.000	1.500	CO1	9	118.0	Bottom	ε_y	0.0034		
	247	-0.100	4.000	1.500	CO1	9	118.0	Bottom	γ_{xy}	0.0027		
332	11689	-0.100	0.000	1.000	CO5	1	0.0	Top	ε_x	0.0003		
	248	-0.100	0.000	1.500	CO1	1	0.0	Top	ε_y	-0.0015		
	132	0.100	0.000	1.500	CO1	9	118.0	Bottom	γ_{xy}	-0.0009		
333	11496	0.100	4.000	2.000	CO1	9	118.0	Bottom	ε_x	-0.0024		
	131	0.100	4.000	1.500	CO1	9	118.0	Bottom	ε_y	0.0034		
	247	-0.100	4.000	1.500	CO1	9	118.0	Bottom	γ_{xy}	-0.0023		
334	201	0.100	0.000	2.500	CO1	9	118.0	Bottom	ε_x	-0.0002		
	248	-0.100	0.000	1.500	CO1	1	0.0	Top	ε_y	-0.0014		
	132	0.100	0.000	1.500	CO1	9	118.0	Bottom	γ_{xy}	0.0014		
335	11502	0.100	4.000	3.000	CO1	1	0.0	Top	ε_x	0.0016		
	11502	0.100	4.000	3.000	CO1	1	0.0	Top	ε_y	0.0016		
	199	0.100	4.000	3.500	CO1	9	118.0	Bottom	γ_{xy}	0.0019		
336	11693	-0.100	0.000	3.000	CO1	1	0.0	Top	ε_x	-0.0004		
	264	-0.100	0.000	3.500	CO1	1	0.0	Top	ε_y	0.0009		
	264	-0.100	0.000	3.500	CO1	9	118.0	Bottom	γ_{xy}	0.0007		
337	11508	0.100	4.000	4.000	CO1	9	118.0	Bottom	ε_x	-0.0025		
	125	0.100	4.000	4.500	CO1	9	118.0	Bottom	ε_y	0.0033		
	245	-0.100	4.000	4.500	CO1	9	118.0	Bottom	γ_{xy}	0.0028		
338	202	0.100	0.000	3.500	CO1	9	118.0	Bottom	ε_x	-0.0003		
	264	-0.100	0.000	3.500	CO1	1	0.0	Top	ε_y	0.0012		
	126	0.100	0.000	4.500	CO1	9	118.0	Bottom	γ_{xy}	-0.0009		
339	11514	0.100	4.000	5.000	CO1	9	118.0	Bottom	ε_x	-0.0023		
	125	0.100	4.000	4.500	CO1	9	118.0	Bottom	ε_y	0.0033		
	245	-0.100	4.000	4.500	CO1	9	118.0	Bottom	γ_{xy}	-0.0022		
340	205	0.100	0.000	5.500	CO1	9	118.0	Bottom	ε_x	-0.0003		
	267	-0.100	0.000	5.500	CO1	1	0.0	Top	ε_y	0.0014		
	126	0.100	0.000	4.500	CO1	9	118.0	Bottom	γ_{xy}	0.0012		
341	11520	0.100	4.000	6.000	CO1	1	0.0	Top	ε_x	0.0016		
	11520	0.100	4.000	6.000	CO1	9	118.0	Bottom	ε_y	-0.0015		
	203	0.100	4.000	6.500	CO1	9	118.0	Bottom	γ_{xy}	0.0019		
342	11699	-0.100	0.000	6.000	CO1	1	0.0	Top	ε_x	-0.0005		
	268	-0.100	0.000	6.500	CO1	1	0.0	Top	ε_y	0.0013		
	268	-0.100	0.000	6.500	CO1	9	118.0	Bottom	γ_{xy}	0.0005		
343	11526	0.100	4.000	7.000	CO1	9	118.0	Bottom	ε_x	-0.0023		
	88	0.100	4.000	7.500	CO1	9	118.0	Bottom	ε_y	0.0030		
	242	-0.100	4.000	7.500	CO1	9	118.0	Bottom	γ_{xy}	0.0027		
344	11701	-0.100	0.000	7.000	CO1	9	118.0	Bottom	ε_x	-0.0004		
	268	-0.100	0.000	6.500	CO1	1	0.0	Top	ε_y	0.0016		
	121	0.100	0.000	7.500	CO1	9	118.0	Bottom	γ_{xy}	-0.0010		
345	11532	0.100	4.000	8.000	CO1	9	118.0	Bottom	ε_x	-0.0022		
	88	0.100	4.000	7.500	CO1	9	118.0	Bottom	ε_y	0.0030		
	242	-0.100	4.000	7.500	CO1	9	118.0	Bottom	γ_{xy}	-0.0021		
346	11703	-0.100	0.000	8.000	CO1	9	118.0	Bottom	ε_x	-0.0005		

Project: CIE5060 Model: V26
Graduation Project

2.2 MAX STRESS RATIO BY SURFACE

Surface No.	Point No.	Point Coordinates [m] X	Y	Z	Load-ing	Layer No.	z [mm]	Side	Stresses [-] Symbol	Existing	Limit	Ratio [-]
	271	-0.100	0.000	8.500	CO1	1	0.0	Top	ε_y	0.0017		
	121	0.100	0.000	7.500	CO1	9	118.0	Bottom	γ_{xy}	0.0009		
347	11538	0.100	4.000	9.000	CO1	1	0.0	Top	ε_x	0.0017		
	11538	0.100	4.000	9.000	CO1	9	118.0	Bottom	ε_y	-0.0017		
	207	0.100	4.000	9.500	CO1	9	118.0	Bottom	γ_{xy}	0.0020		
348	11705	-0.100	0.000	9.000	CO1	1	0.0	Top	ε_x	-0.0006		
	272	-0.100	0.000	9.500	CO1	1	0.0	Top	ε_y	0.0015		
	271	-0.100	0.000	8.500	CO1	9	118.0	Bottom	γ_{xy}	-0.0007		
349	11546	0.100	4.000	10.000	CO1	9	118.0	Bottom	ε_x	-0.0022		
	76	0.100	4.000	10.500	CO1	9	118.0	Bottom	ε_y	0.0027		
	238	-0.100	4.000	10.500	CO1	9	118.0	Bottom	γ_{xy}	0.0027		
350	210	0.100	0.000	9.500	CO1	9	118.0	Bottom	ε_x	-0.0004		
	272	-0.100	0.000	9.500	CO1	1	0.0	Top	ε_y	0.0016		
	62	0.100	0.000	10.500	CO1	9	118.0	Bottom	γ_{xy}	-0.0009		
351	11672	-0.100	4.000	-7.000	CO1	1	0.0	Top	ε_x	-0.0019		
	239	-0.100	0.000	-6.500	CO1	9	90.0	Bottom	ε_y	0.0007		
	237	-0.100	4.000	-6.500	CO1	1	0.0	Top	γ_{xy}	-0.0017		
352	11674	-0.100	4.000	-6.000	CO1	1	0.0	Top	ε_x	-0.0019		
	11674	-0.100	4.000	-6.000	CO1	9	90.0	Bottom	ε_y	-0.0008		
	235	-0.100	4.000	-5.500	CO1	1	0.0	Top	γ_{xy}	-0.0012		
353	11676	-0.100	4.000	-5.000	CO1	1	0.0	Top	ε_x	-0.0020		
	253	-0.100	4.000	-4.500	CO1	9	90.0	Bottom	ε_y	0.0009		
	253	-0.100	4.000	-4.500	CO1	1	0.0	Top	γ_{xy}	-0.0022		
354	11678	-0.100	4.000	-4.000	CO1	1	0.0	Top	ε_x	-0.0021		
	253	-0.100	4.000	-4.500	CO1	9	90.0	Bottom	ε_y	0.0010		
	253	-0.100	4.000	-4.500	CO1	1	0.0	Top	γ_{xy}	0.0016		
355	11680	-0.100	4.000	-3.000	CO1	1	0.0	Top	ε_x	-0.0024		
	251	-0.100	0.000	-3.500	CO1	9	90.0	Bottom	ε_y	0.0006		
	241	-0.100	4.000	-2.500	CO1	1	0.0	Top	γ_{xy}	-0.0013		
356	11682	-0.100	4.000	-2.000	CO1	1	0.0	Top	ε_x	-0.0025		
	249	-0.100	4.000	-1.500	CO1	9	90.0	Bottom	ε_y	0.0016		
	249	-0.100	4.000	-1.500	CO1	1	0.0	Top	γ_{xy}	-0.0027		
357	11684	-0.100	4.000	-1.000	CO1	1	0.0	Top	ε_x	-0.0026		
	249	-0.100	4.000	-1.500	CO1	9	90.0	Bottom	ε_y	0.0016		
	249	-0.100	4.000	-1.500	CO1	1	0.0	Top	γ_{xy}	0.0023		
358	11686	-0.100	4.000	0.000	CO1	1	0.0	Top	ε_x	-0.0029		
	11615	-0.100	3.000	0.500	CO1	1	0.0	Top	ε_y	0.0006		
	257	-0.100	4.000	0.500	CO1	1	0.0	Top	γ_{xy}	-0.0014		
359	11688	-0.100	4.000	1.000	CO1	1	0.0	Top	ε_x	-0.0029		
	247	-0.100	4.000	1.500	CO1	9	90.0	Bottom	ε_y	0.0020		
	247	-0.100	4.000	1.500	CO1	1	0.0	Top	γ_{xy}	-0.0029		
360	11690	-0.100	4.000	2.000	CO1	1	0.0	Top	ε_x	-0.0029		
	247	-0.100	4.000	1.500	CO1	9	90.0	Bottom	ε_y	0.0020		
	247	-0.100	4.000	1.500	CO1	1	0.0	Top	γ_{xy}	0.0028		
361	11692	-0.100	4.000	3.000	CO1	1	0.0	Top	ε_x	-0.0031		
	264	-0.100	0.000	3.500	CO1	9	90.0	Bottom	ε_y	0.0008		
	262	-0.100	4.000	2.500	CO1	1	0.0	Top	γ_{xy}	0.0015		
362	11694	-0.100	4.000	4.000	CO1	1	0.0	Top	ε_x	-0.0029		
	245	-0.100	4.000	4.500	CO1	9	90.0	Bottom	ε_y	0.0019		
	245	-0.100	4.000	4.500	CO1	1	0.0	Top	γ_{xy}	-0.0027		
363	11696	-0.100	4.000	5.000	CO1	1	0.0	Top	ε_x	-0.0028		
	245	-0.100	4.000	4.500	CO1	9	90.0	Bottom	ε_y	0.0019		
	245	-0.100	4.000	4.500	CO1	1	0.0	Top	γ_{xy}	0.0030		
364	11698	-0.100	4.000	6.000	CO1	1	0.0	Top	ε_x	-0.0030		
	268	-0.100	0.000	6.500	CO1	9	90.0	Bottom	ε_y	0.0012		
	266	-0.100	4.000	5.500	CO1	1	0.0	Top	γ_{xy}	0.0016		
365	11700	-0.100	4.000	7.000	CO1	1	0.0	Top	ε_x	-0.0028		
	242	-0.100	4.000	7.500	CO1	9	90.0	Bottom	ε_y	0.0016		
	242	-0.100	4.000	7.500	CO1	1	0.0	Top	γ_{xy}	-0.0024		
366	11702	-0.100	4.000	8.000	CO1	1	0.0	Top	ε_x	-0.0027		
	242	-0.100	4.000	7.500	CO1	9	90.0	Bottom	ε_y	0.0016		
	242	-0.100	4.000	7.500	CO1	1	0.0	Top	γ_{xy}	0.0029		
367	11704	-0.100	4.000	9.000	CO1	1	0.0	Top	ε_x	-0.0029		
	271	-0.100	0.000	8.500	CO1	9	90.0	Bottom	ε_y	0.0015		
	270	-0.100	4.000	8.500	CO1	1	0.0	Top	γ_{xy}	0.0017		

Project: CIE5060 Model: V26
Graduation Project

2.2 MAX STRESS RATIO BY SURFACE

Surface No.	Point No.	Point Coordinates [m] X	Y	Z	Load-ing	Layer No.	z [mm]	Side	Stresses [-] Symbol	Existing	Limit	Ratio [-]
368	11707	-0.100	4.000	10.000	CO1	1	0.0	Top	ε_x	-0.0028		
	272	-0.100	0.000	9.500	CO1	9	90.0	Bottom	ε_y	0.0015		
	11834	-0.100	2.500	10.500	CO1	1	0.0	Top	γ_{xy}	-0.0020		
369	12	1.750	4.000	10.500	CO1	9	98.0	Bottom	ε_x	0.0013		
	76	0.100	4.000	10.500	CO1	1	0.0	Top	ε_y	-0.0024		
	76	0.100	4.000	10.500	CO1	9	98.0	Bottom	γ_{xy}	0.0041		
370	11856	0.100	3.500	10.500	CO1	9	98.0	Bottom	ε_x	0.0013		
	76	0.100	4.000	10.500	CO1	9	98.0	Bottom	ε_y	-0.0026		
	11854	0.100	3.000	10.500	CO1	1	0.0	Top	γ_{xy}	0.0033		
371	11864	1.750	4.000	11.000	CO1	1	0.0	Top	ε_x	0.0010		
	279	1.750	1.000	11.500	CO1	9	90.0	Bottom	ε_y	0.0010		
	11870	1.750	1.500	11.500	CO1	9	90.0	Bottom	γ_{xy}	0.0013		
372	279	1.750	1.000	11.500	CO1	1	0.0	Top	ε_x	-0.0009		
	280	1.750	2.000	12.500	CO3	1	0.0	Top	ε_y	0.0014		
	9540	1.750	2.500	12.500	CO1	1	0.0	Top	γ_{xy}	-0.0023		
373	11887	1.750	4.000	13.000	CO1	1	0.0	Top	ε_x	0.0008		
	280	1.750	2.000	12.500	CO3	1	0.0	Top	ε_y	0.0009		
	275	1.750	4.000	13.500	CO1	9	90.0	Bottom	γ_{xy}	0.0013		
374	11895	1.750	4.000	14.000	CO1	1	0.0	Top	ε_x	0.0004		
	2	1.750	4.000	14.500	CO3	1	0.0	Top	ε_y	-0.0007		
	281	1.750	3.000	13.500	CO1	1	0.0	Top	γ_{xy}	-0.0006		
375	279	1.750	1.000	11.500	CO1	1	0.0	Top	ε_x	-0.0015		
	278	0.100	4.000	11.500	CO1	9	90.0	Bottom	ε_y	-0.0029		
	278	0.100	4.000	11.500	CO1	1	0.0	Top	γ_{xy}	0.0039		
376	11925	-0.100	3.500	11.500	CO1	9	90.0	Bottom	ε_x	0.0009		
	278	0.100	4.000	11.500	CO1	9	90.0	Bottom	ε_y	-0.0029		
	11903	0.100	3.000	11.500	CO1	1	0.0	Top	γ_{xy}	0.0021		
377	11928	0.100	3.500	12.500	CO1	9	98.0	Bottom	ε_x	0.0009		
	277	0.100	4.000	12.500	CO1	9	98.0	Bottom	ε_y	-0.0025		
	277	0.100	4.000	12.500	CO1	1	0.0	Top	γ_{xy}	0.0029		
378	11945	-0.100	3.500	12.500	CO1	9	98.0	Bottom	ε_x	0.0012		
	277	0.100	4.000	12.500	CO1	9	98.0	Bottom	ε_y	-0.0028		
	11931	0.100	3.000	12.500	CO1	9	98.0	Bottom	γ_{xy}	0.0016		
379	275	1.750	4.000	13.500	CO1	1	0.0	Top	ε_x	0.0011		
	276	0.100	4.000	13.500	CO1	9	90.0	Bottom	ε_y	-0.0028		
	275	1.750	4.000	13.500	CO1	1	0.0	Top	γ_{xy}	0.0023		
380	276	0.100	4.000	13.500	CO1	1	0.0	Top	ε_x	0.0007		
	276	0.100	4.000	13.500	CO1	9	90.0	Bottom	ε_y	-0.0027		
	276	0.100	4.000	13.500	CO1	9	90.0	Bottom	γ_{xy}	-0.0012		
385	11959	-0.100	4.000	11.000	CO1	1	0.0	Top	ε_x	-0.0029		
	238	-0.100	4.000	10.500	CO1	9	90.0	Bottom	ε_y	0.0013		
	238	-0.100	4.000	10.500	CO1	1	0.0	Top	γ_{xy}	0.0030		
386	11968	-0.100	4.000	12.000	CO1	1	0.0	Top	ε_x	-0.0028		
	287	-0.100	4.000	11.500	CO3	9	90.0	Bottom	ε_y	-0.0009		
	287	-0.100	4.000	11.500	CO1	1	0.0	Top	γ_{xy}	0.0029		
387	11975	-0.100	4.000	13.000	CO1	1	0.0	Top	ε_x	-0.0025		
	290	-0.100	3.000	13.500	CO1	1	0.0	Top	ε_y	0.0010		
	286	-0.100	4.000	12.500	CO1	1	0.0	Top	γ_{xy}	0.0034		
388	290	-0.100	3.000	13.500	CO1	9	90.0	Bottom	ε_x	-0.0022		
	49	-0.100	4.000	14.500	CO1	9	90.0	Bottom	ε_y	-0.0038		
	285	-0.100	4.000	13.500	CO1	1	0.0	Top	γ_{xy}	0.0036		
389	11985	0.100	4.000	11.000	CO1	1	0.0	Top	ε_x	0.0018		
	76	0.100	4.000	10.500	CO1	9	118.0	Bottom	ε_y	0.0026		
	278	0.100	4.000	11.500	CO1	9	118.0	Bottom	γ_{xy}	0.0020		
390	11985	0.100	4.000	11.000	CO1	9	118.0	Bottom	ε_x	-0.0024		
	76	0.100	4.000	10.500	CO1	9	118.0	Bottom	ε_y	0.0028		
	287	-0.100	4.000	11.500	CO1	9	118.0	Bottom	γ_{xy}	0.0023		
391	11988	0.100	4.000	12.000	CO1	1	0.0	Top	ε_x	0.0017		
	278	0.100	4.000	11.500	CO1	9	118.0	Bottom	ε_y	0.0020		
	277	0.100	4.000	12.500	CO1	9	118.0	Bottom	γ_{xy}	0.0023		
392	11988	0.100	4.000	12.000	CO1	9	118.0	Bottom	ε_x	-0.0021		
	278	0.100	4.000	11.500	CO1	9	118.0	Bottom	ε_y	0.0023		
	286	-0.100	4.000	12.500	CO1	9	118.0	Bottom	γ_{xy}	0.0027		
393	11991	0.100	4.000	13.000	CO1	1	0.0	Top	ε_x	0.0018		

Project: CIE5060 Model: V26
Graduation Project

2.2 MAX STRESS RATIO BY SURFACE

Surface No.	Point No.	Point Coordinates [m] X	Y	Z	Load-ing	Layer No.	z [mm]	Side	Stresses [-] Symbol	Existing	Limit	Ratio [-]
	277	0.100	4.000	12.500	CO1	9	118.0	Bottom	ε_y	0.0019		
	276	0.100	4.000	13.500	CO1	9	118.0	Bottom	γ_{xy}	0.0023		
394	11991	0.100	4.000	13.000	CO1	1	0.0	Top	ε_x	0.0018		
	277	0.100	4.000	12.500	CO1	9	118.0	Bottom	ε_y	0.0021		
	285	-0.100	4.000	13.500	CO1	9	118.0	Bottom	γ_{xy}	0.0026		
395	11996	0.100	4.000	14.000	CO1	1	0.0	Top	ε_x	0.0018		
	35	0.100	4.000	14.500	CO1	1	0.0	Top	ε_y	-0.0024		
	276	0.100	4.000	13.500	CO1	1	0.0	Top	γ_{xy}	0.0019		
396	11996	0.100	4.000	14.000	CO1	1	0.0	Top	ε_x	0.0025		
	35	0.100	4.000	14.500	CO1	1	0.0	Top	ε_y	-0.0024		
	49	-0.100	4.000	14.500	CO1	9	118.0	Bottom	γ_{xy}	0.0052		
397	279	1.750	1.000	11.500	CO1	9	118.0	Bottom	ε_x	-0.0014		
	282	0.100	1.000	11.500	CO1	9	118.0	Bottom	ε_y	-0.0008		
	11919	1.200	1.000	11.500	CO1	1	0.0	Top	γ_{xy}	-0.0025		
398	282	0.100	1.000	11.500	CO1	1	0.0	Top	ε_x	0.0005		
	282	0.100	1.000	11.500	CO1	9	118.0	Bottom	ε_y	-0.0008		
	282	0.100	1.000	11.500	CO1	9	118.0	Bottom	γ_{xy}	-0.0017		
399	11882	1.750	1.333	11.833	CO1	9	118.0	Bottom	ε_x	-0.0014		
	283	0.100	2.000	12.500	CO1	9	118.0	Bottom	ε_y	-0.0016		
	280	1.750	2.000	12.500	CO1	9	118.0	Bottom	γ_{xy}	-0.0034		
400	283	0.100	2.000	12.500	CO1	1	0.0	Top	ε_x	0.0009		
	289	-0.100	2.000	12.500	CO1	9	118.0	Bottom	ε_y	-0.0017		
	283	0.100	2.000	12.500	CO1	9	118.0	Bottom	γ_{xy}	-0.0018		
401	284	0.100	3.000	13.500	CO1	1	0.0	Top	ε_x	0.0009		
	284	0.100	3.000	13.500	CO1	9	118.0	Bottom	ε_y	-0.0018		
	284	0.100	3.000	13.500	CO1	9	118.0	Bottom	γ_{xy}	-0.0016		
402	284	0.100	3.000	13.500	CO1	1	0.0	Top	ε_x	0.0010		
	290	-0.100	3.000	13.500	CO1	9	118.0	Bottom	ε_y	-0.0019		
	284	0.100	3.000	13.500	CO1	1	0.0	Top	γ_{xy}	-0.0019		
403	35	0.100	4.000	14.500	CO1	1	0.0	Top	ε_x	0.0010		
	35	0.100	4.000	14.500	CO1	9	118.0	Bottom	ε_y	-0.0017		
	35	0.100	4.000	14.500	CO1	9	118.0	Bottom	γ_{xy}	-0.0023		
404	35	0.100	4.000	14.500	CO1	9	118.0	Bottom	ε_x	0.0015		
	35	0.100	4.000	14.500	CO1	9	118.0	Bottom	ε_y	-0.0022		
	49	-0.100	4.000	14.500	CO1	1	0.0	Top	γ_{xy}	-0.0021		
406	422	29.800	0.000	10.500	CO1	1	0.0	Top	ε_x	-0.0041		
	2419	31.263	0.000	10.500	CO1	1	0.0	Top	ε_y	0.0025		
	387	32.150	2.000	10.500	CO1	1	0.0	Top	γ_{xy}	-0.0038		
407	437	29.800	4.000	12.500	CO1	1	0.0	Top	ε_x	0.0027		
	437	29.800	4.000	12.500	CO1	1	0.0	Top	ε_y	-0.0027		
	12197	39.062	2.500	12.500	CO1	1	0.0	Top	γ_{xy}	-0.0046		
408	1763	20.897	4.000	10.500	CO1	9	118.0	Bottom	ε_x	0.0034		
	9344	21.887	4.000	12.500	CO3	1	0.0	Top	ε_y	0.0029		
	1949	36.138	4.000	10.500	CO1	1	0.0	Top	γ_{xy}	0.0017		
409	9345	21.392	4.000	12.500	CO1	9	118.0	Bottom	ε_x	0.0033		
	12666	20.404	4.000	13.500	CO1	1	0.0	Top	ε_y	-0.0018		
	12157	38.088	4.000	12.500	CO1	1	0.0	Top	γ_{xy}	0.0030		
410	2436	22.876	0.000	10.500	CO1	1	0.0	Top	ε_x	-0.0052		
	2440	20.897	0.000	10.500	CO1	1	0.0	Top	ε_y	0.0039		
	9543	2.725	2.000	12.500	CO1	9	118.0	Bottom	γ_{xy}	-0.0047		
411	12551	20.405	4.000	14.500	CO1	9	118.0	Bottom	ε_x	0.0032		
	9388	20.897	2.000	12.500	CO7	1	0.0	Top	ε_y	0.0030		
	13235	38.569	3.667	14.167	CO3	1	0.0	Top	γ_{xy}	0.0016		
Maximum Ratio		**0.0000**										

4.1 PARTS LIST

Part No.	Material Description	Thickness t [mm]	Layer Count	Area [m²]	Coating [m²]	Volume [m³]	Weight [t]
1	Lamina properties	6.0	8	64.763	129.525	3.109	6.286
	kern	50.0	1	64.763	0.000	3.238	0.238
Σ		98.0	9	64.763	129.525	6.347	6.524
2	Lamina properties	3.6	4	38.293	76.586	0.551	1.115
	Lamina properties	8.4	4	38.293	0.000	1.287	2.602
	kern	50.0	1	38.293	0.000	1.915	0.141
Σ		98.0	9	38.293	76.586	3.753	3.857

Project: CIE5060 Model: V26
Graduation Project

4.1 PARTS LIST

Part No.	Material Description	Thickness t [mm]	Layer Count	Area [m²]	Coating [m²]	Volume [m³]	Weight [t]
3	Lamina properties	6.0	8	64.763	129.525	3.109	6.286
	kern	50.0	1	64.763	0.000	3.238	0.238
Σ		98.0	9	64.763	129.525	6.347	6.524
4	Lamina properties	3.6	4	38.293	76.586	0.551	1.115
	Lamina properties	8.4	4	38.293	0.000	1.287	2.602
	kern	50.0	1	38.293	0.000	1.915	0.141
Σ		98.0	9	38.293	76.586	3.753	3.857
5	Lamina properties	6.0	8	64.763	129.525	3.109	6.286
	kern	50.0	1	64.763	0.000	3.238	0.238
Σ		98.0	9	64.763	129.525	6.347	6.524
6	Lamina properties	3.6	4	38.293	76.586	0.551	1.115
	Lamina properties	8.4	4	38.293	0.000	1.287	2.602
	kern	50.0	1	38.293	0.000	1.915	0.141
Σ		98.0	9	38.293	76.586	3.753	3.857
7	Lamina properties	18.7	2	113.400	226.800	4.241	8.576
	Lamina properties	5.1	6	113.400	0.000	3.470	7.016
	kern	50.0	1	113.400	0.000	5.670	0.417
Σ		118.0	9	113.400	226.800	13.381	16.009
8	Lamina properties	18.7	2	113.400	226.800	4.241	8.576
	Lamina properties	5.1	6	113.400	0.000	3.470	7.016
	kern	50.0	1	113.400	0.000	5.670	0.417
Σ		118.0	9	113.400	226.800	13.381	16.009
9	Lamina properties	3.6	4	38.293	76.586	0.551	1.115
	Lamina properties	8.4	4	38.293	0.000	1.287	2.602
	kern	50.0	1	38.293	0.000	1.915	0.141
Σ		98.0	9	38.293	76.586	3.753	3.857
10	Lamina properties	18.7	2	113.400	226.800	4.241	8.576
	Lamina properties	5.1	6	113.400	0.000	3.470	7.016
	kern	50.0	1	113.400	0.000	5.670	0.417
Σ		118.0	9	113.400	226.800	13.381	16.009
11	Lamina properties	18.7	2	113.400	226.800	4.241	8.576
	Lamina properties	5.1	6	113.400	0.000	3.470	7.016
	kern	50.0	1	113.400	0.000	5.670	0.417
Σ		118.0	9	113.400	226.800	13.381	16.009
12	Lamina properties	3.6	4	38.293	76.586	0.551	1.115
	Lamina properties	8.4	4	38.293	0.000	1.287	2.602
	kern	50.0	1	38.293	0.000	1.915	0.141
Σ		98.0	9	38.293	76.586	3.753	3.857
13	Lamina properties	18.7	2	113.400	226.800	4.241	8.576
	Lamina properties	5.1	6	113.400	0.000	3.470	7.016
	kern	50.0	1	113.400	0.000	5.670	0.417
Σ		118.0	9	113.400	226.800	13.381	16.009
14	Lamina properties	18.7	2	113.400	226.800	4.241	8.576
	Lamina properties	5.1	6	113.400	0.000	3.470	7.016
	kern	50.0	1	113.400	0.000	5.670	0.417
Σ		118.0	9	113.400	226.800	13.381	16.009
15	Lamina properties	3.6	4	38.293	76.586	0.551	1.115
	Lamina properties	8.4	4	38.293	0.000	1.287	2.602
	kern	50.0	1	38.293	0.000	1.915	0.141
Σ		98.0	9	38.293	76.586	3.753	3.857
16	Lamina properties	18.7	2	113.400	226.800	4.241	8.576
	Lamina properties	5.1	6	113.400	0.000	3.470	7.016
	kern	50.0	1	113.400	0.000	5.670	0.417
Σ		118.0	9	113.400	226.800	13.381	16.009
17	Lamina properties	18.7	2	113.400	226.800	4.241	8.576
	Lamina properties	5.1	6	113.400	0.000	3.470	7.016
	kern	50.0	1	113.400	0.000	5.670	0.417
Σ		118.0	9	113.400	226.800	13.381	16.009
18	Lamina properties	3.6	4	38.293	76.586	0.551	1.115
	Lamina properties	8.4	4	38.293	0.000	1.287	2.602
	kern	50.0	1	38.293	0.000	1.915	0.141
Σ		98.0	9	38.293	76.586	3.753	3.857
19	Lamina properties	18.7	2	113.400	226.800	4.241	8.576
	Lamina properties	5.1	6	113.400	0.000	3.470	7.016
	kern	50.0	1	113.400	0.000	5.670	0.417
Σ		118.0	9	113.400	226.800	13.381	16.009
20	Lamina properties	18.7	2	113.400	226.800	4.241	8.576
	Lamina properties	5.1	6	113.400	0.000	3.470	7.016
	kern	50.0	1	113.400	0.000	5.670	0.417
Σ		118.0	9	113.400	226.800	13.381	16.009
21	Lamina properties	3.6	4	38.293	76.586	0.551	1.115
	Lamina properties	8.4	4	38.293	0.000	1.287	2.602
	kern	50.0	1	38.293	0.000	1.915	0.141

Project: CIE5060 Model: V26
Graduation Project

4.1 PARTS LIST

Part No.	Material Description	Thickness t [mm]	Layer Count	Area [m²]	Coating [m²]	Volume [m³]	Weight [t]
Σ		98.0	9	38.293	76.586	3.753	3.857
22	Lamina properties	18.7	2	113.400	226.800	4.241	8.576
	Lamina properties	5.1	6	113.400	0.000	3.470	7.016
	kern	50.0	1	113.400	0.000	5.670	0.417
Σ		118.0	9	113.400	226.800	13.381	16.009
23	Lamina properties	18.7	2	113.400	226.800	4.241	8.576
	Lamina properties	5.1	6	113.400	0.000	3.470	7.016
	kern	50.0	1	113.400	0.000	5.670	0.417
Σ		118.0	9	113.400	226.800	13.381	16.009
24	Lamina properties	3.6	4	39.000	78.000	0.562	1.136
	Lamina properties	8.4	4	39.000	0.000	1.310	2.650
	kern	50.0	1	39.000	0.000	1.950	0.144
Σ		98.0	9	39.000	78.000	3.822	3.929
25	Lamina properties	6.0	8	64.763	129.525	3.109	6.286
	kern	50.0	1	64.763	0.000	3.238	0.238
Σ		98.0	9	64.763	129.525	6.347	6.524
26	Lamina properties	3.6	4	38.293	76.586	0.551	1.115
	Lamina properties	8.4	4	38.293	0.000	1.287	2.602
	kern	50.0	1	38.293	0.000	1.915	0.141
Σ		98.0	9	38.293	76.586	3.753	3.857
27	Lamina properties	6.0	8	64.763	129.525	3.109	6.286
	kern	50.0	1	64.763	0.000	3.238	0.238
Σ		98.0	9	64.763	129.525	6.347	6.524
28	Lamina properties	3.6	4	38.293	76.586	0.551	1.115
	Lamina properties	8.4	4	38.293	0.000	1.287	2.602
	kern	50.0	1	38.293	0.000	1.915	0.141
Σ		98.0	9	38.293	76.586	3.753	3.857
29	Lamina properties	6.0	8	73.200	146.400	3.514	7.104
	kern	50.0	1	73.200	0.000	3.660	0.269
Σ		98.0	9	73.200	146.400	7.174	7.374
30	Lamina properties	3.6	4	39.000	78.000	0.562	1.136
	Lamina properties	8.4	4	39.000	0.000	1.310	2.650
	kern	50.0	1	39.000	0.000	1.950	0.144
Σ		98.0	9	39.000	78.000	3.822	3.929
31	Lamina properties	6.0	8	64.763	129.525	3.109	6.286
	kern	50.0	1	64.763	0.000	3.238	0.238
Σ		98.0	9	64.763	129.525	6.347	6.524
32	Lamina properties	3.6	4	38.293	76.586	0.551	1.115
	Lamina properties	8.4	4	38.293	0.000	1.287	2.602
	kern	50.0	1	38.293	0.000	1.915	0.141
Σ		98.0	9	38.293	76.586	3.753	3.857
33	Lamina properties	6.0	8	35.195	70.390	1.689	3.416
	kern	50.0	1	35.195	0.000	1.760	0.130
Σ		98.0	9	35.195	70.390	3.449	3.545
34	Lamina properties	3.6	4	19.374	38.749	0.279	0.564
	Lamina properties	8.4	4	19.374	0.000	0.651	1.316
	kern	50.0	1	19.374	0.000	0.969	0.071
Σ		98.0	9	19.374	38.749	1.899	1.952
47	Lamina properties	3.6	6	6.600	13.200	0.143	0.288
	Lamina properties	13.2	2	6.600	0.000	0.174	0.352
	kern	50.0	1	6.600	0.000	0.330	0.024
Σ		98.0	9	6.600	13.200	0.647	0.665
48	Lamina properties	3.6	6	0.800	1.600	0.017	0.035
	Lamina properties	13.2	2	0.800	0.000	0.021	0.043
	kern	50.0	1	0.800	0.000	0.040	0.003
Σ		98.0	9	0.800	1.600	0.078	0.081
49	Lamina properties	3.6	6	6.600	13.200	0.143	0.288
	Lamina properties	13.2	2	6.600	0.000	0.174	0.352
	kern	50.0	1	6.600	0.000	0.330	0.024
Σ		98.0	9	6.600	13.200	0.647	0.665
50	Lamina properties	3.6	6	6.600	13.200	0.143	0.288
	Lamina properties	13.2	2	6.600	0.000	0.174	0.352
	kern	50.0	1	6.600	0.000	0.330	0.024
Σ		98.0	9	6.600	13.200	0.647	0.665
51	Lamina properties	3.6	6	0.800	1.600	0.017	0.035
	Lamina properties	13.2	2	0.800	0.000	0.021	0.043
	kern	50.0	1	0.800	0.000	0.040	0.003
Σ		98.0	9	0.800	1.600	0.078	0.081
52	Lamina properties	3.6	6	0.800	1.600	0.017	0.035
	Lamina properties	13.2	2	0.800	0.000	0.021	0.043
	kern	50.0	1	0.800	0.000	0.040	0.003
Σ		98.0	9	0.800	1.600	0.078	0.081

Project: CIE5060 Model: V26
Graduation Project

4.1 PARTS LIST

Part No.	Material Description	Thickness t [mm]	Layer Count	Area [m²]	Coating [m²]	Volume [m³]	Weight [t]
53	Lamina properties	3.6	6	6.600	13.200	0.143	0.288
	Lamina properties	13.2	2	6.600	0.000	0.174	0.352
	kern	50.0	1	6.600	0.000	0.330	0.024
Σ		98.0	9	6.600	13.200	0.647	0.665
54	Lamina properties	3.6	6	0.800	1.600	0.017	0.035
	Lamina properties	13.2	2	0.800	0.000	0.021	0.043
	kern	50.0	1	0.800	0.000	0.040	0.003
Σ		98.0	9	0.800	1.600	0.078	0.081
55	Lamina properties	3.6	6	6.600	13.200	0.143	0.288
	Lamina properties	13.2	2	6.600	0.000	0.174	0.352
	kern	50.0	1	6.600	0.000	0.330	0.024
Σ		98.0	9	6.600	13.200	0.647	0.665
56	Lamina properties	3.6	6	6.600	13.200	0.143	0.288
	Lamina properties	13.2	2	6.600	0.000	0.174	0.352
	kern	50.0	1	6.600	0.000	0.330	0.024
Σ		98.0	9	6.600	13.200	0.647	0.665
57	Lamina properties	3.6	6	0.800	1.600	0.017	0.035
	Lamina properties	13.2	2	0.800	0.000	0.021	0.043
	kern	50.0	1	0.800	0.000	0.040	0.003
Σ		98.0	9	0.800	1.600	0.078	0.081
58	Lamina properties	3.6	6	0.800	1.600	0.017	0.035
	Lamina properties	13.2	2	0.800	0.000	0.021	0.043
	kern	50.0	1	0.800	0.000	0.040	0.003
Σ		98.0	9	0.800	1.600	0.078	0.081
59	Lamina properties	3.6	6	6.600	13.200	0.143	0.288
	Lamina properties	13.2	2	6.600	0.000	0.174	0.352
	kern	50.0	1	6.600	0.000	0.330	0.024
Σ		98.0	9	6.600	13.200	0.647	0.665
60	Lamina properties	3.6	6	0.800	1.600	0.017	0.035
	Lamina properties	13.2	2	0.800	0.000	0.021	0.043
	kern	50.0	1	0.800	0.000	0.040	0.003
Σ		98.0	9	0.800	1.600	0.078	0.081
61	Lamina properties	3.6	6	6.600	13.200	0.143	0.288
	Lamina properties	13.2	2	6.600	0.000	0.174	0.352
	kern	50.0	1	6.600	0.000	0.330	0.024
Σ		98.0	9	6.600	13.200	0.647	0.665
62	Lamina properties	3.6	6	0.800	1.600	0.017	0.035
	Lamina properties	13.2	2	0.800	0.000	0.021	0.043
	kern	50.0	1	0.800	0.000	0.040	0.003
Σ		98.0	9	0.800	1.600	0.078	0.081
63	Lamina properties	3.6	6	6.600	13.200	0.143	0.288
	Lamina properties	13.2	2	6.600	0.000	0.174	0.352
	kern	50.0	1	6.600	0.000	0.330	0.024
Σ		98.0	9	6.600	13.200	0.647	0.665
64	Lamina properties	3.6	6	0.800	1.600	0.017	0.035
	Lamina properties	13.2	2	0.800	0.000	0.021	0.043
	kern	50.0	1	0.800	0.000	0.040	0.003
Σ		98.0	9	0.800	1.600	0.078	0.081
65	Lamina properties	3.6	6	6.600	13.200	0.143	0.288
	Lamina properties	13.2	2	6.600	0.000	0.174	0.352
	kern	50.0	1	6.600	0.000	0.330	0.024
Σ		98.0	9	6.600	13.200	0.647	0.665
66	Lamina properties	3.6	6	0.800	1.600	0.017	0.035
	Lamina properties	13.2	2	0.800	0.000	0.021	0.043
	kern	50.0	1	0.800	0.000	0.040	0.003
Σ		98.0	9	0.800	1.600	0.078	0.081
101	Lamina properties	3.6	6	6.600	13.200	0.143	0.288
	Lamina properties	13.2	2	6.600	0.000	0.174	0.352
	kern	50.0	1	6.600	0.000	0.330	0.024
Σ		98.0	9	6.600	13.200	0.647	0.665
102	Lamina properties	5.0	8	6.600	13.200	0.264	0.534
	kern	50.0	1	6.600	0.000	0.330	0.024
Σ		90.0	9	6.600	13.200	0.594	0.558
103	Lamina properties	5.0	8	6.600	13.200	0.264	0.534
	kern	50.0	1	6.600	0.000	0.330	0.024
Σ		90.0	9	6.600	13.200	0.594	0.558
104	Lamina properties	5.0	8	6.600	13.200	0.264	0.534
	kern	50.0	1	6.600	0.000	0.330	0.024
Σ		90.0	9	6.600	13.200	0.594	0.558
105	Lamina properties	5.0	8	6.600	13.200	0.264	0.534
	kern	50.0	1	6.600	0.000	0.330	0.024
Σ		90.0	9	6.600	13.200	0.594	0.558
106	Lamina properties	5.0	8	6.600	13.200	0.264	0.534

Project: CIE5060 Model: V26
Graduation Project

4.1 PARTS LIST

Part No.	Material Description	Thickness t [mm]	Layer Count	Area [m²]	Coating [m²]	Volume [m³]	Weight [t]
	kern	50.0	1	6.600	0.000	0.330	0.024
Σ		90.0	9	6.600	13.200	0.594	0.558
107	Lamina properties	5.0	8	6.600	13.200	0.264	0.534
	kern	50.0	1	6.600	0.000	0.330	0.024
Σ		90.0	9	6.600	13.200	0.594	0.558
108	Lamina properties	5.0	8	6.600	13.200	0.264	0.534
	kern	50.0	1	6.600	0.000	0.330	0.024
Σ		90.0	9	6.600	13.200	0.594	0.558
109	Lamina properties	5.0	8	6.600	13.200	0.264	0.534
	kern	50.0	1	6.600	0.000	0.330	0.024
Σ		90.0	9	6.600	13.200	0.594	0.558
110	Lamina properties	5.0	8	6.600	13.200	0.264	0.534
	kern	50.0	1	6.600	0.000	0.330	0.024
Σ		90.0	9	6.600	13.200	0.594	0.558
111	Lamina properties	5.0	8	6.600	13.200	0.264	0.534
	kern	50.0	1	6.600	0.000	0.330	0.024
Σ		90.0	9	6.600	13.200	0.594	0.558
112	Lamina properties	5.0	8	6.600	13.200	0.264	0.534
	kern	50.0	1	6.600	0.000	0.330	0.024
Σ		90.0	9	6.600	13.200	0.594	0.558
113	Lamina properties	5.0	8	6.600	13.200	0.264	0.534
	kern	50.0	1	6.600	0.000	0.330	0.024
Σ		90.0	9	6.600	13.200	0.594	0.558
114	Lamina properties	5.1	4	1.650	3.300	0.034	0.068
	Lamina properties	11.9	4	1.650	0.000	0.079	0.159
	kern	50.0	1	1.650	0.000	0.082	0.006
Σ		118.0	9	1.650	3.300	0.195	0.233
115	Lamina properties	5.1	4	1.650	3.300	0.034	0.068
	Lamina properties	11.9	4	1.650	0.000	0.079	0.159
	kern	50.0	1	1.650	0.000	0.082	0.006
Σ		118.0	9	1.650	3.300	0.195	0.233
116	Lamina properties	5.1	4	1.650	3.300	0.034	0.068
	Lamina properties	11.9	4	1.650	0.000	0.079	0.159
	kern	50.0	1	1.650	0.000	0.083	0.006
Σ		118.0	9	1.650	3.300	0.195	0.233
117	Lamina properties	5.1	4	1.650	3.300	0.034	0.068
	Lamina properties	11.9	4	1.650	0.000	0.079	0.159
	kern	50.0	1	1.650	0.000	0.083	0.006
Σ		118.0	9	1.650	3.300	0.195	0.233
118	Lamina properties	5.1	4	1.650	3.300	0.034	0.068
	Lamina properties	11.9	4	1.650	0.000	0.079	0.159
	kern	50.0	1	1.650	0.000	0.082	0.006
Σ		118.0	9	1.650	3.300	0.195	0.233
119	Lamina properties	5.1	4	1.650	3.300	0.034	0.068
	Lamina properties	11.9	4	1.650	0.000	0.079	0.159
	kern	50.0	1	1.650	0.000	0.082	0.006
Σ		118.0	9	1.650	3.300	0.195	0.233
120	Lamina properties	5.1	4	1.650	3.300	0.034	0.068
	Lamina properties	11.9	4	1.650	0.000	0.079	0.159
	kern	50.0	1	1.650	0.000	0.082	0.006
Σ		118.0	9	1.650	3.300	0.195	0.233
121	Lamina properties	5.1	4	1.650	3.300	0.034	0.068
	Lamina properties	11.9	4	1.650	0.000	0.079	0.159
	kern	50.0	1	1.650	0.000	0.082	0.006
Σ		118.0	9	1.650	3.300	0.195	0.233
122	Lamina properties	5.1	4	1.650	3.300	0.034	0.068
	Lamina properties	11.9	4	1.650	0.000	0.079	0.159
	kern	50.0	1	1.650	0.000	0.083	0.006
Σ		118.0	9	1.650	3.300	0.195	0.233
123	Lamina properties	5.1	4	1.650	3.300	0.034	0.068
	Lamina properties	11.9	4	1.650	0.000	0.079	0.159
	kern	50.0	1	1.650	0.000	0.083	0.006
Σ		118.0	9	1.650	3.300	0.195	0.233
124	Lamina properties	5.1	4	1.650	3.300	0.034	0.068
	Lamina properties	11.9	4	1.650	0.000	0.079	0.159
	kern	50.0	1	1.650	0.000	0.082	0.006
Σ		118.0	9	1.650	3.300	0.195	0.233
125	Lamina properties	5.1	4	1.650	3.300	0.034	0.068
	Lamina properties	11.9	4	1.650	0.000	0.079	0.159
	kern	50.0	1	1.650	0.000	0.082	0.006
Σ		118.0	9	1.650	3.300	0.195	0.233
126	Lamina properties	5.1	4	1.650	3.300	0.034	0.068

Project: CIE5060 Model: V26
Graduation Project

4.1 PARTS LIST

Part No.	Material Description	Thickness t [mm]	Layer Count	Area [m²]	Coating [m²]	Volume [m³]	Weight [t]
	Lamina properties	11.9	4	1.650	0.000	0.079	0.159
	kern	50.0	1	1.650	0.000	0.082	0.006
Σ		118.0	9	1.650	3.300	0.195	0.233
127	Lamina properties	5.1	4	1.650	3.300	0.034	0.068
	Lamina properties	11.9	4	1.650	0.000	0.079	0.159
	kern	50.0	1	1.650	0.000	0.082	0.006
Σ		118.0	9	1.650	3.300	0.195	0.233
128	Lamina properties	5.1	4	1.650	3.300	0.034	0.068
	Lamina properties	11.9	4	1.650	0.000	0.079	0.159
	kern	50.0	1	1.650	0.000	0.083	0.006
Σ		118.0	9	1.650	3.300	0.195	0.233
129	Lamina properties	5.1	4	1.650	3.300	0.034	0.068
	Lamina properties	11.9	4	1.650	0.000	0.079	0.159
	kern	50.0	1	1.650	0.000	0.083	0.006
Σ		118.0	9	1.650	3.300	0.195	0.233
130	Lamina properties	5.1	4	1.650	3.300	0.034	0.068
	Lamina properties	11.9	4	1.650	0.000	0.079	0.159
	kern	50.0	1	1.650	0.000	0.082	0.006
Σ		118.0	9	1.650	3.300	0.195	0.233
131	Lamina properties	5.1	4	1.650	3.300	0.034	0.068
	Lamina properties	11.9	4	1.650	0.000	0.079	0.159
	kern	50.0	1	1.650	0.000	0.082	0.006
Σ		118.0	9	1.650	3.300	0.195	0.233
132	Lamina properties	5.1	4	1.650	3.300	0.034	0.068
	Lamina properties	11.9	4	1.650	0.000	0.079	0.159
	kern	50.0	1	1.650	0.000	0.082	0.006
Σ		118.0	9	1.650	3.300	0.195	0.233
133	Lamina properties	5.1	4	1.650	3.300	0.034	0.068
	Lamina properties	11.9	4	1.650	0.000	0.079	0.159
	kern	50.0	1	1.650	0.000	0.082	0.006
Σ		118.0	9	1.650	3.300	0.195	0.233
134	Lamina properties	5.1	4	1.650	3.300	0.034	0.068
	Lamina properties	11.9	4	1.650	0.000	0.079	0.159
	kern	50.0	1	1.650	0.000	0.083	0.006
Σ		118.0	9	1.650	3.300	0.195	0.233
135	Lamina properties	5.1	4	1.650	3.300	0.034	0.068
	Lamina properties	11.9	4	1.650	0.000	0.079	0.159
	kern	50.0	1	1.650	0.000	0.083	0.006
Σ		118.0	9	1.650	3.300	0.195	0.233
136	Lamina properties	5.1	4	1.650	3.300	0.034	0.068
	Lamina properties	11.9	4	1.650	0.000	0.079	0.159
	kern	50.0	1	1.650	0.000	0.082	0.006
Σ		118.0	9	1.650	3.300	0.195	0.233
137	Lamina properties	5.1	4	1.650	3.300	0.034	0.068
	Lamina properties	11.9	4	1.650	0.000	0.079	0.159
	kern	50.0	1	1.650	0.000	0.082	0.006
Σ		118.0	9	1.650	3.300	0.195	0.233
138	Lamina properties	5.1	4	1.650	3.300	0.034	0.068
	Lamina properties	11.9	4	1.650	0.000	0.079	0.159
	kern	50.0	1	1.650	0.000	0.082	0.006
Σ		118.0	9	1.650	3.300	0.195	0.233
139	Lamina properties	5.1	4	1.650	3.300	0.034	0.068
	Lamina properties	11.9	4	1.650	0.000	0.079	0.159
	kern	50.0	1	1.650	0.000	0.082	0.006
Σ		118.0	9	1.650	3.300	0.195	0.233
140	Lamina properties	5.1	4	1.650	3.300	0.034	0.068
	Lamina properties	11.9	4	1.650	0.000	0.079	0.159
	kern	50.0	1	1.650	0.000	0.083	0.006
Σ		118.0	9	1.650	3.300	0.195	0.233
141	Lamina properties	5.1	4	1.650	3.300	0.034	0.068
	Lamina properties	11.9	4	1.650	0.000	0.079	0.159
	kern	50.0	1	1.650	0.000	0.083	0.006
Σ		118.0	9	1.650	3.300	0.195	0.233
142	Lamina properties	5.1	4	1.650	3.300	0.034	0.068
	Lamina properties	11.9	4	1.650	0.000	0.079	0.159
	kern	50.0	1	1.650	0.000	0.082	0.006
Σ		118.0	9	1.650	3.300	0.195	0.233
143	Lamina properties	5.1	4	1.650	3.300	0.034	0.068
	Lamina properties	11.9	4	1.650	0.000	0.079	0.159
	kern	50.0	1	1.650	0.000	0.082	0.006
Σ		118.0	9	1.650	3.300	0.195	0.233
144	Lamina properties	5.1	4	1.650	3.300	0.034	0.068
	Lamina properties	11.9	4	1.650	0.000	0.079	0.159
	kern	50.0	1	1.650	0.000	0.083	0.006

Project: CIE5060 Model: V26
Graduation Project

4.1 PARTS LIST

Part No.	Material Description	Thickness t [mm]	Layer Count	Area [m²]	Coating [m²]	Volume [m³]	Weight [t]
Σ		118.0	9	1.650	3.300	0.195	0.233
145	Lamina properties	5.1	4	1.650	3.300	0.034	0.068
	Lamina properties	11.9	4	1.650	0.000	0.079	0.159
	kern	50.0	1	1.650	0.000	0.083	0.006
Σ		118.0	9	1.650	3.300	0.195	0.233
146	Lamina properties	5.1	4	1.650	3.300	0.034	0.068
	Lamina properties	11.9	4	1.650	0.000	0.079	0.159
	kern	50.0	1	1.650	0.000	0.083	0.006
Σ		118.0	9	1.650	3.300	0.195	0.233
147	Lamina properties	5.1	4	1.650	3.300	0.034	0.068
	Lamina properties	11.9	4	1.650	0.000	0.079	0.159
	kern	50.0	1	1.650	0.000	0.083	0.006
Σ		118.0	9	1.650	3.300	0.195	0.233
148	Lamina properties	5.1	4	1.650	3.300	0.034	0.068
	Lamina properties	11.9	4	1.650	0.000	0.079	0.159
	kern	50.0	1	1.650	0.000	0.083	0.006
Σ		118.0	9	1.650	3.300	0.195	0.233
149	Lamina properties	5.1	4	1.650	3.300	0.034	0.068
	Lamina properties	11.9	4	1.650	0.000	0.079	0.159
	kern	50.0	1	1.650	0.000	0.083	0.006
Σ		118.0	9	1.650	3.300	0.195	0.233
150	Lamina properties	3.6	6	0.800	1.600	0.017	0.035
	Lamina properties	13.2	2	0.800	0.000	0.021	0.043
	kern	50.0	1	0.800	0.000	0.040	0.003
Σ		98.0	9	0.800	1.600	0.078	0.081
151	Lamina properties	5.0	8	0.800	1.600	0.032	0.065
	kern	50.0	1	0.800	0.000	0.040	0.003
Σ		90.0	9	0.800	1.600	0.072	0.068
152	Lamina properties	5.0	8	0.800	1.600	0.032	0.065
	kern	50.0	1	0.800	0.000	0.040	0.003
Σ		90.0	9	0.800	1.600	0.072	0.068
153	Lamina properties	5.0	8	0.800	1.600	0.032	0.065
	kern	50.0	1	0.800	0.000	0.040	0.003
Σ		90.0	9	0.800	1.600	0.072	0.068
154	Lamina properties	5.0	8	0.800	1.600	0.032	0.065
	kern	50.0	1	0.800	0.000	0.040	0.003
Σ		90.0	9	0.800	1.600	0.072	0.068
155	Lamina properties	5.0	8	0.800	1.600	0.032	0.065
	kern	50.0	1	0.800	0.000	0.040	0.003
Σ		90.0	9	0.800	1.600	0.072	0.068
156	Lamina properties	5.0	8	0.800	1.600	0.032	0.065
	kern	50.0	1	0.800	0.000	0.040	0.003
Σ		90.0	9	0.800	1.600	0.072	0.068
157	Lamina properties	5.0	8	0.800	1.600	0.032	0.065
	kern	50.0	1	0.800	0.000	0.040	0.003
Σ		90.0	9	0.800	1.600	0.072	0.068
158	Lamina properties	5.0	8	0.800	1.600	0.032	0.065
	kern	50.0	1	0.800	0.000	0.040	0.003
Σ		90.0	9	0.800	1.600	0.072	0.068
159	Lamina properties	5.0	8	0.800	1.600	0.032	0.065
	kern	50.0	1	0.800	0.000	0.040	0.003
Σ		90.0	9	0.800	1.600	0.072	0.068
160	Lamina properties	5.0	8	0.800	1.600	0.032	0.065
	kern	50.0	1	0.800	0.000	0.040	0.003
Σ		90.0	9	0.800	1.600	0.072	0.068
161	Lamina properties	5.0	8	0.800	1.600	0.032	0.065
	kern	50.0	1	0.800	0.000	0.040	0.003
Σ		90.0	9	0.800	1.600	0.072	0.068
162	Lamina properties	5.0	8	0.800	1.600	0.032	0.065
	kern	50.0	1	0.800	0.000	0.040	0.003
Σ		90.0	9	0.800	1.600	0.072	0.068
163	Lamina properties	5.1	4	0.200	0.400	0.004	0.008
	Lamina properties	11.9	4	0.200	0.000	0.010	0.019
	kern	50.0	1	0.200	0.000	0.010	0.001
Σ		118.0	9	0.200	0.400	0.024	0.028
164	Lamina properties	5.1	4	0.200	0.400	0.004	0.008
	Lamina properties	11.9	4	0.200	0.000	0.010	0.019
	kern	50.0	1	0.200	0.000	0.010	0.001
Σ		118.0	9	0.200	0.400	0.024	0.028
165	Lamina properties	5.1	4	0.200	0.400	0.004	0.008
	Lamina properties	11.9	4	0.200	0.000	0.010	0.019

Project: CIE5060 Model: V26
Graduation Project

4.1 PARTS LIST

Part No.	Material Description	Thickness t [mm]	Layer Count	Area [m²]	Coating [m²]	Volume [m³]	Weight [t]
	kern	50.0	1	0.200	0.000	0.010	0.001
Σ		118.0	9	0.200	0.400	0.024	0.028
166	Lamina properties	5.1	4	0.200	0.400	0.004	0.008
	Lamina properties	11.9	4	0.200	0.000	0.010	0.019
	kern	50.0	1	0.200	0.000	0.010	0.001
Σ		118.0	9	0.200	0.400	0.024	0.028
167	Lamina properties	5.1	4	0.200	0.400	0.004	0.008
	Lamina properties	11.9	4	0.200	0.000	0.010	0.019
	kern	50.0	1	0.200	0.000	0.010	0.001
Σ		118.0	9	0.200	0.400	0.024	0.028
168	Lamina properties	5.1	4	0.200	0.400	0.004	0.008
	Lamina properties	11.9	4	0.200	0.000	0.010	0.019
	kern	50.0	1	0.200	0.000	0.010	0.001
Σ		118.0	9	0.200	0.400	0.024	0.028
169	Lamina properties	5.1	4	0.200	0.400	0.004	0.008
	Lamina properties	11.9	4	0.200	0.000	0.010	0.019
	kern	50.0	1	0.200	0.000	0.010	0.001
Σ		118.0	9	0.200	0.400	0.024	0.028
170	Lamina properties	5.1	4	0.200	0.400	0.004	0.008
	Lamina properties	11.9	4	0.200	0.000	0.010	0.019
	kern	50.0	1	0.200	0.000	0.010	0.001
Σ		118.0	9	0.200	0.400	0.024	0.028
171	Lamina properties	5.1	4	0.200	0.400	0.004	0.008
	Lamina properties	11.9	4	0.200	0.000	0.010	0.019
	kern	50.0	1	0.200	0.000	0.010	0.001
Σ		118.0	9	0.200	0.400	0.024	0.028
172	Lamina properties	5.1	4	0.200	0.400	0.004	0.008
	Lamina properties	11.9	4	0.200	0.000	0.010	0.019
	kern	50.0	1	0.200	0.000	0.010	0.001
Σ		118.0	9	0.200	0.400	0.024	0.028
173	Lamina properties	5.1	4	0.200	0.400	0.004	0.008
	Lamina properties	11.9	4	0.200	0.000	0.010	0.019
	kern	50.0	1	0.200	0.000	0.010	0.001
Σ		118.0	9	0.200	0.400	0.024	0.028
174	Lamina properties	5.1	4	0.200	0.400	0.004	0.008
	Lamina properties	11.9	4	0.200	0.000	0.010	0.019
	kern	50.0	1	0.200	0.000	0.010	0.001
Σ		118.0	9	0.200	0.400	0.024	0.028
175	Lamina properties	5.1	4	0.200	0.400	0.004	0.008
	Lamina properties	11.9	4	0.200	0.000	0.010	0.019
	kern	50.0	1	0.200	0.000	0.010	0.001
Σ		118.0	9	0.200	0.400	0.024	0.028
176	Lamina properties	5.1	4	0.200	0.400	0.004	0.008
	Lamina properties	11.9	4	0.200	0.000	0.010	0.019
	kern	50.0	1	0.200	0.000	0.010	0.001
Σ		118.0	9	0.200	0.400	0.024	0.028
177	Lamina properties	5.1	4	0.200	0.400	0.004	0.008
	Lamina properties	11.9	4	0.200	0.000	0.010	0.019
	kern	50.0	1	0.200	0.000	0.010	0.001
Σ		118.0	9	0.200	0.400	0.024	0.028
178	Lamina properties	5.1	4	0.200	0.400	0.004	0.008
	Lamina properties	11.9	4	0.200	0.000	0.010	0.019
	kern	50.0	1	0.200	0.000	0.010	0.001
Σ		118.0	9	0.200	0.400	0.024	0.028
179	Lamina properties	5.1	4	0.200	0.400	0.004	0.008
	Lamina properties	11.9	4	0.200	0.000	0.010	0.019
	kern	50.0	1	0.200	0.000	0.010	0.001
Σ		118.0	9	0.200	0.400	0.024	0.028
180	Lamina properties	5.1	4	0.200	0.400	0.004	0.008
	Lamina properties	11.9	4	0.200	0.000	0.010	0.019
	kern	50.0	1	0.200	0.000	0.010	0.001
Σ		118.0	9	0.200	0.400	0.024	0.028
181	Lamina properties	5.1	4	0.200	0.400	0.004	0.008
	Lamina properties	11.9	4	0.200	0.000	0.010	0.019
	kern	50.0	1	0.200	0.000	0.010	0.001
Σ		118.0	9	0.200	0.400	0.024	0.028
182	Lamina properties	5.1	4	0.200	0.400	0.004	0.008
	Lamina properties	11.9	4	0.200	0.000	0.010	0.019
	kern	50.0	1	0.200	0.000	0.010	0.001
Σ		118.0	9	0.200	0.400	0.024	0.028
183	Lamina properties	5.1	4	0.200	0.400	0.004	0.008
	Lamina properties	11.9	4	0.200	0.000	0.010	0.019
	kern	50.0	1	0.200	0.000	0.010	0.001
Σ		118.0	9	0.200	0.400	0.024	0.028

Project: CIE5060 Model: V26
Graduation Project

4.1 PARTS LIST

Part No.	Material Description	Thickness t [mm]	Layer Count	Area [m²]	Coating [m²]	Volume [m³]	Weight [t]
184	Lamina properties	5.1	4	0.200	0.400	0.004	0.008
	Lamina properties	11.9	4	0.200	0.000	0.010	0.019
	kern	50.0	1	0.200	0.000	0.010	0.001
Σ		118.0	9	0.200	0.400	0.024	0.028
185	Lamina properties	5.1	4	0.200	0.400	0.004	0.008
	Lamina properties	11.9	4	0.200	0.000	0.010	0.019
	kern	50.0	1	0.200	0.000	0.010	0.001
Σ		118.0	9	0.200	0.400	0.024	0.028
186	Lamina properties	5.1	4	0.200	0.400	0.004	0.008
	Lamina properties	11.9	4	0.200	0.000	0.010	0.019
	kern	50.0	1	0.200	0.000	0.010	0.001
Σ		118.0	9	0.200	0.400	0.024	0.028
187	Lamina properties	5.1	4	0.200	0.400	0.004	0.008
	Lamina properties	11.9	4	0.200	0.000	0.010	0.019
	kern	50.0	1	0.200	0.000	0.010	0.001
Σ		118.0	9	0.200	0.400	0.024	0.028
188	Lamina properties	5.1	4	0.200	0.400	0.004	0.008
	Lamina properties	11.9	4	0.200	0.000	0.010	0.019
	kern	50.0	1	0.200	0.000	0.010	0.001
Σ		118.0	9	0.200	0.400	0.024	0.028
189	Lamina properties	5.1	4	0.200	0.400	0.004	0.008
	Lamina properties	11.9	4	0.200	0.000	0.010	0.019
	kern	50.0	1	0.200	0.000	0.010	0.001
Σ		118.0	9	0.200	0.400	0.024	0.028
190	Lamina properties	5.1	4	0.200	0.400	0.004	0.008
	Lamina properties	11.9	4	0.200	0.000	0.010	0.019
	kern	50.0	1	0.200	0.000	0.010	0.001
Σ		118.0	9	0.200	0.400	0.024	0.028
191	Lamina properties	5.1	4	0.200	0.400	0.004	0.008
	Lamina properties	11.9	4	0.200	0.000	0.010	0.019
	kern	50.0	1	0.200	0.000	0.010	0.001
Σ		118.0	9	0.200	0.400	0.024	0.028
192	Lamina properties	5.1	4	0.200	0.400	0.004	0.008
	Lamina properties	11.9	4	0.200	0.000	0.010	0.019
	kern	50.0	1	0.200	0.000	0.010	0.001
Σ		118.0	9	0.200	0.400	0.024	0.028
193	Lamina properties	5.1	4	0.200	0.400	0.004	0.008
	Lamina properties	11.9	4	0.200	0.000	0.010	0.019
	kern	50.0	1	0.200	0.000	0.010	0.001
Σ		118.0	9	0.200	0.400	0.024	0.028
194	Lamina properties	5.1	4	0.200	0.400	0.004	0.008
	Lamina properties	11.9	4	0.200	0.000	0.010	0.019
	kern	50.0	1	0.200	0.000	0.010	0.001
Σ		118.0	9	0.200	0.400	0.024	0.028
195	Lamina properties	5.1	4	0.200	0.400	0.004	0.008
	Lamina properties	11.9	4	0.200	0.000	0.010	0.019
	kern	50.0	1	0.200	0.000	0.010	0.001
Σ		118.0	9	0.200	0.400	0.024	0.028
196	Lamina properties	5.1	4	0.200	0.400	0.004	0.008
	Lamina properties	11.9	4	0.200	0.000	0.010	0.019
	kern	50.0	1	0.200	0.000	0.010	0.001
Σ		118.0	9	0.200	0.400	0.024	0.028
197	Lamina properties	5.1	4	0.200	0.400	0.004	0.008
	Lamina properties	11.9	4	0.200	0.000	0.010	0.019
	kern	50.0	1	0.200	0.000	0.010	0.001
Σ		118.0	9	0.200	0.400	0.024	0.028
198	Lamina properties	5.1	4	0.200	0.400	0.004	0.008
	Lamina properties	11.9	4	0.200	0.000	0.010	0.019
	kern	50.0	1	0.200	0.000	0.010	0.001
Σ		118.0	9	0.200	0.400	0.024	0.028
199	Lamina properties	7.0	4	4.000	7.999	0.112	0.226
	Lamina properties	3.0	4	4.000	0.000	0.048	0.097
	kern	50.0	1	4.000	0.000	0.200	0.015
Σ		90.0	9	4.000	7.999	0.360	0.338
200	Lamina properties	7.0	4	4.001	8.002	0.112	0.227
	Lamina properties	3.0	4	4.001	0.000	0.048	0.097
	kern	50.0	1	4.001	0.000	0.200	0.015
Σ		90.0	9	4.001	8.002	0.360	0.338
201	Lamina properties	7.0	4	4.000	7.999	0.112	0.226
	Lamina properties	3.0	4	4.000	0.000	0.048	0.097
	kern	50.0	1	4.000	0.000	0.200	0.015
Σ		90.0	9	4.000	7.999	0.360	0.338
202	Lamina properties	7.0	4	4.000	7.999	0.112	0.226

Project: CIE5060 Model: V26
Graduation Project

4.1 PARTS LIST

Part No.	Material Description	Thickness t [mm]	Layer Count	Area [m²]	Coating [m²]	Volume [m³]	Weight [t]
	Lamina properties	3.0	4	4.000	0.000	0.048	0.097
	kern	50.0	1	4.000	0.000	0.200	0.015
Σ		90.0	9	4.000	7.999	0.360	0.338
203	Lamina properties	7.0	4	4.001	8.002	0.112	0.227
	Lamina properties	3.0	4	4.001	0.000	0.048	0.097
	kern	50.0	1	4.001	0.000	0.200	0.015
Σ		90.0	9	4.001	8.002	0.360	0.338
204	Lamina properties	7.0	4	4.000	7.999	0.112	0.226
	Lamina properties	3.0	4	4.000	0.000	0.048	0.097
	kern	50.0	1	4.000	0.000	0.200	0.015
Σ		90.0	9	4.000	7.999	0.360	0.338
205	Lamina properties	7.0	4	4.000	7.999	0.112	0.226
	Lamina properties	3.0	4	4.000	0.000	0.048	0.097
	kern	50.0	1	4.000	0.000	0.200	0.015
Σ		90.0	9	4.000	7.999	0.360	0.338
206	Lamina properties	7.0	4	4.001	8.002	0.112	0.227
	Lamina properties	3.0	4	4.001	0.000	0.048	0.097
	kern	50.0	1	4.001	0.000	0.200	0.015
Σ		90.0	9	4.001	8.002	0.360	0.338
207	Lamina properties	7.0	4	4.000	7.999	0.112	0.226
	Lamina properties	3.0	4	4.000	0.000	0.048	0.097
	kern	50.0	1	4.000	0.000	0.200	0.015
Σ		90.0	9	4.000	7.999	0.360	0.338
208	Lamina properties	7.0	4	4.000	7.999	0.112	0.226
	Lamina properties	3.0	4	4.000	0.000	0.048	0.097
	kern	50.0	1	4.000	0.000	0.200	0.015
Σ		90.0	9	4.000	7.999	0.360	0.338
209	Lamina properties	7.0	4	4.001	8.002	0.112	0.227
	Lamina properties	3.0	4	4.001	0.000	0.048	0.097
	kern	50.0	1	4.001	0.000	0.200	0.015
Σ		90.0	9	4.001	8.002	0.360	0.338
210	Lamina properties	7.0	4	4.000	7.999	0.112	0.226
	Lamina properties	3.0	4	4.000	0.000	0.048	0.097
	kern	50.0	1	4.000	0.000	0.200	0.015
Σ		90.0	9	4.000	7.999	0.360	0.338
211	Lamina properties	7.0	4	4.000	7.999	0.112	0.226
	Lamina properties	3.0	4	4.000	0.000	0.048	0.097
	kern	50.0	1	4.000	0.000	0.200	0.015
Σ		90.0	9	4.000	7.999	0.360	0.338
212	Lamina properties	7.0	4	4.001	8.002	0.112	0.227
	Lamina properties	3.0	4	4.001	0.000	0.048	0.097
	kern	50.0	1	4.001	0.000	0.200	0.015
Σ		90.0	9	4.001	8.002	0.360	0.338
213	Lamina properties	7.0	4	4.000	7.999	0.112	0.226
	Lamina properties	3.0	4	4.000	0.000	0.048	0.097
	kern	50.0	1	4.000	0.000	0.200	0.015
Σ		90.0	9	4.000	7.999	0.360	0.338
214	Lamina properties	7.0	4	4.000	8.000	0.112	0.226
	Lamina properties	3.0	4	4.000	0.000	0.048	0.097
	kern	50.0	1	4.000	0.000	0.200	0.015
Σ		90.0	9	4.000	8.000	0.360	0.338
215	Lamina properties	7.0	4	4.000	8.000	0.112	0.226
	Lamina properties	3.0	4	4.000	0.000	0.048	0.097
	kern	50.0	1	4.000	0.000	0.200	0.015
Σ		90.0	9	4.000	8.000	0.360	0.338
216	Lamina properties	7.0	4	4.000	8.000	0.112	0.226
	Lamina properties	3.0	4	4.000	0.000	0.048	0.097
	kern	50.0	1	4.000	0.000	0.200	0.015
Σ		90.0	9	4.000	8.000	0.360	0.338
217	Lamina properties	3.6	6	6.600	13.200	0.143	0.288
	Lamina properties	13.2	2	6.600	0.000	0.174	0.352
	kern	50.0	1	6.600	0.000	0.330	0.024
Σ		98.0	9	6.600	13.200	0.647	0.665
218	Lamina properties	3.6	6	0.800	1.600	0.017	0.035
	Lamina properties	13.2	2	0.800	0.000	0.021	0.043
	kern	50.0	1	0.800	0.000	0.040	0.003
Σ		98.0	9	0.800	1.600	0.078	0.081
219	Lamina properties	7.0	4	3.500	7.000	0.098	0.198
	Lamina properties	3.0	4	3.500	0.000	0.042	0.085
	kern	50.0	1	3.500	0.000	0.175	0.013
Σ		90.0	9	3.500	7.000	0.315	0.296
220	Lamina properties	7.0	4	2.500	5.000	0.070	0.142
	Lamina properties	3.0	4	2.500	0.000	0.030	0.061
	kern	50.0	1	2.500	0.000	0.125	0.009

Project: CIE5060 Model: V26
Graduation Project

4.1 PARTS LIST

Part No.	Material Description	Thickness t [mm]	Layer Count	Area [m²]	Coating [m²]	Volume [m³]	Weight [t]
Σ		90.0	9	2.500	5.000	0.225	0.211
221	Lamina properties	7.0	4	1.500	3.000	0.042	0.085
	Lamina properties	3.0	4	1.500	0.000	0.018	0.036
	kern	50.0	1	1.500	0.000	0.075	0.006
Σ		90.0	9	1.500	3.000	0.135	0.127
222	Lamina properties	7.0	4	0.500	1.000	0.014	0.028
	Lamina properties	3.0	4	0.500	0.000	0.006	0.012
	kern	50.0	1	0.500	0.000	0.025	0.002
Σ		90.0	9	0.500	1.000	0.045	0.042
223	Lamina properties	5.0	8	4.950	9.900	0.198	0.400
	kern	50.0	1	4.950	0.000	0.248	0.018
Σ		90.0	9	4.950	9.900	0.445	0.419
224	Lamina properties	5.0	8	0.600	1.200	0.024	0.049
	kern	50.0	1	0.600	0.000	0.030	0.002
Σ		90.0	9	0.600	1.200	0.054	0.051
225	Lamina properties	3.6	6	3.300	6.600	0.071	0.144
	Lamina properties	13.2	2	3.300	0.000	0.087	0.176
	kern	50.0	1	3.300	0.000	0.165	0.012
Σ		98.0	9	3.300	6.600	0.323	0.332
226	Lamina properties	3.6	6	0.400	0.800	0.009	0.017
	Lamina properties	13.2	2	0.400	0.000	0.011	0.021
	kern	50.0	1	0.400	0.000	0.020	0.001
Σ		98.0	9	0.400	0.800	0.039	0.040
227	Lamina properties	5.0	8	1.650	3.300	0.066	0.133
	kern	50.0	1	1.650	0.000	0.083	0.006
Σ		90.0	9	1.650	3.300	0.148	0.140
228	Lamina properties	5.0	8	0.200	0.400	0.008	0.016
	kern	50.0	1	0.200	0.000	0.010	0.001
Σ		90.0	9	0.200	0.400	0.018	0.017
233	Lamina properties	7.0	4	3.500	7.000	0.098	0.198
	Lamina properties	3.0	4	3.500	0.000	0.042	0.085
	kern	50.0	1	3.500	0.000	0.175	0.013
Σ		90.0	9	3.500	7.000	0.315	0.296
234	Lamina properties	7.0	4	2.500	5.000	0.070	0.142
	Lamina properties	3.0	4	2.500	0.000	0.030	0.061
	kern	50.0	1	2.500	0.000	0.125	0.009
Σ		90.0	9	2.500	5.000	0.225	0.211
235	Lamina properties	7.0	4	1.500	3.000	0.042	0.085
	Lamina properties	3.0	4	1.500	0.000	0.018	0.036
	kern	50.0	1	1.500	0.000	0.075	0.006
Σ		90.0	9	1.500	3.000	0.135	0.127
236	Lamina properties	7.0	4	0.500	1.000	0.014	0.028
	Lamina properties	3.0	4	0.500	0.000	0.006	0.012
	kern	50.0	1	0.500	0.000	0.025	0.002
Σ		90.0	9	0.500	1.000	0.045	0.042
237	Lamina properties	5.1	4	1.650	3.300	0.034	0.068
	Lamina properties	11.9	4	1.650	0.000	0.079	0.159
	kern	50.0	1	1.650	0.000	0.083	0.006
Σ		118.0	9	1.650	3.300	0.195	0.233
238	Lamina properties	5.1	4	0.200	0.400	0.004	0.008
	Lamina properties	11.9	4	0.200	0.000	0.010	0.019
	kern	50.0	1	0.200	0.000	0.010	0.001
Σ		118.0	9	0.200	0.400	0.024	0.028
239	Lamina properties	5.1	4	1.650	3.300	0.034	0.068
	Lamina properties	11.9	4	1.650	0.000	0.079	0.159
	kern	50.0	1	1.650	0.000	0.083	0.006
Σ		118.0	9	1.650	3.300	0.195	0.233
240	Lamina properties	5.1	4	0.200	0.400	0.004	0.008
	Lamina properties	11.9	4	0.200	0.000	0.010	0.019
	kern	50.0	1	0.200	0.000	0.010	0.001
Σ		118.0	9	0.200	0.400	0.024	0.028
241	Lamina properties	5.1	4	1.650	3.300	0.034	0.068
	Lamina properties	11.9	4	1.650	0.000	0.079	0.159
	kern	50.0	1	1.650	0.000	0.083	0.006
Σ		118.0	9	1.650	3.300	0.195	0.233
242	Lamina properties	5.1	4	0.200	0.400	0.004	0.008
	Lamina properties	11.9	4	0.200	0.000	0.010	0.019
	kern	50.0	1	0.200	0.000	0.010	0.001
Σ		118.0	9	0.200	0.400	0.024	0.028
243	Lamina properties	5.1	4	1.650	3.300	0.034	0.068
	Lamina properties	11.9	4	1.650	0.000	0.079	0.159
	kern	50.0	1	1.650	0.000	0.083	0.006
Σ		118.0	9	1.650	3.300	0.195	0.233

Project: CIE5060 Model: V26
Graduation Project

4.1 PARTS LIST

Part No.	Material Description	Thickness t [mm]	Layer Count	Area [m²]	Coating [m²]	Volume [m³]	Weight [t]
244	Lamina properties	5.1	4	0.200	0.400	0.004	0.008
	Lamina properties	11.9	4	0.200	0.000	0.010	0.019
	kern	50.0	1	0.200	0.000	0.010	0.001
Σ		118.0	9	0.200	0.400	0.024	0.028
245	Lamina properties	5.1	4	2.333	4.667	0.048	0.096
	Lamina properties	11.9	4	2.333	0.000	0.111	0.225
	kern	50.0	1	2.333	0.000	0.117	0.009
Σ		118.0	9	2.333	4.667	0.275	0.329
246	Lamina properties	5.1	4	0.283	0.566	0.006	0.012
	Lamina properties	11.9	4	0.283	0.000	0.013	0.027
	kern	50.0	1	0.283	0.000	0.014	0.001
Σ		118.0	9	0.283	0.566	0.033	0.040
247	Lamina properties	5.1	4	2.333	4.667	0.048	0.096
	Lamina properties	11.9	4	2.333	0.000	0.111	0.225
	kern	50.0	1	2.333	0.000	0.117	0.009
Σ		118.0	9	2.333	4.667	0.275	0.329
248	Lamina properties	5.1	4	0.283	0.566	0.006	0.012
	Lamina properties	11.9	4	0.283	0.000	0.013	0.027
	kern	50.0	1	0.283	0.000	0.014	0.001
Σ		118.0	9	0.283	0.566	0.033	0.040
249	Lamina properties	5.1	4	2.333	4.667	0.048	0.096
	Lamina properties	11.9	4	2.333	0.000	0.111	0.225
	kern	50.0	1	2.333	0.000	0.117	0.009
Σ		118.0	9	2.333	4.667	0.275	0.329
250	Lamina properties	5.1	4	0.283	0.566	0.006	0.012
	Lamina properties	11.9	4	0.283	0.000	0.013	0.027
	kern	50.0	1	0.283	0.000	0.014	0.001
Σ		118.0	9	0.283	0.566	0.033	0.040
251	Lamina properties	5.1	4	2.333	4.667	0.048	0.096
	Lamina properties	11.9	4	2.333	0.000	0.111	0.225
	kern	50.0	1	2.333	0.000	0.117	0.009
Σ		118.0	9	2.333	4.667	0.275	0.329
252	Lamina properties	5.1	4	0.283	0.566	0.006	0.012
	Lamina properties	11.9	4	0.283	0.000	0.013	0.027
	kern	50.0	1	0.283	0.000	0.014	0.001
Σ		118.0	9	0.283	0.566	0.033	0.040
253	Lamina properties	3.6	6	6.600	13.200	0.143	0.288
	Lamina properties	13.2	2	6.600	0.000	0.174	0.352
	kern	50.0	1	6.600	0.000	0.330	0.024
Σ		98.0	9	6.600	13.200	0.647	0.665
254	Lamina properties	5.0	8	6.600	13.200	0.264	0.534
	kern	50.0	1	6.600	0.000	0.330	0.024
Σ		90.0	9	6.600	13.200	0.594	0.558
255	Lamina properties	5.0	8	6.600	13.200	0.264	0.534
	kern	50.0	1	6.600	0.000	0.330	0.024
Σ		90.0	9	6.600	13.200	0.594	0.558
256	Lamina properties	5.0	8	6.600	13.200	0.264	0.534
	kern	50.0	1	6.600	0.000	0.330	0.024
Σ		90.0	9	6.600	13.200	0.594	0.558
257	Lamina properties	5.0	8	6.600	13.200	0.264	0.534
	kern	50.0	1	6.600	0.000	0.330	0.024
Σ		90.0	9	6.600	13.200	0.594	0.558
258	Lamina properties	5.0	8	6.600	13.200	0.264	0.534
	kern	50.0	1	6.600	0.000	0.330	0.024
Σ		90.0	9	6.600	13.200	0.594	0.558
259	Lamina properties	5.0	8	6.600	13.200	0.264	0.534
	kern	50.0	1	6.600	0.000	0.330	0.024
Σ		90.0	9	6.600	13.200	0.594	0.558
260	Lamina properties	5.0	8	6.600	13.200	0.264	0.534
	kern	50.0	1	6.600	0.000	0.330	0.024
Σ		90.0	9	6.600	13.200	0.594	0.558
261	Lamina properties	5.0	8	6.600	13.200	0.264	0.534
	kern	50.0	1	6.600	0.000	0.330	0.024
Σ		90.0	9	6.600	13.200	0.594	0.558
262	Lamina properties	5.0	8	6.600	13.200	0.264	0.534
	kern	50.0	1	6.600	0.000	0.330	0.024
Σ		90.0	9	6.600	13.200	0.594	0.558
263	Lamina properties	5.0	8	6.600	13.200	0.264	0.534
	kern	50.0	1	6.600	0.000	0.330	0.024
Σ		90.0	9	6.600	13.200	0.594	0.558
264	Lamina properties	5.0	8	6.600	13.200	0.264	0.534

Project: CIE5060 Model: V26
Graduation Project

4.1 PARTS LIST

Part No.	Material Description	Thickness t [mm]	Layer Count	Area [m²]	Coating [m²]	Volume [m³]	Weight [t]
	kern	50.0	1	6.600	0.000	0.330	0.024
Σ		90.0	9	6.600	13.200	0.594	0.558
265	Lamina properties	5.0	8	6.600	13.200	0.264	0.534
	kern	50.0	1	6.600	0.000	0.330	0.024
Σ		90.0	9	6.600	13.200	0.594	0.558
266	Lamina properties	5.1	4	1.650	3.300	0.034	0.068
	Lamina properties	11.9	4	1.650	0.000	0.079	0.159
	kern	50.0	1	1.650	0.000	0.082	0.006
Σ		118.0	9	1.650	3.300	0.195	0.233
267	Lamina properties	5.1	4	1.650	3.300	0.034	0.068
	Lamina properties	11.9	4	1.650	0.000	0.079	0.159
	kern	50.0	1	1.650	0.000	0.082	0.006
Σ		118.0	9	1.650	3.300	0.195	0.233
268	Lamina properties	5.1	4	1.650	3.300	0.034	0.068
	Lamina properties	11.9	4	1.650	0.000	0.079	0.159
	kern	50.0	1	1.650	0.000	0.083	0.006
Σ		118.0	9	1.650	3.300	0.195	0.233
269	Lamina properties	5.1	4	1.650	3.300	0.034	0.068
	Lamina properties	11.9	4	1.650	0.000	0.079	0.159
	kern	50.0	1	1.650	0.000	0.083	0.006
Σ		118.0	9	1.650	3.300	0.195	0.233
270	Lamina properties	5.1	4	1.650	3.300	0.034	0.068
	Lamina properties	11.9	4	1.650	0.000	0.079	0.159
	kern	50.0	1	1.650	0.000	0.082	0.006
Σ		118.0	9	1.650	3.300	0.195	0.233
271	Lamina properties	5.1	4	1.650	3.300	0.034	0.068
	Lamina properties	11.9	4	1.650	0.000	0.079	0.159
	kern	50.0	1	1.650	0.000	0.082	0.006
Σ		118.0	9	1.650	3.300	0.195	0.233
272	Lamina properties	5.1	4	1.650	3.300	0.034	0.068
	Lamina properties	11.9	4	1.650	0.000	0.079	0.159
	kern	50.0	1	1.650	0.000	0.082	0.006
Σ		118.0	9	1.650	3.300	0.195	0.233
273	Lamina properties	5.1	4	1.650	3.300	0.034	0.068
	Lamina properties	11.9	4	1.650	0.000	0.079	0.159
	kern	50.0	1	1.650	0.000	0.082	0.006
Σ		118.0	9	1.650	3.300	0.195	0.233
274	Lamina properties	5.1	4	1.650	3.300	0.034	0.068
	Lamina properties	11.9	4	1.650	0.000	0.079	0.159
	kern	50.0	1	1.650	0.000	0.083	0.006
Σ		118.0	9	1.650	3.300	0.195	0.233
275	Lamina properties	5.1	4	1.650	3.300	0.034	0.068
	Lamina properties	11.9	4	1.650	0.000	0.079	0.159
	kern	50.0	1	1.650	0.000	0.083	0.006
Σ		118.0	9	1.650	3.300	0.195	0.233
276	Lamina properties	5.1	4	1.650	3.300	0.034	0.068
	Lamina properties	11.9	4	1.650	0.000	0.079	0.159
	kern	50.0	1	1.650	0.000	0.082	0.006
Σ		118.0	9	1.650	3.300	0.195	0.233
277	Lamina properties	5.1	4	1.650	3.300	0.034	0.068
	Lamina properties	11.9	4	1.650	0.000	0.079	0.159
	kern	50.0	1	1.650	0.000	0.082	0.006
Σ		118.0	9	1.650	3.300	0.195	0.233
278	Lamina properties	5.1	4	1.650	3.300	0.034	0.068
	Lamina properties	11.9	4	1.650	0.000	0.079	0.159
	kern	50.0	1	1.650	0.000	0.082	0.006
Σ		118.0	9	1.650	3.300	0.195	0.233
279	Lamina properties	5.1	4	1.650	3.300	0.034	0.068
	Lamina properties	11.9	4	1.650	0.000	0.079	0.159
	kern	50.0	1	1.650	0.000	0.082	0.006
Σ		118.0	9	1.650	3.300	0.195	0.233
280	Lamina properties	5.1	4	1.650	3.300	0.034	0.068
	Lamina properties	11.9	4	1.650	0.000	0.079	0.159
	kern	50.0	1	1.650	0.000	0.083	0.006
Σ		118.0	9	1.650	3.300	0.195	0.233
281	Lamina properties	5.1	4	1.650	3.300	0.034	0.068
	Lamina properties	11.9	4	1.650	0.000	0.079	0.159
	kern	50.0	1	1.650	0.000	0.083	0.006
Σ		118.0	9	1.650	3.300	0.195	0.233
282	Lamina properties	5.1	4	1.650	3.300	0.034	0.068
	Lamina properties	11.9	4	1.650	0.000	0.079	0.159
	kern	50.0	1	1.650	0.000	0.082	0.006
Σ		118.0	9	1.650	3.300	0.195	0.233

Project: CIE5060 Model: V26
Graduation Project

4.1 PARTS LIST

Part No.	Material Description	Thickness t [mm]	Layer Count	Area [m²]	Coating [m²]	Volume [m³]	Weight [t]
283	Lamina properties	5.1	4	1.650	3.300	0.034	0.068
	Lamina properties	11.9	4	1.650	0.000	0.079	0.159
	kern	50.0	1	1.650	0.000	0.082	0.006
Σ		118.0	9	1.650	3.300	0.195	0.233
284	Lamina properties	5.1	4	1.650	3.300	0.034	0.068
	Lamina properties	11.9	4	1.650	0.000	0.079	0.159
	kern	50.0	1	1.650	0.000	0.082	0.006
Σ		118.0	9	1.650	3.300	0.195	0.233
285	Lamina properties	5.1	4	1.650	3.300	0.034	0.068
	Lamina properties	11.9	4	1.650	0.000	0.079	0.159
	kern	50.0	1	1.650	0.000	0.082	0.006
Σ		118.0	9	1.650	3.300	0.195	0.233
286	Lamina properties	5.1	4	1.650	3.300	0.034	0.068
	Lamina properties	11.9	4	1.650	0.000	0.079	0.159
	kern	50.0	1	1.650	0.000	0.083	0.006
Σ		118.0	9	1.650	3.300	0.195	0.233
287	Lamina properties	5.1	4	1.650	3.300	0.034	0.068
	Lamina properties	11.9	4	1.650	0.000	0.079	0.159
	kern	50.0	1	1.650	0.000	0.083	0.006
Σ		118.0	9	1.650	3.300	0.195	0.233
288	Lamina properties	5.1	4	1.650	3.300	0.034	0.068
	Lamina properties	11.9	4	1.650	0.000	0.079	0.159
	kern	50.0	1	1.650	0.000	0.082	0.006
Σ		118.0	9	1.650	3.300	0.195	0.233
289	Lamina properties	5.1	4	1.650	3.300	0.034	0.068
	Lamina properties	11.9	4	1.650	0.000	0.079	0.159
	kern	50.0	1	1.650	0.000	0.082	0.006
Σ		118.0	9	1.650	3.300	0.195	0.233
290	Lamina properties	5.1	4	1.650	3.300	0.034	0.068
	Lamina properties	11.9	4	1.650	0.000	0.079	0.159
	kern	50.0	1	1.650	0.000	0.082	0.006
Σ		118.0	9	1.650	3.300	0.195	0.233
291	Lamina properties	5.1	4	1.650	3.300	0.034	0.068
	Lamina properties	11.9	4	1.650	0.000	0.079	0.159
	kern	50.0	1	1.650	0.000	0.082	0.006
Σ		118.0	9	1.650	3.300	0.195	0.233
292	Lamina properties	5.1	4	1.650	3.300	0.034	0.068
	Lamina properties	11.9	4	1.650	0.000	0.079	0.159
	kern	50.0	1	1.650	0.000	0.083	0.006
Σ		118.0	9	1.650	3.300	0.195	0.233
293	Lamina properties	5.1	4	1.650	3.300	0.034	0.068
	Lamina properties	11.9	4	1.650	0.000	0.079	0.159
	kern	50.0	1	1.650	0.000	0.083	0.006
Σ		118.0	9	1.650	3.300	0.195	0.233
294	Lamina properties	5.1	4	1.650	3.300	0.034	0.068
	Lamina properties	11.9	4	1.650	0.000	0.079	0.159
	kern	50.0	1	1.650	0.000	0.082	0.006
Σ		118.0	9	1.650	3.300	0.195	0.233
295	Lamina properties	5.1	4	1.650	3.300	0.034	0.068
	Lamina properties	11.9	4	1.650	0.000	0.079	0.159
	kern	50.0	1	1.650	0.000	0.082	0.006
Σ		118.0	9	1.650	3.300	0.195	0.233
296	Lamina properties	5.1	4	1.650	3.300	0.034	0.068
	Lamina properties	11.9	4	1.650	0.000	0.079	0.159
	kern	50.0	1	1.650	0.000	0.083	0.006
Σ		118.0	9	1.650	3.300	0.195	0.233
297	Lamina properties	5.1	4	1.650	3.300	0.034	0.068
	Lamina properties	11.9	4	1.650	0.000	0.079	0.159
	kern	50.0	1	1.650	0.000	0.083	0.006
Σ		118.0	9	1.650	3.300	0.195	0.233
298	Lamina properties	5.1	4	1.650	3.300	0.034	0.068
	Lamina properties	11.9	4	1.650	0.000	0.079	0.159
	kern	50.0	1	1.650	0.000	0.083	0.006
Σ		118.0	9	1.650	3.300	0.195	0.233
299	Lamina properties	5.1	4	1.650	3.300	0.034	0.068
	Lamina properties	11.9	4	1.650	0.000	0.079	0.159
	kern	50.0	1	1.650	0.000	0.083	0.006
Σ		118.0	9	1.650	3.300	0.195	0.233
300	Lamina properties	5.1	4	1.650	3.300	0.034	0.068
	Lamina properties	11.9	4	1.650	0.000	0.079	0.159
	kern	50.0	1	1.650	0.000	0.083	0.006
Σ		118.0	9	1.650	3.300	0.195	0.233
301	Lamina properties	5.1	4	1.650	3.300	0.034	0.068
	Lamina properties	11.9	4	1.650	0.000	0.079	0.159

Project: CIE5060 Model: V26
Graduation Project

4.1 PARTS LIST

Part No.	Material Description	Thickness t [mm]	Layer Count	Area [m²]	Coating [m²]	Volume [m³]	Weight [t]
	kern	50.0	1	1.650	0.000	0.083	0.006
Σ		118.0	9	1.650	3.300	0.195	0.233
302	Lamina properties	3.6	6	0.800	1.600	0.017	0.035
	Lamina properties	13.2	2	0.800	0.000	0.021	0.043
	kern	50.0	1	0.800	0.000	0.040	0.003
Σ		98.0	9	0.800	1.600	0.078	0.081
303	Lamina properties	5.0	8	0.800	1.600	0.032	0.065
	kern	50.0	1	0.800	0.000	0.040	0.003
Σ		90.0	9	0.800	1.600	0.072	0.068
304	Lamina properties	5.0	8	0.800	1.600	0.032	0.065
	kern	50.0	1	0.800	0.000	0.040	0.003
Σ		90.0	9	0.800	1.600	0.072	0.068
305	Lamina properties	5.0	8	0.800	1.600	0.032	0.065
	kern	50.0	1	0.800	0.000	0.040	0.003
Σ		90.0	9	0.800	1.600	0.072	0.068
306	Lamina properties	5.0	8	0.800	1.600	0.032	0.065
	kern	50.0	1	0.800	0.000	0.040	0.003
Σ		90.0	9	0.800	1.600	0.072	0.068
307	Lamina properties	5.0	8	0.800	1.600	0.032	0.065
	kern	50.0	1	0.800	0.000	0.040	0.003
Σ		90.0	9	0.800	1.600	0.072	0.068
308	Lamina properties	5.0	8	0.800	1.600	0.032	0.065
	kern	50.0	1	0.800	0.000	0.040	0.003
Σ		90.0	9	0.800	1.600	0.072	0.068
309	Lamina properties	5.0	8	0.800	1.600	0.032	0.065
	kern	50.0	1	0.800	0.000	0.040	0.003
Σ		90.0	9	0.800	1.600	0.072	0.068
310	Lamina properties	5.0	8	0.800	1.600	0.032	0.065
	kern	50.0	1	0.800	0.000	0.040	0.003
Σ		90.0	9	0.800	1.600	0.072	0.068
311	Lamina properties	5.0	8	0.800	1.600	0.032	0.065
	kern	50.0	1	0.800	0.000	0.040	0.003
Σ		90.0	9	0.800	1.600	0.072	0.068
312	Lamina properties	5.0	8	0.800	1.600	0.032	0.065
	kern	50.0	1	0.800	0.000	0.040	0.003
Σ		90.0	9	0.800	1.600	0.072	0.068
313	Lamina properties	5.0	8	0.800	1.600	0.032	0.065
	kern	50.0	1	0.800	0.000	0.040	0.003
Σ		90.0	9	0.800	1.600	0.072	0.068
314	Lamina properties	5.0	8	0.800	1.600	0.032	0.065
	kern	50.0	1	0.800	0.000	0.040	0.003
Σ		90.0	9	0.800	1.600	0.072	0.068
315	Lamina properties	5.1	4	0.200	0.400	0.004	0.008
	Lamina properties	11.9	4	0.200	0.000	0.010	0.019
	kern	50.0	1	0.200	0.000	0.010	0.001
Σ		118.0	9	0.200	0.400	0.024	0.028
316	Lamina properties	5.1	4	0.200	0.400	0.004	0.008
	Lamina properties	11.9	4	0.200	0.000	0.010	0.019
	kern	50.0	1	0.200	0.000	0.010	0.001
Σ		118.0	9	0.200	0.400	0.024	0.028
317	Lamina properties	5.1	4	0.200	0.400	0.004	0.008
	Lamina properties	11.9	4	0.200	0.000	0.010	0.019
	kern	50.0	1	0.200	0.000	0.010	0.001
Σ		118.0	9	0.200	0.400	0.024	0.028
318	Lamina properties	5.1	4	0.200	0.400	0.004	0.008
	Lamina properties	11.9	4	0.200	0.000	0.010	0.019
	kern	50.0	1	0.200	0.000	0.010	0.001
Σ		118.0	9	0.200	0.400	0.024	0.028
319	Lamina properties	5.1	4	0.200	0.400	0.004	0.008
	Lamina properties	11.9	4	0.200	0.000	0.010	0.019
	kern	50.0	1	0.200	0.000	0.010	0.001
Σ		118.0	9	0.200	0.400	0.024	0.028
320	Lamina properties	5.1	4	0.200	0.400	0.004	0.008
	Lamina properties	11.9	4	0.200	0.000	0.010	0.019
	kern	50.0	1	0.200	0.000	0.010	0.001
Σ		118.0	9	0.200	0.400	0.024	0.028
321	Lamina properties	5.1	4	0.200	0.400	0.004	0.008
	Lamina properties	11.9	4	0.200	0.000	0.010	0.019
	kern	50.0	1	0.200	0.000	0.010	0.001
Σ		118.0	9	0.200	0.400	0.024	0.028
322	Lamina properties	5.1	4	0.200	0.400	0.004	0.008

Project: CIE5060 Model: V26
Graduation Project

4.1 PARTS LIST

Part No.	Material Description	Thickness t [mm]	Layer Count	Area [m²]	Coating [m²]	Volume [m³]	Weight [t]
	Lamina properties	11.9	4	0.200	0.000	0.010	0.019
	kern	50.0	1	0.200	0.000	0.010	0.001
Σ		118.0	9	0.200	0.400	0.024	0.028
323	Lamina properties	5.1	4	0.200	0.400	0.004	0.008
	Lamina properties	11.9	4	0.200	0.000	0.010	0.019
	kern	50.0	1	0.200	0.000	0.010	0.001
Σ		118.0	9	0.200	0.400	0.024	0.028
324	Lamina properties	5.1	4	0.200	0.400	0.004	0.008
	Lamina properties	11.9	4	0.200	0.000	0.010	0.019
	kern	50.0	1	0.200	0.000	0.010	0.001
Σ		118.0	9	0.200	0.400	0.024	0.028
325	Lamina properties	5.1	4	0.200	0.400	0.004	0.008
	Lamina properties	11.9	4	0.200	0.000	0.010	0.019
	kern	50.0	1	0.200	0.000	0.010	0.001
Σ		118.0	9	0.200	0.400	0.024	0.028
326	Lamina properties	5.1	4	0.200	0.400	0.004	0.008
	Lamina properties	11.9	4	0.200	0.000	0.010	0.019
	kern	50.0	1	0.200	0.000	0.010	0.001
Σ		118.0	9	0.200	0.400	0.024	0.028
327	Lamina properties	5.1	4	0.200	0.400	0.004	0.008
	Lamina properties	11.9	4	0.200	0.000	0.010	0.019
	kern	50.0	1	0.200	0.000	0.010	0.001
Σ		118.0	9	0.200	0.400	0.024	0.028
328	Lamina properties	5.1	4	0.200	0.400	0.004	0.008
	Lamina properties	11.9	4	0.200	0.000	0.010	0.019
	kern	50.0	1	0.200	0.000	0.010	0.001
Σ		118.0	9	0.200	0.400	0.024	0.028
329	Lamina properties	5.1	4	0.200	0.400	0.004	0.008
	Lamina properties	11.9	4	0.200	0.000	0.010	0.019
	kern	50.0	1	0.200	0.000	0.010	0.001
Σ		118.0	9	0.200	0.400	0.024	0.028
330	Lamina properties	5.1	4	0.200	0.400	0.004	0.008
	Lamina properties	11.9	4	0.200	0.000	0.010	0.019
	kern	50.0	1	0.200	0.000	0.010	0.001
Σ		118.0	9	0.200	0.400	0.024	0.028
331	Lamina properties	5.1	4	0.200	0.400	0.004	0.008
	Lamina properties	11.9	4	0.200	0.000	0.010	0.019
	kern	50.0	1	0.200	0.000	0.010	0.001
Σ		118.0	9	0.200	0.400	0.024	0.028
332	Lamina properties	5.1	4	0.200	0.400	0.004	0.008
	Lamina properties	11.9	4	0.200	0.000	0.010	0.019
	kern	50.0	1	0.200	0.000	0.010	0.001
Σ		118.0	9	0.200	0.400	0.024	0.028
333	Lamina properties	5.1	4	0.200	0.400	0.004	0.008
	Lamina properties	11.9	4	0.200	0.000	0.010	0.019
	kern	50.0	1	0.200	0.000	0.010	0.001
Σ		118.0	9	0.200	0.400	0.024	0.028
334	Lamina properties	5.1	4	0.200	0.400	0.004	0.008
	Lamina properties	11.9	4	0.200	0.000	0.010	0.019
	kern	50.0	1	0.200	0.000	0.010	0.001
Σ		118.0	9	0.200	0.400	0.024	0.028
335	Lamina properties	5.1	4	0.200	0.400	0.004	0.008
	Lamina properties	11.9	4	0.200	0.000	0.010	0.019
	kern	50.0	1	0.200	0.000	0.010	0.001
Σ		118.0	9	0.200	0.400	0.024	0.028
336	Lamina properties	5.1	4	0.200	0.400	0.004	0.008
	Lamina properties	11.9	4	0.200	0.000	0.010	0.019
	kern	50.0	1	0.200	0.000	0.010	0.001
Σ		118.0	9	0.200	0.400	0.024	0.028
337	Lamina properties	5.1	4	0.200	0.400	0.004	0.008
	Lamina properties	11.9	4	0.200	0.000	0.010	0.019
	kern	50.0	1	0.200	0.000	0.010	0.001
Σ		118.0	9	0.200	0.400	0.024	0.028
338	Lamina properties	5.1	4	0.200	0.400	0.004	0.008
	Lamina properties	11.9	4	0.200	0.000	0.010	0.019
	kern	50.0	1	0.200	0.000	0.010	0.001
Σ		118.0	9	0.200	0.400	0.024	0.028
339	Lamina properties	5.1	4	0.200	0.400	0.004	0.008
	Lamina properties	11.9	4	0.200	0.000	0.010	0.019
	kern	50.0	1	0.200	0.000	0.010	0.001
Σ		118.0	9	0.200	0.400	0.024	0.028
340	Lamina properties	5.1	4	0.200	0.400	0.004	0.008
	Lamina properties	11.9	4	0.200	0.000	0.010	0.019
	kern	50.0	1	0.200	0.000	0.010	0.001

Project: CIE5060 Model: V26
Graduation Project

4.1 PARTS LIST

Part No.	Material Description	Thickness t [mm]	Layer Count	Area [m²]	Coating [m²]	Volume [m³]	Weight [t]
Σ		118.0	9	0.200	0.400	0.024	0.028
341	Lamina properties	5.1	4	0.200	0.400	0.004	0.008
	Lamina properties	11.9	4	0.200	0.000	0.010	0.019
	kern	50.0	1	0.200	0.000	0.010	0.001
Σ		118.0	9	0.200	0.400	0.024	0.028
342	Lamina properties	5.1	4	0.200	0.400	0.004	0.008
	Lamina properties	11.9	4	0.200	0.000	0.010	0.019
	kern	50.0	1	0.200	0.000	0.010	0.001
Σ		118.0	9	0.200	0.400	0.024	0.028
343	Lamina properties	5.1	4	0.200	0.400	0.004	0.008
	Lamina properties	11.9	4	0.200	0.000	0.010	0.019
	kern	50.0	1	0.200	0.000	0.010	0.001
Σ		118.0	9	0.200	0.400	0.024	0.028
344	Lamina properties	5.1	4	0.200	0.400	0.004	0.008
	Lamina properties	11.9	4	0.200	0.000	0.010	0.019
	kern	50.0	1	0.200	0.000	0.010	0.001
Σ		118.0	9	0.200	0.400	0.024	0.028
345	Lamina properties	5.1	4	0.200	0.400	0.004	0.008
	Lamina properties	11.9	4	0.200	0.000	0.010	0.019
	kern	50.0	1	0.200	0.000	0.010	0.001
Σ		118.0	9	0.200	0.400	0.024	0.028
346	Lamina properties	5.1	4	0.200	0.400	0.004	0.008
	Lamina properties	11.9	4	0.200	0.000	0.010	0.019
	kern	50.0	1	0.200	0.000	0.010	0.001
Σ		118.0	9	0.200	0.400	0.024	0.028
347	Lamina properties	5.1	4	0.200	0.400	0.004	0.008
	Lamina properties	11.9	4	0.200	0.000	0.010	0.019
	kern	50.0	1	0.200	0.000	0.010	0.001
Σ		118.0	9	0.200	0.400	0.024	0.028
348	Lamina properties	5.1	4	0.200	0.400	0.004	0.008
	Lamina properties	11.9	4	0.200	0.000	0.010	0.019
	kern	50.0	1	0.200	0.000	0.010	0.001
Σ		118.0	9	0.200	0.400	0.024	0.028
349	Lamina properties	5.1	4	0.200	0.400	0.004	0.008
	Lamina properties	11.9	4	0.200	0.000	0.010	0.019
	kern	50.0	1	0.200	0.000	0.010	0.001
Σ		118.0	9	0.200	0.400	0.024	0.028
350	Lamina properties	5.1	4	0.200	0.400	0.004	0.008
	Lamina properties	11.9	4	0.200	0.000	0.010	0.019
	kern	50.0	1	0.200	0.000	0.010	0.001
Σ		118.0	9	0.200	0.400	0.024	0.028
351	Lamina properties	7.0	4	4.000	7.999	0.112	0.226
	Lamina properties	3.0	4	4.000	0.000	0.048	0.097
	kern	50.0	1	4.000	0.000	0.200	0.015
Σ		90.0	9	4.000	7.999	0.360	0.338
352	Lamina properties	7.0	4	4.001	8.002	0.112	0.227
	Lamina properties	3.0	4	4.001	0.000	0.048	0.097
	kern	50.0	1	4.001	0.000	0.200	0.015
Σ		90.0	9	4.001	8.002	0.360	0.338
353	Lamina properties	7.0	4	4.000	7.999	0.112	0.226
	Lamina properties	3.0	4	4.000	0.000	0.048	0.097
	kern	50.0	1	4.000	0.000	0.200	0.015
Σ		90.0	9	4.000	7.999	0.360	0.338
354	Lamina properties	7.0	4	4.000	7.999	0.112	0.226
	Lamina properties	3.0	4	4.000	0.000	0.048	0.097
	kern	50.0	1	4.000	0.000	0.200	0.015
Σ		90.0	9	4.000	7.999	0.360	0.338
355	Lamina properties	7.0	4	4.001	8.002	0.112	0.227
	Lamina properties	3.0	4	4.001	0.000	0.048	0.097
	kern	50.0	1	4.001	0.000	0.200	0.015
Σ		90.0	9	4.001	8.002	0.360	0.338
356	Lamina properties	7.0	4	4.000	7.999	0.112	0.226
	Lamina properties	3.0	4	4.000	0.000	0.048	0.097
	kern	50.0	1	4.000	0.000	0.200	0.015
Σ		90.0	9	4.000	7.999	0.360	0.338
357	Lamina properties	7.0	4	4.000	7.999	0.112	0.226
	Lamina properties	3.0	4	4.000	0.000	0.048	0.097
	kern	50.0	1	4.000	0.000	0.200	0.015
Σ		90.0	9	4.000	7.999	0.360	0.338
358	Lamina properties	7.0	4	4.001	8.002	0.112	0.227
	Lamina properties	3.0	4	4.001	0.000	0.048	0.097
	kern	50.0	1	4.001	0.000	0.200	0.015
Σ		90.0	9	4.001	8.002	0.360	0.338

Project: CIE5060 Model: V26
Graduation Project

4.1 PARTS LIST

Part No.	Material Description	Thickness t [mm]	Layer Count	Area [m²]	Coating [m²]	Volume [m³]	Weight [t]
359	Lamina properties	7.0	4	4.000	7.999	0.112	0.226
	Lamina properties	3.0	4	4.000	0.000	0.048	0.097
	kern	50.0	1	4.000	0.000	0.200	0.015
Σ		90.0	9	4.000	7.999	0.360	0.338
360	Lamina properties	7.0	4	4.000	7.999	0.112	0.226
	Lamina properties	3.0	4	4.000	0.000	0.048	0.097
	kern	50.0	1	4.000	0.000	0.200	0.015
Σ		90.0	9	4.000	7.999	0.360	0.338
361	Lamina properties	7.0	4	4.001	8.002	0.112	0.227
	Lamina properties	3.0	4	4.001	0.000	0.048	0.097
	kern	50.0	1	4.001	0.000	0.200	0.015
Σ		90.0	9	4.001	8.002	0.360	0.338
362	Lamina properties	7.0	4	4.000	7.999	0.112	0.226
	Lamina properties	3.0	4	4.000	0.000	0.048	0.097
	kern	50.0	1	4.000	0.000	0.200	0.015
Σ		90.0	9	4.000	7.999	0.360	0.338
363	Lamina properties	7.0	4	4.000	7.999	0.112	0.226
	Lamina properties	3.0	4	4.000	0.000	0.048	0.097
	kern	50.0	1	4.000	0.000	0.200	0.015
Σ		90.0	9	4.000	7.999	0.360	0.338
364	Lamina properties	7.0	4	4.001	8.002	0.112	0.227
	Lamina properties	3.0	4	4.001	0.000	0.048	0.097
	kern	50.0	1	4.001	0.000	0.200	0.015
Σ		90.0	9	4.001	8.002	0.360	0.338
365	Lamina properties	7.0	4	4.000	7.999	0.112	0.226
	Lamina properties	3.0	4	4.000	0.000	0.048	0.097
	kern	50.0	1	4.000	0.000	0.200	0.015
Σ		90.0	9	4.000	7.999	0.360	0.338
366	Lamina properties	7.0	4	4.000	8.000	0.112	0.226
	Lamina properties	3.0	4	4.000	0.000	0.048	0.097
	kern	50.0	1	4.000	0.000	0.200	0.015
Σ		90.0	9	4.000	8.000	0.360	0.338
367	Lamina properties	7.0	4	4.000	8.000	0.112	0.226
	Lamina properties	3.0	4	4.000	0.000	0.048	0.097
	kern	50.0	1	4.000	0.000	0.200	0.015
Σ		90.0	9	4.000	8.000	0.360	0.338
368	Lamina properties	7.0	4	4.000	8.000	0.112	0.226
	Lamina properties	3.0	4	4.000	0.000	0.048	0.097
	kern	50.0	1	4.000	0.000	0.200	0.015
Σ		90.0	9	4.000	8.000	0.360	0.338
369	Lamina properties	3.6	6	6.600	13.200	0.143	0.288
	Lamina properties	13.2	2	6.600	0.000	0.174	0.352
	kern	50.0	1	6.600	0.000	0.330	0.024
Σ		98.0	9	6.600	13.200	0.647	0.665
370	Lamina properties	3.6	6	0.800	1.600	0.017	0.035
	Lamina properties	13.2	2	0.800	0.000	0.021	0.043
	kern	50.0	1	0.800	0.000	0.040	0.003
Σ		98.0	9	0.800	1.600	0.078	0.081
371	Lamina properties	7.0	4	3.500	7.000	0.098	0.198
	Lamina properties	3.0	4	3.500	0.000	0.042	0.085
	kern	50.0	1	3.500	0.000	0.175	0.013
Σ		90.0	9	3.500	7.000	0.315	0.296
372	Lamina properties	7.0	4	2.500	5.000	0.070	0.142
	Lamina properties	3.0	4	2.500	0.000	0.030	0.061
	kern	50.0	1	2.500	0.000	0.125	0.009
Σ		90.0	9	2.500	5.000	0.225	0.211
373	Lamina properties	7.0	4	1.500	3.000	0.042	0.085
	Lamina properties	3.0	4	1.500	0.000	0.018	0.036
	kern	50.0	1	1.500	0.000	0.075	0.006
Σ		90.0	9	1.500	3.000	0.135	0.127
374	Lamina properties	7.0	4	0.500	1.000	0.014	0.028
	Lamina properties	3.0	4	0.500	0.000	0.006	0.012
	kern	50.0	1	0.500	0.000	0.025	0.002
Σ		90.0	9	0.500	1.000	0.045	0.042
375	Lamina properties	5.0	8	4.950	9.900	0.198	0.400
	kern	50.0	1	4.950	0.000	0.248	0.018
Σ		90.0	9	4.950	9.900	0.445	0.419
376	Lamina properties	5.0	8	0.600	1.200	0.024	0.049
	kern	50.0	1	0.600	0.000	0.030	0.002
Σ		90.0	9	0.600	1.200	0.054	0.051
377	Lamina properties	3.6	6	3.300	6.600	0.071	0.144
	Lamina properties	13.2	2	3.300	0.000	0.087	0.176
	kern	50.0	1	3.300	0.000	0.165	0.012
Σ		98.0	9	3.300	6.600	0.323	0.332

Project: CIE5060 Model: V26
Graduation Project

4.1 PARTS LIST

Part No.	Material Description	Thickness t [mm]	Layer Count	Area [m²]	Coating [m²]	Volume [m³]	Weight [t]
378	Lamina properties	3.6	6	0.400	0.800	0.009	0.017
	Lamina properties	13.2	2	0.400	0.000	0.011	0.021
	kern	50.0	1	0.400	0.000	0.020	0.001
Σ		98.0	9	0.400	0.800	0.039	0.040
379	Lamina properties	5.0	8	1.650	3.300	0.066	0.133
	kern	50.0	1	1.650	0.000	0.083	0.006
Σ		90.0	9	1.650	3.300	0.148	0.140
380	Lamina properties	5.0	8	0.200	0.400	0.008	0.016
	kern	50.0	1	0.200	0.000	0.010	0.001
Σ		90.0	9	0.200	0.400	0.018	0.017
385	Lamina properties	7.0	4	3.500	7.000	0.098	0.198
	Lamina properties	3.0	4	3.500	0.000	0.042	0.085
	kern	50.0	1	3.500	0.000	0.175	0.013
Σ		90.0	9	3.500	7.000	0.315	0.296
386	Lamina properties	7.0	4	2.500	5.000	0.070	0.142
	Lamina properties	3.0	4	2.500	0.000	0.030	0.061
	kern	50.0	1	2.500	0.000	0.125	0.009
Σ		90.0	9	2.500	5.000	0.225	0.211
387	Lamina properties	7.0	4	1.500	3.000	0.042	0.085
	Lamina properties	3.0	4	1.500	0.000	0.018	0.036
	kern	50.0	1	1.500	0.000	0.075	0.006
Σ		90.0	9	1.500	3.000	0.135	0.127
388	Lamina properties	7.0	4	0.500	1.000	0.014	0.028
	Lamina properties	3.0	4	0.500	0.000	0.006	0.012
	kern	50.0	1	0.500	0.000	0.025	0.002
Σ		90.0	9	0.500	1.000	0.045	0.042
389	Lamina properties	5.1	4	1.650	3.300	0.034	0.068
	Lamina properties	11.9	4	1.650	0.000	0.079	0.159
	kern	50.0	1	1.650	0.000	0.083	0.006
Σ		118.0	9	1.650	3.300	0.195	0.233
390	Lamina properties	5.1	4	0.200	0.400	0.004	0.008
	Lamina properties	11.9	4	0.200	0.000	0.010	0.019
	kern	50.0	1	0.200	0.000	0.010	0.001
Σ		118.0	9	0.200	0.400	0.024	0.028
391	Lamina properties	5.1	4	1.650	3.300	0.034	0.068
	Lamina properties	11.9	4	1.650	0.000	0.079	0.159
	kern	50.0	1	1.650	0.000	0.083	0.006
Σ		118.0	9	1.650	3.300	0.195	0.233
392	Lamina properties	5.1	4	0.200	0.400	0.004	0.008
	Lamina properties	11.9	4	0.200	0.000	0.010	0.019
	kern	50.0	1	0.200	0.000	0.010	0.001
Σ		118.0	9	0.200	0.400	0.024	0.028
393	Lamina properties	5.1	4	1.650	3.300	0.034	0.068
	Lamina properties	11.9	4	1.650	0.000	0.079	0.159
	kern	50.0	1	1.650	0.000	0.083	0.006
Σ		118.0	9	1.650	3.300	0.195	0.233
394	Lamina properties	5.1	4	0.200	0.400	0.004	0.008
	Lamina properties	11.9	4	0.200	0.000	0.010	0.019
	kern	50.0	1	0.200	0.000	0.010	0.001
Σ		118.0	9	0.200	0.400	0.024	0.028
395	Lamina properties	5.1	4	1.650	3.300	0.034	0.068
	Lamina properties	11.9	4	1.650	0.000	0.079	0.159
	kern	50.0	1	1.650	0.000	0.083	0.006
Σ		118.0	9	1.650	3.300	0.195	0.233
396	Lamina properties	5.1	4	0.200	0.400	0.004	0.008
	Lamina properties	11.9	4	0.200	0.000	0.010	0.019
	kern	50.0	1	0.200	0.000	0.010	0.001
Σ		118.0	9	0.200	0.400	0.024	0.028
397	Lamina properties	5.1	4	2.333	4.667	0.048	0.096
	Lamina properties	11.9	4	2.333	0.000	0.111	0.225
	kern	50.0	1	2.333	0.000	0.117	0.009
Σ		118.0	9	2.333	4.667	0.275	0.329
398	Lamina properties	5.1	4	0.283	0.566	0.006	0.012
	Lamina properties	11.9	4	0.283	0.000	0.013	0.027
	kern	50.0	1	0.283	0.000	0.014	0.001
Σ		118.0	9	0.283	0.566	0.033	0.040
399	Lamina properties	5.1	4	2.333	4.667	0.048	0.096
	Lamina properties	11.9	4	2.333	0.000	0.111	0.225
	kern	50.0	1	2.333	0.000	0.117	0.009
Σ		118.0	9	2.333	4.667	0.275	0.329
400	Lamina properties	5.1	4	0.283	0.566	0.006	0.012
	Lamina properties	11.9	4	0.283	0.000	0.013	0.027
	kern	50.0	1	0.283	0.000	0.014	0.001

Project: CIE5060 Model: V26
Graduation Project

4.1 PARTS LIST

Part No.	Material Description	Thickness t [mm]	Layer Count	Area [m²]	Coating [m²]	Volume [m³]	Weight [t]
Σ		118.0	9	0.283	0.566	0.033	0.040
401	Lamina properties	5.1	4	2.333	4.667	0.048	0.096
	Lamina properties	11.9	4	2.333	0.000	0.111	0.225
	kern	50.0	1	2.333	0.000	0.117	0.009
Σ		118.0	9	2.333	4.667	0.275	0.329
402	Lamina properties	5.1	4	0.283	0.566	0.006	0.012
	Lamina properties	11.9	4	0.283	0.000	0.013	0.027
	kern	50.0	1	0.283	0.000	0.014	0.001
Σ		118.0	9	0.283	0.566	0.033	0.040
403	Lamina properties	5.1	4	2.333	4.667	0.048	0.096
	Lamina properties	11.9	4	2.333	0.000	0.111	0.225
	kern	50.0	1	2.333	0.000	0.117	0.009
Σ		118.0	9	2.333	4.667	0.275	0.329
404	Lamina properties	5.1	4	0.283	0.566	0.006	0.012
	Lamina properties	11.9	4	0.283	0.000	0.013	0.027
	kern	50.0	1	0.283	0.000	0.014	0.001
Σ		118.0	9	0.283	0.566	0.033	0.040
406	Lamina properties	3.6	4	38.293	76.586	0.551	1.115
	Lamina properties	8.4	4	38.293	0.000	1.287	2.602
	kern	50.0	1	38.293	0.000	1.915	0.141
Σ		98.0	9	38.293	76.586	3.753	3.857
407	Lamina properties	3.6	4	19.374	38.749	0.279	0.564
	Lamina properties	8.4	4	19.374	0.000	0.651	1.316
	kern	50.0	1	19.374	0.000	0.969	0.071
Σ		98.0	9	19.374	38.749	1.899	1.952
408	Lamina properties	18.7	2	75.600	151.200	2.827	5.717
	Lamina properties	5.1	6	75.600	0.000	2.313	4.678
	kern	50.0	1	75.600	0.000	3.780	0.278
Σ		118.0	9	75.600	151.200	8.921	10.673
409	Lamina properties	18.7	2	75.600	151.200	2.827	5.717
	Lamina properties	5.1	6	75.600	0.000	2.313	4.678
	kern	50.0	1	75.600	0.000	3.780	0.278
Σ		118.0	9	75.600	151.200	8.921	10.673
410	Lamina properties	18.7	2	106.915	213.829	3.999	8.085
	Lamina properties	5.1	6	106.915	0.000	3.272	6.615
	kern	50.0	1	106.915	0.000	5.346	0.393
Σ		118.0	9	106.915	213.829	12.616	15.094
411	Lamina properties	18.7	2	106.915	213.829	3.999	8.085
	Lamina properties	5.1	6	106.915	0.000	3.272	6.615
	kern	50.0	1	106.915	0.000	5.346	0.393
Σ		118.0	9	106.915	213.829	12.616	15.094
Σ Total				3447.393	6894.786	372.793	417.941

Apendix G: Extra costs rigorously solution

The extra direct costs due to the extra adjustments on the barrier for the rigorously solution are calculated in Table G.1. The direct costs are separated in material costs and costs for labor. The material costs are further specified in the next sections. The labor costs consider mainly the lifting operations which are necessary and some other labor intensive operations. The costs are estimated with price units from a cost expert of Witteveen+Bos. The total values are rounded off to do not present costs with a misleading accuracy.

Table G.1 Extra costs specification rigorously solution

Number	Description	Costs	Costs per slide / per pier	Subtotal
62	Removing the upper beam		€ 10,000	€ 620,000
62	Replacement of the sill beam			
	Removing sill beam (including flushing)	€ 20,000		
	New sill beam[1]	€ 810,000		
	Placing the new sill beam	€ 10,000		
			€ 840,000	€ 52,000,000
65	Increasing a rabbet			
	Disassemble the cylinders and other installations	€ 12,000		
	Removing the extending parts, cardan girders and cylinders	€ 10,000		
	Increasing a rabbet[2]	€ 210,000		
	Replace the extending parts, cardan girders and cylinders	€ 10,000		
	Reassembly of the cylinders and other installations	€ 15,000		
			€ 257,000	€ 17,000,000
				€ 70,000,000

1 Costs new sill beam

The costs for the new sill beam are calculated in Table G.2. A rounded value of the total material costs for the new sill beam is used in Table G.1.

Table G.2 Calculation of costs for new sill beam

Parameter	Value	
Total surface (m^2)	17.22	
Length (m)	39	
Volume (m^3)	671.58	
Material price (€/m^3)	1200	
Price per sill beam(€)	**€ 805,896**	**€ 810,000**

The total surface of a cross section of the new sill beam is calculated in Table G.3 on the basis of the dimensions which are shown in Figure G.1.

Table G.3 Surface new sill beam

Width (m)	Length (m)	Number	Surface (m^2)
9.7	4	1	38,8
8.3	2,6	-1	-21.58
Total surface (m^2)			**17.22**

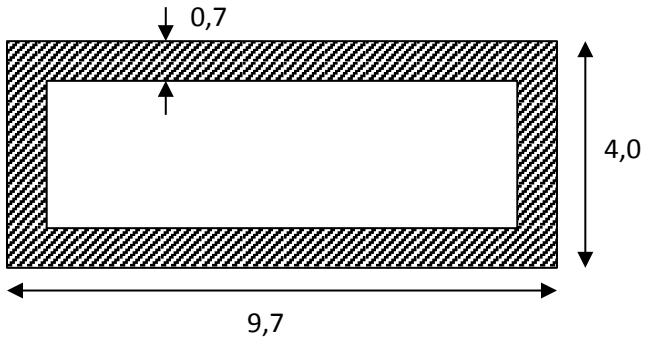


Figure G.1 Dimensions new sill beam (in meters)

2 Increasing a rabbet

The costs for increasing a rabbet are calculated in Table G.4. A rounded value of the total material costs for increasing a rabbet is used in Table G.1.

Table G.4 Calculation of costs for increasing a rabbet

Parameter	Value	
Total surface (m^2)	25.88	
Increase (m)	10.1	
Volume (m^3)	261.388	
Material price (€/m^3)	800	
Price per pier(€)	**€ 209,110**	**€ 210,000**

The total surface of a cross section of the pier is calculated in Table G.5 on the basis of the dimensions which are shown in Figure G.2.

Table G.5 Surface piers

Surface nr.	Width (m)	Length (m)	Number	Surface (m^2)
1	**1.4**	5.0	1	7.00
2	**1.6**	2.4	2	7.68
3	**1.6**	1.1	4	7.04
4	**0.8**	1.3	4	4.16
Total surface (m^2)				**25.88**

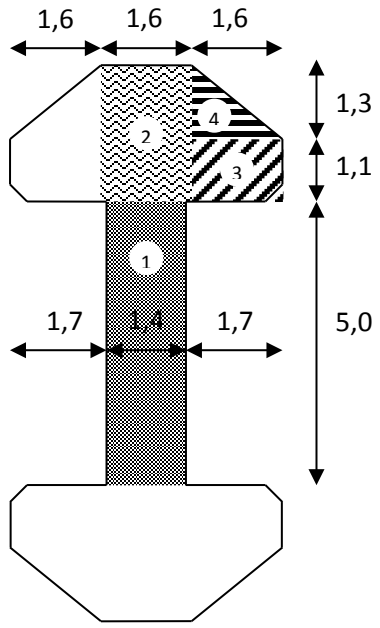


Figure G.2 Dimensions pier (in meters)

Apendix H: Information provided on DVD

The following information is provided on DVD as attachment to this report:

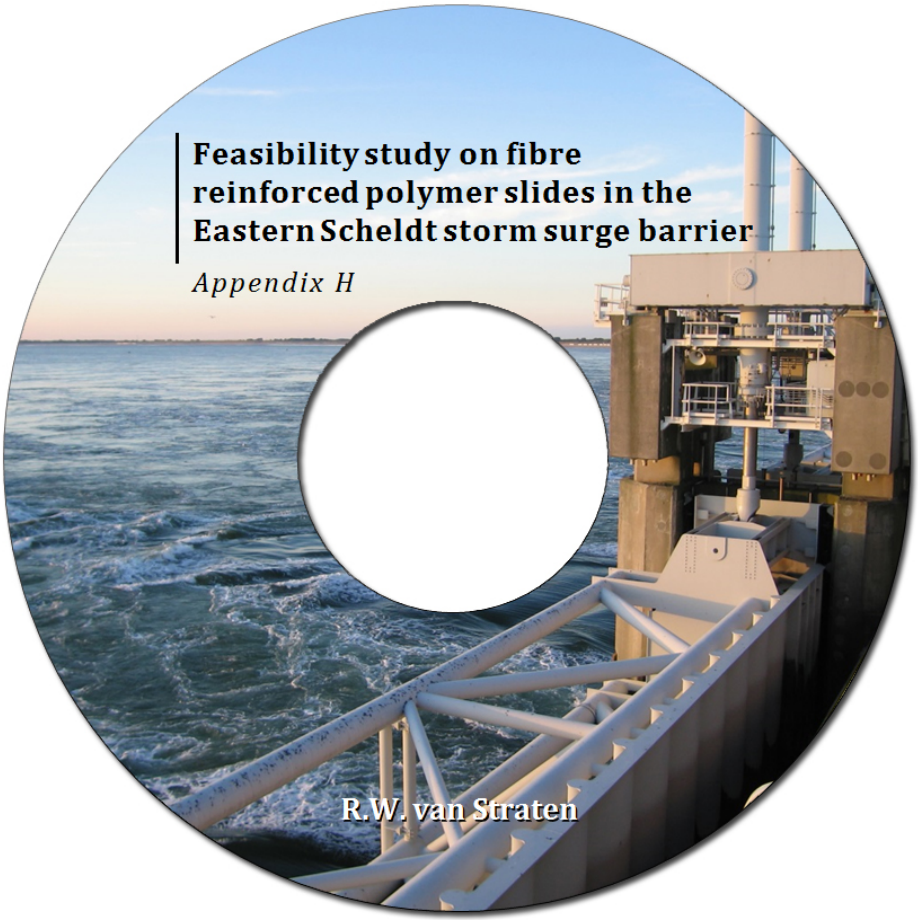
- FEA Models of the variant study, see Table H.1
- FEA Models of final design (only important ones), see Table H.2
- Final report in PDF and DOCX format

Table H.1 FEA Models of the variant study (chapter 8)

Variant	Description of model
Variant 1	Sandwich
Variant 2	Horizontally curved shell
Variant 3.1	Straight box girder
Variant 3.2	Box girder with thickening
Variant 3.3	Box girder with extra thickening

Table H.2 FEA Models of the final design (chapter 10)

Version	Description of model
V2	Infinity stiff line support at both sides
V3	Line support with finite stiffness at both sides
V4	Surface support with finite stiffness at both sides
V7	Stiff end structure with extra horizontal plates
V8	Line support with finite stiffness at bottom of slide
V10	Nodal support in longitudinal direction
V12	Gaps in horizontal plates (r=1)
V14	Improvement of size of gaps (r1=0,75, r2=0,5)
V15	Horizontal plates divided in separate compositions
V16	Second order calculation of V15
V17	Adjustment of separation of horizontal plates
V18	Extra horizontal plate at bottom of slide
V23	Extra loads, exceeds strain limit
V24	Thickness outer sandwich adjusted
V26	Thickness outer sandwich optimized



Feasibility study on fibre reinforced polymer slides in the Eastern Scheldt storm surge barrier

Appendix H

R.W. van Straten